REPORT UAG - 24
PART I

WORLD DATA CENTER A
for
Solar-Terrestrial Physics

DATA ON SOLAR - GEOPHYSICAL ACTIVITY ASSOCIATED WITH THE MAJOR GROUND LEVEL COSMIC RAY EVENTS OF 24 JANUARY AND 1 SEPTEMBER 1971

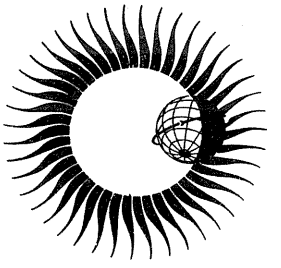

DECEMBER 1972

WORLD DATA CENTER A

National Academy of Sciences

2101 Constitution Avenue, N. W. Washington, D. C. U.S.A., 20418

World Data Center A consists of the Coordination Office

and eight subcenters:

World Data Center A
Coordination Office
National Academy of Sciences
2101 Constitution Avenue, N.W.
Washington, D. C., U.S.A. 20418
Telephone (202) 961-1478

Solar and Interplanetary Phenomena, Ionospheric Phenomena, Flare-Associated Events, Geomagnetic Variations, Magnetospheric and Interplanetary Magnetic Phenomena, Aurora, Cosmic Rays, Airglow:
World Data Center A
for Solar-Terrestrial Physics
National Oceanic and Atmospheric Administration
Boulder, Colorado, U.S.A. 80302
Telephone (303) 499-1000 Ext. 6467

Geomagnetism, Seismology, Gravity (and Upper Mantle Project Archives):
World Data Center A:
Geomagnetism, Seismology and Gravity
Environmental Data Service, NOAA
Boulder, Colorado, U.S.A. 80302
Telephone (303) 499-1000 Ext. 6311

Glaciology:
World Data Center A:
Glaciology
U. S. Geological Survey
1305 Tacoma Avenue South
Tacoma, Washington, U.S.A. 98402
Telephone (206) 383-2861 Ext. 318

Longitude and Latitude:
World Data Center A:
Longitude and Latitude
U. S. Naval Observatory
Washington, D. C., U.S.A. 20390
Telephone (202) 698-8422

Meteorology (and Nuclear Radiation):
World Data Center A:
Meteorology
National Climatic Center
Federal Building
Asheville, North Carolina, U.S.A. 28801
Telephone (704) 254-0961

Oceanography:
World Data Center A:
Oceanography
National Oceanic and Atmospheric Administration
Rockville, Maryland, U.S.A. 20852
Telephone (202) 426-9052

Rockets and Satellites:
World Data Center A:
Rockets and Satellites
Goddard Space Flight Center
Code 601
Greenbelt, Maryland, U.S.A. 20771
Telephone (301) 982-6695

Tsunami:
World Data Center A:
Tsunami
National Oceanic and Atmospheric Administration
P.O. Box 3887
Honolulu, Hawaii, U.S.A. 96812
Telephone (808) 546-5698

Notes:

(1) World Data Centers conduct international exchange of geophysical observations in accordance with the principles set forth by the International Council of Scientific Unions. WDC-A is established in the United States under the auspices of the National Academy of Sciences.
(2) Communications regarding data interchange matters in general and World Data Center A as a whole should be addressed to: World Data Center A, Coordination Office (see address above).
(3) Inquiries and communications concerning data in specific disciplines should be addressed to the appropriate subcenter listed above.

WORLD DATA CENTER A
for
Solar-Terrestrial Physics

REPORT UAG - 24 PART I

DATA ON SOLAR - GEOPHYSICAL ACTIVITY ASSOCIATED WITH THE MAJOR GROUND LEVEL COSMIC RAY EVENTS OF 24 JANUARY AND 1 SEPTEMBER 1971

compiled by

Helen E. Coffey and J. Virginia Lincoln
WDC-A for Solar-Terrestrial Physics
Boulder, Colorado

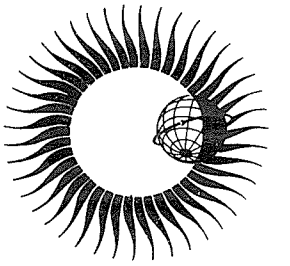

Prepared by World Data Center A for
Solar-Terrestrial Physics, NOAA, Boulder, Colorado
and published by

U.S. DEPARTMENT OF COMMERCE
NATIONAL OCEANIC AND ATMOSPHERIC ADMINISTRATION

ENVIRONMENTAL DATA SERVICE
Asheville, North Carolina, USA 28801

DECEMBER 1972

SUBSCRIPTION PRICE: $9.00 a year; $2.50 additional for foreign mailing; single copy price varies.* Checks and money orders should be made payable to the Department of Commerce, NOAA. Remittance and correspondence regarding subscriptions should be sent to the National Climatic Center, Federal Building, Asheville, NC 28801, Attn: Publications.

*PRICE THIS ISSUE $2.00

FOREWORD

This data compilation is the sixth in the series of special compilations which have been produced under the auspices of World Data Center A for Solar-Terrestrial Physics. The first five have concerned the solar-terrestrial events of May 23, 1967, October 24 - November 6, 1968, November 18, 1968, November 2-10, 1969, and March 8, 1970. Judging from the references made to these publications in journal papers and from many informal contacts, these kinds of reports seem to be filling a need for a publication medium for collecting in one place rather detailed data for a particular event, with discussions and interpretations by those responsible for the observations.

To be useful such publications should be started rather soon after the event has taken place, giving hardly time for extensive consideration by international bodies. We at WDC-A for Solar-Terrestrial Physics, therefore, proposed this report after only informal consultation with what in our judgment was a representative international sample of leading solar-terrestrial scientists.

The periods selected were those including the ground-level cosmic ray increases of January 24, 1971 and September 1, 1971.

The many contributors are thanked for their submissions. The compilers wish to acknowledge with special thanks the typing and correcting of the manuscript by Miss J. May Starr.

Helen E. Coffey

J. Virginia Lincoln

TABLE OF CONTENTS

TABLE OF CONTENTS

* Article covers both the January and September events.

Table of Contents (Continued)

* Article covers both the January and September events.

Table of Contents (Continued)

* Article covers both the January and September events.

1. INTRODUCTION AND BACKGROUND DATA

by

Helen E. Coffey
World Data Center A for Solar-Terrestrial Physics
NOAA, Boulder, Colorado 80302

Since this report covers two separate cosmic ray events, we have tried to devote a separate section to each event. In some cases, however, comparisons of the two events were made, making it difficult to place the paper in a one event category. To avoid reproducing the same paper in both sections, these papers are found in the first section on the January event. An asterisk in the Table of Contents indicates a two event paper.

Data from earlier publications of "Solar-Geophysical Data" relating to the events are reproduced for the readers' convenience in the introductory paragraphs. For further explanations concerning these data, see the Descriptive Text, "Solar-Geophysical Data", Number 330 (Supplement), February, 1972.

General Activity:

Solar activity on January 24, 1971 is shown in the solar maps in Figure 1 reprinted from the monthly publication "Solar-Geophysical Data". An historical account of the development of the region wherein the large flare occurred is given in Table 1.

Table 1

McMATH REGION 11128 CMP DATE 21.3

				CALCIUM PLAGE DATA					SUNSPOT DATA								9.1 CM	
YR	MO	DA	MC NO.	LAT	CMD	L	AREA	INT	MW NO.	LAT	CMD	L	MAG.	H	AREA	CNT	C	INT	FLUX
71	1	14	11128	N20	E80	227	3000	3.0	18281	N17	E80	227	BP		250	1	H	24	13
		15	11128	N20	E75	222	4700	3.5	18281	N18	E75	222	(BP)	5	630	21	E	35	19
		16							18281	N18	E58	225	(BP)	6	560	8	E	48	26
									18284	N19	E76	207	(B	2					
		17	11128	N20	E46	224	5300	3.5	18281	N19	E48	222	(BP)	5	640	21	E	51	27
									18284	N18	E63	207	BF)	1					
		18	11128	N20	E32	224	5700	3.0	18281	N19	E35	222	(D)	6					
									18284	N19	E46	211	(B)	3					
		19	11128	N20	E21	223	5600	3.5	18281	N19	E21	222	(BP)	6	930	46	E	54	29
									18284	N19	E32	211	(B)	3	10	1	A		
		20	11128	N20	E08	223	6000	3.5	18281	N18	E09	222	(BY)	6	990	36	E	47	25
									18284	N18	E20	211	(B)	4	30	8	D		
		21							18281	N19	W06	222	(BP)	6	640	45	E	39	20
									18284	N19	E06	210	(BP)	5	160	25	D		
		22	11128	N20	W15	220	6200	3.5	18298	N28	W28	228	(BP)	1	0	3	B	38	20
									18281	N19	W28	228	(BP)	5	850	52	E		
									18284	N19	W12	212	(BP)	5	490	21	D		
		23	11128	N20	W30	222	6000	3.5	18298	N28	W34	224	(B)	1				34	18
									18281	N19	W34	224	(BP)	5	660	31	D		
									18284	N20	W23	213	(BP)	5	350	20	D		
		24	11128	N20	W45	220	5800	3.5	18298	N24	W59	233	(BP	1				62	32
									18281	N19	W49	223	(BP)	5	410	22	D		
									18284	N20	W38	212	(B)	4	300	5	D		
		25	11128	N20	W60	222	5700	3.5	18298	N22	W70	234	(B)	1				23	12
									18281	N18	W59	223	(BP)	5	480	8	E		
									18284	N19	W49	213	(B)	4	60	1	H		
		26							18298	N22	W83	232	BF					24	12
									18281	N18	W75	224	(BP)	4	230	7	E		
									18284	N20	W64	213	(BP)	4	50	1	H		
		27	11128	N18	W80	217	4000	3.5	18281	N19	W90	224	AF		90	1	H	13	7
									18284	N20	W83	217	BP		10	1	H		

JANUARY 24, 1971 (P=-8.54, B_o=-5.38, L_o=186.75)

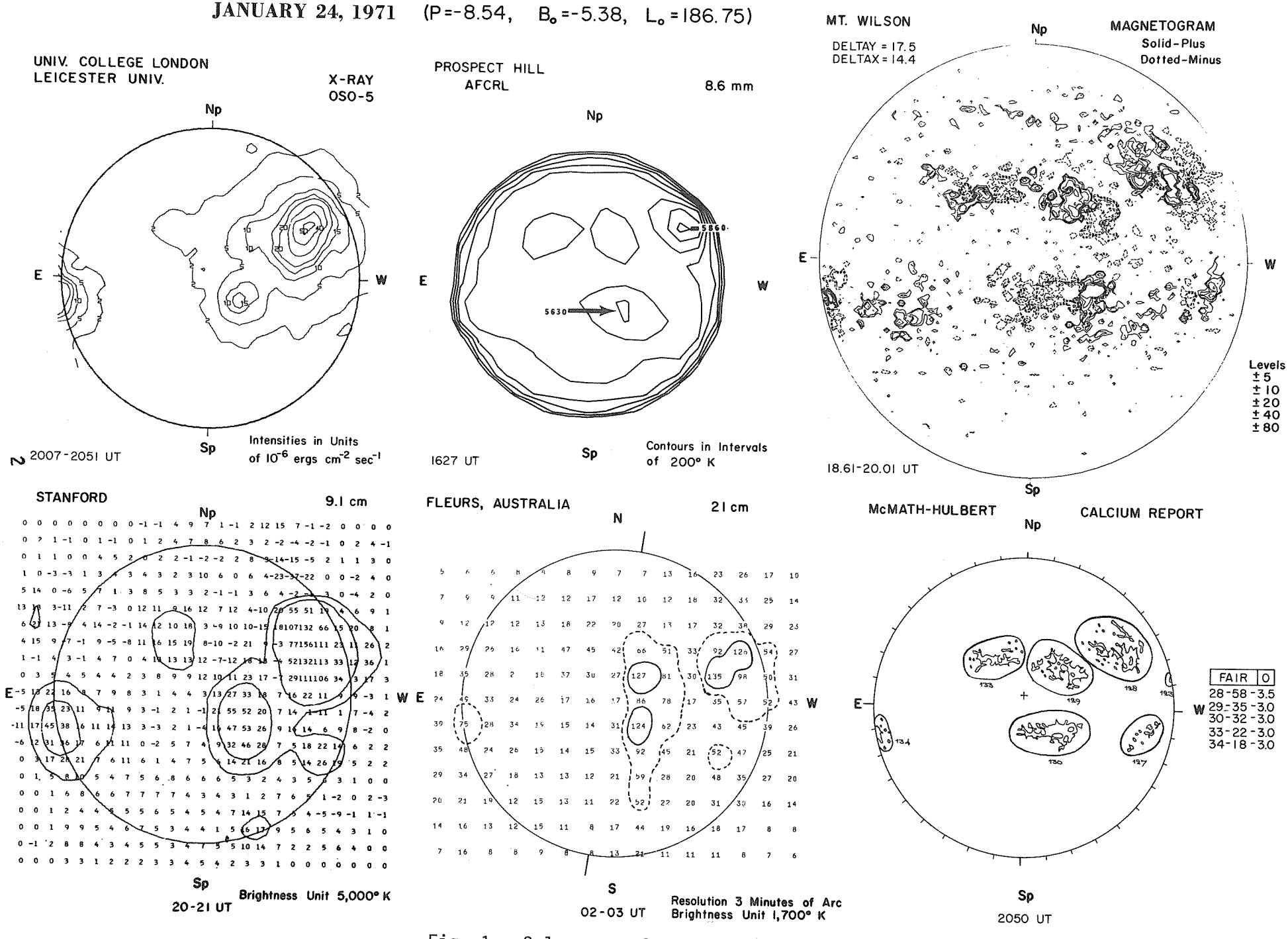

Fig. 1. Solar maps for January 24, 1971.

The final Relative Sunspot Numbers (R_z) and the observed 2800 MHz flux (S_a) for the period January 21-30, 1971 are given below; the monthly means for January are: $\bar{R}_z$ = 91.3, $\bar{S}_a$ = 170.1.

	R_z	S_a		R_z	S_a
Jan 21	131	178.7	Jan 26	109	164.9
22	125	180.6	27	121	166.7
23	120	182.9 (month's peak)	28	109	166.2
24	120	177.0	29	108	160.7
25	112	168.6	30	95	163.0

Shortly before the cosmic ray ground level increase, a confirmed grouped flare with two brightenings occurred, Group 36350, with maxima at 2331 and 2316 UT on January 24 and 0250 UT on January 25 (in time order as published in "Solar-Geophysical Data"):

Universal Time			Location							
Start	End	Max Phase	Approx. Lat	Mer Dist.	Central Distance	Duration Min	Importance	Meas. Area Sq. Deg.	Remarks
2215	0020	2331	N18	W49	0.806	125	3B	18.77	FKU 2213
2309	0024	2316	N19	W50	0.818	75	*1B	3.92	U 2223
2346	0324	0250	N19	W51	0.827	218	*3F	8.31	EFIJU 4115

* Second Brightening

where in Remarks:

E = Two or more brilliant points
F = Several eruptive centers
I = Very extensive active region
J = Plage with flare shows marked intensity variations
K = Several intensity maxima
U = Close and somewhat parallel bright filaments (|| or Y shape).

The first number represents the number of stations reporting. The second and third numbers give the weighting functions for the average importance and the average measured area. The fourth number is the number of stations reporting at the time of the event.

Sudden ionospheric disturbances during this time were:

Jan	Universal Time Start	End	Max	Imp.	Wide Spread Index	Number of Station Reports by Type SWF	SCNA	SEA	SPA	LF-SPA	SES	SFD
24	2038	2146	2104	2-	5	1		3	5	1	3	
	2310	2358	2327	2+	5	5	1		7	4	4	
25	0927	0942	0934	1-	1				1			

Spectral observations at the time of the event are given in Table 2.

Table 2

JAN. 1971	TIMES OF OBSERVATION START UT	TIMES OF OBSERVATION END UT	STATION	EVENTS: CENTIMETRIC BAND START UT	CENTIMETRIC BAND END UT	CENTIMETRIC BAND INT.	DECIMETRIC BAND START UT	DECIMETRIC BAND END UT	DECIMETRIC BAND INT.	METRIC BAND START UT	METRIC BAND END UT	METRIC BAND INT.	DEKAMETRIC BAND START UT	DEKAMETRIC BAND END UT	DEKAMETRIC BAND INT.	SPECTRAL TYPE
24	2022	2400	CULG				2037.5	2038	1							IIIG
			HARV				2044	2052	2							IIIGG
			CULG				2045	2052	1	2048	2050	1				I
			CULG							2113		1				IIIB,W
			CULG							2134.5		1				IIIB,W
			CULG							2136	2136.5	1				IIIG,U
			HARV							2136		2				IIIG
			HARV							2140	2141	1				IIIG
			CULG							2140	2141	1				IIIG,W
			HARV							2146	2240	1				IN
			HARV				2220	2355	1	2240	2359	1				I
			CULG				2225.5		1							IIIB,W
			CULG							2231		1				IIIB,W
			CULG							2234.5	2235	2				IIIG,U
			HARV							2235		3				IIIG
			HARV				2306	2318	3	2307	2324	3				IIIGG
			CULG				2307	2325	1	2307	2325	1				IIIG,U
			CULG										2310		1	SWF
			CULG	2310	2345	1	2310	0050	1							IV
			HARV				2310	2359 D	3	2314	2359 D	3				IV
			CULG				2310.5	2312	1							UNCLF
			CULG				2315.5	2353	3	2320.5	2353	2				IIIH
			HARV							2315.6	2342	3	2320	2335		II
			CULG							2320	0250	1				IV
			HARV				2327	2329	3	2327	2329	3				IIIGG
			CULG							2340	0300	1				I
			HARV							2343	2345	2	2343	2345	2	IIIGG,RD
			CULG				2347.5	2350.5	1							IIIG
25	0000	0725	CULG							0009	0725	1				IIIN,RS,DP
			CULG							0048	0050.5	1				IIIG
			CULG							0116.5	0118.5	1				IIIG
			CULG							0120.5		2				IIIB,U
			CULG							0129.5	0130	1				IIIG
			CULG							0134	0136	1				IIIG
			CULG							0134.5	0135	2				IIIG,U
			CULG							0135.5	0136	2				IIIG,U
			CULG							0246		2				IIIB
			CULG							0329		2	0329		2	IIIB
			CULG				0517.5	0518	1							IIIG
			CULG							0554	0555	1				IIIG
			CULG							0633	0634	2				IIIG
			WEIS							0835.0	1025.0	1				IS

Table 3 gives the outstanding solar radio emission occurrences during the cosmic ray ground level event.

Table 3

JAN. 1971	FREQUENCY STATION	TYPE	STARTING TIME UT	TIME OF MAXIMUM UT	DURATION MINUTES	FLUX DENSITY 10^{-22} Wm^{-2} Hz^{-1} PEAK	FLUX DENSITY MEAN	INT	REMARKS
24	9400 HUAN	5	2035	2048.4	90	31.8	18.7		
	8800 SGMR	22	2036	2048.3	28.4	22.0	5.5		
	4995 SGMR	22	2036.2	2047.5	31.3	67.6	16.4		
	2800 OTTA	21	2036	2230	180 D	18.0			
	2695 SGMR	22	2037	2047.5	36	42.9	10.7		
	2800 OTTA	4	2040	2047.5	15	52.0	26.0		
	960 PENN	45	2042.1	2045.5		25.9			
	2695 BOUL	40	2044	2049	14			2	
	10700 PENN	3	2045.3	2048.7	11	13.9	7.4		
	4995 BOUL	3	2046.5	2049	10			1	
	1415 SGMR	1	2047.1	2048.2	7.9	5.5	1.4		
	606 SGMR	4	2047	2047.4	7.2	13.5	3.8		
	408 SANM	45	2049.4	2049.7	2.4	67.0	13.5		
	2800 OTTA	29	2055		65	24.0	11.0		
	18 MCMA	41	2131	2137	9			1	
	200 HIRA	45	2233.8	2233.8	.5	830.0	410.0		
	4995 MANI	47	2303.8	2323.2	29.1	6300.0	2500.0		
	3750 TYKW	47	2303	2324	52	3540.0	850.0		
	2695 PENT		2303	2324	33 D	2375.0			
	2695 MANI	47	2303.8	2323.2	29.1	2300.0	1280.0		
	2665 CRON	4	2303.5	2324	91.5			3	
	2000 TYKW	47	2303	2324	57	1270.0	390.0		
	9400 TYKW	47	2304	2322.4	51	6900.0	1400.0		
	4995 CRON	41	2304	2323.5	83.5			3	
	1415 MANI	47	2304.9	2320.3	28	640.0	460.0		
	1000 TYKW	45	2304	2322.1	55	810.0	250.0		
	500 HIRA	45	2304.7	2322.5	80	650.0	100.0		
	4995 BOUL	45	2305.5	2324.5	41.5D			3	
	2695 BOUL	45	2305	2325	41.5D			3	
	1420 CRON	4	2305	2325	54.5			3	
	200 HIRA	45	2305	2320	70	1000.0	100.0		
	1420 BOUL	4	2306	2325	40 D			2	
	8800 MANI	47	2307.6	2323.1	25.3	9100.0	3300.0		
	606 MANI	47	2307.6	2322.2	25.1	1330.0	540.0		
	208 VORO	45	2315	2320	28	580.0	188.0		
	606 MANI	30	2323.7	2323.7	112.8	280.0	102.0		
	8800 MANI	29	2332.9	2332.9	95.3	1000.0	360.0		
	4995 MANI	29	2332.9	2332.9	95.3	1040.0	310.0		
	2695 MANI	29	2332.9	2332.9	95.3	770.0	285.0		

Table 3 continued

JAN. 1971	FREQUENCY STATION	TYPE	STARTING TIME UT	TIME OF MAXIMUM UT	DURATION MINUTES	FLUX DENSITY 10^{-22} Wm^{-2} Hz^{-1} PEAK	FLUX DENSITY 10^{-22} Wm^{-2} Hz^{-1} MEAN	INT	REMARKS
	1415 MANI	29	2332.9	2332.9	103.6	480.0	196.0		
	606 MANI	4	2349	2350	2.8	127.0	64.0		
	9400 TYKW	29	2355		225	185.0	50.0		
	3750 TYKW	29	2355		225	140.0	40.0		
	1000 TYKW	29	2359		175	15.0	7.0		
	2000 TYKW	29	2400		180	30.0	14.0		
25	1000 TYKW	45	--	0020	24	35.0	14.0		
	1000 TYKW	5	0026	0030.5	8	12.0	5.0		
	1000 TYKW	5	0038	0039.6	4	6.0	3.0		
	2000 TYKW	5	0047	0048.6	5	29.0	7.0		
	1000 TYKW	5	0047	0048.7	8	80.0	13.0		
	1420 CRON	8	0048	0049.5	4			2	
	1000 TYKW	45	0057	0058.5	6	16.0	5.0		
	1000 TYKW	5	0108	0111	22	12.0	5.0		
	1000 TYKW	45	0130	0148.5	22	14.0	5.0		
	606 MANI	22	0153.2	0157.9	10.8	17.0	5.3		
	1000 TYKW	45	0154	0157.5	35	42.0	13.0		
	606 MANI	4	0242.5	0246.3	6.2	18.1	5.7		
	9400 TYKW	45	0254	0254.2	3	28.0	9.0		
	8800 MANI	4	0254	0254.2	2.2	18.6	7.4		
	4995 MANI	4	0254	0254.2	2.2	11.2	5.6		
	3750 TYKW	45	0254	0254.2	4	8.0	3.0		
	1000 TYKW	5	0309	0313	15	14.0	7.0		
	221 ABST	41	0700		120	9.0			
	204 KIEV	44	0700 E		420 D	87.0	16.0		
	200 GORK	44	0700 E		135		40.0		
	100 GORK	44	0700 E		162		25.0		
	600 UCCL	1	0806	0806.2	.8	7.0	4.0		
	260 ONDR	41	0810	1059	370	40.0			
	1490 BERL	22	0819.5	0836.5	25.5U	10.0	3.1		
	600 UCCL	20	0851.8	0922.5	97	13.0	5.0		
	100 GORK	6	0900 E	0907	.9E	700.0	150.0		
	200 GORK	44	0915		195 D		25.0		
	100 GORK	44	0942		189 D		5.0		
	650 GORK	21	0919.2		48		2.0		
	420 KIEL	48	0920	1003	60	260.0	150.0		
	408 TRST	47	0920	1003.5	60	230.0			
	650 GORK	3	0927.5	0929.9	6.4	22.0	9.5		
	600 UCCL	3	0927.8	0930.5	7.5	65.0	30.0		
	536 ONDR	45	0927.5	0930	10	180.0			
	2950 GORK	1	0928.3	0928.6	1	6.0	3.0		

Explorers 33 and 35 2-12 Å X-ray data for January 24 are also listed:

University of Iowa

Date 1971	Onset U.T.	Maximum U.T.	Peak-Ratio to Quiet Sun	Remarks and Values of Maximum Flux F(2-12 A°) in erg (cm^2 sec)$^{-1}$
24 January	--	1729	4-	Onset not observed
	1807	1827	4	
	2034	2105	4	
	2307	2329	60	0.190 Major electron, proton, alpha particle event

Magnetograms of geomagnetic storms on January 27-28, 1971 associated with the January 24 event are shown in Figure 2. Stations included are Leirvogur, Great Whale River, Meanook, College, Kakioka, Tangerang, San Juan and Honolulu.

MAGNETOGRAMS OF GEOMAGNETIC STORMS

27-28 JANUARY 1971

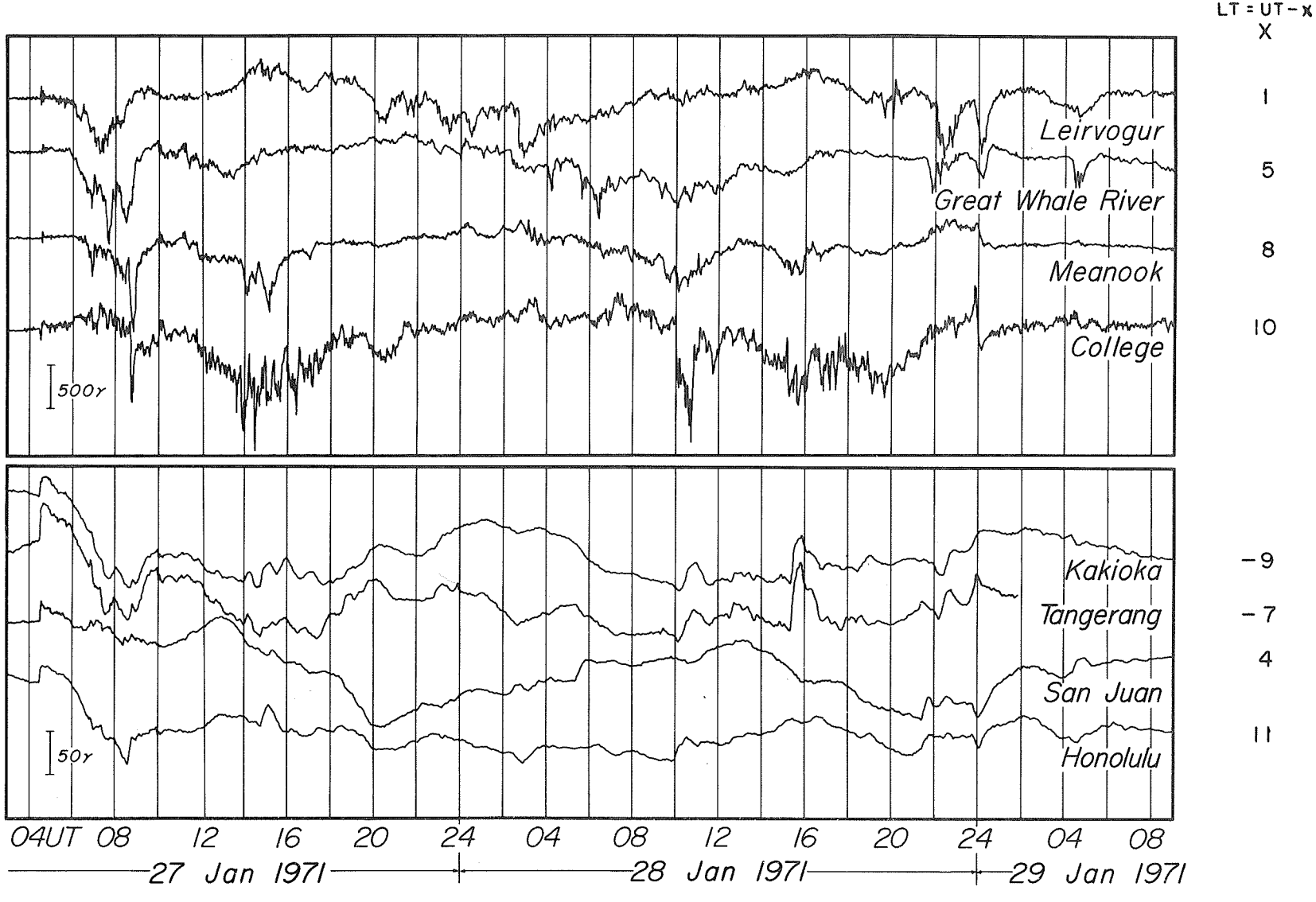

Fig. 2.

2. SOLAR REGION OF JANUARY 1971

Evolution of Solar Active Regions (Hα and K Faculae and Spots)

by

G. Godoli, V. Sciuto, M. L. Sturiale and R. A. Zappala
Osservatorio Astrofisico di Catania
Consiglio Nazionale delle Ricerche, Italia

Three main separate active regions were present on the solar disk during the 24 January 1971 event.

These regions are the McMath region 11128 located at N20 and Carrington longitude 220 degrees, the McMath region 11129 located at N12 and Carrington longitude 189 degrees and the McMath region 11130 located at S14 and Carrington longitude 186 degrees.

In Figures 1a and 1b daily maps of Hα and K faculae associated with these regions are shown.

In Figures 2a and 2b the daily maps of sunspots associated with these faculae are shown.

The maps of Hα faculae were drawn using a A600 Durst projector from the heliograms of the Catania Hα patrol and of the Rome Photographic Journal of the Sun. In the Catania Hα patrol one heliogram is made each five minutes with filters fed by a single aspherical lens (15 cm/222 cm) from 75 minutes after sunrise to sunset. Beginning with May 1971 a Zeiss filter is used. The filtergrams are 20.5-21 mm in diameter. The maps were drawn at 150 mm and reduced photographically.

The maps of K faculae were drawn, using the same projector, from the Catania K spectroheliograms and from the Rome Photographic Journal of the Sun. Catania spectroheliograms are taken daily with a spectroheliograph fed by the Steinheil refractor (33 cm/347 cm). The spectroheliograms are 31.5-32 mm in diameter. Also in this case the maps were drawn at 150 mm and reduced photographically.

The maps of sunspots were made using the same projector from the Catania white light patrol and from the Rome Photographic Journal of the Sun. In the Catania white light patrol one heliogram is made each hour with the Cooke refractor (15 cm/223 cm) using the GH 649 Kodak emulsion + OG2 Schott filter. The heliograms are 20.5-21 mm in diameter. The maps were drawn at 150 mm.

From the maps of Hα and K faculae the evolution curves of these phenomena were deduced (Figures 3, 4 and 5). The projected area Ap is given in 10^{-4} of the solar disk. The corrected area Ac = 1/2 Ap sec h is given in 10^{-4} of the solar hemisphere.

McMath active region 11128 that appeared at the East limb on January 14, 1971 is that associated with the geophysical event of January 24. Hα and K faculae associated with this region are described in Figures 1 and 3 for four transits on the disk from December 18, 1970 to March 21, 1971.

The sunspot group associated with these faculae, described in Figure 2a, lasted three rotations from January 14, 1971 to March 21, 1971. The sunspot group according to Mt. Wilson Observatory was βp type on its appearance on January 14, 1971.

Hα and K faculae associated with the McMath active region 11129 located at N12, 189 degrees are described in Figures 1 and 4 for three transits on the disk, from December 21, 1970 to February 26, 1971.

The sunspot group associated with these faculae, described in Figure 2b, was visible only during the transit from January 17, 1971 to January 29, 1971. The sunspot group according to Mt. Wilson Observatory was βp type on its appearance on January 17, 1971.

Hα and K faculae associated with the McMath active region 11130 located at S14, 186 degrees are described in Figures 1 and 5 for three transits on the disk, from December 22, 1970 to February 26, 1971.

The sunspot group associated with these faculae described in Figure 2b lasted two rotations from January 17, 1971 to February 25, 1971. The sunspot group according to Mt. Wilson Observatory was βp type on its appearance on January 17, 1971.

We notice that as far as it concerns the facula and spot activity all three regions reached their maxima during the same transit. Moreover, around 23 or 24 January all three regions showed a peak of activity.

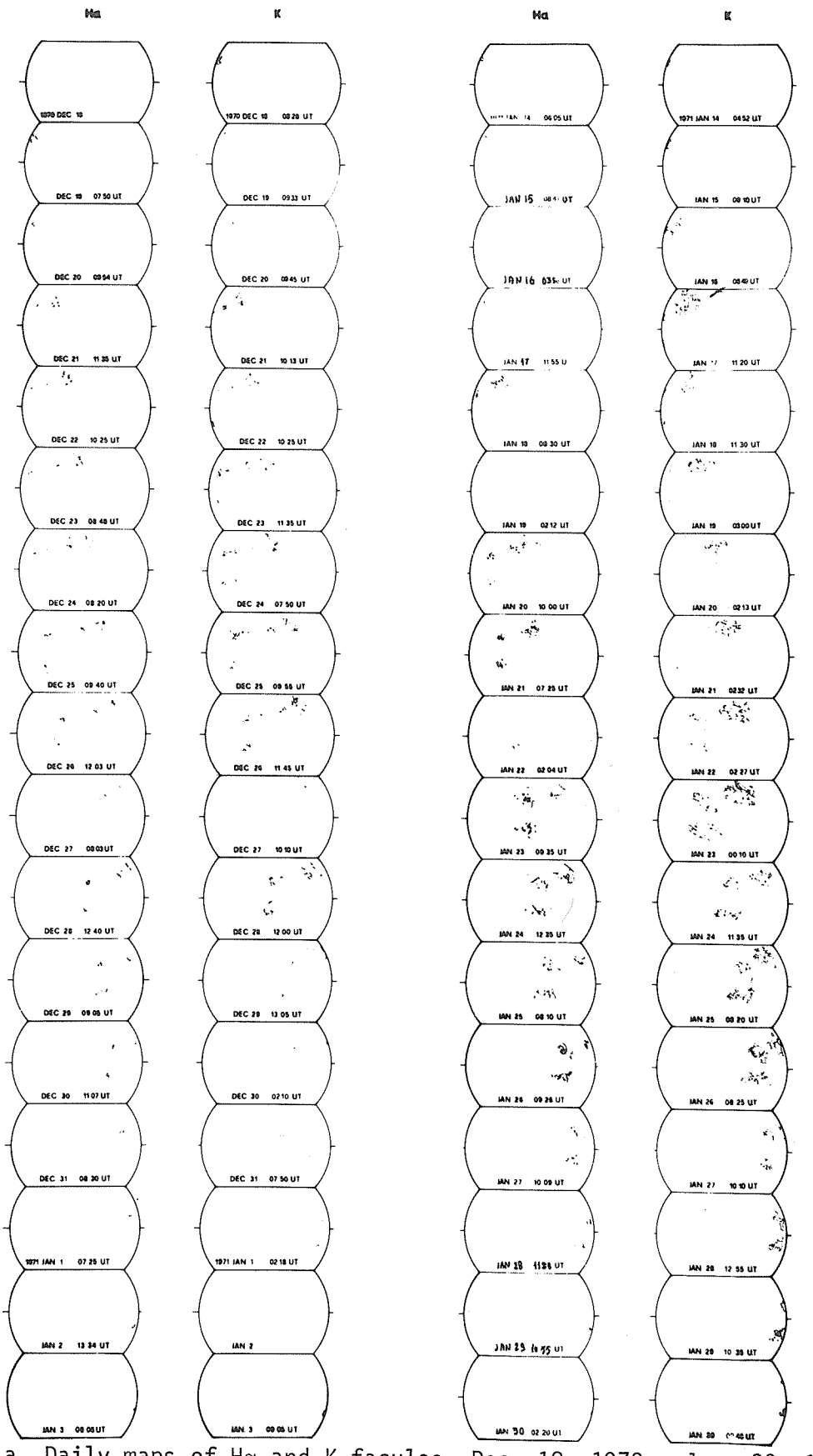

Fig. 1a Daily maps of Hα and K faculae, Dec. 18, 1970 - Jan. 30, 1971, associated with the three main active regions present on the solar disk during the 24 January 1971 event.

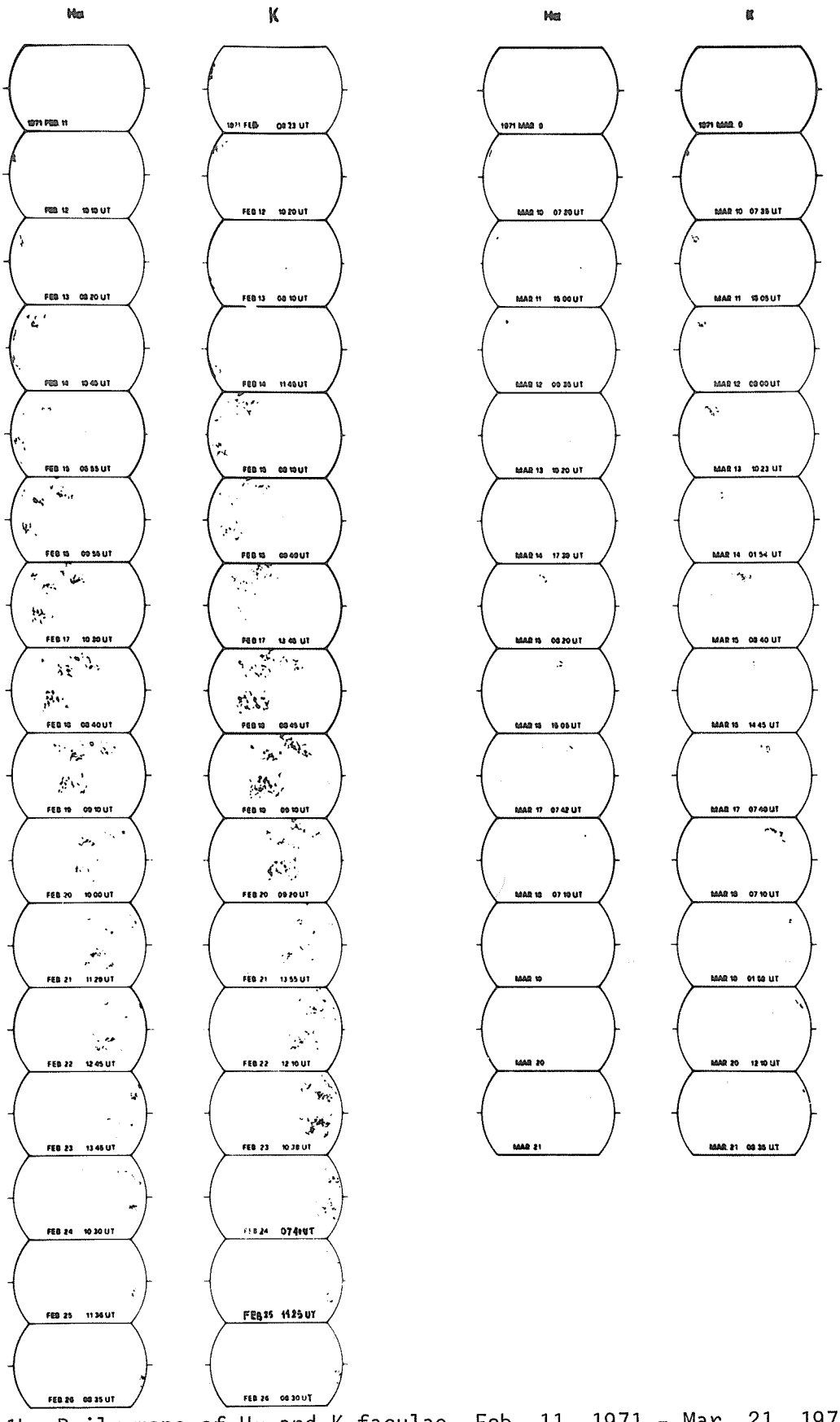

Fig. 1b Daily maps of Hα and K faculae, Feb. 11, 1971 - Mar. 21, 1971, associated with the three main active regions present on the solar disk during the 24 January 1971 event.

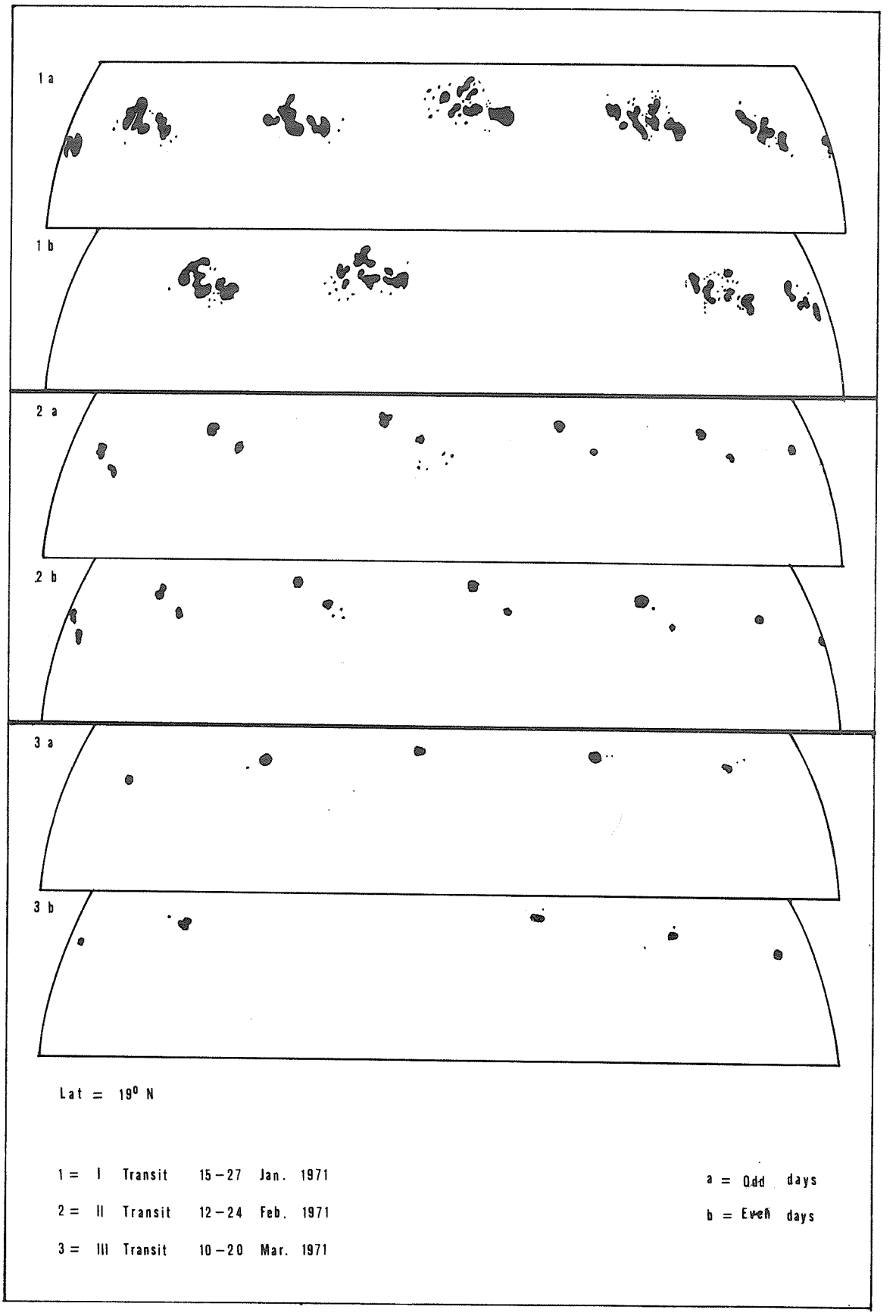

Fig. 2a Daily maps of the N19 sunspots during the three transits of this active region which was present on the solar disk during the 24 January 1971 event.

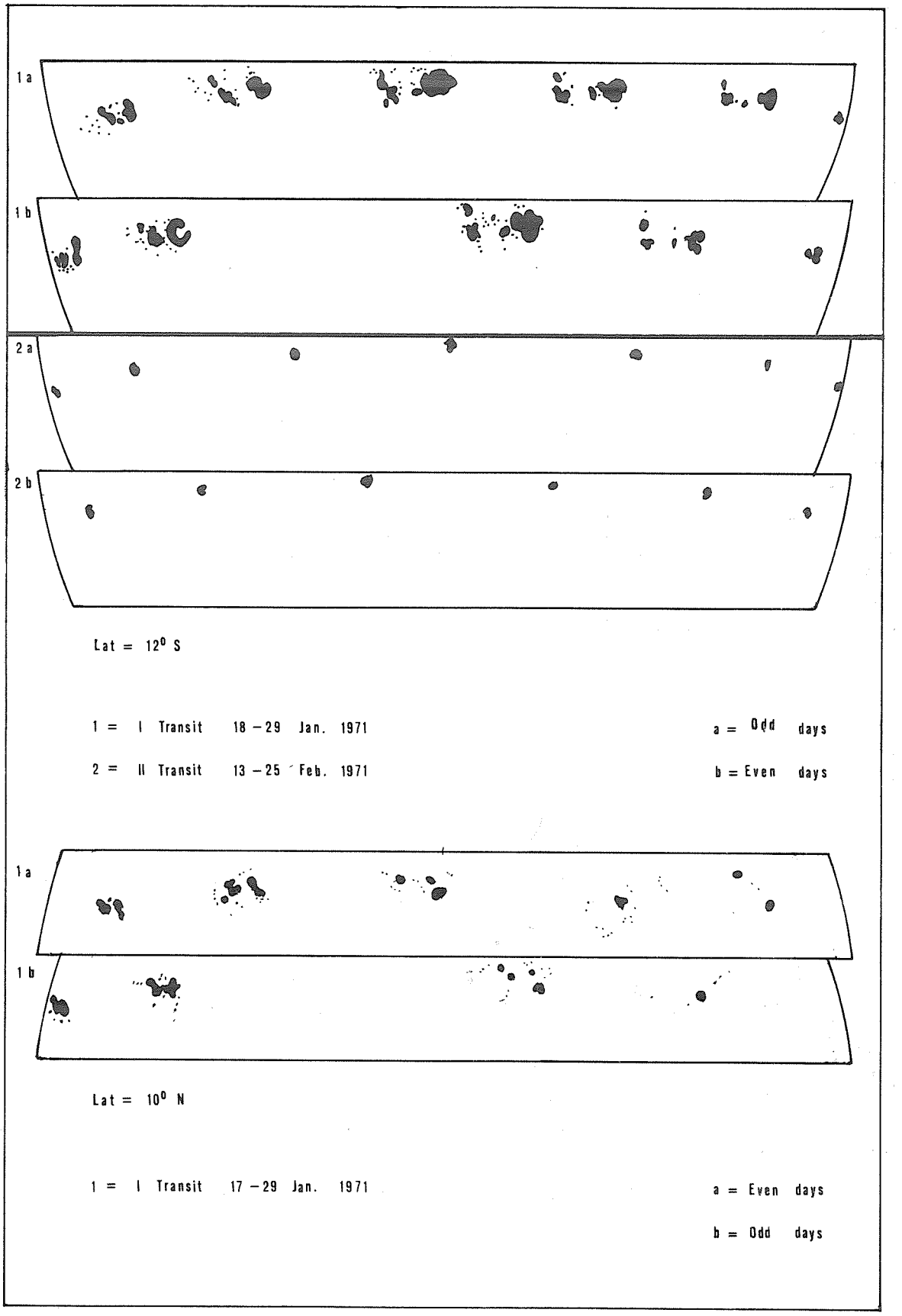

Fig. 2b Daily maps of the S12 and N10 sunspots during the transits of these active regions which were present on the solar disk during the 24 January 1971 event.

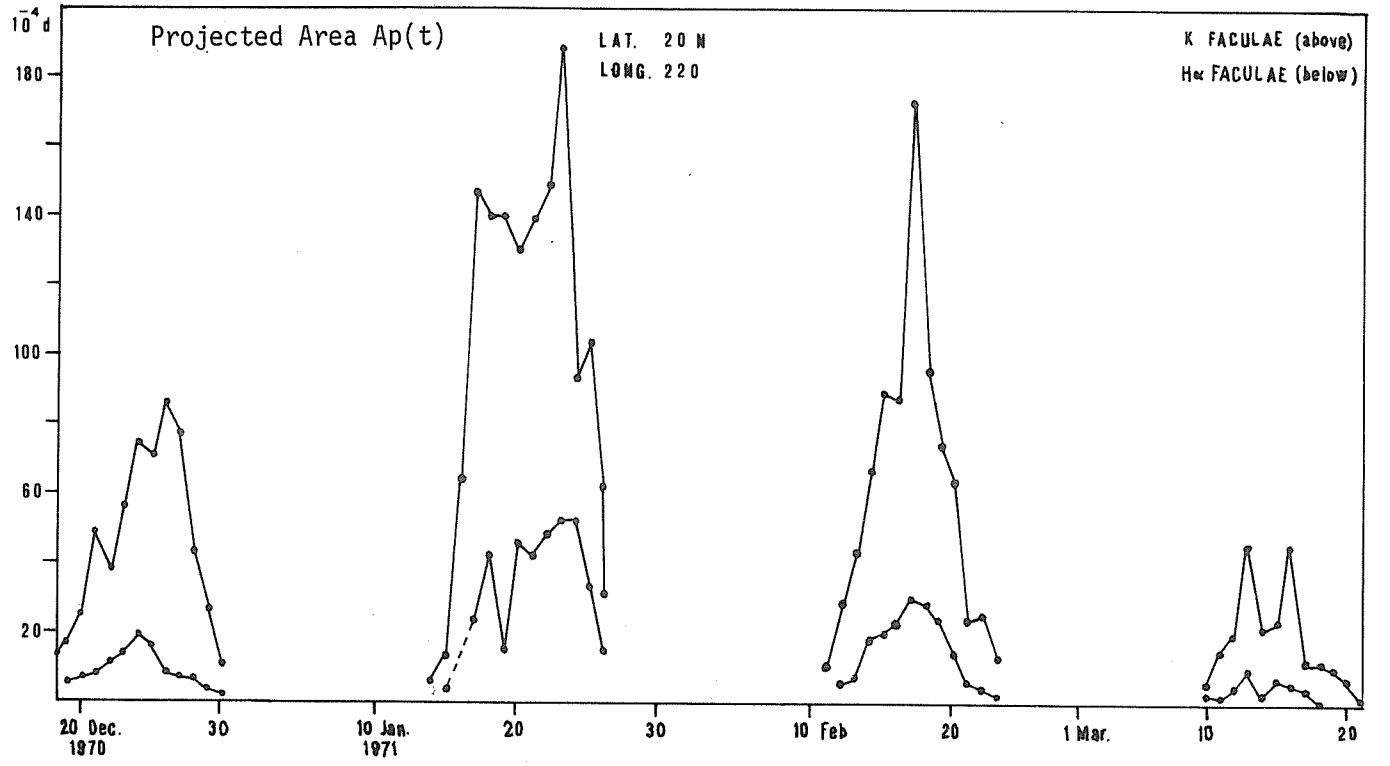

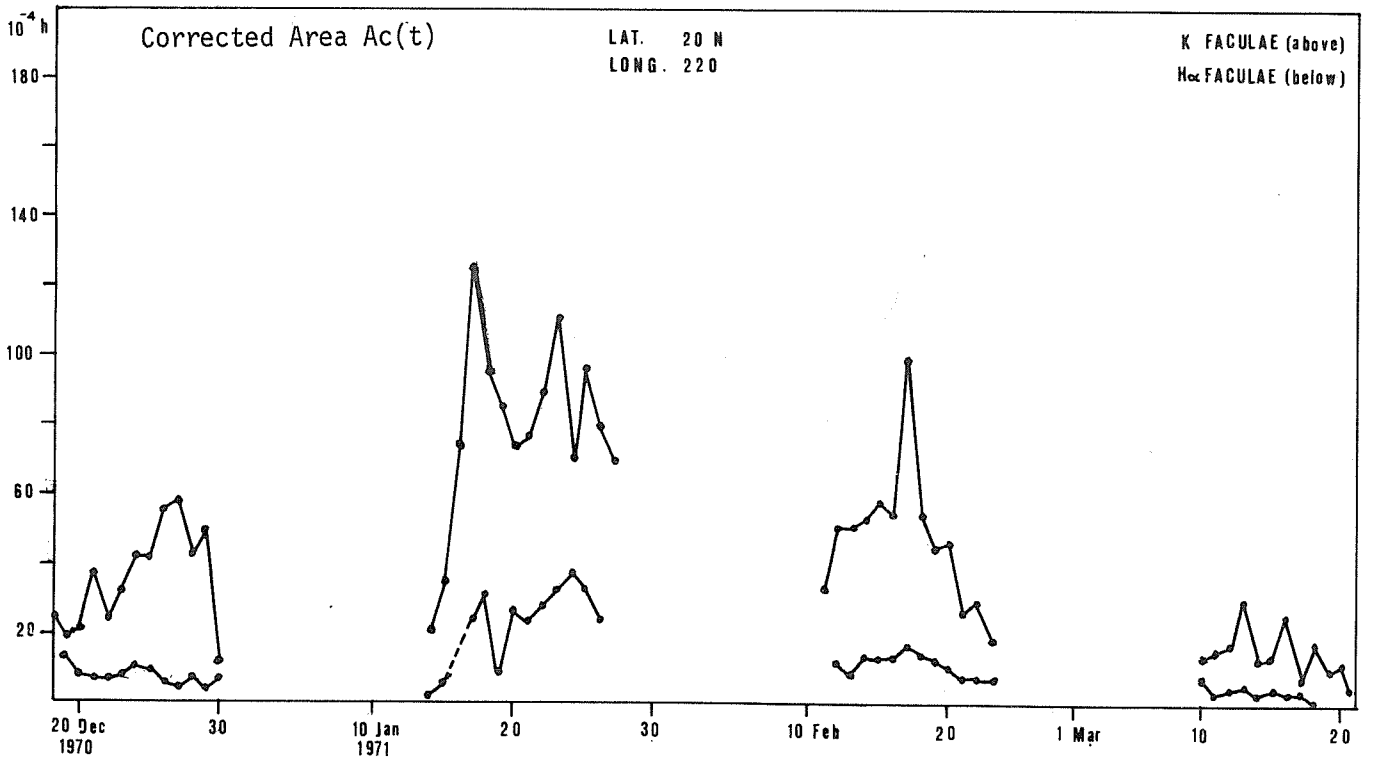

Fig. 3 Evolution curve of Hα and K facula at N20.

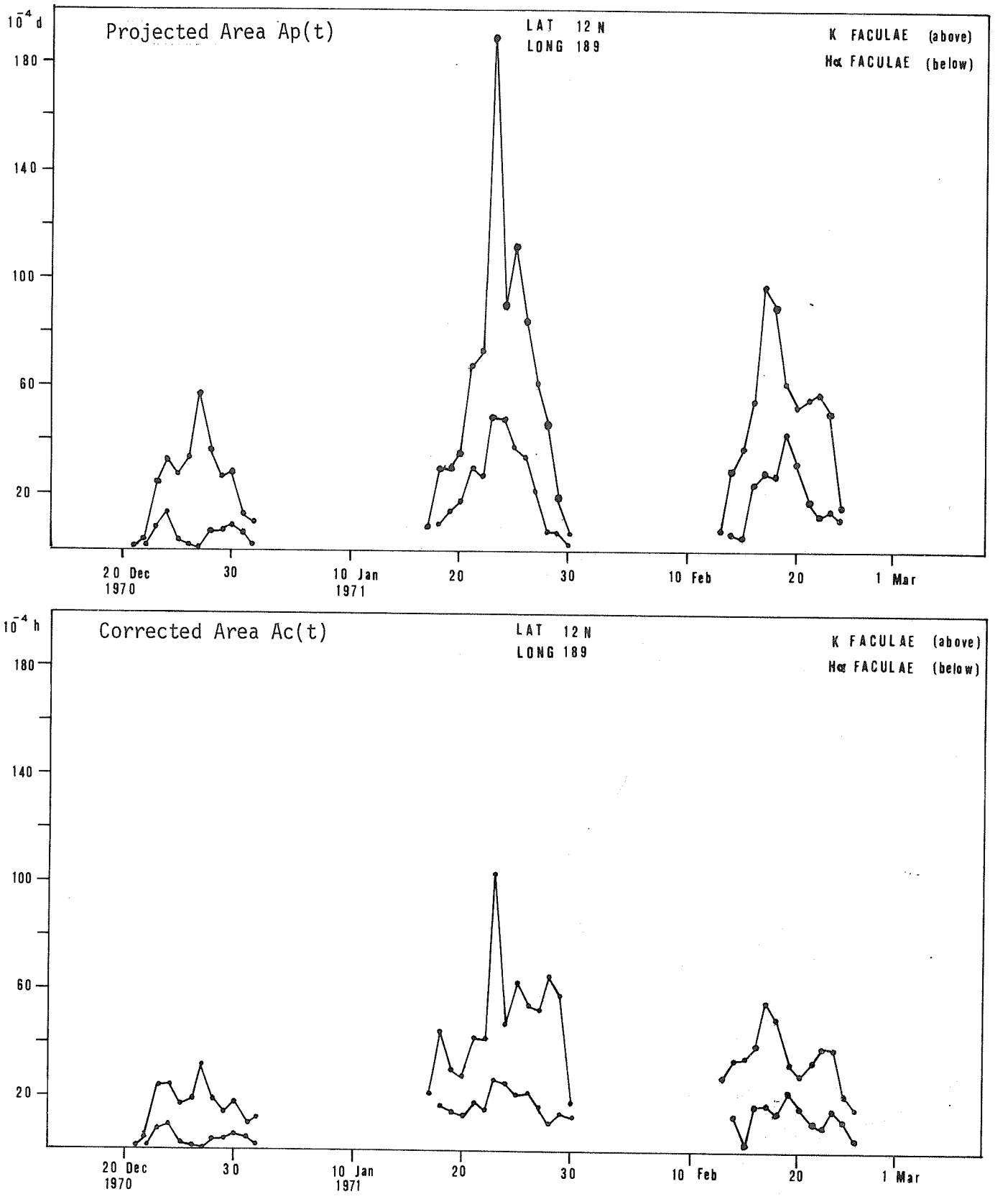

Fig. 4 Evolution curve of Hα and K facula at N12.

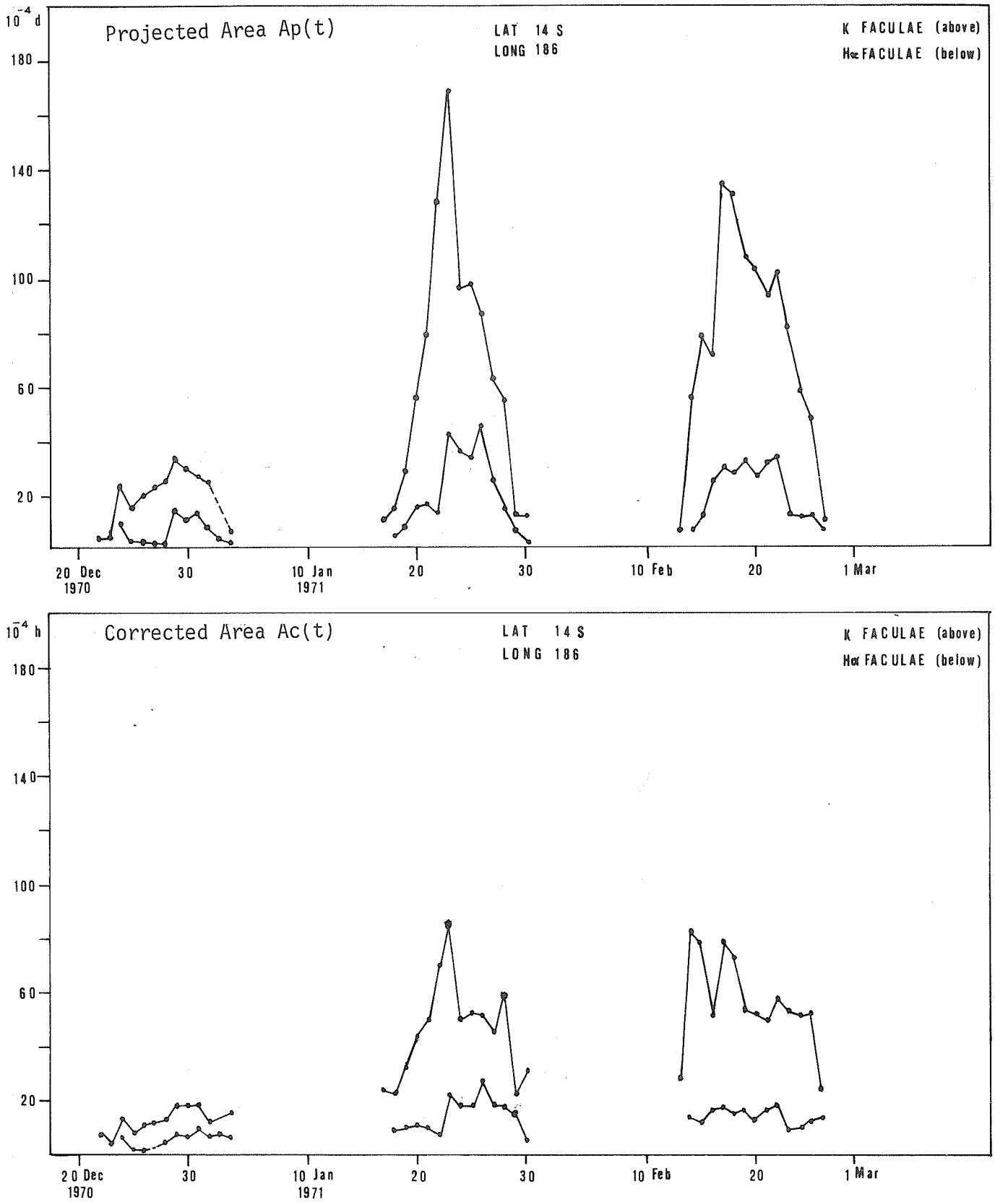

Fig. 5 Evolution curve of Hα and K facula at S14.

Optical and Ground Level Phenomena Associated with the Cosmic Ray Increase of January 24, 1971

by

Marcos E. Machado
Observatorio Nacional de Fisica Cosmica
San Miguel, Argentina

Several investigations have shown that the occurrence of flares, particularly those producing energetic proton emission, are intimately related to the strength and configuration of the magnetic field in the region of occurrence. They appear, in general, in those places where the magnetic field gradient increases, as has been shown by Severny and coworkers. On the basis of these results, Alfven and Carlqvist [1967] developed their theory of solar flares.

Even if no magnetic field measurements are available, as is the case at the San Miguel Observatory, one can estimate the possible occurrence of a solar flare by observing the sunspot configuration. During the days 20 to 24 January, 1971 we observed the evolution of the sunspot groups contained in the McMath Region 11128; the eastern group born on January 19 grew rapidly until January 24, the day when the proton flare occurred. Because of very bad weather conditions, we could not get white-light photographs again until January 30, and thus were not able to investigate the later evolution of the sunspot group. See Figure 1.

As mentioned above, we have no magnetic measurements of the region. However, it was considered very probable that the two sunspots, each belonging to a different group, yet having on January 24 a common penumbra, would have different polarities, thereby constituting a δ configuration. The approaching of such regions produces an increase in the magnetic field gradient, propitious for the appearance of energetic flares.

Calling 128A the older region and 128B the one born on January 19, we can show the evolution of the sunspot schematically in the following way:

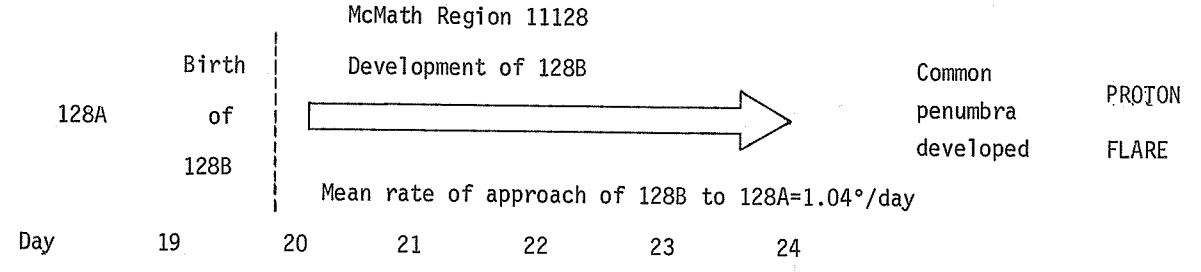

The rate of approach is measured from the decreasing distance between the leading sunspot of the group 128B and the follower of group 128A; these collided on January 24. The development of 128B was measured and is tabulated in Table 1.

Table 1

Measured Area of the Sunspot Group 11128 and of the Leading Sunspot in 128B

Day	Total Area	Leading Sunspot in 128B**		
		Total	Penumbra	Umbra
20	1384	88	73	15
21*	1319	240	149	91
22	1424	297	212	85
23*	1212	248	194	54
24	2016	215	161	54

* Poor quality plates.

** Area measured in millionths of solar hemisphere.

We can see that the time when the flare occurred was not the time of maximum area covered by the leading sunspot in 128B. This fact is in accordance with the conclusions of Martres et al. [1968], who determined that more flares generally appear when the sunspot configuration and area varies,

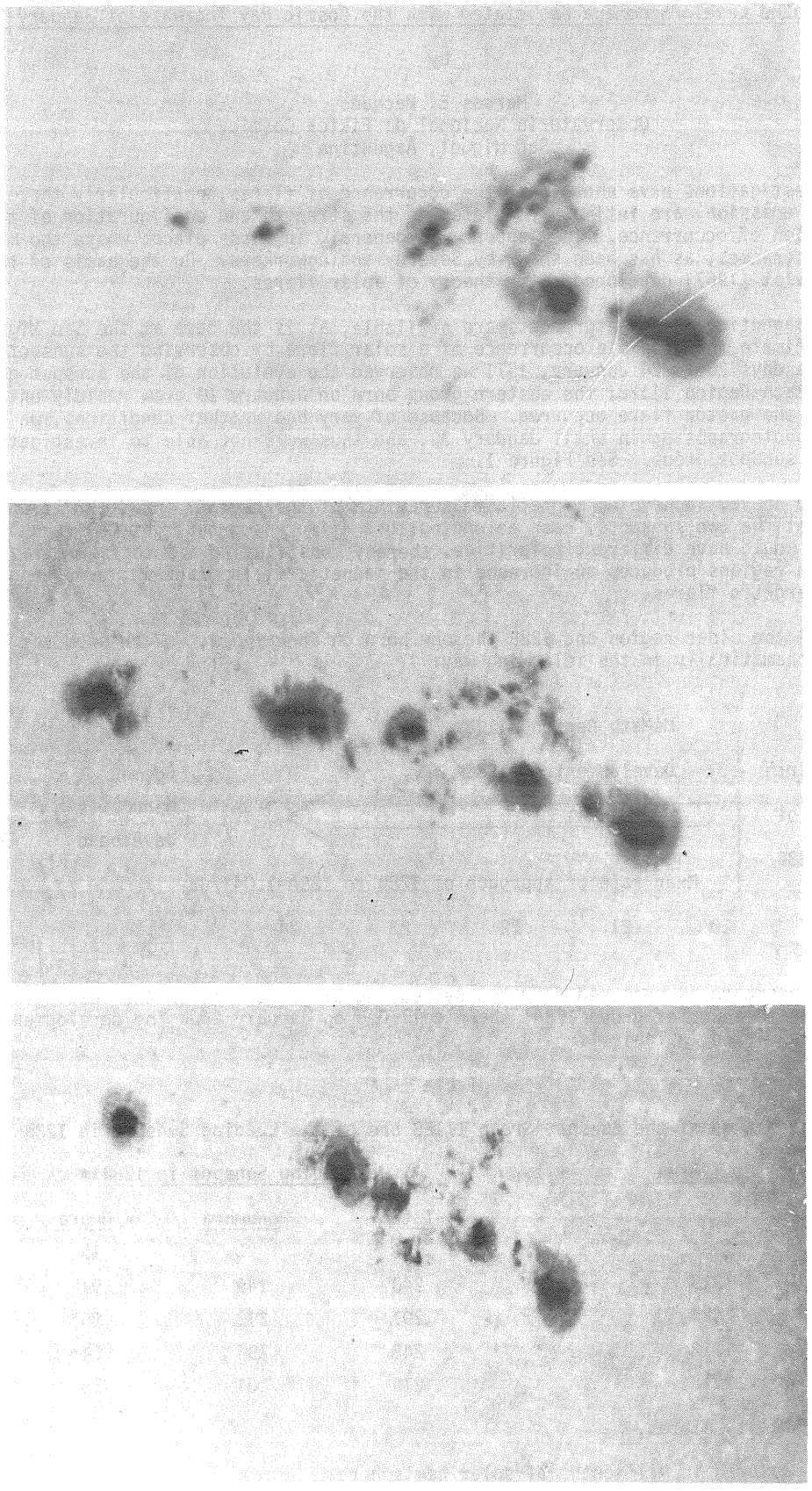

Fig. 1. White-light photographs showing the evolution of the sunspot region 11128.

with no correlation with the maximum area of the group. We believe, in fact, that the conspicuous phenomenon related to the proton flare of January 24 is the approach of the two sunspots.

The arrival of charged particles, with energies of a few hundred Mev's produced by the flare could be detected by a super neutron monitor, type 6-NM-64, at the Scientific Base General Belgrano in the Antarctic Region. In Figure 2 we see simultaneous observations made at the Antarctic base and at Buenos Aires with the 18-NM-64 monitor of the Institute of Astronomy and Space Physics (IAFE). They show significant differences. The rigidity cut-off of Base General Belgrano and Buenos Aires are 0.75 GV and 10.6 GV, respectively. The lack of recorded increase in other than the high geomagnetic latitude observatory shows that the particle energies were not very great.

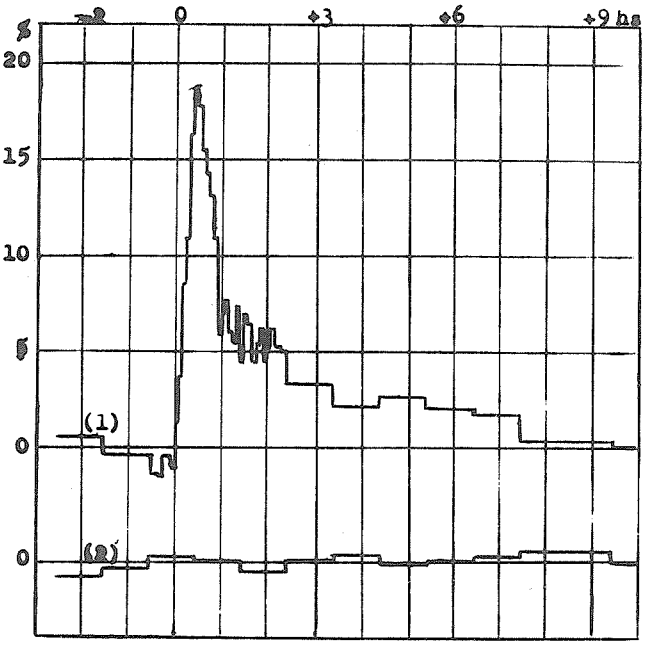

(1) BASE GENERAL BELGRANO (ANTARCTICA)

(2) BUENOS AIRES

Fig. 2. Simultaneous neutron monitor observations at Buenos Aires and Base General Belgrano. (By courtesy of H.S. Ghielmetti and J. Sahade [Ghielmetti, 1971]). The maximum occurred very close to 0000 UT, Jan. 25, 1971.

Svestka [1970] and Najita and Orrall [1970] have shown that the penetration of very energetic particles into the lowest chromospheric and upper photospheric layers of the Sun can explain the continuous emissions of flares in the optical and UV region. This hypothesis is strongly supported by the analysis made by Machado [1971] of line intensities in white-light flare spectra.

The white-light emission only occurs when the particle spectra is very hard. Both protons and electrons might participate in this process, but the electrons will, in general, lose their energy very rapidly due to synchroton emission. However, if the electron distribution is very anisotropic, they could play an important role in this process as has been studied by Syrovatskii and Shmeleva [1971] and mentioned by Svestka [1971].

With the observed range of energies in the proton emission, white-light flare emission would be produced with a very hard power-law spectra ($\gamma \simeq 2$) which has been observed in some cases [see e.g. Svestka, 1971].

We have no knowledge of any white-light observations of this flare, but we would not be surprised if no such emission were observed, since a very large proton flare on September 2, 1966 with $\gamma > 4$ in the energy range above 100 Mev [Svestka and Simon, 1969] subsequently showed no white-light emission.

Acknowledgements

I wish to thank very much Lic. H. Ghielmetti for the neutron monitor data and for helpful discussions in its respect. My thanks are also due to Dr. J. J. Hennessey, S.J. from Manila Observatory, for sending me a copy of their Hα plate of the flare. Finally, I wish to express my thanks to Mr. M. Peralta from our Observatory for his great help in the reduction of data.

REFERENCES

ALFVEN, H. and P. CARLQVIST 1967 Currents in the Solar Atmosphere and a Theory of Solar Flares, Solar Phys., 1, 220-228.

GHIELMETTI, H. S. 1971 Cosmic Ray Increases at the Antarctic Base of General Belgrano, Inform. Bull. Southern Hemisphere, 19, 32-33.

MACHADO, M. E. 1971 Evidence for the Photospheric Origin of the Flare Optical Continuum, Solar Phys., 17, 389-391.

MARTRES, M.-J., R. MICHARD, I. SORU-ISCOVICI and T. T. TSAP 1968 Etude de la localisation des eruptions dans la structure magnetique evolutive des regions actives solaires, Solar Phys., 5, 187-206.

NAJITA, K. and F. Q. ORRALL 1970 White Light Events as Photospheric Flares, Solar Phys., 15, 176-194.

SVESTKA, Z. 1970 The Phase of Particle Acceleration in the Flare Development, Solar Phys., 13, 471-489.

SVESTKA, Z. and P. SIMON 1969 Proton Flare Project, 1966, Solar Phys., 10, 3-59.

SYROVATSKII, S. I. and O. P. SHMELEVA 1971 Heating of Plasma by Energetic Electrons and Non-Thermal Emission in Solar Flares, P. N. Lebedev Physical Institute, Preprint.

Sunspots and H-Alpha Plage Associated with the GLE Event of 24 January 1971

by

Patrick S. McIntosh
NOAA Environmental Research Laboratories
Boulder, Colorado 80302

The identification of the active region source for the energetic particle event on 24 January 1971 is without question the complex active center then located at N19 W49 (McMath #11128). The flare at 2303 U.T. (start of major radio bursts) [Solar-Geophysical Data] was isolated in time from any other major events and the arrival of the ground-level energetic particles occurred less than an hour after the beginning of the optical event [Solar-Geophysical Data]. This report presents the daily photographs of the sunspot group and H-alpha plage with only a minimal analysis of the evolution of the active region.

It has been repeatedly established that major solar flares prefer to occur in active regions with complex sunspot and magnetic field configurations. More specifically, proton flares and, by close association, flares with type IV radio bursts prefer regions that were formed by the blending of two or more sunspot groups [Kopecký and Křivský, 1966; Antalová, 1967; Kleczek and Olmr, 1967]. The closer the two groups occur, the more likely they will create a complex magnetic configuration and produce a great flare [Martres, 1968; Křivský and Obridko, 1969]. McIntosh and Donnelly [1970] found that five well-observed white light flares all occurred close to the line of magnetic polarity reversal situated between sunspot groups that were in the process of colliding. All of these flares were also proton flares. To this writer's knowledge the flare of 24 January 1971 was not observed in white light, yet the evolution of the active region closely resembled the evolutions of white-light flare sunspot groups. The discontinuous nature of white light patrol observations allows that this flare might have produced white light emission.

McMath Region #11128 was located at N19 and Carrington longitudes from 205 to 230 degrees. These heliographic coordinates have been outstanding for producing great active centers throughout this solar cycle, although there have been lengthy periods when little or no activity was present at this location

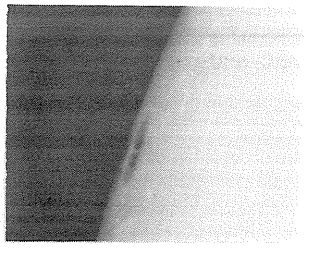

14 Jan. 1971 1548 U.T.

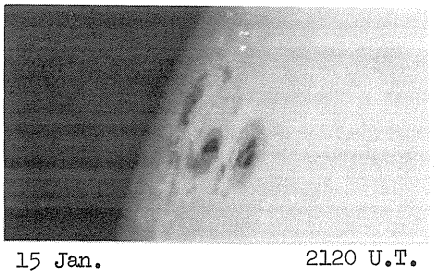

15 Jan. 2120 U.T.

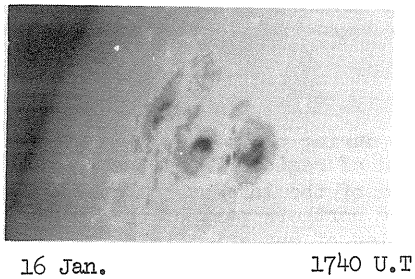

16 Jan. 1740 U.T.

Fig. 1 The east-limb passage of McMath region #11128 as seen in white light from Sacramento Peak Observatory patrol films (left) and the new Sacramento Peak Vacuum Tower Telescope (above). The tower operated at 20-in aperture while the patrol was with a 6-in lens. Note the small bipolar spot group just east of the main group on 16 January, best seen in the Tower photograph above taken at about 1700 U.T.

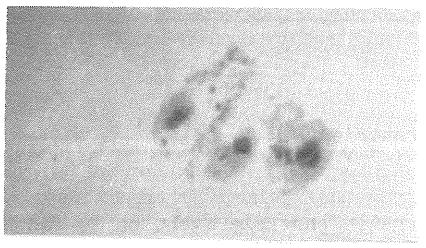

17 Jan. 1971 1510 U.T.

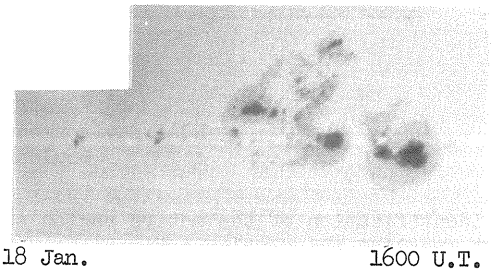

18 Jan. 1600 U.T.

30
ARC SEC

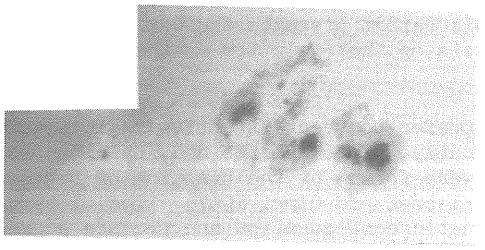

17 Jan. 2005 U.T.

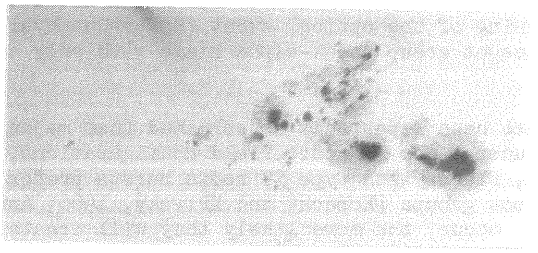

19 Jan. 1550 U.T.

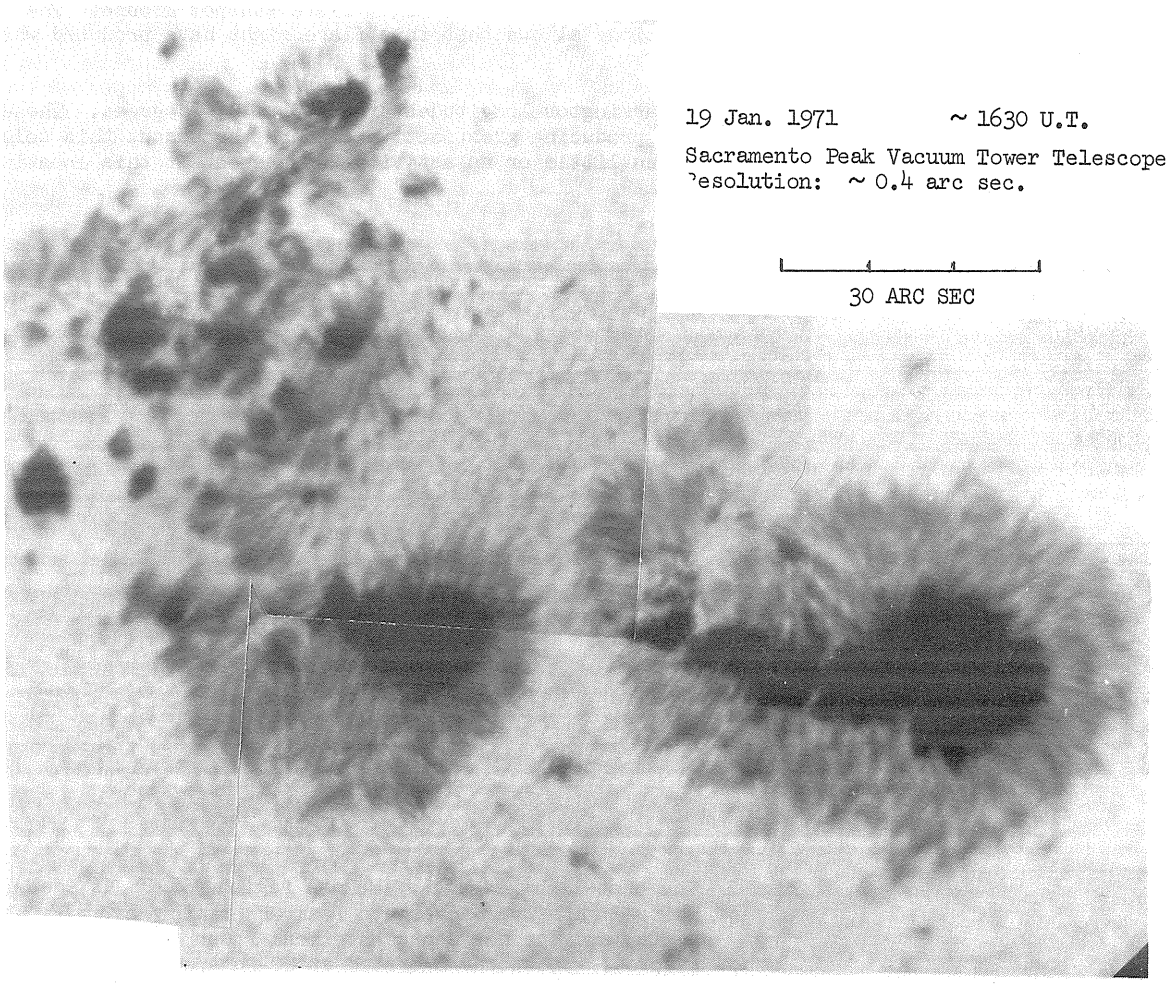

19 Jan. 1971 ~ 1630 U.T.

Sacramento Peak Vacuum Tower Telescope
Resolution: ~ 0.4 arc sec.

30 ARC SEC

Fig. 2 Sacramento Peak white light photographs of McMath region #11128 during period just prior to outbreak of vigorous new sunspot group at following end of region. Note the variability of the small spots trailing the region, the rotation of the largest follower spot, and the growth of numerous small spots and penumbra in the northern part of the trailer. The fine structure on the 19th indicates strong twisting of magnetic field patterns near the line of polarity reversal.

on the sun. These coordinates were the first to produce a great complex of two or more active centers during this cycle, and from May, 1965 through January, 1966 no other location on the sun competed with this area in terms of flares and active centers. Memorable regions at this location include the proton-flare groups of July, 1966, May, 1967, and March, 1970. Clearly, this has been one of the preferred active longitudes during the past decade.

The appearance of McMath Region #11128 at east limb on 14 January 1971 did not represent a returning region, although it appeared among some remnants of old plages #11089 and 11091. The sunspot group (Figure 1) already was large and complex. The presence of two large, symmetric leader spots, both of the proper leading (negative) polarity for the northern hemisphere in cycle 20, suggests that already the region was the product of at least two regions having merged. An additional, very small bipolar group trailed the large region. This small group was quite variable in the number and position of spots during the period from east limb (16 January) until the emergence at this position of a strong bipolar set of spots on 20 January (Figure 3).

The area between the twin leaders and the large follower spot in the original group contained large amounts of penumbra associated with many small umbrae, some within and many outside the patches of penumbra. These features changed rapidly from day to day. On 19 January the fine structure of this region was recorded at high resolution at Sacramento Peak (Figure 2) and showed evidence of strong twisting of magnetic field lines in the vicinity of the line of magnetic polarity reversal. Maps of the magnetic field of this region occur elsewhere in this compilation, but the basic magnetic field distribution can be successfully inferred from the H-alpha photographs of Figure 7. The plage corridor marking the line of polarity reversal exhibited a reversed S-shape winding from east of the twin leaders to a point north of the pair, then abruptly turning east and passing through the midst of the spots toward the top of the Sacramento Peak Vacuum Tower photo in Figure 2.

The character of the active center changed with the rapid growth of new spots and plage east of the large sunspots, beginning at about 0900 U.T. on 20 January. Large spots with only rudimentary penumbra appeared by 2025 U.T. (Figure 3) and the new group had become a large McIntosh-type Dai group by 1645 U.T. on the 21st (Figure 4). The high resolution enlargement in Figure 5 shows that the strong emerging magnetic fields caused an alignment of photospheric granules into lanes running from spots of one polarity to spots of the opposite polarity, mimicking the alignment of the arch-filament system observed in H-alpha at the same position, shown for 21 January in Figure 7. It appears that the size of the photospheric granules within the group was smaller than those lying outside the region.

It is normal behavior for the leader and following spots of a new sunspot group to diverge in longitude as the group ages. In the case of a new group emerging very near an older group, this divergence leads to a collision between the two groups [Martres, 1968]. Such a collision can be seen in Figure 6. The new eastern group reached maximum area on 22 January and the leading spot steadily moved westward until it collided with the followers of the large western group on 24 January. As with the white light flares reported by McIntosh and Donnelly [1970], the proton flare occurred on the day of closest approach of the two groups. The Sacramento Peak Vacuum Tower photograph for the 24th showed that "bridges" of penumbral filaments formed between the colliding spots some hours prior to the flare and the penumbra near the point of collision became darker than is normally observed for penumbra. Such dark penumbra has been noted previously for proton-flare sunspot groups, and in all cases the dark structures were associated with a line of polarity reversal during an interval of rapidly increasing gradient in the longitudinal magnetic field across that line [McIntosh, 1969a, 1969b, 1970].

A comparison of the photographs for 22 and 23 January in Figure 6 shows that both the leader and follower spots of the new group rotated through 90° during this day, as if a twisting of the magnetic fields from this group was associated with the imminent collision with the older group to the west. Conspicuous sunspot rotation was also observed prior to the collision of sunspot groups associated with the great white-light flare of 23 May 1967 [McIntosh, 1969b].

There is one important difference between the flare of 24 January 1971 and the white-light flares reported by McIntosh and Donnelly [1970]. The white light flares occurred within 10 arc seconds of the longitudinal neutral line that lay between the colliding groups. The proton flare on 24 January 1971 lay close to the neutral line within the large old group and west of the neutral line between the groups (see the photographs by McCabe elsewhere in this compilation). Thus, we may speculate that the collision of the two sunspot groups resulted in a deformation of the magnetic fields associated with the old western group such that energy was stored and released within the twisted field topology partially mapped in the sunspot fine structure of Figure 2.

The sunspot photographs on the days following the proton flare show an overall decay of the activity complex, except for the growth of new spots and penumbra immediately south and east of the original pair of leader spots. This new growth was centered on the longitudinal neutral line associated with the flare. Since the growth of these spots was already evident on photographs taken before the flare on 24 January, it seems likely that this growth represented emerging magnetic flux that may have triggered the instability leading to the release of flare energy. Could this sunspot growth be a direct result of the magnetic field deformation caused by the collision between the two sunspot groups?

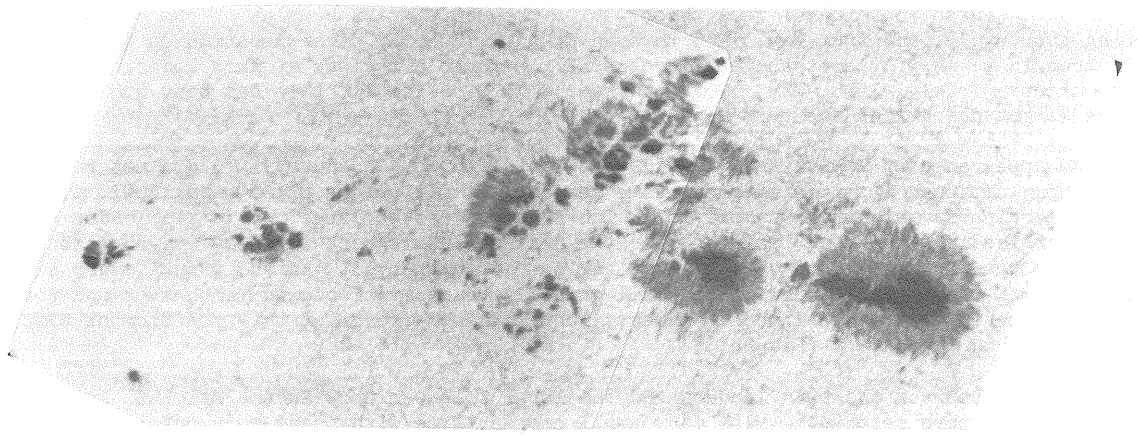

Fig. 3 Sacramento Peak Vacuum Tower photo on 20 January 1971, 2025 U.T. A strong new bipolar spot group has just emerged at left.

30 ARC SEC

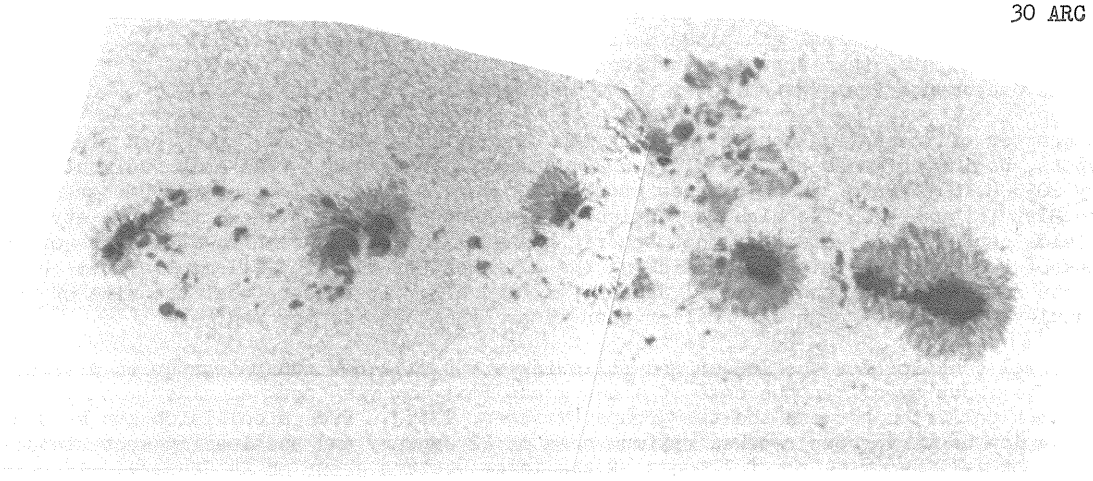

Fig. 4 Sacramento Peak Vacuum Tower photo for 21 January 1971 at 1645 U.T. The spot group at left continues rapid growth.

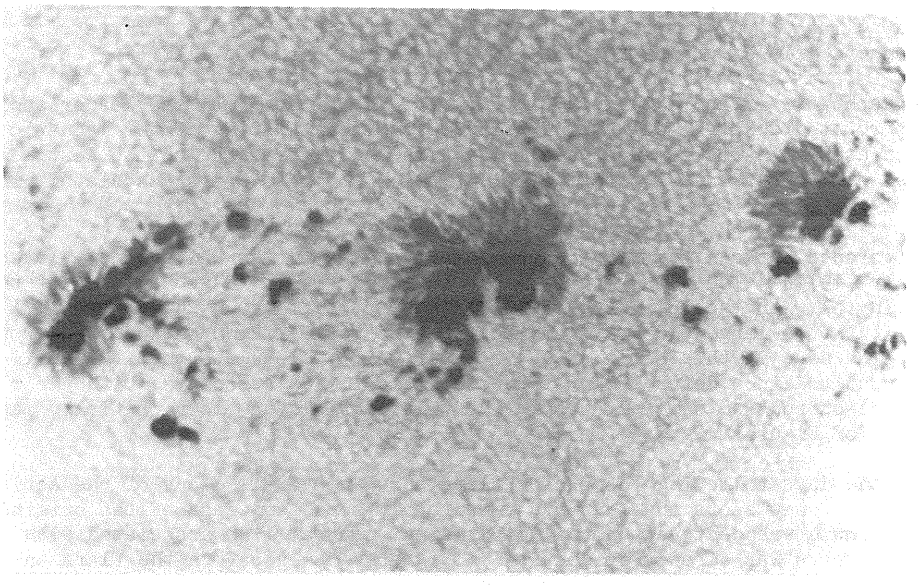

Fig. 5 A contrasty enlargement from Fig. 4 showing granulation, interior to the new and rapidly-growing group, aligned into chains running from spots of one polarity to spots of the opposite polarity.

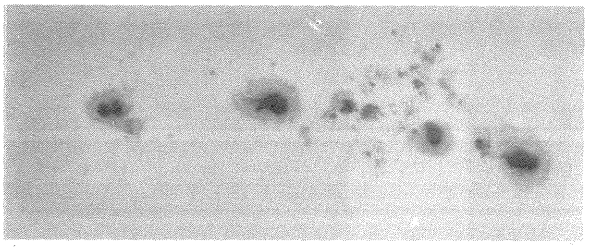

22 Jan. 1971 1650 U.T.

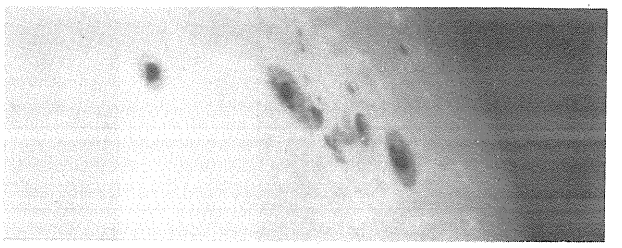

25 Jan. 2100 U.T.

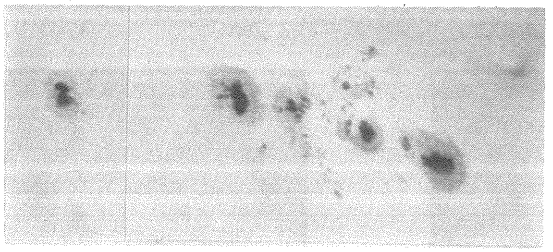

23 Jan. 1805 U.T.

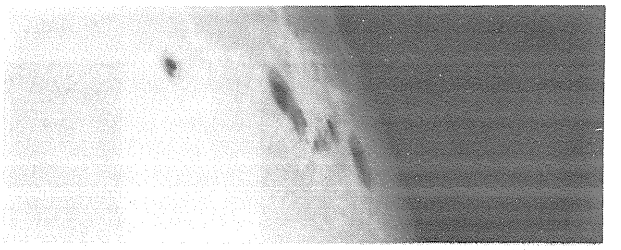

26 Jan. 1532 U.T.

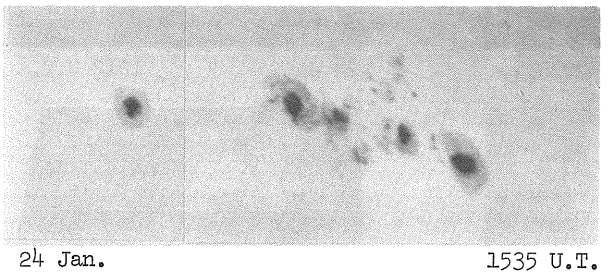

24 Jan. 1535 U.T.

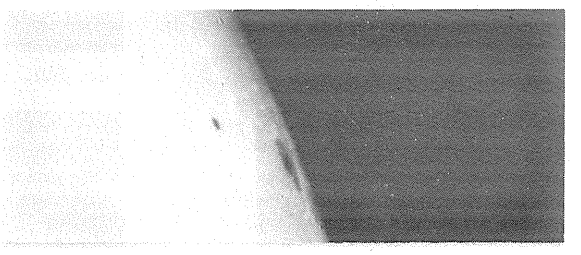

27 Jan. 1511 U.T.

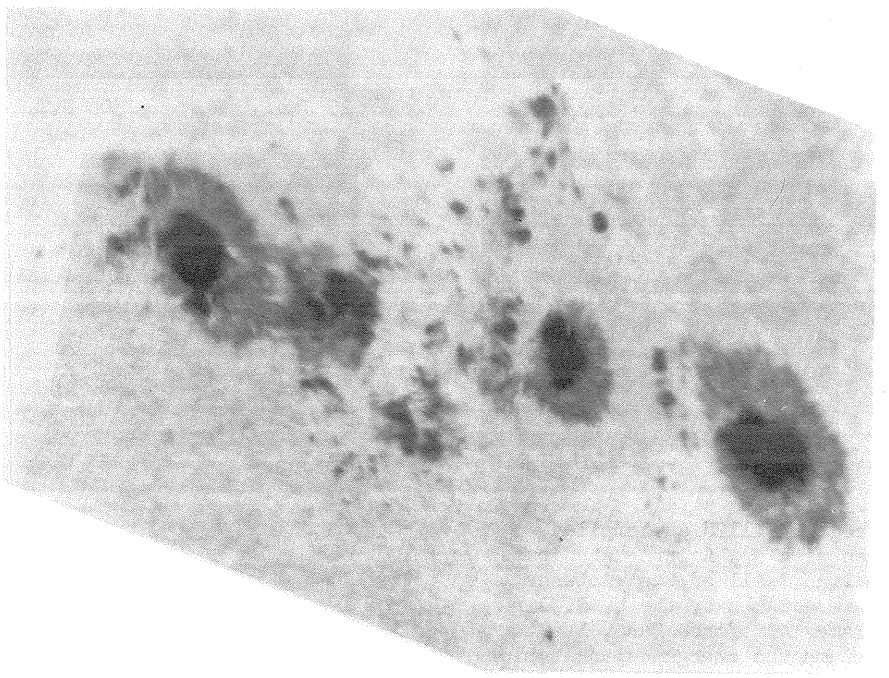

24 Jan. 1971 1648 U.T.

The leader spot of the new bipolar group (far left) is in the process of "colliding" with the follower spot of the older group. Note the bridges of penumbra spanning the narrow gap between them. The penumbra of the old follower spot appears darker than normal. Sacramento Peak Vacuum Tower photograph.

Fig. 6 Passage of McMath region #11128 over the western part of the solar disk, showing the approach and collision of the new bipolar spot group with the older region. Note the 90° rotations of the leader and follower spots of the new group between the 22nd and 23rd. Small photos are from Sac Peak white-light patrol.

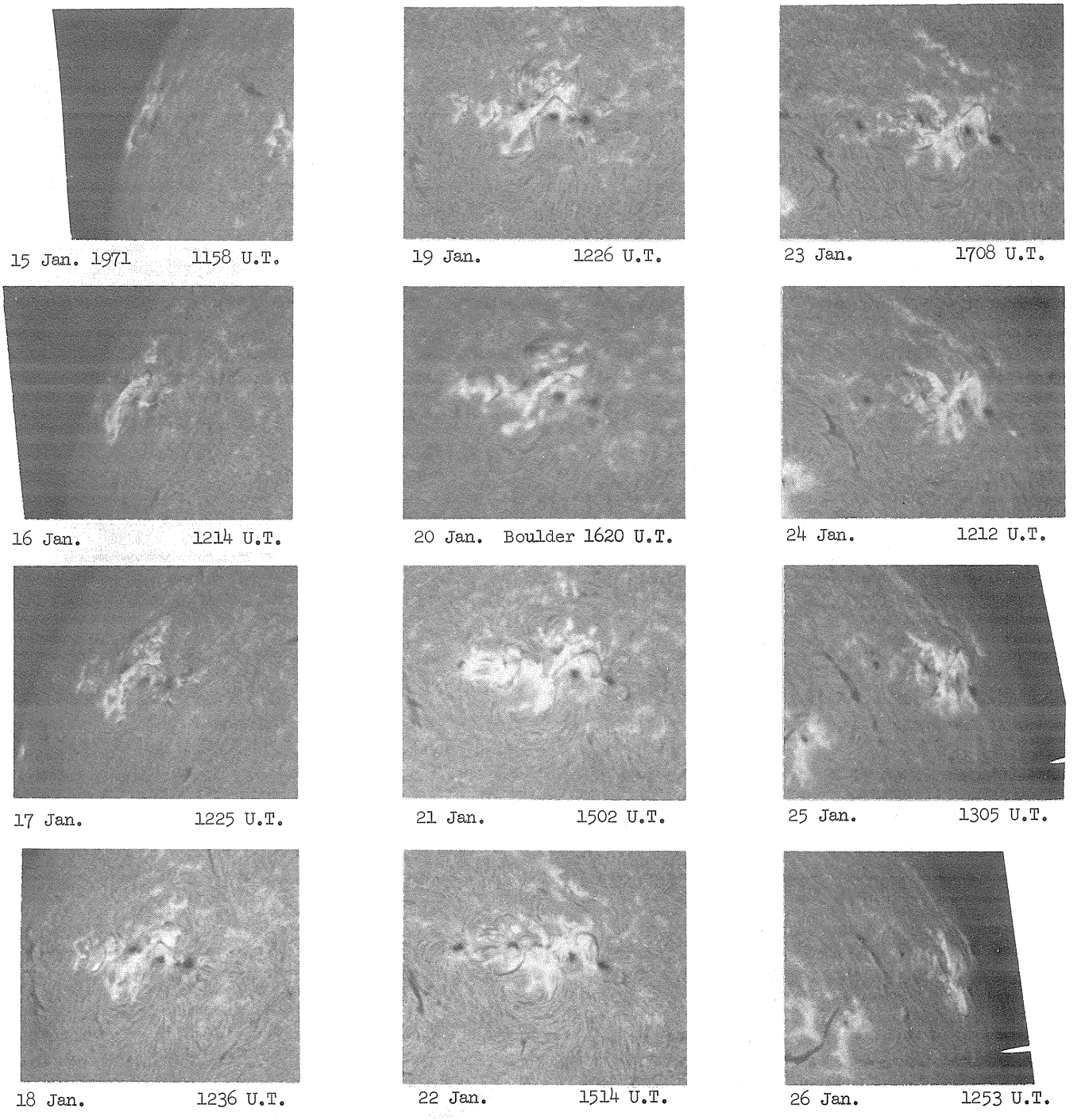

Fig. 7 The disk passage of McMath region #11128 as compiled from patrol filtergrams taken with a $\frac{1}{2}$-Angstrom bandpass filter tuned to the H-alpha line. All of the pictures except the one from Boulder were taken by the U. S. Air Force solar observatory at Ramey Air Force Base, Puerto Rico. Note in the center column the emergence and rapid growth of new plage and spots at the following end of the region. The merging of this area with the original plage leads to the heating of the chromosphere between them, as seen in the righthand column. The proton flare occurred late on 24 January in this area of "collision."

This report was greatly assisted by the generous sharing of observations by Dr. David Rust of the Sacramento Peak Observatory, Joe Hirman of the NOAA observing staff at the NASA S.P.A.N. observatory on Gran Canary Island, and by Capt. Jimmie Smith, USAF Officer In Charge at the 4th Weather Wing solar observatory at Ramey Air Force Base, Puerto Rico.

REFERENCES

ANTALOVÁ, A. 1967 — The photospheric situation connected with the development of flares accompanied by the type IV radio bursts, Bull. Astron. Inst. Czech., 18, 61.

KLECZEK, J. and OLMR, J. 1967 — Type IV bursts and associated active regions, Bull. Astron. Inst. Czech., 18, 68.

KOPECKÝ, M. and KŘIVSKÝ, L. 1966 — Proton flares and types of spot groups in the 11-yr cycle, Bull. Astron. Inst. Czech., 17, 360.

KŘIVSKÝ, L. and OBRIDKO, V. 1969 — Large-scale mutual relations of spot groups in proton complex, Solar Phys., 6, 418.

MARTRES, M. J. 1968 — Origine des régions actives solaires 'anomales', IAU Symposium 35 (Structure and Development of Solar Active Regions), edited by K. O. Kiepenheuer, D. Reidel, Dordrecht, Holland, 25-32.

McINTOSH, P. S. 1969a — Birth and development of the sunspot group associated with the proton flare of July 1966, Annals of the IQSY, 3, 40-43.

McINTOSH, P. S. 1969b — Sunspots associated with the proton flare of 23 May 1967, World Data Center A, Upper Atmosphere Geophysics Report UAG-5, 14-19, February 1969.

McINTOSH, P. S. 1970 — Sunspots associated with the proton flares of late October 1968, World Data Center A, Upper Atmosphere Geophysics Report UAG-8, 22-29, March 1970.

McINTOSH, P. S. and DONNELLY, R. F. 1970 — Relationships among white-light flares, magnetic fields, and EUV bursts, Bull. Amer. Astron. Soc., 2, 330.

1971 — Solar-Geophysical Data, 323 Part II; 319 Part I, U.S. Department of Commerce, (Boulder, Colorado, U.S.A., 80302).

H-Alpha Synoptic Chart for January 1971

by

Patrick S. McIntosh
NOAA Environmental Research Laboratories
Boulder, Colorado 80302

The large-scale distribution of solar magnetic fields is mapped in considerable detail by the position of filaments and filament channels observed in good-quality H-alpha filtergrams [McIntosh, 1970, 1972a]. The synoptic chart of the entire solar surface for the solar rotation centered on the disk passage of McMath Region #11128 is presented below. This chart is an early version of the charts that are now being used to derive more detailed magnetic field information for periods when magnetographs were operating at low resolution, or not operating at all [McIntosh, 1972b]. The definition of the cellular organizations of large-scale magnetic fields is better on these charts than on synoptic charts of measured magnetic fields, and the lines of polarity reversal can be traced continuously over much greater distances. Since the chart below was constructed during the early stages of work on the mapping procedures, it may be incomplete and perhaps inaccurate in some areas.

The area of interest for this compilation is located just right of center, with the colliding sunspot groups [see McIntosh, elsewhere in this compilation] at N19 and Carrington longitude 220°. The solid lines are the locations of filament channels and the dashed lines are areas of extrapolated, or estimated, polarity reversal.

The magnetic field flux imbalance (deficit?) computed for McMath Region #11128 [Rust, this compilation] might be explained by this synoptic chart. Rust measured an excess of flux of the negative polarity, presumably emanating from the large leader sunspots. Perhaps this flux excess existed in lines of force connecting the spots to the large-scale area of positive polarity immediately west of the active region.

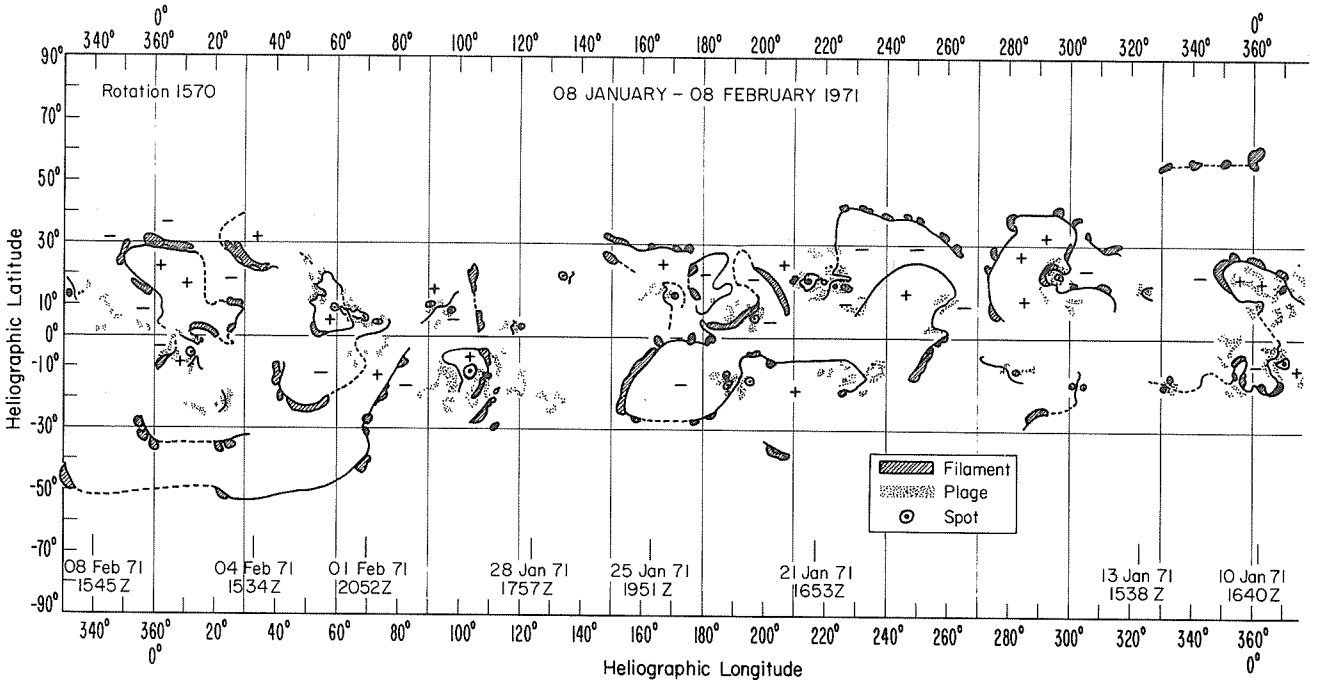

Fig. 1 Synoptic chart of the total sun constructed by plotting positions of H-alpha features associated with lines of magnetic polarity reversal [from McIntosh, 1972a].

REFERENCES

McINTOSH, P. S. 1970 Techniques for inferring solar magnetic polarities from H-alpha observations, AIAA Paper No. 70-1369 at AIAA Observation and Prediction of Solar Activity Conference, Huntsville, Alabama, November 16-18, 1970.

McINTOSH, P. S. 1972a Large-scale solar magnetic fields and H-alpha patterns, paper presented at Asilomar Solar Wind Conference, Pacific Grove, California, March 21-26, 1971, Solar Wind, ed. C. P. Sonett, P. J. Coleman and J. M. Wilcox, NASA SP308, pp. 136-140.

McINTOSH, P. S. 1972b Solar magnetic fields derived from hydrogen-alpha filtergrams, Topical Review in Rev. Geophys. and Space Phys., 11, 837.

RUST, D. M. 1972 Solar magnetic fields in McMath Region #11128, this compilation.

Hα Observations of the Solar Flare, January 24-25, 1971

by
Marie McCabe
Institute for Astronomy
University of Hawaii
Honolulu, Hawaii

McMath Region 11128 was first seen at the East limb at 20°N on January 14, 1971, associated with a bipolar spot group. Three days later, a new Hα plage appeared immediately East of this region and developed rapidly as the region crossed the disk. The two main spots of the new group separated from each other, the leading one approaching the following spot of the more mature group. By January 24th the region was at a mean distance of 45° west of the central meridian.

At Haleakala Observatory Hα flare patrol observations using the 0.5Å Halle filter were obtained during the following hours:

January 24: 1759-2039, 2122-2238, 2311-2400 UT
January 25: 0001-0107 UT

The 10 cm Zeiss filter (0.25Å bandpass) telescope was in operation from 2323-2352 UT, with sets of exposures taken at 1 min intervals. Each set consisted of center-line and off-band (± 5/8Å) frames of the active region. Figures 1 and 2 show selected frames from each of these telescopes, during the progress of the proton flare which was reported in "Solar-Geophysical Data" [1971] to have commenced at 2309 UT with a maximum at 2316 UT. Prior to the main event there were several other flares one of which is seen in the first set of exposures at 1833 UT (Figure 2); the off-band frames show the sunspot configuration.

The flare occurred within the main spot group and showed filamentary structure which curved around and between the three larger spots, later obscuring the center one and covering part of the umbra of the leading one. There was minor activity in the following group at points a, b, and c (Fig. 2), commencing at 2322, 2325, and 2330 UT, respectively.

Our first observations show the flare consisting of a few bright patches which coalesced forming one long and one arch-shaped filament; the latter extended gradually along one side to become parallel to the former, by which time the characteristic shape of a proton producing flare is obvious. Scattered brightenings appeared to the south (d in Fig. 2) from 2324 UT, but there was no evidence of high velocities either along the solar surface or in the line of sight which would have indicated a spray-like feature. Some prominence activity was observed from around 2343 UT when the filament (e in Fig. 2) appeared in the off-band blue frames, while the center line pictures showed brightening along the eastern border of the filament for a few minutes.

Due to mostly poor seeing conditions, the resolution of these photographs is not very high, but a close examination reveals structure between the flare filaments which can be interpreted as a loop prominence system, commencing at about 2334 UT at line center. Exposures at 2345 UT (Fig. 2) show this feature. Region 11128 was too far on to the disk to show any material projected beyond the limb and we had no coronal observations from January 26-28 when the region crossed the limb. The only other activity on the disk during this flare consisted of the temporary appearance of two small plage regions south of the solar equator but at about the same longitude as 11128. One of these is marked f on the disk exposure in Figure 1 and was present from before 2311 UT; the other was a few degrees to the east and commenced at 2315 UT. They were both gone by 2330 UT.

The complex system of 80 MHz radio sources associated with the flare have been studied in detail by Riddle and Sheridan [1971]. The first type II burst was clearly associated with the commencement of the optical flare, but it is difficult to relate the second major event - type II and type IV, starting at about 2320 UT - to a specific optical feature.

The observations described above were obtained as a result of support received from NASA Contract NGL 12-001-011 and NSF grant GA 25903.

REFERENCES

RIDDLE, A. C. and K. V. SHERIDAN — 1971 — Evolution of a Jet-like Structure in the Late Phase of a Complex Solar Outburst, Proc. Astron. Soc. Australia, 2, 1, 62. (Reprinted on pages 93-97.)

1971 — Solar-Geophysical Data, 323 Part II, U.S. Department of Commerce, (Boulder, Colorado, U.S.A. 80302).

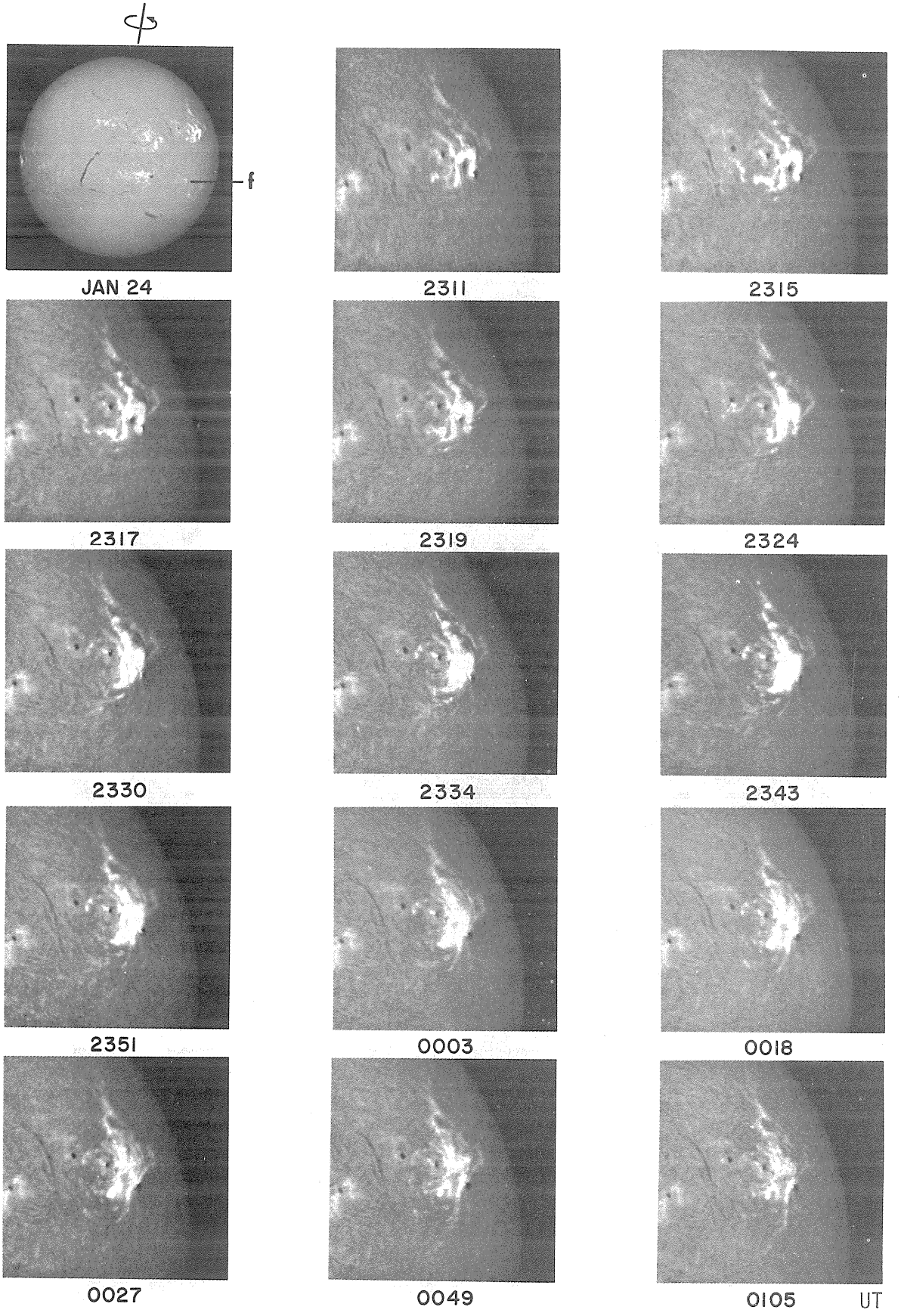

Fig. 1 - Hα Flare Patrol Observations, Jan. 24-25, 1971.

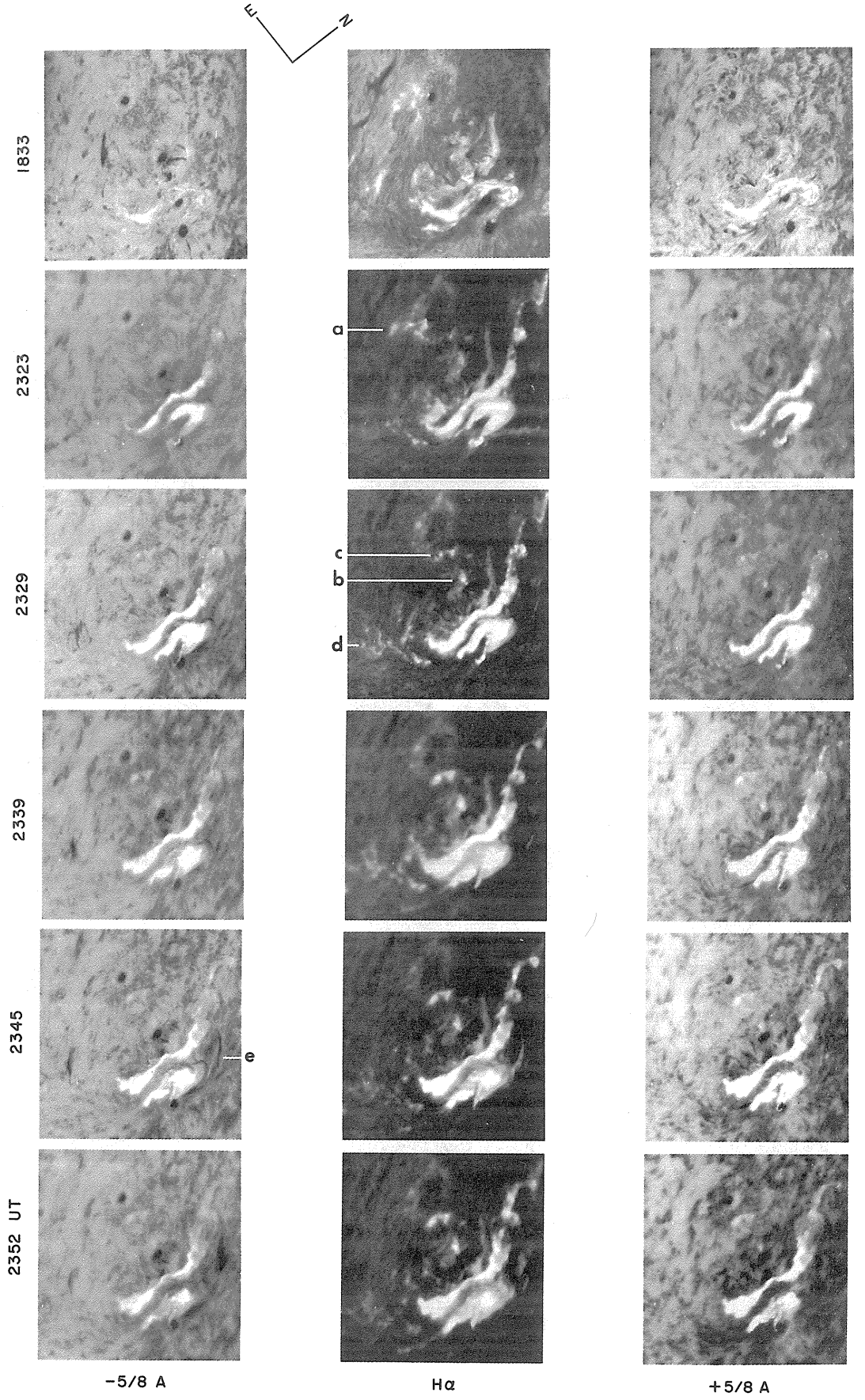

Fig. 2 - On and Off-band (± 5/8Å) Hα Exposures, Jan. 24, 1971.

Development of Activity in McMath 11128 and the 24 January 1971 Flare

by

Harold Zirin
Big Bear Solar Observatory, Hale Observatories
California Institute of Technology
Carnegie Institution of Washington

The development of McMath 11128 is a fascinating example of the role of magnetic field reconnection and solar activity. When this active region came over the limb on January 14, it was an ordinary active region. The sunspots in the leading part, consisting of two "p" spots ("p1" and "p2") and one "f" spot ("f1") remained almost identical for the entire period. However on January 19 a new sunspot group developed in the following part of the region and rapidly spread to overtake the "f" spot of the first group. In the subsequent reconnection of fields, a considerable amount of activity took place, finally leading up to the great flare of the 24th.

The material for our discussion is provided by coverage with four telescopes: two refractors at Big Bear which give large scale on-band and off-band Hα; a patrol refractor in Pasadena giving back-up coverage with a small image, and the Tel Aviv photoheliograph covering the Pasadena night. Fairly continuous coverage is available during the disk passage of the region.

The development of the region is shown in Figure 1. We number the "p" spots "p1" and "p2" in the leading group, and "p3" in the follower; "f1" in the lead group (best seen January 22) and "f3" in the follower.

The emerging flux region to be designated Mt. Wilson 18284 was first seen by us on the 19th at 0700 UT on the Tel Aviv films. Its further growth was followed at Tel Aviv on the 20th. We have no film on the 21st, but on the 22nd it could be seen as a rapidly expanding bipolar region. By that time the lead spot "p3" of 18284 had pushed deep into the "f" plage of 18281, almost touching the second "p" spot "p2" of that group.

On January 22nd "p3" had reconnected to the "f" plage of the older group. A number of bipolar flares took place this day, with branches in "p3" and "f1". Note that there was no cancellation between the colliding "p" and "f" polarity, just reconnection. In fact the "f" spot even grew a bit. At the same time the big filament curling around "p1" and "p2" curled into a much tighter arc as the "f" plage pushed forward. The region along the filament grew considerably brighter, until on the morning of the 24th the filament was completely surrounded by bright plage, a situation often preceding flares.

On the 23rd at 1929 UT a flare occurred with a "p" branch in the N arc of the filament and "f" branch near spot "f1". On the 24th the filament had also encroached on the penumbra of "p2" so that it was sharply cut off. A precursor flare occurred along the filament at 2046 UT, accompanied by an expulsion from the "p1" spot and an impulsive radio burst. At 2230 UT gradual brightening started all over the area. There was very little motion of the filament, which just appeared to fade out. This is verified by the simultaneous off-band (-½Å) films and a λ scan from -1 to +1Å at 2300 UT. The real brightening starts at 23 hr 08 min 45 sec, the two strands starting to separate at 2310 UT. The bright "p" strand curled out from the N arc of the filament to cover the spot "p2", while the bright "f" strand spread over the entire "f" plage, but interestingly enough did not remain parallel to the filament. The most energetic part of the flare seems to have been a bifurcation of the filament near its northernmost arc, where some new flux has pushed up; it was here the "f" strand broke away from the filament.

On the 25th some structural change could be seen. The plage under the big filament was no longer bright, but the filament was back in place. The spot "p1" was split in two, and the spot "p2", over which the flare had occurred, was much diminished in size. On the 26th "p2" had disappeared. It may be no accident that the most significant spot changes in five days occurred after this big flare.

In summary, there is some evidence that the expansion of Mt. Wilson 18284 into Mt. Wilson 18281 gave rise to stresses which ultimately caused the great flare of 24 January 1971, but the case is not proven. The flare was also marked by intrusion of a filament onto a spot penumbra and rapid decline of that spot. The flares between "p3" and "f1" on the 22nd are a nice example of field reconnection.

This work was supported by NASA and NSF. I am indebted to Dr. J. Vorpahl for several valuable discussions.

BIG BEAR SOLAR OBSERVATORY

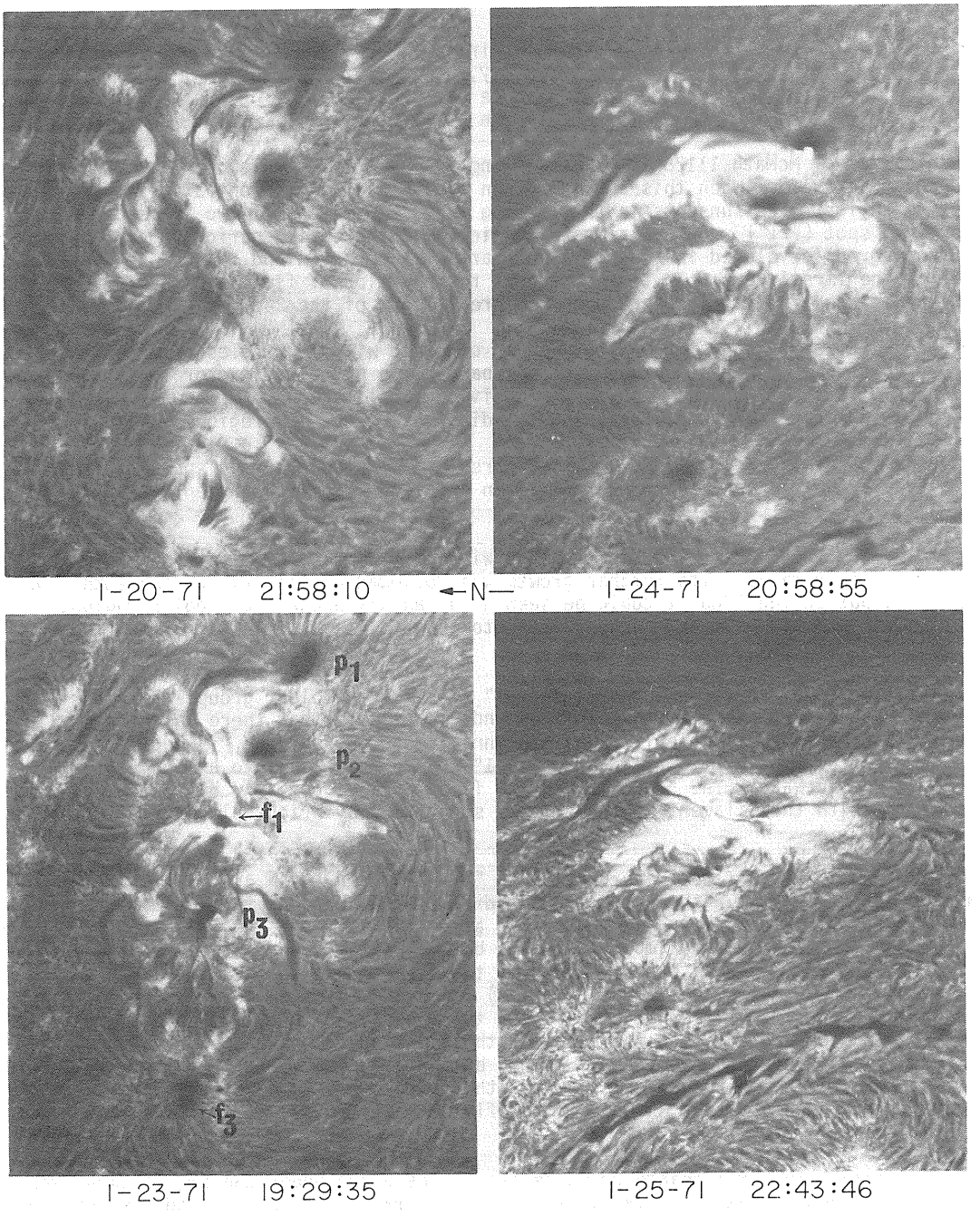

Fig. 1. Four stages in the development of McMath 11128.
(W top, N left)

1/20/71: The emerging flux region Mt. Wilson 18284 is seen at the bottom.

1/23/71: Mt. Wilson 18284 has grown into a serious bipolar group; its leader "p3" shares a penumbra with the follower "f1" of 18281, and the filament around that group has been compressed.

1/24/71: Just before the flare the filament is completely enveloped by plage and has moved closer to "p2". The follower spot "f1" has broken up.

1/25/71: After the flare the size of spot "p2" is greatly reduced.

BIG BEAR SOLAR OBSERVATORY
Proton Flare
January 24, 1971

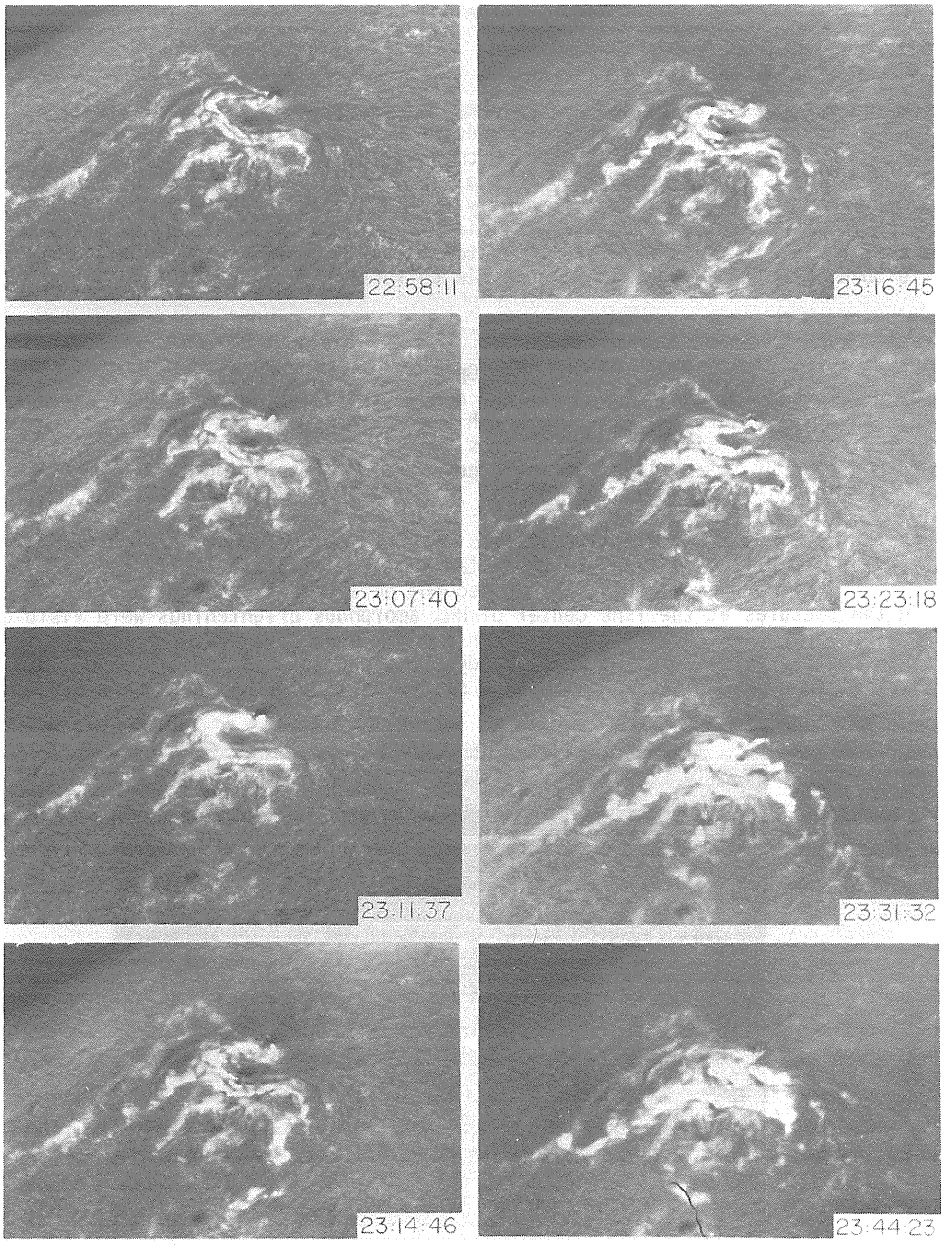

Fig. 2. Development of the flare. The print at 23 hr 11 min 37 sec was redone at a different time from the others and is too contrasty; the actual flare brightness at that time is no greater than at 23 hr 14 min 46 sec directly following. Note the steady separating of the two bright strands in the course of the flare. The lower strand fills the area of following polarity between "p3" and the filament; the "p" strand fills the area inside the filament. The "f" side of the leading part of the filament plays no part in the flare.

Flare of January 24 - 25, 1971

by

F. Moriyama
Tokyo Astronomical Observatory

Introduction

A large flare occurred at N18 W49 in an E-type sunspot group on January 24-25, 1971. We observed this flare at the Tokyo Astronomical Observatory using a 14 cm SECASI monochromatic heliograph at the center of Hα (pass band 0.75Å) and a 20 cm equatorial refractor equipped with a Halle filter (pass band 0.5Å) at the center as well as in the wings of Hα. Unfortunately, because of unfavorable weather, photographic records were obtained only for the decaying phase of the flare, Figure 1. Mr. Ohki of the Goto Optical Co. took several pictures of the flare around the maximum phase with an Hα interference filter (pass band 2.4Å) mounted on a 7.5 cm refractor. The photographic aspect of the flare observed at the two observatories is collectively presented in this report.

Development of Flare

Figure 2 shows pictures taken at the Goto Optical Co. In the first two prints, the flare appeared in two bright ropes: the one (F1) described a semicircle surrounding the north-west side of the central spot (S2), the other (F2) extended north and south across the eastern part of the sunspot group. The two ropes were similar in brightness, and the central spot was partly covered by F1. Between 2322 and 2335 UT, F1 evolved into a rather straight rope lying to the west of the central spot.

The apparent area of the flaring region was measured to be 1130 millionths of the solar disk at 0013 UT on January 25 when the observation started at Mitaka, and the flare was classified as importance 3n. Hα filtergrams showing the subsequent development of the flare are given in Figures 3 and 4. In the pictures at the line center of Hα, amorphous brightenings were visible superposed on the main flare ropes, which were prominent in the off-band pictures. On the original negatives, one can see threadlike formations (L) which bridged the gap between the two main flare ropes. They lasted until the end of the flare, and may be a system of loop prominences seen projected on the disk.

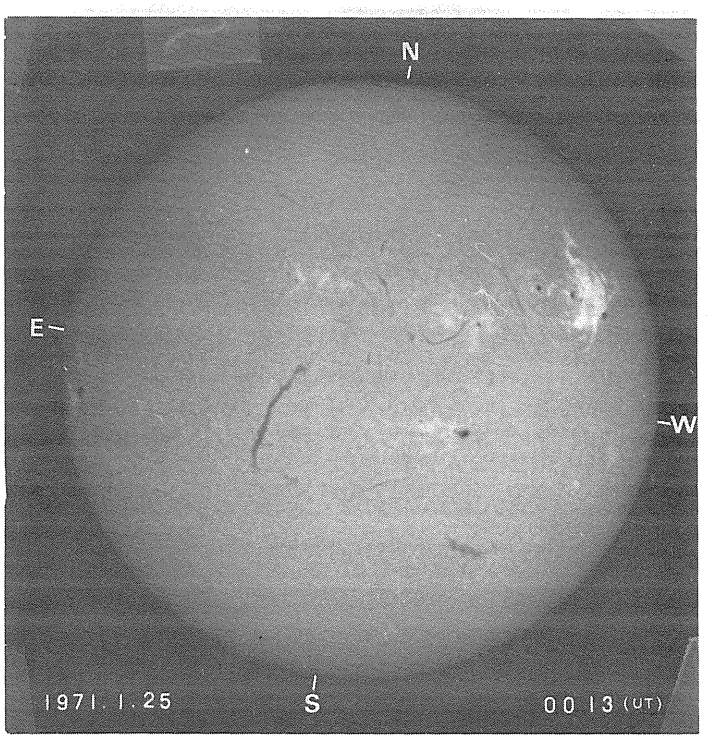

Fig. 1. Hα-filtergram taken with SECASI monochromatic heliograph at the Tokyo Astronomical Observatory on Jan. 25, 1971.

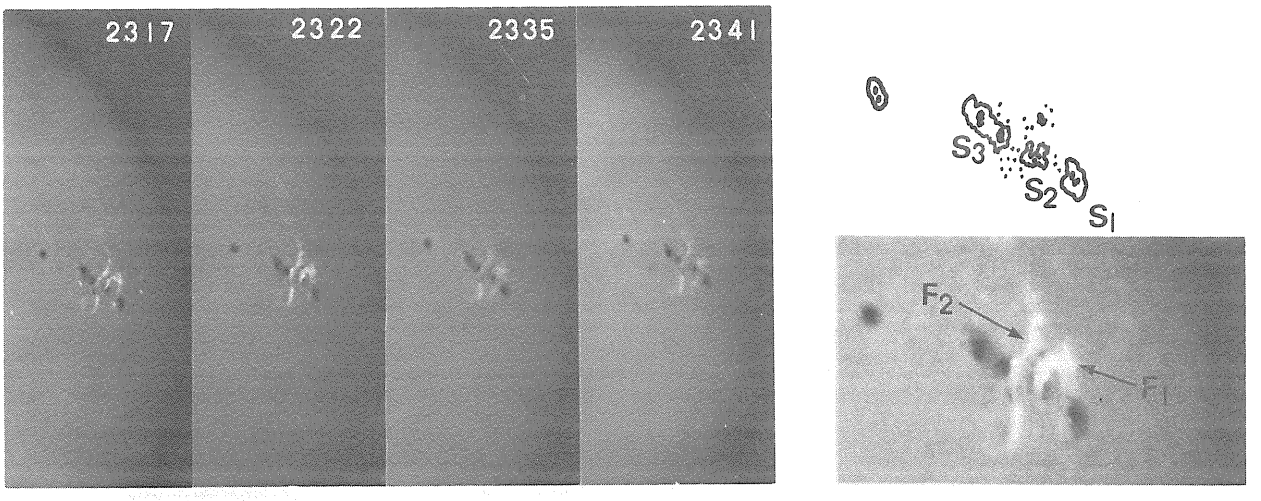

Fig. 2. Flare observed with a broad band filter (pass band 2.4A) at the Goto Optical Co. on Jan. 24, 1971.

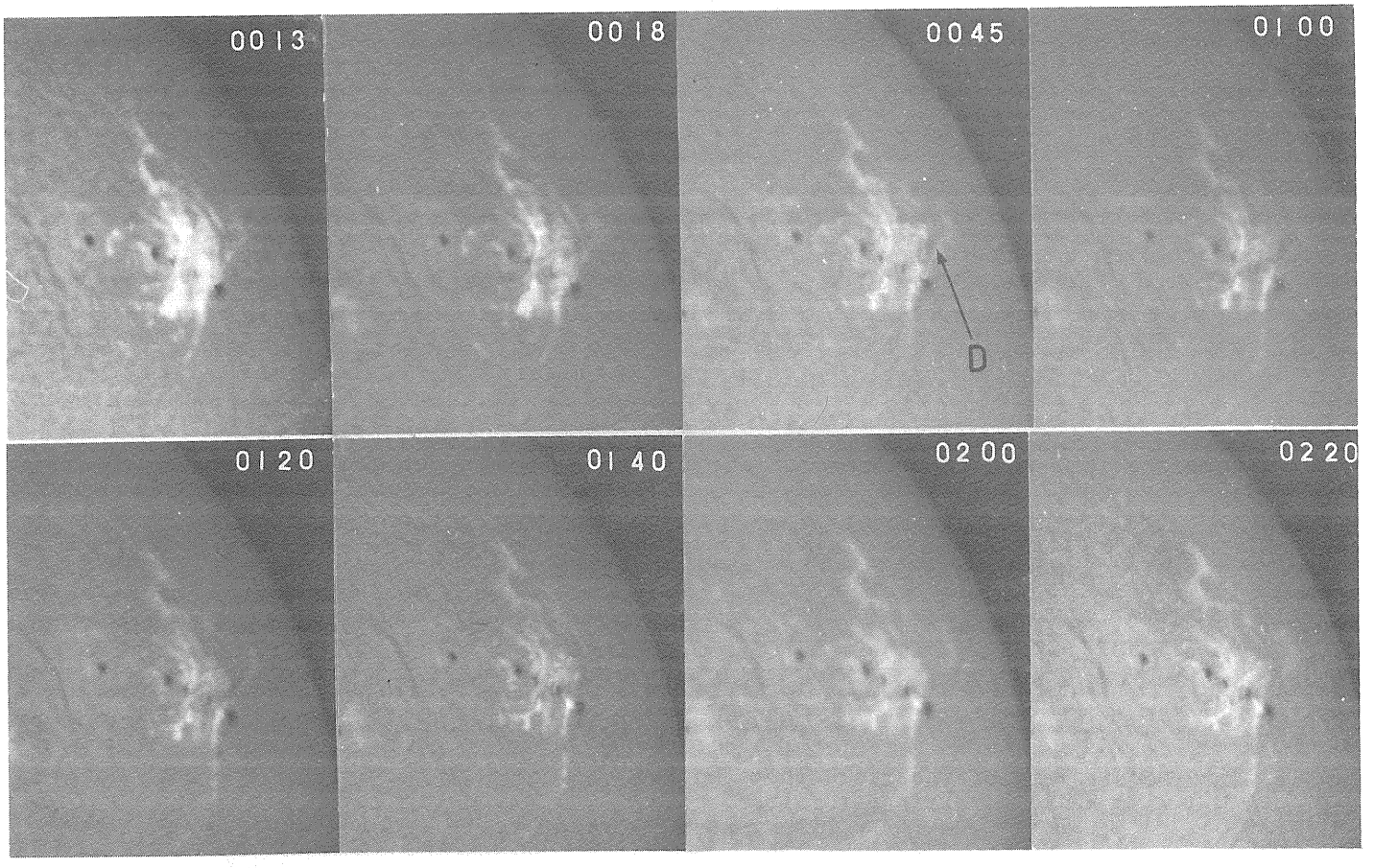

Fig. 3. Flare observed with SECASI monochromatic heliograph at the Tokyo Astronomical Observatory on Jan. 25, 1971.

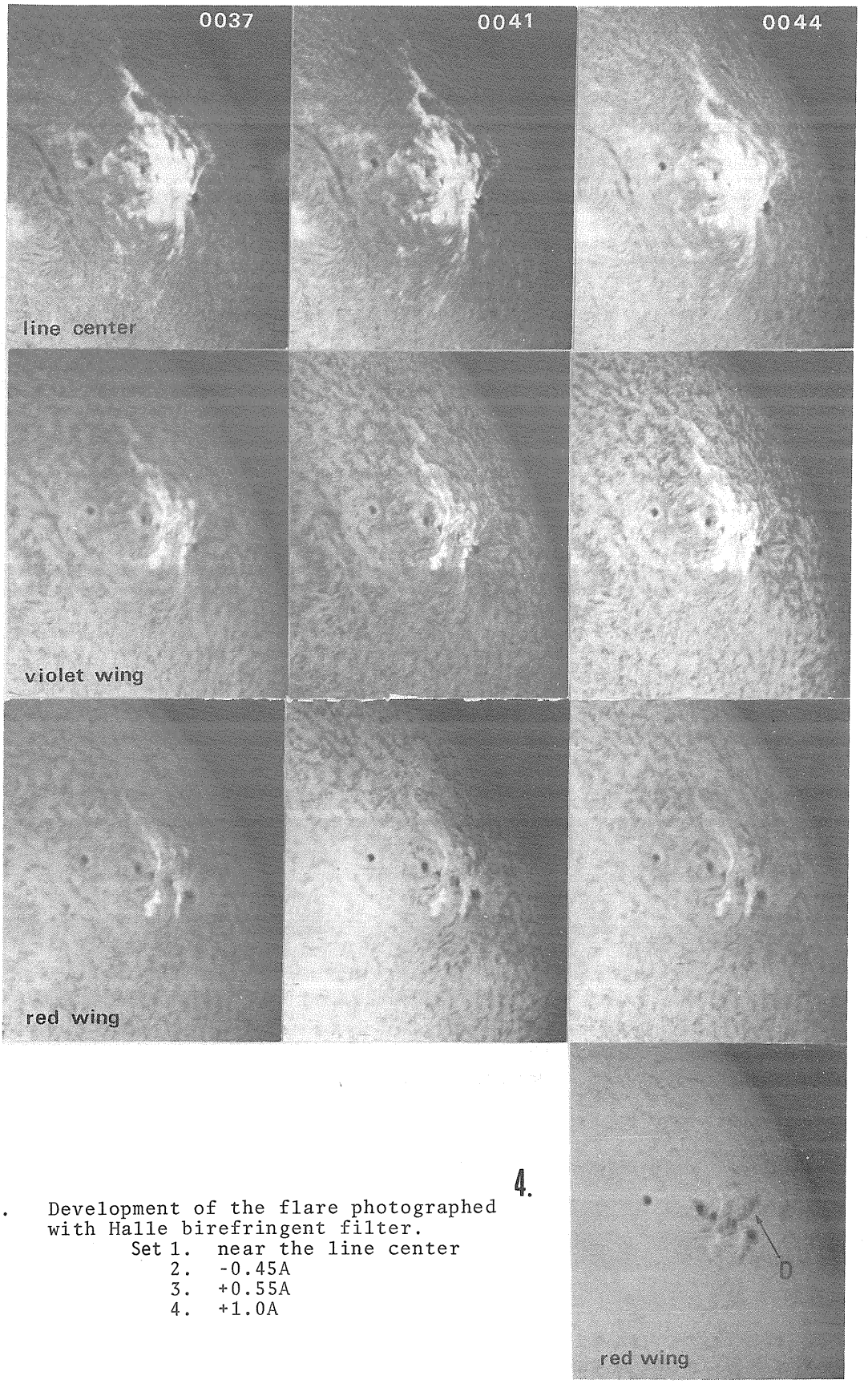

Fig. 4. Development of the flare photographed with Halle birefringent filter.
Set 1. near the line center
2. -0.45A
3. +0.55A
4. +1.0A

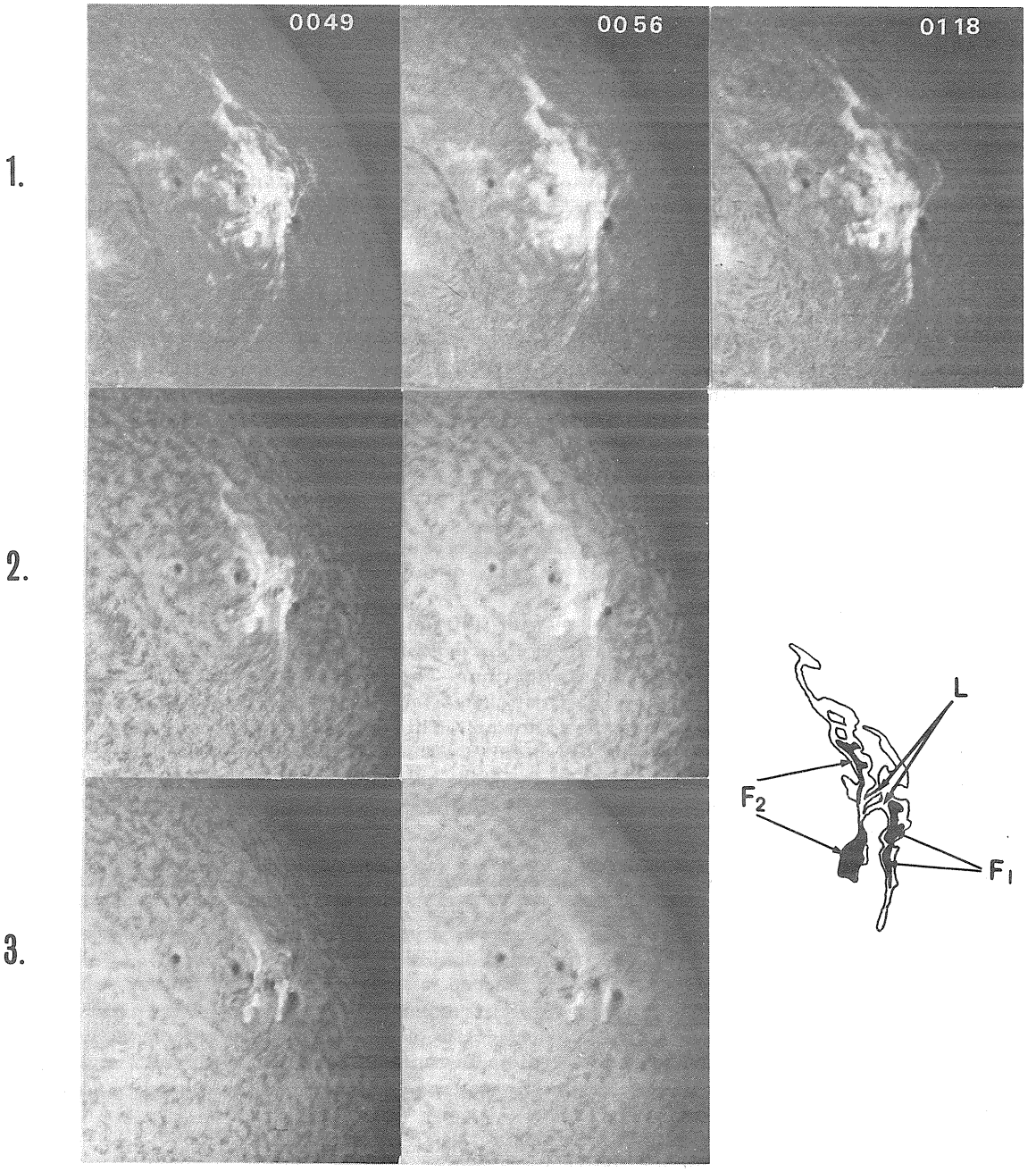

The violet image of the flare was more enhanced than the red image in Set 3, but this asymmetry might possibly be caused by a shift of the wavelength scale of the Halle filter due to imperfect temperature control. Judging from the appearance of the chromospheric structure in the off-band photographs, we estimate the shift to be approximately 0.05Å.

A dark surge (D) was seen near F1 at 0045 UT, Figure 3. Although largely obscured by bright features, it can be traced back till 0013 UT. The surge was most noted in the +1.0Å off-band picture at 0044 UT, which showed the surge to originate in the north side of the central spot, and disappeared at 0145 UT.

At about 0220 UT the brightness of the region did not change, and we may consider the flare ended.

Acknowledgement

The author is grateful to Mr. K. Ohki for kindly providing pictures taken at the Goto Optical Co.

The Flare of 24-25 January 1971 Observed at Manila

by

Francis Heyden, S.J. and Danilo Balboa
Manila Observatory, P.O. Box 1231, Manila, Philippines

The flare was observed visually with the Halle filter. Spectroheliograms were taken in Hα and K (Ca II). White light photographs were taken at Manila and Baguio. Continuous observation of the sun was maintained until 0212 UT of 25 January. At the time of the flare the sun was at a rather low altitude, approximately 20° above the southeastern horizon.

The 2B flare occurred at N19W50 in a region of several sunspots (Figures 1 to 4), Boulder region 128A or McMath region 11128. Starting time was observed visually at 2309 UT on 24 January 1971. Two maxima were observed, the first at 2316 with an estimated area of 280 millionths of the disk, and the second at 2322 with an estimated area of 450 millionths.

Three spectroheliograms were taken during the flare: one in Hα (Figures 5 and 6) at 2357 UT on 24 January and two in K (Figures 7, 8 and 9) at 0005 and 0024 on 25 January. Although the Hα spectroheliogram was taken after the two maxima, there is a considerable amount of detail, some of which is common to the white light photographs. There is a definite overlay of a bright cloud that shows a ribbon structure and which appears also on the K spectroheliograms taken at 0005 and at 0024 UT. The last coincides with the visual estimate of the end of the event.

The white light photographs were taken with Unitron four-inch F15 refractors at Manila and at Baguio. Both of them have been fitted with eyepieces which give approximately 30 X enlargement to permit direct reading of the film without projection. The four enlargements (Figures 1 to 4) show some rather interesting features. The first pair of sunspots show light bridges quite narrow across the leader and quite broad across the follower. This latter is most involved with the flare and on its light bridge there appears a distinct brightening about twenty minutes before the end of the flare at 0024. This same brightening of this area of the light bridge is seen on the photograph taken at Baguio at 2354 near the time of the Hα spectroheliogram (Figures 5 and 6).

While the Wilson effect [Tandberg-Hanssen, 1967] seems very pronounced on the sunspots, a decided change occurs on the eastern edge of the following spot of the second pair. At 2321 (Figure 2) twelve minutes after the estimated beginning of the flare, the penumbra is still missing completely. About twenty-four hours earlier at 2342 on 23 January, a very bright loop had encroached over the eastern edge of this same spot, which also appeared double at that time (Figure 1). Between the white light photograph at 2321 on 24 January and the one taken at 0005 on 25 January some slight changes have occurred. The K spectroheliogram corresponds to the ending of the flare. An enlargement of the flare is shown in Figure 9, but many of the details of the original have been washed out. On the white light photographs taken at Manila and Baguio a few minutes earlier (Figures 2 and 4) there is another area of brightening appearing on the northwest edge of the following spot of the second pair. This spot is also involved in the flare.

The very bright encroachment (Figure 1) which can be seen also on the white light photograph taken at Baguio at 0010 on 24 January (Figure 10) does not show the duplicity that was noted twenty-four hours later in Manila. Possibly the duplicity is only apparent. No reports on this feature by other observers are available at Manila Observatory. Possibly it is due to an overlap of the sunspot areas 128A and 128B. An overlay (Figure 11) showing the position of the sunspots with respect to the area of the flare has been prepared to give some idea of the relative positions of the features mentioned in the other Figures.

The spectroheliograms in Hα and K (Ca II) were taken by Adalric Arinque. The Baguio white light photographs were taken by Simeon Dicang.

REFERENCE

Tandberg-Hanssen, E. 1967 Solar Activity, Blaisdell, Waltham, Mass., 189.

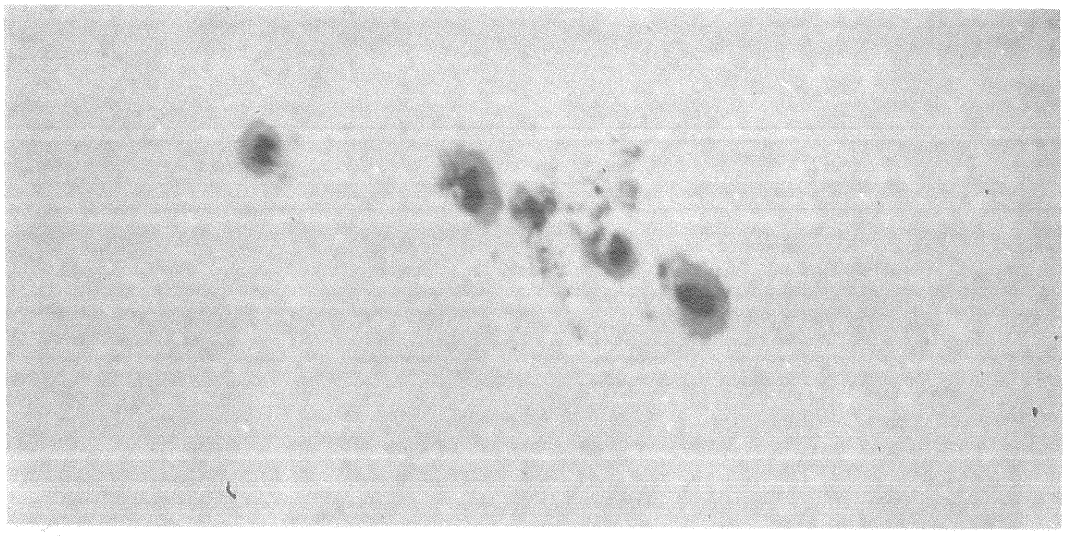

Fig. 1. Sunspots at 2342 UT, 23 Jan. 1971

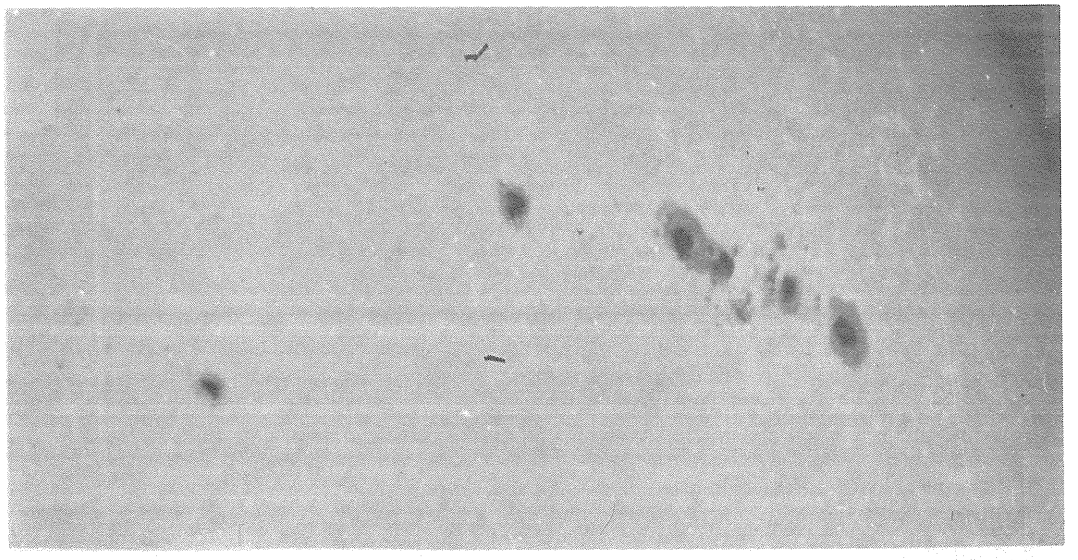

Fig. 2. Sunspots at 2321 UT, 24 Jan. 1971

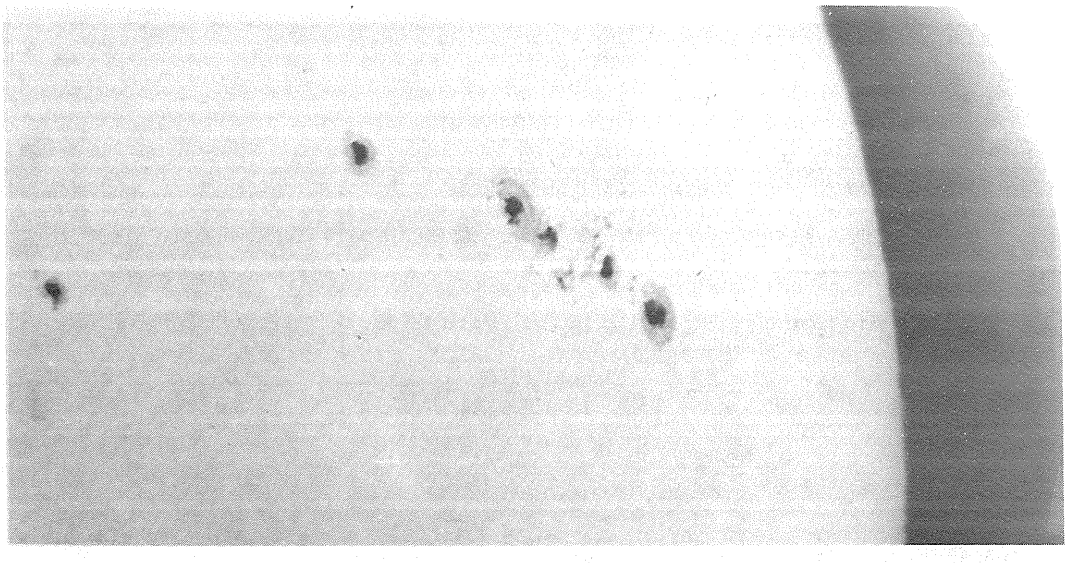

Fig. 3. Sunspots at 0005 UT, 25 Jan. 1971

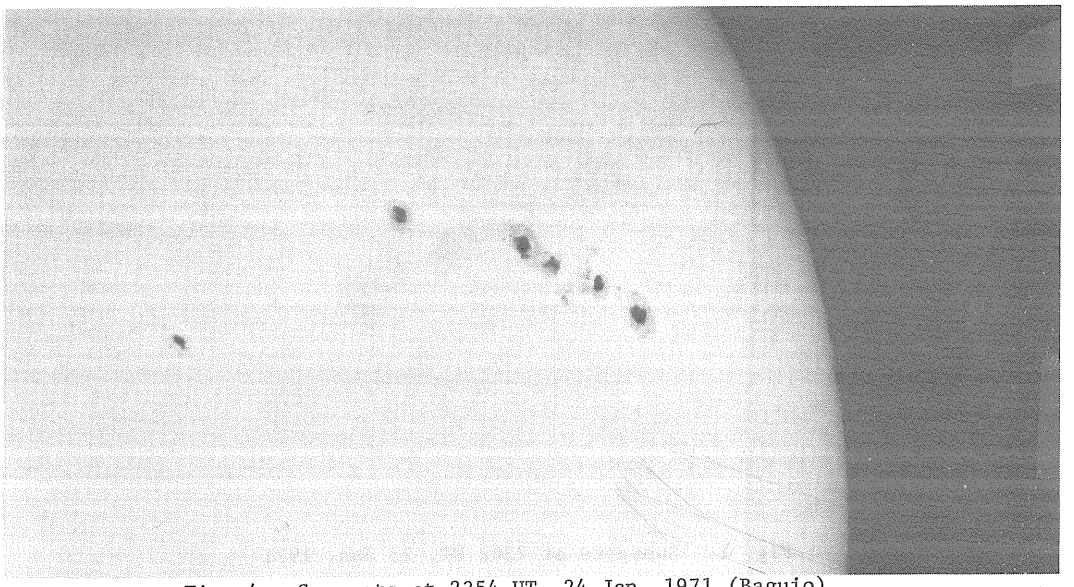

Fig. 4. Sunspots at 2354 UT, 24 Jan. 1971 (Baguio)

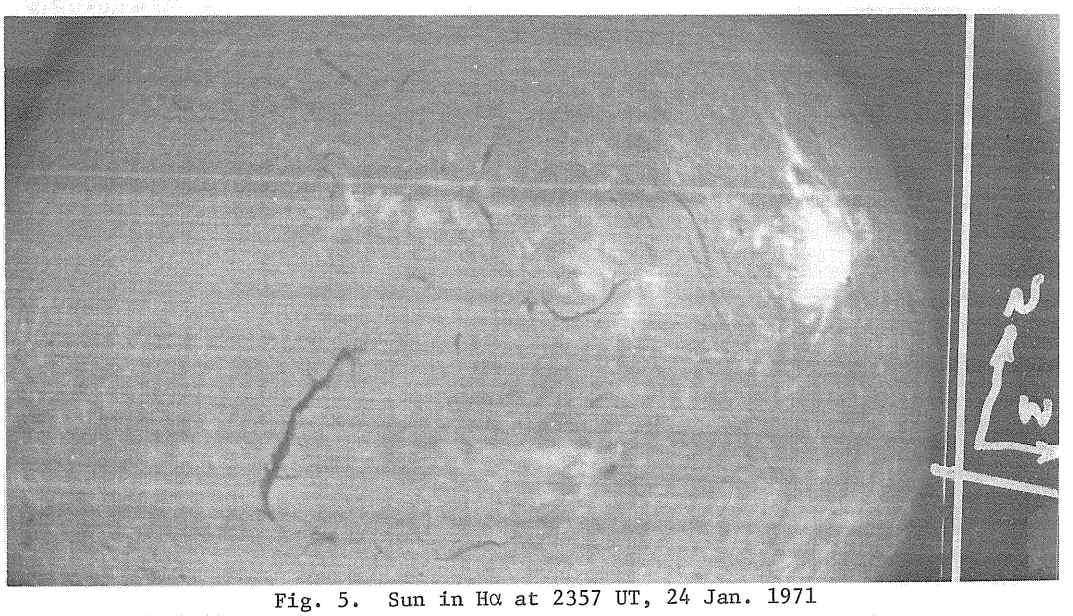

Fig. 5. Sun in Hα at 2357 UT, 24 Jan. 1971

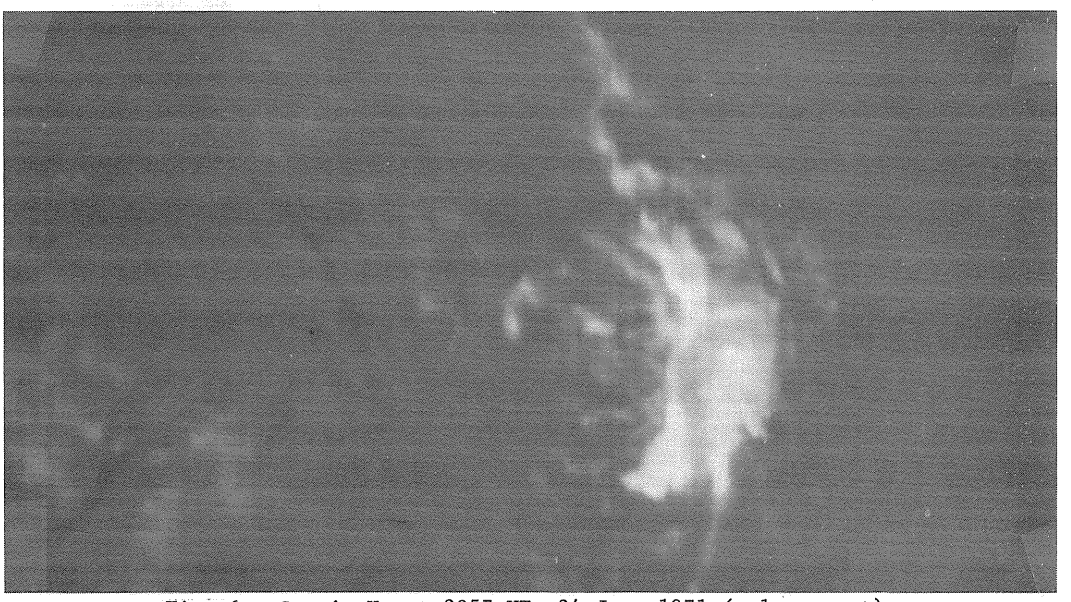

Fig. 6. Sun in Hα at 2357 UT, 24 Jan. 1971 (enlargement)

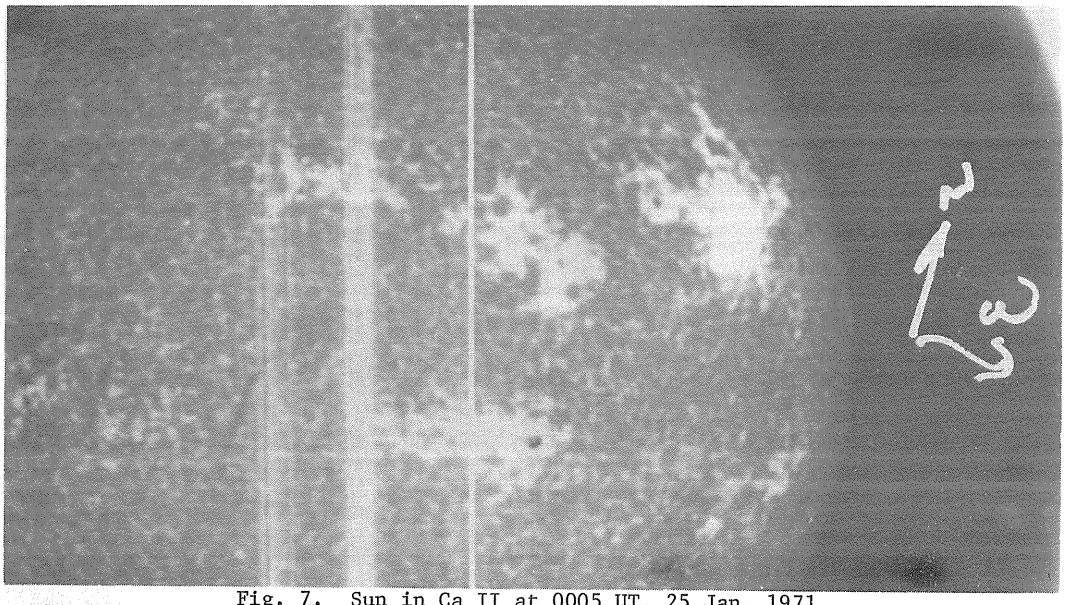

Fig. 7. Sun in Ca II at 0005 UT, 25 Jan. 1971

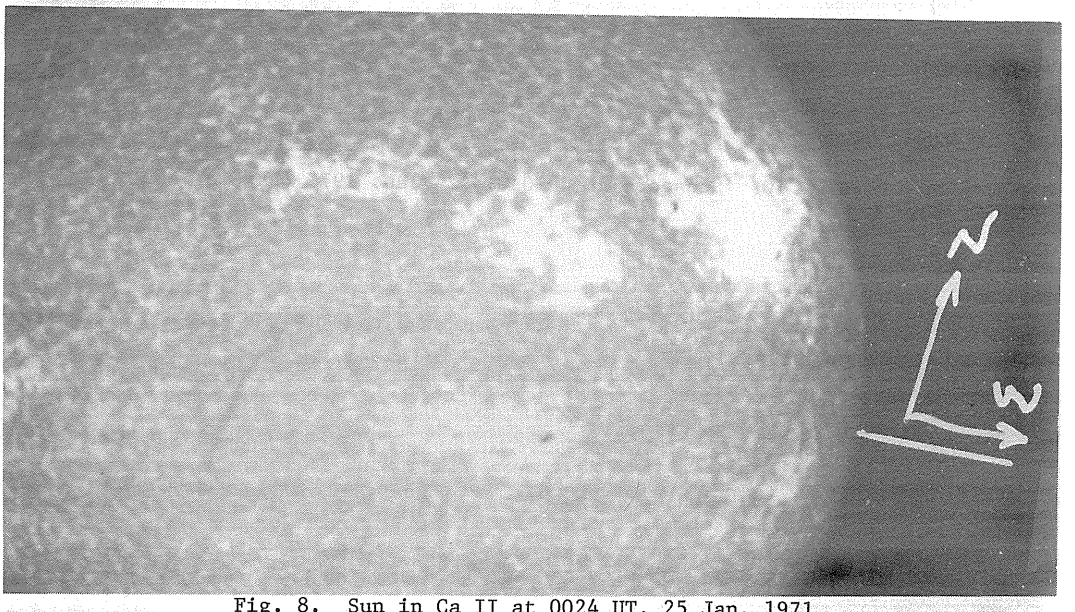

Fig. 8. Sun in Ca II at 0024 UT, 25 Jan. 1971

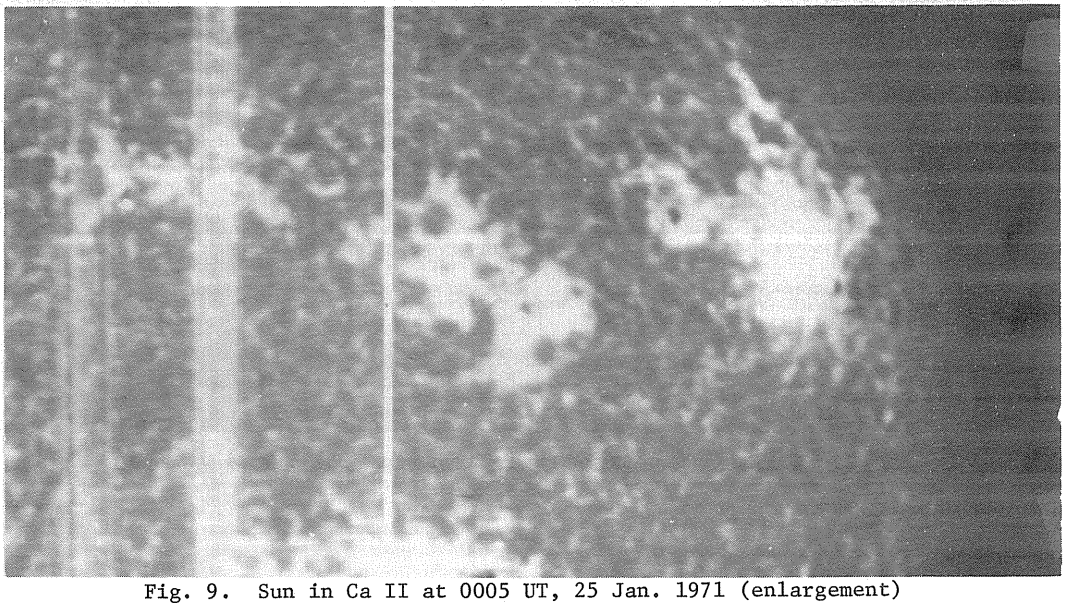

Fig. 9. Sun in Ca II at 0005 UT, 25 Jan. 1971 (enlargement)

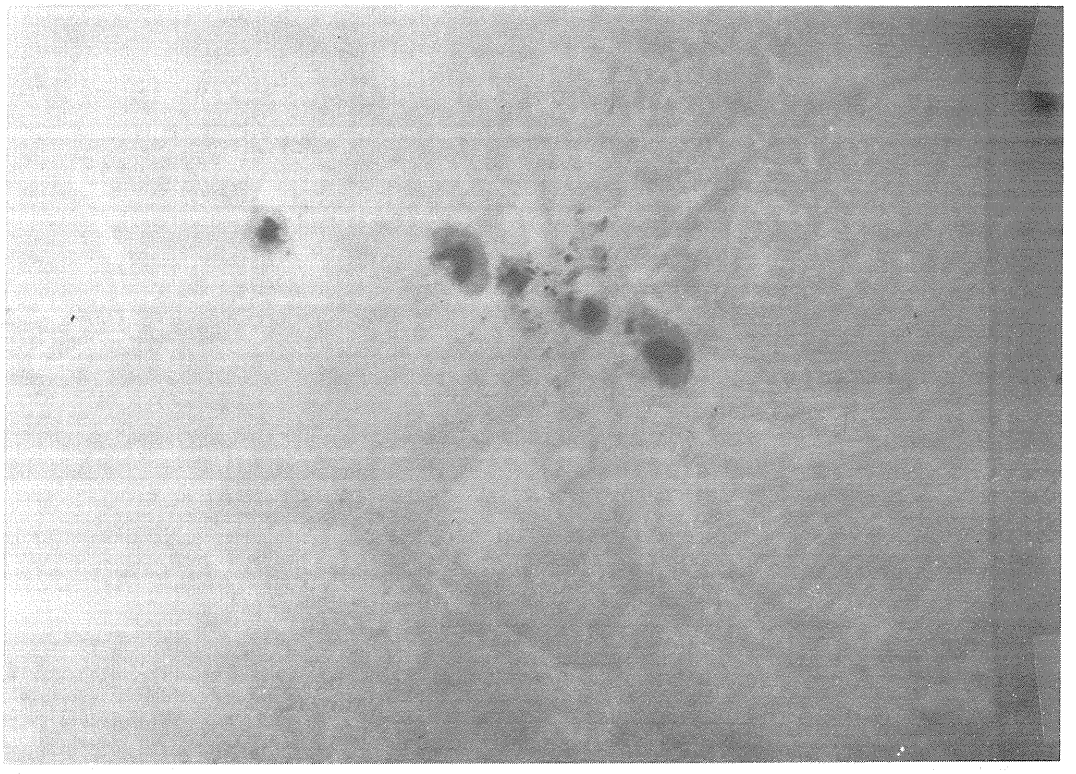

Fig. 10. Sunspots at 0010 UT, 24 Jan. 1971 (Baguio)

Fig. 11. Sunspots superposed on Hα flare of 2357 UT, 24 Jan. 1971

Development of the Large-Scale Situation in which the Proton-Flare of January 24, 1971 Took Place

by

V. Bumba
Astronomical Institute of the Czechoslovak
Academy of Sciences, Ondrejov
and
J. Sýkora
Astronomical Institute of the Slovak
Academy of Sciences, Skalnate Pleso

1. Introduction:

Recently in several notes [Bumba 1971a; Bumba 1971b; Bumba et al. 1972] it was demonstrated that during the descending part of cycle of solar activity No. 19, the location of large particle-emitting flares was closely related to the large-scale distribution of photospheric magnetic fields. These large-scale magnetic field patterns are also connected with the systematic distribution of magnetic field and flare activity in heliographic longitude [Bumba 1971a] and therefore with the development of complexes of activity [Bumba et al. 1972]. Very often the magnetic fields of one polarity in an activity complex become expanded into large, regular (or semiregular) drop-shaped structures extending often more than 100° of heliographic longitude [Ambroz et al. 1971]. The opposite polarity forms a complementary figure. The center of gravity of the major flare activity, and of particle-emitting flares, is never connected with the head of these patterns formed from older magnetic fields, but is usually anchored to the eastern part of this drop-shaped magnetic field body. The regular large-scale distribution of magnetic fields is practically repeated by the distribution of the green corona intensity, which has the same spatial relationship to large flares as in the case of magnetic fields [Bumba, Sýkora, 1971].

2. Development of the Large-scale Situation in which the Studied Proton-flare Took Place:

Information about the development of the large-scale situation in which the proton-flare of January 24, 1971 took place is shown in Figure 1. This complex figure presents a time-series of synoptic charts, plotted in latitude and longitude, centered on the longitude of the proton-flare region of the January 24 event (220°) and with the arrow indicating the solar rotation during which the flare took place (1570). Figures 1a and 1b show the negative and positive polarity magnetic fields, respectively, drawn from daily Mt. Wilson magnetic maps. Figure 1c presents the Solar Activity Fraunhofer Institute maps. Figure 1d shows geomagnetic data taken from the Göttingen daily geomagnetic character figures, shifted four days to take into account the travel time of solar particles.

Studying the magnetic field distribution, we find the same behavior as in the preceding cycle, although the large-scale characteristic features of the magnetic field body are not so well pronounced. On the negative polarity maps, two streams of concentrated fields with synodic rotation close to 27 days are seen. In the center of the figure in northern heliographic latitude where the flare occurred, the indication of a drop-shaped feature with its tail stretched out to the southern hemisphere may be seen in its development. Again, the flare did not appear in the region of the head of this feature but in its eastern part, about 90° from the head. The complementary patterns of the positive polarity are not as spectacular as during the previous cycle. Consider the Carrington period of synodic rotation of positive polarity features connected with the flare. As in previous cases the fast redistribution of negative polarity following the flare occurrence is seen in opposition to the relative stability of the positive polarity patterns.

The development of calcium plages and spot groups in the given longitudinal and time interval shows that the proton-flare region seems to be the last large manifestation of activity in this longitudinal interval. The fast disappearance of activity in the western stream of negative polarity once more speaks in favor of the idea that the fields in the head of drop-shaped large-scale field body are older, being the remains of activity which took place there several rotations earlier.

Concerning the enhancement of the geomagnetic activity in the previous nineteenth cycle, it was as a rule closely related to the streams of older positive polarity magnetic fields [Bumba, 1971c; Bumba, 1971b; Ambroz et al. 1971]. For the first time during this period of the two recent cycles, the recurrent geomagnetically enhanced time intervals correlate with the streams of negative polarity magnetic field, as is seen in Figure 1d compared with Figures 1a, 1b and 1c. This important fact is studied and discussed separately.

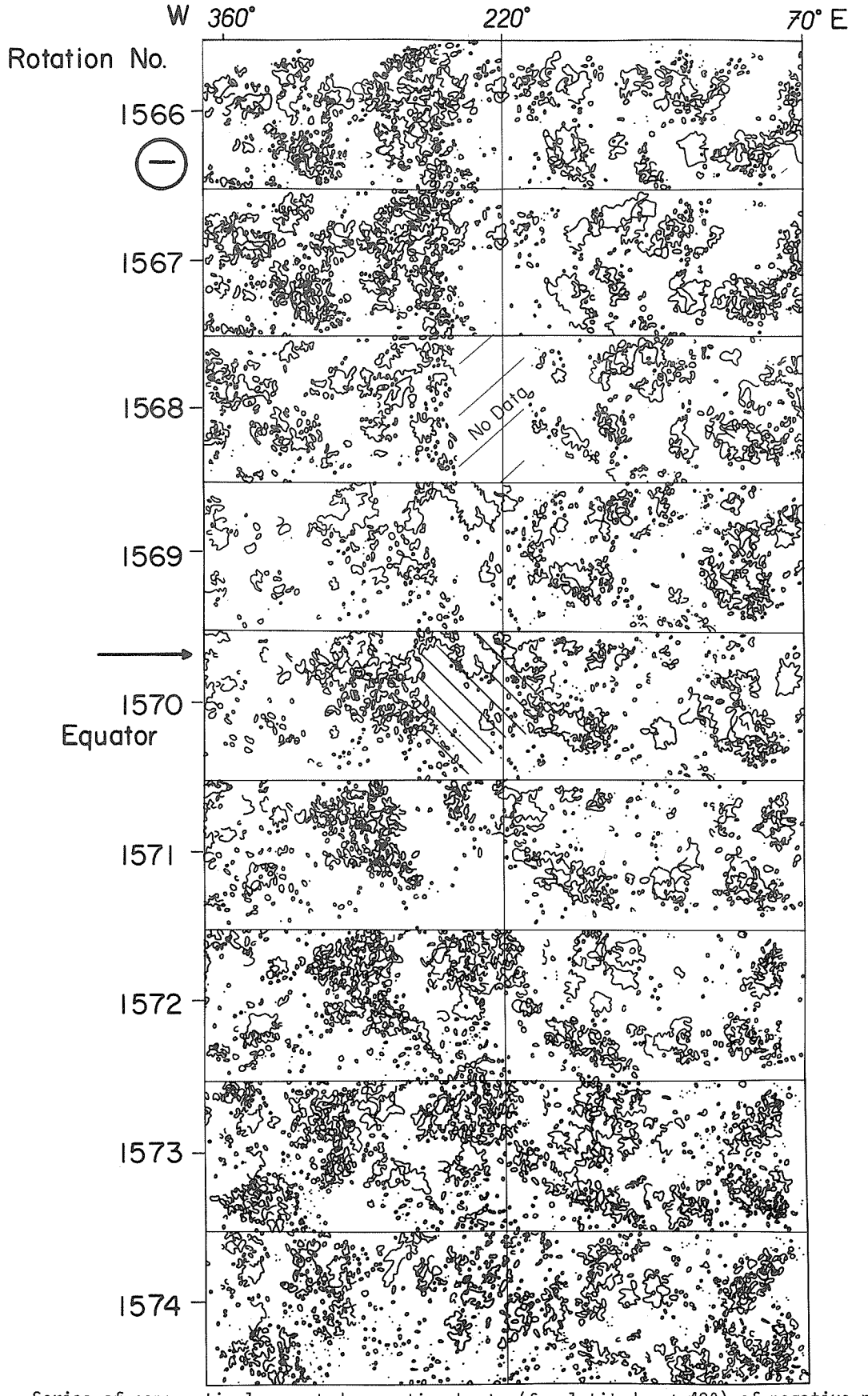

Fig. 1a. Series of consecutively mounted synoptic charts (for latitudes ± 40°) of negative polarity magnetic fields for rotations Nos. 1566-1575. For integration two consecutive maps, one of which is repeated, are always overlapped. The rotation with the proton-flare which took place close to the indicated heliographic longitude 220° (N 19°) is shown by an arrow.

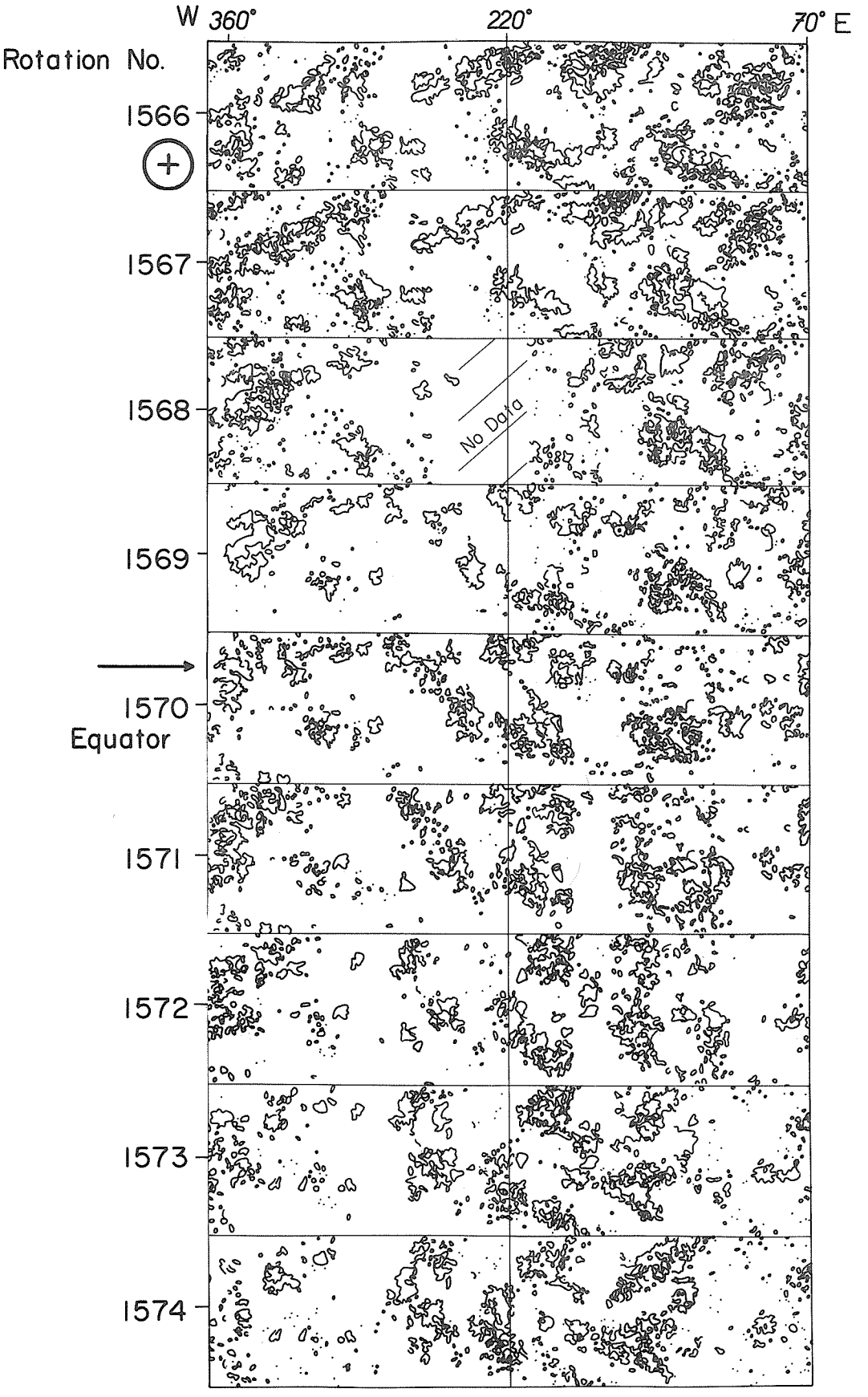

Fig. 1b. The same series of consecutively mounted magnetic synoptic charts as in Fig. 1a for positive polarity fields.

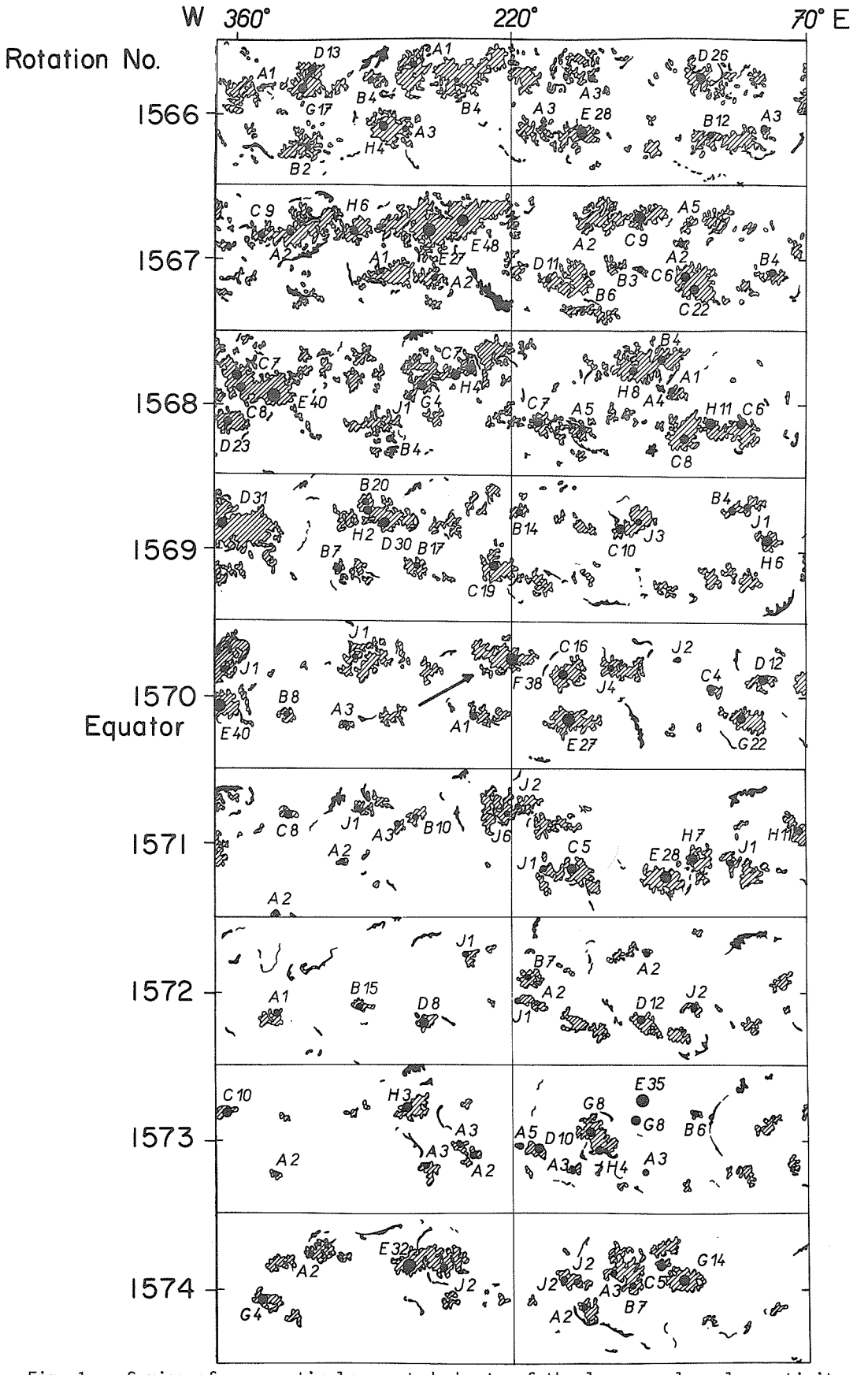

Fig. 1c. Series of consecutively mounted charts of the large-scale solar activity distribution (Fraunhofer Institute, Freiburg) without overlapping of maps for rotations Nos. 1566-1574. Active region F 38 in which the proton-flare occurred is indicated by an arrow.

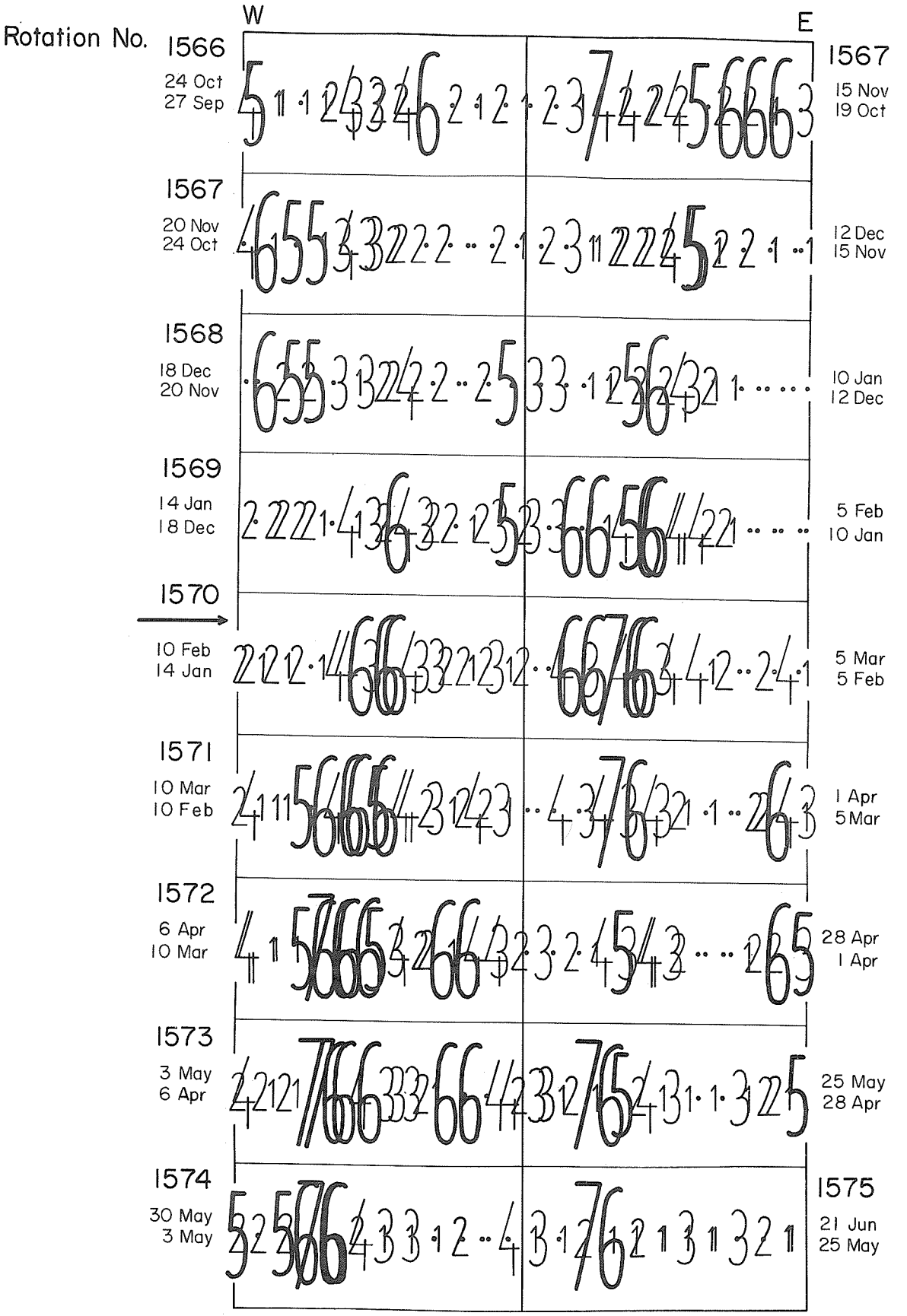

Fig. 1d. Series of consecutively mounted charts of geomagnetic activity distribution (Institut für Geophysik, Göttingen) for the same time interval with the same overlapping of charts. The four days, needed by the particles to arrive at the Earth, are taken into account.

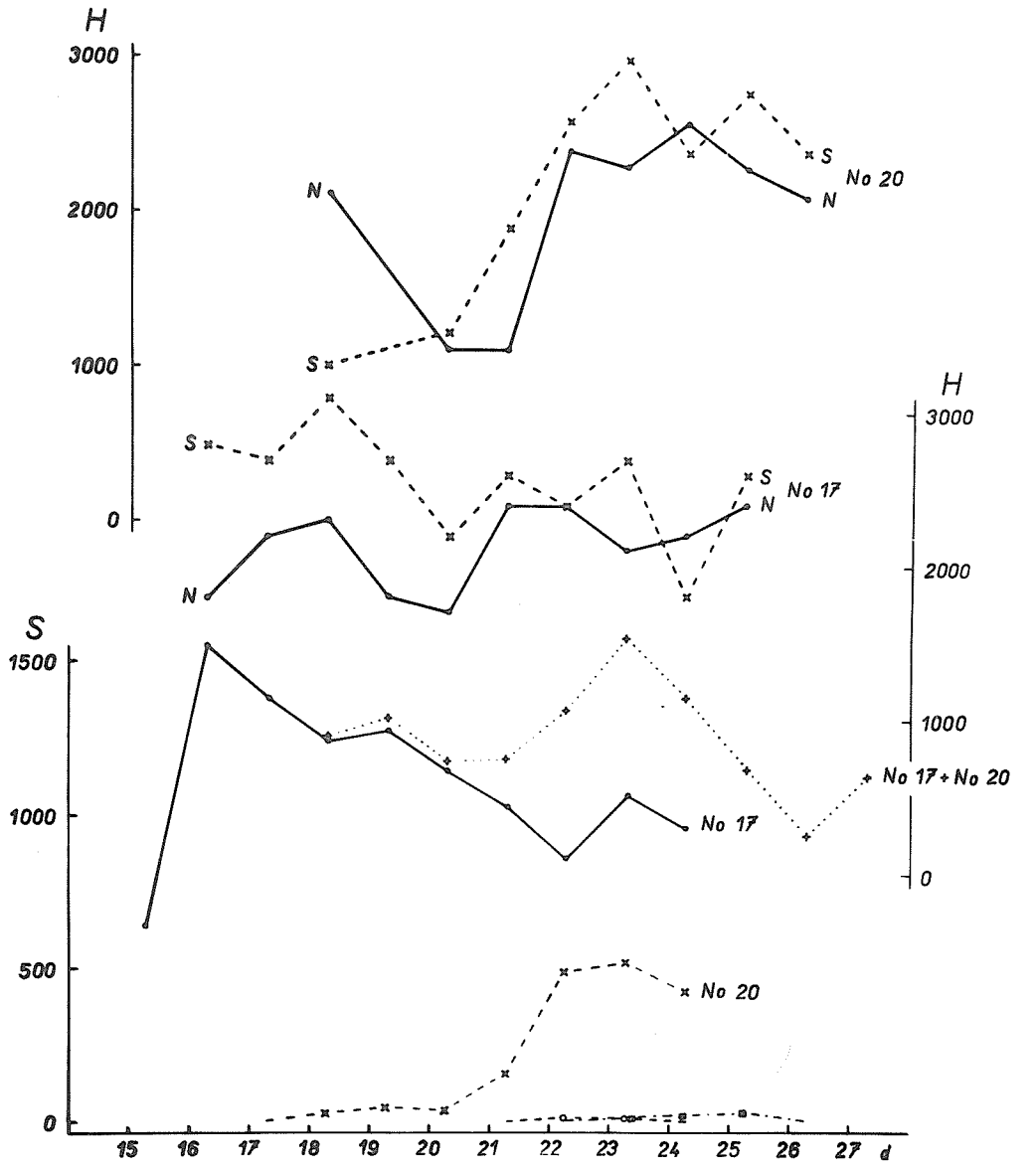

Fig. 2. The development of spot area and magnetic field intensity in two sunspot groups (No. 17 + No. 20) forming the proton-flare region. On the bottom the changes of the area in 10^{-6} of the visible solar hemisphere taken from the "Magnetic Field of Sunspots" published by the Pulkovo Observatory of the U.S.S.R. Academy of Sciences. The small areas of satellite groups are drawn too. The middle part shows changes of the maximum negative (S) and positive polarity (N) magnetic field intensity in the leading and following part of the main spot group No. 17. The top shows the same for the newly developed group No. 20.

3. Development of the Proton-flare Region:

We believe that to understand the physics and the trigger mechanism of the studied flare the interesting development of the proton-flare sunspot groups has to be described. The main group (No. 17), as seen for example in the "Magnetic Field of Sunspots" published by the Pulkovo Observatory of the U.S.S.R. Academy of Sciences, appeared well developed, bipolar, with some indications of magnetic field complexity when at the limb. Until January 21 both polarities were separated in two pronounced rows. On January 18 several degrees east of this main group a small bipolar group (No. 20) developed. On January 21 this sunspot group started to grow rapidly and on January 23 it reached its maximum area. During the same time interval very small satellite groups appeared north of the main group (No. 28, 29, 30). Simultaneous with this growth the main group (No. 17) became more complex. On January 24 both groups seemed to interact mutually and on this day their area diminished rapidly. This area decrease continued until they passed the western limb. The described development of both groups is seen in Figure 2, which shows the daily values of area of each group until it was no longer possible to separate them. The changes of maximum intensity of the main spots in both groups are also presented in Figure 2. Note the higher values of the southern (lead-

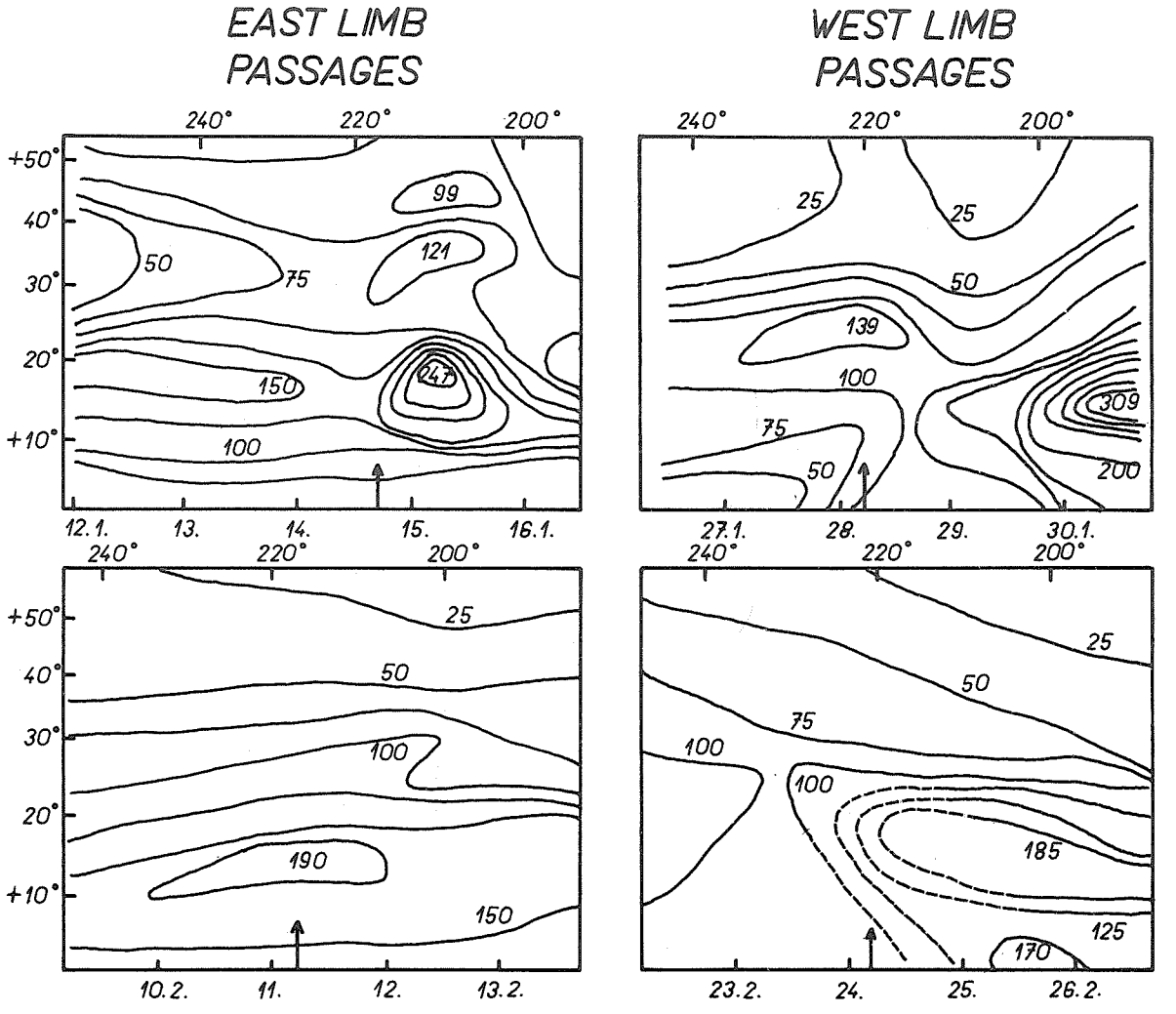

Fig. 3. Coronal situation above the proton-flare region for the rotation with the flare and the next rotation. Lines of equal mean intensity of the green (λ 5303 A) coronal emission in absolute coronal units above the studied solar region are shown. The isophotes are drawn with the distance of 25 absolute units, the intensity being unified to the Pic-du-Midi photometric scale using the method described by Sykora [1971]. Heliographic coordinates are indicated. Also, the passage of the region on the limb is shown by the date and an arrow.

ing) polarity throughout the whole transit of both groups on the disk with the exception of the day with the proton-flare. The same results were obtained by Krivsky [1972]. Also, the enhancement of flare activity reported by him as starting on January 18 and once more on January 24 is probably related to the described phases of development of the two groups forming the proton-flare region.

4. Coronal Situation Above the Proton-flare Region:

Not enough observational data exist to follow the large scale distribution of the coronal green emission (λ 5303 A). Thus, in Figure 3 only the situation as it was observed on the east and west solar limb around the day of the studied region's passage (indicated by the arrow) and one rotation after is shown. The peak of emission intensity (247 coronal absolute units) at the east limb on January 15 probably indicates the future development of the sunspot group No. 20. The peak of intensity (309 units) at the west limb on January 30 does not belong to the studied region; it is connected with another group, separated from the proton-flare region. The fact that the coronal situation after the flare occurrence becomes calm very fast seems to be meaningful.

REFERENCES

AMBROZ, P., V. BUMBA, R. HOWARD and J. SÝKORA — 1971 — Opposite Polarities in the Development of Some Regularities in the Distribution of Large-scale Magnetic Fields, Howard (ed.), Solar Magnetic Fields, 696.

BUMBA, V. — 1971a — Large-scale Negative Polarity Magnetic Fields on the Sun and Particle Emitting Flares, Submitted to the Proceedings of the Solar Wind Conference, Asilomar, Pacific Grove, California, March 21-26, 1971.

BUMBA, V. — 1971b — Large-scale Regularities in Solar Magnetic Field Distribution and Occurrence of Large Flares, Submitted to the Proceedings of the 6th Regional Consultation on Solar Physics, Gyula, Hungary, September 6-11, 1971.

BUMBA, V. — 1971c — Solar Large-scale Positive Polarity Magnetic Fields and Geomagnetic Disturbances, Submitted to the Proceedings of the Solar Wind Conference, Asilomar, Pacific Grove, California, March 21-26, 1971.

BUMBA, V., L KRIVSKY and J. SÝKORA — 1972 — Development and Spatial Structure of Proton-flares Near the Limb and Coronal Phenomena. IV Proton-flare from Nov. 2, 1969 and its Active Region, Bull. Astr. Inst. Czech., 23, 85.

BUMBA, V. and J. SÝKORA — 1971 — Svjaz krupnomasshtabnogo raspredelenija solnetschnych magnitnych polej i korony s bolshimi vspyshkami i solnetschnym vetrom, Submitted to the Proceedings of the Interkosmos Conference, Moscow, November 15-19, 1971.

KRIVSKY, L. — 1972 — Trends of Development of the Proton Active Region about January 24, 1971, Bull. Astr. Inst. Czech., 23, in press.

SÝKORA, J. — 1971 — Some Remarks on the Summary Use of Existing Corona Measurements, Bull. Astr. Inst. Czech., 22, 12.

Magnetic Fields in McMath Region 11128

by

David M. Rust
Sacramento Peak Observatory
Air Force Cambridge Research Laboratories
Sunspot, New Mexico 88349

ABSTRACT

The magnetic fields in the region which produced a 3B flare on January 24, 1971, were measured with a non-saturating magnetograph on January 18 - 20. Other data reveal only minor changes during the intervening days in the gross structure of the magnetic field in the western part of the region where the flare occurred. Utilizing this knowledge, I have computed the current-free fields for the low corona over the region. The computed fields provide considerable aid in understanding diverse phenomena of the flare, including the observed pattern of Hα brightening, the post-flare loops and the escape of protons from the seat of the flare.

1. Instrumentation

On January 18, 19 and 20, 1971, I measured the longitudinal component of the photospheric magnetic fields in McMath Region 11128. These observations were made with the Doppler-Zeeman Analyzer (DZA), a photoelectric instrument similar in some respects to the Babcock magnetograph used at Mount Wilson. The chief difference between the DZA and the Babcock magnetograph is that the DZA splits the light passing through the entrance slit of the spectrograph into two beams representing incoming light of opposing senses of circular polarization. At the output of the spectrograph, the central wavelength of each of the two images of a selected spectral line is measured photoelectrically and recorded on magnetic tape. The recordings ('R' and 'L') of the central wavelengths of the right- and left-circularly polarized images of the spectral line are processed in a digital computer to produce contour maps of the longitudinal velocities and longitudinal magnetic fields over selected regions of the solar disk. Velocities are computed from the average of the L and R wavelength shifts and magnetic fields are computed from the difference, L - R. Because the L and R shifts are measured independently of each other, the DZA magnetic signal does not saturate in intense fields, contrary to the behavior of a Babcock magnetograph. The brightness in the wings of the line and the coordinates of each observation point on the solar disk, are recorded along with the L and R signals. For a more complete description of the instrument, the reader should see the articles by Dunn [1971] and Evans [1966].

2. Observations

I chose to make all the observations in the FeI line at 5250.218 Å because of its high sensitivity to the Zeeman effect ($g\lambda^2 = 83$). As Harvey and Livingston [1969] have pointed out, the line is extremely temperature sensitive and measurements made with conventional magnetographs must be increased by a factor of up to 2.5 due to the correlation between temperature-induced line profile changes and the longitudinal magnetic field. The DZA measurements suffer somewhat from the same fault, but to a lesser degree [Hollars, 1970]. The magnetic field intensities indicated on the maps, therefore, should be increased by perhaps 50%, the error depending upon the unknown sub-telescopic fine structure of the fields. Table 1 gives other observational details.

Table 1 Observational Parameters

Scan No.	Date	Time (UT)	Aperture (arc sec)	Step between Observations (arc sec)	Image Quality
1	1/18	1548 - 1601	4 x 4"	10"	fair
2	1/18	1601 - 1614	4 x 4	10	fair
3	1/19	1534 - 1552	4 x 4	4	good
4	1/19	1552 - 1610	4 x 4	4	good
5	1/20	2022 - 2030	8 x 10	8	poor
6	1/20	2030 - 2038	8 x 10	8	poor
7	1/20	2039 - 2047	8 x 10	8	poor
8	1/20	2047 - 2055	8 x 10	8	poor

Figures 1, 2 and 3 show maps of the longitudinal component of the magnetic field for scans 1, 3 and 6 made on January 18, 19 and 20, 1971, respectively. The contour levels start at ± 10 G and increase by factors of two up to a -1280 G contour on each map. Solid lines enclose positive fields

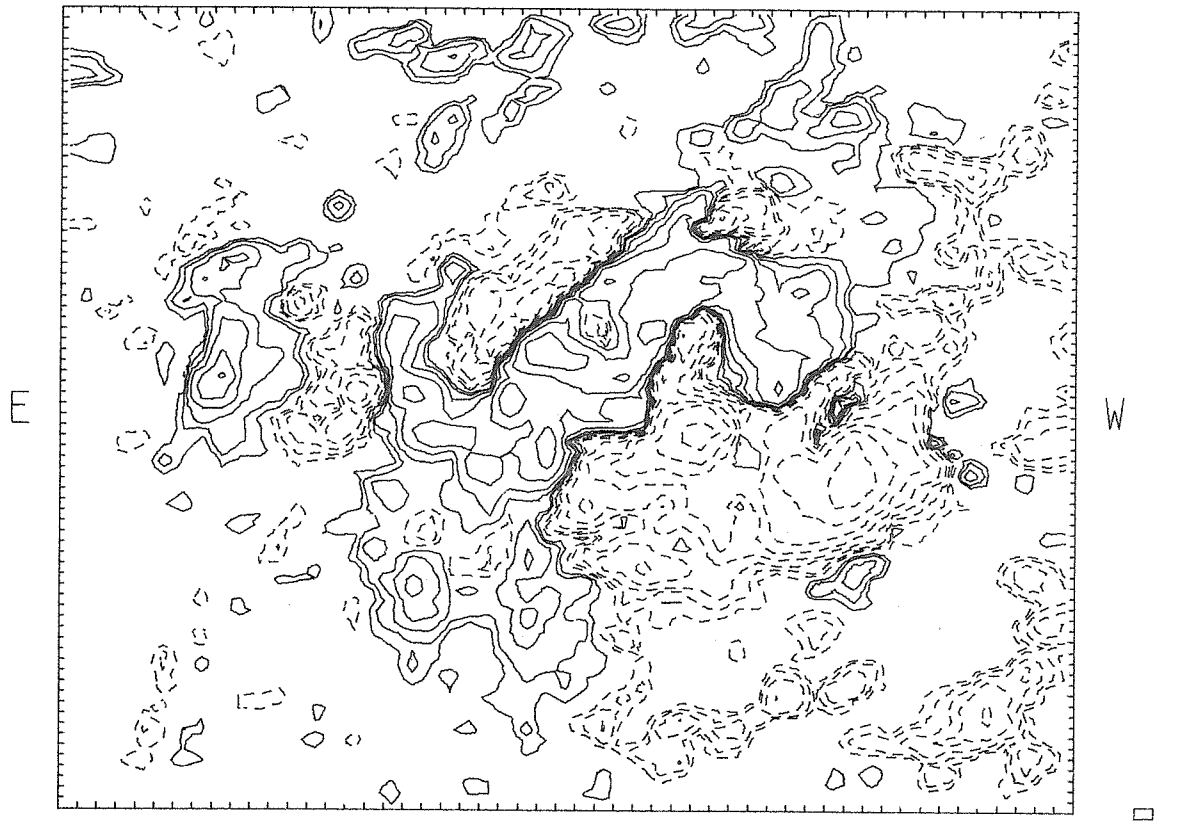

Fig. 1. McMath Region 11128 magnetic fields at 1601 UT, January 18, 1971.

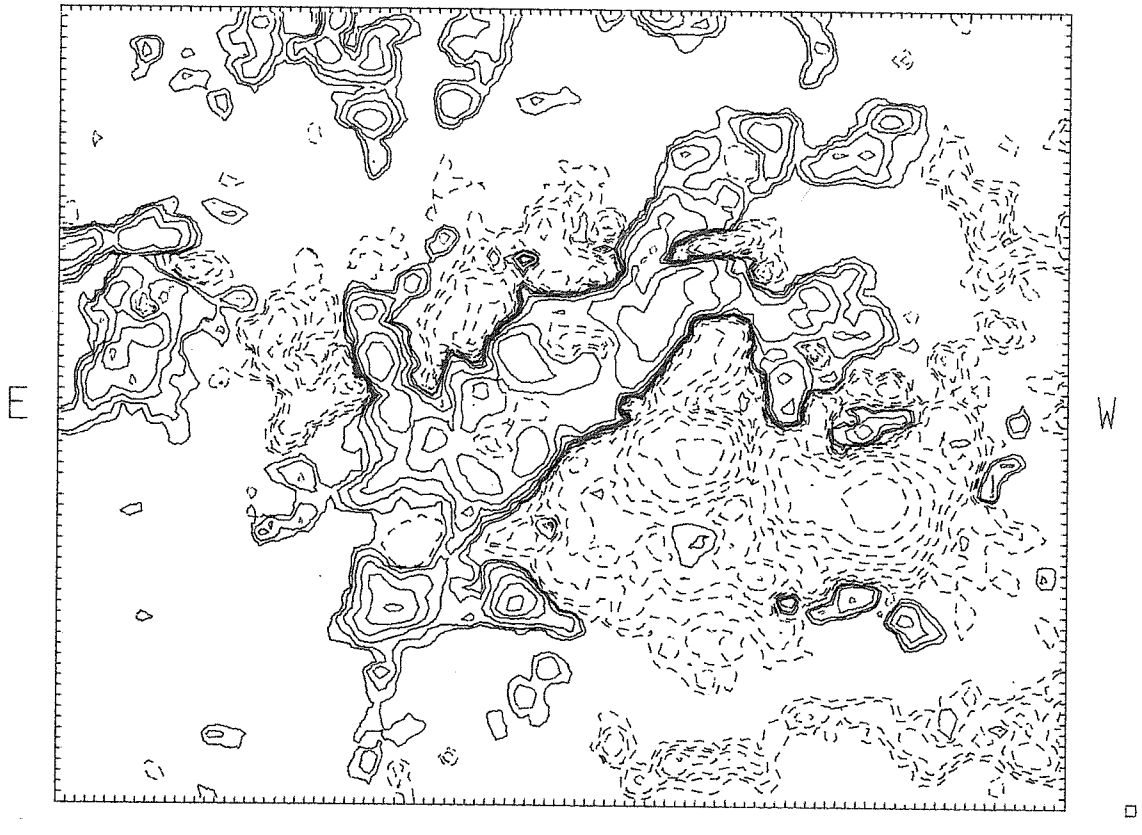

Fig. 2. Magnetic fields in the same region at 1552 UT, January 19, 1971.

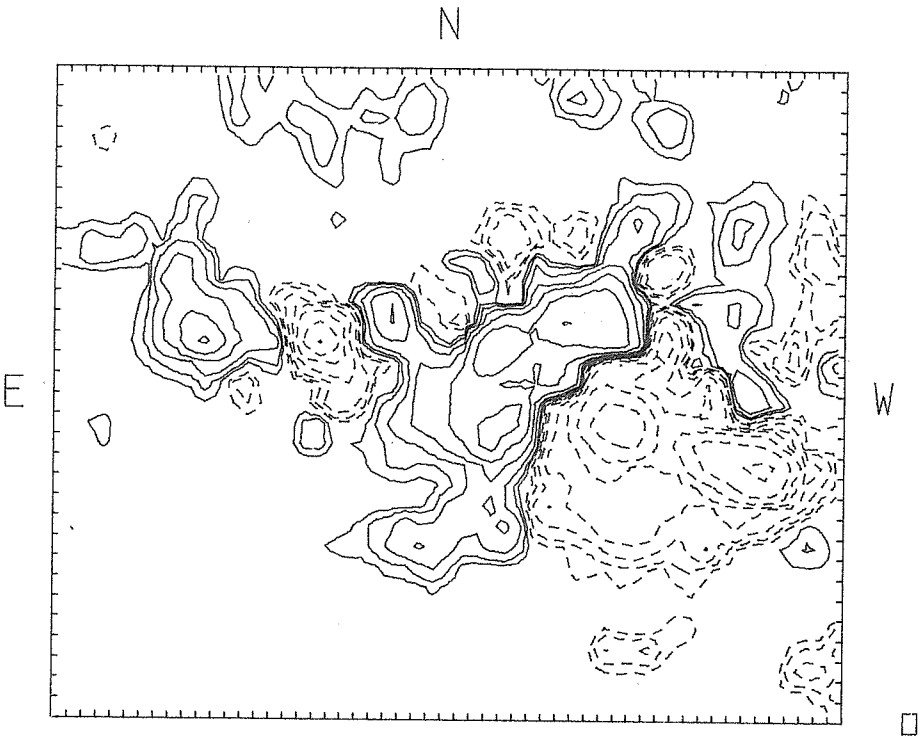

Fig. 3. McMath Region 11128 magnetic fields at 2038 UT, January 20, 1971.

and dashed lines enclose negative fields. As with the Mount Wilson magnetograms, this convention is reversed when the fields within an area already contoured are locally decreasing; i.e., we have a way to distinguish a 'valley' from a 'hill'. Geocentric north is toward the top of the maps and east is on the left. All of the maps show the fields in a 300 by 400 arc sec area. Due to cloudiness and some haste in setting-up for the observations, the maps for the three days do not represent a homogeneous set of data and cannot profitably be examined for detailed changes from day-to-day. However, much can be learned from a detailed examination of the individual maps.

The most intense field in McMath Region 11128 was in the large, negative-polarity, leading sunspot. The DZA measurements for both January 18 and 19 indicated a field of -1900 G there. The visual field measurements from Mount Wilson indicated fields of -2600 G and -2900 G on January 18 and 19, respectively. The differences between the two types of measurement probably are not significant, since the aperture of the DZA averages the field over a relatively large area while the observer making visual measurements selects the point of most intense field in the spot. The DZA should be considered principally as a flux measuring device, therefore. The integrated positive flux through the region on both days was 10^{22} maxwells, and the integrated negative flux was -1.4×10^{22} maxwells. The meaning and reality, even, of the flux deficit of 4×10^{21} maxwells are among the most intriguing and difficult problems in the study of solar magnetism. In the calculations of lines of magnetic force described below, I assume the flux difference is real. The fieldline calculations are based on data from January 20, when the measured net flux was 3×10^{21} maxwells.

When compared with the map of the fields for January 20 (Figure 3), the higher resolution of the magnetograms from January 18 and 19 is obvious. The gross structure of the magnetic fields is the same on all three days, however. In the first two maps, one may especially notice how complex the fields are in comparison with most active centers. The leading spot of negative polarity is surrounded by 'satellites' of opposite polarity. These satellites will always be closely associated with small flares and surges and may serve as the starting points for large flares [Rust, 1972]. However, as Figures 1 and 2 show, the satellites change significantly from day-to-day, and it is therefore impossible to associate any of these features with the 3B flare of January 24.

Notice the region of steep horizontal gradients in the field that appears at the NW (hooked) extreme of the inversion line that runs diagonally across the center of Figure 2. It is possible to follow this region on the magnetograms of the succeeding days up to January 24, when the first bright points of the flare at 2309 UT occurred there. From a topological point of view, it is probably impossible to construct a set of lines of magnetic force near such a region of intertwined polarities

without admitting to the presence of at least one true neutral point in the magnetic fields in the low corona or upper chromosphere there. Of course, there are theoretical reasons for supposing that flares start at such neutral points, but more important for the discussion that follows is the fact that matter accelerated at such a point will have access to fieldlines leading to many other sections of the active region.

3. Fieldline calculations; the flare of January 24

An examination of Mount Wilson magnetograms and Hα photographs from January 20 to 24 showed that the western part of McMath Region 11128 (the part where the 3B flare occurred) did not change its gross structure during that period. Therefore, I computed the lines of magnetic force that would stretch over the region if there were no electric currents in the lower corona. The input data for the calculation are the fields measured by DZA on January 20, 1971 (see Figure 3). The fields observed on that day may be regarded as the radial component of the magnetic field in the photosphere, since the region was near disk center then. Figure 4 shows the coordinates of the scanned region on that day and outlines the principal sunspots. The method of calculating the current-free fieldlines and the limitations of such calculations have been discussed by Schmidt [1964] and by Rust [1970]. A most important characteristic of the computed lines of force that must be borne in mind when comparing the fields with other data on the flare is that these current-free fields are incapable of energy release. The field lines computed with the aid of the Schmidt program and shown in Figure 5 represent the lowest energy state of the magnetic fields over the active region. The distribution of the poles in the photosphere, as shown in Figure 3, uniquely determines the fields shown in Figure 5.

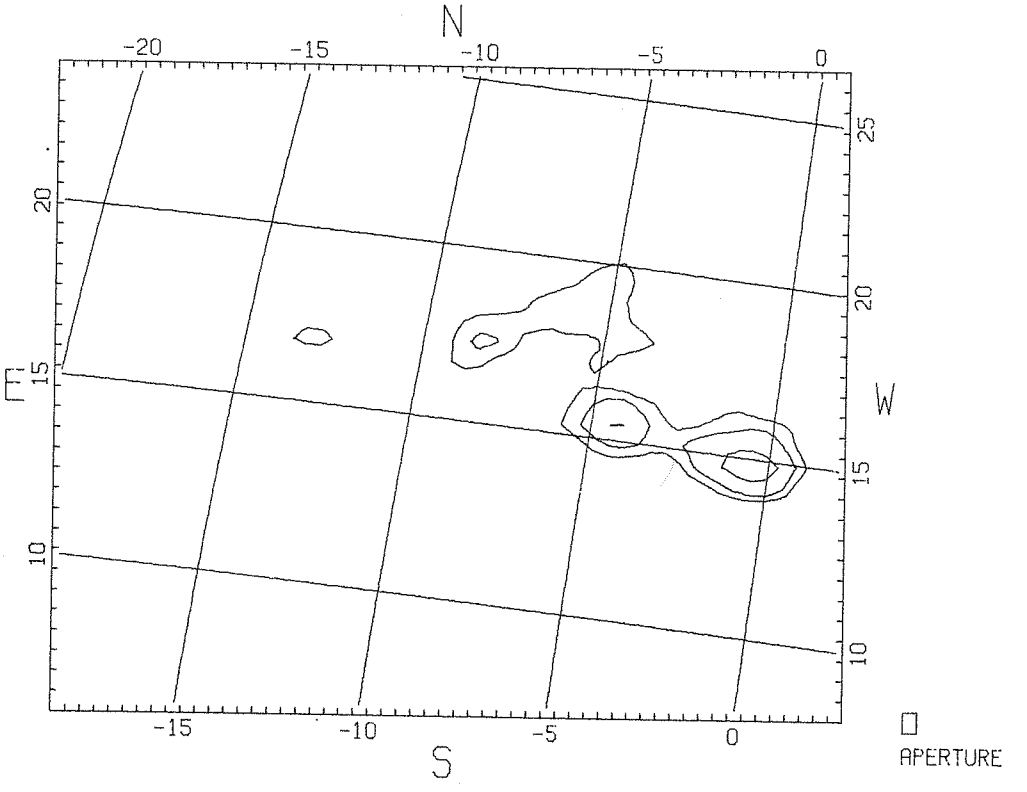

Fig. 4. Sunspot outlines and solar coordinates for McMath Region 11128 at 2038 UT, January 20, 1971

The reader may immediately notice several interesting features of the fieldlines in Figure 5 that will help understand the 3B flare of January 24. Most noticeable are the lines of force opening into space from the leading, negative-polarity spot. The open lines generally curve gently to the east and one has no difficulty in his mind in connecting these lines of force from the flaring region at 49° west longitude with the spiral fields of the solar sector structure that will help guide to the earth the high-energy protons emitted at the beginning of the flare. The open fieldlines stem from the same region of the leading spot as do fieldlines passing through the region where the flare started. High-energy protons may diffuse from closed fieldlines extending from the region where they were accelerated to adjacent, open fieldlines that they may follow into interplanetary space.

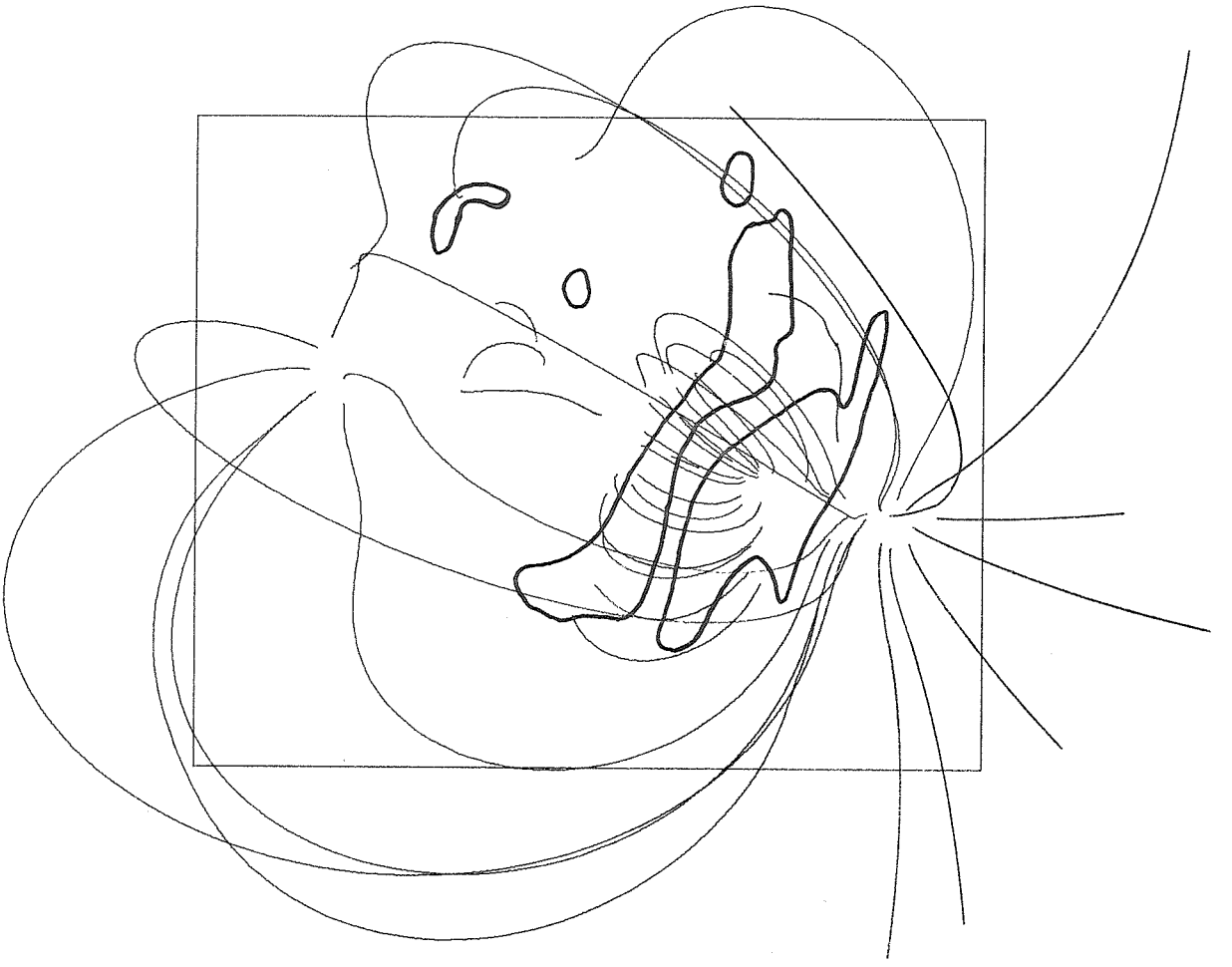

Fig. 5. Lines of force computed from the magnetogram shown in Fig. 3.

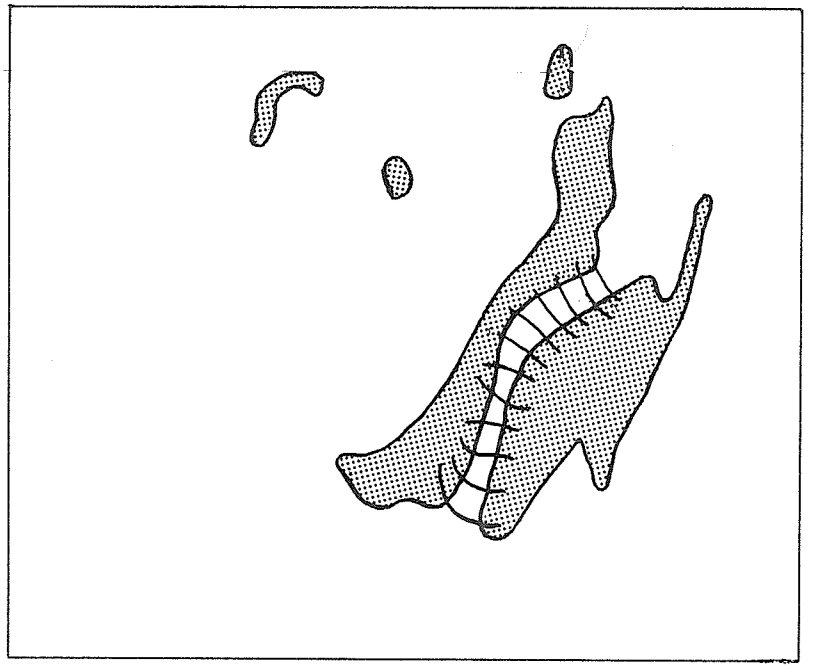

Fig. 6. Flare patches (shaded areas) and post-flare loops at 2345 UT, January 24, 1971

As a check on the possibility that matter was ejected from the region of the leading spot during the flare, one should follow the high loops that curve over the region to the small patches of positive field in the northeast. If material were to follow these lines of force and strike the chromosphere, there would be some flare brightenings far removed from the two ribbons of the main body of the flare (see Figure 6).

Dr. Marie McCabe of the Institute of Astronomy in Hawaii has kindly allowed me to examine a preprint of her Hα observations of the flare. Her discussion of the observations appears elsewhere in this volume [McCabe, 1972]. Her observations show that there were indeed a number of sporadic brightenings of isolated points in the northeast region. The brightenings occurred in positive field regions, as closely as I can tell from maps made on January 20 and extrapolated to January 24. As we should expect, also, the leader spot was partially obscured by Hα emission during the flare.

In Figure 5, it is interesting to note, the lines of force from the leader spot either spread outward toward the earth or curve high over the closest positive fields. Instead of stopping there, the fieldlines extend to the positive fields on the eastern edge of the region. The leader spot is not connected magnetically to the two principal ribbons of the flare. As shown in McCabe's observations, these ribbons are parallel with and close by the principal inversion line of the region. The current-free fields show a system of low-lying loops connecting these ribbons. It is well known from the work by Bruzek [1964] that the brightest ribbons of major flares outline the locus of the intersections of post-flare loops and the solar surface. As Figure 6 shows (it has been drawn from McCabe's observations) there was indeed a system of low-lying loops seen to connect the bright ribbons of the flare. These loops coincide very closely with the computed fieldlines shown in Figure 5.

The flare started at 2309 UT, and McCabe saw the loops at 2345 UT, a sufficiently long time after the onset of the flare to allow the magnetic fields, now drained of their convertible energy, to assume the current-free configuration shown in Figure 5. A remarkable correspondence between post-flare loops and lines of magnetic force computed with the Schmidt program has been noted earlier by Rust and Roy [1971]. Roy [1972] has shown convincingly that the growth of loops coincides with sets of successively higher fieldlines computed from center-of-the-disk magnetic observations.

4. Summary

The usefulness of moderate-resolution magnetograms and current-free field calculations is evident from this preliminary analysis of data from the January 24, 1971 proton flare. A more detailed study of Hα films and of the associated radio and high energy phenomena is planned in order to discover how far one may apply the rather crude techniques used here to the flare problem. Sakurai [1970] derived a model field configuration for proton flares that bears a striking resemblance to the current-free fields shown in Figure 5. The fact that his work was based entirely upon Type IV radio data and Hα observations of major flares seems to lend credibility to the picture derived here.

5. Acknowledgements

I am especially grateful to Dr. Marie McCabe for allowing me to examine her analysis of the January 24 flare prior to publication. I am also grateful to Dr. Harold Zirin and the staff of the Big Bear Solar Observatory for the use of their Hα films of the flare. Dr. Robert Howard of Hale Observatories allowed me to make copies of the Mount Wilson sunspot drawings and magnetograms.

REFERENCE

BRUZEK, A. 1964 On the association between loop prominences and flares, Astrophys. J., 140, 746.

DUNN, R. B. 1971 Sacramento Peak magnetograph, Solar Magnetic Fields, R. HOWARD, ed., Reidel, Dordrecht, Holland, 65.

EVANS, J. W. 1966 Solar magnetographs, Atti del Convegno sui Campi Magnetici Solari, G. BARBERA, Florence, 123.

HARVEY, J. W. and W. LIVINGSTON 1969 Magnetograph measurements with temperature-sensitive lines, Solar Phys., 10, 283.

HOLLARS, D. 1970 Private communication.

MCCABE, M. 1972 Hα observations of the solar flare, January 24-25, 1971, this volume, p. 28.

ROY, J. -R. 1972 The magnetic configuration of the 18 November 1968 loop prominence system, Solar Phys., in press.

RUST, D. M. 1970 Magnetic fields in quiescent solar prominences II. Photospheric sources, Astrophys. J., 160, 315.

RUST, D. M. 1972 Flares and changing magnetic fields, Solar Phys., 25, 141.

RUST, D. M. and J. -R. ROY 1971 Coronal magnetic fields above active regions, Solar Magnetic Fields, R. HOWARD, ed., Reidel, Dordrecht, Holland, 569.

SAKURAI, K. 1970 On the magnetic configuration of sunspot groups which produce solar flares, Planet. Space Sci., 18, 33.

SCHMIDT, H. U. 1964 On the observable effects of magnetic energy storage and release connected with solar flares, AAS-NASA Symp. Phys. Solar Flares, W. N. NESS, ed., NASA SP-50, U. S. Government Printing Off., Washington, 107.

A Study of the Coronal Active Region Associated with the Eruptive Flare of January 24, 1971

by

P. R. SenGupta
Tripura Engineering College
Tripura, India

The eruptive flare of January 24, which occurred at 2307 UT, was associated with the McMath plage region 11128. This is concluded from the reported location of the associated optical flare. The optical flare which started at 2309 UT was of importance 1B. The X-ray flare belonged to Type III (Eruptive) flare according to the author's classification [SenGupta, 1971b]. A number of intense radio bursts covering a wide range of frequency were also observed during the flare. That the flare was of eruptive nature is confirmed from the Solar Particle Events recorded simultaneously by particle detectors on several satellites within a few hours after the flare.

Table 1 shows the time history of the Coronal Active Region Associated with McMath plage region 11128. Daily physical data of the active region calculated from the daily 9.1 cm Radio-Spectroheliogram made by Stanford University Radio Astronomy Laboratory and published in "Solar-Geophysical Data" [319, 1971], employing the physical model of the Plage Associated Active Regions and the empirical formula derived by the author [SenGupta, 1971a], are listed in the first two columns of Table 1. $T_{e\ max}$ is the maximum electron temperature and Y_i the total emission measure of the region.

Table 1

Calculated and Observed Physical Data for the Active Region Associated with McMath Region 11128

Date Jan. 1971	$T_{e\ max}$ (10^6 °K)	Y_i (10^{48}cm^{-3})	Recorded 9.1 cm flux from the region	No. of X-ray flares from the region recorded by NRL detectors	No. of 2-12 Å flares from the region reported by University of Iowa experiment
14	2.3	14	13	Nil	Nil
15	2.4	20	19	1	1
16	2.5	28	26	1	1
17	2.6	30	27	1	Nil
18	2.7	32	?	2	Nil
19	2.7	35	29	3	1
20	2.7	29	25	?	Nil
21	2.7	25	20	4	1
22	2.65	25	20	2	1
23	2.6	20	18	1	Nil
24	3.0	45	32	7	4
25	2.4	14	12	Nil	Nil
26	2.3	12	12	Nil	Nil
27	2.2	6	7	Nil	Nil

9.1 cm flux from the region listed in column 3 is also from the same issue of the "Solar-Geophysical Data". NRL X-ray flare data in column 4 are from the continuous daily plots in "Solar-Geophysical Data" [323, 1971]. The University of Iowa X-ray flare data in column 5 are also from the same issue of "Solar-Geophysical Data". The number in both cases is taken from the correspondence with optical flares from the region. There are fewer flares in column 5 than in column 4 because the University of Iowa reports only those flares in which peak flux exceeds the preflare level by a factor of four or more.

It is easy to see from the Table that there were two superimposed phases of activity. The first phase reached a peak on January 18-19 with a peak temperature and emission measure of 2.7×10^6 °K and 35×10^{48} cm^{-3}, respectively, and showed a decline from January 20. But before the activity could decline to the background undisturbed coronal level, a second and more intense phase of activity showed up which had a very fast growth and an equally fast decay. Comparing the growth and the decay rates of the two phases, we find in Table 1 that while it took five days for the first phase to increase the electron temperature from 2.3 to 2.7×10^6 °K, i.e. by 0.4×10^6 °K, in the second

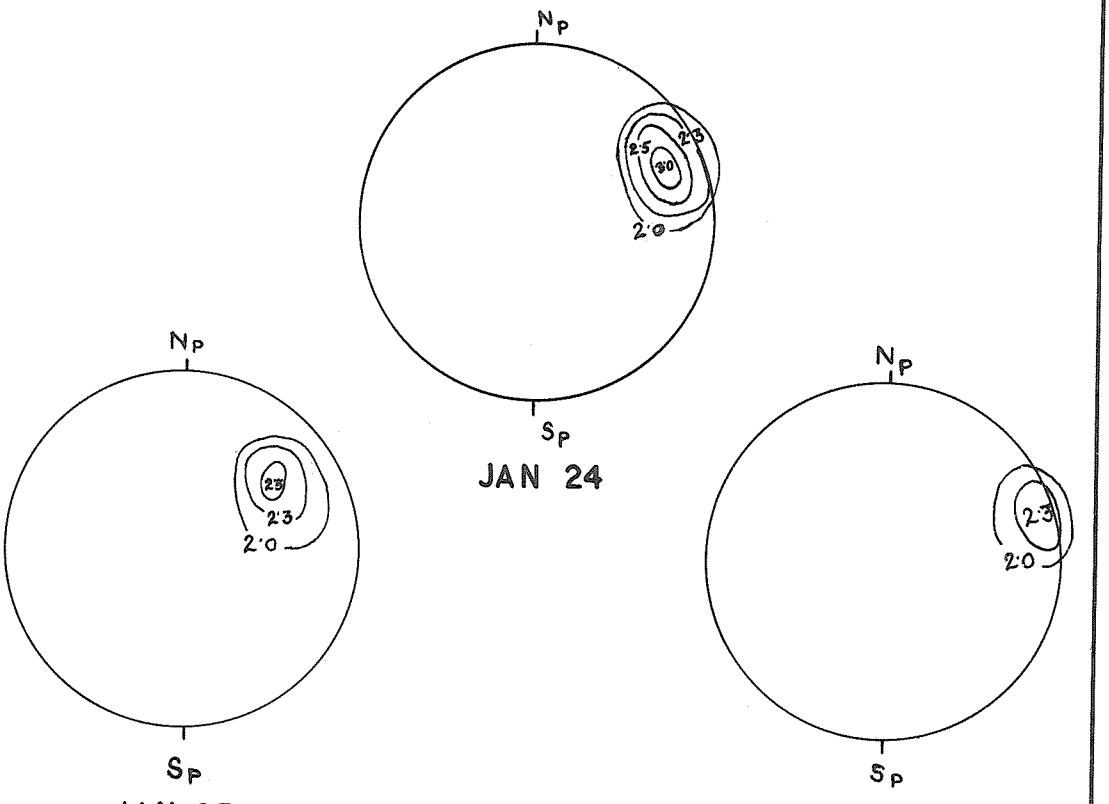

FIG1. INDEX OF ACTIVITY LEVEL OF McMATH REGION 11128 IN TERMS OF CALCULATED ELECTRON TEMPERATURES. TEMPERATURES ARE IN UNITS OF 10^{6}°K.

TIME 2000-2100 UT

phase it took only one day for an equal increase in temperature. The decay of the second phase is more significant. In one day the electron temperature decreased by 0.6×10^6 °K and the emission measure was reduced to less than 30% of the previous day's value. It is significant to note that the great eruptive flare occurred at 2307 UT on January 24. The daily physical data in Table 1, as also in Figure 1, correspond to 2000-2100 UT. Hence, the data on January 24 correspond to the activity about two hours before the great eruption, while the data on January 25 correspond to the activity level about twenty hours after the flare. Altogether, seven X-ray flares were recorded by NRL detectors on January 24. The decline in the activity may thus be well attributed, at least partly, to the release of energy in the eruptive flares of January 24.

Data in columns 3, 4 and 5 are also in conformity with the behavior of the Active Region described above.

Figure 1 gives a picture of the growth and decay of the second phase of the activity in terms of area and the distribution of electron temperature in the region. The figures on the contours represent the calculated electron temperature in 10^6 °K.

REFERENCES

SENGUPTA, P. R. 1971a A method of calculating 0-20 Å solar X-ray flux and its spectral distribution using 9.1 cm. spectroheliogram, Solar Physics, 17, 160-173.

SENGUPTA, P. R. 1971b A study of solar X-ray flares, Proc. Visitors' Programme on Space Physics, Delhi University, July, 1971, Solar Radiations and the Earth, Ed. J. N. TANDON, Hindustan Publishing Co., 1972.

1971 Solar-Geophysical Data, 319 Part I; 323 Part II, U.S. Department of Commerce, (Boulder, Colorado, U.S.A. 80302).

3. SOLAR RADIO EVENTS

On the S-Component and Noise Storms in January, 1971

by

A. Böhme and A. Krüger
German Academy of Sciences
Central Institute for Solar-Terrestrial Physics
(Heinrich-Hertz-Institute)
Berlin-Adlershof, GDR

This report is restricted to a representation of radio flux and polarization data referring to the development of the active regions before the occurrence of the proton event on January 24, 1971. The observed data are shown in Table 1, and are condensed in form of synthetic spectral diagrams of the S-component and the noise storm emission (Figure 1).

It is widely believed that the S-component and noise storm spectra carry some significance about conditions facilitating the outflow of high and medium energetic solar particles, respectively [cf. also Sakurai, 1971]. However, it is indicated by the present examples that the observing conditions by directivity and angular dependence of the emission properties are not always favorable for an exact prediction of energetic events.

The January 1971 Period

The last decade of January 1971 was characterized by an increase of the S-component up to about 130 solar units at the spectral maximum near 10 cm wavelength. Apparently this increase was preferably due to the influence of the active region on the northern hemisphere which produced the proton flare on January 24 (cf. Figure 1).

In contrast to the long-period character of the S-component, the noise storm component exhibits stronger time fluctuations. As a consequence of the higher directivity, the radiation is only visible under special geometrical conditions similar to the intermittent flash of light from a light-house. Therefore, optimal conclusions from noise storm data can be drawn from observations near the central meridian [cf. also Böhme and Krüger, 1971]. But at present it seems not yet clear whether the effects of short-term (day-to-day) variability are due to changes of the ray direction or to changes of the emitted intensity itself.

A strong source of ordinary circular polarization was very briefly seen on the 20th and 21st of January. Proposing an origin at the northern solar hemisphere, the sense of circular polarization was opposite to that which could be expected from the leading spot hypothesis. It should be noticed that at longer wavelengths the degree of polarization decreased. Especially at 113 MHz there was not always a close (hourly) correlation between the magnitudes of the fluxes and the degree of polarization.

REFERENCES

BÖHME, A. and A. KRUGER 1971 Data on Solar-Geophysical Activity Associated with the Major Geomagnetic Storm of March 8, 1970, World Data Center A - Upper Atmosphere Geophysics Report UAG-12, NOAA, Boulder, Colorado, 71.

SAKURAI, K. 1971 Data on Solar-Geophysical Activity Associated with the Major Geomagnetic Storm of March 8, 1970, World Data Center A - Upper Atmosphere Geophysics Report UAG-12, NOAA, Boulder, Colorado, 52.

Table 1

Daily Flux and Polarization Data, Heinrich-Hertz-Institute

Jan. 1971	9500	3000	1490	510	287	234	113	68	40 MHz
11	297 -	141	99 -	-	24	39	63 L	<	< l
12	292 -	144	103 -	35	27	54	67 L	<	< l
13	292 -	140	101 l	39	28	51	54 l	70	130 l
14	294 -	152	96 l	32	17	16	32 l	<	170 l
15	295 -	148	- l	32	18	21	2 0	<	< 0
16	(314)-	(-)	(101 l)	(81)	(49)	(39)	(39 0)	(-)	(180 0)
17	302 -	153	- 0	32	12	8	2 0	<	< 0
18	308 l	154	103 l	32	15	9	2 l	<	< 0
19	304 l	164	101 l	32	14	14	15 L	<	< l
20	307 l	158:	122:l	32	22	47	670 L	270	< 0
21	301 r	176	109 l	32	29	71	140 L	70	< l
22	298 r	177	109 0	32	12	12	2 l	<	< 0
23	314 r	183	114 0	35	11	10	17 r	<	< 0
24	313 r	174	112 0	32	10	8	2 r	<	< 0
25	305 r	160	111 0	35	15	12	7 l	<	< 0
26	307 -	161	104 0	32	10	8	2 0	<	< 0
27	309 0	161	104 0	32	10	8	2 0	<	< 0
28	307 0	161	104 0	32	11	8	2 0	<	< 0
29	306 0	-	123 0	32	12	12	12 r	<	< 0
30	297 r	-	121 0	32	12	13	12 r	<	< 0
31	299 0	156	121 l	32	17	20	21 r	70	< r

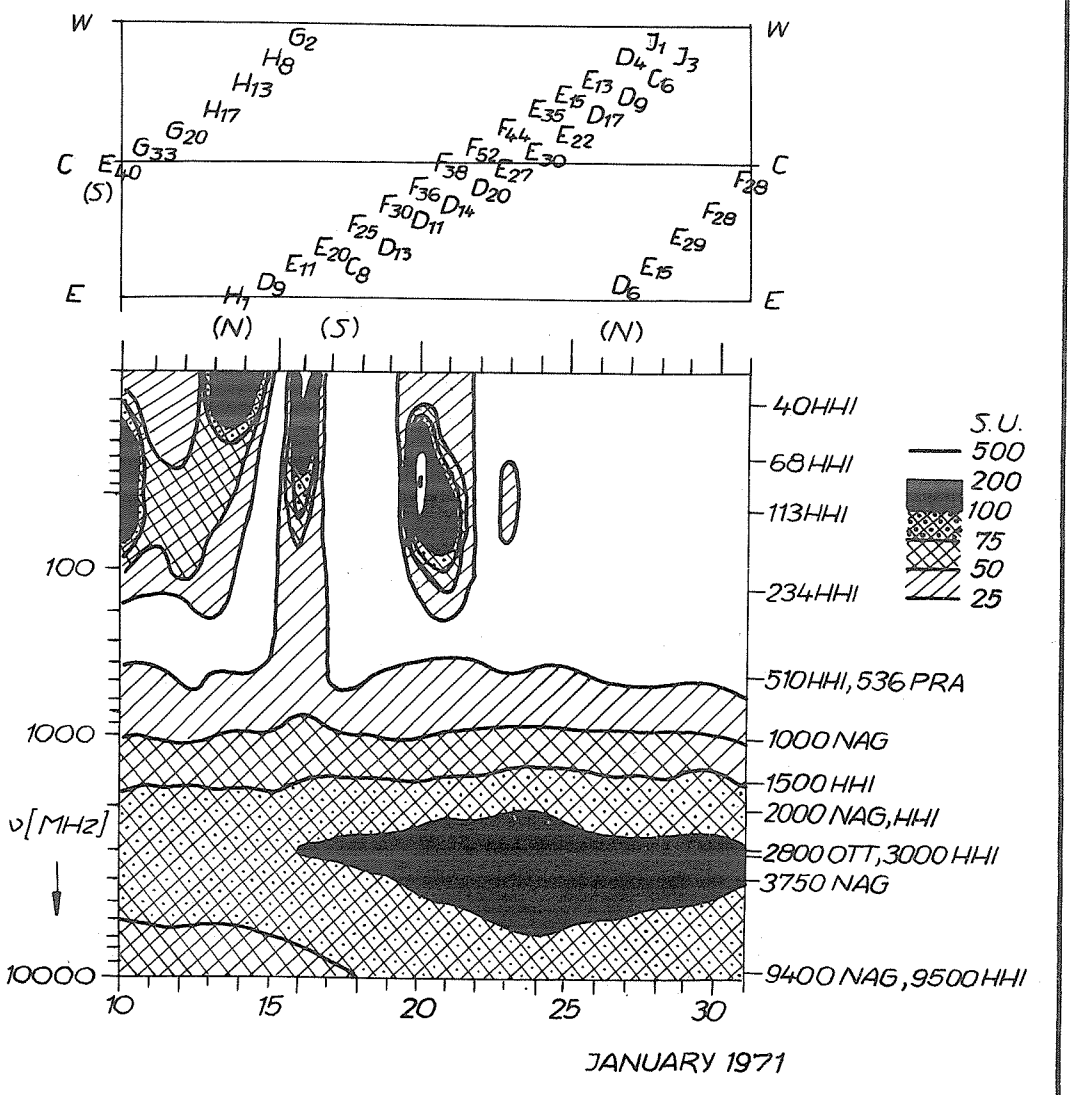

Fig. 1 Spectral diagram of S-and noisestorm components and major spot groups (top)

Millimeter Wave Spectroheliograms Associated with the January 24, 1971 Solar Terrestrial Event

by

Larry E. Telford
Air Force Cambridge Research Laboratories
L. G. Hanscom Field, Bedford, Massachusetts 01730

8.6 mm spectroheliograms have been taken on a daily basis (weather and equipment permitting) since the Summer, 1968. In March, 1971, 20 mm spectroheliograms were added to the daily routine. The 8.6 mm and 20 mm spectroheliograms are taken concurrently using a dual frequency feed system on the AFCRL 29-Foot Millimeter Wave Antenna. This submission represents a collection of 8.6 mm spectroheliograms covering approximately two weeks prior to the event.

The following comments apply to the spectroheliograms presented in Figures 1 and 2:

1. All spectroheliogram radio brightness temperatures are to be multiplied by ten, i. e., 520 = 5200°K.
2. All spectroheliogram radio brightness temperatures are antenna temperatures corrected for atmospheric attenuation but not corrected for antenna pattern effects.
3. The 8.6 mm antenna pattern and radiometer parameters are given in the latest "Solar-Geophysical Data Descriptive Text".
4. The contour levels for the plotted spectroheliograms are:
   Figs. 1 and 2 - 2500°K, 4600°K and up in 200°K increments.
5. The times associated with each spectroheliogram is the time the center grid point was observed. The spectroheliogram observation sequence starts at the upper left corner of the plotted grid and ten seconds are spent at each grid point. The sequence moves from left to right for each line. Using this sequence, the exact observation time for each grid point can be calculated.

In addition to the plotted spectroheliograms, Table 1 represents the output of a data reduction computer program which interpolates the original radio brightness temperature grid and searches for maxima with a fixed set of searching constraints. The table represents the heliographic location and enhancement, or temperature above the average surface background temperature, for each maxima found for each spectroheliogram. In reproducing the table, all maxima with enhancements less than 100°K were ignored. Since the input grid data are not corrected for antenna effects, the maxima locations are not accurate when the region is greater than ± 45° from Central Meridian at 8.6 mm. Within these limits, the locations are accurate to ± 2° in heliographic coordinates.

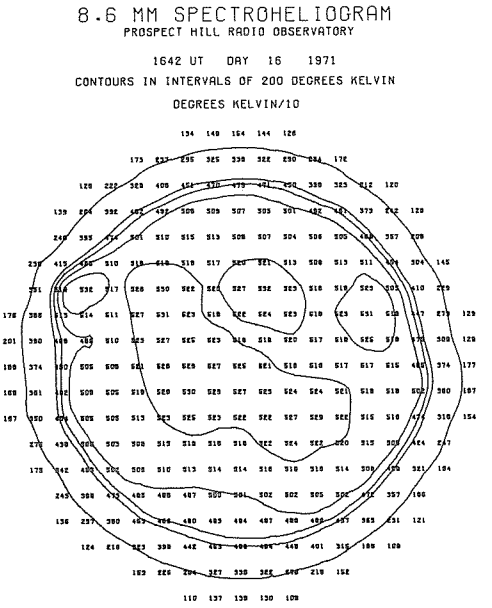
8.6 MM SPECTROHELIOGRAM
PROSPECT HILL RADIO OBSERVATORY
1642 UT DAY 16 1971
CONTOURS IN INTERVALS OF 200 DEGREES KELVIN
DEGREES KELVIN/10

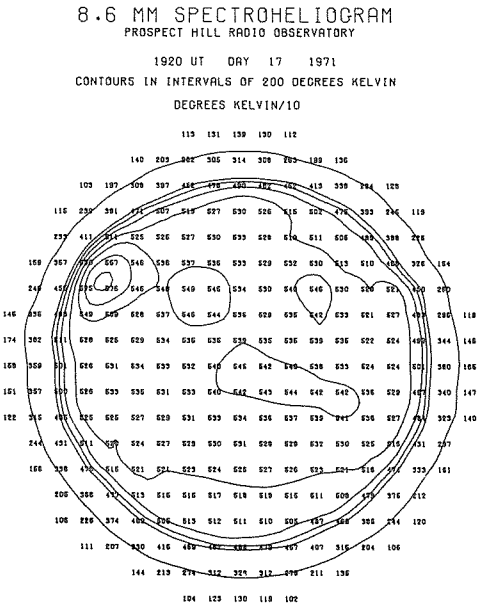
8.6 MM SPECTROHELIOGRAM
PROSPECT HILL RADIO OBSERVATORY
1920 UT DAY 17 1971
CONTOURS IN INTERVALS OF 200 DEGREES KELVIN
DEGREES KELVIN/10

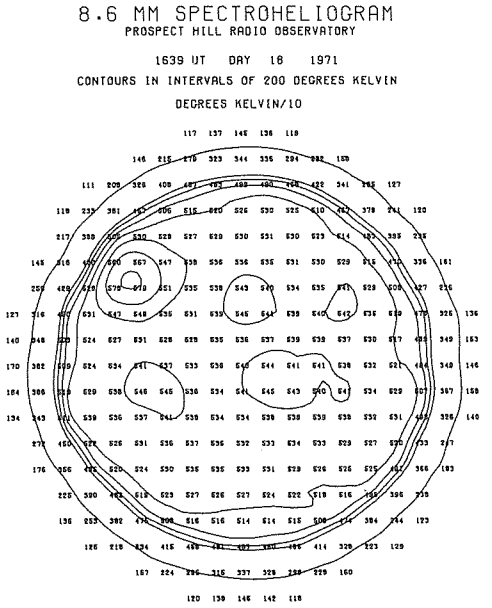
8.6 MM SPECTROHELIOGRAM
PROSPECT HILL RADIO OBSERVATORY
1639 UT DAY 18 1971
CONTOURS IN INTERVALS OF 200 DEGREES KELVIN
DEGREES KELVIN/10

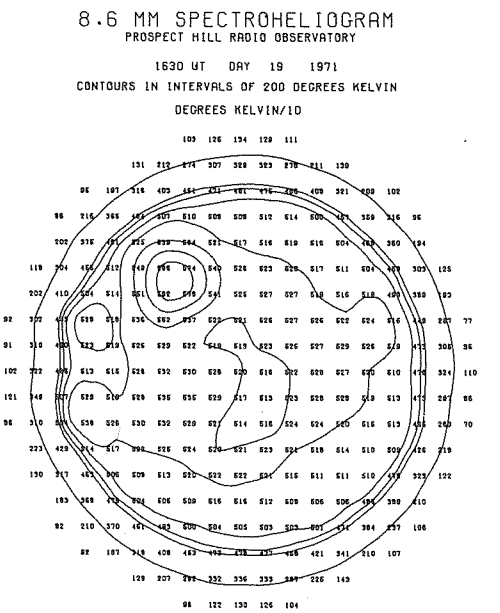
8.6 MM SPECTROHELIOGRAM
PROSPECT HILL RADIO OBSERVATORY
1630 UT DAY 19 1971
CONTOURS IN INTERVALS OF 200 DEGREES KELVIN
DEGREES KELVIN/10

Figure 1.

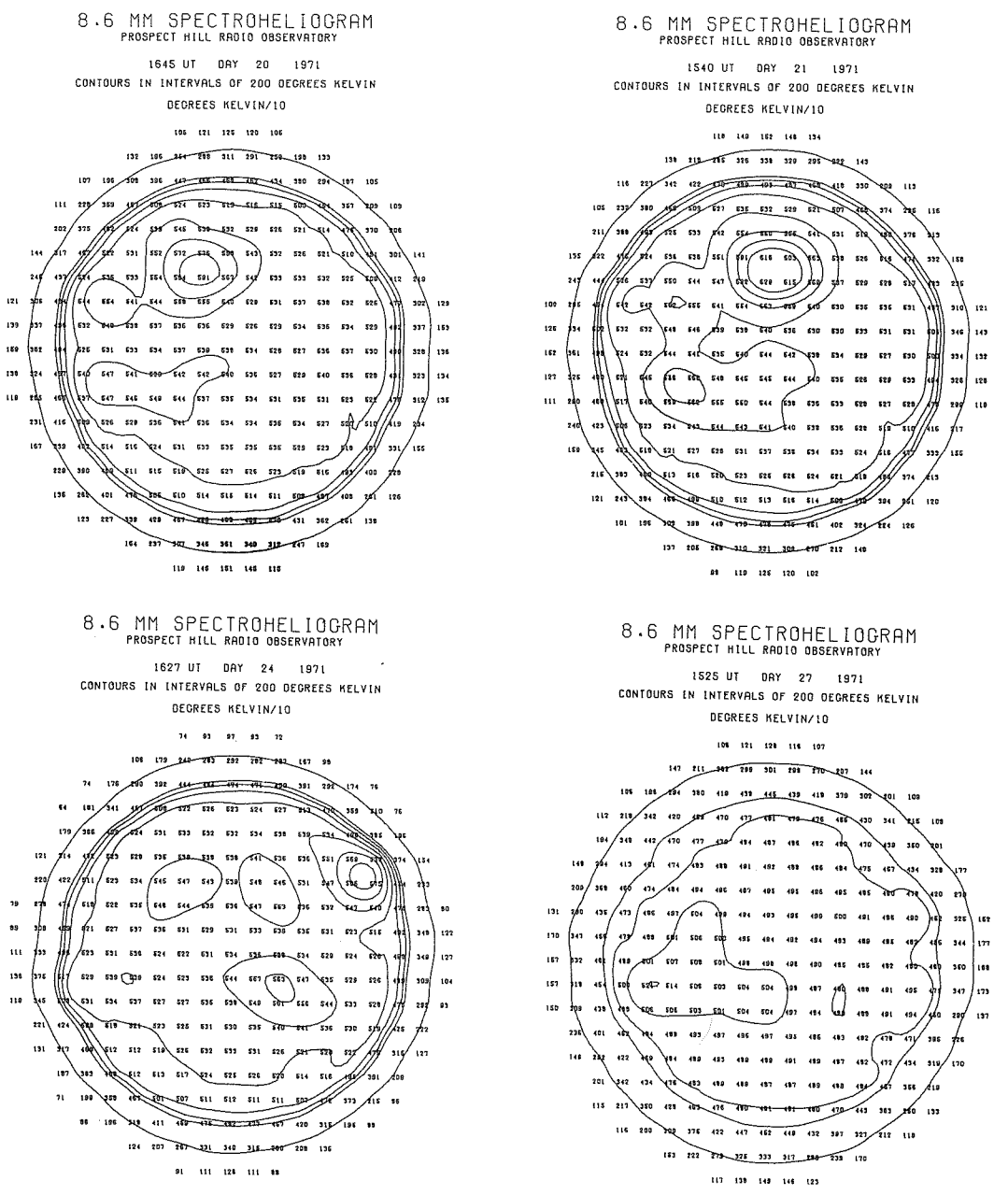
8.6 MM SPECTROHELIOGRAM
PROSPECT HILL RADIO OBSERVATORY
1645 UT DAY 20 1971
CONTOURS IN INTERVALS OF 200 DEGREES KELVIN
DEGREES KELVIN/10
8.6 MM SPECTROHELIOGRAM
PROSPECT HILL RADIO OBSERVATORY
1540 UT DAY 21 1971
CONTOURS IN INTERVALS OF 200 DEGREES KELVIN
DEGREES KELVIN/10
8.6 MM SPECTROHELIOGRAM
PROSPECT HILL RADIO OBSERVATORY
1627 UT DAY 24 1971
CONTOURS IN INTERVALS OF 200 DEGREES KELVIN
DEGREES KELVIN/10
8.6 MM SPECTROHELIOGRAM
PROSPECT HILL RADIO OBSERVATORY
1525 UT DAY 27 1971
CONTOURS IN INTERVALS OF 200 DEGREES KELVIN
DEGREES KELVIN/10

Figure 2.

TABLE I

Day 16

JANUARY 16, 1971 1642 UT

$L_o = 283^o$, $B_o = -5^o$

L	LAT	CMD	8 mm
290	17N	07W	180 K
227	18N	56E	290 K
257	15N	26E	190 K
323	12N	40W	170 K
265	03S	18E	160 K
304	10S	21W	150 K

Day 17

JANUARY 17, 1971 1920 UT

$L_o = 270^o$, $B_o = -5^o$

L	LAT	CMD	8 mm
225	20N	45E	600 K
257	16N	13E	215 K
292	16N	22W	175 K
270	01S	00	160 K
284	05S	14W	150 K
300	07S	30W	140 K

Day 18

JANUARY 18, 1971 1639 UT

$L_o = 257^o$, $B_o = -5^o$

L	LAT	CMD	8 mm
222	18N	35E	520 K
286	15N	29W	115 K
256	12N	01E	135 K
278	01S	21W	100 K
229	05S	28E	150 K
286	05S	29W	100 K
203	09S	54E	130 K

Day 19

JANUARY 19, 1971 1630 UT

$L_o = 244^o$, $B_o = -5^o$

L	LAT	CMD	8 mm
222	20N	22E	775 K
189	12N	55E	160 K
188	07S	56E	240 K

TABLE I Continued

Day 20

JANUARY 20, 1971 1645 UT

$L_o = 239^o$, $B_o = -5^o$

L	LAT	CMD	8 mm
221	18N	10E	604 K
191	12N	40E	220 K
188	07S	43E	190 K
207	11S	24E	170 K

Day 21

JANUARY 21, 1971 1540 UT

$L_o = 218^o$, $B_o = -5^o$

L	LAT	CMD	8 mm
218	18N	00	970 K
189	11N	29E	260 K
165	11N	53E	90 K
189	08S	29E	325 K

Day 24

JANUARY 24, 1971 1627 UT

$L_o = 178^o$, $B_o = -5^o$

L	LAT	CMD	8 mm
221	20N	43W	623 K
158	12N	20E	190 K
190	12N	12W	230 K
143	06S	35E	100 K
192	08S	14W	365 K

Day 27

JANUARY 27, 1971 1525 UT

$L_o = 138^o$, $B_o = -6^o$

L	LAT	CMD	8 mm
156	11N	18W	125 K
100	05S	38E	330 K
133	09S	05E	180 K
187	07S	49W	100 K

REFERENCES

1972 Solar-Geophysical Data, Descriptive Text, Number 330 (Supplement), February, 1972, U. S. Department of Commerce, (Boulder, Colorado, U.S.A. 80302), 21.

Dynamic Radio Spectra of the Solar Flare of 1971 January 24 2300 UT

by

A. Maxwell
Harvard Radio Astronomy Station, Fort Davis, Texas 79734

During 1971, the solar dynamic radio-spectrum analyzer at the Harvard Radio Astronomy Station, Fort Davis, Texas, operated over the complete band 10-2000 MHz. Descriptions of the equipment will be found elsewhere [Thompson 1961, Maxwell 1971]. The receivers in the band 500-2000 MHz were put into operation in 1970 and are connected to a steerable 85-ft antenna, whose large collecting area permits solar bursts in this band to be recorded at high sensitivity.

The two records of Figure 1 show the radio outburst that was recorded at Fort Davis on 1971 January 24. Type III emission began at 23hr 06min 40sec. Type IV emission was first seen in the decimeter band at 2310 UT and it then gradually spread to lower bands. A type II burst, with a clearly recognizable fundamental and second harmonic, commenced in the meter band at 23hr 15min 30sec and was followed by complex bursts with "herringbone" and reverse drift structure that continued until 2346 UT. The type IV emission continued until sunset at 2355 UT. (At Culgoora, in Australia, the type IV burst was reported to have continued on the meter band until 0250 UT on the following day, January 25.) According to the NOAA Monthly Bulletin of Solar-Geophysical Data, the radio burst was accompanied by a large optical flare that was located at N16 W49 on the solar disk. The flare commenced at about 2215 UT on January 24, brightened to reach an importance classification of 3B at about 2308 UT, and died away at about 0300 UT on the following day, January 25.

REFERENCES

MAXWELL, A. 1971 Solar Phys., 16, 224.

THOMPSON, A. R. 1961 Astrophys. J., 133, 643.

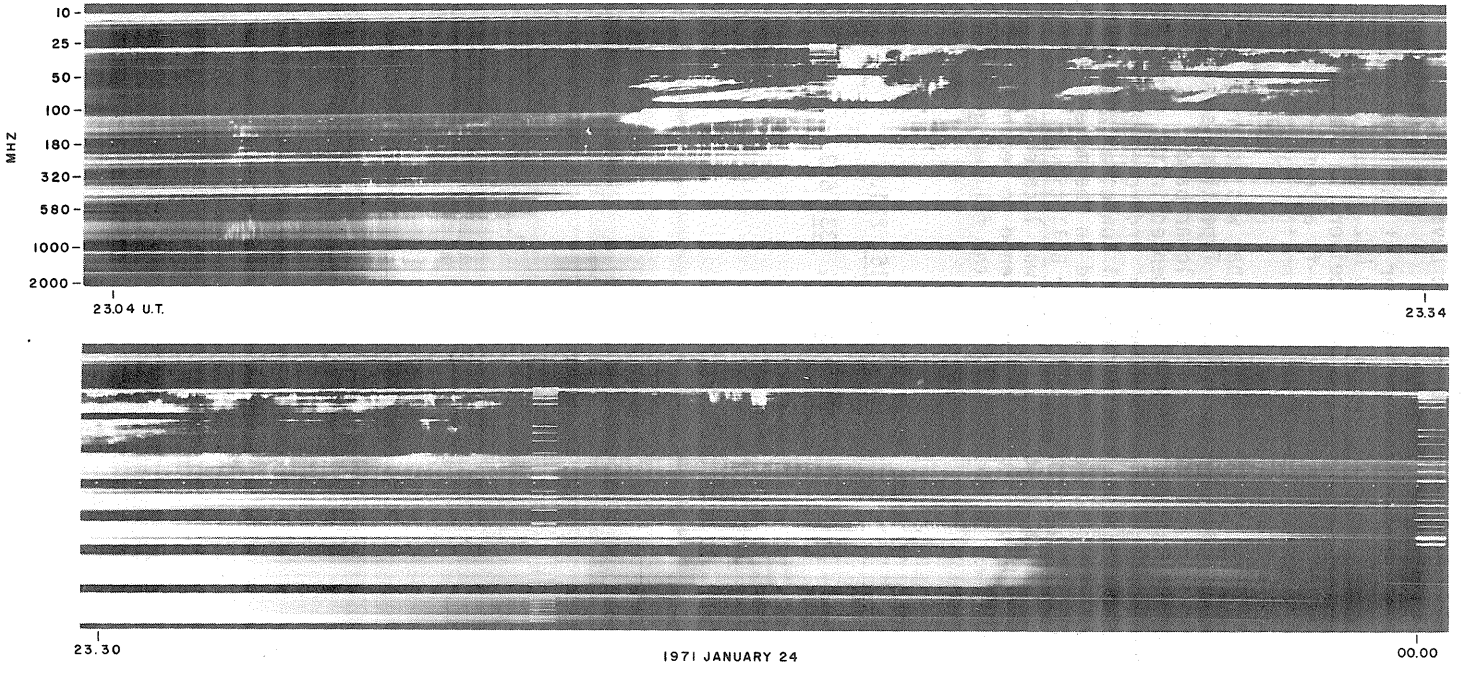

Fig. 1. Dynamic spectra of the solar radio burst recorded at the Harvard Radio Astronomy Station, Fort Davis, Texas.

Radio Burst Observations of 24 January 1971 Solar Proton Flare

by

William R. Barron
Air Force Cambridge Research Laboratories
Bedford, Massachusetts

On 24 January 1971 a 3B solar flare was observed in McMath Region 11128, reaching a maximum at 2331 UT. This flare was the source of energetic particles and subsequent ground level phenomena.

Radio emission associated with this flare was observed at the Manila Observatory, Republic of the Phillipines, at discrete frequencies in the 606 - 8800 MHz interval [Hennessey, 1969; Badillo, 1970]. Table 1 gives data pertaining to the radio burst.

Table 1

Freq. (MHz)	Start Time (UT)	Peak Time (UT)	Duration (min.)	Peak Flux ($\times 10^{-22}$ W/m^2/Hz)	Mean Flux
8800	2304.3*	2323.1	28.6*	11900*	4200*
4995	2303.8	2323.2	29.1	7050*	3200*
2695	2303.8	2323.2	29.1	2400*	1200*
1415	2304.3*	2323.2*	28.6*	720*	500*
606	2307.6	2323.2	16.1*	1400*	540*

The data values marked with an asterisk (*) are final values supplied by Reverend V. J. Badillo of the Manila Observatory. The analog record of the burst is illustrated in Figure 1.

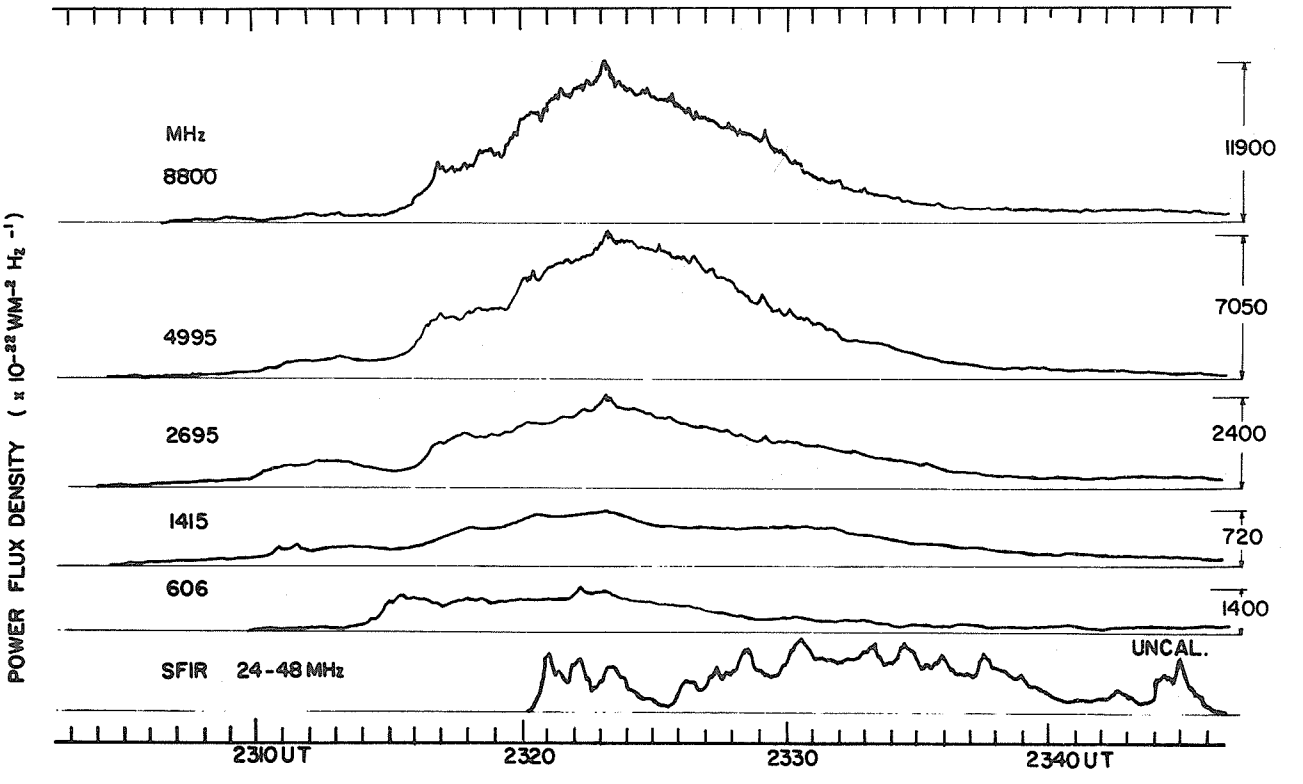

GREAT RADIO BURST OBSERVED ON 24 JANUARY 1971
AT THE MANILA OBSERVATORY, R. P.

FIG. 1

The spectral plot of the peak fluxes of the burst is shown in Figure 2. Also included in the plot is the 2695 MHz peak flux observed at the Dominion Radio Astrophysical Observatory, Penticton, British Columbia [NOAA, 1971 a]. This is included to show the agreement between the two observatories. The peak flux spectrum (U-shaped), flux amplitudes, and flux rise times (>5 minutes) all bear the characteristics of a solar proton radio burst [Castelli et al., 1967; O'Brien, 1970].

The least squares best fit cubic curve determined from the data values is plotted in Figure 2. The maximum and minimum of this curve are

$$F_{max} = 8374 \text{ MHz}, \sim 3.5 \text{ cm}$$

$$F_{min} = 1064 \text{ MHz}, \sim 28.1 \text{ cm}$$

The integrated radio burst flux densities, found by multiplying the burst mean flux by the duration in seconds, are given in Table 2.

Table 2

Frequencies	Integrated Flux Densities $x10^{-16}$ Joules/m^2/Hz
8800	12.9
4995	8.9
4695	4.1
1415	2.5
606	3.0

These integrated flux densities fall into the 10^{-17}-10^{-15} Joules/m^2/Hz range which is sufficient for ground level proton events to occur [Straka et al., 1970]. The reported riometer absorption at 30 MHz was

Godhavn, Greenland	9.7 dB	[Cormier, 1972]
Shepherd's Bay, NWT, Canada	6.2 dB	

The 3B flare reached maximum at 2331 UT at a position of N18 W49 on the visible solar disk. The heliographic longitude of this position was 222.8°. This is in a region of heliographic longitudes which has a history of producing solar proton flares [Straka et al., 1970; Dodson et al., 1968].

In the 100 - 245 MHz frequency interval, noise storm activity was reported by several observatories [NOAA, 1971 a] during the days just prior to the 24th, on the 24th, and on the 25th until approximately 14 hours after the flare. The noise storm activity ceased to be observed at 1400 UT on the 25th and continued to be quiet until 29 January. This decline in solar activity is also noted in dekameter band activity following the intense type IV and type II bursts associated with the 3B flare [NOAA, 1971 b]. No activity whatsoever was reported in the 24 - 48 MHz band by either the Manila Observatory or Sagamore Hill from 0634 UT on 25 January to 1350 UT on 29 January [Geophysics and Space Data Bulletin, 1971].

During the period of January 26 - 28 the level of radio burst activity was also quite low in the 606 - 8800 MHz frequency interval. The lowest level of activity occurred on the 27th. Experience at the AFCRL Sagamore Hill Radio Observatory has shown that a decrease of activity in this given frequency range is a characteristic of post-proton flare periods.

Summary

The 3B solar flare of 24 January 1971 occurred in a heliographic region known to be productive of proton flares. The U-shaped frequency spectrum, peak fluxes, and flux rise times all met criteria established as being characteristic of solar proton flares which are accompanied by PCA events. The reported absorptions of 6.2 dB and 9.7 dB meant that a ground level PCA event had taken place after the flare. For a period of about 4 days after the flare, radio burst activity was very reduced.

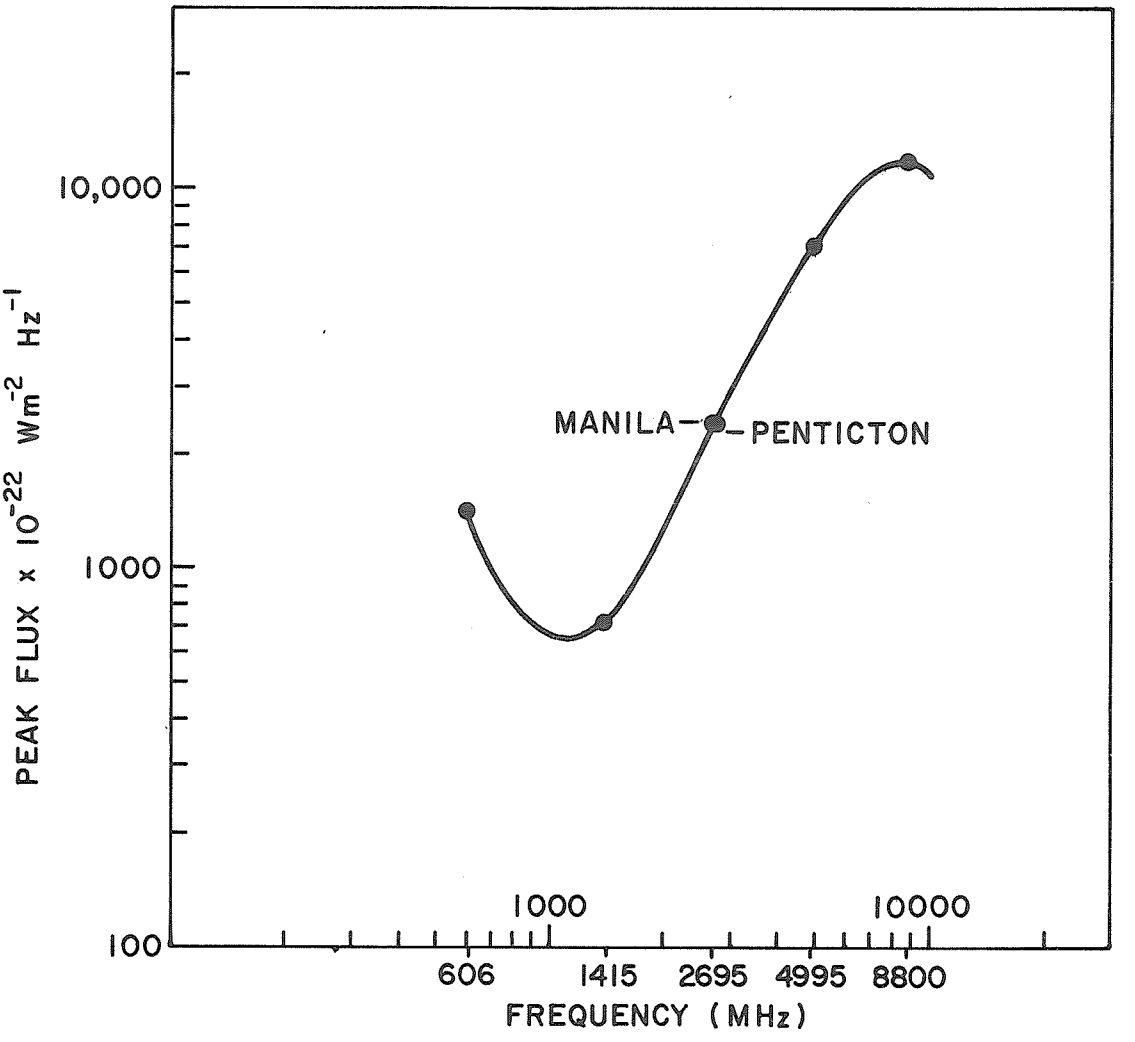

FIG. 2 PEAK FLUX SPECTRUM OF SOLAR RADIO BURST OBSERVED 24 JANUARY 1971, MANILA OBSERVATORY, R.P. AT 2323 UT.

REFERENCES

BADILLO, V. J. 1970 Solar Studies at Manila Observatory, AFCRL Report 70-0358.

CASTELLI, J. P., J. AARONS and G. A. MICHAEL 1967 Flux Density Measurements of Radio Bursts of Proton-Producing Flares and Non-Proton Flares, J. Geophys. Res., 72.

CORMIER, R. 1972 (private communication)

DODSON, H. W. and R. HEDEMAN 1968 Some Patterns in the Development of Centers of Solar Activity, 1962-66, Structure & Development of Solar Active Regions, IAU Symposium No. 35, Published by D. Reidel Pub. Co.

HENNESSEY, J. J. 1969 Solar Work at Manila Observatory, Solar Physics, 9, No. 2.

O'BRIEN, W. E. 1970 The Prediction of Solar Proton Events Based on Solar Radio Emissions, AFCRL-70-0425; 23 Jul 70, Environmental Research Papers, No. 328.

STRAKA, R. M. and W. R. BARRON 1970 Multifrequency Solar Radio Bursts as Predictors for Proton Events, AGARD Conference Proceedings No. 49, Edited by V. AGY, Published January 1970.

1971 Geophysics and Space Data Bulletin, A. L. CARRIGAN, Editor, Vol VIII, No. 1, First Quarter 1971, AFCRL-71-0339, Space Reports No. 119.

1971 a Solar-Geophysical Data, 323 Part II, July 1971, U.S. Department of Commerce, (Boulder, Colorado, U.S.A. 80302).

1971 b Solar-Geophysical Data, 319 Part I, February 1971, U.S. Department of Commerce, (Boulder, Colorado, U.S.A. 80302).

The Solar Microwave Burst of January 24-25, 1971

by

Haruo Tanaka and Shinzo Énomé
The Research Institute of Atmospherics
Nagoya University

Time histories of the burst as observed at Toyokawa are shown in the Figure, which indicates comparatively smooth and simple profiles of the burst at four frequencies: 1000, 2000, 3750 and 9400 MHz. Details of numerical values related to this burst are tabulated in Table 1. Within the observed frequencies the spectrum is characterized by the flux being roughly proportional to the frequency. Polarization percentages at the time of maximum flux are also designated in the final column of the Table. Although we have failed to measure polarization at 3750 MHz, the sense of polarization was probably right-handed at 9400, 3750 and 2000 MHz. At 1000 MHz the sense was left-handed (40%) in the main peak, but in the secondary hump occurring around 2350 UT the sense reversed to right-handed (20%). We have no spatial information of the burst source in the main peak owing to the unfavorable time of occurrence for interferometer observations.

Table 1

Date	Freq.	Starting Time	Time of Max.	Duration	Type	Max. Flux Dens. $10^{-22}Wm^{-2}Hz^{-1}$		Polarization
Jan.	MHz	UT	UT	Min.		Peak	Mean	
24	9400	2304	2322.4	51	C+	6900	1400	25% R
	3750	2303	2324	52	C+	3540	850	-
	2000	2303	2324	57	C+	1270	390	≃ 30% R
	1000	2304	2322.1	55	C	810	250	40% L

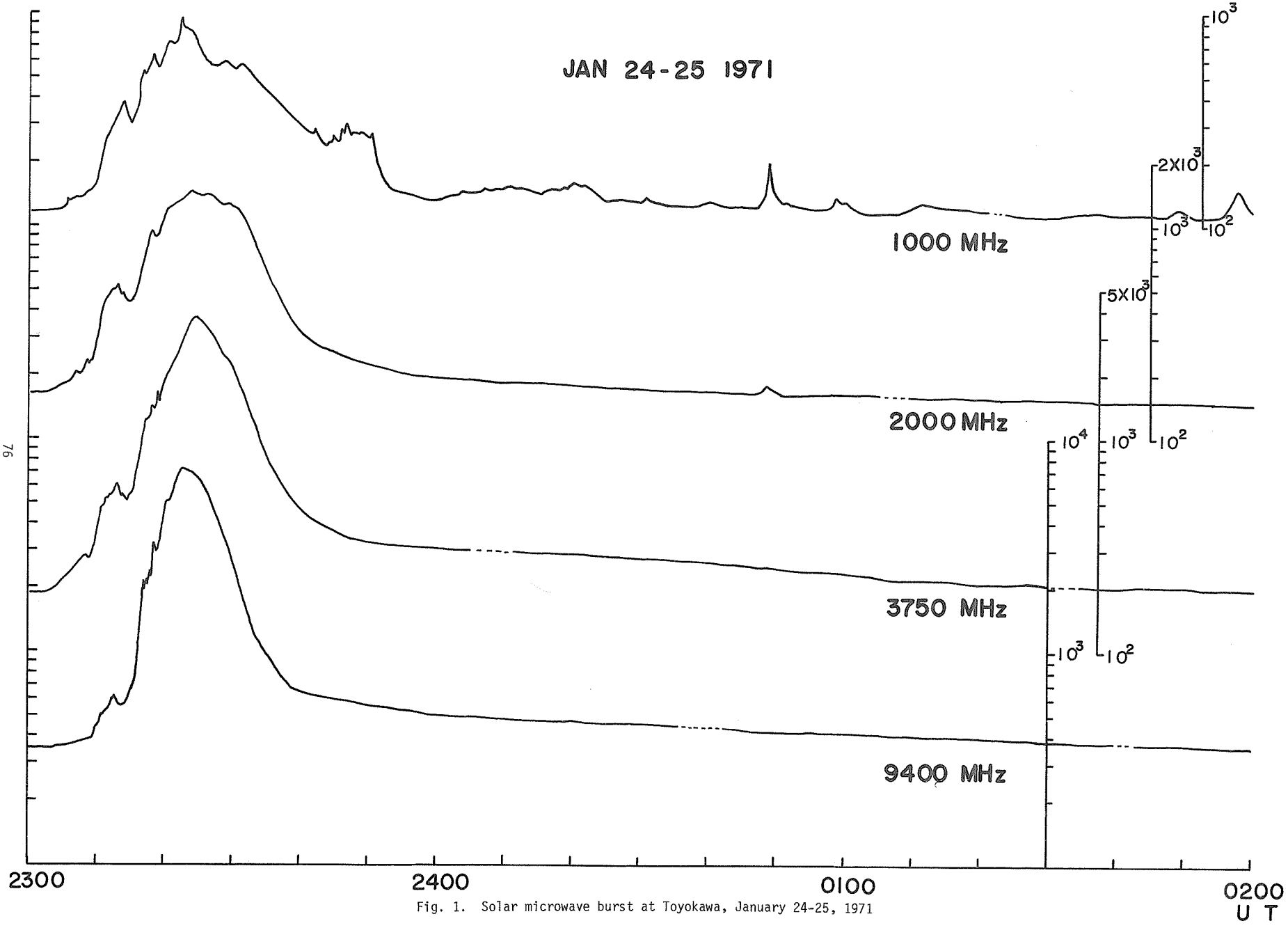

Fig. 1. Solar microwave burst at Toyokawa, January 24-25, 1971

The Slowly Varying Component of the Frequencies of 2695 MHz, 606 MHz and 536 MHz during the Period of the Proton Flare Events of January 24 and September 1, 1971

by

A. Tlamicha and J. Olmr
Astronomical Institute
of
The Czechoslovak Academy of Sciences
Ondrejov, Czechoslovakia

Because of the observation schedule at The Ondrejov Observatory, the radiotelescopes were not in operation at the time of the proton flares of January 24 and September 1. Thus, we can say nothing about the active radio component during the above-mentioned proton flares. Since the slowly varying component originates from discrete sources that exist in the neighborhood of sunspot active regions, we therefore try to examine not only the active radio component, but also the slowly varying component.

In order to have a richer spectrum, we examined the slowly varying component on the frequencies of 2695 MHz (Sagamore Hill), 606 MHz (Sagamore Hill), 536 MHz (Ondrejov) and 260 MHz (Ondrejov). The period examined includes December 1, 1970 to December 31, 1971 (see Figure 1). The results confirm there is good correlation between the radio flux on the wavelengths mentioned above and sunspot area [Covington, 1948; Tanaka, 1958].

We have taken into account (see Figure 2) the reduced sunspot area of every group from Solnechnye Dannye (Moscow) and the definitive relative sunspot numbers for the years 1970 and 1971 (Sunspot Numbers, Swiss. Federal Observatory, Zürich). It appears from the graph that a very high correlation exists between the flux density on the frequency of 2695 MHz and sunspot area and relative sunspot numbers. A considerable strengthening of the slowly varying component appears on the frequency of 2695 MHz in the period from January 21 to 24 (Table 1). It agrees very well with the supposition of the storage of energy before the proton flare.

On the other hand, at the end of August we observed at this frequency a decrease after strong enhancement (Table 2). The active center of the proton flare by this time had passed from the visible solar disk 3 days earlier.

Surprisingly, the correlation between the main maxima of sunspot area (and relative sunspot number) and the maxima of flux density on the frequencies of 606 MHz, 536 MHz and 260 MHz is also very strong. The base level on 260 MHz is remarkably constant. One observes an extraordinary enhancement in the period from January 9 to 25 (Table 1). We can say nothing for the second event since there are no measurements on 260 MHz from August 27-31.

It is conspicuous that in the period before both proton flares the behavior of the component of radiation on 260 MHz was of the sort that cannot be overlooked. The flux density was enhanced and the active radio component was manifested by strong noise storms. Such centers of storm radiation can be supposed to be stores of particles of low energy escaping from the Sun and coming to the earth [Böhme A. and A. Krüger, 1971]. The behavior of the base level components on all mentioned frequencies and the active radio component on 536 MHz and 260 MHz is presented.

In the Tables 3 and 4 for the noise storms in January and August are given, besides the starting time and duration, also the variability and types of noise storm as classified after Tlamicha et al. [1964]. The noise storms were very intense, particularly on 9, 10, 11 and 12 January 1971 and on August 20-24, 1971. We also examined the active radio component on 9400 MHz, 808 MHz and 536 MHz during January and August at the Ondrejov Observatory. In Tables 5 and 6 the values of the bursts on the frequencies 9400 MHz and 808 MHz are on a relative scale while the values on the frequency 536 MHz are expressed in units of $10^{-22} Wm^{-2} Hz^{-1}$.

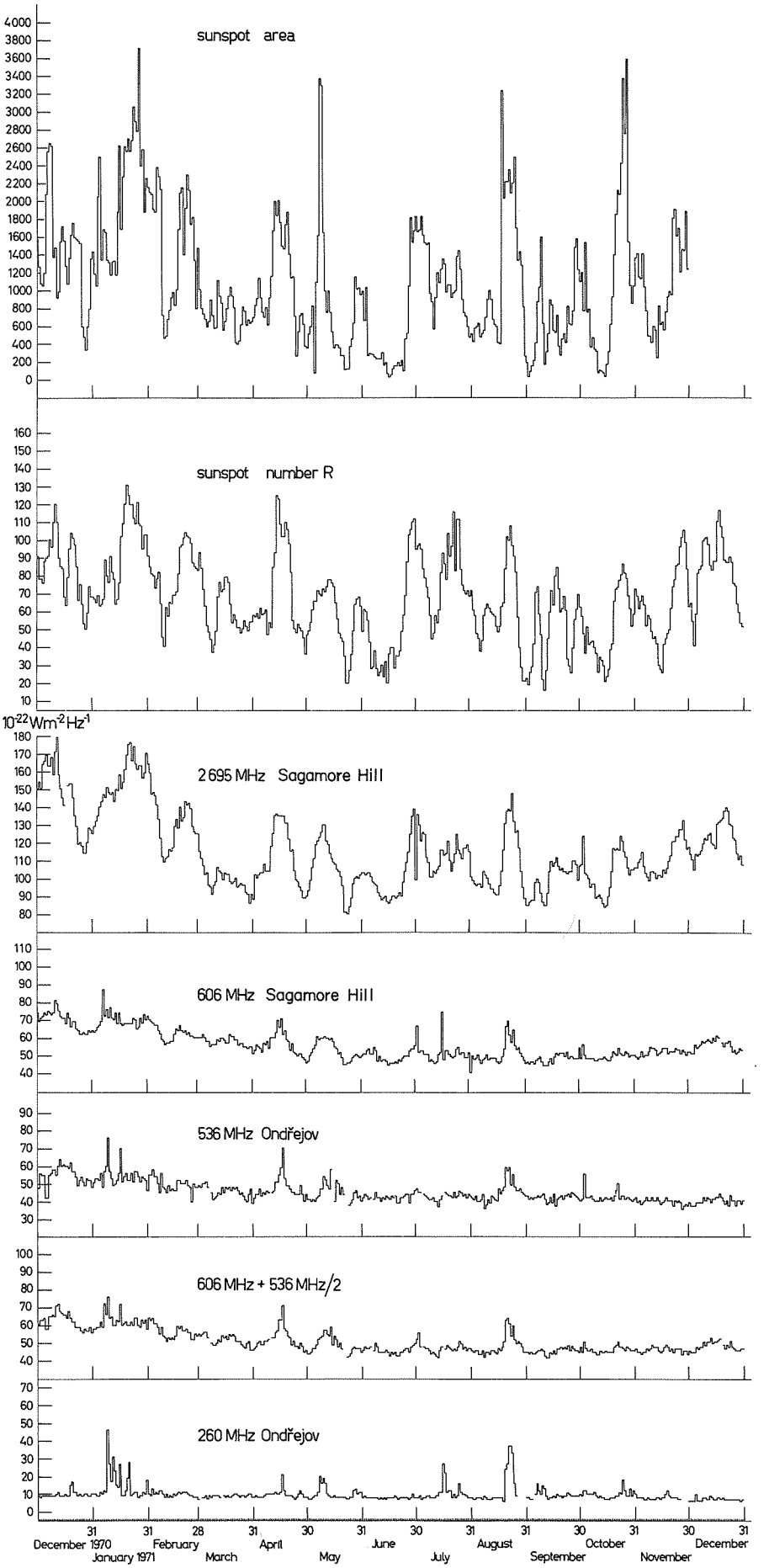
sunspot area
sunspot number R
$10^{-22} Wm^{-2} Hz^{-1}$
2695 MHz Sagamore Hill
606 MHz Sagamore Hill
536 MHz Ondřejov
606 MHz + 536 MHz/2
260 MHz Ondřejov
31 December 1970
31 January 1971
28 February
31 March
30 April
31 May
30 June
31 July
31 August
30 September
31 October
30 November
31 December

Fig. 1

Table 1

Proton event of January 24, 1971

Daily means of solar radio flux density from January 1 to January 31, 1971

Date January 1971	2695 MHz (Sagamore Hill)	606 MHz (Sagamore Hill)	536 MHz (Ondrejov)	260 MHz (Ondrejov)
1	125	64	51	10
2	129	63	53	10
3	132	64	53	9
4	135	66	52	9
5	140	67	56	11
6	143	69	48	10
7	147	87	57	12
8	145	72	60	11
9	151	76	76	46
10	148	71	57	27
11	147	77	53	17
12	148	71	49	31
13	143	70	50	23
14	150	74	52	15
15	149	68	56	14
16	158	74	70	27
17	150	68	51	9
18	154	67	54	9
19	161	68	56	12
20	169	68	52	19
21	175	68	52	28
22	176	68	56	9
23	166	68	51	10
24	174	71	57	11
25	164	70	57	11
26	161	65	54	8
27	163	66	51	9
28	163	71	54	9
29	156	68	53	11
30	159	73	52	10
31	170	70	46	18

Table 2

Proton event of September 1, 1971

Daily means of solar radio flux density from August 1 to September 1

Date	2695 MHz (Sagamore Hill)	606 MHz (Sagamore Hill)	536 MHz (Ondrejov)	260 MHz (Ondrejov)
Aug. 1	101	50	42	8
2	99	48	41	7
3	97	49	43	7
4	96	51	40	8
5	97	48	40	8
6	97	46	41	8
7	95	48	44	7
8	104	47	36	9
9	102	51	38	8
10	100	48	41	7
11	97	49	39	7
12	94	49	43	7
13	94	49	42	8
14	92	49	41	8
15	91	47	40	8
16	91	46	47	8
17	96	47	44	8
18	104	50	46	8
19	116	54	48	6
20	131	67	59	24
21	138	70	57	27
22	139	62	59	37
23	138	58	49	37
24	148	65	55	33
25	132	56	48	16
26	126	54	46	9
27	127	55	46	-
28	117	52	47	-
29	104	50	45	-
30	95	48	44	-
31	89	46	43	-
Sep. 1	85	47	43	8

Table 3

Noise storms at Ondrejov on 260 MHz - January 1971

Date	Start UT	Duration Min.	Intensity	Variability	Type
Jan. 4	0820	250	65	0	M weak
6	0820	330	50	0	"
8	0810	340	65	0	"
9	0820	350	85	3	NC
10	0830	370	80	3	NC
11	0810	360	50	3	NC
12	0810	300	65	3	NC
17	0810	350	70	1	M weak
18	0820	340	70	1	M very weak
19	0820	350	80	0	"
21	0810	360	75	2	NC
22	0918	282	100	1	M weak
25	0810	370	40	1	M
29	0820	360	50	1	M
31	0840	320	105	2	NS
Feb. 2	0810	230	>55	1	M
8	0820	360	60	0	M weak
9	0830	360	60	1	M weak
17	0910	340	>60	1	M very weak
19	1010	240	100	1	M very weak
27	0650	490	>40	1	M

Table 4

Noise storms at Ondrejov on 260 MHz - August 1971

Date	Start UT	Duration Min.	Intensity	Variability	Type
Aug. 5	0939	141	60	1	NB
19	1007.5	200	30	0	M
20	0600	580	>130	2	ND
21	0640	530	> 95	2	NC
22	0620	430	>120	1	NC
23	0610	560	50	2	NC
24	0610	560	50	2	NC
27	1234	61	110	?	M
Sep. 5	1310	130	50	No class.	No class.
6	0625	525	75	1	NB
7	1100	520	70	1	ND
8	0630	450	60	1	ND
9	<1109.5	241.5	50	1	NC
10	0640	320	65	2	M
11	1050	210	50	0	M
14	0650	500	45	1	NS
16	0808	79	65	1	NB
24	0740	140	35	1	M
28	1308.5	121.5	75	0	M

Types:
M = Group of bursts
NS = Noise storm in progress
C = Complex

Table 5

List of extraordinary events at Ondrejov during January 1971

Date	Start UT	Duration Min.	Intensity 9400 MHz	808 MHz	536 MHz
			Relative units	Relative units	$10^{-22}Wm^{-2}Hz^{-1}$
14	1121	9	>4.1		
	1123	9		>2.6	
	1121	9			235
21	1318	11	1.7		
	1319			1.8	
	1320				70
22	1105.5	8.5	1.8		
	1106	>14		>2.8	
	1106	>14			>120
23	1252.5	2.5			235
25	0927.5	10			180
26	1327	3		1.6	
	1327.5	2.5			60

Table 6

List of extraordinary events at Ondrejov during August 1971

Date	Start UT	Duration Min.	Intensity 9400 MHz	808 MHz	536 MHz
			Relative Units	Relative Units	$10^{-22}Wm^{-2}Hz^{-1}$
8	1154	1.5	1.3		
	1214	5.5	1.2		
	1157	2		1.2	
	1209	4.5		1.3	
21	0933.5	3.5	1.6		
	0934	3.5		2.3	
	0934.5	0.5			190
22	0750	8	3.8		
	0750	8		2.0	
	0747	28			>260
23	0943	3	1.9		
	0943	7		2.0	

In conclusion, we can say that we propose the possibility that the big storms before proton events may be an indication of the storage of energy manifested by the proton events of January 24 and September 1, 1971.

The authors wish to thank Dr. L. Krivský, from whose initiative this work was begun and for his valuable suggestions during the preparing of this paper.

REFERENCES

BÖHME A. and A. KRÜGER	1971	Characteristics of Noise Storms and S-component of Solar Radio Emission in March, 1970. World Data Center A, Report UAG-12, Part I, 71-75.
COVINGTON, A. E. and W. J. MEDD	1948	Simultaneous Observations of Solar Radio Noise on 1.5 Meters and 10.7 Centimeters, J. Roy. Astron. Soc., 43, 106-110.
KRÜGER, A., W. KRÜGER and G. WALLIS	1964	Das zeitliche und spektrale Verhalten der langsam veränowslishen Komponente der solaren Radiostrahlung im gegenwärtigen Fleckenzyklus, Zeitschrift für Astrophysik, 59, 37-55.
KUNDU, M. R.	1964	Solar Radio Astronomy, 1964, pp 201 and following.
TANAKA, H.	1964	Eleven-year Variation of the Spectrum of Solar Radio Emission on Microwave Region, Proceedings of the Research Institute of Atmospherics, Nagoya University, 11, 41-51.
TLAMICHA, A., L. KRIVSKY and J. OLMR	1964	Classification of Solar Radio Noise Storms (Ondrejov 1959-1961), Bull. of Czech. Obs., 15, No. 2, 49-52.

Dekameter Burst of 24 January 1971

by

V. L. Badillo
Manila Observatory
P. O. Box 1231, Manila
Philippines

The solar dekameter burst accompanying the Ground Level Event (GLE) of 24 January 1971 is shown in Figures 1 and 2 as recorded by the Swept Frequency Interferometer Radiometer (SFIR) at Manila about one hour after local sunrise. The instrument has two outputs: (1) one showing the flux integrated over the spectral band 24-48 MHz and permitting a measurement of intensity variation as in Figure 1, and (2) a dynamic spectrograph as in Figure 2 permitting identification of the type of burst, among other things. Data in the dekameter band provides information on activities and conditions in the sun's upper corona.

The envelope of the total flux curve shows three main maxima, A, B and C, each of which show fine structure. A rather striking symmetry is indicated whose physical significance is still to be found. The spectrograph shows type IV radiation on which are superposed type II and type III bursts. Change in intensity is also indicated in the spectrograph by intensification of fringe pattern, fringe reversal (brought about by a clipping circuit when saturation is reached) and fringe washout (due to saturation of the IF circuit). A close correspondence can be seen between the fine structure of the total flux curve and the events depicted in the spectrograph.

The dekameter burst has a more impulsive character than the cm bursts, also recorded at Manila. Bursts 1, 2 and 3 in the main maximum A can be identified as a type III followed by two type II bursts with drift rates of 0.25 and 0.20 MHz/sec respectively. These bursts can be interpreted as manifestations of streams of energetic electrons moving radially outward and exciting successively lower frequencies. The three bursts would then represent three streams, the fastest being followed by successively slower streams. Burst 3 does not seem to be a harmonic of burst 2. Clouds of relativistic electrons are responsible for the type III burst. Using the Baumbach-Allen model with electron densities increased by a factor of 10 (for coronal densities above an active region) the velocities of the electron clouds responsible for bursts 2 and 3 are of the order of 2000 km/sec.

The dekameter burst is very evident starting at 2320.5 UT, but faint traces can be discerned at 2316 in the spectrograph and as early as 2304 in the total power curve, which is about the start time for the cm burst. The GLE of 24 January 1971 is thus accompanied by type IV radiation from the cm to dekameter bands. Hopefully the data from the dekameter burst may help to a better understanding of the mechanisms responsible for Ground Level Events.

We thank the following: J. P. Castelli and J. J. Hennessey for their encouragement, J. E. Salcedo for careful measurements and Air Force Cambridge Research Laboratories for supporting this.

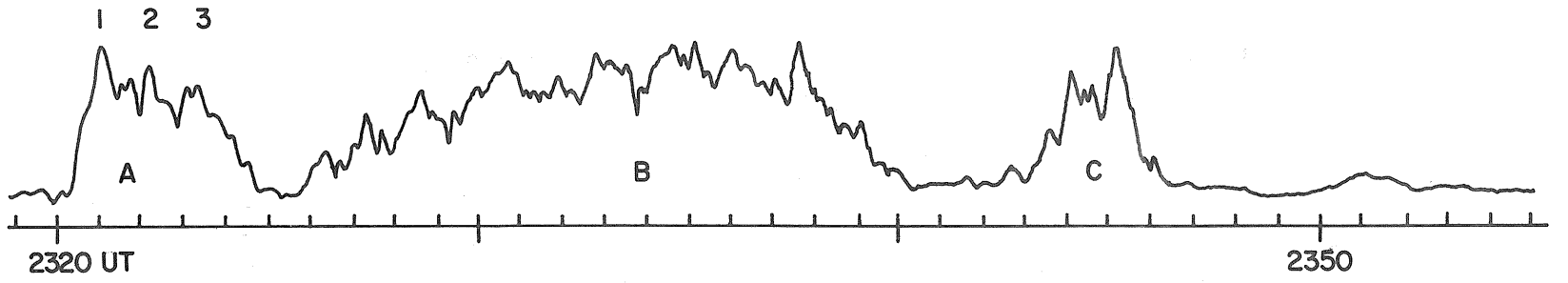

Fig. 1. Flux of 24 January 1971 dekameter burst integrated over 24-48 MHz band. (Flux is in relative units).

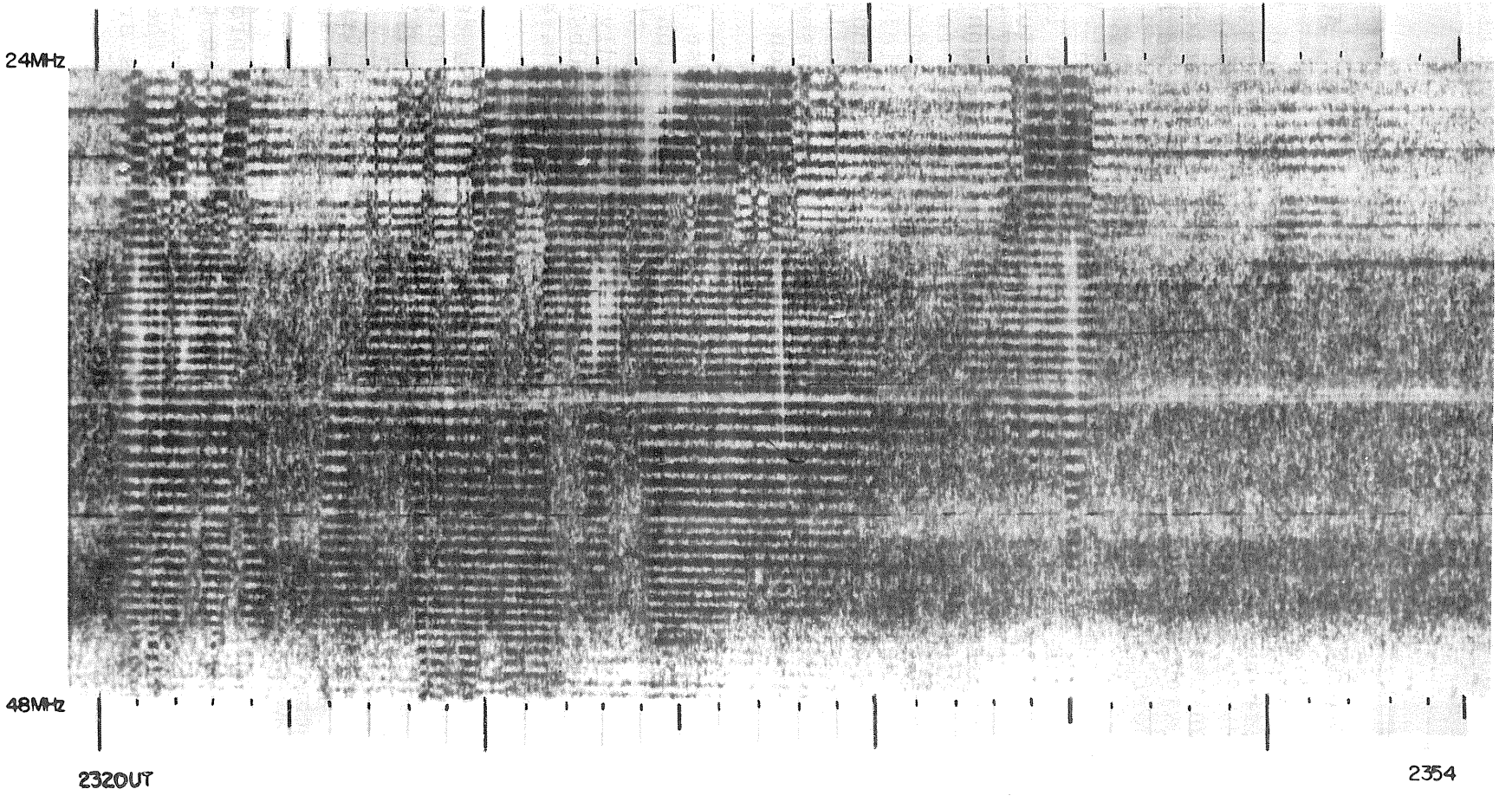

Fig. 2. Type IV dekameter event recorded by a 24-48 MHz SFIR on 24 January 1971 at Manila Observatory, R. P.

Culgoora Radioheliograph and Spectrograph Observations of the Event of 1971 January 24

by

A.C. Riddle and I.D. Palmer
Division of Radiophysics, CSIRO, Sydney, Australia

The event of 1971 January 24 was observed at Culgoora, in its entirety with the 8 MHz to 8 GHz spectrograph and from $23^h16^m30^s$ U.T. by the 80 MHz radioheliograph. Sections of these data have been utilized in two papers [Riddle and Sheridan 1971; Palmer et al. 1972], published elsewhere and reproduced below in this UAG report.

Riddle and Sheridan [1971] described briefly the observations and gave a model for the sources seen in the late phase of the event. A feature of their model was the postulated injection of electrons, with energies in the 50 to 500 keV range, on to the interplanetary field lines over the period 00^h to 04^h U.T. Palmer et al. [1972] related the radio data to the initial acceleration of mildly relativistic protons and electrons and their subsequent injection on to interplanetary field lines. Here we add a more detailed comparison of spectrum and heliograph records in the early phase (23^h16^m to 23^h47^m) to facilitate comparison with other data. In the process of this comparison more definite associations have been made between features on the spectrum and radioheliograph data.

The Culgoora spectrum for the early phase is shown in Figure 1(b). The flux of each radioheliograph source seen during the same period is shown in Figure 1(a). In the analysis which follows use was also made of a spectrum kindly provided by Dr. Alan Maxwell from the Harvard, Fort Davis, Observatory which enabled us to determine spectral details in areas where the Culgoora record is obscured by saturation.

The positions of the heliograph sources, derived from computer analysis, are shown in Figure 2, where an indication of the time of occurrence is given for the moving sources.

The fundamental emission from the first type II event was seen only briefly at 80 MHz and the high-frequency component of the split band was responsible for source A. The lower-frequency component of the harmonic split band was responsible for source B, which appeared to move with a projected speed comparable with that of the shock causing the type II event [Riddle and Sheridan 1971]. However, source C, which corresponds to the high-frequency component of the harmonic of the first type II, was almost stationary, as are many type II sources observed with the radioheliograph.

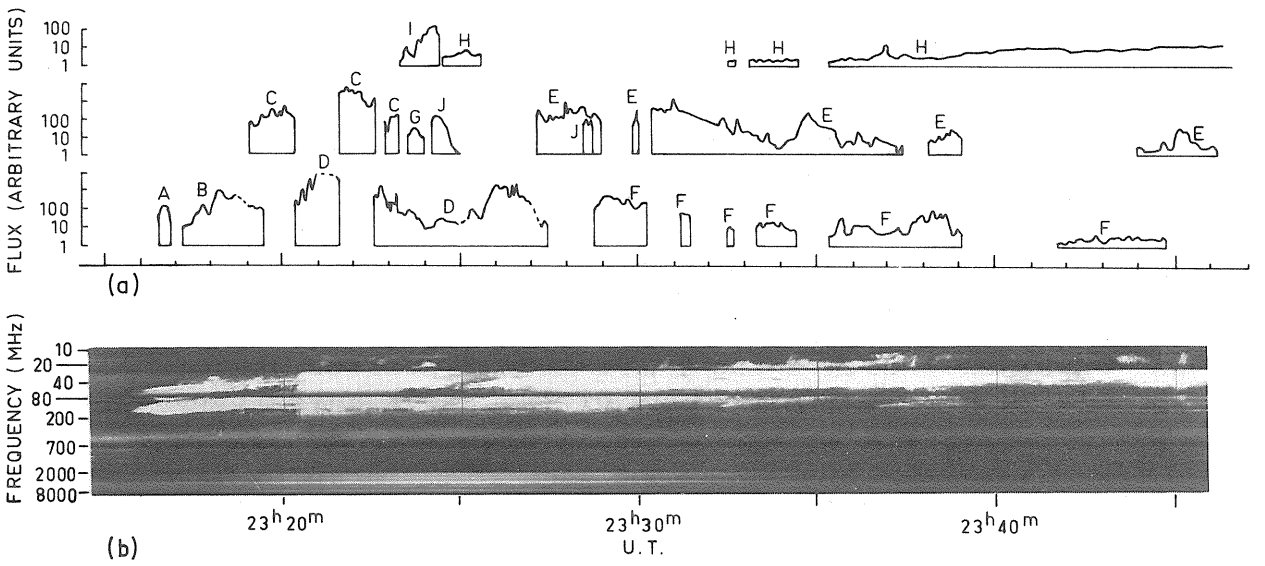

Fig. 1 The early phase of the event of 1971 January 24.
(a) Computer-derived 80 MHz flux values for each radio-heliograph source plotted on a logarithmic scale in arbitrary units. Unless sources present simultaneously have similar flux values only the strongest source is recorded. Dashed profiles indicate missing data. Positions for the sources are shown in Figure 2.
(b) The radio spectrum, 8 MHz to 8 GHz.
(After Riddle and Sheridan. 1971.)

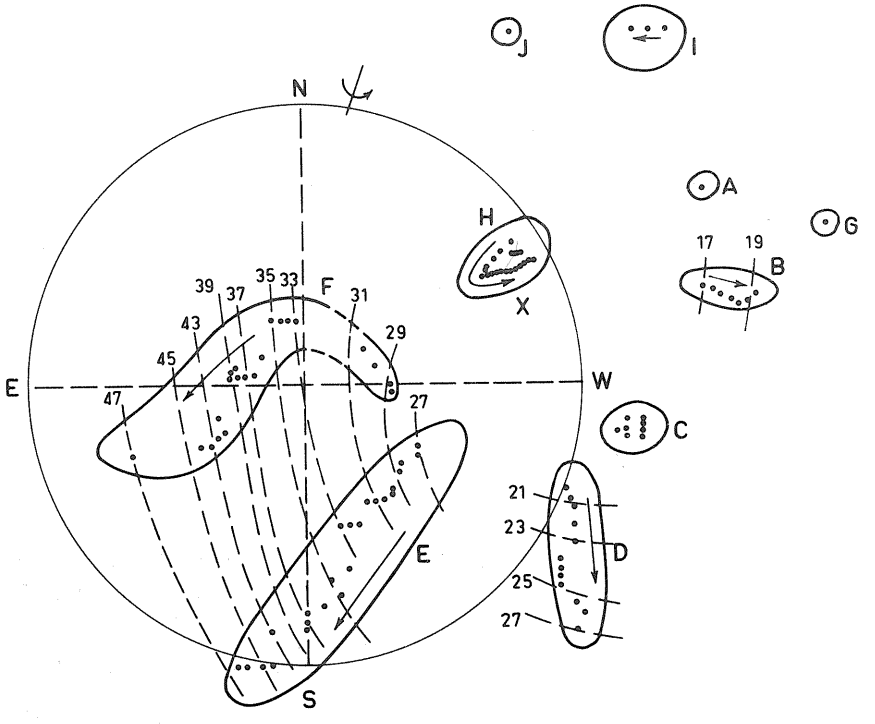

Fig. 2 Positions of peak brightness for 80 MHz sources during the early phases of the event of 1971 January 24. Points are plotted for every half-minute during the time a source was continuously visible and the dashed lines indicate the time (in minutes after 23^h00^m) at which the source was at a particular position.
(After Riddle and Sheridan, 1971.)

The continuum or type-V-like feature (which includes repeated type III events on the Harvard spectrum) commencing at $23^h20^m30^s$ corresponded to source D, the position of which changed continuously over the period 23^h20^m to 23^h27^m, as though influenced by the first shock front [Riddle and Sheridan 1971]. Only the harmonic of the second type II passed through 80 MHz (23^h26^m to 23^h27^m) and was responsible for the final brightening of the source D. Later portions of the second type II event possibly were represented by source E, although both E and F appear also to be related to the continuum from 23^h28^m onwards. Both E and F are moving sources and are apparently 80 MHz manifestations of the shock wave responsible for the second type II event. Drifting features seen on the spectrum passing through 80 MHz at 23^h35^m and 23^h38^m and herringbone features at 23^h32^m, 23^h38^m and 23^h45^m caused enhancement of sources E or F without any obvious change in their position. The source J corresponds at 23^h28^m to a drifting feature visible on the Harvard spectrum and probably gives evidence of northward propagation of the shock fronts. The source H became highly polarized towards the end of the early phase and persisted as a storm source for many hours. It is the only source common to both the early and late phase of the event.

Overall the spectral and radioheliograph data for the early stage of the event can be related well to a double explosive event having one flash phase at about 23^h09^m and another at about 23^h20^m, each with a resultant shock front. The moving radioheliograph sources can be related directly to one or the other of two shock fronts, which apparently propagate in quite different directions. In the case of sources E and F emissions represented by a wide variety of spectral features originate within, or close to, the second shock front; in the case of D there is distinct evidence of electrons accelerated in the second flash phase interacting with the shock wave produced by the first flash.

REFERENCES

Riddle, A.C. and K.V. Sheridan 1971 Evolution of a jet-like structure in the late phase of a complex solar outburst, Proc. A.S.A., 2, 62-65.

Palmer, I.D., S.F. Smerd, and A.C. Riddle 1972 Solar radio observations of the proton event of 1971 January 24, Proc. A.S.A., 2, 103-105.

Solar Radio Observations of the Proton Event of 1971 January 24 *

by

I.D. PALMER, S.F. SMERD AND A.C. RIDDLE
Division of Radiophysics, CSIRO, Sydney

On 1971 January 24 a 3B flare at 18°N., 49°W. was associated with the acceleration of protons to relativistic energies; it was one of the rare events recorded by ground-level neutron monitors. Excellent radio coverage was obtained with single-frequency radiometers in the range 1000-9400 MHz, and at Culgoora with the 8-8000 MHz spectrograph and the 80 MHz radioheliograph. At the Earth relativistic protons and electrons arrived very promptly from the flare, whose site was near the foot of the nominal interplanetary field line which connects to the Earth.

In this paper we relate the time sequence and the positions of the solar radio bursts to the times and places where the energetic particles were accelerated and injected on to interplanetary field lines. This is the first time that an analysis of such an event has used the positions of the radio bursts in the corona. We show from the radio data that there were two separate explosive events, identified by two flash phases, which occurred ≈10 min apart. Both explosions gave rise to a coronal shock wave, and these propagated away from the flare site in markedly different directions. The microwave observations indicate that particle acceleration to relativistic energies was associated with the first event, while the subsequent particle release, as deduced from cosmic ray data recorded near the Earth, occurred during the second event. We propose that the shock wave of the first event was responsible for the acceleration of the relativistic particles and that the shock wave of the second event enabled their release on to interplanetary field lines which connected to the Earth.

RADIO OBSERVATIONS

The radio spectrum recorded at Culgoora during the 1971 January 24 event has been discussed by Riddle and Sheridan[1] (see their Figure 1). Two type II bursts (both showing fundamental and harmonic structure) appeared at 23^h16^m and 23^h25^m. Their frequency drifts imply the release of shocks from near the surface of the Sun at 23^h10^m and 23^h20^m, respectively. We take these times as defining those of two flash phases in this double event.[1]

In the case of the first flash phase this interpretation is supported by the observation at 23^h10^m of the initial impulsive rise at the microwave frequencies (see below), and of the 0.5-3Å hard X-ray burst between 23^h04^m and $23^h12^m.2$.[2] The absence of type III bursts suggests that the accelerated sub-relativistic electrons were magnetically confined low in the corona. The identification of the second flash phase is supported by several fast-drift bursts which accompanied the sudden onset at $23^h20^m.5$ of a broad-band metre-wave continuum, probably of type V.[1] The absence of a distinct impulsive microwave burst suggests that the sub-relativistic electrons did not have access to the low corona.

The microwave single-frequency traces recorded at Toyokawa at frequencies of 9400, 3750, 2000 and 1000 MHz, and reproduced here by courtesy of Dr. H. Tanaka, are given in Figure 1. The 80 MHz flux density is shown for comparison. The impulsive first flash-phase burst at 23^h10^m was followed by a much larger outburst which peaked at 23^h23^m; both can be regarded as part of the first event, and distinct from the second event, which begins with the second flash.

The 80 MHz positional data obtained from the heliograph,[1] as summarized in Figure 2, shows the envelopes of the brightest points of the first type II burst (A, B and C), the continuum (D), and the second type II burst (D, E and F). Source movement is indicated by an arrow within the envelope. Notice that the 80 MHz source positions indicate that the two shock waves travelled away from the flare site in approximately orthogonal directions.

SOLAR COSMIC RAYS

The recording of this event by neutron monitors indicates that protons with energy of ≈1 GeV first arrived at the Earth at $23^h35^m.2$.[2] Subtracting their theoretical transit time over 1.3 A.U.[3] suggests that they were injected at the Sun into the interplanetary field at 23^h23^m. This figure is based on the assumption that the first particles to reach the Earth had suffered negligible delay due to scattering, and therefore were effectively collimated (pitch angle ≈0°) along the diverging spiral interplanetary field.

In this event spacecraft observations near Earth also revealed the presence of mildly-relativistic electrons. When interpreted similarly to that above, the onset times of the 0.3-0.9 MeV and >80 keV electron events, viz. 23^h33^m,[4] and 23^h41^m,[5] imply injection times of 23^h21^m and 23^h25^m, respectively.

In order to test whether any appreciable diffusive delay (due to scattering in the interplanetary medium) might be inherent in the transit time of the first-arriving particles, a simple isotropic

*Editor's Note: Permission has been received from the authors and editors of the Astronomical Society of Australia to reprint this article.

diffusion model (with diffusion coefficient independent of radial distance from the Sun) was employed to fit the rise of intensity of the proton event as recorded by the Alert neutron monitor.[6] The best fit implies an impulsive injection at 23^h22^m with an error of a few minutes, and is thus in good agreement with the values above derived from transit times. We conclude therefore that the injection at the Sun of mildly-relativistic protons and electrons occurred between 23^h20^m and 23^h25^m, i.e. during the decay of the microwave type IV burst as shown in Figure 1. (Note that particle injection times are shown delayed by 8 min to agree with the radio observations.)

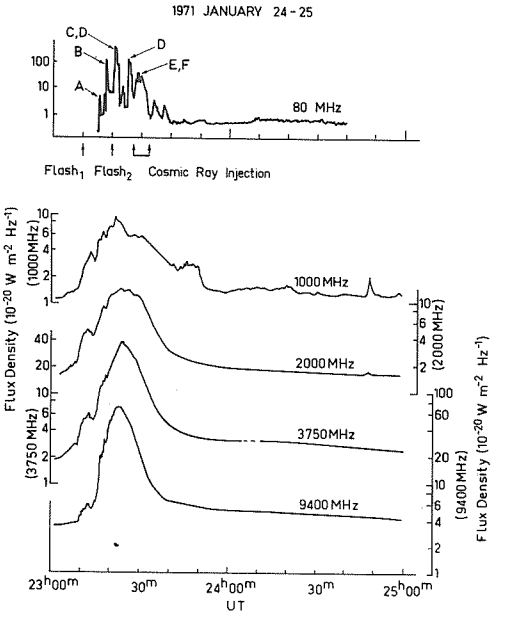

Fig. 1. Flux density profiles obtained from Toyokawa for the event of 1971 January 24-25 at frequencies of 9400, 3750, 2000 and 1000 MHz. The 80 MHz profile from the Culgoora heliograph is also given, and the peaks are labelled by their positions in Figure 2. The two flash phases and the period of cosmic ray injection are also indicated. The cosmic ray injection is shown 8 min after the time at the Sun, since all the other times refer to the arrival of electromagnetic radiation at the Earth.

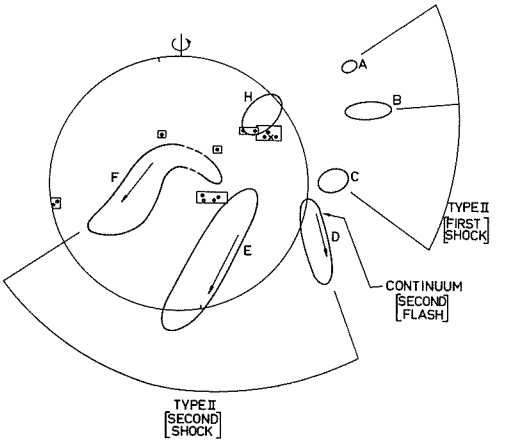

Fig. 2. Radioheliograph positions at 80 MHz of various radio bursts in the event of 1971 January 24-25, superposed on the Boulder sunspot map.

DISCUSSION

We now interpret these pieces of evidence in terms of the acceleration, storage and release of relativistic particles in this event (with the particle injection time still delayed by 8 min).

The rise of the microwave type IV burst is evidence of gradual particle acceleration from 23^h16^m to 23^h23^m (see Figure 1). It is likely that during this time protons as well as electrons were accelerated to relativistic energies perhaps as a consequence of some form of wave-particle interaction associated with the first shock. If the peak in the microwave outburst at 23^h23^m signifies the end of particle acceleration, this leaves 5-10 min before the relativistic particles were injected on to interplanetary field lines which connected to the Earth. The injection time, 8-13 min after the second explosion (at 23^h20^m) is near the time at which the second shock wave reached the upper corona. We propose that the second shock wave, by virtue of its quite different direction of travel relative to the first, released the energetic particles (which had been trapped during their acceleration) between H, D, E and F (Figure 2). The particle release may have culminated, at about 23^h28^m, in a 'bursting' of the magnetic trap due to the expanding hot gas behind the second shock. (A similar interpretation was placed[7] on another event in which the 'bursting' of the condensation was detected by coronagraph observations.) Those relativistic particles released from the magnetic trap on to field lines that connected with the interplanetary field high above equatorial regions near longitude 50°W. should have found a direct magnetic connection to Earth.

The radio records were examined for indications of the release of mildly relativistic electrons in the corona at this time. The only possible evidence is a fairly sudden enhancement in continuum radiation which spans the frequency range between the fundamental and the harmonic of the second type II burst (20-150 MHz).

Riddle and Sheridan[1] described several moving sources appearing some hours later in this event and stretching to the west of region H (see Figure 2) in the form of a jet. They attributed this to the escape of mildly-relativistic electrons along a streamer above H. This streamer would serve as a suitable escape route for the cosmic rays observed at the Earth.

Figure 3 illustrates a model of the three phases of the particle acceleration and release described above.

The authors would like to thank Dr. H. Tanaka for providing the microwave records from Toyokawa, and Dr. G. M. Simnett and Dr. R. P. Lin for the onset times of the 0.3-0.9 MeV and >80 keV electron events, respectively.

REFERENCES

[1]Riddle, A.C. and Sheridan, K.V., Proc. ASA, 2, 62 (1971).

[2]Solar Geophysical Data, U.S. Dept. Commerce, 319, Part 1 (March 1971).

[3]Webber, W.R., 'The Physics of Solar Flares', NASA SP-50, 215 (1964).

[4]Simnett, G.M., private communication.

[5]Lin, R.P., private communication.

[6]Cline, T.L. and McDonald, F.B., Sol. Phys. 5, 507 (1968).

[7]Hansen, R.T., Garcia, C.J., Grognard, R.J.-M. and Sheridan, K.V., Proc. ASA, 2, 57 (1971).

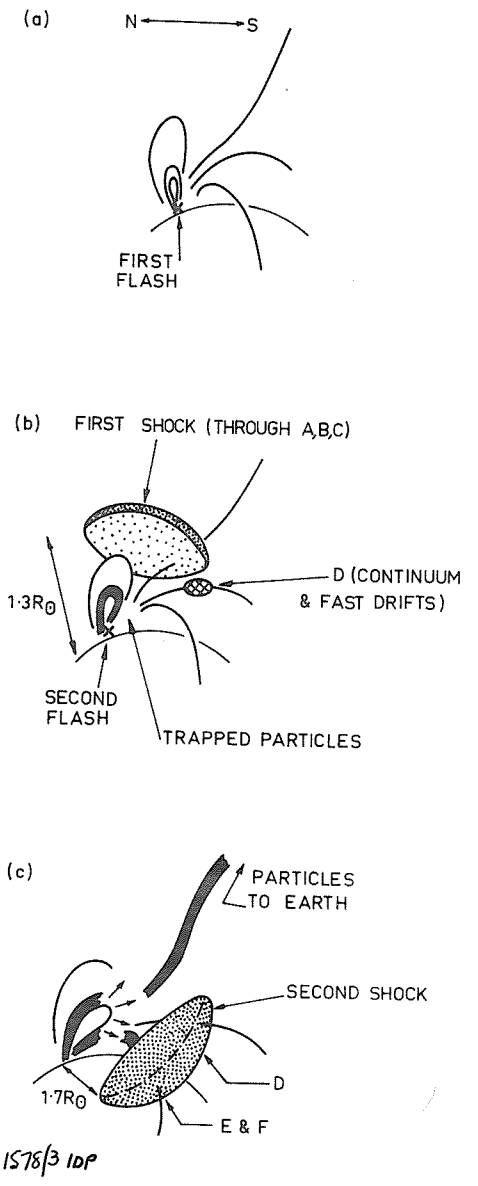

Fig. 3. Illustrating the model of the acceleration and release of energetic particles:

(a) The coronal magnetic field configuration at the first flash phase at 23^h10^m showing the flare (X) below closed loops of strong field, but with open field lines nearby.

(b) The situation at the time of the second flash phase at 23^h20^m, showing the trapped particles (shaded loop) accelerated behind the first shock wave, and the appearance of the continuum and associated fast drift bursts in the 80 MHz region D.

(c) The bursting of the magnetic trap behind the second shock wave at $\sim 23^h28^m$. Energetic particles are released towards the Earth.

Reprinted from
Proceedings of the Astronomical Society of Australia
Volume 2, Number 1, pages 62-65, July 1971

Evolution of a Jet-like Structure in the Late Phase of a Complex Solar Outburst *

A. C. RIDDLE AND K. V. SHERIDAN
Division of Radiophysics, CSIRO, Sydney

A new feature in the form of a jet formed by close juxtaposition of a number of highly polarized, separately resolved 80 MHz sources was observed as the late phase of a very complex outburst on 1971 January 25. We present here a source model which, we think, can explain the observed source properties. The early phase, also complex and involving numerous moving sources, will be described first.

THE EARLY PHASE

(a) *Observations other than radio*

A flare of importance 2B was observed[1] to start at position N.19°, W.49° in McMath region 11128 on January 24, 23^h09^m U.T. The maximum intensity of the flare was at 23^h16^m, and by January 25, 00^h24^m the flare was over. A distinctive feature of this region was a row of five large sunspots formed by coalescence of previously separate regions and extending over some 20° in longitude between latitudes 17° and 19°N. The magnetic-field distribution at the surface was correspondingly complex.

The event was accompanied by a large solar proton burst detected at ground level by neutron monitors.

An intense solar X-ray burst was also recorded, between 0.5 and 20 Å, by the Explorer 37 satellite.[1]

(b) *Radio observations*

The event was recorded from its beginning by the 8 MHz to 8 GHz Culgoora radiospectrograph. The intense activity began at $23^h15^m30^s$ with the sudden onset of the first type II burst (see Figure 1 (c)*). After 23^h20^m a more intense continuum burst appeared superimposed on this type II burst. A second type II burst commenced at about 23^h25^m. These intense emissions, characterizing the early phase of the event, finished at about 23^h47^m.

Observations with the 80 MHz radioheliograph[2] commenced at $23^h16^m30^s$ U.T.—near flare maximum but just prior to the major radio emissions at 80 MHz (see Figure 1 (a)). For the next 30 min a multitude of sources provided a spectacular radioheliograph display. Figure 2 (a)† shows a number of individual sources which, on the whole, moved outward from a central point (the flare centre); in part the morphology is reminiscent of previously reported arch structure.[3–5] The positions of the peak brightness of these sources are plotted in Figure 3 for the intervals during which the sources were observed, as shown in Figure 1 (b).

(c) *Discussion*

The first type II event shows split-band fundamental and harmonic radiation. From the spectrum we derive a starting time for the initiating disturbance (presumably a shock wave) of 23^h07^m, close to the starting time of the flare, and a radial velocity of ≈1200 km/s. Source A (Figures 1 (b) and 3) is the source of the upper-frequency band of the fundamental radiation, while source B accounts for the lower band of the second harmonic radiation. A line joining sources A and B is approximately normal to a radius through the flare centre, a relationship which has been previously noted.[6] The identification of source C is uncertain; it may be that of the upper band of the second harmonic. The projected velocity of source B is ≈1000 km/s, which, on the assumption of radial propagation, gives a source velocity of ≈1250 km/s, in good agreement with the velocity derived from the spectrum.

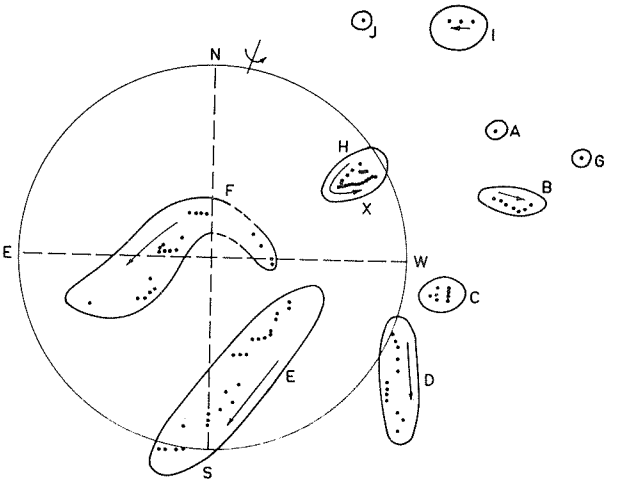

Figure 3. Positions of peak brightness for 80 MHz sources during the early phase of the event of 1971 January 24/25. Points are plotted for every half-minute during the time a source was continuously visible (see Figure 1 (b)). All points representing the same source are enclosed by a line and identified with a letter. The arrows show the direction of motion of each source. The large circle represents the solar photosphere and X the site of the flare at N.19° W.49°.

The harmonic radiation of the second type II burst appears as source E, which moved at a projected velocity of 950 km/s. From the spectrum we derived a radial velocity of ≈2000 km/s and a starting time of ~23^h20^m for the initiating disturbance. This was also the starting time of the metre-wave continuum burst (possibly of type V) identified as source D. The common starting time suggests a possible connection between these two bursts. This could be another explosive flare phase resulting in the ejection of fast electrons and a much slower shock front. The former could be responsible for the continuum burst when crossing the shock front of the first type II burst; the latter could become the source of the second type II burst. No distinct optical event has been reported at that time.

The radioheliograph sources F to J are not clearly related to any distinct features on the photographic

*See Plate III.
†See Plate IV.

*Editor's Note: Permission has been received from the authors and Journal to reprint this article.

PLATE III

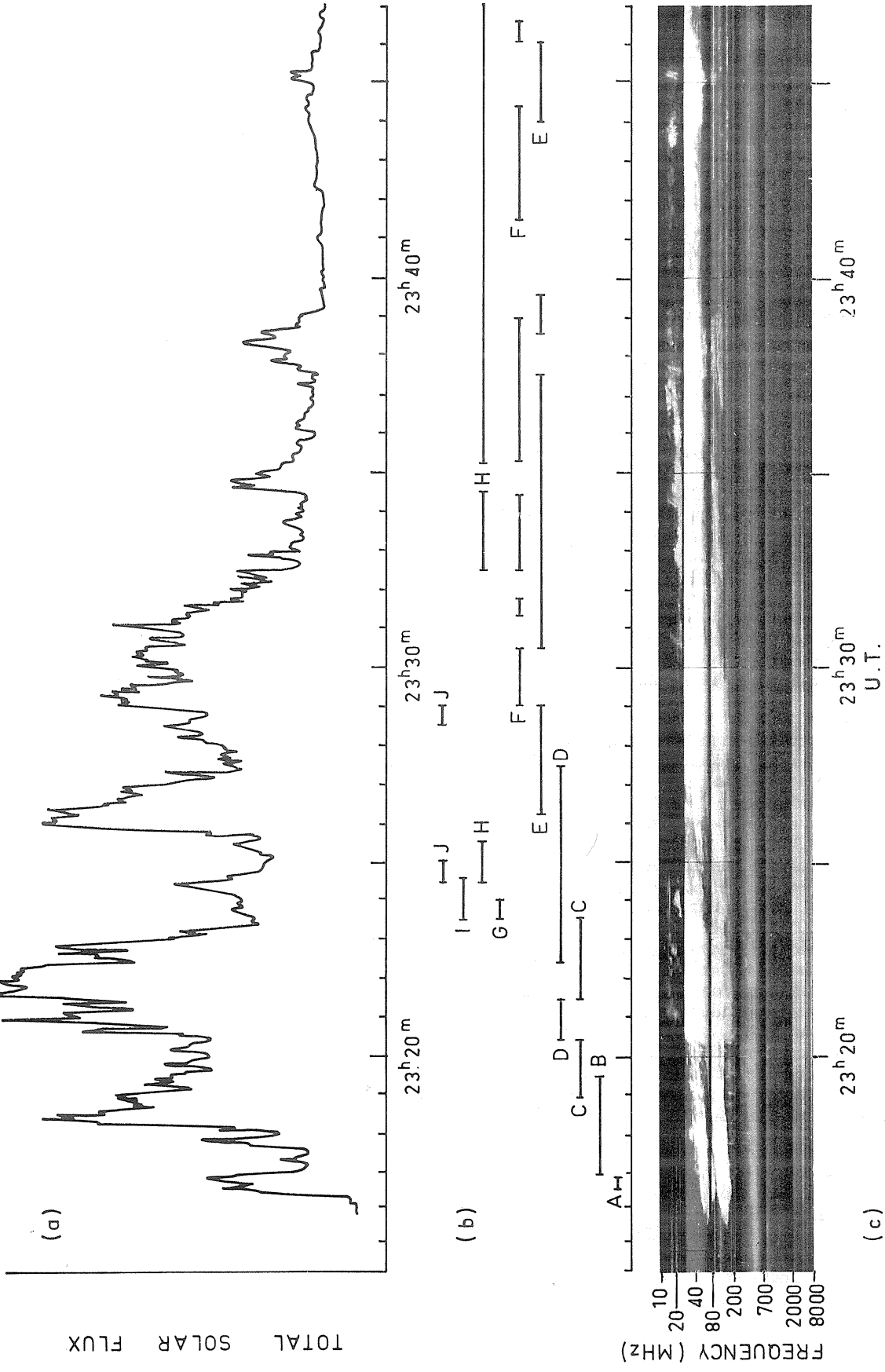

Figure 1. The early phase of the event of 1971 January 24/25.
(a) The total flux density at 80 MHz plotted on a pseudo-logarithmic scale.
(b) A bar chart showing the time duration of sources identified at 80 MHz. The positions of the sources are shown in Figure 3.
(c) The radio spectrum, 8 MHz to 8 GHz.

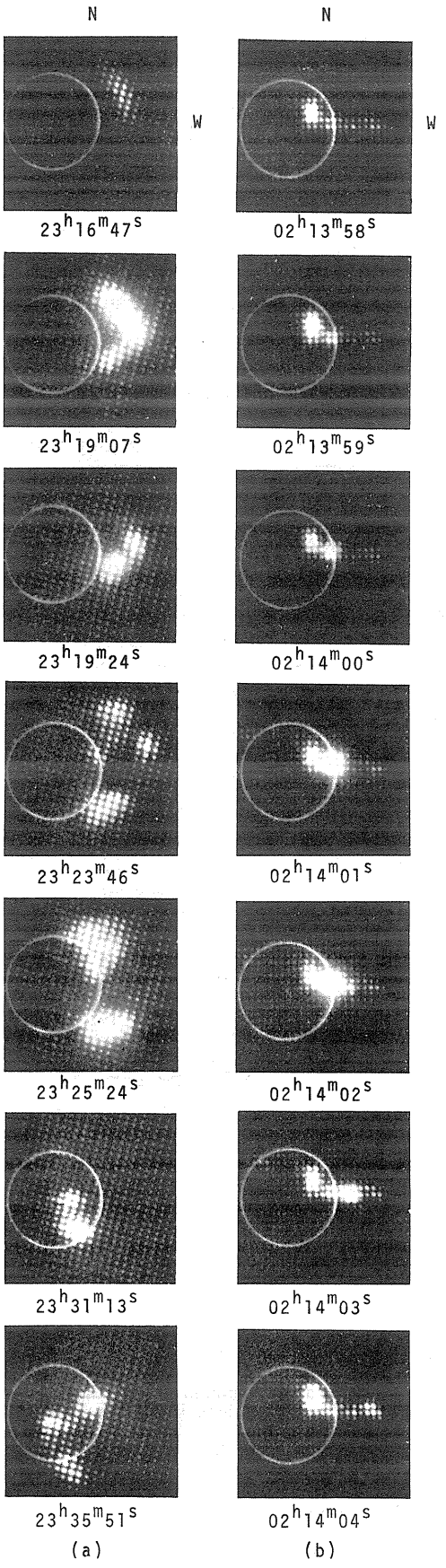

Figure 2. Selected 80 MHz 1-sec. heliograms for the event of 1971 January 24/25.

(a) The early phase of the event.

(b) A sequence of sequential brightenings in the late phase.

spectrum; photometric analysis of the spectrum may lead to further identifications.

The early phase of the event shows features and raises problems already mentioned in other papers[5] and no new hypotheses will be presented here other than the suggestion above of a possible connection between the continuum burst at 23^h20^m and the second type II burst at 23^h25^m.

THE LATE PHASE

(a) *Observations*

After 23^h47^m the spectrum at frequencies near 80 MHz showed much reduced activity with weak type IV continuum emission, type I and occasional type III bursts. On the heliograph up to four sources were visible at any one time. These sources were positioned close to a line running west from the centre of the disk (see Figure 2 (b)). Most sources were moving farther west with time. This new type of structure will be referred to as the jet. There were no reports[1] of significant optical activity.

The positions of peak emission of heliograph sources in the jet were calculated up till the cessation of observation on January 25, 04^h00^m. The east-west coordinate of these positions is plotted in Figure 4 as a function of time. While only four sources were apparent on the heliograph at any one time, Figure 4 shows that at least seven sources existed at different times. Five of the sources were moving with velocities ranging from 50 to 200 km/s. Except for source 6 the moving sources could have originated from a common position between the two stationary sources (1

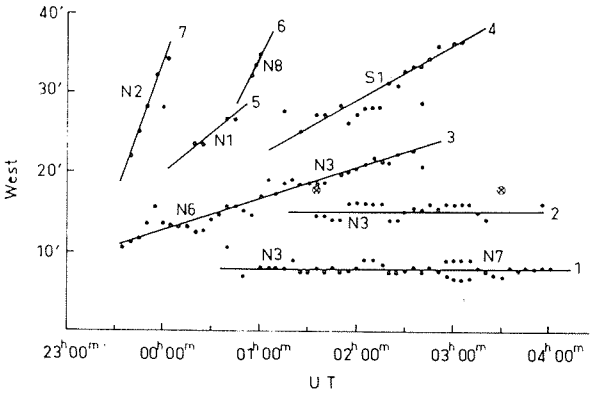

Figure 4. Source positions west of the centre of the Sun as a function of time during the late phase of the event of 1971 January 24/25. Symbols such as N3 show the north-south position coordinate in minutes of arc. Two type III bursts are indicated by ⊗.

and 2) at the time of flare commencement. The degree of L.H. circular polarization of the sources 1, 2 and 4 to 6 was consistently 80-90%, whilst that of source 3 increased from an initial value of ≈40% to about 80% during the period 23^h35^m to 00^h00^m U.T. Source 7 was too weak relative to the other close sources for reliable polarization measurements, and both type III sources at 01^h35^m and 03^h30^m were unpolarized.

Ionospheric refraction was apparently quite constant during the existence of the jet as most sources maintained a steady north-south position within 2′ arc. The source at 8′ W. also maintained its east-west coordinate within 2′ arc.

(b) *Analysis*

On viewing the heliograph film at speed the authors noted a number of occasions on which the sources in the jet seemed to brighten in succession from east to west. The brightenings typically doubled the flux density of each source in turn; each brightening lasted for one or two seconds and the sequence took ≈7 sec to complete. One such occurrence is shown in Figure 2 (b) in which all four sources brightened. On other occasions only three of the sources brightened. In the period 01^h55^m to 02^h25^m, for most of which suitable data were available, there were three occurrences of four sources brightening in sequence and eight when only three sources brightened.

Assuming the sequential brightenings to be a real effect, we calculated the projected velocity of the causal agent. Velocities of 0.4c to 0.6c (c is the velocity of light) are typical of the 11 cases. The true velocity will be greater than the projected velocity by an amount depending on the geometry.

We tested for coincidences between jet source brightenings and type III bursts to see if the energy range of the jet source electrons (≳100 keV) extended down to typical type III values (≈40 keV). Only two out of seven weak type III events corresponded in time with brightenings. There is certainly no close association.

(c) *Discussion*

The radiation mechanism for the moving sources in the jet is presumably synchrotron radiation (in the x-mode), since most of the sources occur at positions far above the 80 MHz plasma level. The high degree of polarization is compatible[7] with the mildly relativistic energies of the jet source electrons; it also requires small viewing angles with respect to the magnetic field and would favour anisotropic and asymmetric pitch angle distributions. Since all sources are of like polarity it is probable that the electrons are travelling along open field lines.

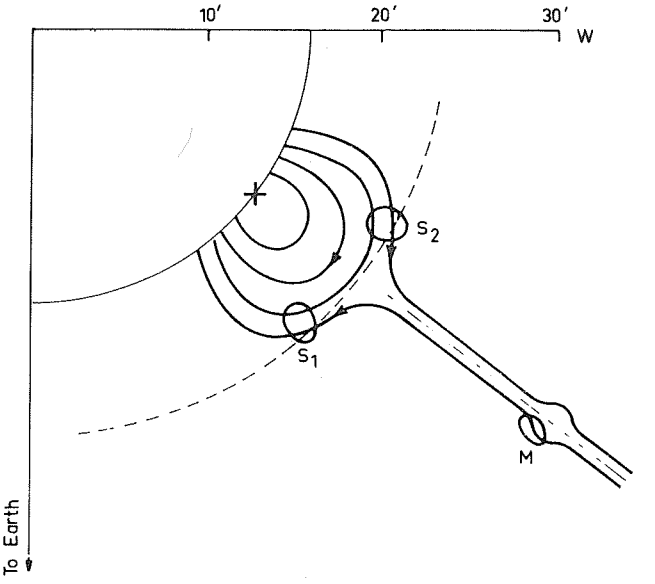

Figure 5. A model of the magnetic field for the event of 1971 January 24/25. The view represents a cross section through the active region in a plane parallel to the equatorial plane. The photosphere is seen as a full line quadrant, the 80 MHz plasma level as a dashed curve, the neutral sheet as a dash-dot line, and X marks the site of the flare. Possible stationary sources are denoted by S1 and S2 and a moving source by M. A view in a higher, or lower, plane may show a different moving source.

The stationary sources are probably continuum storms radiated at the plasma level (in the o-mode). Since they have the same (L.H.) polarization as the moving sources the magnetic fields through the stationary and the moving sources must have opposite line-of-sight components.

For the moving sources we hypothesize a disturbance moving outward along the very extended neutral sheet in a helmet structure above the unusually long sunspot group. The disturbance, which could be a plasmoid ejected by the flare or a loop retracting outwards after reconnection of field lines in the neutral sheet, travels with the local Alfvén velocity. Energetic electrons moving on field lines close to the neutral sheet see the disturbance as a bulging region of higher magnetic field. The higher field, and perhaps also the wider range of possible viewing angles, result in the observer seeing much enhanced radiation over that from other points on the electrons' trajectory. This radiation would correspond to a moving source. Brightenings of the source are the result of extra electrons with a narrow range of velocity. In order that the brightenings occur with the observed timing the electrons must have energies >50 keV. On the high-energy side, electrons with energies >500 keV would have increasingly directive radiation patterns and may escape observation.

The differing velocities of the moving sources make it unlikely that they follow the same path. In view of the complex nature of the magnetic field in the spot group it is possible that several disturbances, or different parts of a broad disturbance, could be propagating seemingly independently in different parts of the neutral sheet. The various projected velocities could arise from different Alfvén velocities (due to differences in the local magnetic field and electron density), or from differing directions of motion.

One such moving source (designated by M) is illustrated in Figure 5. The solid lines represent the magnetic field, viewed from the north pole, in a section parallel to the equator through the region of most intense magnetic field. Also marked on the solid lines by S1 and S2 are the positions at which continuum storms could exist. It is suggested that S1 corresponds to the heliograph source 1 and that source 2, which is also stationary, could be either S2 or a moving source travelling directly along the line of sight.

For the type III bursts which occurred during the jet phase to be visible to the west of sources 1 and 2, as observed (see Figure 4), the plasma level in the region where the type III bursts originated must be considerably higher than in the section shown, or the bursts could be harmonic radiation from the 40 MHz plasma level. Both are possible in the present model.

The injection point of electrons must be situated so as to excite any or all of the sources. A position near the photosphere below S1 is a suitable point. Which sources would be excited by a particular group of electrons would depend on the combination of lines along which the electrons were injected into the complex network of closed and open fields.

The model outlined above appears to account at least qualitatively for all the significant observations.

The authors wish to thank Miss Marie McCabe (University of Hawaii) for her generosity in supplying optical data, the staff of the Culgoora Observatory, and Dr S. F. Smerd for his valuable contributions.

[1] Solar Geophys. Data, No. 318 Part I, U.S. Dept. Commerce, (February 1971)
[2] Wild, J. P. (ed.), '*The Culgoora Radioheliograph*', *Proc. IREE Aust.*, **28**, No. 9 (1967).
[3] Wild, J. P., *Solar Phys.*, **9**, 260 (1969).
[4] Kai, K., *Solar Phys.*, **11**, 310 (1970).
[5] Wild, J. P., *Proc. ASA*, **1**, 365 (1970).
[6] Dulk, G. A., *Aust. J. Phys.*, **24**, 177 (1971).
[7] Dulk, G. A., *Proc. ASA*, **1**, 372 (1970).

Radio Bursts Associated with Solar Proton Flare on January 24, 1971

by

Kunitomo Sakurai
Radio Astronomy Branch
Laboratory for Extraterrestrial Physics
NASA/Goddard Space Flight Center
Greenbelt, Maryland 20771

1. Introduction

Solar flares which produce high-energy particles, so-called solar cosmic rays, generally accompany radio bursts of spectral type IV. It is known that the microwave component of these bursts is a good indicator of the generation of high-energy particles in solar flares [e.g., Kundu and Haddock, 1960; Sakurai and Maeda, 1961].

In this paper, we will consider some characteristics of solar radio bursts as obtained by satellite and ground-based observations on January 24, 1971. In case of the solar flare on January 24, 1971, the result of decametric radio bursts as observed at the Clark Lake Observatory only will be shown.

2. Radio Bursts at Decametric Frequencies on January 24, 1971

The solar flare which produced solar cosmic rays occurred at 2307 UT on January 24, 1971. Its location was N19 and W50 in latitude and longitude, respectively. Type II and IV radio bursts at decametric frequencies were associated with this flare as shown in Figure 1. These were observed at the Clark Lake Observatory. Type II and IV radio bursts at these frequencies started at about 2316 and 2324 UT, respectively. Thus, about ten minutes after the start of the flare, these radio bursts started.

3. Discussion

It is known that intense emission of type IV radio bursts at decametric frequencies is a good indicator of the occurrence of solar proton events [e.g., Sakurai and Kita, 1966]. In the case of the January 24, 1971 event, an intense decametric burst was observed as shown in Figure 1. Although the data on high frequency radio emission are not available, this burst may have been accompanied by intense type IV radio bursts at microwave and decimetric frequencies.

4. Acknowledgement

I would like to thank Dr. R. G. Stone and Dr. J. Fainberg for their supply of the valuable data on solar radio emission for this event. Comments by Dr. J. Fainberg are appreciated.

REFERENCES

KUNDU, M. R. and F. T. HADDOCK 1960 Nature, 186, 610.

SAKURAI, K. and K. KITA 1966 Pub. Astron. Soc. Japan, 18, 355.

SAKURAI, K. and H. MAEDA 1961 J. Geophys. Res., 66, 1966.

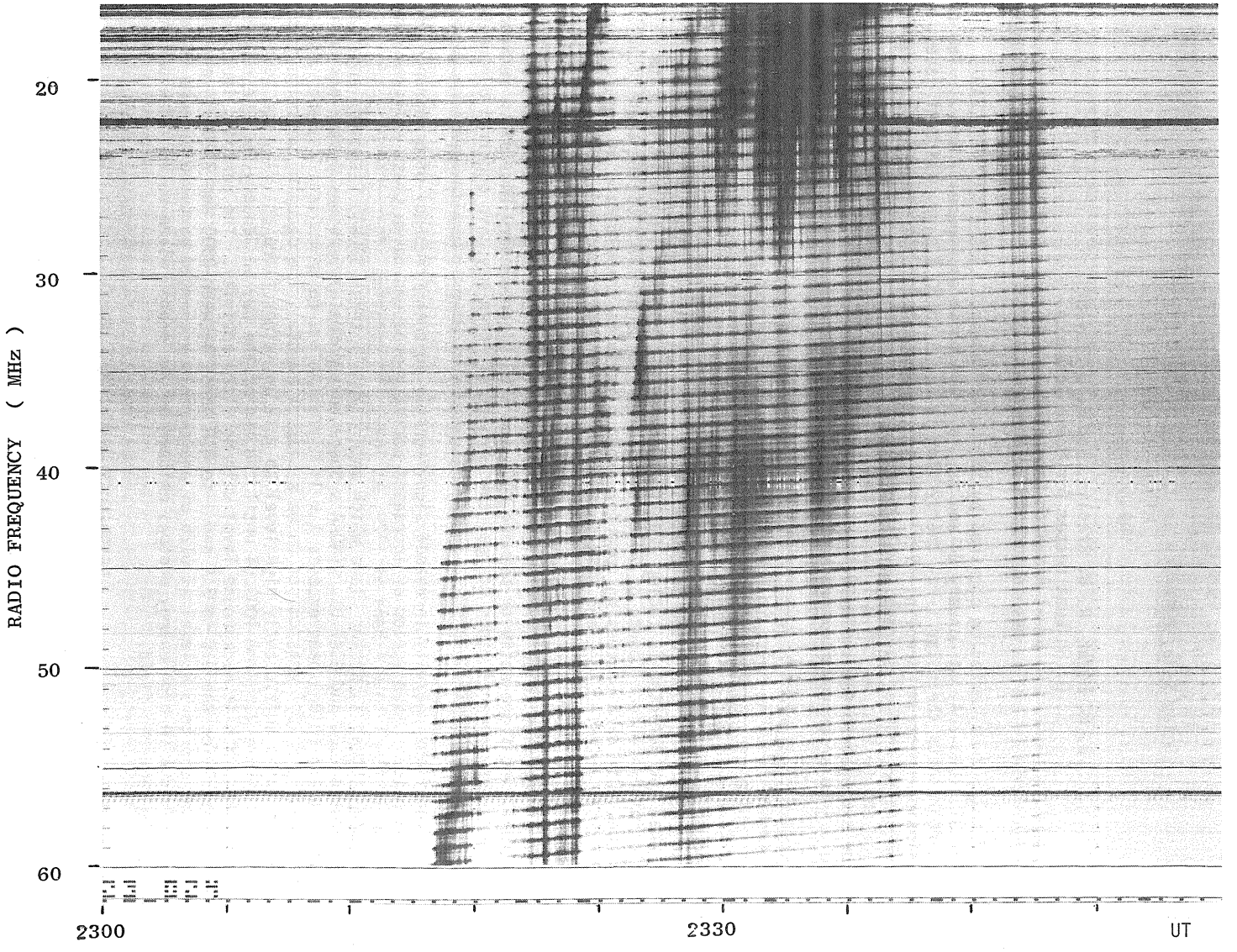

Fig. 1. Record of decametric radio bursts on January 24, 1971.

4. SPACE OBSERVATIONS

Solar X-Ray Emission on January 24-25, 1971

by

D. M. Horan, R. W. Kreplin, and R. G. Taylor
E. O. Hulburt Center for Space Research
Naval Research Laboratory
Washington, D.C. 20390

The records of solar X-ray emission obtained by the Naval Research Laboratory's SOLRAD 9 satellite (Explorer 37, 1968-17A) on January 24 and 25, 1971 are shown as Figures 1 and 2. The top curve on each plot represents the solar X-ray energy flux in the 8 to 20 Å band. In both cases, a gray-body solar emission spectrum [Kreplin, 1961] with a 2×10^6 °K color temperature was assumed in converting from ionization chamber current levels to energy flux units. The third curve from the top represents solar energy flux in the 0.5 to 3 Å band based on a gray-body emission spectrum with a 10×10^6 °K color temperature for the emitting solar region. The curve is quite intermittent because the 0.5 to 3 Å solar energy flux is usually below the threshold level of the detector.

The X-ray emission is plotted in units of ergs/cm^{2}sec on a logarithmic scale. The abscissa is linear with the integers denoting hours in Universal Time (UT). Charged particle interference with the X-rays sensors, which can cause the plotted flux values to be higher or lower than the actual flux, is indicated by the lowest data curve. The ionization chamber current caused by the charged particle background is digitized and recorded as a "count." The number of "counts" plotted is linearly related to the current generated in the 0.5 to 3 Å ionization chamber by penetrating charged particles when the detector is facing away from the sun. Counts of 10 to 15 indicate negligible particle interference. Counts of 20 to the maximum value of 127 indicate significant particle interference. The data processing computer program inhibits the plotting of data obviously contaminated by particle interference, and this feature causes randomly spaced data gaps of 30 minutes duration or less.

In Figure 1, the record of solar X-ray emission in the 1 to 8 Å and 8 to 20 Å bands shows a high background but virtually no flare activity between 0000 and 1150 UT on January 24, 1971. Between 1150 and 1706 UT there were several minor flares; the largest of which may have occurred during the 1418 to 1453 UT darkness interval.

After 1706 UT, the flare activity increased significantly in both frequency of occurrence and magnitude of X-ray emission. This period of increased activity produced three Class M flares which reached peak emission in the 1 to 8 Å band at 1729, at 1820, and sometime after 2049 UT; and culminated in the large, Class X, proton flare which saturated all three SOLRAD 9 sensors and reached a peak flux level between 2323 and 2347 UT. (NOAA's Space Environmental Services Center has defined a flare whose flux in the 1 to 8 Å band exceeds 1×10^{-2} ergs/cm^{2}sec to be a Class M event, and a flare whose flux exceeds 1×10^{-1} ergs/cm^{2}sec to be a Class X event.) The decaying emission from the Class X flare continued at a sufficiently high level to mask any minor flare activity for several hours into January 25, Figure 2. From 1000 UT until the end of the day on January 25, the record of solar X-ray emission shows a high background level with no flare activity. The periodic increases in the plotted X-ray level for the 0.5 to 3 Å and 1 to 8 Å bands between 0300 and 1120 UT, and the apparent decrease in the 0.5 to 3 Å level at 0125 UT are certainly charged particle effects in the detectors, and probably due to high energy protons emitted by the proton flare rather than particles trapped in the Earth's magnetic field.

REFERENCES

HORAN, D. M. and R. W. KREPLIN 1972 The SOLRAD 10 Satellite, Explorer 44, 1971-058A, NRL Report # 7408.

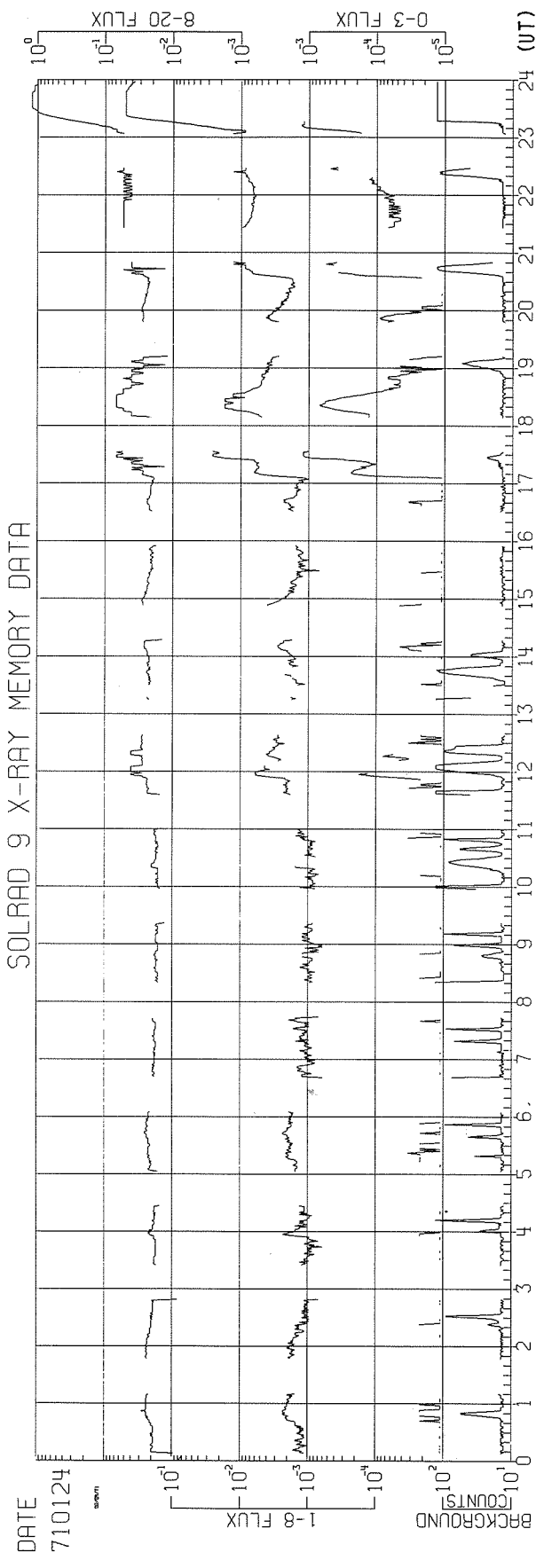

Fig. 1. Solar X-ray flux on January 24, 1971.

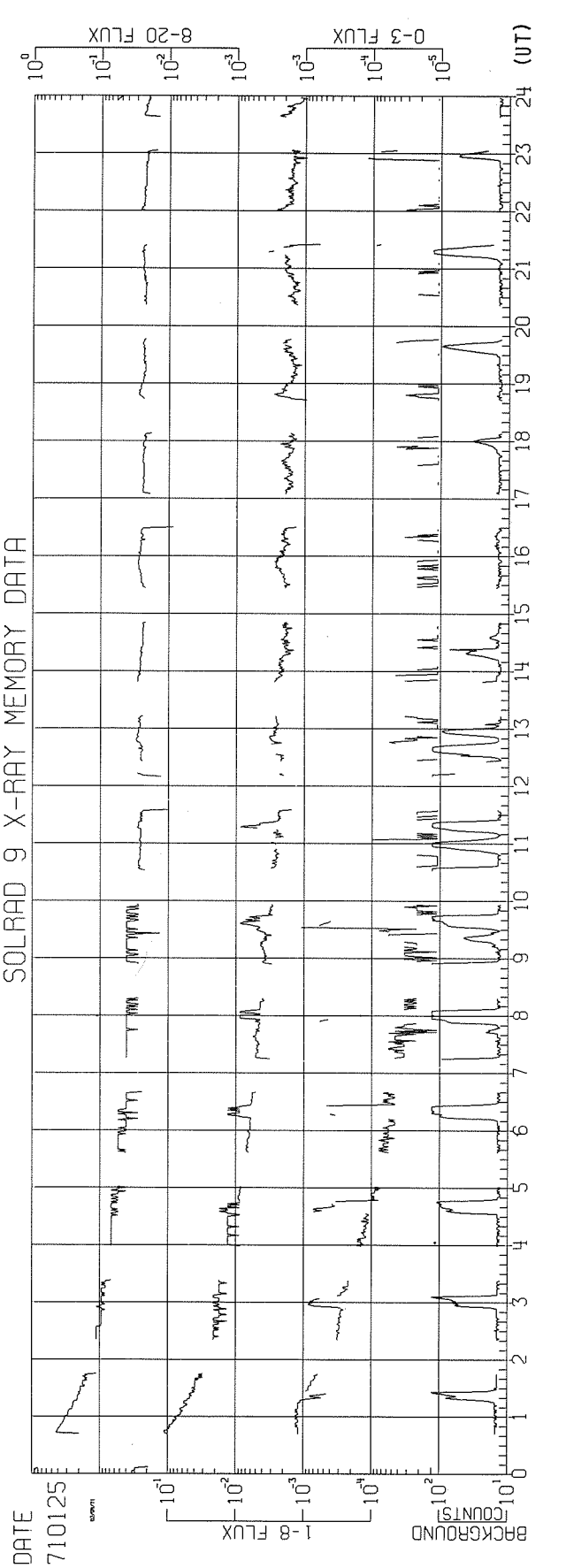

Fig. 2. Solar X-ray flux on January 25, 1971.

IMP V Observations on the Solar Flare Particle Events of January 24 and September 1 of 1971

by

M. Van Hollebeke, J. R. Wang, and F. B. McDonald
NASA, Goddard Space Flight Center, Greenbelt, Maryland

Introduction

Detailed observations of the solar particle events of January 24 and September 1, 1971, were made with the Goddard Cosmic Ray Experiment on IMP V. These were among the larger events of the current cycle. Both exhibited a rapid rise and a lengthy decay that extended over a three-week period. Detailed examination of the arrival times, and proton/alpha ratio, however, show important differences.

The detector system provides spectral information on 0.5-20 Mev electrons, and 1-80 Mev/nucleon proton and helium nuclei. In particular the experiment is designed to study both galactic and solar cosmic rays and therefore gives rather precise onset times for the various energy intervals. Table 1 gives the particle onset times as well as some solar parameters associated with the two flare events.

Table 1. Details of the Flares

	Event	
	Jan. 24, 1971	Sept. 1, 1971
Particle Onset near Earth (U.T.):		
0.5-1 Mev electron --	2333 $\pm$ 3	2002 $^{+0}_{-3}$
19-80 Mev proton --	0001 $\pm$ 3 (Jan. 25)	2055 $\pm$ 3
4-19 Mev proton --	0031 $\pm$ 3 (Jan. 25)	2130 $\pm$ 3
Flare:		
McMath Plage --	11128	11482*
Class --	3B	
Position --	N19W49	~S12W120*
Hα (U.T.)		
Start --	2300	
Max. --	2320	
End --	0020 (Jan. 25)	
Type II onset (U.T.) --	2316	1934
Type IV onset (U.T.) --	2310 2320	1937
2-12 Å X-ray (U.T.):		
Onset --	2307	1930
Max --	2329	2009
Remark --	Strong	Weak
Geomagnetic Activity:		
Onset SC (U.T.) --	0430 (Jan. 27)	1645 (Sept. 4)

*Assumed origin of the associated flare.

The Event of January 24, 1971

The first 0.5-1 Mev electrons, 19-80 Mev and 4-19 Mev protons associated with this flare were observed to arrive at 2333 UT (Jan. 24), 0001 UT (Jan. 25) and 0031 UT (Jan. 25), respectively. The intensity-time profiles of these particles are plotted in Figure 1. These data points are averages over 1 hour interval. The initial rise-time was very rapid, and the detector observing electrons and 19-80 Mev protons saturated about 2-3 hours after the onset. The 6-19 Mev proton intensity reached a broad maximum around 2300 UT on January 25. Both protons and electron intensities decayed more or less exponentially during the January 26-January 30 period. The decay time constants of 0.5-1 Mev electrons, 19-80 Mev and 6-19 Mev protons were ~28 hours, ~20 hours, and ~17 hours, respectively. After about January 30, the decay times for all particles either became very large or the decay mode was not exponential. The entire event lasted for more than 3 weeks. There was a sudden commencement at ~0430 UT on January 27, which produced only small effects in the particle intensities.

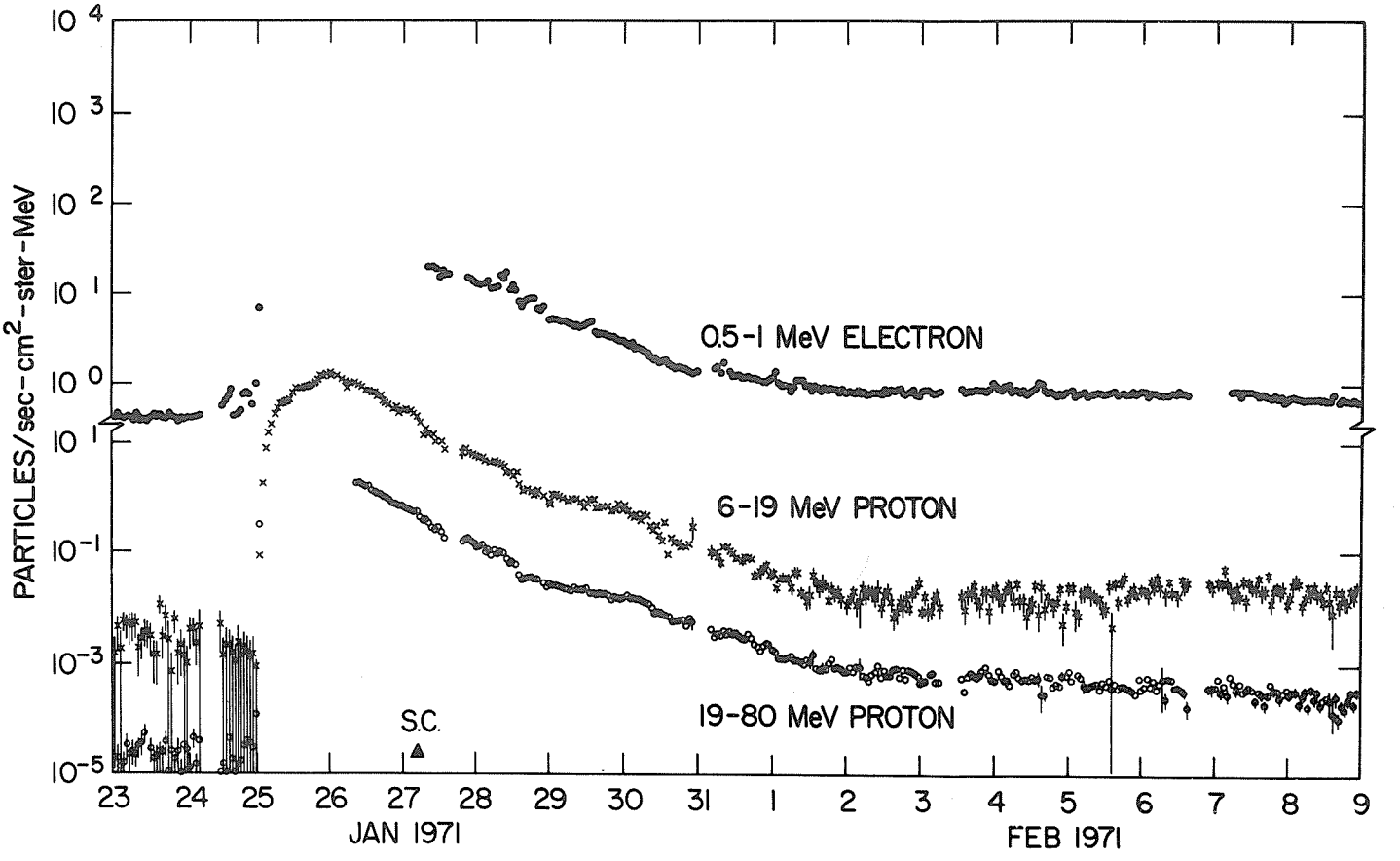

Fig. 1. Intensity-time variations of 0.5-1 Mev electrons, 6-19 Mev and 19-80 Mev protons for the flare-associated event of January 24, 1971. The data were averaged over 1-hour intervals.

Figure 2 shows both the proton and alpha differential energy spectra averaged over 24 hours during the decay phase. It is clear that the proton intensity distribution does not obey power-law-in-energy representation over the entire energy range of 1-80 Mev. In the limited energy range of 4-20 Mev, the proton spectrum could be described by the form of E^{-n}, with n = 2.7. On the other hand, the alpha energy spectrum appears to be well represented by $\sim E^{-4.1}$ over the energy range of 1-80 Mev/nuc. The steeper energy spectrum of alpha particles as compared to that of protons for a given flare-associated event has been observed by many authors in the past years [Teegarden, personal communication; Hsieh and Simpson, 1970; Lanzerotti, 1971].

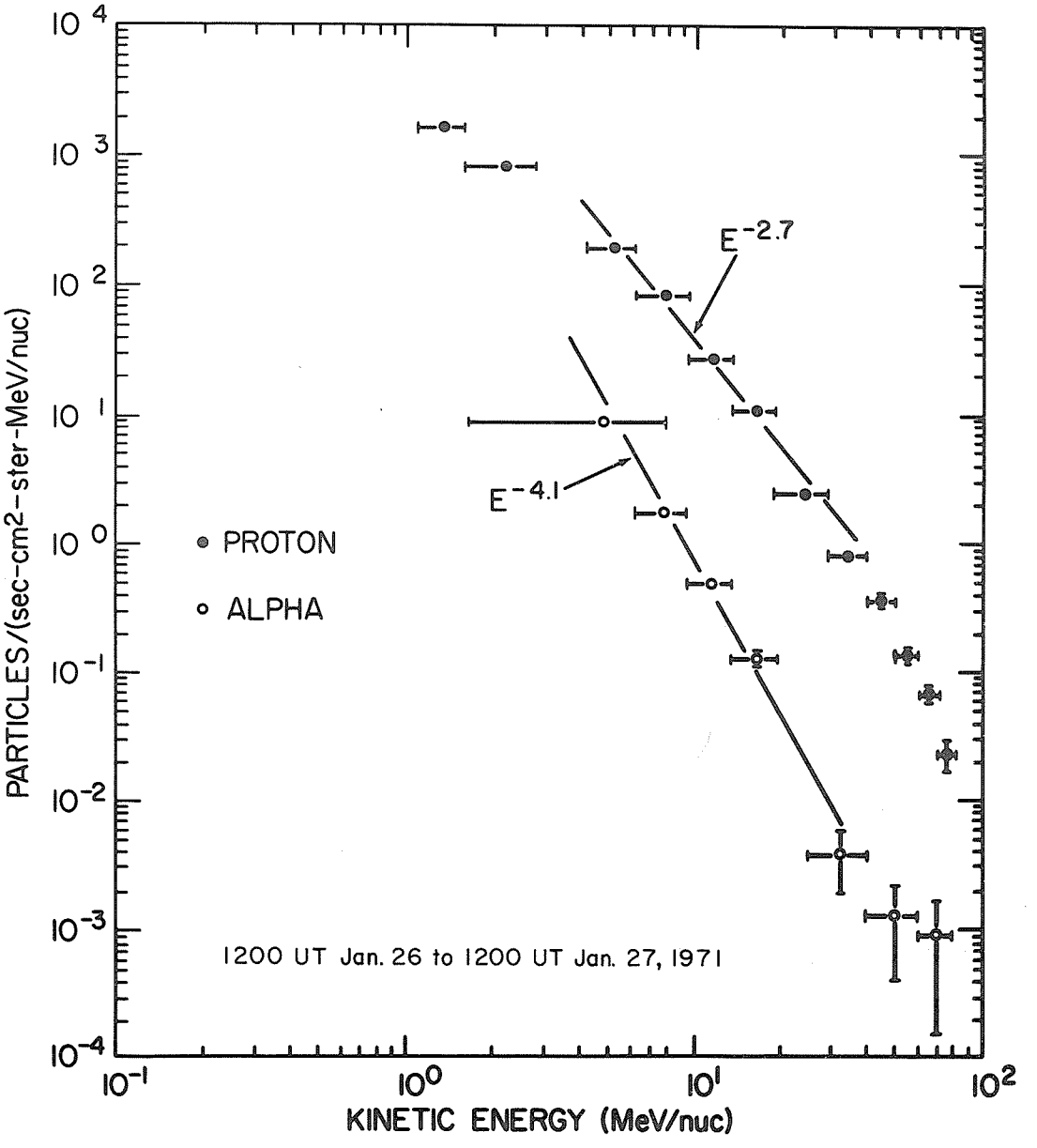

Fig. 2. The differential energy spectra of protons and alpha particles for January 24 event. Both proton and alpha intensities were averaged over 24 hours during the early part of the decay phase.

Figure 3 gives the variations with time of proton intensities in both 6-19 Mev and 19-80 Mev energy intervals and of the proton spectral index in the energy range of 4-19 Mev. The data points in this plot were averaged over a time period of 6 hours. Initially, the spectrum is hard and gradually becomes softer as the intensity increases, the spectral index reaching a maximum value of 2.7. The spectral index then decreases as the intensity steadily decreases. The hardening of the energy spectrum during the decay phase is consistent with the observational results of Rao et al. [1971], that the further away from the population longitude the measurement is made, the harder the energy spectrum one obtains.

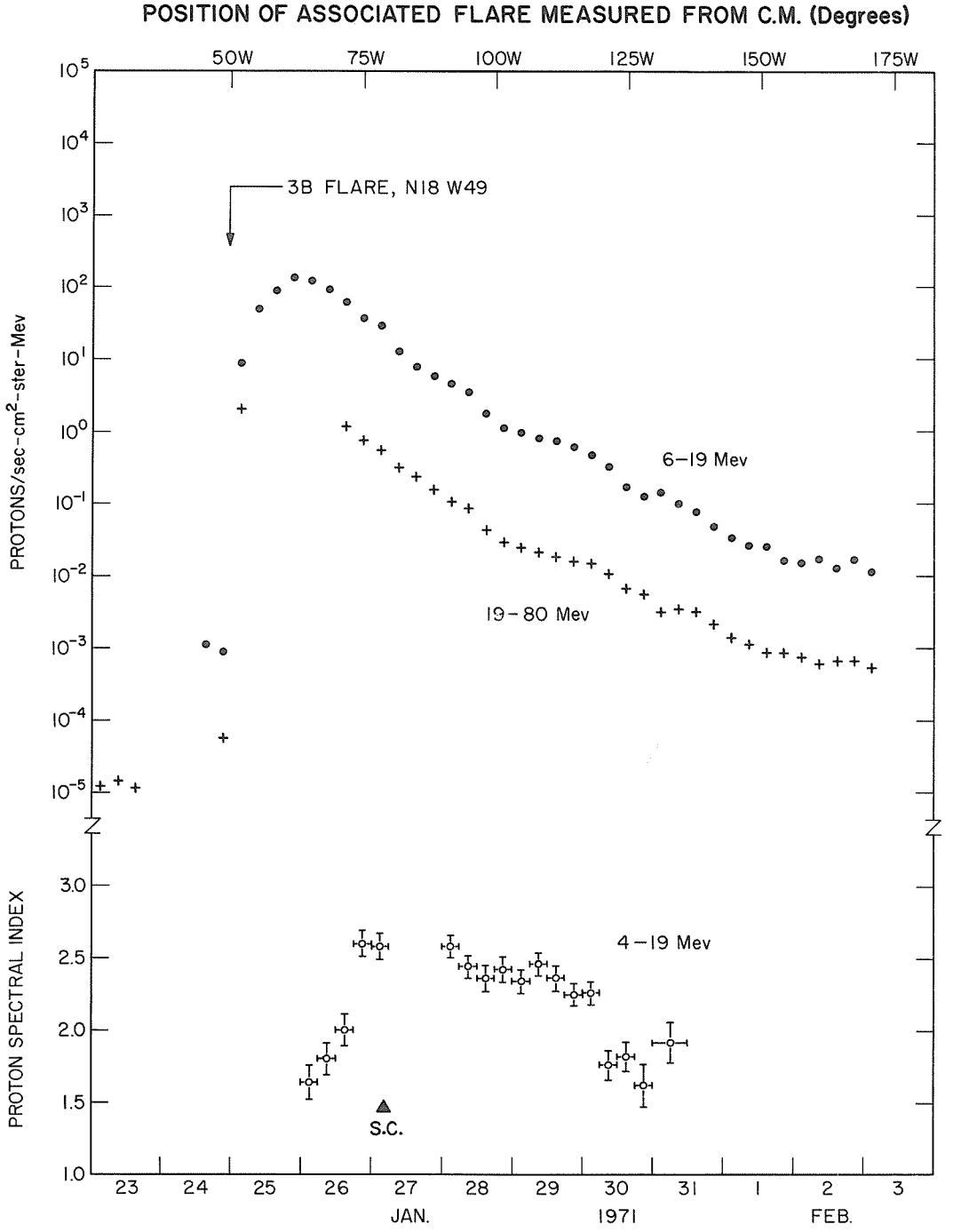

Fig. 3. The 6-hour averages of 6-19 Mev and 19-80 Mev proton intensities are plotted here as a function of both time and the position of the associated flare. The time variation of proton spectral index in the energy range of 4-19 Mev is also shown.

In Figure 4 we have plotted both the 6-19 Mev to 19-80 Mev proton ratio and the proton-to-alpha ratio in the same 6-19 Mev/nuc range as a function of both time and flare position. The 6-19 Mev to 19-80 Mev proton ratio clearly decreases with time in decay phase. This implies that the hardening of proton spectrum with time shown in Figure 2 extends to energy of ~80 Mev. On the other hand, the proton-to-alpha ratio in the energy range of 6-19 Mev/nuc displays an initial rapid rise, and then increases very slowly with time. The ratio has a value of ~50 on January 26 when both proton and alpha intensities begin to decay and increases to ~70 on January 30. The average ratio over the entire event is 56.

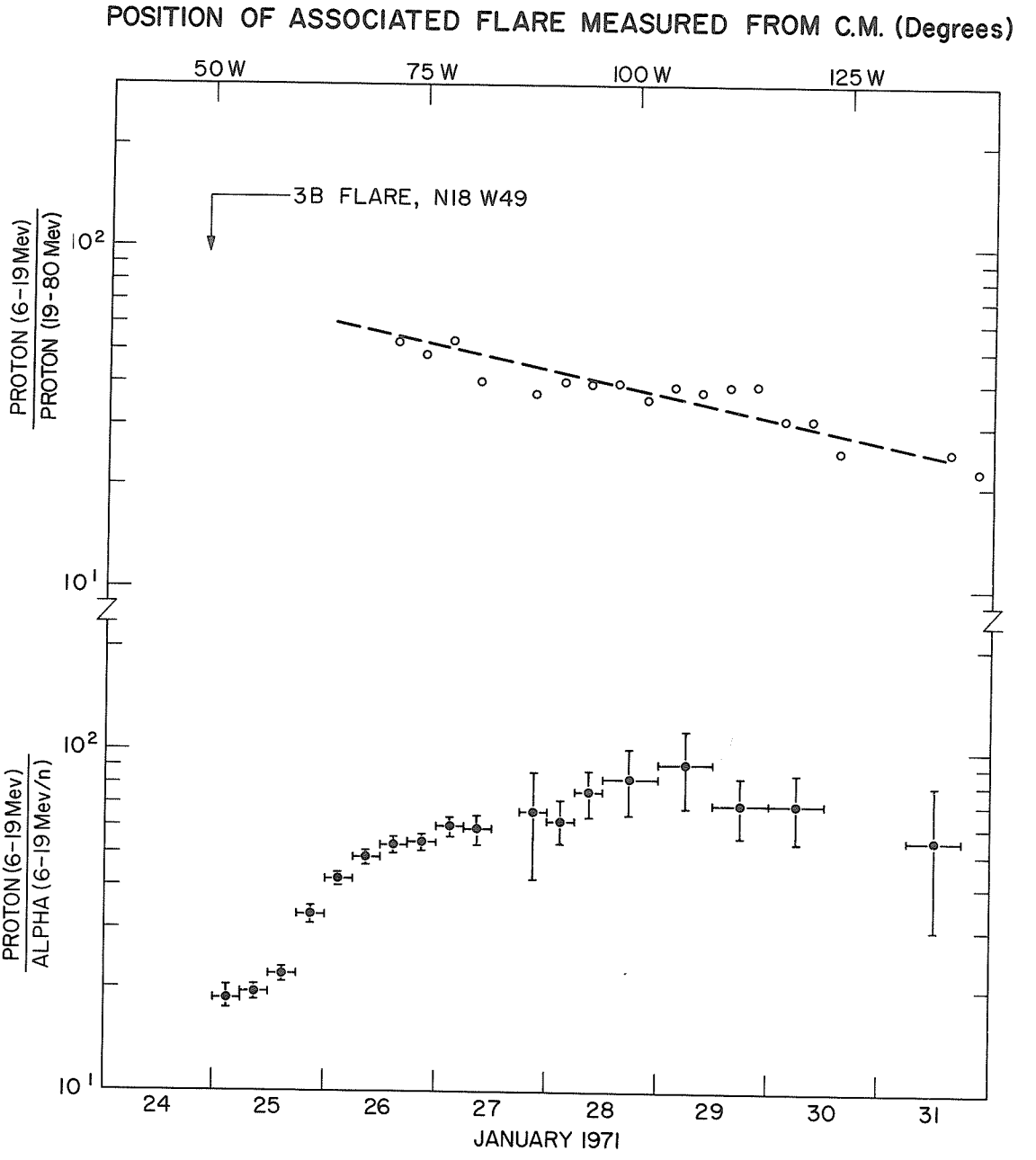

Fig. 4. The intensity ratios of both 6-19 Mev to 19-80 Mev protons and proton-to-alpha particles in the energy range of 6-19 Mev/nuc are plotted as a function of time and flare position. The time variations of the two ratios are quite different during the decay phase.

The Event of September 1, 1971

This particle event could not be positively associated with an optical flare on the visible solar disk. There were Type II, Type IV, and soft X-ray bursts at about the right time which could be related to the flare. Later in this section, we shall present arguments suggesting that this particle event originated from a flare about 30° behind the west limb.

The onsets of 0.5-1 Mev electrons, 19-80 Mev and 4-19 Mev protons were observed to be ~2002 UT, 2055 UT, and 2130 UT, respectively. The intensity-time variations of these particles are shown in Figure 5. The initial intensity rise of 0.5-1 Mev electrons is comparable to that of the January 24 event. However, the protons in both the 19-80 Mev and 6-19 Mev energy intervals appear to have longer initial rise-times than those of January 24 event. The 6-19 Mev proton intensity maximum was reached only some 10 hours after the onset and the time of maximum intensity was better defined when compared to the event on January 24. About 3 days after the particle onsets, there was a geomagnetic storm sudden commencement. The small but distinct simultaneous drop in both electron and proton intensities around ~2000 UT on September 4 perhaps was related to the passage of an interplanetary shock wave. Protons in both 6-19 Mev and 19-80 Mev energy ranges have approximately the same decay time constant of ~21 hours, whereas 0.5-1 Mev electrons have a longer decay time of ~25 hours during the period from ~1200 UT September 2 to ~1200 UT September 6.

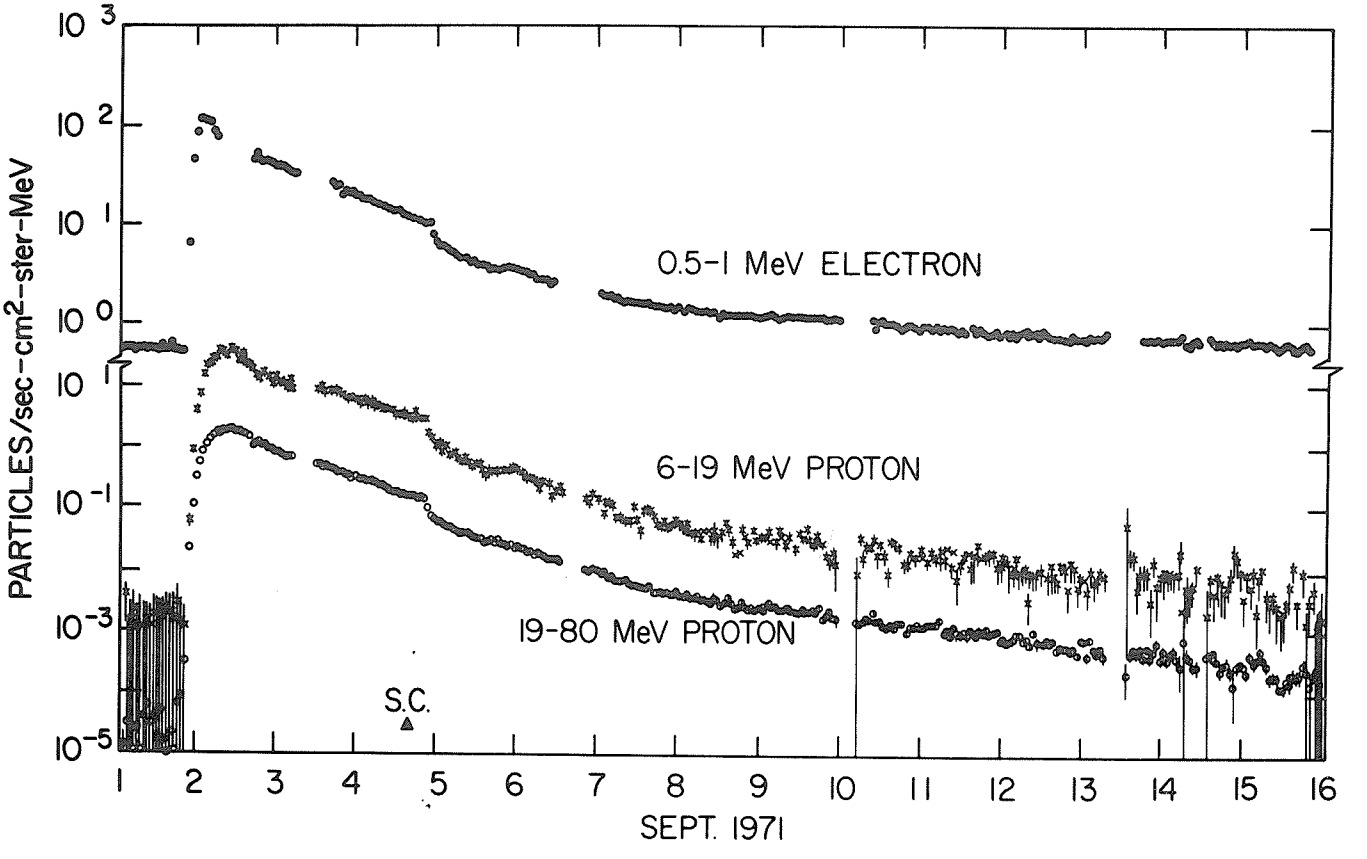

Fig. 5. Intensity-time variations of 0.5-1 Mev electrons, 6-19 and 19-80 Mev protons for the event of September 1, 1971. The data are averaged over 1-hour intervals.

Figure 6 shows both proton and alpha differential energy spectra measured during the time interval from 1200 UT, September 2 to 2400 UT September 3. Again, the alpha particle spectrum appears to obey a power law in energy quite well, whereas the proton spectrum does not. Both proton and alpha energy spectra are harder compared to those of the January 24 event and have spectral indices of ~2.0 and ~2.9, respectively, in the energy range of 4-40 Mev/nuc. Once more, we have steeper alpha spectrum for this event.

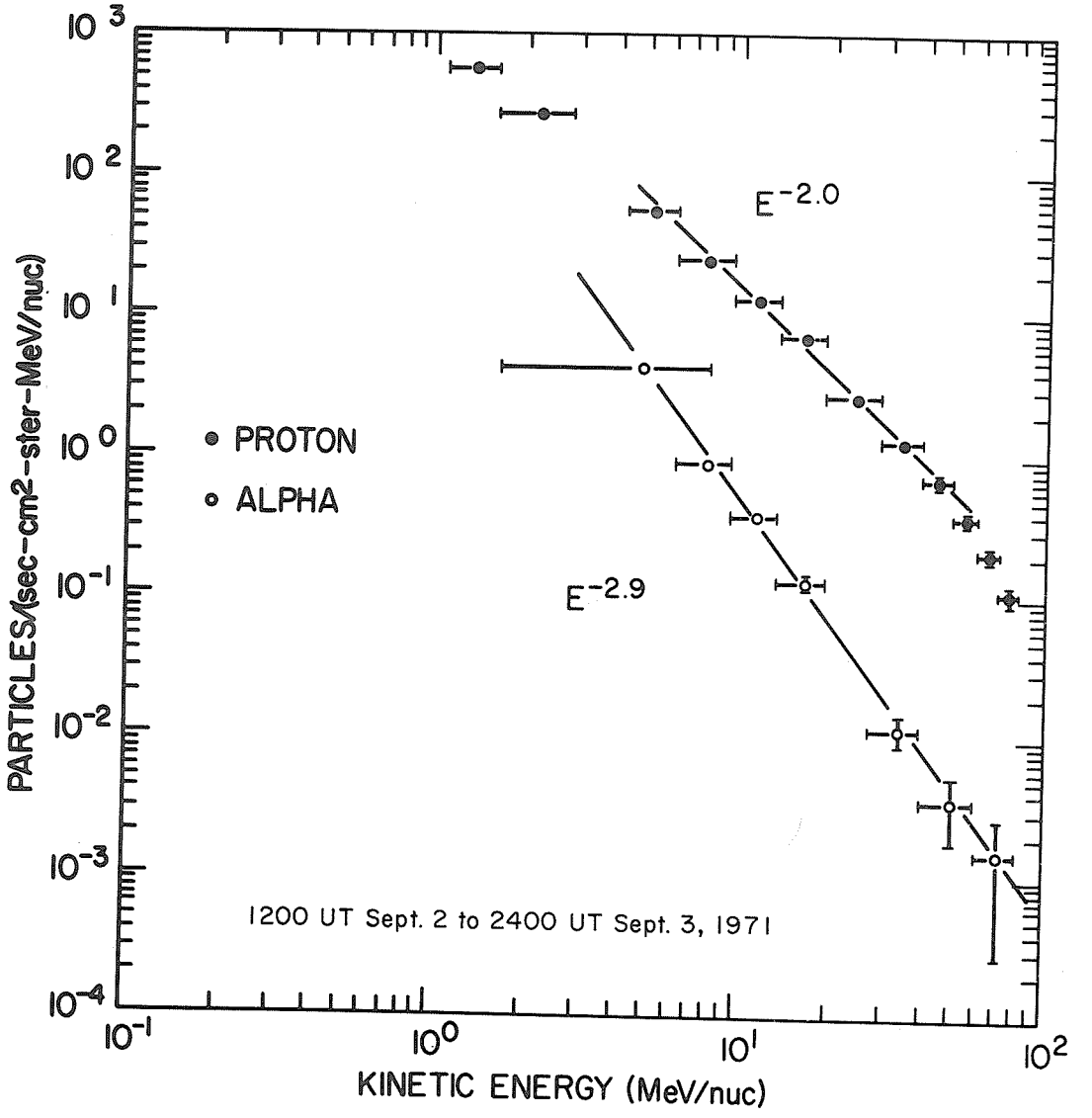

Fig. 6. The proton and alpha differential energy spectra from the event of September 1. Both proton and alpha intensities are averaged over 36 hours during the early part of the decay phase.

The 6-hour averages of 6-19 Mev and 19-80 Mev proton intensities and of the proton spectral index in the energy range of 4-19 Mev are plotted in Figure 7 as a function of time. Clearly, the time variation of the spectral index is quite similar to that of the previous event. During the initial intensity rise, the spectrum becomes softer and softer showing the effect of velocity dispersion. The spectral index reaches a maximum value of ~2 when the particle intensity started to decay. It decreases with time slowly during the decay phase.

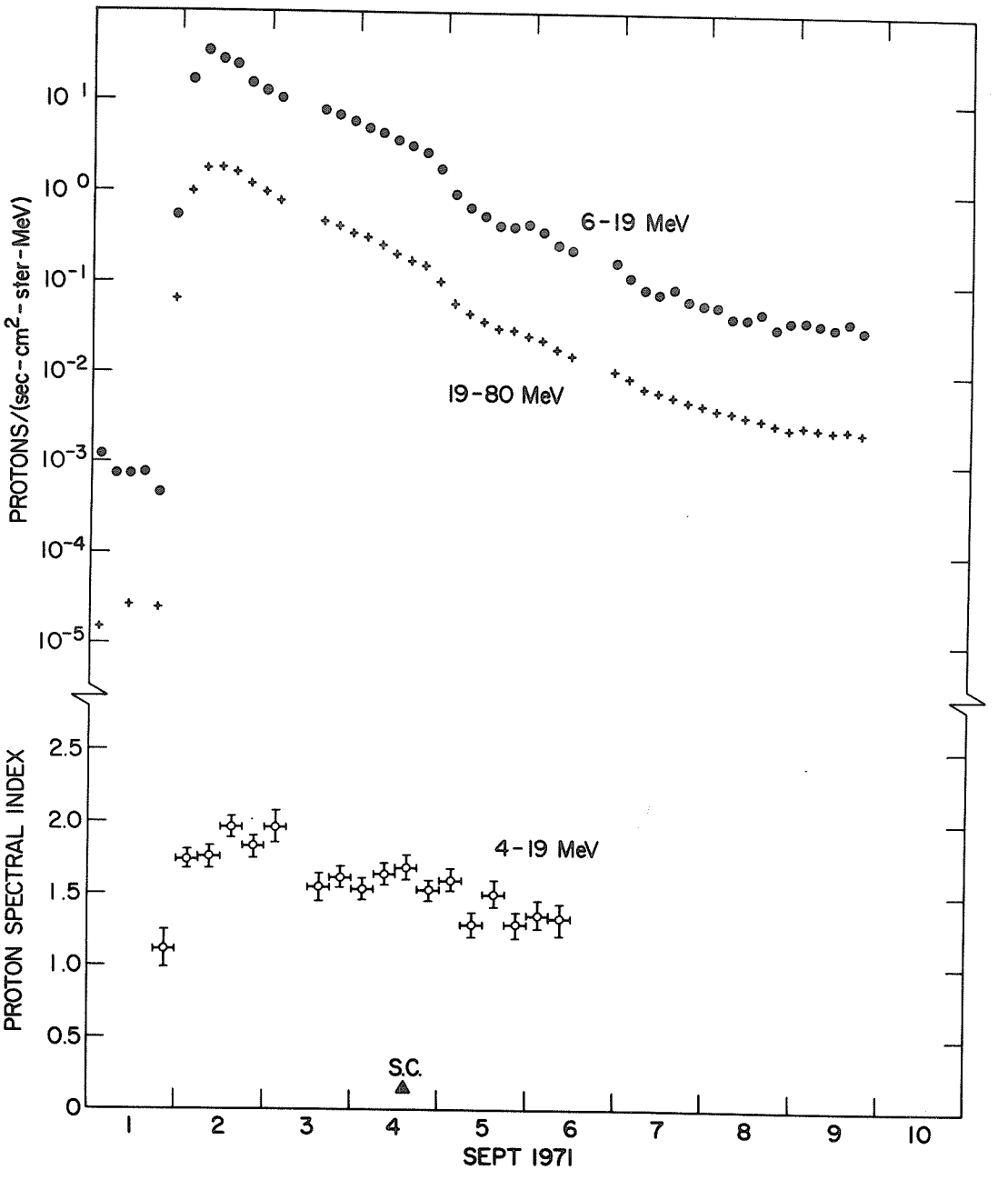

Fig. 7. The 6-hour averages of 6-19 Mev and 19-80 Mev proton intensities are plotted as a function of time. The time variation of proton spectral index in the energy range of 4-19 Mev is also shown.

Figure 8 gives the ratios of both 6-19 to 19-80 Mev protons and proton-to-alpha particles in the energy range of 6-19 Mev/nuc. Although the data points are very scattered, the average 6-19 Mev to 19-80 Mev proton ratio appears to show a general slow decrease with time. This again indicates the general hardening of spectrum up to ~80 Mev, but the rate of this spectral hardening is less rapid than the previous event. The proton-to-alpha ratio on the bottom half of Figure 8 shows a different pattern compared to the event of January 24. During the initial intensity increase, it decreases rapidly. In the decay phase it shows a slight increase with time, although, within errors, a time-independent ratio could also be consistent with data. The overall average ratio is ~40.

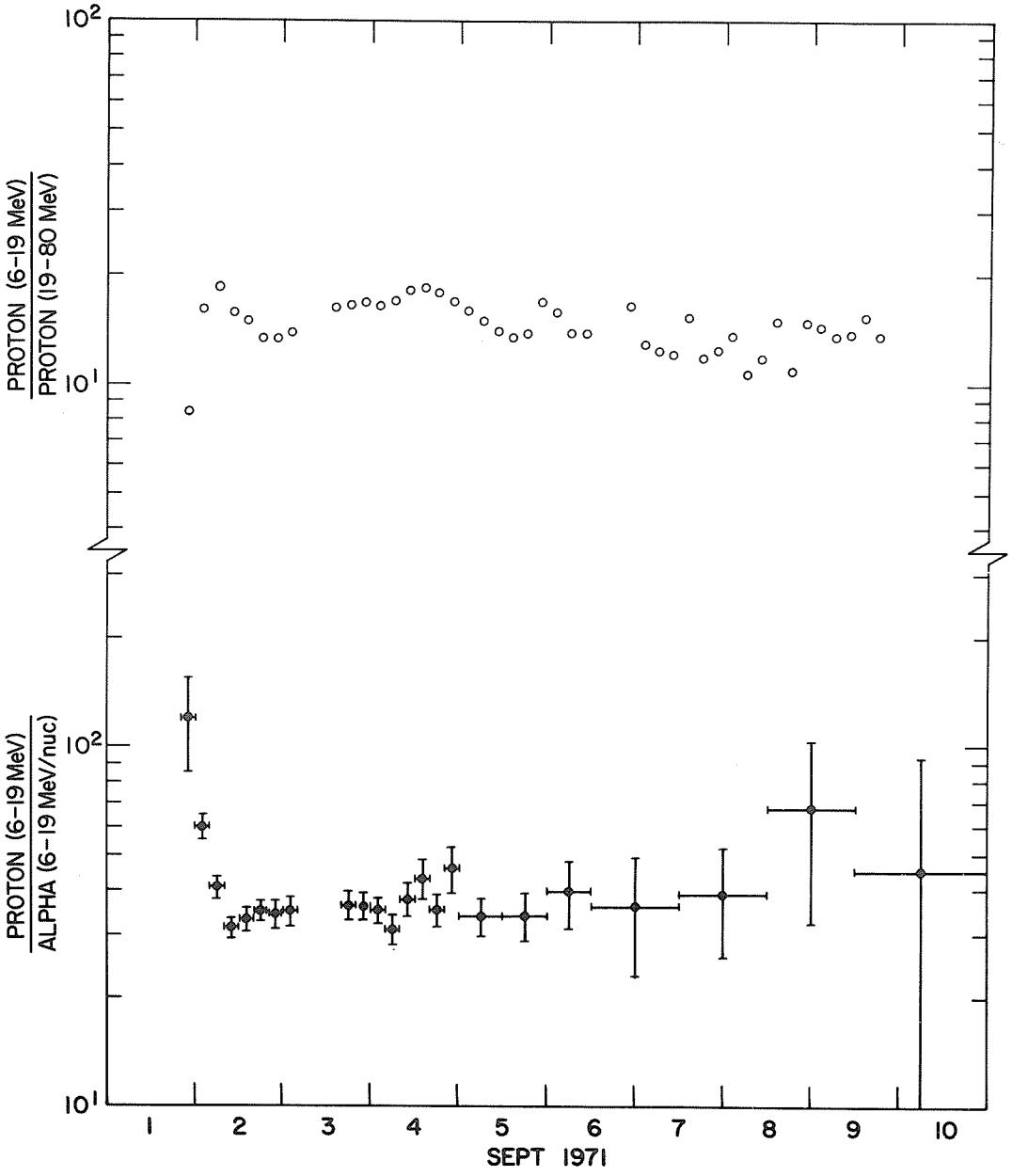

Fig. 8. The intensity ratios of both 6-19 Mev to 19-80 Mev and proton-to-alpha particles in the energy range of 6-19 Mev/nuc are plotted as a function of time. The difference in the time variation of the two ratios, although not as strong as that of January 24 event, is present.

Our belief that this event could be originated from a backside flare is based upon the following observations:

a. The McMath Plage region 11482 was at the position of ~W120 of central meridian at the time of the flare. During its passage on the visible solar disk, the activity of this region, both in terms of optical flare production and flux of 9 cm radio waves was quite outstanding.

b. Within several hours before the time of particle intensity increase, there was no optical flare of reasonable size and brightness which could be considered as being reasonable for the huge particle fluxes observed near the Earth. Although there are both Type II and Type IV radio bursts associated with the particle event, it is possible that these are produced by a flare just behind the limb [Smerd, 1970]. The observed weak soft X-ray burst listed in Table 1 could result from the edge of a large radiation region centered around McMath Plage 11482.

c. Both the proton and alpha particle spectra in the energy range of 4-40 Mev/nuc are hard compared to those of particle events originating from western hemisphere on the visible solar disk. For most cases, we found that protons associated with flares at positions far away from ~W50 generally have harder energy spectrum than those near ~W50 heliolongitude.

d. At the time of this event, the positions of Pioneers 6, 7, 8 and 9 spacecraft relative to the assumed position of the flare (~W120 of central meridian) are at ~E120, ~W50, ~W160 and ~W110, respectively. Therefore, particle intensities observed by Pioneers 6 and 7, as well as IMP V, should be comparable. Those measured by Pioneers 8 and 9 should be somewhat less comparable (after the effect due to interplanetary spiral magnetic field is taken into account). The data from Pioneer 7 were not available during the event [Solar-Geophysical Data]. However, a preliminary comparison of proton intensities measured by IMP V, Pioneers 6, 8, and 9 is consistent with our assumption on the position of the flare.

From all the above considerations, it is very likely that this particle event originates from McMath Plage region 11482 at ~W120.

Discussion

There are several features from the above description which we consider to be significant. First of all, the variation of the proton-to-alpha ratio in the energy range of 6-19 Mev/nuc during the time of initial intensity rise was completely different for the two events. Whereas the ratio increases for the event of January 24, it decreases for the event of September 1. This strongly suggests that the condition of the diffusive region between the source and the Earth may be quite different for the two time periods. In fact, Englade [1971] has pointed out that the parallel diffusion coefficients for protons and alpha particles at a given energy per nucleon depend critically upon both the power-law exponent of the interplanetary magnetic field power spectrum and the correlation length of the field. Thus, depending upon these magnetic field parameters at the time of particle measurements, it is possible to have the proton-to-alpha ratio either increasing or decreasing with time in the early part of the particle event.

Secondly, during the decay phase of both events, while the proton-to-alpha ratio (6-19 Mev/nuc) appears to increase with time, the 6-19 Mev to 19-80 Mev proton ratio is observed to decrease with time. The 6-19 Mev/nuc alpha particles have the same speed as, but higher rigidity than, the 6-19 Mev protons. Compared to 19-80 Mev protons, however, they have about the same rigidity but less speed. If the diffusion coefficient in both solar corona and interplanetary medium is an increasing function of both speed and rigidity, then one expects the proton-to-alpha ratio to stay constant or decrease slightly with time during the decay phase. The observed increase of the ratio with time suggests that, because of the difference in proton and alpha differential energy spectra, the effect of adiabatic deceleration in the interplanetary medium and/or the ionization loss in the solar corona is operating. For the case of adiabatic deceleration, the alpha particles would decay faster than protons because the energy spectrum for alpha particles is steeper than that for protons [Forman, 1971]. On the other hand, the energy loss in the solar corona could also give rise to the observed phenomenon, because (1) for both events, the positions of the associated flares moved away from ~W50 heliolongitude, and (2) the ionization loss is the same for both protons and alpha particles at a given energy per nucleon. As time goes on in the decay phase, we are observing proton-to-alpha ratio at progressively higher kinetic energy (Mev/nuc) as particles travel a longer distance across the solar disk.

Thirdly, if the first arriving particles travel ~1.3 A.U. along the interplanetary spiral magnetic field lines between the sun and the Earth, then the transit times are ~12 min, ~34 min and ~71 min for 0.7 Mev electrons, ~50 Mev and ~11 Mev protons, respectively. The expected transit time difference between 0.5-1 Mev electrons and 19-80 Mev protons is ~22 min, and that between 0.5-1 Mev electrons and 4-19 Mev protons is ~59 min. These time differences are consistent with the observed results of the January 24 event. However, the event of September 1 gives much larger transit time differences of ~53 min and ~88 min than those expected from a simultaneous near-sun release of all flare particles. The onsets of >45 kev electrons (which has the effective energy response of ~100 kev assuming electron energy spectrum of $\sim E^{-3}$) for those events were ~2333 ±2 UT on January 24 and ~2000 $^{+2}/_{-5}$ UT on September 1 [R. P. Lin, personal communication]. These results imply [Sullivan, 1970; Lin and Anderson, 1967] that particles of different species and energy may not be injected into interplanetary medium simultaneously. It is not completely clear whether this non-simultaneous particle injection is due to the evolutionary particle acceleration [Sullivan, 1970] or the diffusion-storage of the energetic particles in the solar corona. Undoubtedly, this phenomenon deserves more detailed study.

REFERENCES

ENGLADE, R. C. 1971 J. Geophys. Res. 76, 768

FORMAN, M. A. 1971 12th Intern. Conf. on Cosmic Rays, 2, 511

HSIEH, K. C. and J. A. SIMPSON 1970 Ap. J., 162, L191

LANZEROTTI, L. J. 1972 NASA/TM-X02440, 193

LIN, R. P. and D. A. ANDERSON 1967 Solar Physics, 1, 446.

RAO, U. R., K. G. MC CRACKEN, R. P. BUKATA, and E. P. KEATH 1971 12th Intern. Conf. on Cosmic Rays, 2, 519

SMERD, S. F. 1970 Proc. ASA, 1, 305

SULLIVAN, J. D. 1970 Thesis, University of Chicago

1971 Solar-Geophysical Data, 318 Part I, U.S. Department of Commerce, (Boulder, Colorado, U.S.A. 80302).

Energetic Electron and Proton Solar Particle Observations on OGO-5, January 24-30, 1971*

by

H. I. West, Jr., R. M. Buck and J. R. Walton
Lawrence Livermore Laboratory, University of California
Livermore, California 94550

and

R. G. D'Arcy, Jr.
Bartol Foundation of the Franklin Institute
Swarthmore, Pennsylvania 19081

Introduction

Neutron monitors [Solar-Geophysical Data No. 319, Part I, p. 97, March 1971] indicated the arrival of solar particles of cosmic energy at the earth at about 2330 UT January 24, 1971. At that time OGO-5 was outbound on the morning side of the earth. Our instruments on OGO-5 detected the first arrival of solar particles at 2336 UT at which time OGO-5 was located at R = 10.27 R_E, λ_m = 41.6°, ϕ_{GSE} = 254°, λ_{GSE} = 67.5°, ϕ_{GSM} = 262°, and λ_{GSM} = 42.2°, where the coordinates are radial distance, magnetic latitude, solar ecliptic azimuth and elevation, and solar magnetospheric azimuth and elevation. OGO-5 did not return to the magnetosphere until January 27, hence was able to provide uninterrupted coverage during this early evolution of the solar particle event. The data coverage in this report extends through January 30, 1971.

Instrumentation

These data were obtained by the LLL electron and proton spectrometer experiment on OGO-5. The electron analyzer consisted of two magnetic 180°-first-order-focusing spectrometers. Solid state detectors in the focal plane provided both particle detection and secondary energy analysis. Shielded background detectors provided an accurate measure of the background. Data were obtained from energy channels centered at 79, 158, 266, 479, and 822 kev. Channels were also available at 1530 and 2830 kev. However, the 1530-kev channel at this time was somewhat noisy (OGO-5 was launched March 4, 1968) and the 2830-kev channel was at background.

Protons were obtained from a range energy telescope and a single adjacent detector located in the larger of the electron spectrometer magnets in line with the entrance aperture of the electron spectrometer. The electron spectrometer magnet served the dual purpose of electron broom. Energy channels were P_1 (0.1 - 0.15 Mev), P_2 (0.23 - 0.57 Mev), P_3 (0.56 - 1.35 Mev), P_4 (1.35 - 5.4 Mev), P_5 (5.6 - 13.3 Mev), P_6 (14 - 46 Mev), and P_7 (43 - ∿94 Mev). In addition an omnidirectional channel derived from the background detector for the 2830-kev electron channel provided a proton channel O_1 ($\gtrsim$ 100 Mev). The geometrical factors for these channels were (P_1, 2.06 x 10^{-3} cm^2-sr), P_2, 1.3 x 10^{-2} cm^2-sr), (P_3, 1.3 x 10^{-2} cm^2-sr), (P_4, 1.3 x 10^{-2} cm^2-sr), (P_5, 1.25 x 10^{-2} cm^2-sr), (P_6, 1.72 x 10^{-2} cm^2-sr), (P_7, 1.98 x 10^{-2} cm^2-sr), and (O_1, ∿0.6 x 4π cm^2). The logical rearrangement of the various logic elements of the proton telescope allowed the evaluation of the backgrounds but in general the background evaluation was more subjective than for the electron spectrometer.

In order to obtain directional information on the earth-sun oriented satellite, the apertures of the spectrometers were scanned relative to the satellite at 3°/second through an excursion of 230°. The axis of the scan was about the radius vector passing through the center of the earth with the experiment aperture looking out perpendicular to the scan axis.

Since the experiment had been in use 3 years at the time of these observations, the experiments diagnostic procedures were important. An inflight pulse generator insured us that the logic levels were correct and that the logic was functioning properly. In addition the data obtained in the outer radiation belt were credible.

Orbit

At launch on March 4, 1968, OGO-5's orbit was inclined at 31° and perigee and apogee were 1.04 R_E and 24 R_E (geocentric). At the time of these observations the orbit was inclined at 54° and perigee and apogee were 4.8 R_E and 20.2 R_E (geocentric). Table 1 gives the location of the satellite during these observations.

*Work performed under the auspices of the U. S. Atomic Energy Commission funded in part under NASA P.O. S-70014-G.

Table 1

Position of OGO-5

UT	R	λ_m	ϕ_{GSE}	λ_{GSE}	ϕ_{GSM}	λ_{GSM}
2400/24	10.631	41	261	69	265	43
0200/25	12.32	37	291	70	281	48
0400/25	13.81	34	313	67	296	53
0600/25	15.117	32	326	63	313	57
1200/25	17.802	35	344	53	341	52
1800/25	19.739	30	354	41	340	37
2400/25	20.288*	7	359	32	344	28
1200/26	18.097	- 4	7	11	7	11
1800/26	15.179	- 7	12	- 4	13	0
2400/26	10.738	-34	22	-28	31	-16
0200/27	8.882	-45	29	-41	42	-27
0400/27	6.921	-51	50	-60	63	-46
0600/27	5.242	-33	144	-63	130	-56
0724/27	4.815*	- 1	179	-29	175	-29
0800/27	4.935	13	186	-12	185	-13
1000/27	6.327	49	203	32	205	31
1200/27	8.269	62	222	56	226	54
1800/27	13.439	49	306	68	291	52
2400/27	18.939	- 5	3	15	355	15
1200/28	20.162	20	354	36	352	35
1430/28	20.256*	21	356	32	351	31
2400/28	18.647	- 9	4	14	357	14
1200/29	12.751	-29	14	-16	15	-15
1800/29	7.382	-46	40	-56	55	-42
2000/29	5.585	-43	118	-69	104	-47
2142/29	4.846*	-12	175	-31	161	-26
2400/29	5.928	32	197	23	205	13
0200/30	7.806	47	214	51	231	34
0400/30	9.729	49	239	65	251	48
1200/30	15.678	47	326	61	320	59
1800/30	18.383	36	341	50	325	41

* Apogee and perigee.

Electron Observations

OGO-5 was at 10.45 R_E on the morning side of the earth at the start of the event. It had just exited from an encounter with high latitude (λ_m = 42°) plasma sheet particles and from 2336 UT January 24 to 0100 UT January 25 was able to make good electron observations before again encountering plasma sheet particles (11.5 R_E). In general all data obtained during the encounters with particles of magnetospheric origin have been eliminated. At times, even interplanetary, there were occasional gusts of particles in E_1. No attempt was made to preserve the structure in the averaging of the data.

The data average during the period of rapidly changing fluxes at the start was 9.6 minutes, later to be extended to 1.2 hour. The experiment scanned continuously during the six days of observations. No sign of any appreciable deviation from isotropy showed during this period. All data were of course, corrected for backgrounds, the most subjective periods being within a few hours of the start when the relativistic particle fluxes were highest and towards the end of the observations when the solar particle counts were not greatly above background.

The data in Figure 1 show strong time-of-flight effects. This becomes more evident by examining the differential energy spectra in Figure 2. By 2142 UT January 25 a power law spectrum ($E^{-3.00}$) prevailed. After that the spectrum hardened slightly, the exponent being 2.66 at 0400 UT January 27, 2.55 at 0400 UT January 28, and 2.67 at 0300 UT January 29. There is no significant difference between these values.

Proton Observations

The proton results are shown in Figures 3 and 4, Figure 3 giving the time history and Figure 4 integral spectra. Similarly, as for the electrons the data are 9.6 minutes or 1.2 hour averages as the details of the structure dictate. We have not plotted channels P_1 and P_2. These channels often saw gusts of particles and the structure would be lost in the plot. Also there was some anisotropy in the data, the effect being greatest at the lower energies. The background effects for all P-channels have been evaluated and subtracted for both Figures 3 and 4. For O_1, the galactic background level of 3.1 counts/sec was included in Figure 3 but was subtracted for Figure 4. Similar to the electrons these data show strong time-of-flight effects.

Discussion

A periodic structure ($\sim$ 5 hours) shows up in both the electron and proton data for the first day after the onset of arrival of the particles. Since the periodicity is not dependent upon energy or type of particle the data suggest a filamentary structure in the interplanetary medium.

Early on January 27 a Forbush decrease began [Solar-Geophysical Data No. 319, Part 1, p. 98, March 1971] terminating towards the end of January 29. Possibly the drop in the flux of the more energetic protons (including the > 100 Mev-channel) starting $\sim$ 0400 UT January 27 is associated with the Forbush decrease. However, at this time OGO-5 was well inside the magnetosphere ($\sim$ 7 R_E) encountering trapped radiation between 0630 UT and 0900 UT. The solar proton flux continued to decrease until $\sim$ 1500 UT (R = 11.6, λ_m = 44°, ϕ_{GSM} = 267°, and λ_{GMS} = 60°). It is possibly significant that as the flux returned to its original decay curve at 2300 UT (R = 15.4, λ_m = 36°, ϕ_{GMS} = 302°, λ_{GMS} = 44°) the directional distribution of the protons changed from isotropy to a modulation in the OGO-5 data of $\sim$ 4/1. The data as averaged at this time (in Figure 3) reflect, predominately, the flux of particles from the sunward direction. At this time we can be reasonably assured that OGO-5 was outside of the magnetosphere. It would appear that the flux of protons in the magnetosphere more nearly followed the flux of protons directed towards the sun than away from the sun. The solar protons stayed modulated until $\sim$ 1300 UT January 28 (R = 20.2, ϕ_{GSE} = 356°, λ_{GSE} = 33°). Possibly some of the drop in counting rates at this time may have been due to a loss of the most advantageous look direction. During the solar particle event the electrons were isotropic and showed no effects during the magnetospheric encounters, except of course, when trapped radiation or gusts of plasma sheet radiation were encountered. These radiations were easily detected and excluded from the plot in Figures 1. It would appear that when properly analyzed these solar particle data will have something to say about magnetospheric entry and clearly they can contribute to our knowledge of the interplanetary transport of energetic charged particles.

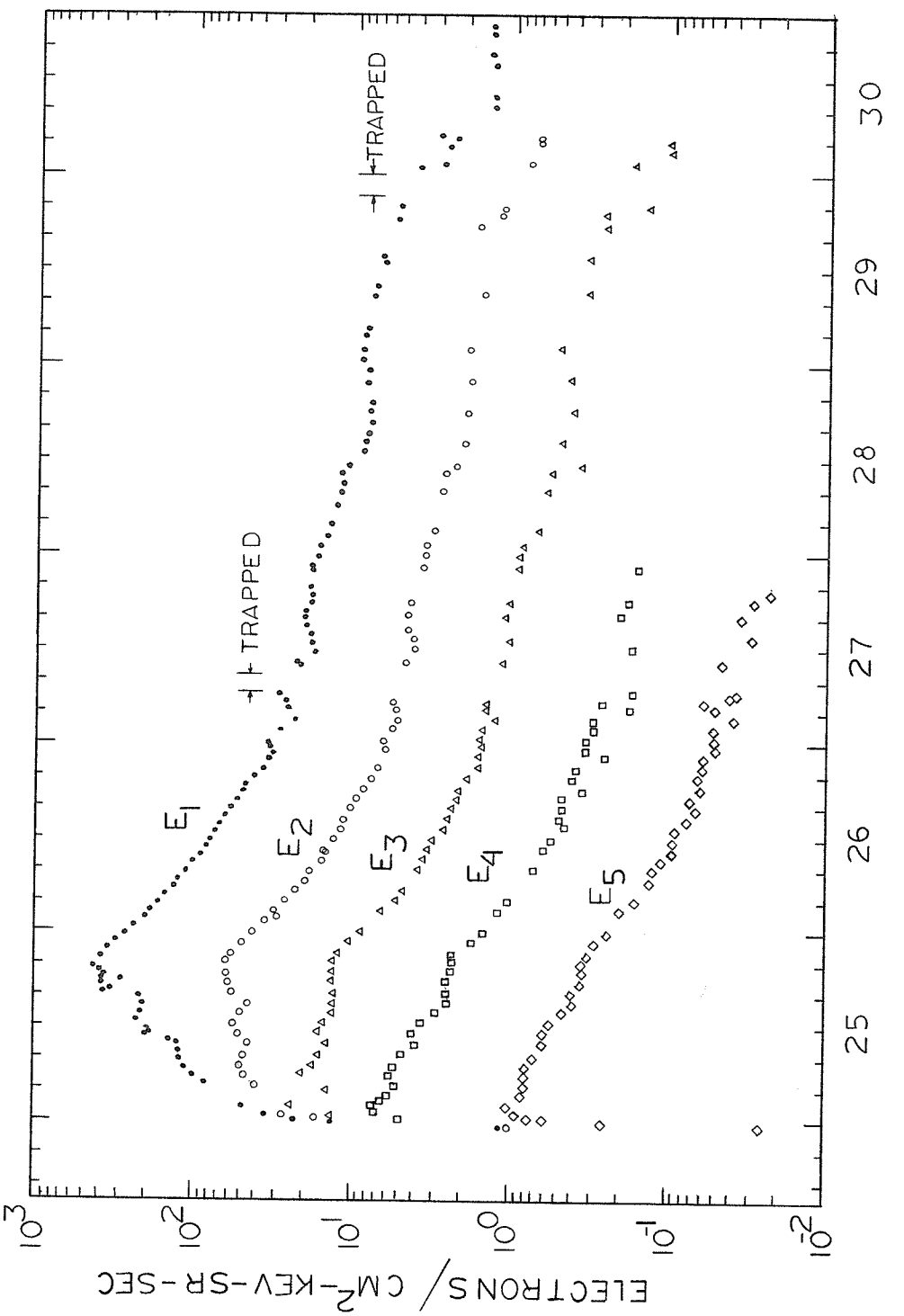

Fig. 1. Time profile of the differential electron fluxes as observed by the magnetic electron spectrometer on OGO-5.

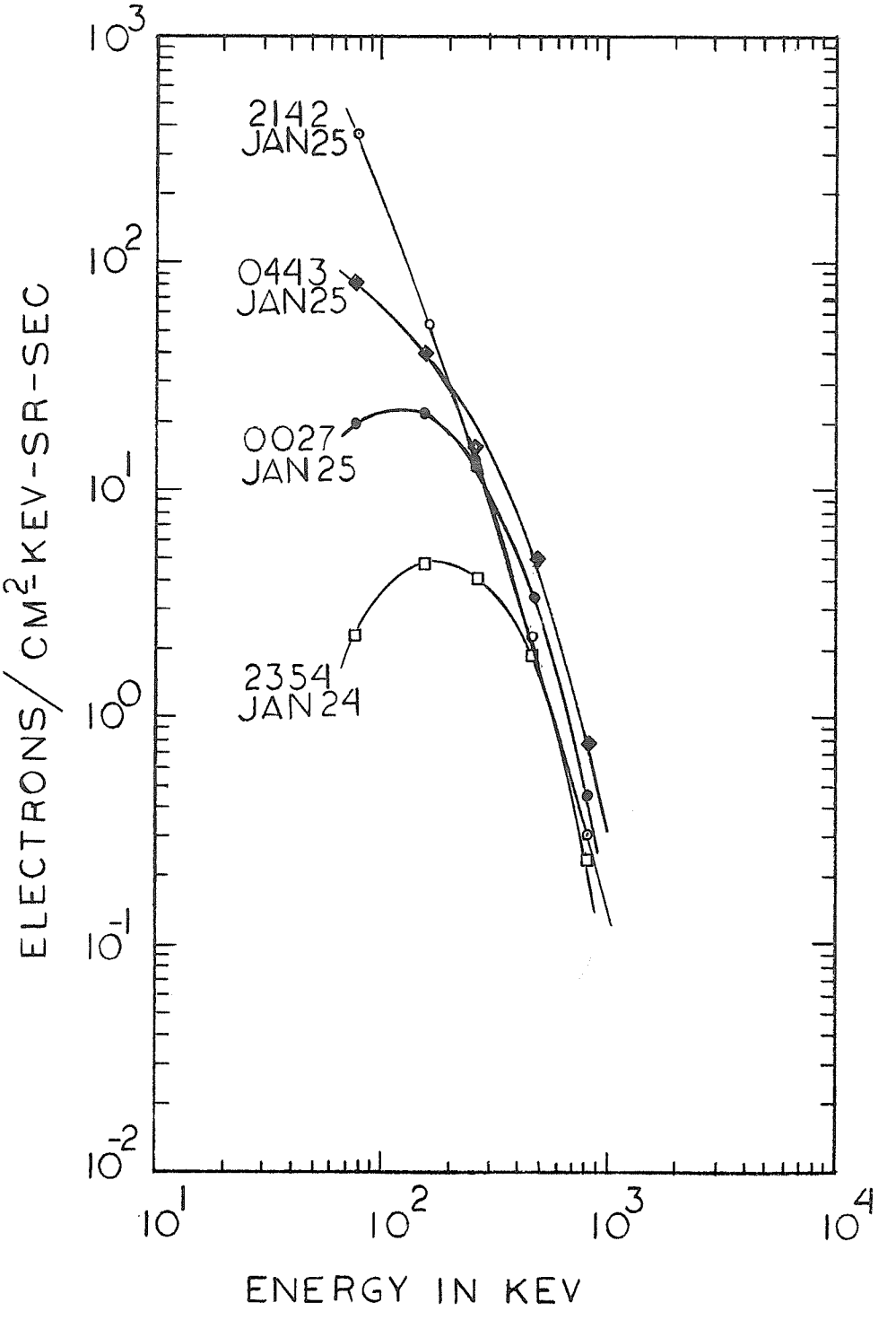

Fig. 2. Differential electron spectra during the early part of the event. The spectrum was essentially constant after 2400 UT January 25.

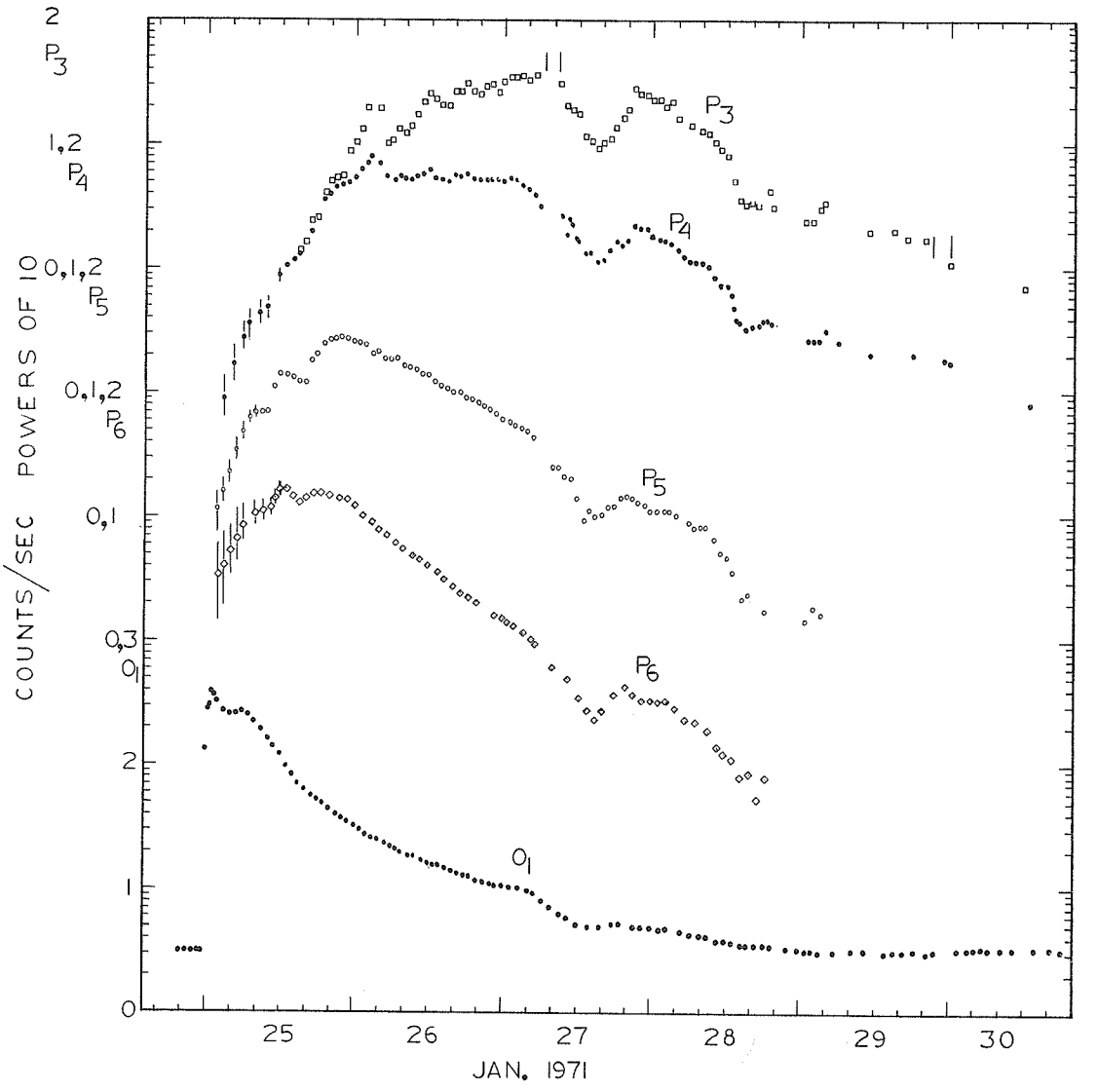

Fig. 3. Time profile of the proton fluxes as observed by the range energy telescope on OGO-5. The geometrical factors are given in the text.

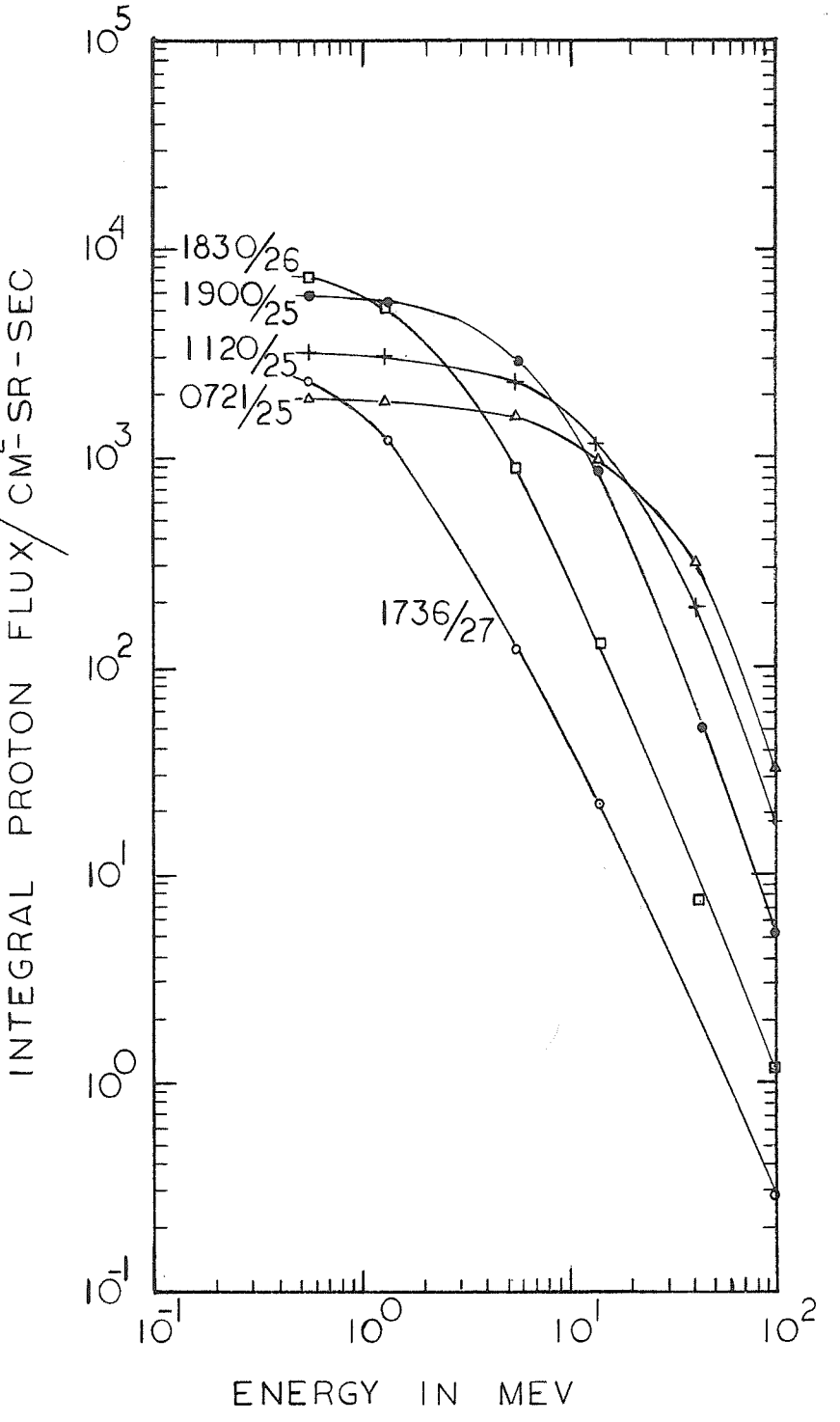

Fig. 4. Integral proton spectra during the particle event.

Proton and Alpha Particle Fluxes Measured Aboard OV5-6

by

G. K. Yates and J. G. Kelley
Air Force Cambridge Research Laboratories
L. G. Hanscom Field, Bedford, Massachusetts

and

B. Sellers and F. A. Hanser
Panametrics, Inc., Waltham, Massachusetts

Satellite OV5-6 (International designation 1969-046B) measures solar fluxes of protons and alpha particles. The perigee is 16,341 km and the apogee is 112,196 km. Thus, for most of the time the instruments are outside the earth's magnetosphere. The data presented here do not include fluxes within this region. The orbit was described in greater detail in an earlier report in this series [Yates et al., 1971].

The proton-alpha particle detector on OV5-6 consists of two totally depleted silicon surface barrier detectors in a telescope configuration. The detectors each have a 2 cm^2 area and are separated by 2.54 cm. The outer one is 200 microns thick and the inner one 750 microns. The outer detector is shielded from light by 0.6 mil of aluminum foil. In the coincidence mode of operation, the telescope has a geometric factor of 0.52 cm^2-sr, with a detection cone of 30° half angle. The average angle of detection is 17°. A coincidence is set by an energy loss window on the first detector and a threshold on the second detector. The resulting coincidences detect protons and alpha particles (principally) in the following ranges: protons 5.3 to 8 Mev, 8 to 17 Mev, 17 to 40 Mev, and 40 to 100 Mev; alpha-particles 20 to 32 Mev, 32 to 68 Mev, and 68 to 100 Mev. The telescope cycles sequentially through these seven ranges, each range is counted and then read out. The complete cycle is completed in approximately two minutes. The telescope looks in the equatorial plane of the satellite.

The satellite spin axis is stable and is directed toward 0^h and 40^m RA and 32° declination in celestial coordinates. In January 1971 the sun appeared twenty degrees above (+20°) the satellite's equator. Since the spin period at this time was approximately 4.7 seconds, the telescope accumulated counts in a given particle energy range for approximately two satellite rotations.

The figure shows 30 minute averages of the data from the four coincidence proton channels and the lowest energy alpha particle channel. Fluxes are given in particles/cm^2-sec-sr-Mev; most gaps correspond to periods of no telemetry; points when the satellite was within the trapped radiation belt are omitted.

Armstrong and Krimigis [1971] have shown that there is an inverse correlation between the proton/alpha-particle flux ratio and the hardness of the proton energy spectrum. These data agree with their results. A comparison of the two lower proton energy intervals in the figure shows that the January event was harder than the September event given in Part II, p. At 1200 hours UT, January 25, the proton/alpha-particle flux ratio in the 5 to 8 Mev/nucleon interval was 12.

REFERENCES

ARMSTRONG, T. P. and S. M. KRIMIGIS — 1971 — Statistical study of solar protons, alpha particles, and $Z \geq 3$ nuclei in 1967-1968, J. Geophys. Res., 76, 4230-4244.

YATES, G. K., L. KATZ, J. G. KELLEY, B. SELLERS, F. A. HANSER and P. R. MOREL — 1971 — Proton, alpha and bremsstrahlung fluxes measured aboard OV5-6, Upper Atmospheric Geophysics Report, UAG-12, Pt I, p. 139-146.

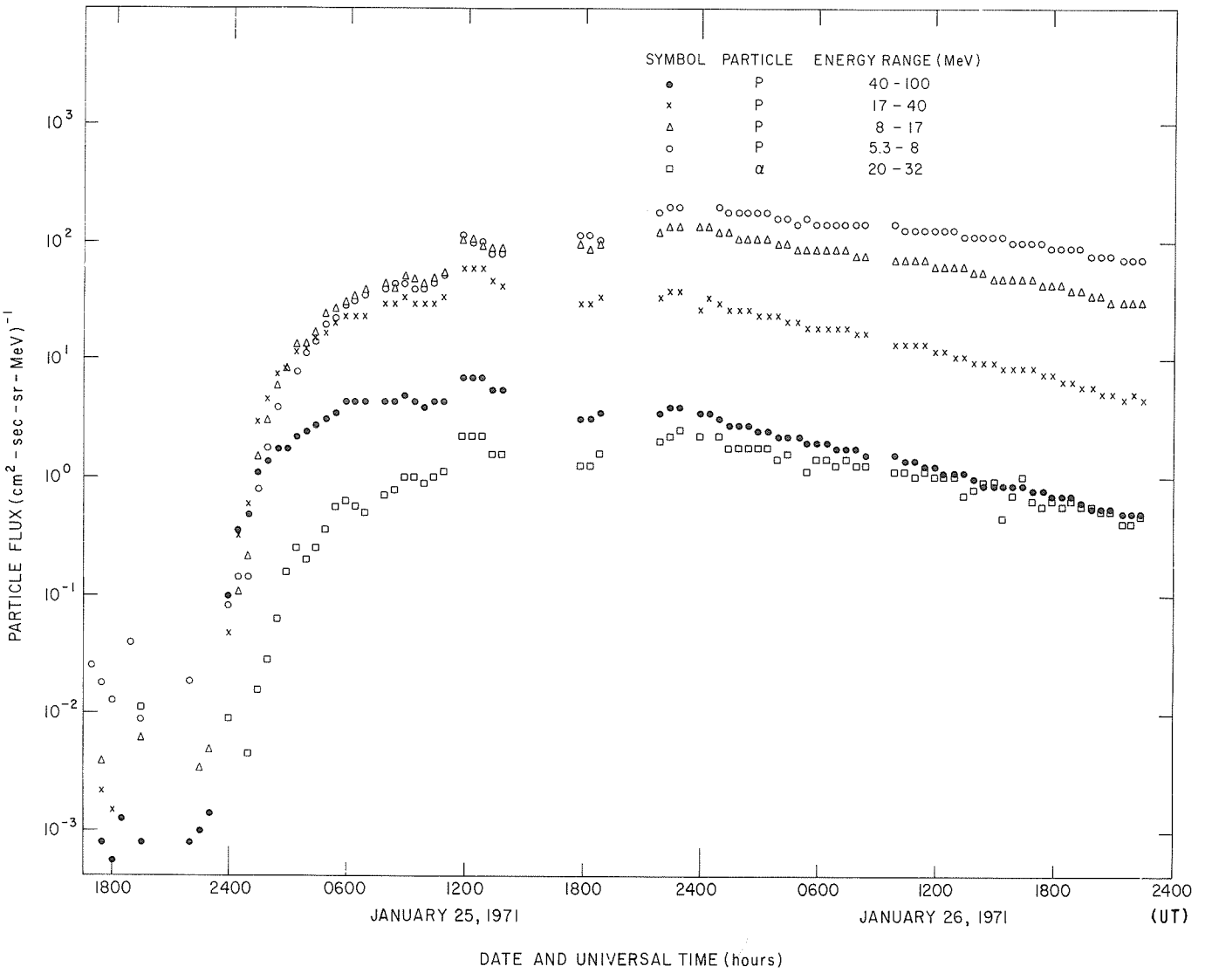

FIGURE I. TIME VARIATION OF PARTICLE FLUXES (30 minute AVERAGES)

Particle Observations during the 24 January 1971 Event

by

J. W. Kohl
The Johns Hopkins University
Applied Physics Laboratory
Silver Spring, Maryland

Presented here are observations of solar proton and alpha particles detected by solid state detectors of the Solar Proton Monitoring Experiment (SPME) on board IMP-G (Explorer 41) during the time period 24 January through 1 February 1971.

Background

IMP-G (Explorer 41) is in a highly elliptical orbit with apogee at ~170 × 10^3 km, perigee at ~250 km, and an inclination of 84°. The orgital period is ~80 hours and during the time period shown in the following figures completed ~2 1/2 orbits. From 24 January through 1 February 1971 the orbital plane was at a sun-earth-spacecraft angle of ~156° at ~2200 hours LT.

There are three groups of integral detectors with threshold energies of >60 Mev, >30 Mev, and >10 Mev. A description of these detector systems and their characteristics has been previously published in "Solar-Geophysical Data", Descriptive Text [197?]. There is also a single detector with two discrimination levels which measures protons and alphas in the differential ranges $1 \lesssim E_p \lesssim 10$ Mev and $4 \lesssim E_\alpha \lesssim 36$ Mev, respectively. The characteristics of this detector have been previously discussed by J. C. Armstrong and C. O. Bostrom [1971]. No additional comments on detector characteristics will be presented in this report.

The data for all channels will be presented as hourly averages. Perigee effects such as passage through the trapped radiation zones have been edited out. Also, a background value (an average of several days prior to 24 January) has been subtracted from the >60 Mev, >30 Mev, and >10 Mev values. No background values have been subtracted from the $1 \lesssim E \lesssim 10$ Mev/nucleon channels because of their variability prior to the event.

Observations

The data for protons >60 Mev, >30 Mev, and >10 Mev for the time period 24 January through 1 February 1971 are presented in Figure 1. From every-point data, which is not shown, it can be seen that all three detectors begin their initial rise within ~6 minutes of each other at ~ 2336 UT on 24 January. The fluxes then increase to their maximum; 89, 407, 1170 protons/cm^{2}sec ster for the >60, >30, >10 Mev detectors, respectively. The fluxes then seem to remain on a plateau for a length of time longer for lower energies. The decay period, which exhibits some modulating effects, extends from ~3 to ~7 days, depending on energy. Shown on this same figure, for convenience, are the 3-hour Kp averages. Also indicated is a sudden-storm-commencement at 0430 UT on 27 January. All three channels indicate the arrival as a sudden decrease in intensity.

Figure 2a shows the intensity-time profile for the two differential channels. Except for the ledge early on the 25th, the intensity-time profiles exhibit essentially similar characteristics. The event onset for the ~1-10 Mev/nucleon channels is ~2347 UT on the 24th - some 10 minutes after the higher energy integral channels. The maximum intensities are 3.936 and 161 particles/cm^{2}sec ster for the ~1-10 Mev/nucleon protons and alphas, respectively. The ratio of alphas-to-protons for the same time intervals is shown in Figure 2b. It can be seen that prior to the event the alpha/proton ratio has a large spread about ∿.06 and at the start of the event the spread in the ratios become smaller to form a smooth curve. The ratio is then seen to fall to a minimum of ∿.015 at about the time of the sudden-storm-commencement. At this time also, the spread begins to increase. As the recovery phase develops, the value of the alpha/proton ratio and the spread in values increase to approximately the pre-event values.

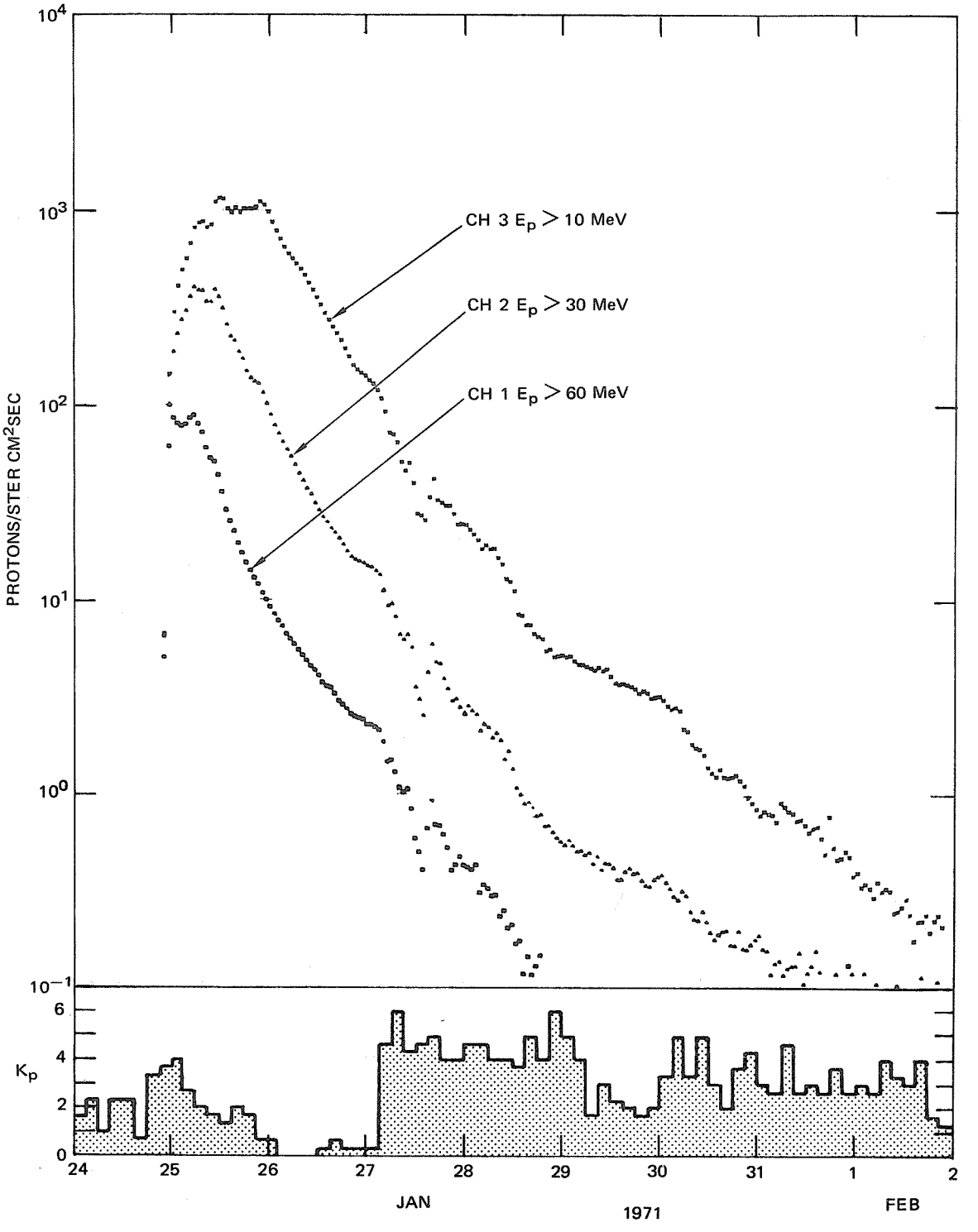

Fig. 1. EXPLORER 41 HOURLY AVERAGES 1971 CH 1, 2, 3

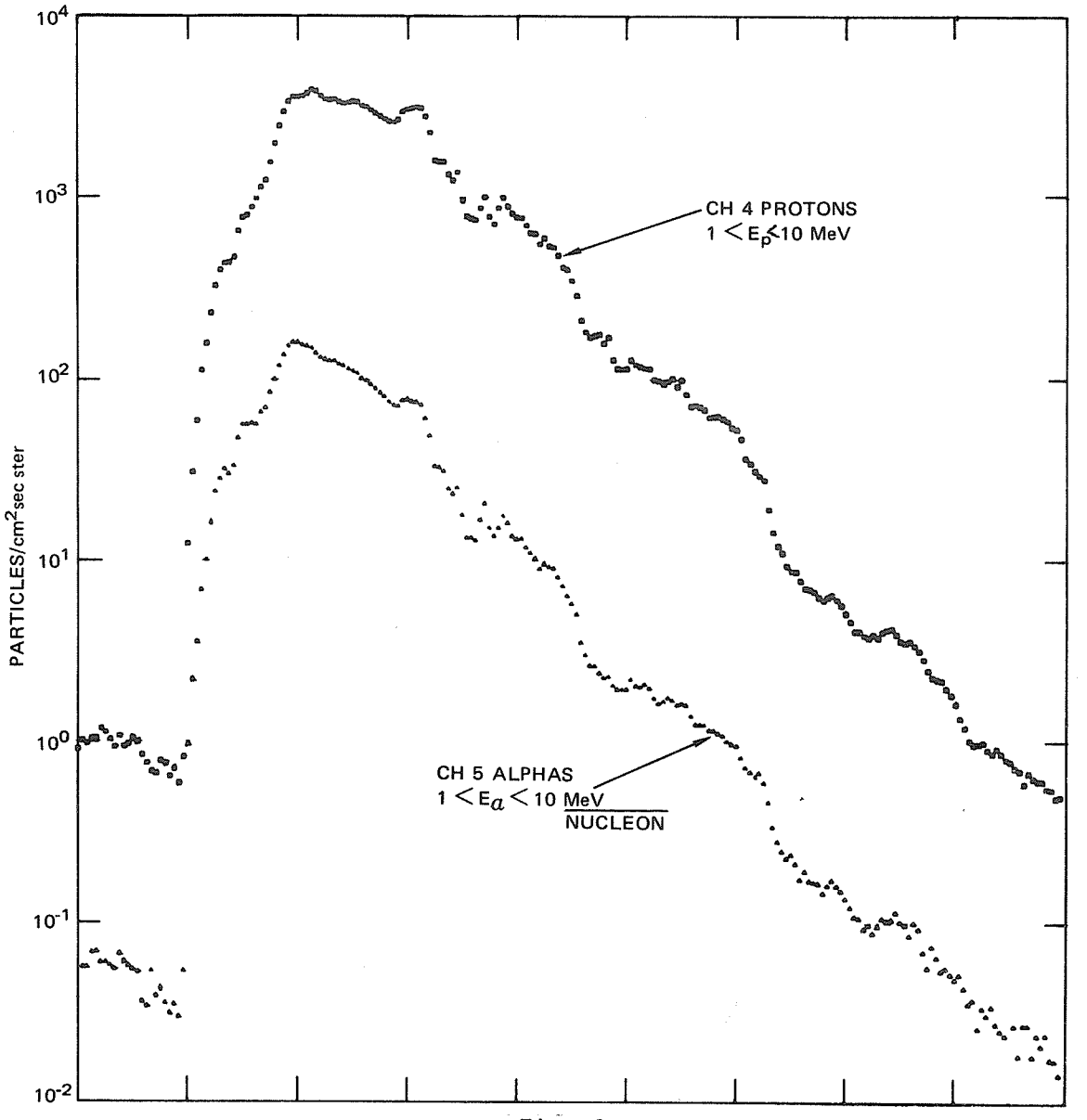

Fig. 2a

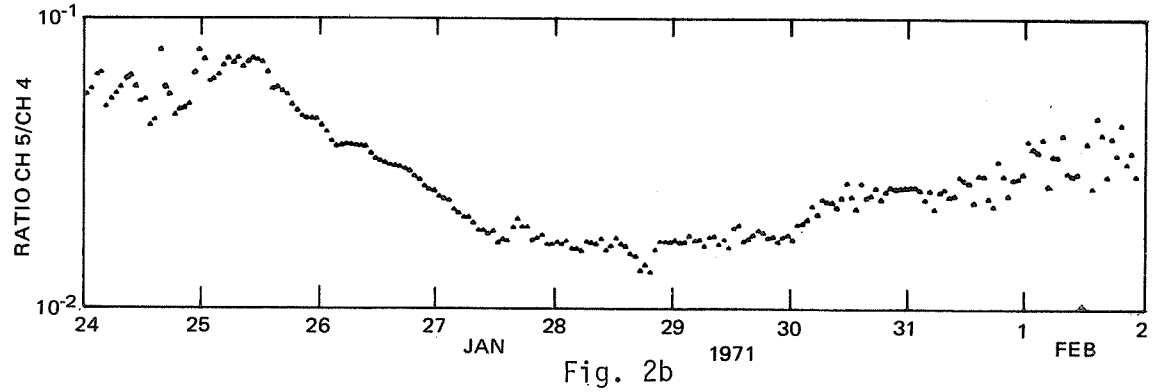

Fig. 2b

Fig. 2. EXPLORER 41 HOURLY AVERAGES CH 4, 5

REFERENCES

ARMSTRONG J. C. and C. O. BOSTROM 1971 Solar Protons and Alpha Particles in the March 6-9, 1970 Events, World Data Center A, Upper Atmosphere Geophysics, Report UAG-12, 134.

1972 Solar-Geophysical Data, Descriptive Text, 330 Supplement, U.S. Department of Commerce, (Boulder, Colorado, U.S.A. 80302).

Solar Electrons, Protons, and Alpha Particles in the 24 January 1971 Event

by

L. J. Lanzerotti and C. G. Maclennan
Bell Laboratories
Murray Hill, New Jersey

Editor's Note: The authors did not have time to submit discussion of their data, but kindly sent the following four Figures presenting the event as seen on detectors on the Explorer 41 satellite.

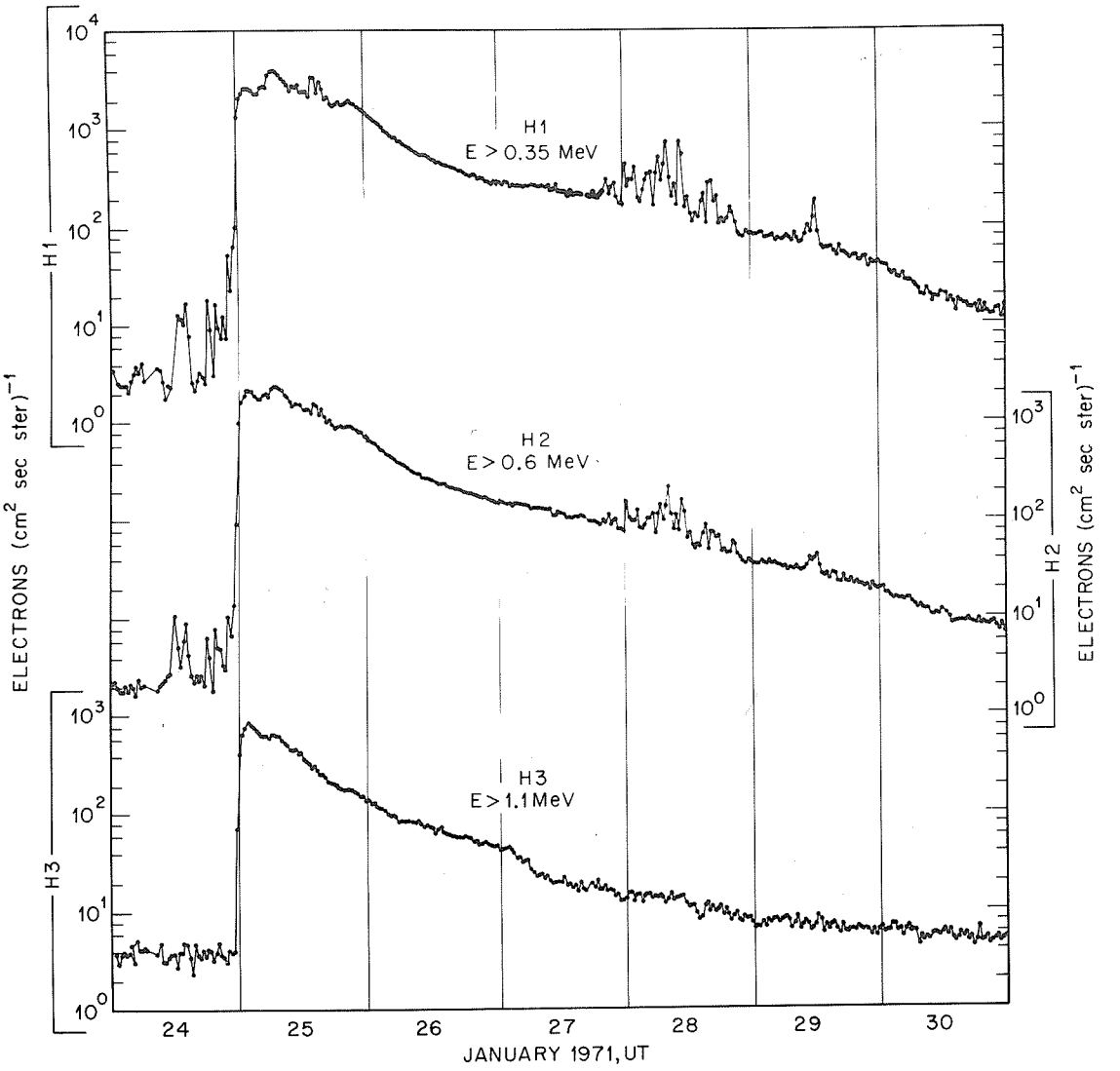

Fig. 1. Time history of the electron fluxes in three integral electron channels as measured by a four element solid state detector telescope on the Explorer 41 satellite.

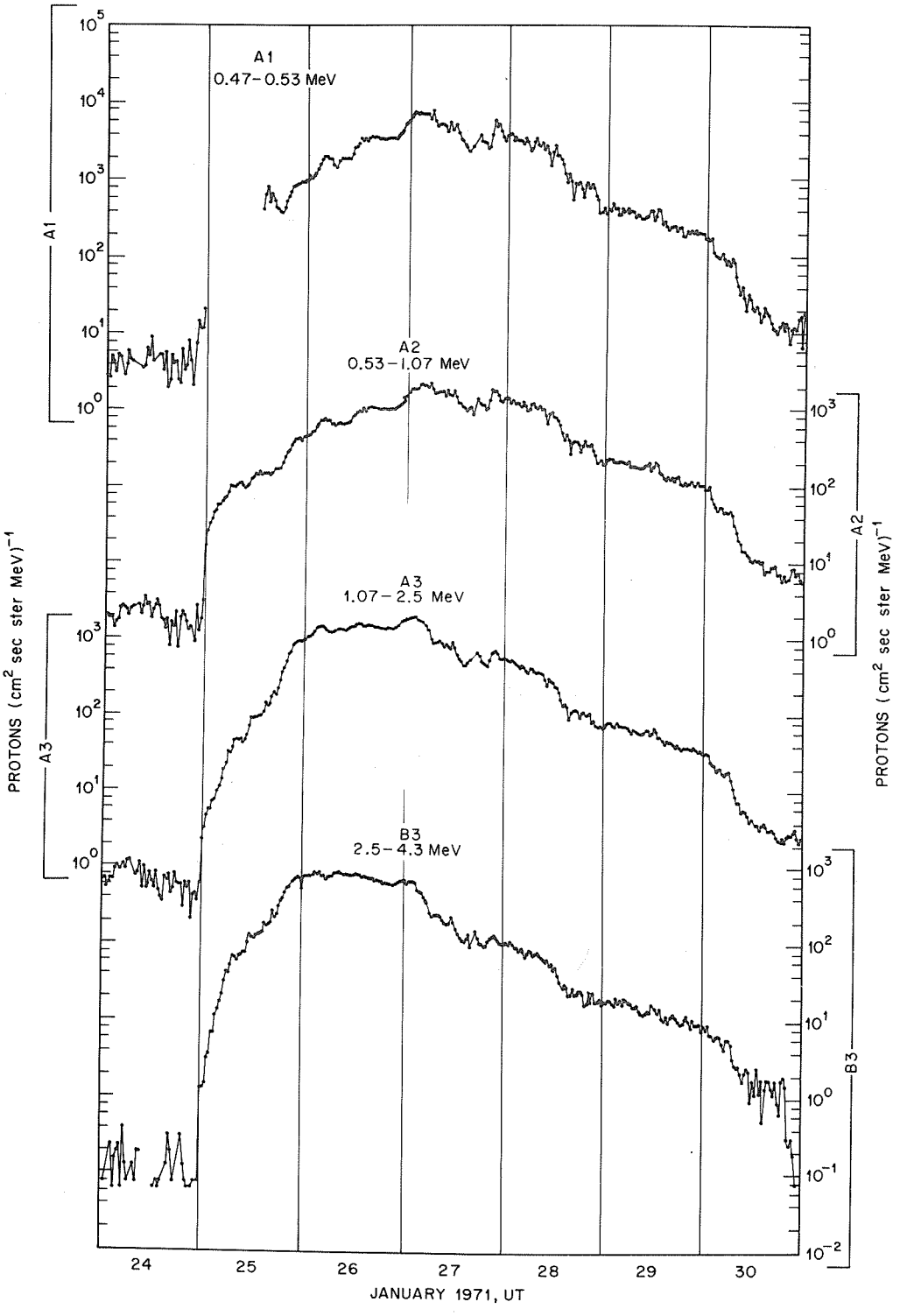

Fig. 2. Time history of the proton fluxes in four differential channels.

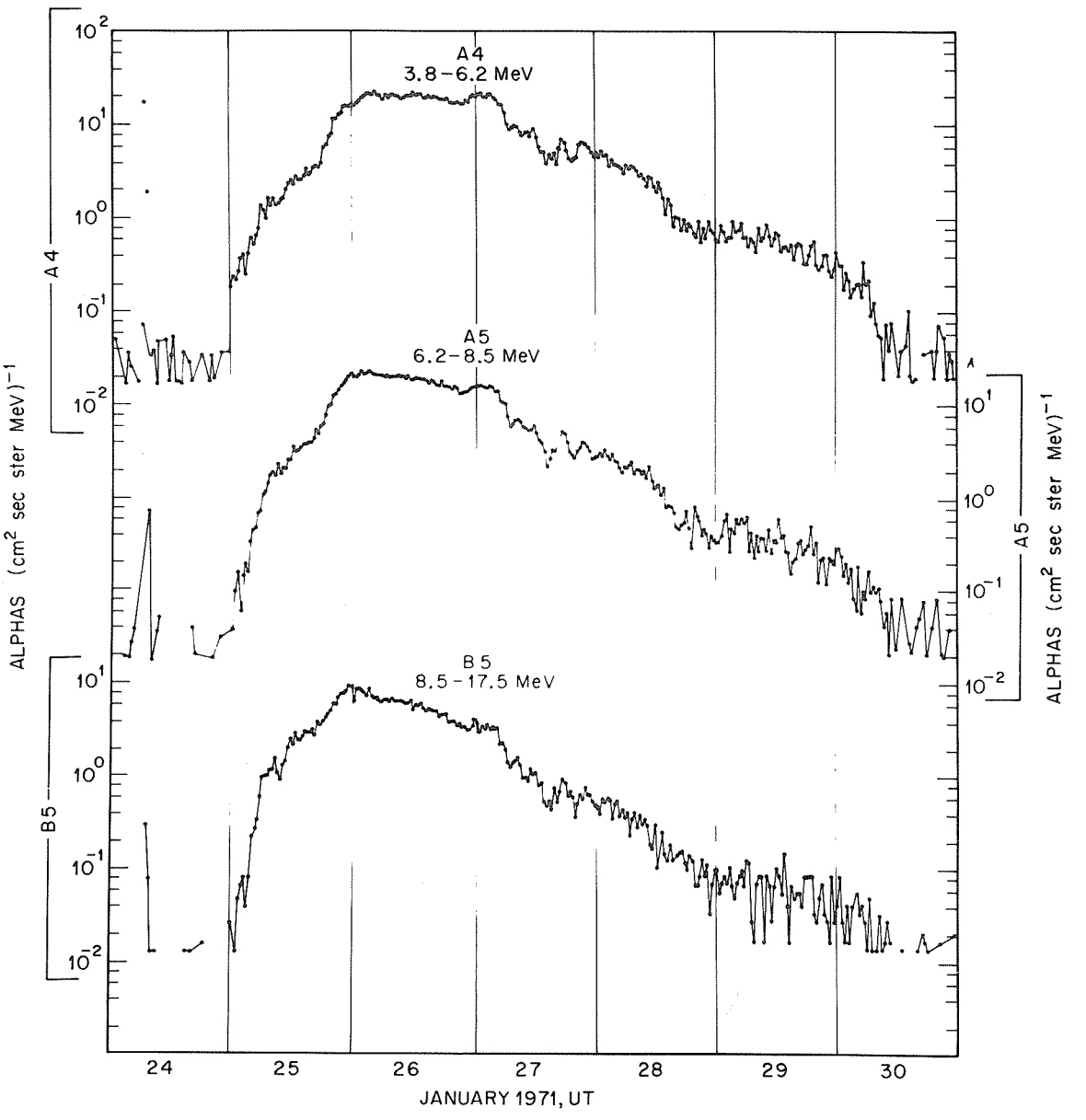

Fig. 3. Time history of the alpha particle fluxes in three differential channels.

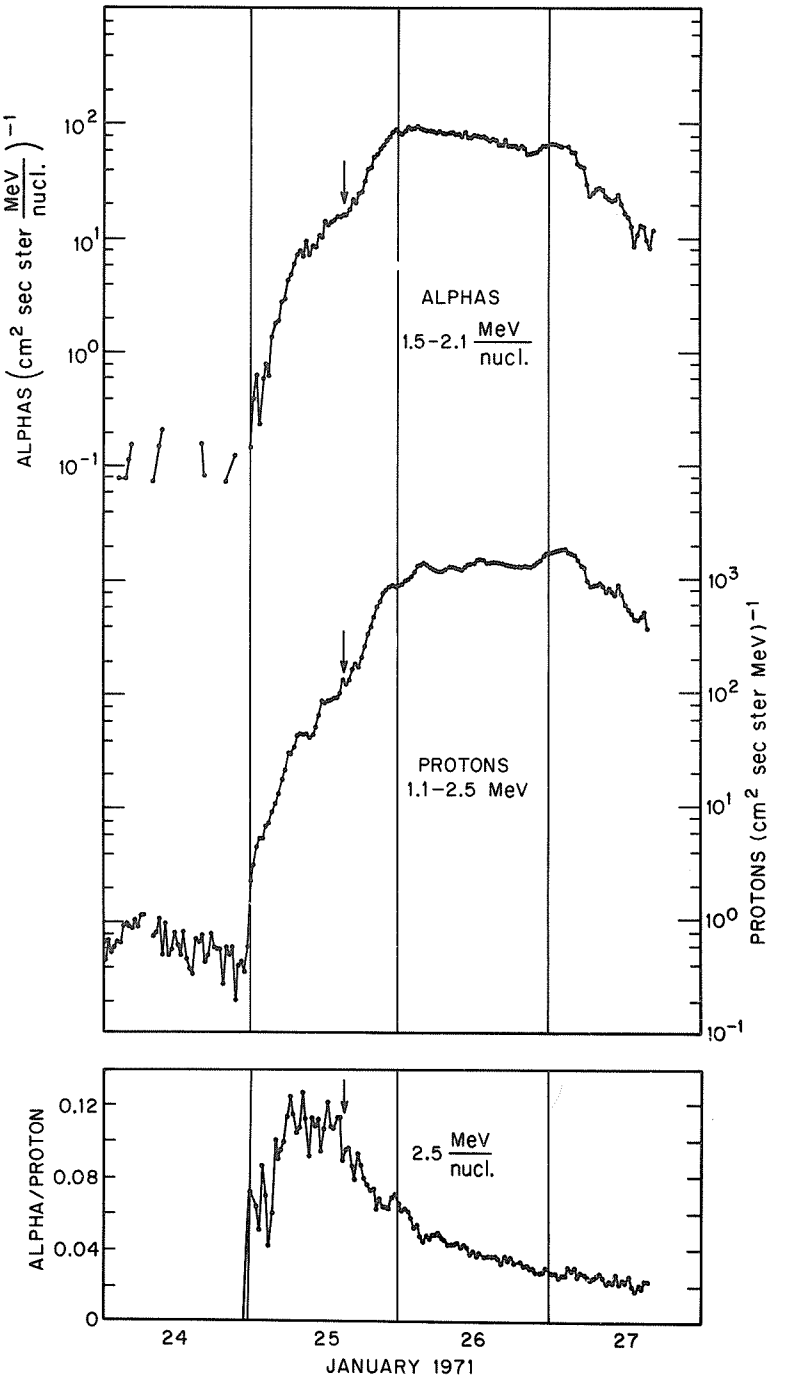

Fig. 4. Time history of the alpha and proton fluxes in two differential channels and the alpha-to-proton flux ratio for the onset of the event. The alpha-to-proton ratio is substantially enhanced during the first day of the event. (This figure is taken from a paper by Lanzerotti, Maclennan, and Graedel, Astrophys. J., 173, L39-43, University of Chicago Press, 1972. Permission to reprint this figure has been given by the authors and the Journal. Copyright 1972, The American Astronomical Society. All rights reserved. Printed in U.S.A.).

The Distant Interplanetary Magnetic Field Measured by Pioneer 8 during the Period January 20 to 30, 1971

by

A. Castelli[+] and F. Mariani[+*]
[+]Laboratorio Plasma nello Spazio
Consiglio Nazionale delle Ricerche
Istituto di Fisica dell'Università
Roma, Italia

[*]Istituto di Fisica dell'Università
L'Aquila, Italia

and

N. F. Ness
NASA, Goddard Space Flight Center
Greenbelt, Maryland U.S.A.

In the time interval from January 20 to 30, 1971 the Pioneer 8 space probe was on its heliocentric orbit East of the Sun-Earth line at an angular distance of about 70 degrees: the geometry of the orbit is shown in Figure 1.

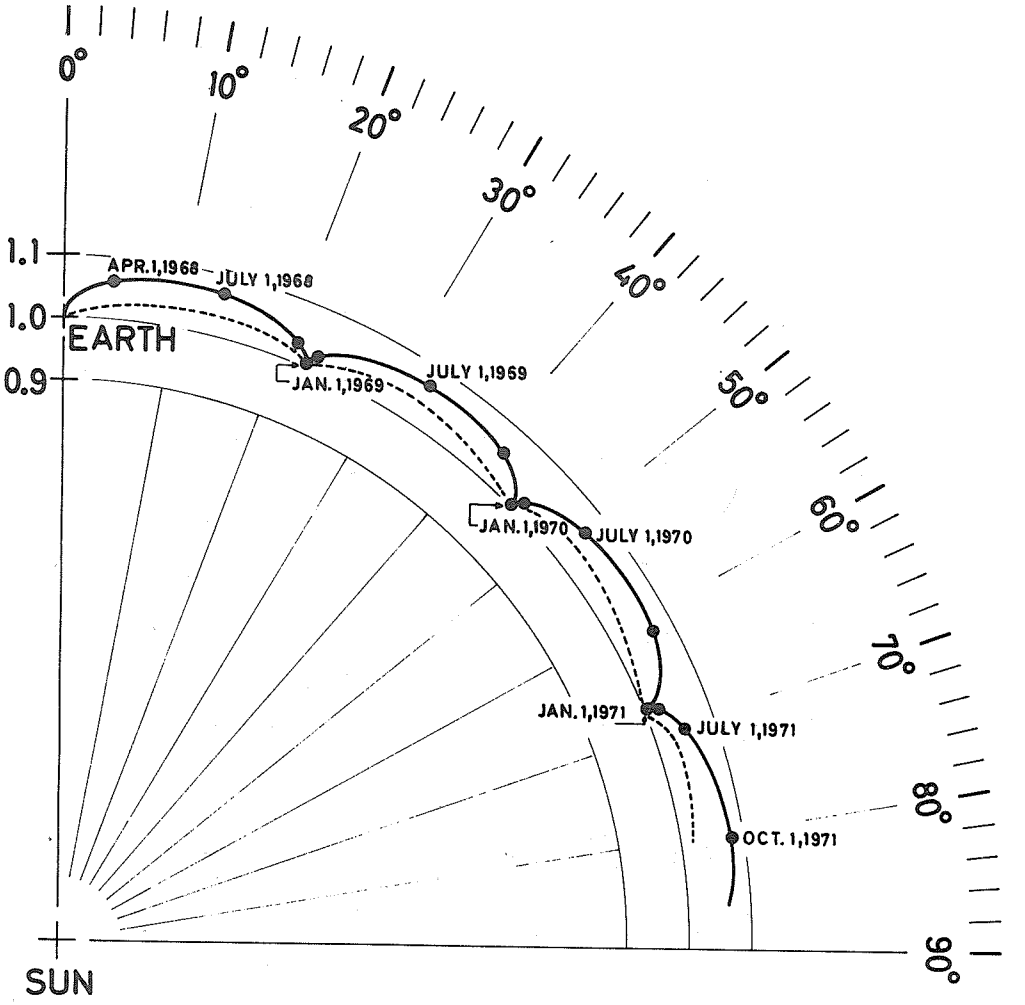

Fig. 1. The trajectory of Pioneer 8 on the ecliptic plane, referred to the Sun-Earth line. The figure is slightly different from that published in a previous report [UAG-12, Part III, p. 409] because now the Sun-Earth line distance is taken as a time invariable unit, incorporating its annual variation. To allow reconstruction of the heliocentric absolute distance the dashed line tracing the trajectory gives the absolute Sun-Earth distance in units of that at the beginning of the flight.

The average time interval between each field value is about 7 seconds. Each vector component is the average of four consecutive measurements computed on board the spacecraft by a special computer, the Time-Average Unit. The total time coverage was about 45% of the time.

Hourly averages of the field elements are shown in Figure 2. More details are shown in Figures 3 and 4 where five minutes averages are shown for days 22 to 26 January.

Except for the first two days the field character is near to that of the spiral away from the Sun.

The incomplete time coverage does not allow clear statements on the field behavior, although higher levels of the field strength, as well as of its fluctuations, is suggested for days 23 to 25.

A shock-like step increase of the field intensity is possibly observed at 0142 UT of January 23, as shown in Figure 5 where one-minute averages are plotted for the first 4 hours of the day.

The definitions of the values plotted are as follows:

$\bar{F}$, the average field computed by the averages $\bar{x}$, $\bar{y}$, $\bar{z}$ of the field components.

$\bar{\bar{F}}$, the average field magnitude computed by the individual field magnitudes. According to their definitions, $\bar{\bar{F}}$ is always greater than or equal to $\bar{F}$.

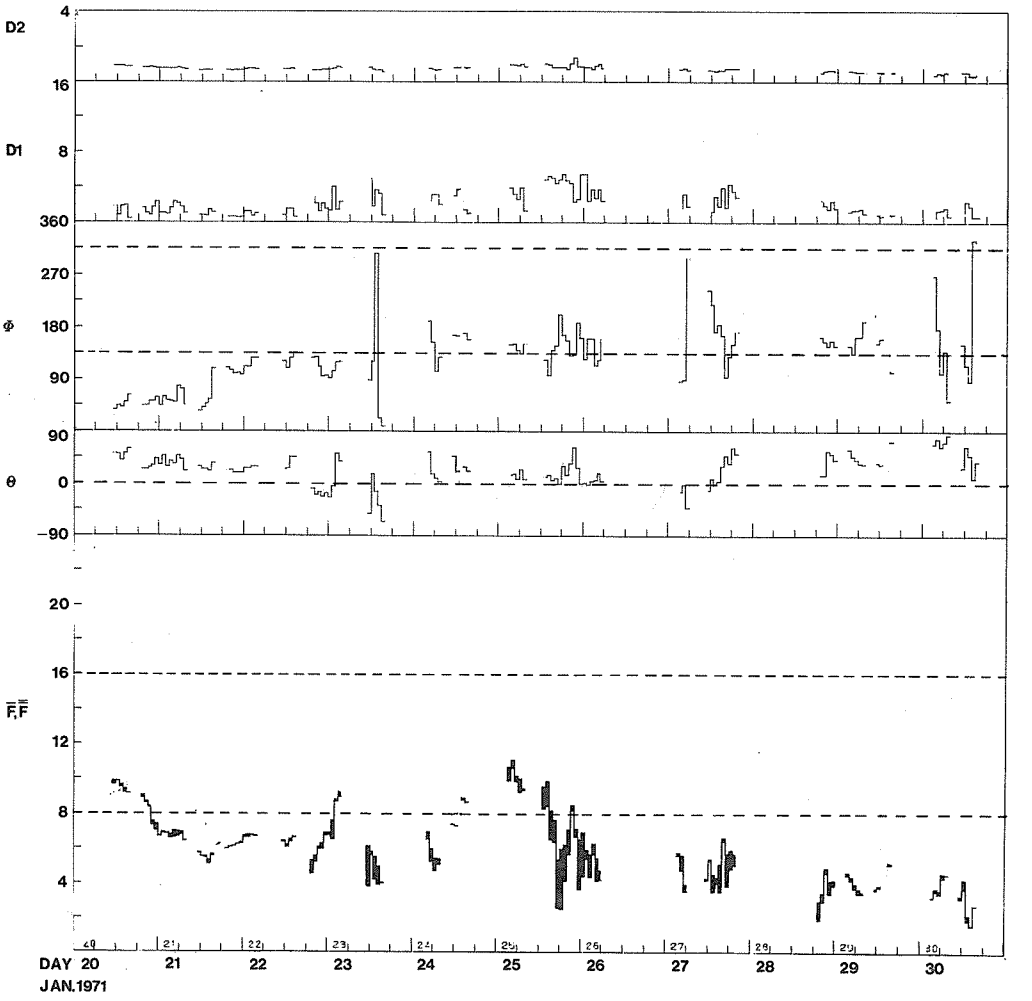

Fig. 2. Hourly average field magnitude ($\bar{F}$, $\bar{\bar{F}}$), orientation (θ, Φ) and RMS deviations D1 and D2. Magnitude and deviations are in gammas; angles in degrees. The time is given as day of year (1st of January = day 1) and calendar day.

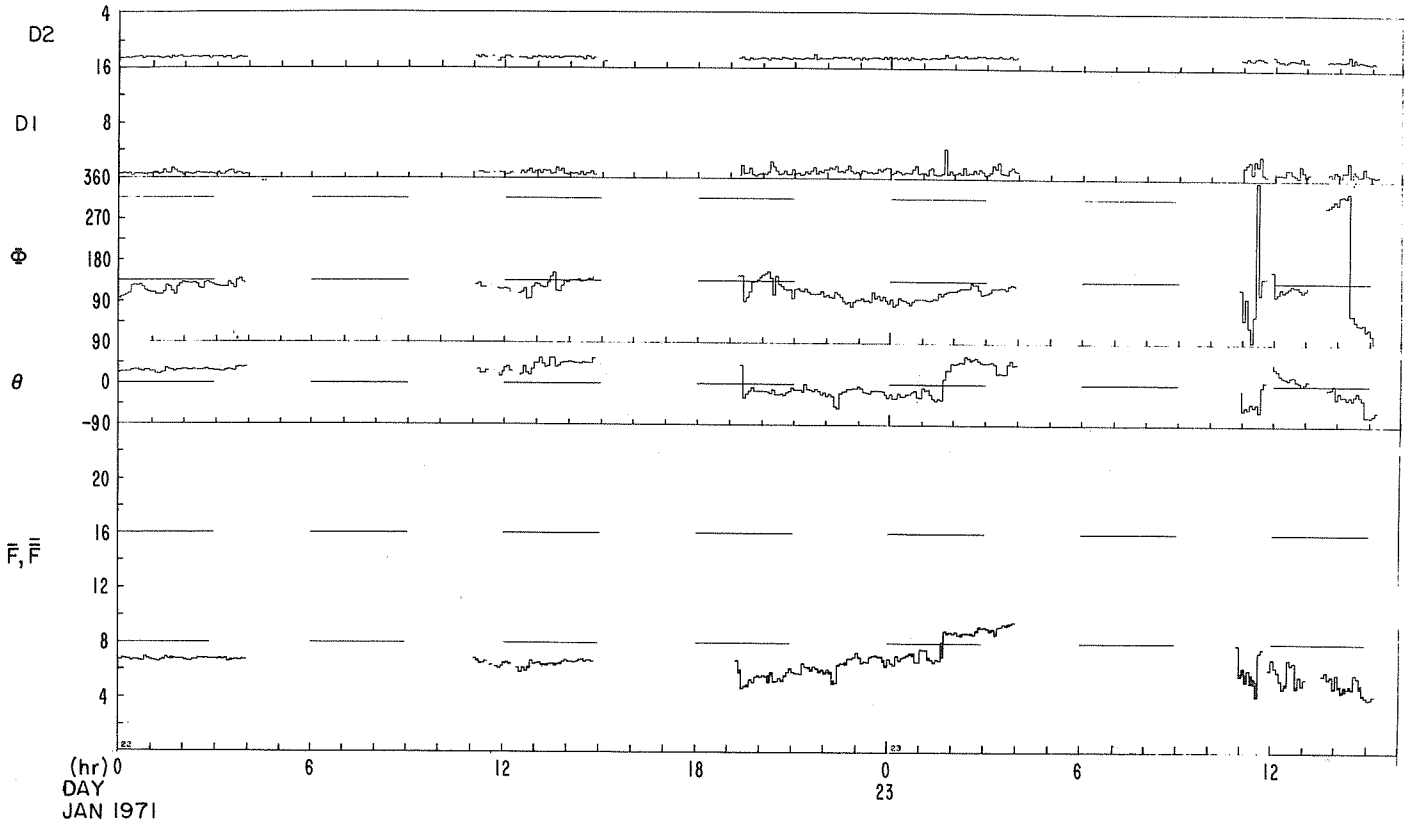

Fig. 3. Five-minute average field magnitude ($\bar{F}$, $\bar{\bar{F}}$), orientation (θ, Φ) and RMS deviations D1 and D2 for January 22 and 23.

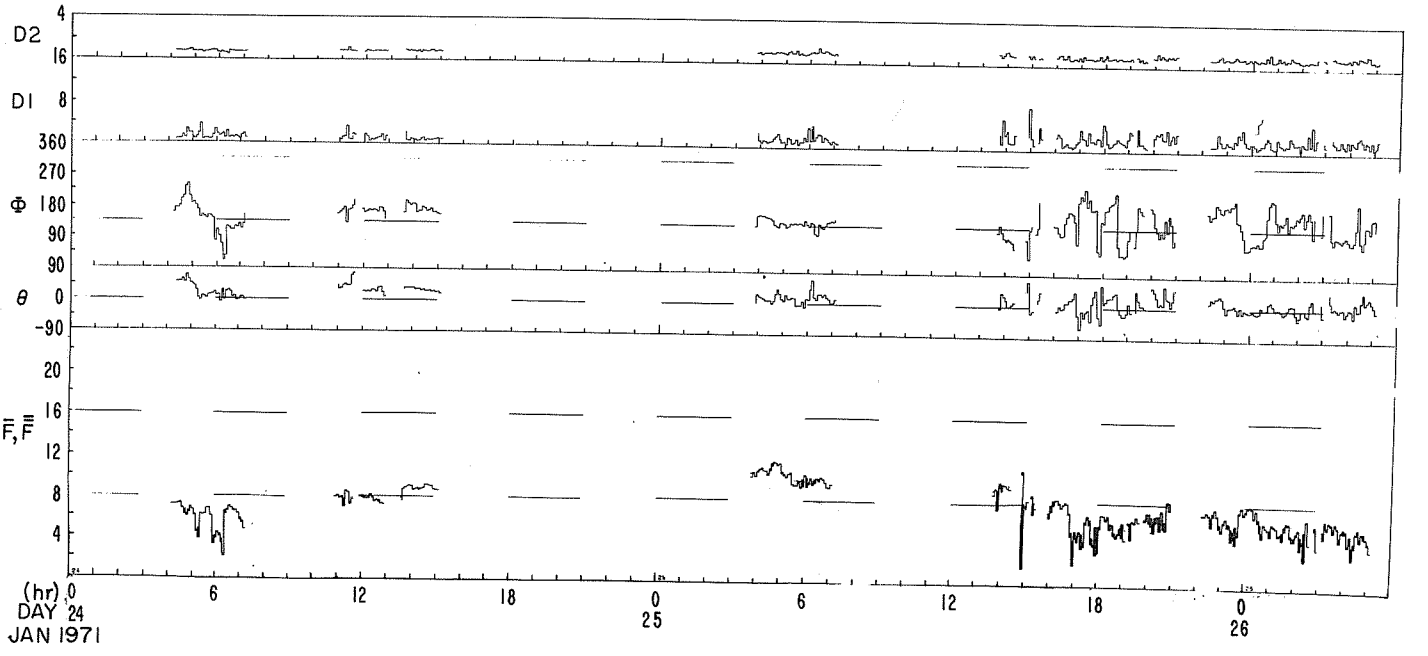

Fig. 4. Same as for Fig. 3, for January 24 and 25, and the first few hours of January 26.

θ and Φ, i.e. the inclination (+ north, - south) and the azimuth of the field vector on the ecliptic plane (0° towards Sun, 90° east and 180° away from Sun).

Also, the RMS deviations are given, according to the following definition:

$$D = \left\{ \frac{1}{n} \sum_{i=1}^{n} [(x_i - \bar{x})^2 + (y_i - \bar{y})^2 + (z_i - \bar{z})^2] \right\}^{\frac{1}{2}}$$

where x_i, y_i, z_i are individual values of the three field components.

D1, the same as D computed over the averaging time interval.

D2, the average of the 30 sec RMS deviation D.

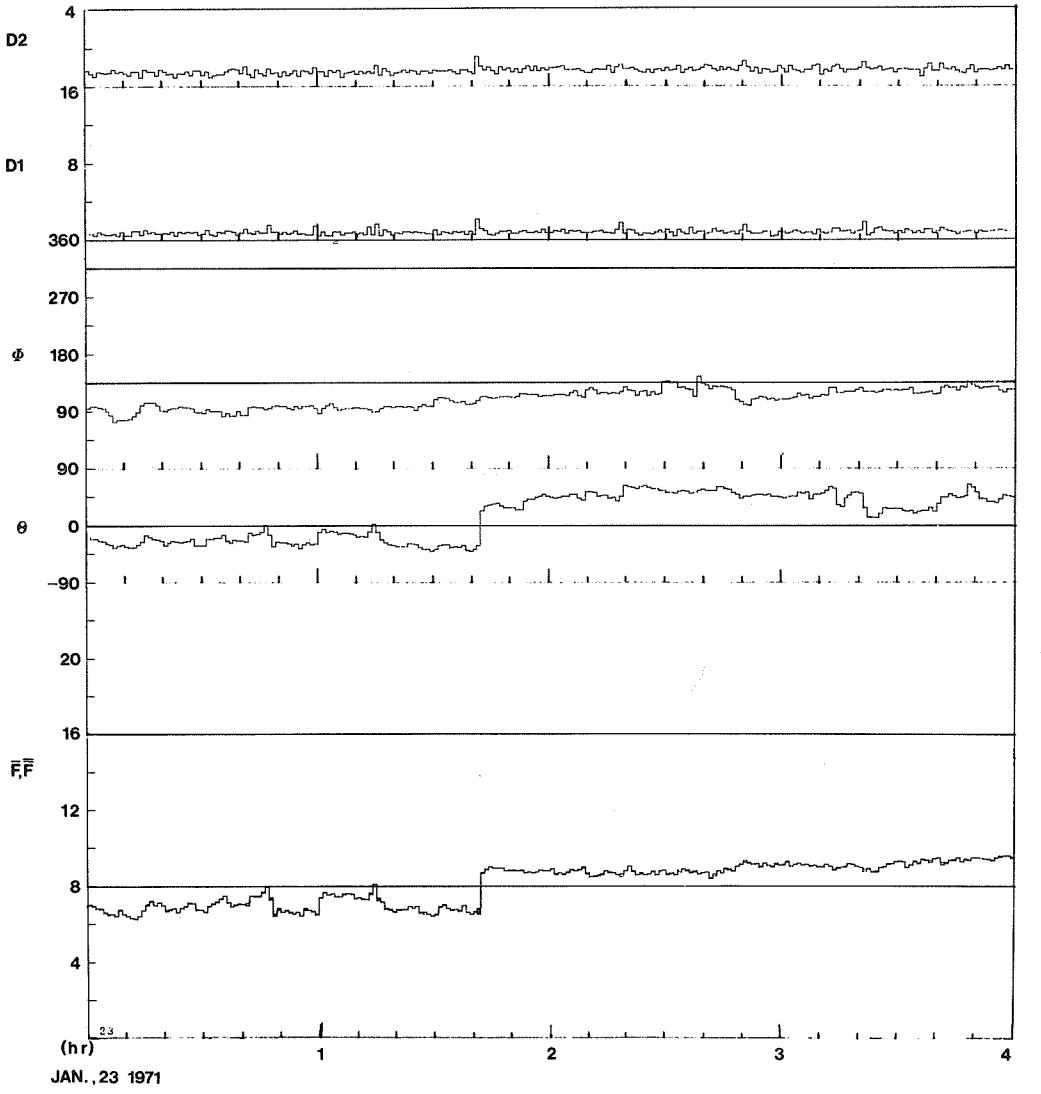

Fig. 5. One-minute average of field elements for January 23 between 0000 and 0400 UT. The abrupt increase of field strength at 0142 UT has to be noticed.

5. COSMIC RAYS

Tables of Neutron Monitor Data and Selected Graphs for the January 24, 1971 Event

by

Helen E. Coffey
World Data Center A for
Solar-Terrestrial Physics
NOAA, Boulder, Colorado 80302

Cosmic ray neutron monitor data for the January 24-25, 1971 event are presented both in tabulated form and graphical displays. In many cases the data for this period were forwarded to us upon special request. We thank all the reporting observatories for their cooperation.

Table 1 lists the stations, their equipment, geographic coordinates, cut-off rigidities, scaling factors, pressure coefficients, mean station pressure in mm Hg and multiplication factors, if any. Following this is Table 2 which presents the hourly values for January 24-25, 1971 from the 41 stations, listed in cut-off rigidity order. The incompleteness of the data is due to the lag in compiling cosmic ray data. The data does however cluster around the period we are most interested in, i.e., 2300-0200 UT.

Graphical displays of selected stations show both the variation of data with cut-off rigidity and a quick graphical look at the event. These include: a.) Dumont d'Urville fifteen-minute data given in percentage deviations for 1800 UT January 24 - 0800 UT January 25 (Figure 1); Port aux Francais five-minute data in percentage deviations for 1800 UT January 24 - 0800 UT January 25 (Figure 2); and c.) Durham five-minute data for 2000 UT January 24 - 0400 UT January 25 (Figure 3).

Finally, Table 3 presents 23 individual stations data in 5-, 10-, and 15-minute hourly rates. Information pertinent to each station is given in the headings. All data is pressure corrected except for Rome, Belgrano, Apatity and Oulu. Average hourly pressure values are given for Rome and Oulu. No pressure values were available for Belgrano and Apatity.

The 23 stations listed in cut-off rigidity order are:

Station	Cutoff rigidity	Hourly rate
Dumont d'Urville	0.01	Fifteen-minute
Fort Churchill	0.21	Five-minute
Tixie Bay	0.53	" "
Kiruna	0.54	" "
Apatity	0.65	Fifteen-minute
General Belgrano	0.75	Five-minute
Oulu	0.81	" "
Deep River	1.02	" "
Sanae	1.02	Ten-minute
Port aux Francais	1.19	Five-minute
Mt. Washington	1.24	" "
Durham	1.41	" "
Uppsala	1.43	" "
Magadan	2.10	Fifteen-minute
Leeds	2.20	Five-minute
Kiel	2.29	" "
Moscow	2.46	Fifteen-minute
Irkutsk	3.74	Five-minute
Lomnicky Stit	4.00	Ten-minute
Dallas	4.35	Five-minute
Rome	6.32	Fifteen-minute
Mt. Norikura	11.39	Fifteen-minute
Tokyo/Itabashi	11.61	Ten-minute

Table 1

	Station	Equip.	Geographic Coordinates Lat.	East	Cutoff Rigidity	Scaling Factors	Pressure Coefficient	Mean Station Pressure mm HG	Real Counts
ALE	Alert	SNM	82.5 N	297.6	0.0	--	0.987%/mm Hg	725	100x tabulated
DUM	Dumont D'urville	SNM	66.4 S	140.0	0.01	--	.99 %/mm Hg	---	200x "
INU	Inuvik	SNM	68.35N	226.2	0.18	--	.987%/mm Hg	758	100x "
CHU	Fort Churchill	NM	58.75N	265.9	0.21	--	--	1010mb	40x "
	Syowa Base	SNM	69.03S	39.6	0.42	--	--	980mb	100x "
GOO	Goose Bay	SNM	53.33N	299.5	0.52	--	.987%/mm Hg	758	100x "
	Tixie Bay	SNM	71.55N	128.9	0.53	--	-.96 %/mm Hg	758	100x "
	Kiruna	SNM	67.83N	20.4	0.54	--	-.99 %/mm Hg	720	100x "
	Norilsk	SNM	69.26N	88.05	0.63	64	-.69 %/mb	1005mb	---
APA	Apatity	NM	67.55N	33.3	0.65	--	--	---	---
BEL	General Belgrano	SNM	77.97S	321.2	0.75	--	--	---*	32x "
OUL	Oulu	SNM	65.0 N	25.4	0.81	--	.735%/mb	1000mb	100x "
DEE	Deep River	SNM	46.1 N	282.5	1.02	--	.987%/mm Hg	747	300x "
	Sanae	SNM	70.46S	357.51	1.02	--	.73 %/mb	980mb	10x "
OTT	Ottawa	NM	45.4 N	284.4	1.08	6.4	--	---	---
CAL	Calgary	SNM	51.08N	245.9	1.09	--	.7718%/mb	---	100x "
BEG	Bergen	NM	60.4 N	5.3	1.13	16	.74 %/mb	990mb	---
SUL	Sulphur Mountain	SNM	51.2 N	244.39	1.14	--	.7665%/mb	---	100x "
POR	Port aux Francais	SNM	49.35S	70.2	1.19	--	1.01	---	400x "
MTW	Mt. Washington	NM	44.3 N	288.7	1.24	--	Pressure Corrected		
DUR	Durham	SNM	43.1 N	289.1	1.41	--	Pressure Corrected		
UPP	Uppsala	NM	58.85N	17.92	1.43	--	-.986%/mm Hg	757.75	10x "
	Magadan	SNM	60.11N	151.01	2.1	64	-.74 %/mb	982mb	---
LEE	Leeds	NM	53.82N	358.4	2.2	--	--	---	100x "
KIE	Kiel	SNM	54.33N	10.1	2.29	--	.961%/mm Hg	755	100x "
MOS	Moscow	SNM	55.47N	37.3	2.46	--	-.71 %/mb	---	200x "
	Utrecht	SNM	52.08N	5.13	2.76	--	.99 %/mm Hg	760	100x "
LIN	Lindau	SNM	51.6 N	10.1	3.0	--	--	780	100x "
CLI	Climax	NM	39.37N	253.8	3.03	100	-.96 %/mm Hg	504	---
IRK	Irkutsk	SNM	52.42N	104.3	3.74	64	-.74 %/mb	---	---
LOM	Lomnicky Stit	NM	49.2 N	20.22	4.0	8	--	---	---
PRE	Predigstuhl	SNM	47.7 N	12.88	4.30	--	-.9 %/mm Hg	625	100x "
DAL	Dallas	NM	32.78N	263.20	4.35	--	--	---	120x
HER	Hermanus	SNM	34.42S	19.2	4.90	--	.72 %/mb	1015mb	100x "
PIC	Pic-du-Midi	SNM	42.93N	0.2	5.36	--	.93 %/mm Hg	---	100x "
USH	Ushuaia	NM	54.8 S	291.7	5.68	8	--	750	-3000x "
ROM	Rome	SNM	41.9 N	12.5	6.32	100	.92 %/mm Hg	---*	---
	Mexico City	SNM	19.33N	260.8	9.53	--	-.96 %/mm Hg	584	64x "
MTN	Mt. Norikura	SNM	36.12N	137.5	11.39	64	-.85 %/mm Hg	540	---
	Tokyo/Itabashi	SNM	35.67N	139.75	11.61	64	-.7 %/mb	1013.3mb	--
HUA	Huancayo	NM	12.05S	284.6	13.45	100	-.96 %/mm Hg	518	---

*Uncorrected for pressure.

Table 2

January 24, 1971

HOUR	13	14	15	16	17	18	19	20	21	22	23	24
ALERT	6737	6722	6775	6745	6746	6747	6762	6753	6762	6752	6722	7019
TERRE ADELIE	1951	1953	1958	1950	1955	1951	1949	1964	1965	1968	1969	2129
INUVIK					6493	6485	6513	6528	6494	6478	6480	6727
CHURCHILL										5977	5969	6171
SYOWA BASE												2647
GOOSE BAY	6555	6520	6535	6542	6542	6539	6544	6495	6528	6520	6527	6803
TIXIE BAY	6637	6665	6675	6655	6664	6659	6645	6654	6671	6654	6667	6821
KIRUNA	6597	6608	6576	6586	6567	6583	6589	6579	6589	6578	6598	6938
NORILSK	5581	5569	5565	5587	5592	5576	5598	5593	5593	5598	5591	5716
APATITY												8661
BELGRANO											6932	7164
OULU	3497	3483	3481	3499	3498	3490	3515	3518	3510	3495	3516	3648
DEEP RIVER	6467	6471	6460	6458	6479	6475	6479	6468	6461	6485	6463	6722
SANAE											14231	14683
OTTAWA	2864	2837	2833	2780	2829	2906	2843	2833	2820	2839	2831	2926
CALGARY	10709	10707	10672	10646	10648	10664	10640	10642	10644	10665	10629	11733
BERGEN	530	534	544	527	535	524	537	542	533	531	543	549
SULPHUR MT	7997	7959	7933	7941	7954	7950	7947	7959	7931	7943	7973	8987
KERGUELEN	1847	1842	1836	1833	1828	1828	1824	1819	1837	1848	1838	1893
MT WASHINGTON									2068	2085	2090	2212
DURHAM									1398	1396	1401	1453
UPPSALA	5612	5645	5603	5635	5620	5637	5599	5581	5645	5602	5574	5804
MAGADAN											7217	7431
LEEDS	6325	6307	6310	6307	6289	6313	6303	6307	6316	6295	6315	6437
KIEL	5943	5927	5933	5919	5909	5913	5925	5909	5940	5917	5923	6019
MOSCOW								4491	4510	4488	4505	4626
UTRECHT	6015	6003	6003	5994	5974	5982	5994	5994	6012	6010	6012	6086
LINDAU	3669	3665	3654	3653	3646	3641	3667	3645	3657	3651	3651	3696
CLIMAX	3839	3863	3878	3840	3828	3833	3862	3860	3881	3853	3842	3914
IRKUTSK										10125	10256	10261
LOMNICKY STIT										4981	4982	4986
PREDIGTSTUHL	3599	3585	3616	3625	3600	3622	3597	3611	3595	3552	3543	3571
DALLAS										5937	5985	6011
HERMANUS	973	978	981	977	971	981	982	976	970	979	976	984
PIC DU MIDI	2384	2386	2386	2387	2386	2392	2397	2405	2404	2392	2386	2397
USHUAIA	271	290	228	302	274	344	283	268	294	270	244	298
ROME	2940	2967	2996	2961	2960	2945	2951	2964	2940	2897	2875	2891
MEXICO CITY	843	841	847	840	836	842	841	851	838	849	847	845
MT NORIKURA											10173	10197
TOKYO/ITABASHI											3480	3451
HUANCAYO	1714	1723	1717	1726	1708	1721	1727	1712	1714	1706	1720	1713

Table 2 (continued)

January 25, 1971

01	02	03	04	05	06	07	08	09	10	11	12	AVERAGE
7359	7064	6931	6863	6826	6793	6770	6799	6786	6771	6762	6795	6823.4
2223	2067	2032	2014	1998	1998	2000	1993	1986	1970	1964	1979	1995.2
7063	6796	6680	6622	6564	6579	6552	6535	6540	6544	6525	6533	6586.5
6515	6279	6125	6060	6073	6029	6045	6021	6033	6028	6038	6032	6093.0
2778	2649	2585	2594	2544	2549							2620.8
7201	6831	6705	6643	6637	6607	6583	6579	6606	6601	6601	6596	6618.3
7187	6921	6823	6811	6741	6743	6717	6694	6685	6675	6659	6658	6724.2
7389	7012	6818	6769	6737	6726	6686	6688	6668	6661	6626	6641	6700.3
5990	5860	5745	5713	5646	5651	5613	5616	5587	5596	5602	5588	5640.2
9155	8769	8590	8603	8617								8732.5
7725	7358	7220	7160	7196	7176	7225	7215	7238	7222	7252	7212	7235.3
3846	3683	3595	3598	3576	3562	3562	3562	3560	3567	3556	3542	3556.6
7056	6767	6658	6585	6575	6526	6524	6521	6528	6523	6531	6519	6550.0
15418	14843	14486	14314	14363	14348							14585.7
3041	2955	2881	2930	2916	2899	2840	2865	2821	2865	2858	2903	2871.4
12157	11306	11024	10917	10823	10758	10803	10773	10745	10784	10793	10779	10860.8
592	557	552	540	543	540	546	548	547*	546	536	544	542.5
9433	8605	8297	8189	8134	8102	8104	8061	8076	8045	8069	8037	8151.0
1990	1926	1901	1880	1875	1867	1874	1867	1871	1865	1866	1859	1863.0
2364	2203	2164	2132	2130								2160.7
1494	1445	1422	1417	1410								1426.1
6068	5819	5746	5719	5655	5682	5693	5734	5665	5689	5689	5636	5681.3
7508	7374	7374	7273	7237	7252	7230	7227	7210	7215			7295.7
6483	6427	6399	6367	6366	6358	6380	6387	6409	6422	6388	6374	6357.6
6084	6009	5986	5965	5986	5983	5985	5987	6000	5989	5972	5973	5962.3
4541	4516	4526	4546	4517	4542						4494	4525.2
6096	6064	6042	6026	6043	6028	6038	6069	6074	6072	6054	6059	6030.7
3698	3664	3669	3677	3676	3690	3686	3695	3705	3704	3688	3693	3672.5
3940	3900	3879	3852	3866	3867	3869	3862	3881	3875	3877	3888	3868.7
10183	10208	10280	10322	10456	10344	10227	10240	10259	10227	10232	10214	10255.6
4952	5003	4930	4945	4892	4988	4953	4886	4998	4955	4923	4963	4955.6
3582	3573	3564	3579	3574	3593	3598	3622	3658	3657	3655	3659	3601.2
5987	5990	5994	5971	5965	5941	5948	5967	5964	5974	5959	5995	5972.5
976	983	982	980	982	984	982	985	993	973	979	981	942.0
2398	2406	2405	2409	2402	2427	2422	2422	2430	2430	2429	2426	2404.5
244	298	285	258	287	347	272	259	290	214	268	294	282.6
2877	2851	2848	2838	2852	2857	2831	2830	2827	2835	2837	2858	2892.8
850	846	839	842	843	842	843	851	848	841	848	852	844.3
10303	10290	10235	10227	10212								10233.8
3503	3505	3518	3515	3488								3494.3
1721	1731	1717	1719	1711	1733	1714	1729	1716	1732	1716	1716	1719.0

Table 3

DUMONT DURVILLE 66.4S 140.02E ANTARCTICA

NEUTRON MONITOR 9-NM-64

CORRECTED FOR BAROMETRIC PRESSURE

COEFFICIENT 9.9 PER CENT PER CM HG

MULTIPLY INDICATED NUMBERS BY 200

FIFTEEN-MINUTE HOURLY RATES

JANUARY 24-25, 1971

TIME U.T.	MINUTES AT END OF INTERVAL 15	30	45	60
1200-1300	488	488	485	488
1300-1400	489	486	486	489
1400-1500	491	490	486	491
1500-1600	489	485	486	490
1600-1700	485	488	487	492
1700-1800	489	485	486	491
1800-1900	488	491	484	489
1900-2000	494	488	492	488
2000-2100	487	489	494	493
2100-2200	489	492	494	491
2200-2300	490	497	490	492
2300-2400	493	496	555	585
0000-0100	585	555	548	536
0100-0200	524	520	513	511
0200-0300	509	513	506	506
0300-0400	501	506	501	503
0400-0500	498	498	502	500
0500-0600	501	500	499	501
0600-0700	500	499	502	502
0700-0800	501	498	499	498
0800-0900	499	497	497	496
0900-1000	496	491	493	493
1000-1100	489	494	495	492
1100-1200	493	497	495	499

Table 3 (continued)

FORT CHURCHILL 58.75N 265.90E CANADA

NEUTRON MONITOR NM-64

BAROMETER REFERENCE 1010 MILLIBARS

ATTENUATION LENGTH 137.2 MILLIBARS

REAL COUNTS 40 TIMES TABULATED COUNTS

FIVE-MINUTE BAROMETER CORRECTED HOURLY RATES

JANUARY 24-25, 1971

TIME U.T.	MINUTES AT END OF INTERVAL 05	10	15	20	25	30	35	40	45	50	55	60	AVERAGE
1900	1508	1498	1497	1501	1484	1491	1488	1489	1495	1496	1488	1495	1494.1
2000	1481	1499	1487	1505	1486	1481	1492	1492	1490	1498	1479	1491	1490.3
2100	1470	1478	1501	1492	1495	1510	1494	1494	1489	1506	1483	1521	1494.3
2200	1490	1495	1478	1491	1488	1484	1488	1484	1519	1495	1497	1497	1492.2
2300	1496	1495	1486	1498	1501	1484	1494	1546	1616	1640*	1672	1690	1551.7
2400	1672	1669	1667	1657	1657	1621	1619	1596	1588	1615	1594	1591	1628.8
0100	1604	1583	1578	1566	1583	1555	1576	1547	1550*	1550*	1566	1540	1566.5
0200	1527	1547	1525	1546	1535*	1526	1528	1507	1536	1537	1531	1534	1531.6
0300	1516	1496	1517	1520*	1520*	1521	1511	1519	1516	1516	1519	1520	1515.8
0400	1537	1516	1529	1513	1521	1505	1516	1508	1522	1516	1523	1513	1518.2
0500	1510	1518	1503	1495	1517	1487	1501	1507	1498	1537	1493	1519	1507.1
0600	1516	1497	1521	1517	1515	1515	1507	1497	1507	1505	1516	1522	1511.3
0700	1505	1486	1497	1500	1529	1533	1498	1517	1510*	1503	1486	1506	1505.7
0800	1495	1518	1505	1488	1507	1506	1514	1529	1503	1514	1506	1513	1508.3
0900	1492	1504	1501	1508	1532	1510	1498	1492	1526	1506	1500	1516	1507.1
1000	1500	1510	1511	1515	1504	1506	1521	1496	1525	1507	1505	1514	1509.6
1100	1511	1509	1516	1496	1512	1492	1512	1511	1490	1509	1511	1530	1508.0
1200	1503	1508*	1513	1507	1511	1510	1494	1502	1503	1494	1508	1488	1503.4
1300	1522	1524	1501	1508	1519	1497	1519	1514	1507	1513	1514	1513	1512.7

TIXIE BAY 71.58N 128.9E USSR

NEUTRON MONITOR 18-NM-64

PRESSURE CORRECTED TO 758 MM HG

BAROMETRIC COEFFICIENT -0.96 PER CENT PER MM HG

RECALCULATING COEFFICIENT 100

FIVE-MINUTE HOURLY RATES

JANUARY 24-25, 1971

TIME U.T.	MINUTES AT END OF INTERVAL 05	10	15	20	25	30	35	40	45	50	55	60	AVERAGE
2200	551	557	555	550	554	554	552	554	555	555	545	565	555.6
2300	567	558	552	557	549	555	558	559	579	594	605*	601	560.1
2400	592	599	600	601*	600	603*	606*	601	602	600	596	601	600.1
0100	590*	590*	587*	582	577	582	579	577	578	572	574	569	579.8
0200	570	571	567	575	572	565	565	566	565	570	572	565	568.6
0300	574	574	575	565	573	564	572	570	564	565	561	555	567.6
0400	557	562	563*	560	559	558	562	570*	562	571	565	558	561.8
0500	559	563	564	563	561	564*	554	567	566	569	557	561	562.0
0600	560	562	557	553	555	564	556	566*	563	559	564	559	559.8
0700	553	559	558	559	561	559	553	555	565	556	559	555	557.8
0800	557	564	548	563	556	561	557	558	556	561	556	547	557.0
0900	551	561	556	557	556	562	560	553	557	555	550	557	556.3
1000	559	557	552	551	557	551	554	559	553	557	555	554	555.0
1100	551	550	560	559	547	558	553	553	550	558	556	552	554.8
1200	558	561*	556	562	558	557	559	555	549	552	552	550	555.5
1300	559	556	566	555	563	553	555	561	561	555	557	552	557.8

Table 3 (continued)

KIRUNA 67.83N 20.43E SWEDEN

NEUTRON MONITOR 12-NM-64

CORRECTED TO 720 MM HG

COEFFICIENT -0.99 PER CENT PER MM HG

REAL COUNTS 10 TIMES TABULATED COUNTS

FIVE-MINUTE HOURLY RATES

JANUARY 24-25, 1971

TIME U.T.	MINUTES AT END OF INTERVAL 05	10	15	20	25	30	35	40	45	50	55	60	AVERAGE
2200	5663	5669	5664	5669	5661	5639	5726	5713	5643	5678	5631	5656	5667.7
2300	5674	5690	5700	5694	5689	5637	5722	5639	5696	5746	5685	5648	5685.0
2400	5689	5660	5665	5635	5668	5667	5707	5772	6246	6536	6721	6761	5977.3
0100	6780	6625	6487	6476	6366	6296	6229	6244	6290	6238	6139	6237	6367.3
0200	6158	6178	6094	6093	6064	6040	5982	5996	6033	5936	5976	5957	6042.3
0300	5882	5864	5952	5903	5855	5851	5899	5830	5906	5835	5874	5852	5875.3
0400	5856	5879	5848	5851	5825	5879	5829	5820	5742	5822	5818	5820	5832.4
0500	5809	5841	5754	5788	5795	5855	5763	5831	5845	5776	5811	5797	5805.4
0600	5782	5816	5786	5742	5817	5835	5792	5760	5820	5816	5819	5762	5795.6
0700	5769	5813	5742	5767	5748	5744	5709	5742	5749	5780	5798	5789	5762.5
0800	5780	5742	5753	5838	5799	5767	5716	5759	5762	5793	5742	5795	5770.5
0900	5782	5776	5766	5786	5761	5722	5818	5776	5776	5744	5736	5776	5768.3
1000	5774	5757	5763	5714	5794	5796	5754	5810	5804	5733	5725	5753	5764.8
1100	5710	5766	5743	5699	5753	5732	5752	5780	5691	5749	5733	5754	5738.5
1200	5732	5765	5718	5713	5749	5741	5757	5722	5782	5716	5795	5747	5744.8
1300	5766	5732	5739	5719	5705	5737	5774	5780	5841	5750	5737	5761	5753.4
1400	5775	5777	5728	5734	5697	5720	5705	5731	5726	5737	5700	5746	5731.3
1500	5749	5746	5769	5698	5756	5741	5717	5764	5782	5758	5729	5775	5748.7
1600	5725	5678	5738	5686	5694	5728	5689	5705	5720	5675	5709	5683	5702.5
1700	5720	5751	5676	5767	5696	5702	5730	5730	5760	5720	5720	5669	5720.1
1800	5716	5751	5686	5762	5729	5693	5717	5738	5702	5731	5719	5751	5724.6

APATITY 67.5N 33.3E USSR

NEUTRON MONITOR

UNCORRECTED FOR PRESSURE

FIFTEEN-MINUTE HOURLY RATES

JANUARY 24-25, 1971

TIME U.T.	MINUTES AT END OF INTERVAL 15	30	45	60
2300		2063	2121	2377
2400	2360	2297	2260	2248
0100	2214	2198	2187	2170
0200	2151	2138	2151	2150
0300	2149	2138	2164	2152
0400	2153	2157	2156	2151

Table 3 (continued)

BELGRANO 77.96S 38.8W ANTARCTIC

NEUTRON MONITOR 6-NM-64

UNCORRECTED FOR PRESSURE

REAL COUNTS 32 TIMES TABULATED COUNTS

FIVE-MINUTE HOURLY RATES

JANUARY 24-25, 1971

TIME U.T.	MINUTES AT END OF INTERVAL 05	10	15	20	25	30	35	40	45	50	55	60	AVERAGE
2200-2300	580	588	585	567	574	585	581	581	582	576	562	581	577.7
2300-2400	573	572	573	579	579	578	574	588	601	629	643	675	597.0
0000-0100	690	684	671	664	657	644	615	622	626	616	612	624	643.8
0100-0200	608	621	619	607	613	618	608	612	618	612	612	610	613.2
0200-0300	605	623	616	603	604	596	585	598	599	595	596	600	601.7
0300-0400	599	583	590	602	599	583	608	597	602	601	592	604	596.7
0400-0500	598	594	596	589	607	618	586	596	608	601	602	601	599.7
0500-0600	596	603	591	598	596	597	595	598	598	595	598	611	598.0
0600-0700													602.1
0700-0800													601.3
0800-0900													603.2
0900-1000													601.9
1000-1100													604.3
1100-1200													601.0

OULU 65.0N 25.4E FINLAND

NEUTRON MONITOR 9-NM-64

UNCORRECTED FOR PRESSURE

FIVE-MINUTE HOURLY RATES

JANUARY 24-25, 1971

TIME U.T.	MINUTES AT END OF INTERVAL 05	10	15	20	25	30	35	40	45	50	55	60	PRESSURE
0000-0100	470	476	481	483	468	481	477	476	473	478	475	477	993.4
0100-0200	479	481	480	473	474	472	471	475	482	476	480	476	993.4
0200-0300	476	481	478	487	477	477	474	474	482	478	480	477	993.0
0300-0400	479	478	482	476	488	474	479	476	478	478	483	482	992.4
0400-0500	477	479	486	483	479	482	482	476	484	483	481	484	992.2
0500-0600	481	487	480	480	475	474	482	482	477	482	479	481	992.2
0600-0700	477	475	481	482	480	481	479	486	481	482	482	484	992.1
0700-0800	484	490	476	476	476	478	478	486	477	474	483	477	992.1
0800-0900	475	483	482	483	484	473	474	479	474	480	490	481	992.2
0900-1000	486	478	479	477	478	489	481	484	478	478	478	474	992.2
1000-1100	480	480	482	475	471	479	475	483	478	474	477	480	992.2
1100-1200	482	476	480	480	479	476	483	482	478	471	476	482	992.3
1200-1300	481	490	486	472	482	490	481	490	474	476	480	483	992.3
1300-1400	474	483	477	487	480	478	480	487	478	482	481	479	992.0
1400-1500	478	483	482	480	483	478	479	486	483	488	482	481	991.8
1500-1600	478	477	486	480	491	498	481	488	482	481	481	488	991.6
1600-1700	480	480	491	487	486	480	490	483	487	484	487	493	991.0
1700-1800	480	483	490	487	489	488	492	484	480	490	484	493	990.3
1800-1900	492	495	494	496	491	499	497	493	488	492	505	490	989.5
1900-2000	499	503	498	494	501	497	489	500	498	501	490	502	988.7
2000-2100	499	490	501	496	500	498	506	500	498	502	500	502	987.9
2100-2200	500	505	500	498	501	508	503	502	498	496	491	496	987.2
2200-2300	508	505	502	499	510	505	499	506	505	510	510	503	986.6
2300-2400	509	499	502	503	504	511	506	520	537	559	580	589	985.9
0000-0100	580	577	565	563	559	559	566	552	551	541	552	548	985.0
0100-0200	546	550	543	546	543	540	536	541	539	529	533	528	984.0
0200-0300	533	532	528	530	527	529	520	526	528	531	534	532	983.2
0300-0400	528	523	531	541	531	530	529	535	531	535	537	534	982.6
0400-0500	535	526	526	534	533	528	533	532	534	526	531	532	982.1

Table 3 (continued)

0500-0600	532	533	537	529	530	520	531	523	531	532	533	533	981.6
0600-0700	533	530	530	529	532	537	538	527	530	542	536	531	981.1
0700-0800	534	537	538	536	538	537	535	532	541	531	527	535	980.5
0800-0900	543	536	535	533	538	535	543	541	534	533	538	536	979.9
0900-1000	538	548	535	545	539	537	544	541	542	544	540	537	979.3
1000-1100	533	546	535	537	542	543	544	542	537	537	545	542	978.9
1100-1200	546	533	540	542	538	543	537	540	533	538	540	549	978.5
1200-1300	540	542	540	547	543	545	544	542	547	546	548	553	978.3
1300-1400	548	547	546	544	546	542	546	543	543	539	554	539	978.2
1400-1500	537	541	541	546	548	548	550	546	543	543	550	547	977.9
1500-1600	537	542	545	549	543	543	547	542	556	542	536	545	977.8
1600-1700	545	538	545	542	551	548	544	547	546	542	544	548	977.7
1700-1800	549	541	549	551	539	552	538	547	542	548	554	547	977.6
1800-1900	546	555	553	543	546	549	539	539	550	550	544	545	977.5
1900-2000	552	543	546	547	548	543	539	541	550	552	544	547	977.6
2000-2100	548	542	540	541	541	545	541	540	536	547	545	549	977.9
2100-2200	538	543	539	545	541	542	544	539	540	550	548	543	978.4
2200-2300	536	535	538	539	547	532	544	531	536	534	537	532	979.1
2300-2400	537	541	544	535	541	534	537	538	539	543	539	539	979.7

DEEP RIVER 46.1N 77.3W CANADA

NEUTRON MONITOR 48-NM-64

REAL COUNTS 300 TIMES TABULATED COUNTS

FIVE-MINUTE BAROMETER CORRECTED HOURLY RATES

JANUARY 24-25, 1971

TIME U.T.	MINUTES AT END OF INTERVAL 05	10	15	20	25	30	35	40	45	50	55	60	AVERAGE
2200-2300	6423	6430	6483	6471	6483	6453	6453	6453	6470	6482	6482	6482	6464
2300-2400	6446	6505	6499	6480	6474	6427	6527	6775	6912	7089	7243	7255	6719
0000-0100	7298	7262	7120	7089	7094	7064	7040	7033	6991	6925	6866	6890	7056
0100-0200	6866	6883	6864	6834	6752	6752	6757	6710	6715	6685	6690	6707	6768
0200-0300	6689	6665	6682	6710	6662	6656	6685	6644	6603	6626	6666	6619	6659
0300-0400	6590	6601	6583	6606	6618	6590	6590	6561	6538	6585	6573	6596	6586
0400-0500	6578	6618	6542	6577	6583	6646	6593	6529	6564	6580	6557	6552	6577
0500-0600	6511	6557	6511	6546	6534	6511	6562	6585	6493	6505	6510	6510	6528
0600-0700	6526	6520	6526	6521	6538	6526	6480	6533	6526	6538	6526	6538	6525
0700-0800	6549	6549	6503	6533	6510	6498	6526	6520	6485	6531	6502	6513	6518
0800-0900	6536	6536	6541	6525	6525	6479	6548	6548	6491	6507	6530	6548	6526
0900-1000	6525	6513	6513	6520	6543	6582	6513	6530	6491	6531	6520	6520	6525
1000-1100	6508	6515	6510	6516	6505	6562	6562	6482	6557	6529	6610	6524	6532
1100-1200	6547	6507	6484	6565	6496	6502	6497	6538	6515	6503	6510	6527	6516
1200-1300	6579	6505	6528	6563	6546	6518	6536	6559	6577	6577	6537	6543	6547
1300-1400	6491	6498	6563	6504	6493	6512	6523	6518	6548	6566	6549	6532	6525

SANAE 70.3S 02.35W ANTARCTICA

NEUTRON MONITOR 3-NM-64

CORRECTED TO 980 MILLIBARS

COEFFICIENT 0.73 PER CENT PER MILLIBAR

REAL COUNTS 10 TIMES TABULATED VALUES

TEN-MINUTE HOURLY RATES

JANUARY 24-25, 1971

TIME U.T.	MINUTES AT END OF INTERVAL 10	20	30	40	50	60	AVERAGE
2200-2300	2354	2388	2388	2367	2354	2380	2371.8
2300-2400	2307	2342	2377	2442	2590	2625	2447.2
2400-0100	2570	2597	2601	2579	2544	2527	2569.7

0100-0200	2489	2500	2448	2509	2443	2454 2473.8
0200-0300	2375	2401	2419	2445	2428	2418 2414.3
0300-0400	2328	2442	2398	2407	2350	2389 2385.7
0400-0500	2352	2422	2427	2387	2383	2392 2393.8
0500-0600	2333	2416	2430	2381	2394	2394 2391.3

PORT AUX FRANCAIS 49.35S 70.25E KERGUELEN ISLAND

NEUTRON MONITOR 18-NM-64

CORRECTED FOR BAROMETRIC PRESSURE

COEFFICIENT 10.1 PER CENT PER CM HG

MULTIPLY INDICATED NUMBERS BY 40

FIVE-MINUTE HOURLY RATES

JANUARY 24-25, 1971

TIME U.T.	MINUTES AT END OF INTERVAL 05	10	15	20	25	30	35	40	45	50	55	60
1200-1300	1544	1541	1548	1539	1542	1536	1541	1540	1521	1550	1548	1536
1300-1400	0000	0000	1531	1556	1542	1548	1554	1522	1535	1514	1526	1535
1400-1500	1542	1535	1530	1541	1526	1535	1539	1521	1526	1532	1527	1520
1500-1600	1517	1525	1522	1522	1532	1530	1526	1532	1523	1528	1537	1535
1600-1700	1538	1516	1510	1526	1521	1531	1533	1535	1519	1517	1508	1531
1700-1800	1537	1526	1514	1544	1510	1534	1533	1521	1517	1505	1510	1520
1800-1900	1507	1516	1519	1521	1507	1526	1516	1532	1531	1515	1532	1518
1900-2000	1523	1509	1512	1506	1519	1513	1508	1531	1507	1522	1510	1530
2000-2100	1529	1516	1546	1534	1539	1525	1517	1523	1522	1527	1529	1549
2100-2200	1539	1553	1536	1546	1540	1539	1539	1554	1537	1537	1553	1537
2200-2300	1530	1537	1544	1540	1550	1537	1520	1531	1507	1534	1516	1517
2300-2400	1540	1516	1529	1553	1531	1523	1538	1588	1658	1651	1665	1656
0000-0100	1660	1679	1682	1664	1662	1665	1648	1665	1616	1649	1639	1635
0100-0200	1624	1626	1605	1624	1615	1602	1608	1593	1604	1578	1591	1582
0200-0300	1588	1604	1589	1566	1595	1593	1584	1576	1572	1578	1586	1580
0300-0400	1567	1586	1576	1558	1583	1576	1561	1557	1564	1559	1547	1568
0400-0500	1567	1570	1570	1573	1555	1576	1557	1568	1551	1555	1555	1551
0500-0600	1558	1555	1561	1548	1574	1554	1551	1547	1559	1568	1544	1557
0600-0700	1551	1558	1549	1568	1567	1550	1574	1580	1565	1576	1554	1562
0700-0800	1557	1549	1561	1562	1558	1570	1559	1544	1546	1550	1571	1550
0800-0900	1562	1544	1571	1570	1578	1563	1546	1552	1585	1556	1542	1559
0900-1000	1555	1549	1555	1558	1569	1553	1544	1564	1543	1561	1544	1553
1000-1100	1561	1570	1547	1554	1562	1565	1549	1546	1556	1570	1553	1549
1100-1200	1557	1553	1555	1556	1561	1548	1560	1550	1534	1546	1530	1535

MT WASHINGTON 44.3N 288.7E NEW HAMPSHIRE

IGY NEUTRON MONITOR

CORRECTED FOR BAROMETRIC PRESSURE

FIVE-MINUTE HOURLY RATES

JANUARY 24-25, 1971

TIME U.T.	MINUTES AT END OF INTERVAL 05	10	15	20	25	30	35	40	45	50	55	60	AVERAGE
2000-2100	172	170	174	171	172	171	174	170	173	173	174	172	172.3
2100-2200	175	172	174	174	174	171	176	175	172	174	175	174	173.8
2200-2300	175	175	174	173	174	172	173	175	176	173	171	177	174.1
2300-2400	174	175	173	171	173	174*	175	187	196	203	207	203	184.3
2400-0100	204	208	207	204	202	196	195	192	191	187	185	193	196.9
0100-0200	194	189	185	185	183	183	180	183	182	181	179	180	183.6
0200-0300	181	185	177	183	184	181	182	179	174	179	181	177	180.3
0300-0400	176	180	181	177	176	175	179	179	178	178	176	177	177.6
0400-0500	180	175	178	180	174	179	178	174	178	179	179	175	177.5

Table 3 (continued)

DURHAM 43.1N 289.1E NEW HAMPSHIRE

NEUTRON MONITOR 12-NM-64

CORRECTED FOR BAROMETRIC PRESSURE

FIVE-MINUTE HOURLY RATES

JANUARY 24-25, 1971

TIME U.T.	MINUTES AT END OF INTERVAL 05	10	15	20	25	30	35	40	45	50	55	60	AVERAGE
2000-2100	116	117	116	116	116	116	117	118	117	118	116	115	116.6
2100-2200	117	117	116	117	116	117	115	117	117	115	117	115	116.3
2200-2300	118	119	117	115	118	117	115	117	117	114	119	117	116.8
2300-2400	117	117	118	116	116	117	117	122	127	129	129	128	121.1
2400-0100	129	128	126	129	124	126	123	122	122	122	123	121	124.5
0100-0200	122	121	122	120	120	122	121	119	120	120	118	120	120.4
0200-0300	120	119	119	118	118	118	118	120	119	118	119	117	118.5
0300-0400	119	117	116	117	118	120	118	117	121	117	119	117	118.1
0400-0500	117	119	115	118	117	119	117	119	118	118	119	115	117.5

UPPSALA 59.85N 17.58E SWEDEN

IGY NEUTRON MONITOR

CORRECTED TO 757.75 MM HG

COEFFICIENT -0.986 PER CENT PER MM HG

SCALING FACTOR 2.5

FIVE-MINUTE HOURLY RATES

JANUARY 24-25, 1971

TIME U.T.	MINUTES AT END OF INTERVAL 05	10	15	20	25	30	35	40	45	50	55	60	AVERAGE
2200	1800	1816	1798	1803	1868	1788	1806	1804	1825	1814	1798	1871	1815.9
2300	1814	1788	1840	1846	1799	1789	1791	1799	1807	1830	1828	1783	1809.5
2400	1852	1870	1859	1791	1786	1797	1840	1940	1966	1982	1908	1987	1881.5
0100	2007	2047	1956	1940	1967	1931	1949	1937	2003	1990	1940	1934	1966.5
0200	1938	1901	1899	1920	1894	1869	1878	1906	1857	1868	1868	1838	1886.3
0300	1881	1862	1808	1851	1856	1886	1842	1897	1865	1876	1878	1846	1862.3
0400	1824	1871	1870	1816	1897	1838	1869	1848	1847	1878	1885	1801	1853.7
0500	1805	1822	1829	1825	1854	1860	1907	1882	1857	1857	1821	1794	1842.8
0600	1858	1809	1866	1844	1836	1852	1851	1871	1781	1848	1827	1855	1841.5
0700	1811	1829	1904	1865	1802	1860	1813	1890	1841	1821	1869	1840	1845.4
0800	1820	1824	1868	1854	1853	1854	1820	1945	1884	1884	1863	1838	1858.9
0900	1774	1835	1823	1875	1797	1889	1878	1826	1813	1875	1837	1810	1836.0
1000	1852	1827	1847	1832	1821	1820	1868	1852	1814	1915	1818	1860	1843.8
1100	1818	1871	1836	1804	1842	1850	1862	1835	1882	1908	1802	1820	1844.2
1200	1820	1834	1842	1805	1863	1853	1828	1829	1807	1856	1764	1819	1826.7
1300	1870	1822	1805	1809	1867	1817	1804	1848	1887	1795	1801	1809	1827.8
1400	1829	1869	1840	1895	1829	1799	1880	1783	1840	1803	1827	1855	1837.4
1500	1797	1842	1830	1802	1858	1821	1821	1894	1843	1787	1824	1897	1834.7
1600	1826	1855	1827	1798	1802	1806	1828	1797	1849	1788	1867	1826	1822.4
1700	1856	1849	1800	1844	1789	1774	1847	1849	1810	1820	1831	1797	1822.2
1800	1801	1848	1816	1889	1840	1850	1802	1855	1783	1820	1817	1880	1833.4

Table 3 (continued)

MAGADAN 60.11N 151.01E USSR

NEUTRON MONITOR 18-NM-64

CORRECTED TO 980 MILLIBARS

BAROMETRIC COEFFICIENT -0.74 PER CENT PER MILLIBAR

RECALCULATING COEFFICIENT 64

FIFTEEN-MINUTE HOURLY RATES

JANUARY 24-25, 1971

TIME U.T.	MINUTES AT END OF INTERVAL 15	30	45	60
2200	1801	1810	1802	1804
2300	1796	1800	1867	1968
2400	1910	1892	1860	1846
0100	1845	1841	1845	1843
0200	1845	1841	1845	1843
0300	1829	1812	1814	1818
0400	1816	1810	1800	1811
0500	1812	1808	1815	1817
0600	1814	1811	1800	1805
0700	1801	1814	1814	1798
0800	1811	1792	1805	1802
0900	1796	1818	1795	1806

LEEDS 53.8N 01.5W ENGLAND

IGY NEUTRON MONITOR

REAL COUNTS 100 TIMES TABULATED COUNTS

FIVE-MINUTE BAROMETER CORRECTED RATES

JANUARY 24-25, 1971

TIME U.T.	MINUTES AT END OF INTERVAL 05	10	15	20	25	30	35	40	45	50	55	60	AVERAGE
0000-0100	522	525	526	526	525	526	527	528	529	525	531	524	526.2
0100-0200	523	528	530	529	523	526	526	526	528	530	529	526	527.0
0200-0300	525	525	530	527	527	527	531	531	526	520	528	532	527.3
0300-0400	530	528	524	533	523	527	527	527	527	521	528	530	527.0
0400-0500	530	531	524	528	526	521	528	524	522	528	523	522	525.8
0500-0600	525	525	530	530	531	527	523	523	532	524	529	525	527.1
0600-0700	525	525	526	526	523	530	530	526	526	527	531	516	526.0
0700-0800	523	528	524	525	523	523	524	527	522	523	527	529	524.8
0800-0900	527	524	529	525	520	528	527	523	526	528	523	530	525.9
0900-1000	523	531	527	527	527	530	529	524	524	523	528	524	526.5
1000-1100	527	526	529	530	522	525	525	534	530	528	530	523	527.4
1100-1200	523	528	535	526	529	527	522	518	530	525	532	528	527.0
1200-1300	526	522	529	527	528	529	525	525	526	529	531	528	527.0
1300-1400	523	525	527	531	520	522	526	524	530	524	530	526	525.6
1400-1500	526	527	527	524	529	531	526	527	523	525	519	527	525.8
1500-1600	529	524	530	522	526	528	528	523	526	525	525	522	525.6
1600-1700	524	529	521	522	526	525	522	525	522	523	522	528	524.1
1700-1800	529	525	523	523	526	526	527	529	528	528	531	519	526.1
1800-1900	528	524	523	524	525	523	526	531	521	528	525	525	525.3
1900-2000	525	518	519	530	531	525	526	526	528	529	526	524	525.6
2000-2100	526	524	528	529	525	525	527	528	526	522	528	528	526.3
2100-2200	524	526	525	521	525	526	521	524	526	527	527	523	524.6
2200-2300	527	524	529	520	527	526	524	530	530	520	528	528	526.3
2300-2400	531	522	523	519	530	527	529	536	556	556	552	556	536.4
0000-0100	547	548	547	540	538	539	537	537	536	538	536	540	540.3
0100-0200	533	538	546	532	536	534	540	533	535	531	535	533	535.6
0200-0300	536	532	539	533	532	531	530	533	534	535	532	532	533.3
0300-0400	528	527	538	532	529	531	531	527	528	538	531	528	530.6

Table 3 (continued)

0400-0500	530	530	533	534	527	533	531	535	530	526	530	527	530.6
0500-0600	526	530	528	534	527	532	535	524	530	534	530	527	529.8
0600-0700	531	526	534	534	533	526	529	531	532	537	531	534	531.7
0700-0800	529	534	533	531	533	535	535	528	535	534	528	533	532.3
0800-0900	531	533	532	535	532	531	534	537	540	536	532	536	534.1
0900-1000	533	535	536	536	539	531	537	535	533	532	533	544	535.2
1000-1100	533	529	530	534	532	533	533	533	529	532	534	535	532.3
1100-1200	537	529	526	529	530	530	533	530	536	527	535	534	531.2
1200-1300	530	528	533	526	538	529	522	526	538	526	531	529	529.8
1300-1400	532	526	531	531	530	527	528	529	523	529	525	526	528.0
1400-1500	522	534	0	531	528	530	531	524	521	531	538	525	*528.7
1500-1600	525	531	528	0	0	532	526	527	525	533	527	524	*528.0
1600-1700	532	531	529	0	528	528	526	526	522	528	531	528	*528.0
1700-1800	530	530	530	526	528	526	523	532	532	534	525	525	528.5
1800-1900	531	530	524	527	536	534	526	529	530	534	529	528	529.9
1900-2000	531	529	535	534	530	529	528	530	528	530	530	525	529.9
2000-2100	532	526	525	532	524	529	525	529	525	524	528	528	527.2
2100-2200	529	532	530	530	525	528	527	528	526	529	526	528	528.3
2200-2300	530	529	528	530	527	526	531	530	529	533	536	526	529.6
2300-2400	532	523	532	526	522	526	526	526	528	533	527	530	527.4

KIEL 54.33N 10.10E GERMANY

NEUTRON MONITOR 18-NM-64

FIVE-MINUTE BAROMETER CORRECTED RATES

JANUARY 24-25, 1971

TIME U.T.	MINUTES AT END OF INTERVAL											
	05	10	15	20	25	30	35	40	45	50	55	60
2200	4916	4894	4916	4859	4877	4929	4953	4897	4934	4919	4938	4924
2300	4952	4926	4882	4935	4873	4870	4934	5034	5127	5156	5128	5145
2400	5094	5107	5077	5033	5045	5061	4996	5052	5055	4979	5019	5043
0100	4969	5024	4909	5020	4977	5003	4949	5000	4949	4973	5037	5019
0200	5018	4952	4958	4950	4959	4907	4986	4970	4969	4989	4937	4960
0300	4942	4973	4966	4936	4991	4939	4990	4916	4891	4923	4960	4963
0400	4961	4970	4956	4999	4918	5003	4927	4976	4955	4954	4963	4975
0500	4981	4976	4943	4920	4947	4992	4964	4905	4986	4995	4927	4958
0600	4936	4990	4953	4930	4955	5005	4951	4954	4940	5010	5006	5024
0700	4998	4965	4953	4972	4972	4998	4964	4962	4976	4940	4934	4993
0800	4978	4958	4987	4938	4993	4984	4938	4933	5002	4992	4992	4972
0900	4979	4953	5013	4990	4976	4958	5040	4955	4946	4952	4943	4902
1000	4885	4903	4940	5018	4952	4903	4923	5000	4928	4931	4944	4909
1100	4954	4974	4946	4965	4912	4936	4957	4937	4943	4939	4959	4941
1200	4985	4972	4962	4911	4920	4947	4935	4899	4929	4933	4939	4933
1300	4987	4934	4932	5024	4893	4977	4960	4958	4938	4944	4960	4915

Table 3 (continued)

MOSCOW 55.47N 37.3E USSR

NEUTRON MONITOR SNM

CORRECTED FOR PRESSURE

BAROMETRIC COEFFICIENT -0.71 PER CENT PER MILLIBAR

RECALCULATING COEFFICIENT 64

FIFTEEN-MINUTE HOURLY RATES

JANUARY 24-25, 1971

TIME U.T.	MINUTES AT END OF INTERVAL 15	30	45	60
2000	1124	1124	1112	1131
2100	1117	1127	1135	1131
2200	1130	1122	1124	1112
2300	1121	1113	1122	1149
2400	1177	1165	1143	1141
0100	1134	1135	1139	1133
0200	1128	1130	1126	1132
0300	1131	1133	1130	1132
0400	1128	1134	1140	1144
0500	1115	1132	1140	1130
0600	1135	1131	1133	1143

IRKUTSK 52.45N 104.03E USSR

NEUTRON MONITOR 18-NM-64

CORRECTED TO MILLIBARS

BAROMETRIC COEFFICIENT -0.74 PER CENT PER MILLIBAR

RECALCULATING COEFFICIENT 64

FIVE-MINUTE HOURLY RATES

JANUARY 24-25, 1971

TIME U.T.	MINUTES AT END OF INTERVAL 05	10	15	20	25	30	35	40	45	50	55	60	AVERAGE
2200	835	851	843	843	827	856	849	840	850	840	844	847	843.8
2300	844	851	847	842	847	844	855	863	859	871	862	871	854.7
2400	851	854	854	854	856	855	860	859	848	868	849	853	855.1
0100	851	850	848	849	850	862	848	847	846	838	845	849	848.6
0200	853	851	863	848	855	855	853	848	848	849	840	845	850.7
0300	859	866	862	833	848	855	868	855	865	860	855	854	856.7
0400	850	872	863	858	867	861	853	855	865	859	858	861	860.2
0500	861	857	866	860	868	861	967	865	862	867	859	863	871.3
0600	852	863	857	848	872	865	854	879	866	860	855	873	862.0
0700	860	846	850	851	862	856	856	855	346	852	841	852	852.3
0800	863	850	856	861	854	848	849	850	354	850	851	854	853.3
0900	855	849	860	851	853	851	868	850	851	860	860	851	854.9
1000	853	846	850	846	854	861	850	855	861	856	844	851	852.3
1100	855	851	845	853	850	849	864	844	850	858	856	857	852.7
1200	854	855	844	854	849	851	864	845	843	848	852	855	851.2
1300	848	962	849	851	853	859	856	853	855	867	854	857	863.7

Table 3 (continued)

LOMNICKY STIT 49.2N 20.22E CZECHOSLOVAKIA

IGY NEUTRON MONITOR

SCALING FACTOR 8

TEN-MINUTE BAROMETER CORRECTED RATES

JANUARY 24-25, 1971

TIME U.T.	MINUTES AT END OF INTERVAL 10	20	30	40	50	60	AVERAGE
2200	816	840	832	838	842	832	830.1
2300	814	834	814	840	838	842	830.3
2400	827	836	819	856	821	827	831.1
0100	825	832	829	831	816	818	825.3
0200	827	863	823	832	820	836	833.8
0300	823	822	844	834	803	803	821.6
0400	835	841	814	814	820	821	824.1
0500	805	804	827	815	820	819	815.3
0600	843	833	814	834	834	830	831.3
0700	822	807	821	835	827	841	825.5
0800	844	834	827	832	816	832	831.0
0900	828	850	834	823	819	844	833.0
1000	821	817	837	813	831	836	825.9
1100	823	804	824	828	828	817	820.4
1200	841	833	810	831	834	814	827.2

DALLAS 32.78N 96.80W TEXAS

NEUTRON MONITOR NM-64

REAL COUNTS 40 TIMES TABULATED COUNTS

FIVE-MINUTE BAROMETER CORRECTED HOURLY RATES

JANUARY 24-25, 1971

TIME U.T.	MINUTES AT END OF INTERVAL 05	10	15	20	25	30	35	40	45	50	55	60
1800	1485	1490	1504	1483	1500	1493	1509	1482	1503	1489	1472	1472
1900	1484	1493	1497	1497	1507	1485	1490	1469	1482	1485	1487	1485
2000	1484	1491	1487	1498	1484	1493	1493	1486	1496	1491	1475	1485
2100	1489	1477	1487	1497	1490	1500	1485	1476	1478	1470	1474	1488
2200	1494	1487	1497	1517	1500	1485	1488	1511	1496	1506	1476	1497
2300	1509	1490	1488	1503	1509	1477	1503	1518	1493	1519	1519	1507
2400	1483	1491	1492	1498	1500	1493	1497	1506	1503	1489	1497	1511
0100	1523	1512	1493	1497	1504	1496	1482	1496	1478	1500	1492	1500
0200	1505	1501	1490	1499	1511	1476	1510	1500	1491	1499	1503	1497
0300	1500	1513	1496	1493	1497	1496	1485	1515	1495	1474	1469	1481
0400	1498	1500	1486	1493	1488	1491	1497	1491	1494	1506	1473	1478
0500	1485	1500	1482	1487	1482	1476	1494	1488	1476	1486	1487	1478
0600	1487	1498	1487	1482	1481	1479	1494	1498	1464	1487	1486	1499
0700	1487	1488	1498	1503	1492	1497	1498	1484	1488	1501	1483	1481
0800	1497	1484	1492	1496	1500	1494	1495	1490	1464	1482	1502	1493
0900	1497	1494	1486	1485	1493	1485	1490	1499	1519	1497	1499	1477
1000	1506	1496	1495	1494	1483	1489	1479	1471	1479	1502	1492	1490
1100	1491	1493	1514	1497	1508	1488	1498	1508	1498	1485	1501	1505
1200	1500	1507	1499	1503	1491	1507	1498	1501	1490	1511	1506	1487
1300	1477	1499	1488	1507	1495	1473	1501	1481	1507	1491	1497	1488
1400	1492	1487	1496	1495	1505	1502	1505					

Table 3 (continued

ROME 41.9N 12.5E ITALY

NEUTRON MONITOR 9-NM-64

UNCORRECTED FOR PRESSURE

PROVISIONAL BAROMETRIC COEFFICIENT 9.2 PER CENT PER CM HG

SCALING FACTOR 100

FIFTEEN-MINUTE HOURLY RATES

JANUARY 24-25, 1971

TIME U.T.	MINUTES AT END OF INTERVAL 15	30	45	60	PRESSURE
0100	714	714	719	718	757.2
0200	715	717	728	712	757.1
0300	708	709	710	715	757.1
0400	723	721	712	715	756.9
0500	710	720	718	720	756.6
0600	729	713	714	721	756.4
0700	718	725	728	728	756.0
0800	727	719	727	723	755.9
0900	725	728	729	723	755.6
1000	725	726	732	727	755.4
1100	725	736	741	736	754.1
1200	737	735	732	736	753.8
1300	738	739	742	748	753.0
1400	745	752	758	741	752.6
1500	743	739	741	738	753.1
1600	741	738	739	742	753.3
1700	739	735	737	734	753.8
1800	748	731	735	737	754.3
1900	743	739	742	740	754.4
2000	735	735	736	734	755.0
2100	721	726	727	723	756.0
2200	721	715	718	721	756.8
2300	726	726	716	723	756.8
2400	725	717	715	720	757.1
0100	711	718	710	712	757.9
0200	713	710	713	712	758.2
0300	715	704	713	706	758.4
0400	710	707	718	717	758.5
0500	716	715	709	717	758.5
0600	705	706	713	707	759.0
0700	700	715	703	712	759.2
0800	705	710	706	706	759.3
0900	698	713	710	714	759.2
1000	707	709	711	710	758.8
1100	710	715	716	717	757.8
1200	714	716	719	716	757.6
1300	713	711	717	716	757.1
1400	722	725	720	723	756.5
1500	724	721	723	720	756.4
1600	718	717	720	717	756.3
1700	727	719	734	729	755.7
1800	733	734	736	728	755.3
1900	741	722	735	730	755.0
2000	740	721	734	728	755.2
2100	727	733	735	733	755.5
2200	728	735	732	736	755.5
2300	733	739	724	731	755.8

MT NORIKURA 36.11N 137.55E JAPAN

NEUTRON MONITOR 4-NM-64

PRESSURE CORRECTED TO 540 MM HG

COEFFICIENT -0.85 PER CENT PER MM HG

SCALE OF 64

FIFTEEN-MINUTE HOURLY RATES

JANUARY 24-25, 1971

TIME U.T.	MINUTES AT END OF INTERVAL 15	30	45	60	AVERAGE
2200-2300	2536	2531	2552	2554	2543.2
2300-2400	2539	2557	2544	2557	2549.2
2400-0100	2557	2582	2582	2582	2575.7
0100-0200	2588	2564	2569	2569	2572.5
0200-0300	2577	2557	2557	2544	2558.7
0300-0400	2572	2539	2562	2554	2556.7
0400-0500	2526	2572	2580	2534	2553.0

ITABASHI 35.75N 139.71E JAPAN

NEUTRON MONITOR 9-NM-64

PRESSURE CORRECTED TO 1013.3 MILLIBARS

COEFFICIENT -0.70 PER CENT PER MILLIBAR

SCALE OF 64

TEN-MINUTE HOURLY RATES

JANUARY 24-25, 1971

TIME U.T.	MINUTES AT END OF INTERVAL 10	20	30	40	50	60	AVERAGE
2200-2300	584	589	579	577	575	576	580.0
2300-2400	575	576	574	575	575	576	575.1
2400-0100	574	579	587	593	585	585	583.8
0100-0200	585	592	583	578	589	578	584.1
0200-0300	579	595	581	587	586	590	586.3
0300-0400	584	589	591	584	586	581	585.8
0400-0500	583	583	580	579	586	577	581.3

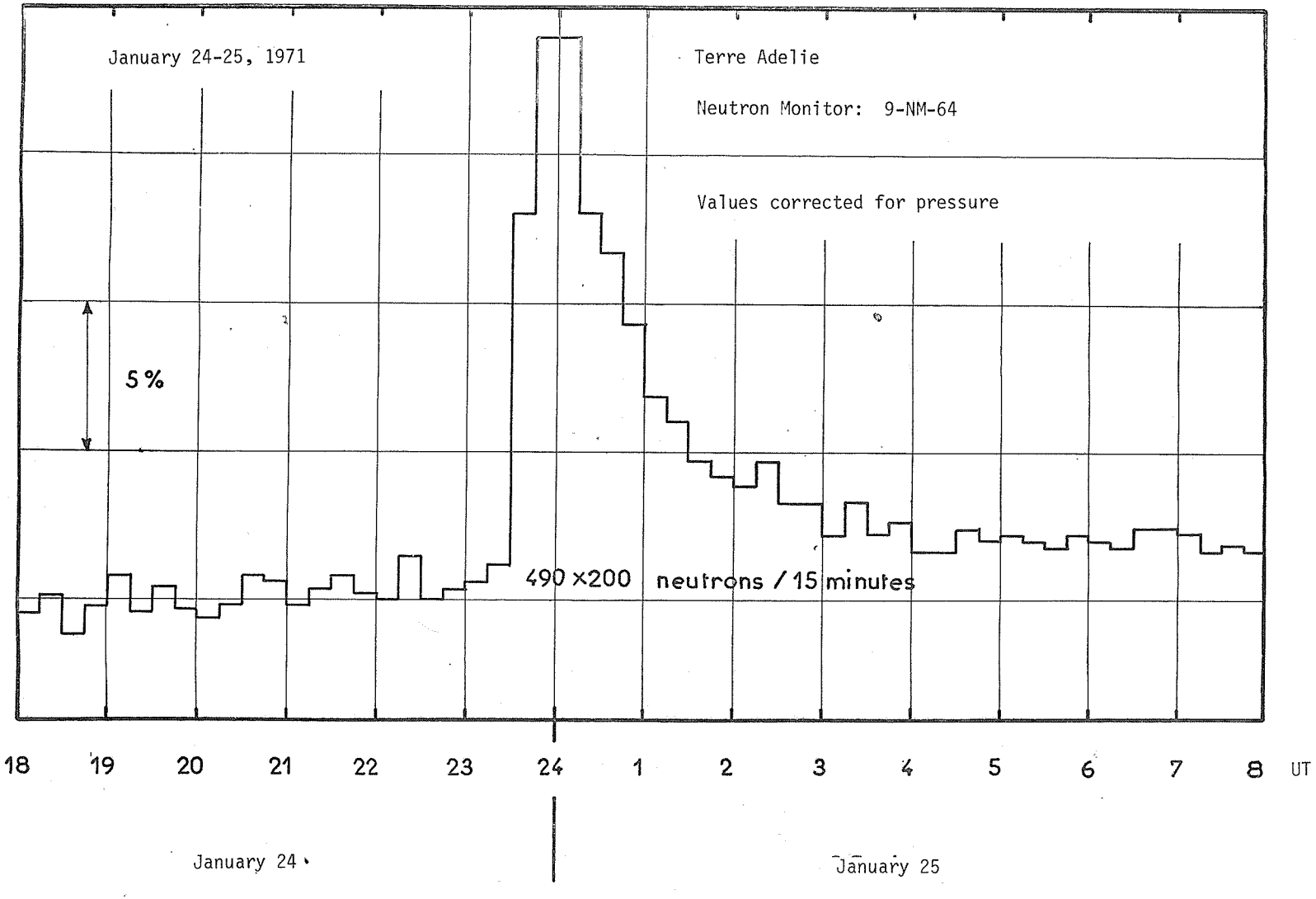

Fig. 1. January 24-25, 1971 Neutron Monitor Data from Dumont d'Urville. (Cut-off Rigidity = 0.01).

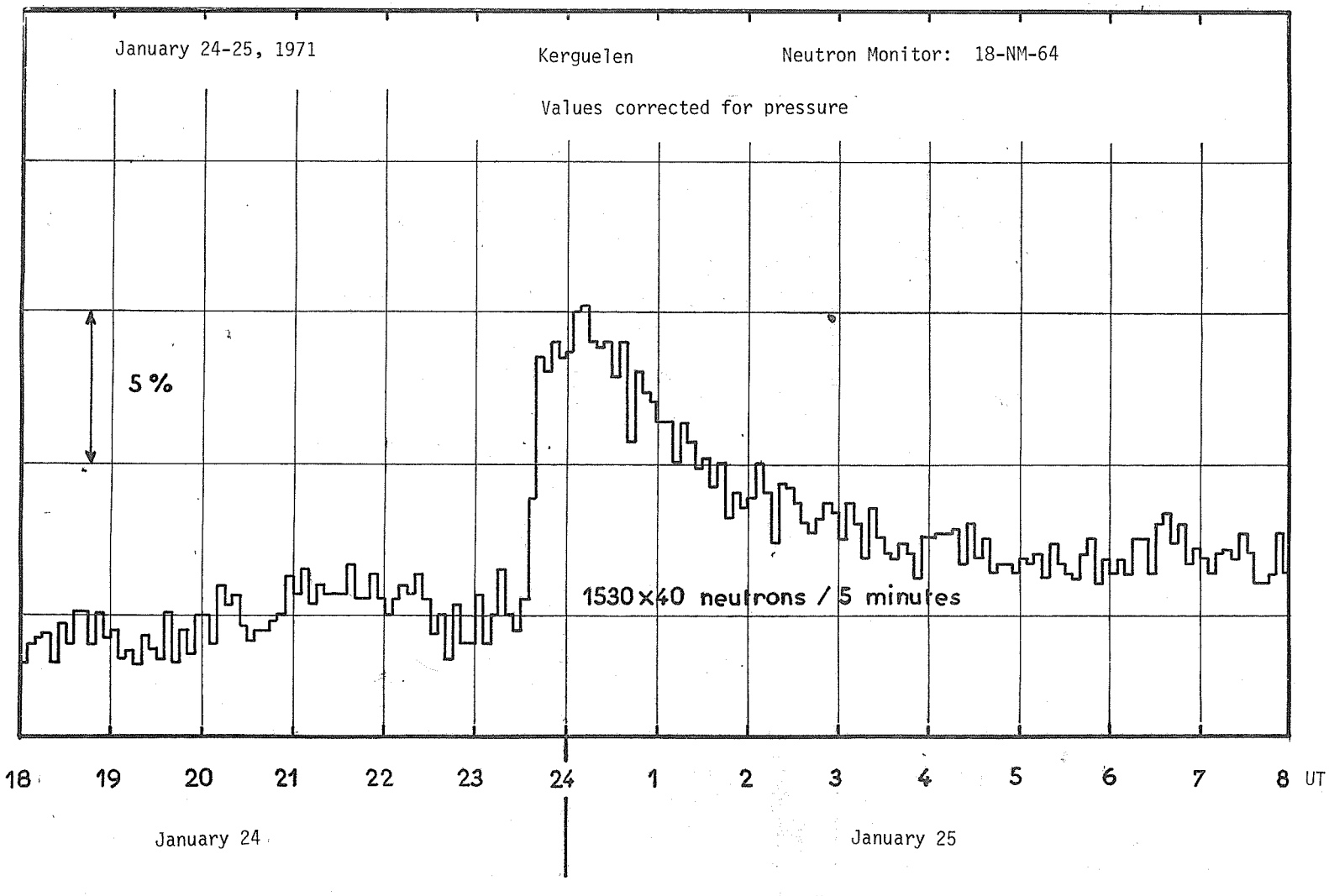

Fig. 2. January 24-25, 1971 Neutron Monitor Data from Port aux Francais. (Cut-off Rigidity = 1.19).

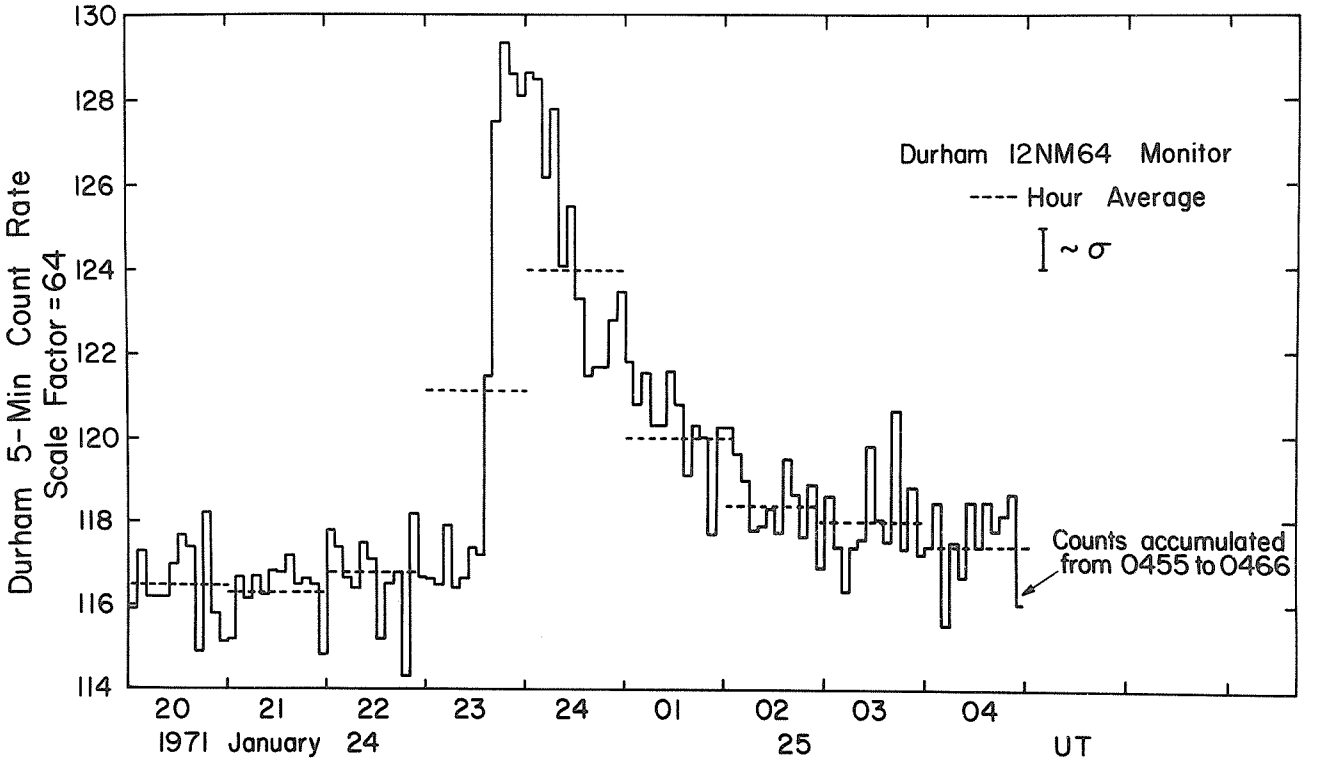

Fig. 3. January 24-25, 1971 Neutron Monitor Data from Durham.
(Cut-off Rigidity = 1.41).

Cosmic-Ray Trajectory Calculations for Selected High Latitude Stations Appropriate for the Solar Cosmic-Ray Events in 1971

by

M. A. Shea and D. F. Smart
Air Force Cambridge Research Laboratories
Bedford, Massachusetts

It has been shown by Gall et al. [1968] that the external magnetic sources controlling the fields in the earth's magnetic cavity can have an effect on the amount of geomagnetic bending cosmic-ray particles of rigidities less than a few GeV undergo in their passage through the magnetosphere to arrive at a specific location on the earth. This effect, which is particularly significant for particles arriving at high latitude ($\Lambda > 55^{\circ}$) stations, is also a function of local time. Consequently, it is important to account for the variation in the amount of geomagnetic bending in trying to ascertain the interplanetary flux and direction from the data recorded by ground-level detectors [Shea and Smart, 1970]. The purpose of this paper is to present the results of a set of cosmic-ray trajectory calculations detailing the approach directions for the high latitude ground-level cosmic-ray stations observing the cosmic-ray events of January 24 and September 1, 1971. These calculations have been made for the local time of each station during each event.

The accuracy of these types of calculations is highly dependent upon the magnetic field model parameters utilized and the relative merits of the various field model configurations are presently a matter of debate in the scientific community [Morfill, 1971]. Since the results of this type of calculation are highly dependent on the model used, it is necessary to describe in some detail the manner in which the magnetic fields are combined and the trajectories calculated in this field. The quiescent magnetospheric model we have used is based on the model derived by Williams and Mead [1965] and contains magnetic fields of both internal and external origin. The cosmic-ray trajectory calculations were restricted to the domain of the earth's magnetic cavity (i.e. the magnetosphere) represented by a boundary generated by a surface of revolution about the earth-sun line composed on the day side by a hemisphere of radius 13.9 earth radii centered at -3.5 earth radii and extended into a truncated cone whose generators form an angle of 15.3 degrees with the earth-sun line. Within this domain the magnetic field at any point in the magnetosphere is considered to be composed of an internal field ($\bar{B}_{int}$) represented by the Gaussian expansion with IGRF coefficients [IAGA Commission 2, Working Group 4, 1969] and an external field ($\bar{B}_{ext}$) as developed by Williams and Mead [1965].

The external field consists of sources due to currents flowing on the magnetopause and in the magnetospheric tail. It is explicit in this model that the solar wind is flowing perpendicular to the dipole axis and that these external fields are a function of position in dipole coordinates and local time. Perturbations of the geomagnetic field or any possible contributions due to ring currents are not included in this model. The expressions for the external sources were limited to two terms based on the work of Gall et al. [1969] who have shown by field line tracing that this limitation generates a magnetopause which nearly coincides with the boundary as described previously and as shown in Figure 1.

The magnetic field at any point inside the magnetosphere is given by the equation

$$\bar{B}_{total} = \bar{B}_{int}\,(R, \textcircled{H}, \bar{\Phi}) + \alpha \bar{B}_{ext}\,(r, \theta, \gamma)$$

$$\bar{B}_{ext} = \bar{B}_{s}\,(r, \theta, \gamma) + \bar{B}_{cs}\,(r, \theta, \gamma).$$

The internal field is expressed in geocentric coordinates, R, $\textcircled{H}$, $\bar{\Phi}$, while the Williams and Mead external field, symmetric with respect to the geomagnetic equator and the noon-midnight meridian, is computed in geomagnetic coordinates (r, θ, γ). At each iteration step the geomagnetic components of the external field are transformed by using the matrix α into geographic components. γ is the local time measured in degrees which corresponds to the angle in geomagnetic coordinates between the meridian of the anti-solar point and the meridian of the current particle position.

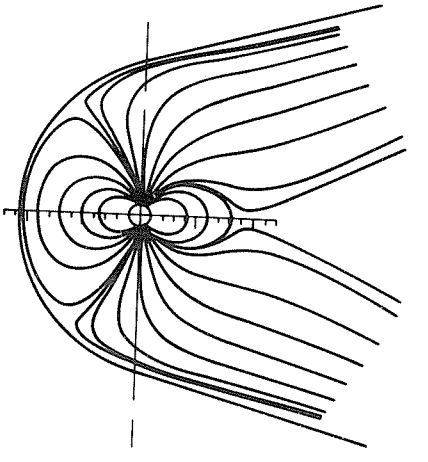

Fig. 1. Illustration of field lines in the model magnetosphere.

A tail configuration of R_1 = 10 earth radii and R_2 = 40 earth radii (the inward and outward termination points of the neutral sheet in the tail, respectively) and $\bar{B}_{cs}$ (the tail field associated with the current sheet) adjusted to 40 γ was utilized.

The cosmic-ray trajectories were calculated in the following manner. For each station the differential equation describing the motion ($\ddot{\bar{r}} = (q/m)\ \dot{\bar{r}} \times \bar{B}$) of a charged particle of mass m and charge q in the previously described magnetic field was solved at selected rigidities by using the Runge-Kutta integration method (See McCracken et al. [1962] for details of this process). In these calculations the step length employed in the Runge Kutta process was about 1/100 of the distance traversed during a Larmor gyration. The particles were started at an altitude of 30 km in the radial (vertical) direction with the calculations for each station made at the local mean solar time corresponding to the particle increase (0000 UT for the event of January 24-25, 1971, and 2100 UT for the event of September 1, 1971). The asymptotic directions of approach* were calculated at the position where (1) the orbit penetrated the magnetopause or (2) the orbit extended into the magnetospheric tail to a distance greater than 20 earth radii. Orbits that intersected the solid earth, or failed to reach an allowed solution by 100,000 iterative steps were declared "forbidden".

The asymptotic cones of acceptance for relativistic solar protons (0.09-10.0 GV) for selected high latitude stations appropriate for 0000 UT and 2100 UT are illustrated in Figures 2 and 3, respectively. Inspection of these figures shows that although these calculations were made for time periods separated by only three hours, noticeable differences in the amount of geomagnetic bending can be seen for some of these stations.

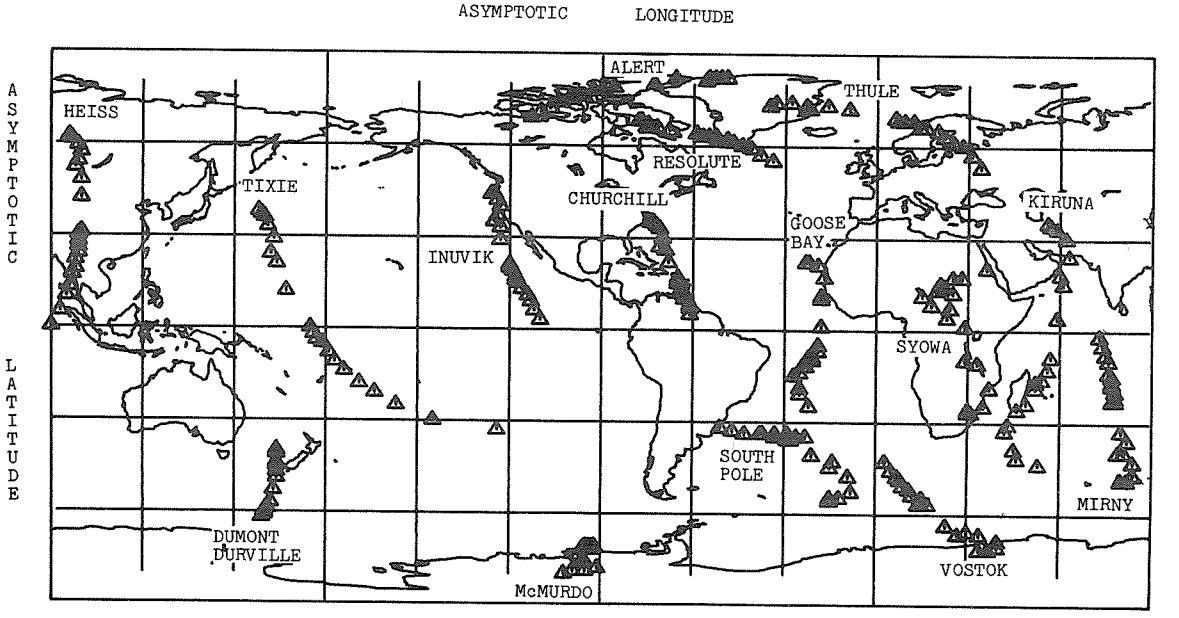

Fig. 2. Illustration of the asymptotic directions of approach for selected high latitude stations at 0000 UT. These directions are appropriate for the high energy particle event of January 24-25, 1971.

*In this paper the asymptotic direction of approach is given as the direction of a geocentric radial vector parallel to the particle velocity vector at the position where the calculation is made. These are not truly "asymptotic" in the classical sense of the word since further magnetic bending will occur due to the interplanetary magnetic field.

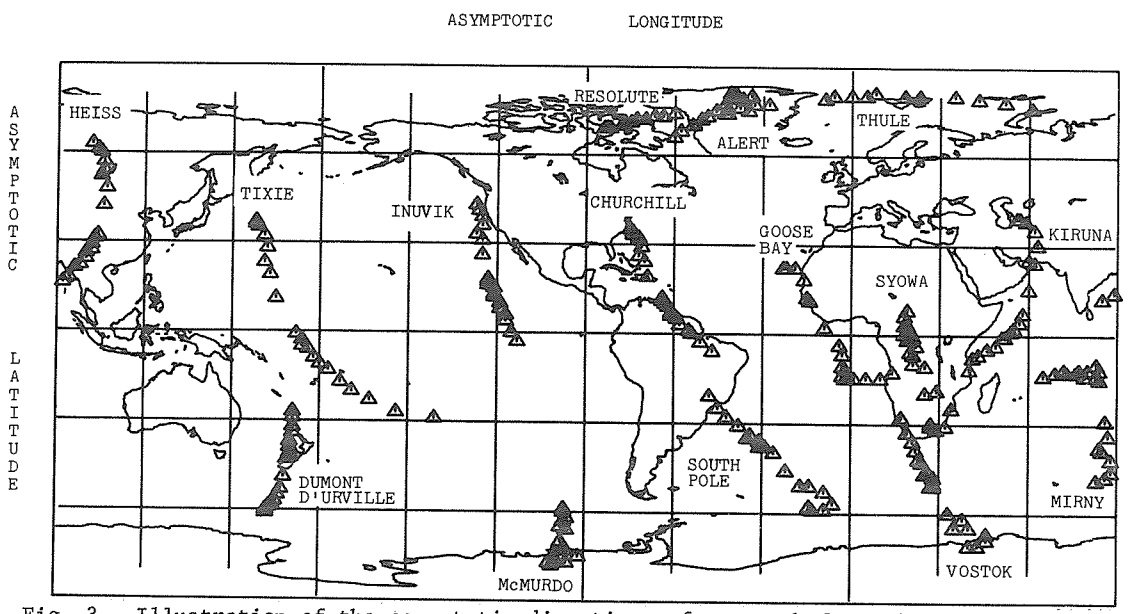

Fig. 3. Illustration of the asymptotic directions of approach for selected high latitude stations at 2100 UT. These directions are appropriate for the high energy particle event of September 1, 1971.

The following tables contain the asymptotic directions of approach for selected high latitude neutron monitors. Negative asymptotic longitudes indicate that the particle trajectory does not cross the Greenwich meridian. Longitude values larger than 360 degrees are indicative of a large longitudinal drift of the particle as it traverses the magnetic cavity. The notation "R" and "F" mean a re-entrant or failed orbit respectively. All calculations were made for the local time of the station correponding to the particle increase.

REFERENCES

GALL, RUTH, JAIME JIMENEZ, and LUCILLA CAMACHO (1968) Arrival of low-energy cosmic rays via the magnetospheric tail, J. Geophys. Res., 73, 1593-1605.

GALL, RUTH, SILVIA BRAVO, JAIME JIMENEZ, and ADOLFO OROZCO (1969) Modelos del campo-geomagnetico para el estudio de la propagacion de la radiacion cosmica, Anales del Instituto de Geofisca, U.N.A.M., 14, 1-22.

IAGA COMMISSION 2, WORKING GROUP 4 (1969) International geomagnetic reference field 1965.0, J. Geophys. Res., 74, 4407.

McCRACKEN, K. G., U. R. RAO, and M. A. SHEA (1962) The trajectories of cosmic rays in a high simulation of the geomagnetic field, Mass. Inst. Technology Tech. Rept. 77, August 1962.

MORFILL, G. E. (1971) A comment on trajectory calculations in the Williams and Mead geomagnetic field model, Planet. Space Sci., 19, 1016-1018.

SHEA, M. A., and D. F. SMART (1970) The effect of the asymmetric magnetosphere on the response of high-latitude neutron monitors to solar particle events, Acta Physica, Academiae Scientiarum Hungaricae, 29, Suppl. 2 (Proceedings of the 11th International Conference on Cosmic Rays, Budapest 1969), 539-543.

WILLIAMS, D. J., and G. D. MEAD (1965) Nightside magnetosphere configuration as obtained from trapped electrons at 1100 kilometers, J. Geophys. Res., 70, 3017-3029.

ALERT, CANADA

Geographic Latitude = 82.50 N
Geographic Longitude = 62.33 W
UT = 0000 LT = 1951

Rigidity (GV)	Asymptotic LAT	LONG
10.00	82	-50
9.00	82	-53
8.00	83	-56
7.00	83	-55
6.00	83	-52
5.00	82	-57
4.00	82	-67
3.00	81	-73
2.00	79	-86
1.90	79	-87
1.80	78	-91
1.70	78	-94
1.60	78	-94
1.50	77	-97
1.40	76	-100
1.30	75	-101
1.20	74	-105
1.10	73	-108
1.00	71	-110
0.90	69	-113

RESOLUTE, CANADA

Geographic Latitude = 74.69 N
Geographic Longitude = 94.91 W
UT = 0000 LT = 1740

Rigidity (GV)	Asymptotic LAT	LONG
10.00	68	-79
9.00	68	-79
8.00	68	-87
7.00	68	-77
6.00	68	-75
5.00	67	-74
4.00	67	-72
3.00	66	-68
2.00	64	-60
1.90	64	-58
1.80	64	-57
1.70	64	-56
1.60	63	-54
1.50	63	-52
1.40	62	-50
1.30	61	-48
1.20	60	-45
1.10	59	-42
1.00	58	-38
0.90	56	-35

THULE, GREENLAND

Geographic Latitude = 76.55 N
Geographic Longitude = 68.84 W
UT = 0000 LT = 1925

Rigidity (GV)	Asymptotic LAT	LONG
10.00	73	-35
9.00	74	-35
8.00	74	-33
7.00	74	-28
6.00	74	-23
5.00	73	-22
4.00	73	-17
3.00	72	-10
2.00	70	7
1.90	69	8
1.80	69	9
1.70	68	12
1.60	67	15
1.50	66	16
1.40	65	20
1.30	64	22
1.20	62	26
1.10	60	28
1.00	57	31
0.90	54	34

VOSTOK, ANTARCTICA

Geographic Latitude = 78.47 S
Geographic Longitude = 106.87 E
UT = 0000 LT = 0707

Rigidity (GV)	Asymptotic LAT	LONG
10.00	-72	35
9.00	-73	38
8.00	-72	41
7.00	-70	41
6.00	-67	35
5.00	-68	28
4.00	-66	31
3.00	-64	23
2.00	-58	17
1.90	-58	15
1.80	-58	15
1.70	-56	15
1.60	-55	12
1.50	-55	12
1.40	-52	11
1.30	-52	9
1.20	-49	8
1.10	-48	7
1.00	-46	5
0.90	-44	3

DUMONT D'URVILLE, ANTARCTICA

Geographic Latitude = 66.67 S
Geographic Longitude = 140.02 E
UT = 0000 LT = 0920

Rigidity (GV)	Asymptotic LAT	LONG
10.00	-62	159
9.00	-62	160
8.00	-61	160
7.00	-60	161
6.00	-59	162
5.00	-58	162
4.00	-56	163
3.00	-54	163
2.00	-50	164
1.90	-49	164
1.80	-49	164
1.70	-48	164
1.60	-47	164
1.50	-47	164
1.40	-46	164
1.30	-45	164
1.20	-44	164
1.10	-43	165
1.00	-42	165
0.90	-40	165

McMURDO, ANTARCTICA

Geographic Latitude = 77.85 S
Geographic Longitude = 166.72 E
UT = 0000 LT = 1107

Rigidity (GV)	Asymptotic LAT	LONG
10.00	-79	261
9.00	-80	258
8.00	-80	259
7.00	-80	265
6.00	-78	270
5.00	-76	264
4.00	-77	265
3.00	-75	263
2.00	-73	267
1.90	-72	265
1.80	-73	265
1.70	-73	267
1.60	-72	266
1.50	-72	266
1.40	-72	267
1.30	-72	266
1.20	-71	267
1.10	-71	268
1.00	-71	268
0.90	-71	268

MIRNY, ANTARCTICA

Geographic Latitude = 66.55 S
Geographic Longitude = 93.00 E
UT = 0000 LT = 0612

Rigidity (GV)	Asymptotic LAT	LONG
10.00	-50	81
9.00	-49	83
8.00	-47	85
7.00	-44	85
6.00	-41	82
5.00	-41	80
4.00	-37	83
3.00	-33	80
2.00	-24	79
1.90	-23	78
1.80	-22	78
1.70	-20	79
1.60	-19	77
1.50	-18	78
1.40	-15	77
1.30	-14	76
1.20	-11	76
1.10	-8	76
1.00	-6	75
0.90	-2	74

HEISS ISLAND, USSR

Geographic Latitude = 80.33 N
Geographic Longitude = 57.80 E
UT = 0000 LT = 0351

Rigidity (GV)	Asymptotic LAT	LONG
10.00	62	97
9.00	62	98
8.00	60	99
7.00	57	100
6.00	54	99
5.00	52	99
4.00	48	101
3.00	43	100
2.00	32	100
1.90	30	100
1.80	29	100
1.70	27	100
1.60	24	99
1.50	23	99
1.40	20	98
1.30	17	97
1.20	14	97
1.10	10	96
1.00	5	93
0.90	0	90

SOUTH POLE, ANTARCTICA

Geographic Latitude = 89.98 S
Geographic Longitude = 0.00 E
UT = 0000 LT = 0000

Rigidity (GV)	Asymptotic LAT	LONG
10.00	-55	-15
9.00	-56	-15
8.00	-56	-12
7.00	-53	-9
6.00	-48	-9
5.00	-45	-16
4.00	-43	-14
3.00	-41	-21
2.00	-36	-24
1.90	-36	-27
1.80	-36	-29
1.70	-36	-29
1.60	-34	-30
1.50	-35	-34
1.40	-35	-33
1.30	-34	-38
1.20	-34	-38
1.10	-34	-44
1.00	-33	-47
0.90	-33	-52

INUVIK, CANADA

Geographic Latitude = 68.35 N
Geographic Longitude = 133.73 W
UT = 0000 LT = 1505

Rigidity (GV)	Asymptotic LAT	LONG
10.00	44	-127
9.00	44	-126
8.00	43	-125
7.00	41	-124
6.00	37	-124
5.00	36	-126
4.00	34	-124
3.00	29	-124
2.00	22	-121
1.90	21	-121
1.80	20	-120
1.70	19	-119
1.60	17	-119
1.50	16	-119
1.40	15	-117
1.30	13	-117
1.20	11	-115
1.10	9	-114
1.00	6	-112
0.90	3	-110

CHURCHILL, CANADA

Geographic Latitude = 58.75 N
Geographic Longitude = 94.09 W
UT = 0000 LT = 1744

Rigidity (GV)	Asymptotic LAT	LONG
10.00	36	-74
9.00	35	-74
8.00	35	-73
7.00	33	-71
6.00	30	-70
5.00	28	-71
4.00	26	-70
3.00	22	-69
2.00	17	-66
1.90	16	-66
1.80	16	-65
1.70	15	-64
1.60	14	-64
1.50	13	-64
1.40	12	-63
1.30	11	-63
1.20	10	-62
1.10	9	-62
1.00	7	-62
0.90	6	-61

MAWSON, ANTARCTICA

Geographic Latitude = 67.60 S
Geographic Longitude = 62.88 E
UT = 0000 LT - 0412

Rigidity (GV)	Asymptotic LAT	LONG
10.00	-36	48
9.00	-37	50
8.00	-36	52
7.00	-32	55
6.00	-26	55
5.00	-22	50
4.00	-22	52
3.00	-12	49
2.00	-3	50
1.90	0	50
1.80	2	48
1.70	2	47
1.60	4	48
1.50	7	47
1.40	8	45
1.30	11	47
1.20	12	44
1.10	16	44
1.00	19	44
0.90	22	42

SYOWA, ANTARCTICA

Geographic Latitude = 69.03 S
Geographic Longitude = 39.60 E
UT = 0000 LT = 0238

Rigidity (GV)	Asymptotic LAT	LONG
10.00	-26	30
9.00	-27	30
8.00	-27	32
7.00	-26	36
6.00	-19	38
5.00	-11	34
4.00	-11	30
3.00	1	30
2.00	4	24
1.90	7	25
1.80	13	26
1.70	14	22
1.60	8	18
1.50	14	20
1.40	15	22
1.30	12	16
1.20	17	26
1.10	15	22
1.00	17	29
0.90	20	36

GOOSE BAY, CANADA

Geographic Latitude = 53.33 N
Geographic Longitude = 60.42 W
UT = 0000 LT = 1958

Rigidity (GV)	Asymptotic LAT	LONG
10.00	22	-23
9.00	22	-23
8.00	23	-22
7.00	22	-20
6.00	17	-17
5.00	11	-18
4.00	10	-18
3.00	2	-19
2.00	-5	-19
1.90	-7	-20
1.80	-9	-21
1.70	-9	-22
1.60	-10	-22
1.50	-13	-23
1.40	-13	-25
1.30	-15	-26
1.20	-16	-27
1.10	-19	-26
1.00	-21	-25
0.90	-25	-23

TIXIE BAY, USSR

Geographic Latitude = 71.55 N
Geographic Longitude = 128.90 E
UT = 0000 LT = 0836

Rigidity (GV)	Asymptotic LAT	LONG
10.00	38	159
9.00	37	159
8.00	36	160
7.00	34	162
6.00	29	163
5.00	25	163
4.00	21	165
3.00	13	167
2.00	0	175
1.90	-2	176
1.80	-4	177
1.70	-6	179
1.60	-9	182
1.50	-12	184
1.40	-14	187
1.30	-18	191
1.20	-21	196
1.10	-25	203
1.00	-30	216
0.90	-33	237

KIRUNA, SWEDEN

Geographic Latitude = 67.83 N
Geographic Longitude = 20.43 E
UT = 0000 LT = 0122

Rigidity (GV)	Asymptotic LAT	LONG
10.00	35	57
9.00	35	58
8.00	33	60
7.00	30	62
6.00	24	63
5.00	19	61
4.00	16	62
3.00	5	60
2.00	-10	57
1.90	-13	56
1.80	-16	54
1.70	-17	53
1.60	-20	52
1.50	-24	49
1.40	-26	47
1.30	-31	44
1.20	-34	42
1.10	-39	46
1.00	-42	47
0.90	-45	53

APATITY, USSR

Geographic Latitude = 67.55 N
Geographic Longitude = 33.33 E
UT = 0000 LT - 0213

Rigidity (GV)	Asymptotic LAT	LONG
10.00	34	68
9.00	33	69
8.00	31	71
7.00	28	74
6.00	22	74
5.00	16	72
4.00	12	73
3.00	2	72
2.00	-12	69
1.90	-14	70
1.80	-16	72
1.70	-17	71
1.60	-16	75
1.50	-13	80
1.40	-12	82
1.30	-3	91
1.20	-2	95
1.10	-3	106
1.00	-3	115
0.95	-2	121
0.90	-1	128

GENERAL BELGRANO, ANTARCTICA

Geographic Latitude = 77.97 S
Geographic Longitude = 38.80 W
UT = 0000 LT = 2125

Rigidity (GV)	Asymptotic LAT	LONG
10.00	-28	-18
9.00	-28	-20
8.00	-30	-20
7.00	-30	-17
6.00	-25	-13
5.00	-16	-15
4.00	-13	-20
3.00	-3	-16
2.00	6	-14
1.90	5	-13
1.80	7	-11
1.70	10	-8
1.60	10	-7
1.50	9	-5
1.40	9	3
1.30	7	4
1.20	4	13
1.15	0	16
1.10	-2	15
1.05	-7	21
1.00	-14	25
0.95	-19	24
0.90	-32	29

OULU, FINLAND

Geographic Latitude = 65.00 N
Geographic Longitude = 25.40 E
UT = 0000 LT = 0142

Rigidity (GV)	Asymptotic LAT	LONG
10.00	28	61
9.00	27	62
8.00	26	64
7.00	22	67
6.00	16	68
5.00	9	66
4.00	5	67
3.00	-7	66
2.00	-17	74
1.90	-15	79
1.80	-11	85
1.70	-7	87
1.60	-1	92
1.50	-3	101
1.40	-2	107
1.30	-3	116
1.20	0	127
1.15	0	132
1.10	3	144
1.05	6	153
1.00	9	164
0.99	10	169
0.98	11	174
0.97	13	180
0.96	14	186
0.95	16	192
0.94	16	198
0.93	17	203
0.92	17	208
0.91	17	215
0.90	17	225

SANAE, ANTARCTICA

Geographic Latitude = 70.30 S
Geographic Longitude = 2.35 W
UT = 0000 LT = 2350

Rigidity (GV)	Asymptotic LAT	LONG
10.00	-18	4
9.00	-18	2
8.00	-20	2
7.00	-20	4
6.00	-17	9
5.00	-8	10
4.00	-3	5
3.00	3	11
2.00	11	29
1.90	10	31
1.80	8	31
1.70	9	36
1.60	13	50
1.50	12	58
1.40	12	63
1.30	10	88
1.20	4	100
1.19	4	101
1.18	3	104
1.17	2	107
1.16	1	111
1.15	-1	116
1.14	-3	122
1.13	-6	131
1.12	-10	142
1.11	-14	163
1.10	-37	246
1.09	-34	256
1.08	-26	268
1.07	-12	283
1.06	5	316
1.05	-25	321
1.04	-1	322
1.03	5	330
1.02	-13	328
1.01	-18	348
1.00	-28	345
0.99	-50	0
0.98	R	R
0.97	6	63
0.96	0	152
0.95	1	110
0.94	R	R
0.93	-35	13
0.92	-25	8
0.91	-10	315
0.90	-5	24

DEEP RIVER, CANADA

Geographic Latitude = 46.10 N
Geographic Longitude = 77.50 W
UT = 0000 LT = 1850

Rigidity (GV)	Asymptotic LAT	LONG
10.00	8	-44
9.00	8	-44
8.00	7	-43
7.00	6	-40
6.00	0	-38
5.00	-7	-38
4.00	-9	-37
3.00	-18	-31
2.00	-25	-13
1.90	-26	-8
1.80	-28	-1
1.70	-27	3
1.60	-26	8
1.50	-24	20
1.40	-20	29
1.30	-11	40
1.29	-7	42
1.28	-2	42
1.27	5	43
1.26	8	49
1.25	10	57
1.24	14	67
1.23	19	79
1.22	21	90
1.21	21	100
1.20	20	111
1.19	17	122
1.18	12	136
1.17	1	157
1.16	-22	205
1.15	10	121
1.14	-13	336
1.13	-15	330
1.12	-20	343
1.11	R	R
1.10	R	R
1.09	20	82
1.08	-12	361
1.07	-17	352
1.06	-26	28
1.05	3	87
1.04	4	232
1.03	6	102
1.02	14	150
1.01	R	R
1.00	R	R
0.99	18	196
0.98	4	67
0.97	R	R
0.96	5	218
0.95	4	54
0.94	-10	224
0.93	R	R
0.92	R	R
0.91	-7	91
0.90	R	R

SULPHUR MOUNTAIN, CANADA

Geographic Latitude = 51.20 N
Geographic Longitude = 115.61 W
UT = 0000 LT = 1618

Rigidity (GV)	Asymptotic LAT	LONG
10.00	7	-95
9.00	7	-94
8.00	6	-92
7.00	2	-89
6.00	-5	-86
5.00	-12	-85
4.00	-15	-81
3.00	-28	-69
2.00	-31	-43
1.90	-29	-37
1.80	-25	-32
1.70	-21	-29
1.60	-17	-22
1.50	-9	-11
1.40	-3	1
1.39	-3	3
1.38	-2	5
1.37	-2	7
1.36	-1	10
1.35	0	13
1.34	1	18
1.33	0	26
1.32	-3	36
1.31	-6	48
1.30	0	74
1.29	-5	116
1.28	-12	278
1.27	-18	352
1.26	-21	40
1.25	-16	295
1.24	16	154
1.23	3	216
1.22	R	R
1.21	R	R
1.20	R	R
1.19	8	158
1.18	16	117
1.17	-2	202
1.16	-30	362
1.15	12	143
1.14	R	R
1.13	-1	144
1.12	R	R
1.11	-7	91
1.10	3	174
1.09	19	126
1.08	-18	340
1.07	10	133
1.06	R	R
1.05	-21	36
1.04	R	R
1.03	R	R
1.02	R	R
1.01	R	R
1.00	R	R
0.99-0.90	R	R

KERGUELEN ISLAND

Geographic Latitude = 49.35 S
Geographic Longitude = 70.22 E
UT = 0000 LT = 0441

Rigidity (GV)	Asymptotic LAT	LONG
10.00	-4	82
9.00	-3	83
8.00	-3	85
7.00	1	89
6.00	8	94
5.00	16	96
4.00	18	99
3.00	29	116
2.00	28	151
1.90	26	156
1.80	23	168
1.70	14	181
1.60	7	190
1.50	-4	207
1.49	-7	210
1.48	-10	214
1.47	-13	219
1.46	-17	225
1.45	-21	233
1.44	-25	244
1.43	-28	259
1.42	-28	281
1.41	-22	308
1.40	-11	323
1.39	8	318
1.38	-8	364
1.37	-5	225
1.36	-24	345
1.35	11	169
1.34	-4	319
1.33	-10	349
1.32	12	94
1.31	4	204
1.30	27	110
1.29	-26	31
1.28	0	336
1.27	R	R
1.26	-35	17
1.25	14	106
1.24	-9	351
1.23	-31	14
1.22	-13	38
1.21	-1	122
1.20	-16	47
1.19	-38	29
1.18	-32	40
1.17	R	R
1.16	R	R
1.15	-7	222
1.14	-3	197
1.13	R	R
1.12	15	129
1.11	R	R
1.10	R	R
1.09	R	R
1.08	F	F
1.07	-22	47
1.06	22	95
1.05-0.95	R	R
0.94	14	152
0.93-0.90	R	R

ALERT, CANADA

Geographic Latitude = 82.50 N
Geographic Longitude = 62.33 W
UT = 2100 LT = 1651

Rigidity (GV)	Asymptotic LAT	LONG
10.00	81	-40
9.00	81	-41
8.00	81	-42
7.00	81	-38
6.00	81	-35
5.00	79	-38
4.00	79	-41
3.00	78	-44
2.00	76	-46
1.90	75	-47
1.80	74	-49
1.70	74	-50
1.60	74	-50
1.50	73	-52
1.40	73	-52
1.30	72	-54
1.20	71	-55
1.10	70	-57
1.00	68	-59
0.90	67	-61

RESOLUTE, CANADA

Geographic Latitude = 74.69 N
Geographic Longitude = 94.91 W
UT = 2100 LT = 1440

Rigidity (GV)	Asymptotic LAT	LONG
10.00	69	-84
9.00	69	-84
8.00	69	-84
7.00	69	-84
6.00	69	-83
5.00	69	-83
4.00	69	-83
3.00	70	-82
2.00	71	-78
1.90	71	-78
1.80	71	-77
1.70	72	-76
1.60	72	-75
1.50	72	-74
1.40	72	-72
1.30	73	-70
1.20	73	-67
1.10	74	-64
1.00	74	-60
0.90	75	-55

THULE, GREENLAND

Geographic Latitude = 76.55 N
Geographic Longitude = 68.84 W
UT = 2100 LT = 1625

Rigidity (GV)	Asymptotic LAT	LONG
10.00	74	-42
9.00	75	-43
8.00	76	-42
7.00	76	-39
6.00	76	-35
5.00	75	-36
4.00	77	-33
3.00	78	-29
2.00	80	-10
1.90	80	-8
1.80	80	-7
1.70	81	0
1.60	81	5
1.50	81	9
1.40	81	19
1.30	81	24
1.20	80	35
1.10	80	44
1.00	78	52
0.90	77	61

VOSTOK, ANTARCTICA

Geographic Latitude = 78.47 S
Geographic Longitude = 106.87 E
UT = 2100 LT = 0407

Rigidity (GV)	Asymptotic LAT	LONG
10.00	-71	40
9.00	-71	43
8.00	-70	46
7.00	-67	46
6.00	-65	40
5.00	-65	35
4.00	-63	39
3.00	-60	34
2.00	-52	29
1.90	-51	27
1.80	-51	28
1.70	-49	28
1.60	-47	26
1.50	-46	26
1.40	-44	25
1.30	-42	24
1.20	-39	22
1.10	-37	22
1.00	-33	20
0.90	-29	18

DUMONT D'URVILLE, ANTARCTICA

Geographic Latitude = 66.67 S
Geographic Longitude = 140.02 E
UT = 2100 LT = 0620

Rigidity (GV)	Asymptotic LAT	LONG
10.00	-61	162
9.00	-60	163
8.00	-60	163
7.00	-59	164
6.00	-57	165
5.00	-56	166
4.00	-53	167
3.00	-50	168
2.00	-44	170
1.90	-43	170
1.80	-42	170
1.70	-41	170
1.60	-40	170
1.50	-39	170
1.40	-37	171
1.30	-36	171
1.20	-34	171
1.10	-32	171
1.00	-30	171
0.90	-27	171

McMURDO, ANTARCTICA

Geographic Latitude = 77.85 S
Geographic Longitude = 166.72 E
UT = 2100 LT = 0807

Rigidity (GV)	Asymptotic LAT	LONG
10.00	-78	261
9.00	-78	259
8.00	-78	259
7.00	-78	264
6.00	-76	268
5.00	-73	264
4.00	-73	264
3.00	-70	262
2.00	-66	265
1.90	-66	263
1.80	-66	263
1.70	-65	264
1.60	-64	264
1.50	-64	263
1.40	-63	264
1.30	-62	263
1.20	-61	264
1.10	-60	264
1.00	-59	263
0.90	-58	263

MIRNY, ANTARCTICA

Geographic Latitude = 66.55 S
Geographic Longitude = 93.00 E
UT = 2100 LT = 0312

Rigidity (GV)	Asymptotic LAT	LONG
10.00	-49	84
9.00	-48	86
8.00	-46	88
7.00	-43	88
6.00	-39	86
5.00	-39	85
4.00	-34	88
3.00	-29	86
2.00	-15	84
1.90	-14	83
1.80	-13	84
1.70	-11	83
1.60	-14	80
1.50	-12	80
1.40	-13	78
1.30	-13	77
1.20	-13	74
1.10	-12	72
1.00	-13	69
0.90	-14	65

HEISS ISLAND, USSR

Geographic Latitude = 80.33 N
Geographic Longitude = 57.80 E
UT = 2100 LT - 0051

Rigidity (GV)	Asymptotic LAT	LONG
10.00	63	102
9.00	62	104
8.00	60	106
7.00	57	107
6.00	54	106
5.00	52	106
4.00	48	108
3.00	42	107
2.00	32	104
1.90	31	103
1.80	30	103
1.70	28	102
1.60	26	101
1.50	25	100
1.40	22	99
1.30	21	97
1.20	18	95
1.10	16	93
1.00	14	89
0.90	12	86

SOUTH POLE, ANTARCTICA

Geographic Latitude = 89.98 S
Geographic Longitude = 0.00 E
UT = 2100 LT = 2100

Rigidity (GV)	Asymptotic LAT	LONG
10.00	-59	15
9.00	-60	13
8.00	-60	-10
7.00	-57	-6
6.00	-53	-9
5.00	-51	-17
4.00	-51	-15
3.00	-47	-23
2.00	-41	-26
1.90	-39	-29
1.80	-38	-31
1.70	-39	-31
1.60	-36	-32
1.50	-35	-35
1.40	-35	-35
1.30	-32	-38
1.20	-31	-38
1.10	-28	-42
1.00	-25	-45
0.90	-22	-48

INUVIK, CANADA

Geographic Latitude = 68.35 N
Geographic Longitude = 133.73 W
UT = 2100 LT = 1205

Rigidity (GV)	Asymptotic LAT	LONG
10.00	43	-128
9.00	43	-127
8.00	42	-126
7.00	40	-125
6.00	36	-126
5.00	34	-127
4.00	32	-125
3.00	27	-126
2.00	18	-123
1.90	17	-123
1.80	17	-123
1.70	16	-122
1.60	13	-122
1.50	12	-121
1.40	10	-120
1.30	8	-120
1.20	6	-118
1.10	4	-117
1.00	0	-116
0.90	-3	-113

CHURCHILL, CANADA

Geographic Latitude = 58.75 N
Geographic Longitude = 94.09 W
UT = 2100 LT = 1444

Rigidity (GV)	Asymptotic LAT	LONG
10.00	35	-75
9.00	34	-75
8.00	34	-74
7.00	32	-73
6.00	29	-72
5.00	26	-72
4.00	24	-71
3.00	20	-70
2.00	12	-65
1.90	11	-64
1.80	10	-64
1.70	10	-63
1.60	8	-62
1.50	7	-61
1.40	5	-59
1.30	3	-58
1.20	2	-56
1.10	0	-54
1.00	-3	-51
0.90	-6	-48

MAWSON, ANTARCTICA

Geographic Latitude = 67.60 S
Geographic Longitude = 62.88 E
UT = 2100 LT = 0112

Rigidity (GV)	Asymptotic LAT	LONG
10.00	-38	48
9.00	-39	50
8.00	-38	53
7.00	-34	56
6.00	-30	54
5.00	-28	47
4.00	-28	49
3.00	-23	42
2.00	-20	40
1.90	-18	39
1.80	-17	36
1.70	-18	35
1.60	-18	36
1.50	-15	33
1.40	-17	31
1.30	-15	31
1.20	-15	27
1.10	-13	26
1.00	-13	24
0.90	-12	20

SYOWA, ANTARCTICA

Geographic Latitude = 69.03 S
Geographic Longitude = 39.60 E
UT = 2100 LT = 2338

Rigidity (GV)	Asymptotic LAT	LONG
10.00	-30	28
9.00	-32	27
8.00	-32	29
7.00	-31	33
6.00	-26	35
5.00	-19	30
4.00	-20	26
3.00	-11	25
2.00	-6	20
1.90	-7	21
1.80	-5	22
1.70	-2	21
1.60	-2	19
1.50	-2	20
1.40	2	20
1.30	0	18
1.20	4	20
1.10	3	18
1.00	7	18
0.90	9	19

GOOSE BAY, CANADA

Geographic Latitude = 53.33 N
Geographic Longitude = 60.42 W
UT = 2100 LT = 1658

Rigidity (GV)	Asymptotic LAT	LONG
10.00	22	-23
9.00	23	-23
8.00	23	-22
7.00	22	-20
6.00	18	-16
5.00	12	-15
4.00	11	-14
3.00	3	-10
2.00	-5	-4
1.90	-7	-4
1.80	-11	-3
1.70	-12	-3
1.60	-14	-4
1.50	-16	-3
1.40	-16	-2
1.30	-15	1
1.20	-16	5
1.10	-15	10
1.00	-13	14
0.90	-10	21

TIXIE BAY, USSR

Geographic Latitude = 71.55 N
Geographic Longitude = 128.90 E
UT = 2100 LT = 0536

Rigidity (GV)	Asymptotic LAT	LONG
10.00	37	159
9.00	36	159
8.00	35	160
7.00	32	161
6.00	28	162
5.00	23	162
4.00	20	164
3.00	11	166
2.00	-1	173
1.90	-4	174
1.80	-5	175
1.70	-6	176
1.60	-10	179
1.50	-12	181
1.40	-14	184
1.30	-17	187
1.20	-20	192
1.10	-23	197
1.00	-27	206
0.90	-30	219

KIRUNA, SWEDEN

Geographic Latitude = 67.83 N
Geographic Longitude = 20.43 E
UT = 2100 LT = 2222

Rigidity (GV)	Asymptotic LAT	LONG
10.00	39	57
9.00	39	58
8.00	38	60
7.00	35	63
6.00	30	63
5.00	26	61
4.00	24	62
3.00	16	60
2.00	7	58
1.90	5	58
1.80	3	56
1.70	3	55
1.60	1	55
1.50	-2	53
1.40	-2	51
1.30	-4	49
1.20	-5	47
1.10	-8	43
1.00	-9	41
0.90	-12	40

APATITY, USSR

Geographic Latitude = 67.55 N
Geographic Longitude = 33.33 E
UT = 2100 LT = 2313

Rigidity (GV)	Asymptotic LAT	LONG
10.00	37	68
9.00	36	69
8.00	35	71
7.00	32	73
6.00	26	74
5.00	21	71
4.00	19	73
3.00	9	70
2.00	-2	68
1.90	-5	67
1.80	-7	65
1.70	-8	64
1.60	-10	64
1.50	-13	61
1.40	-14	60
1.30	-18	58
1.20	-20	58
1.10	-27	59
1.00	-31	60
0.95	-34	62
0.90	-37	64

GENERAL BELGRANO, ANTARCTICA

Geographic Latitude = 77.97 S
Geographic Longitude = 38.80 W
UT = 2100 LT = 1825

Rigidity (GV)	Asymptotic LAT	LONG
10.00	-29	-15
9.00	-31	-15
8.00	-32	-14
7.00	-31	-11
6.00	-25	-9
5.00	-14	-12
4.00	-12	-15
3.00	1	-14
2.00	15	-13
1.90	15	-12
1.80	18	-9
1.70	23	-2
1.60	24	0
1.50	25	2
1.40	28	14
1.30	26	18
1.20	24	29
1.15	20	34
1.10	17	34
1.05	11	40
1.00	1	41
0.95	-5	41
0.90	-24	37

OULU, FINLAND

Geographic Latitude = 65.00 N
Geographic Longitude = 25.40 E
UT = 2100 LT = 2242

Rigidity (GV)	Asymptotic LAT	LONG
10.00	31	61
9.00	30	62
8.00	30	64
7.00	26	66
6.00	21	68
5.00	15	66
4.00	12	66
3.00	1	65
2.00	-10	65
1.90	-13	66
1.80	-17	67
1.70	-18	68
1.60	-20	68
1.50	-25	73
1.40	-27	75
1.30	-31	80
1.20	-33	90
1.15	-34	92
1.10	-33	104
1.05	-26	112
1.00	-16	119
0.99	-9	122
0.98	2	124
0.97	15	125
0.96	30	126
0.95	32	137
0.94	31	145
0.93	30	150
0.92	29	154
0.91	28	160
0.90	28	167

SANAE, ANTARCTICA

Geographic Latitude = 70.30 S
Geographic Longitude = 2.35 W
UT = 2100 LT = 2050

Rigidity (GV)	Asymptotic LAT	LONG
10.00	-15	4
9.00	-16	2
8.00	-17	2
7.00	-18	4
6.00	-14	8
5.00	-3	9
4.00	4	5
3.00	11	12
2.00	21	32
1.90	20	34
1.80	18	34
1.70	16	39
1.60	13	50
1.50	7	54
1.40	2	56
1.30	-13	66
1.20	-25	66
1.19	-26	66
1.18	-27	66
1.17	-29	67
1.16	-30	68
1.15	-32	68
1.14	-26	75
1.13	-6	94
1.12	-7	109
1.11	-9	122
1.10	-10	135
1.09	-10	147
1.08	-9	160
1.07	-6	173
1.06	-3	188
1.05	-2	49
1.04	-16	370
1.03	-7	360
1.02	-41	32
1.01	-12	22
1.00	-30	347
0.99	2	138
0.98	R	R
0.97	1	126
0.96	-36	30
0.95	-9	34
0.94	9	165
0.93	-27	70
0.92	R	R
0.91	15	120
0.90	-9	354

DEEP RIVER, CANADA

Geographic Latitude = 46.10 N
Geographic Longitude = 77.50 W
UT = 2100 LT = 1550

Rigidity (GV)	Asymptotic LAT	LONG
10.00	6	-42
9.00	6	-42
8.00	6	-40
7.00	4	-37
6.00	-1	-32
5.00	-9	-29
4.00	-11	-25
3.00	-21	-12
2.00	-23	11
1.90	-20	15
1.80	-17	20
1.70	-12	23
1.60	-8	26
1.50	-2	35
1.40	6	44
1.30	10	64
1.29	11	67
1.28	9	74
1.27	5	82
1.26	0	91
1.25	-6	101
1.24	-3	124
1.23	-10	158
1.22	-19	230
1.21	-39	75
1.20	-17	94
1.19	-6	225
1.18	8	186
1.17	-25	97
1.16	10	382
1.15	R	R
1.14	0	256
1.13	-25	213
1.12	-1	219
1.11	23	180
1.10	19	122
1.09	-27	68
1.08	-1	182
1.07	R	R
1.06	R	R
1.05	12	126
1.04	R	R
1.03	R	R
1.02	12	184
1.01	6	127
1.00	R	R
0.99	-12	207
0.98	2	154
0.97	-24	68
0.96	-13	219
0.95	-34	73
0.94	8	147
0.93	R	R
0.92	R	R
0.91	R	R
0.90	R	R

SULPHUR MOUNTAIN, CANADA

Geographic Latitude = 51.20 N
Geographic Longitude = 115.61 W
UT = 2100 LT = 1318

Rigidity (GV)	Asymptotic LAT	LONG
10.00	7	-95
9.00	6	-94
8.00	5	-92
7.00	1	-88
6.00	-6	-85
5.00	-13	-84
4.00	-16	-78
3.00	-28	-64
2.00	-32	-23
1.90	-30	-13
1.80	-26	-4
1.70	-21	3
1.60	-11	4
1.50	10	7
1.40	20	27
1.39	19	32
1.38	18	38
1.37	15	45
1.36	9	53
1.35	0	61
1.34	-14	70
1.33	-32	80
1.32	-1	60
1.31	18	138
1.30	18	121
1.29	-21	52
1.28	-16	348
1.27	R	R
1.26	11	202
1.25	-28	53
1.24	13	171
1.23	-25	62
1.22	-2	46
1.21	-6	74
1.20	-16	213
1.19	-8	79
1.18	R	R
1.17	-32	77
1.16	-32	59
1.15	-6	34
1.14	R	R
1.13	13	166
1.12	1	230
1.11	R	R
1.10	R	R
1.09	4	129
1.08	R	R
1.07	R	R
1.06	R	R
1.05	R	R
1.04	R	R
1.03	R	R
1.02	R	R
1.01	R	R
1.00	R	R

KERGUELEN ISLAND

Geographic Latitude = 49.35 S
Geographic Longitude = 70.22 E
UT = 2100 LT = 0141

Rigidity (GV)	Asymptotic LAT	LONG
10.00	-6	79
9.00	-6	80
8.00	-5	82
7.00	-2	85
6.00	-6	88
5.00	13	86
4.00	14	86
3.00	26	105
2.00	26	138
1.90	25	144
1.80	22	155
1.70	15	168
1.60	9	175
1.50	2	188
1.49	0	190
1.48	-2	193
1.47	-4	196
1.46	-6	199
1.45	-9	203
1.44	-12	207
1.43	-15	212
1.42	-18	217
1.41	-21	222
1.40	-24	228
1.39	-26	235
1.38	-27	243
1.37	-28	251
1.36	-28	260
1.35	-27	270
1.34	-25	280
1.33	-20	294
1.32	-12	314
1.31	5	350
1.30	15	376
1.29	-1	32
1.28	22	92
1.27	-12	58
1.26	-5	36
1.25	9	13
1.24	21	174
1.23	-2	55
1.22	19	128
1.21	R	R
1.20	2	168
1.19	15	128
1.18	R	R
1.17	-15	81
1.16	3	216
1.15	-15	81
1.14	R	R
1.13	-30	76
1.12	R	R
1.11	R	R
1.10	2	22
1.09	R	R
1.08	R	R
1.07	-5	213
1.06	-24	77
1.05	9	189
1.04-0.98	R	R
0.97	F	F
0.96-0.90	R	R

Relativistic Solar Cosmic Rays on January 24-25, 1971

by

M. A. Pomerantz and S. P. Duggal
Bartol Research Foundation
of
The Franklin Institute

1. Introduction

The most prominent feature of the January 24, 1971, ground-level event (GLE) is that it displayed a heretofore unobserved sectorial pattern of anisotropy that was limited to a narrow and stable region. Furthermore, it is also the first for which it is possible to distinguish between two rival candidates for the parent flare, in the same location within 3°, with reported onset times differing by only one minute, and each visible in Hα for longer than one hour. The analysis whereby the relevant injection and propagation characteristics have been determined is described in detail elsewhere [Duggal and Pomerantz, 1972].

2. Observations

Two neighboring but apparently distinct solar flares, of importance 3B (N16, W49) and 1B (N19, W50), were eligible for identification as the source of the relativistic particles that reached the earth on January 24-25, 1971. Although the closest reported onset times [Solar-Geophysical Data, 1971] differed by only one minute (2308 UT and 2309 UT, respectively), maximum Hα intensity was attained by the 3B flare about 14 minutes after the optical maximum of the less energetic flare. The total duration of both flares was ≥1.25 hours. The angle between the base of the nominal garden hose field line passing through the earth and the flare locations is estimated to be ≃28°.

The neutron monitor observations at the three stations (Thule, McMurdo and South Pole) comprising the Bartol polar network are plotted in Figure 1. Although the interval between the onset and the time of maximum was quite short (about 8 minutes at Thule), the availability of data from these high counting rate neutron monitors in two-minute intervals (with the exception of Swarthmore, the minimum readout period at other stations is 5 minutes) has made it possible to analyze certain basic features of this GLE that could otherwise not have been studied.

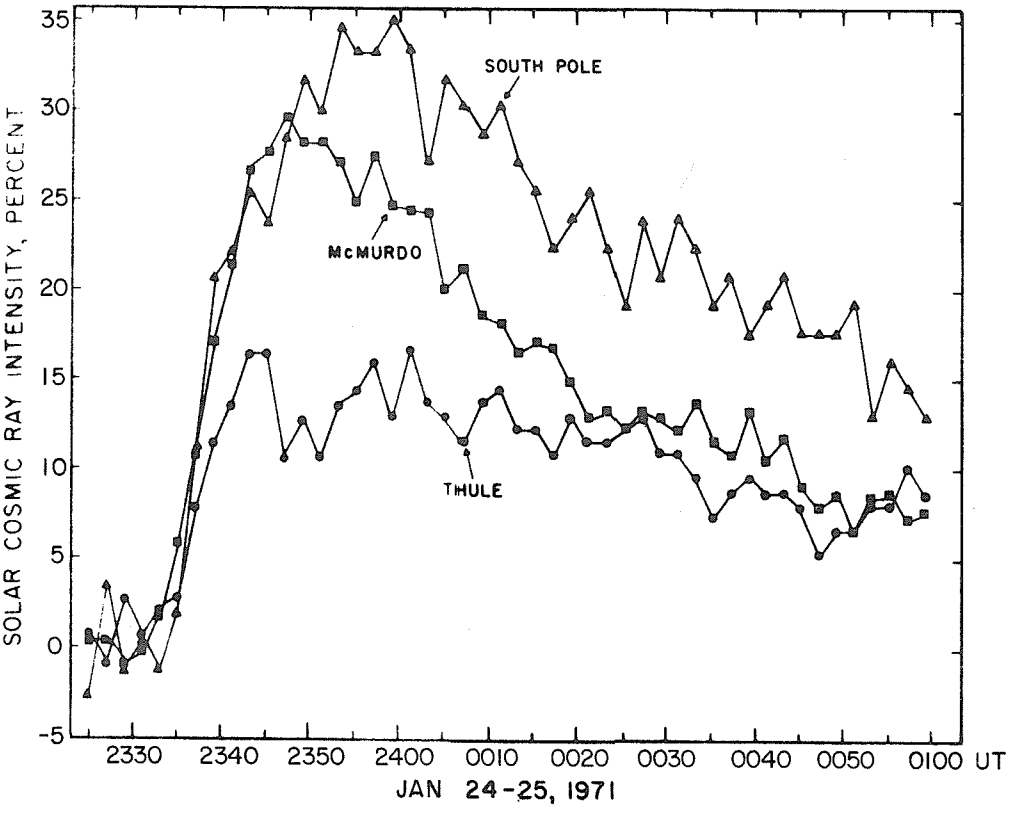

Fig. 1. Nucleonic intensity in two-minute intervals at the Bartol polar stations during the GLE of January 24-25, 1971, expressed as percent of the galactic background prior to onset.

The January 24-25, 1971, GLE occurred during a period in which the galactic cosmic ray flux was still recovering from a major cosmic ray storm that commenced on January 12. It was followed, four days after, by an unusual Forbush decrease that displayed an abnormal north-south anisotropy [Pomerantz and Duggal, 1972]. A measurable neutron flux enhancement was observed at all stations having a geomagnetic cutoff below ≃5 GV.

The data shown in Figure 1 represent the nucleonic intensity arising from solar cosmic rays after correction for atmospheric pressure changes by the application of two pressure coefficients, α_1 and α_2, appropriate for solar and galactic cosmic rays [Baird et al., 1967; Wilson et al., 1967].

3. Results of Analysis

A. Spectrum

Figure 2 is a plot of the dependence upon threshold rigidity P_c of the relative enhanced nucleonic intensity in the hour 0100-0200 UT, an epoch during which the solar particle flux was essentially isotropic. The data indicate that the effective atmospheric cutoff was about 1.2 GV. The scatter among the points representing stations with lower geomagnetic threshold rigidities appears to be ascribable to possible anisotropies in the recovery phase of the on-going cosmic ray storm, this affects the base period. Also involved are imperfect corrections for atmospheric effects, since only our own observations were subjected to the two pressure coefficient procedures.

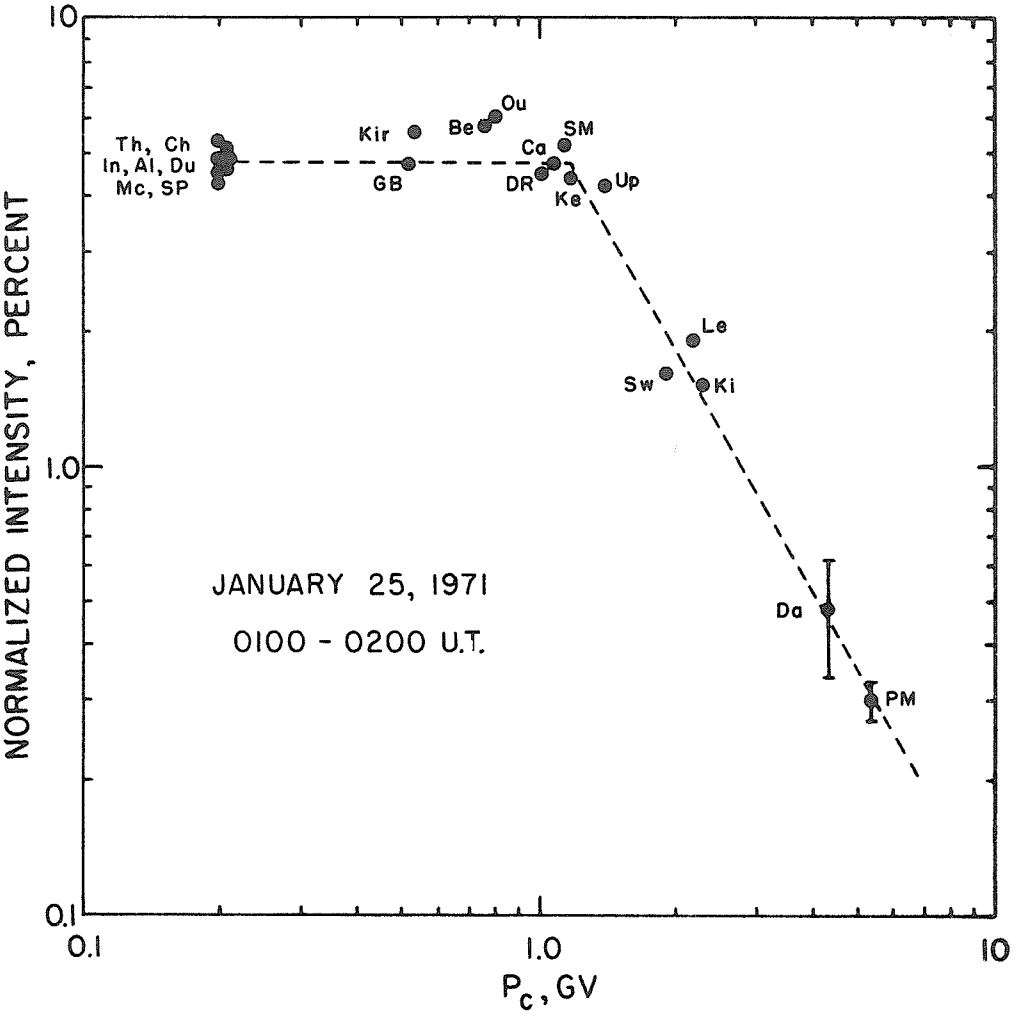

Fig. 2. Data from 21 neutron monitors, normalized to a standard pressure, plotted as a function of threshold rigidity. The slope of the inclined dashed line corresponds to a primary spectral index $\gamma = 5.0 \pm 0.3$.

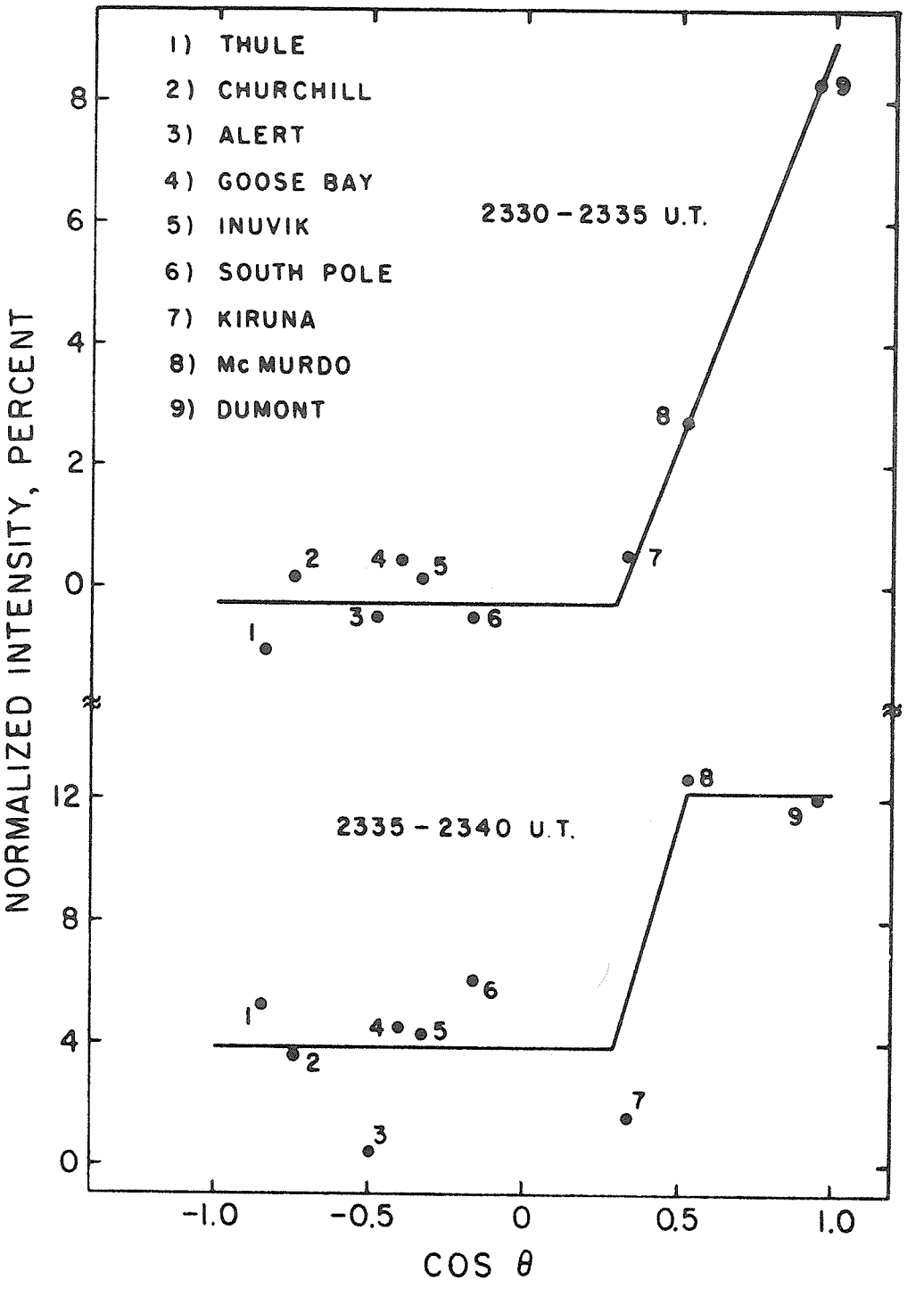

Fig. 3. Nucleonic intensity at 9 selected stations, normalized to a standard pressure, during two 5-minute intervals when solar cosmic rays first reached the earth on January 24, 1971, plotted as a function of cos θ, where the pitch angle θ is the angle between the effective direction of viewing and the assumed axis of symmetry.

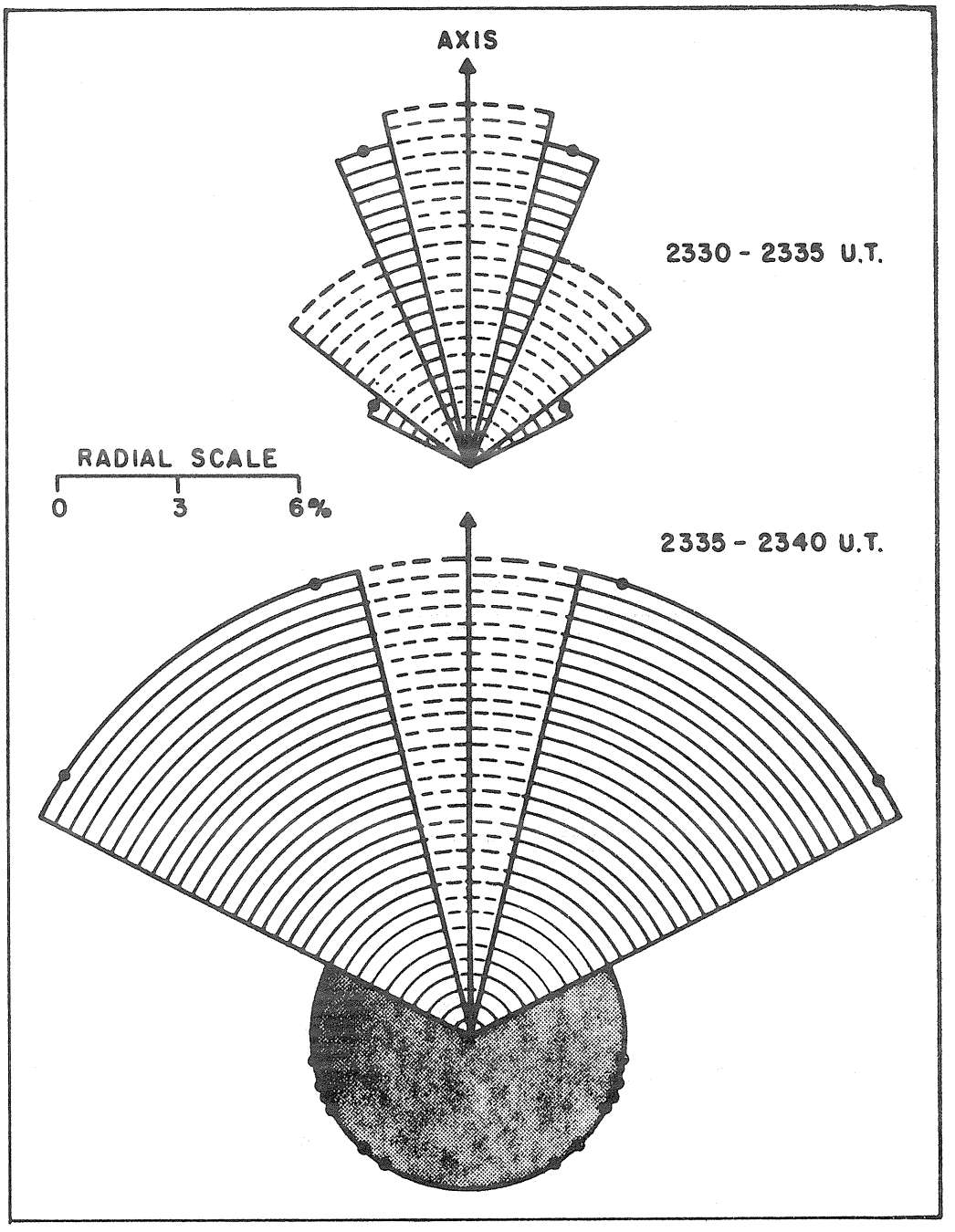

Fig. 4. Polar plot showing sectorial structure of the particle flux with respect to the axis of symmetry during the same intervals as in Figure 3.

On the basis of these data and the coupling coefficients given by Lockwood and Webber [1967], the value of the spectral index in a power law representation ($dI/dP = kP^{-\gamma}$) of the differential primary solar particle spectrum is $\gamma = 5.0 \pm 0.3$.

B. Spatial Distribution

An examination of the data recorded at nine stations with appropriately narrow asymptotic cones reveals that the flux was anisotropic during the period 2330-0100 UT. However, the anisotropy was limited to a narrow region between two essentially isotropic sectors. Since large departures from the magnitude of the intensity increases recorded at other stations were observed at only two sites, McMurdo and Dumont in Antarctica, estimation of the precise direction of the axis of symmetry is precluded. Hence a nominal value of the location of the axis at geographical latitude 50° south and longitude 135° east was assumed in the annalysis.

The theoretical prediction that, with the usual magnetic field power spectral densities in the interplanetary space, the solar particle flux depends on the cosine of the pitch angle has also been verified experimentally [Duggal et al., 1971; Maurer et al., 1972]. Consequently, in Figure 3, the normalized intensity enhancements recorded at the nine stations in two intervals close to the onset of the relativistic solar particle precipitation are plotted as a function of cos θ, where the pitch angle θ is the angle between the effective direction of viewing and the axis of symmetry.

The sectorial structure in the distribution of the particle flux with respect to the axis of symmetry immediately following the onset (i.e., the two 5-minute intervals indicated in Figure 3), as depicted schematically in Figure 4, is striking. There is a larger uncertainty in the sector close to the axis, since it was necessary to estimate the intensity at Dumont in shorter intervals from 15-minute readouts.

The history, in successive quarter hour intervals, of the development of the anisotropy, culminating in the final isotropic state, is shown in Figure 5. The dashed lines bridge the transition from large flux to a lower level, since the shapes of the curves in this anisotropic region are indeterminate owing to the lack of suitably-located stations. Thus, the domain of the anisotropy, centered near 60° from the axis of symmetry, extended over only about 10° for the entire 1½ hour interval following onset before complete isotropy set in.

C. Parent Flare Identification

As noted earlier, two concurrent flares were eligible for identification as the source of the solar cosmic rays. A detailed theoretical analysis of the propagation characteristics revealed that the actual time of emission of relativistic particles from the sun was 2320 ± 0001 UT. This estimated time of maximum is almost coincident (within two minutes) with the observed maximum phase of Hα brightness of the 3B flare which is identified by the analysis as the source of the relativistic particles.

4. Conclusion

The results summarized above have clearly established that, at least in this event, solar protons with energies of about 0.5 Gev were not released simultaneously with the onset of the chromoshperic eruption on the sun. Instead, the ejection time was close to the flash phase of the 3B flare.

On account of the short duration of the January 24-25, 1971, event which was marked by a large anisotropy, a detailed comparison between the predictions of different diffusion models that have been proposed thus far is not feasible. Furthermore, although the pitch angle distribution of the solar particles was unusual, the diffusion coefficient and the outer boundary of the scattering region were not different from those determined for other events, i.e., $(11 \pm 4) \times 10^{21}$ cm^2/sec and 1.8 ± 0.3 AU, respectively.

In summary, this abnormal GLE is the first in which the bulk of the anisotropy was limited to a very narrow region. For the entire 1½ hour interval before isotropy set in, the anisotropy, which was as great as 60%, was limited to a 10° cone centered about 60° from the spiral magnetic field line. Outside this anisotropic sector, the scattering was independent of pitch angle.

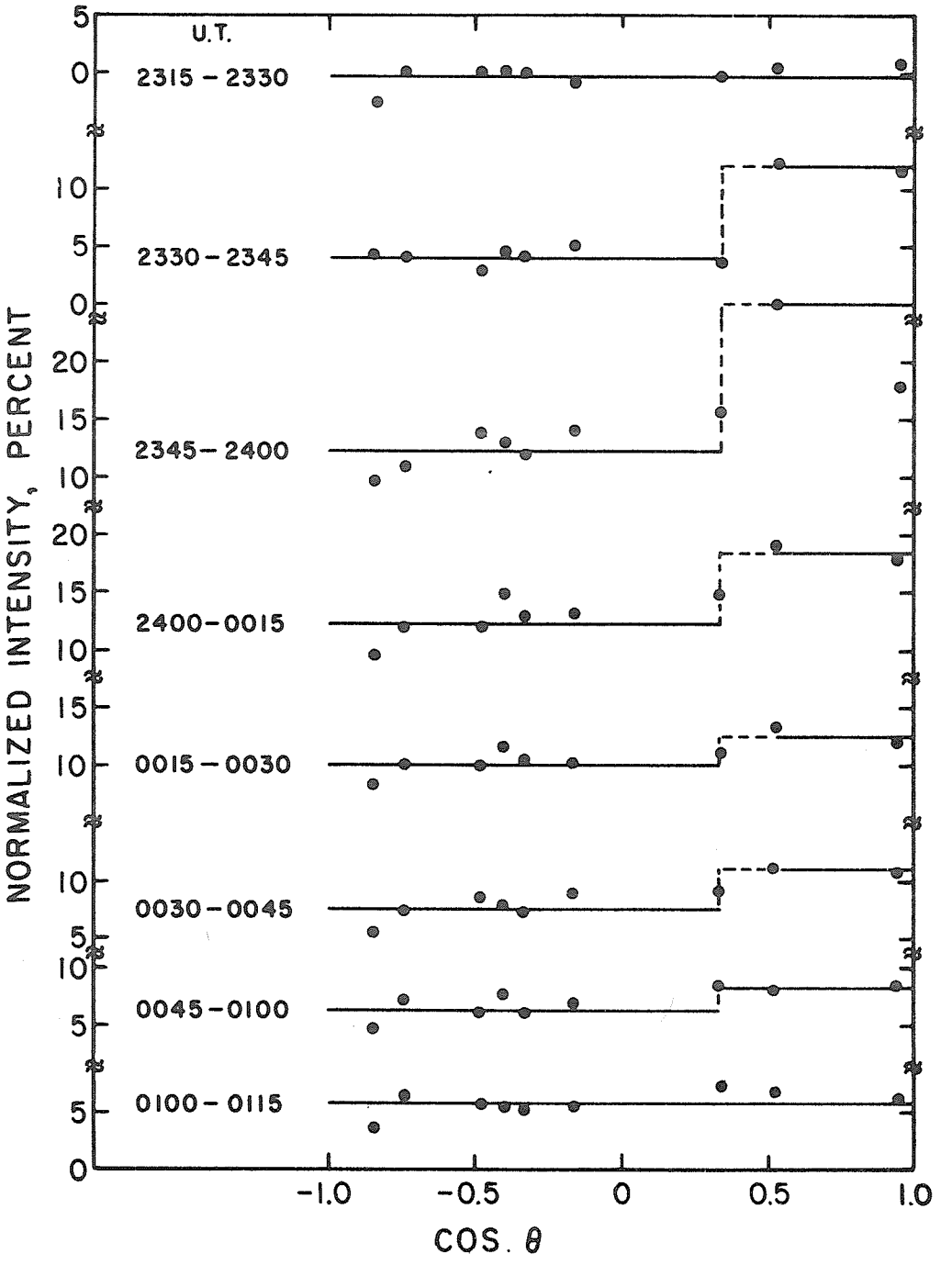

Fig. 5. History of the development of the anisotropy from onset to the isotropic stage of the January 24-25, 1971, GLE. The domain of anisotropy indicated by the dashed lines, centered near 60° from the axis of symmetry, extended over only about 10°.

REFERENCES

BAIRD, G. A., G. G. BELL, S. P. DUGGAL and M. A. POMERANTZ — 1967 — Solar Phys., 2, 491.

DUGGAL, S. P and M. A. POMERANTZ — 1971 — Proc. Int. Conf. Cosmic Rays, 12th, 2, 533.

DUGGAL, S. P. and M. A. POMERANTZ — 1972 — Solar Phys., to be published.

LOCKWOOD, J. A. and W. R. WEBBER — 1967 — J. Geophys. Res., 72, 3395.

MAURER, R. H., S. P. DUGGAL and M. A. POMERANTZ — 1972 — J. Geophys. Res., to be published.

POMERANTZ, M. A. and S. P. DUGGAL — 1972 — J. Geophys. Res., 77, 263.

WILSON, B. G., T. MATHEWS and R. H. JOHNSON — 1967 — Phys. Rev. Letters, 18, 675.

1971 — Solar-Geophysical Data, 323 Part II, U.S. Department of Commerce, (Boulder, Colorado, U.S.A. 80302).

The Ground Level Increase and Variations of Cosmic Rays on January 24-30, 1971

by

N. P. Chirkov, V. I. Ipatjev, G. V. Skripin,
G. G. Todikov, and A. T. Filippov
Institute of Cosmophysical Research and Aeronomy, Yakutsk Branch
Siberian Department of the Academy of Sciences of the USSR, Yakutsk, U.S.S.R.

On January 24, 1971 at the very end of the day the increase of solar cosmic rays was registered by the Siberian net of stations. Coordinates of stations, their threshold rigidity [Shea et al., 1968] and the intensity amplitudes are listed in the Table. The stations are equipped with neutron supermonitors.

	Station	Rigidity (GV)	Geographical Latitude	Longitude	Amplitude (%) Jan 24	Jan 25
1.	Tixie Bay	0.52	71.5°N	128.9°E	8.1	8.0
2.	Norilsk	0.60	69.3	88.1	-	5.5
3.	Yakutsk	1.85	62.0	129.7	9.8	5.4
4.	Magadan	2.15	60.1	151.0	7.8	3.9
5.	Novosibirsk	2.85	54.8	83.0	-	2.2
6.	Irkutsk	3.75	52.4	104.0	2.8	1.5
7.	Khabarovsk	5.55	48.5	135.2	-	0.2

Five and fifteen-minute intensity values during the flare are given in Figure 1, and hour values during the flare accompanied by two Forbush decreases are presented in Figure 2. Data are corrected for barometric pressure. In Figure 1 the statistical errors are indicated. Five-minute data from station Deep River are presented for a comparison.

It is evident from Figure 1 that the cosmic ray increase started at 2340-2345 UT and reached its maximum at 2350-2400 UT. The amplitude increase at high latitude stations was 9-13 percent.

A small intensity increase (about 2 percent) at the end of 2200 UT in Tixie Bay and (2-3 percent) at the end of 2100 UT and at the beginning of 2200 UT in Yakutsk was observed.

In Figure 3 the dependence of the amplitude increase on threshold rigidity is given. Crosses are amplitudes defined for the period of time 2345-2400 UT, January 24, and they are given in the next to last column of the Table. Points are amplitudes determined based on Figure 2 for 0100 UT, January 25, and they are listed in the last column. For a zero level a mean intensity value for 2200 UT and 2300 UT, January 24 was taken in the latter case. From Figure 3 it is seen that the dependence of the amplitude increase on rigidity has the form $A(P) \sim P^{-\gamma}$, where $\gamma = 1.85 \pm 0.05$. From Figure 1 and 3 it is also seen that in Tixie Bay at 2340-2400 UT, January 24, i.e. at the increase maximum and at the beginning of the first hour, January 25, intensity was lower than could be expected from the latitudinal effect. This fact is explained below.

Let us assume according to Krymsky [1969] that the time dependence of intensity during the flare has the form

$$n(R_0^+, t) = B\tau^{\frac{3}{2+\alpha}} e^{-\frac{1}{\tau}}$$

where B is constant, and

$$\tau = \frac{2+\alpha}{\left(\frac{R_0^+}{R_\odot}\right)^{2-\alpha} + 1} \cdot \frac{Dt}{R_\odot^2}$$

Here R_0^+ is a distance from the Sun to the Earth, $R_\odot$ is the Sun's radius, D is the diffusion coefficient, t is the time from the increase commencement. Parameter α is a characteristic of a dependence of diffusion coefficient on distance: $D(r) \sim r^\alpha$. If $\alpha = 0$ the equation for n changes into the usual diffusion equation. If assume $\alpha = 0.25$-0.50 and take 2335-2340 UT, January 24, for increase commencement, we make the estimated and experimental curves for Tixie Bay and Deep River agree. Then we obtain a diffusion coefficient of $(2\text{-}3)\times10^{22}$ cm^2/sec.

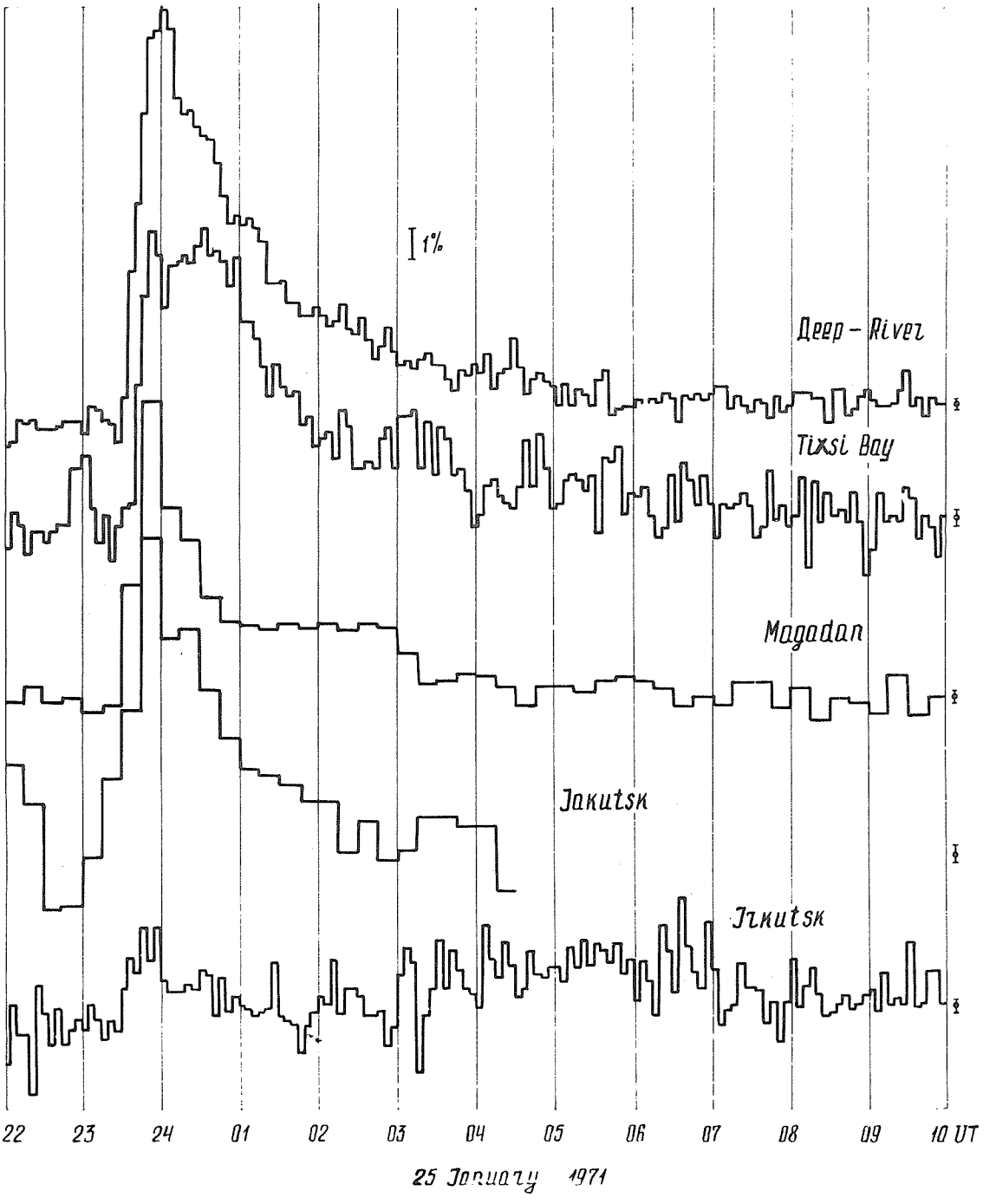

Fig. 1. Cosmic ray intensity variations during the flare on January 24, 1971 in Tixie Bay, Magadan, Yakutsk, Irkutsk, and Deep River.

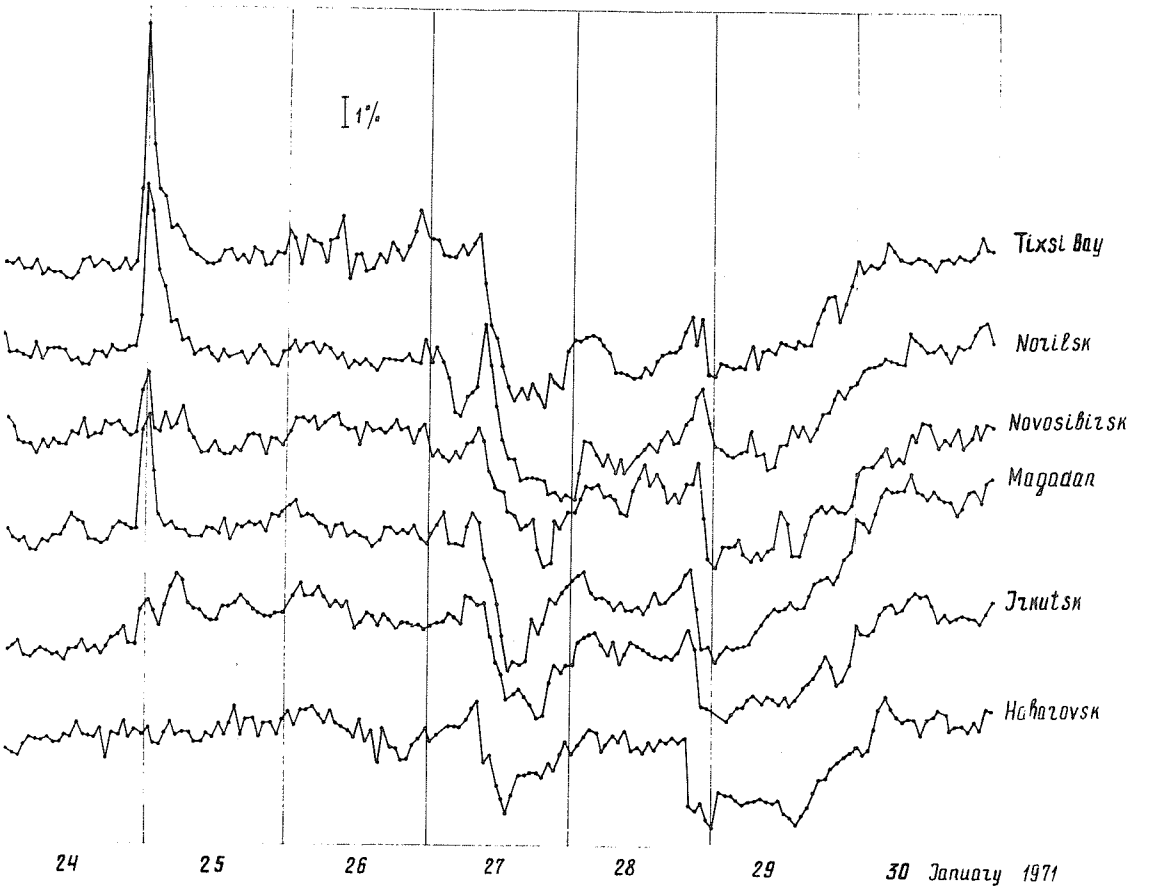

Fig. 2. Cosmic ray intensity variations during the period January 24-30, 1971 in Tixie Bay, Norilsk, Novosibirsk, Magadan, Irkutsk, and Khabarovsk.

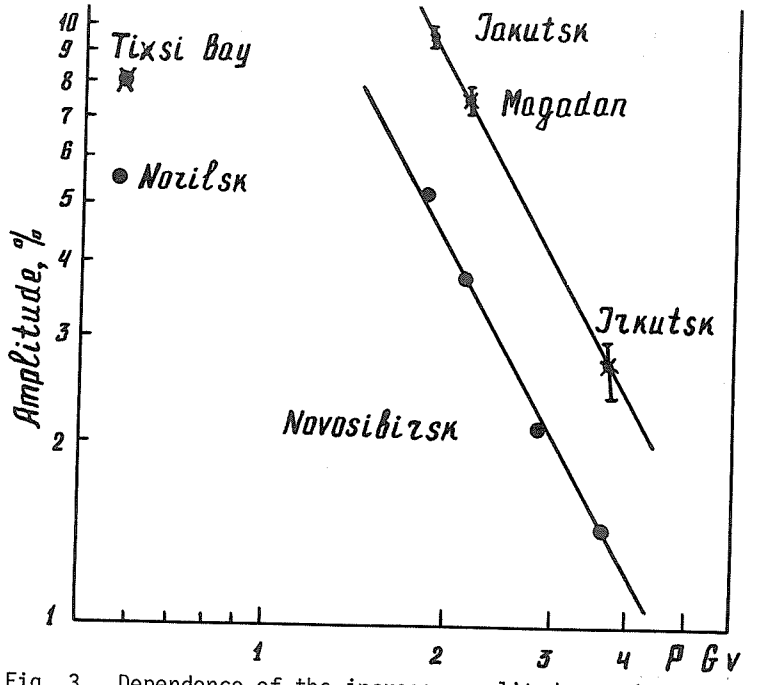

Fig. 3. Dependence of the increase amplitude on threshold rigidity.

Variations of cosmic ray intensity of the order of an hour or less are of great interest. In order to study them we have smoothed out five-minute data from several stations using the method of sliding means in 3 points, at first, then in 12 points. After that we have subtracted from the first line of smoothed values the second one. The results are presented in Figure 4 from which it is clear that the variations of cosmic ray intensity occur at all the noted stations with an amplitude reaching 1 percent and with periods of 20-60 minutes. Under our method of treatment the periods of more than 60 minutes, or less than 20 minutes, are almost expected. Variations during the increase are also distorted. At the same time from Figure 4 it is evident that in Tixie Bay before the increase and at the increase commencement the 50-55-minute variations with amplitudes of 1.0-1.5 percent occurred. A lower value of intensity was in Tixie Bay at the flare maximum and it can be explained that a minimum value of the 55-minute wave accounts for that period.

Cosmic ray variations with periods of 20-60 minutes have been found by us earlier in Chirkov and Ipatjev [1969], where the nature of their origin was discussed. It was shown that their amplitude-frequency spectrum coincided with that of inhomogeneities of the interplanetary magnetic field.

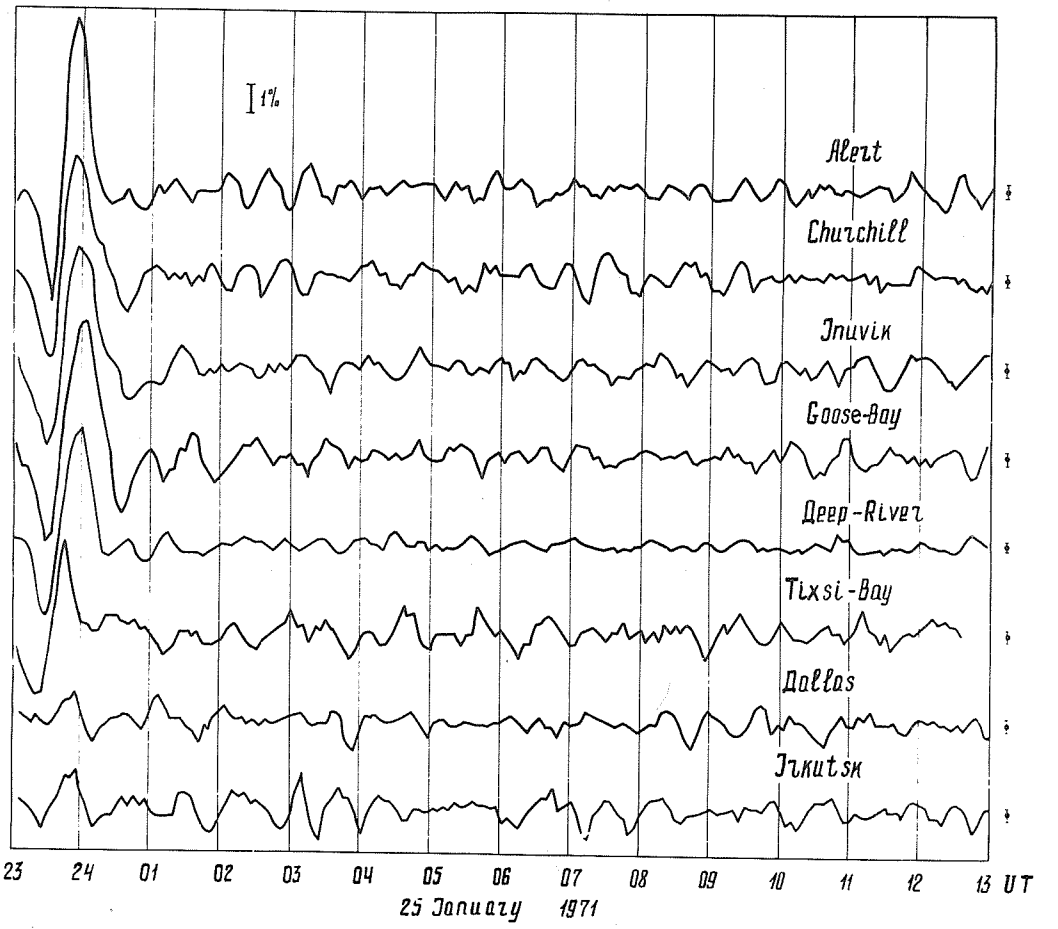

Fig. 4. Cosmic ray intensity variations during the period 2300 UT January 24 - 1300 UT January 25, 1971 in Alert, Churchill, Inuvik, Goose Bay, Deep River, Tixie Bay, Dallas, and Irkutsk.

REFERENCES

CHIRKOV, N. P., and V. I. IPATJEV 1969 Microvariations of Cosmic Ray Intensity, Acta Physica Academiae Scientiarum Hungaricae 29, Suppl. 2, 257-260.

KRYMSKY, G. F. 1969 Modulyatsia kosmicheskikh luchei v mezhplanetnom prostranstve, Izd. "Nauka", Moscow.

SHEA, M. A., D. F. SMART, and J. R. MCCALL 1968 A Five Degree by Fifteen Degree World Grid of Trajectory Determined Vertical Cutoff Rigidities, Canadian J. of Physics, 46, 10, 4, 1098-1103.

Upper Cutoff in the Proton Spectrum of January 24 and September 1, 1971 Events

by

Dj. Heristchi, J. Pérez Peraza+ and G. Trottet
Laboratoire de Physique Cosmique
Verrières le Buisson [France]

In an earlier publication, [Heristchi and Trottet, 1971] arguments have been advanced in favor of the existence of an upper cutoff in the spectrum of solar protons in the case of the events of January 28, 1967 and March 30, 1969. This quantity, even when it is determined in the Earth's environment, is directly related to the Source Spectrum, for, contrary to other parameters of the Source Spectrum, it is almost unaffected by the propagation of particles in the interplanetary medium. When the magnitude of this upper cutoff is of a few GV it can be evaluated from Neutron Monitor (NM) data. As the "Specific Yield Function" for protons (SYF) increases with the rigidity, the neutron monitor is a particularly good means of this measurement. The purpose of this paper is to determine the upper cutoff during the January 24-25, 1971 and September 1-2, 1971 events.

A first method consists in using the world-wide network of NM as a rigidity spectrometer while adding the presence of a maximum rigidity in the proton spectrum [Heristchi and Trottet, 1971]. Mountain stations are ignored and a double correction of the barometric effect is applied. The percentage increase (F) for one NM may be formulated as follows [Palmeira et al., 1970]:

$$F = \frac{A_1}{N_g} \int_{P_c}^{P_m} P^{-\mu} S(P)\, dP \qquad (1)$$

where P is the magnetic rigidity of the protons, A_1 a constant, N_g the counting rate due to galactic cosmic rays with a standard NM located in a place of magnetic rigidity P_c, P_m the upper cutoff, $P^{-\mu}$ the differential spectrum of the primary solar protons and S(P) the SYF. Here we use for N_g the values obtained by Carmichael et al. [1966], for P_c the values calculated by Shea et al. [1965], and the Lockwood and Webber's [1967] SYF which is represented by power laws in different rigidity bands.

By using for each time interval the percentage increase at several NM stations located in different geomagnetic latitudes and by applying the least square method, it is possible to determine A_1, μ and P_m. By writing equation (1) as a function of energy, we obtain:

$$F = \frac{A_2}{N_g} \int_{E_c}^{E_m} E^{-\gamma} S(E)\, dE \qquad (2)$$

where E_c corresponds to P_c for protons.

This method is only applicable for an isotropic event. In the case of a noticeable anisotropy or of a lack of data we can proceed as follows [Heristchi et al., 1972]. The ratio R = F1/F2 of the percentage increases at two stations viewing in similar mean asymptotic directions and located in different P_c is calculated. From equation (1) this ratio is computed as a function of P_m for different values of μ. Two examples of the curves $R = f(P_m,\mu)$ are shown on Figure 1.

By choosing three or two pairs of stations in different cutoffs, it is possible to determine P_m and μ. We consider three stations with P_{c1}, P_{c2} and P_{c3} ($P_{c1} < P_{c2} < P_{c3}$) in order to have P_m near P_{c3} and substantially larger than P_{c1} and P_{c2}. P_m and μ are determined, from R_1 = F1/F2 and R_2 = F1/F3, by means of an iterative method. Starting from one P_m larger than P_{c3}, μ is determined by using R_1. The knowledge of μ allows one then to find P_m from R_2. This new P_m is used to obtain a new μ and so on. This method is rapidly convergent. Evidently if μ is deduced from other measurements, R_2 is sufficient to evaluate P_m and vice versa.

In order to estimate the magnitude of P_m, it would be possible to search from which cutoff the event is not registered. The preciseness of this procedure is not sufficient to determine P_m, but it can be used to corroborate the results deduced from the preceding methods.

+ On leave from the E.S.F.M. of the Instituto Politécnico Nacional, México.

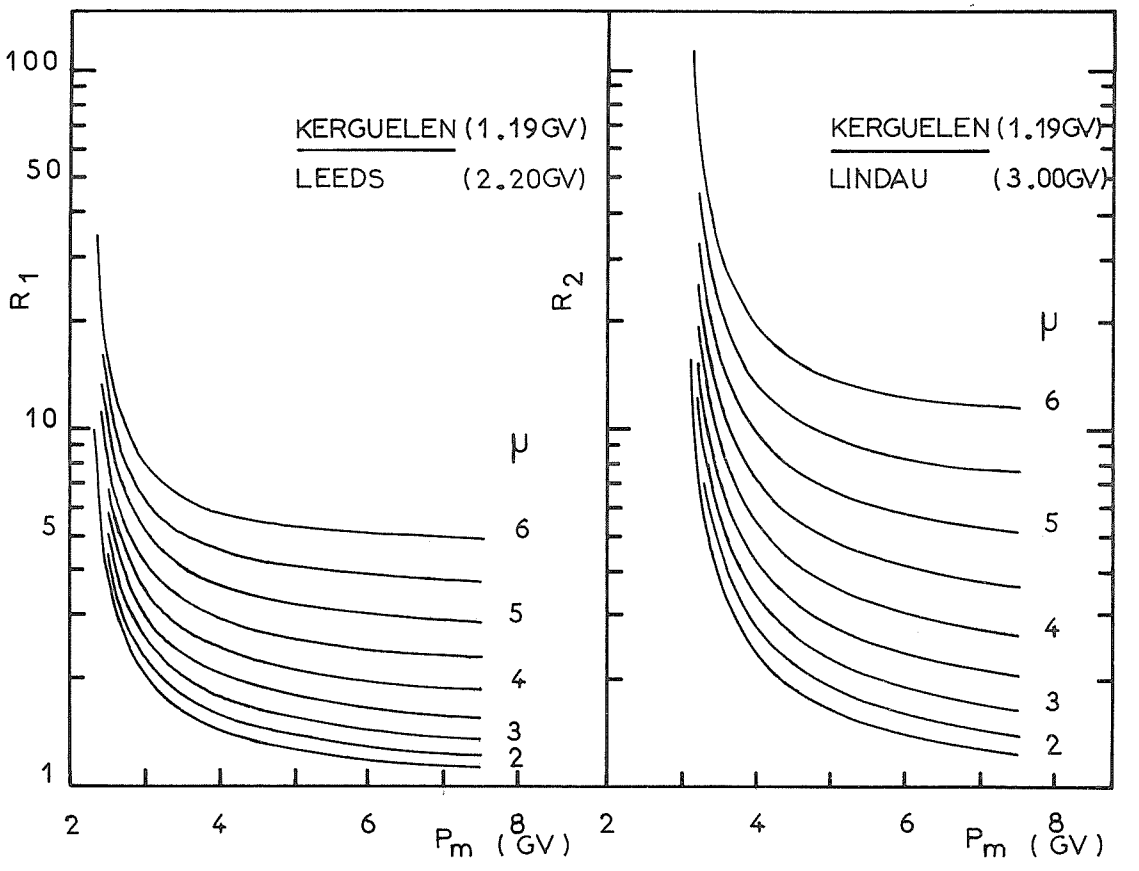

Fig. 1. Expected ratios of relative enhancements of two pairs of stations versus P_m for different values of μ.

January 24-25, 1971 event

The time variations recorded at different NM stations during this event are shown in Figure 2. As this event is not very anisotropic, the first method has been applied to the hourly counting rates of several NM. Since records of low latitude stations show that the galactic background varies during the event, this method has been applied in two different ways:

- The background variations have been neglected (background = mean level before the event).
- A variable background for all the stations has been deduced proportionally to Rome's smoothed variations.

The results are similar in both cases and for different hours.
We obtain:

$$P_m = (3.5 - 4.0) \pm 0.6 \text{ GV} \; ; \; \mu = (3.7 - 3.9) \pm 0.4$$

$$E_m = (2.7 - 3.0) \pm 0.5 \text{ Gev}; \; \gamma = (2.7 - 2.8) \pm 0.4$$

In Figure 3 the percentage increases between 0000 UT and 0100 UT on January 25 is plotted against P_c, and the Figure shows the predicted curves of various forms of the differential spectrum. These curves indicate that the best agreement with the experimental points is obtained with an upper cutoff in the differential spectrum.

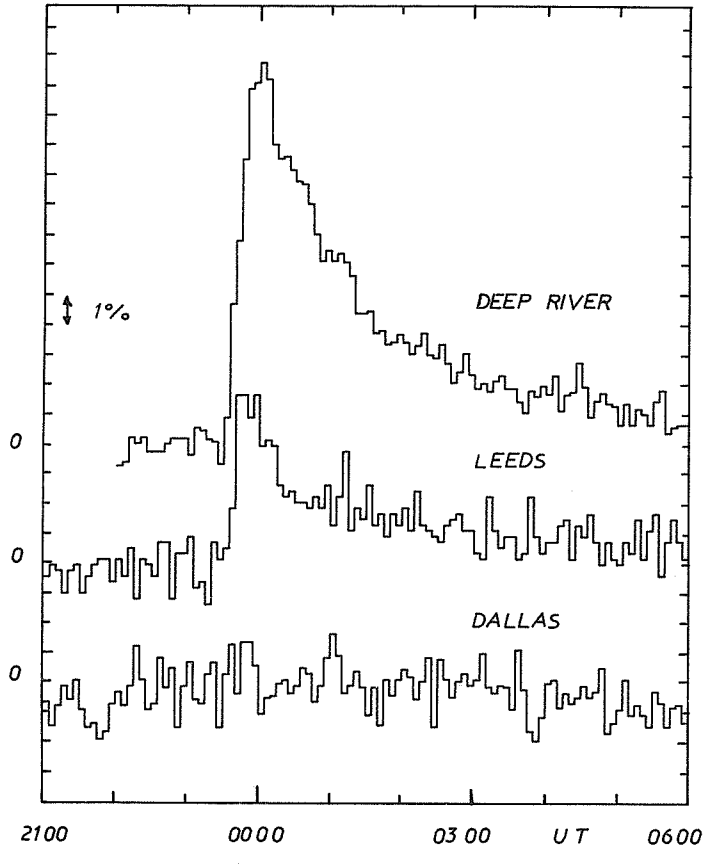

Fig. 2. Time variations of three typical stations on January 24-25, 1971.

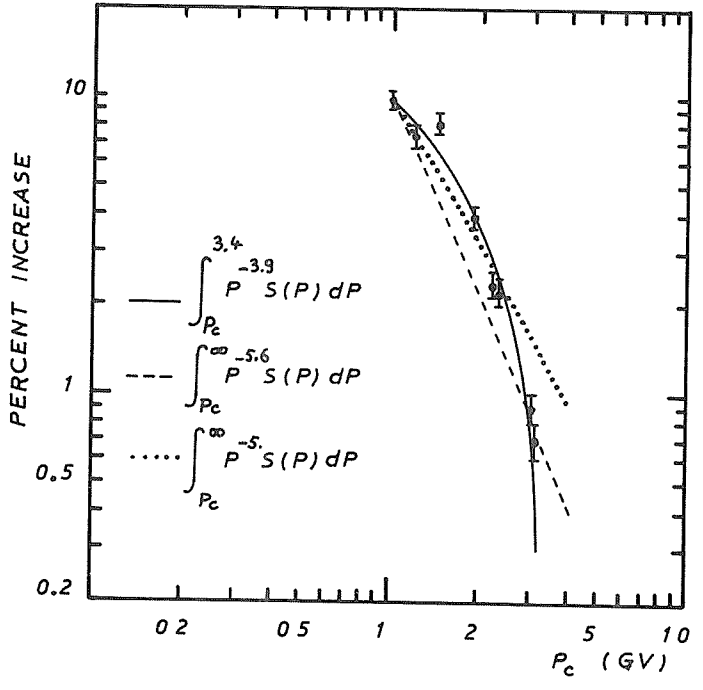

Fig. 3. Percentage increase in the sea level NM at 0100 UT on January 25, 1971, compared with different theoretical curves. The percentage increases of polar stations (1 GV) have been averaged.

Considering that this event is slightly anisotropic the second method has been applied to two groups of three stations. The results are:

- from Kerguelen (1.2 GV), Leeds (2.2 GV), Lindau (3.0 GV).

$$P_m = 4.0 \pm 0.6 \text{ GV} \; ; \; \mu = 4.0 \pm 0.4$$

- from Oulu (1.0 GV), Kiel (2.3 GV), Lindau (3.0 GV).

$$P_m = 4.6 \pm 0.6 \text{ GV} \; ; \; \mu = 4.6 \pm 0.4$$

Within the errors all these results are in agreement.

However, from balloon measurements in the 100-500 Mev energy band, Charakhchyan [1972] has found $\gamma = 3.8$ to 4.2 corresponding to $\mu = 4.8$ to 5.2, values larger than ours. This difference is partly due to the correction which has been applied for the nuclear interaction of 100-500 Mev protons in the atmosphere, and partly to a possible decrease of the P_c of the stations, for the Kp index reaches a value of 4 during the event.

September 1-2, 1971 event

In Figure 4 the counting rates of several NM during the event are plotted against time. Both methods have been applied to the hourly percentage increase and to their sum through 2000 to 2400 UT. Using P_m, so deduced, μ can be evaluated from R_1 = Deep River (1.0 GV)/ Swarthmore (1.9 GV). All the results are shown in Table 1. It follows from this Table:

- The values of P_m and μ, deduced from the different methods, are all consistent:
- E_m and P_m remain substantially constant in time.
- γ and μ increase with time. This can be explained by the propagation of particles in interplanetary space.

Figure 5 is equivalent to Figure 3 for this event. Here again, it is clear that the best agreement with the experimental points is obtained with an upper cutoff in the differential spectrum.

A small increase is visible on Pic-du-Midi's hourly and fifteen minutes records between 2100 and 2200 UT. However, only one of the three sections of this NM shows this increase, so it cannot be due to the event. Moreover, as it can be seen from Figure 4, there is no increase in Dallas's records. It is to be noted that during this event there is an enhanced diurnal variation and that the magnetic activity is very low.

Table 1

Universal time	First method				Second method		
	E_m	γ	P_m	μ	P_m+	μ+	μ++
2000-2100	2.5	1.3	3.3	1.6			
2100-2200	2.4	2.6	3.2	3.5	3.2	3.2	2.6
2200-2300	2.1	2.8	2.9	3.8	2.9	4.2	3.6
2300-2400	2.1	3.2	2.9	4.4			4.0
Sum	2.3	2.7	3.1	3.6	3.0	3.6	3.6

\+ From Kiruna, Leeds and Utrecht.
++ From Deep River and Swarthmore by using P_m from fourth column.

The two events discussed here show upper cutoffs of the same order of magnitude as in the case of the events of 28 January 1967 and 30 March 1969. Preliminary results obtained on other events, recorded by Neutron Monitors, indicate that the upper cutoffs are of a few GV except for the February 23, 1956 event, the P_m of which is larger [Heristchi et al., 1972].

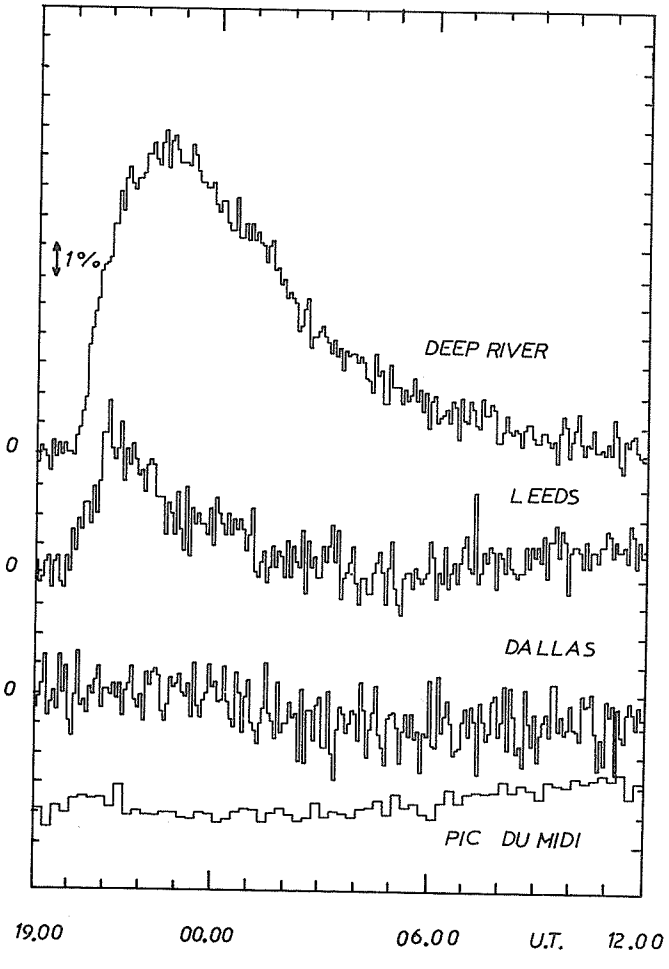

Fig. 4. Time variations of four typical stations on September 1-2, 1971.

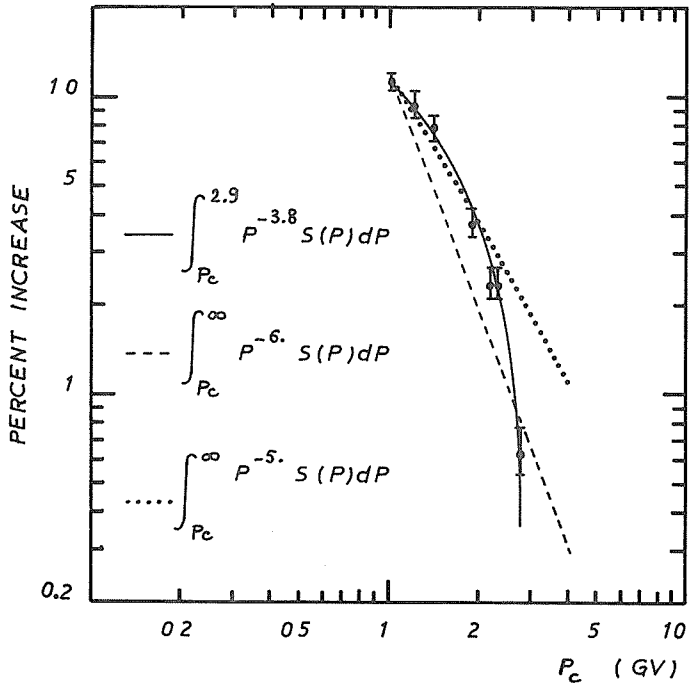

Fig. 5. The same as Figure 3 at 2300 UT on September 1, 1971.

Acknowledgement

We are indebted to the laboratories which supplied us with the data used in this paper, and to Dr. A. N. Charakhchyan for providing us with information. One of us [J.P.P.] wishes to thank the Conacyt-Cofaa of México and the French Ministry of Foreign Affairs for financial support through a scholarship.

REFERENCES

CARMICHAEL, H., M BERCOVITCH, J. F. STELJES and M. MAGIDIN — 1966 — Latitude Survey in North America, Proceedings of the Ninth International Conference on Cosmic Rays, 1, 553.

CHARAKHCHYAN, A. N. — 1972 — To be published in IZV. Acad. Nauk. SSSR, ser. fiz. and Private Communication.

HERISTCHI, Dj., J. PEREZ PERAZA and G. TROTTET — 1972 — To be published.

HERISTCHI, Dj. and G. TROTTET — 1971 — Upper Cutoff in the Spectrum of Solar Particles. Physical Review Letters, 26, 197.

LOCKWOOD, J. A. and W. R. WEBBER — 1967 — Differential Response and Specific Yield Functions of Cosmic-Ray Neutron Monitors. J. Geophys. Res. 72, 3395.

PALMEIRA, P.A.R., R. P. BUKATA and P. T. GRONSTAL — 1970 — Determination of the Solar-flare Cosmic-ray Rigidity Spectrum using Neutron Monitor Network, Can. J. Phys., 48, 419.

SHEA, M. A., D. F. SMART, K. G. McCRACKEN and U. R. RAO — 1965 — Cosmic Ray Tables, IQSY Instruction Manual No. 10.

The Ground Level Cosmic Ray Increase of January 24, 1971 Recorded by the Neutron Monitor in Bergen, Norway

by

R. Amundsen and H. Trefall
Department of Physics
University of Bergen, Norway

The Bergen neutron monitor data for the January 24, 1971 event is presented in Figure 1. The graph presents hourly values and is plotted as a percentage of the pre-event average count-rate. The data are pressure corrected to 990 mb (coefficient 0.74%/mb) and represent the mean of two sections. The 100% level is at 8560 counts per hour for the January event. The standard deviation is shown on the graph.

The neutron monitor station in Bergen is at sea level, and the geographical position is N60°24' latitude and E5°24' longitude. The cut-off rigidity is 1.2 GV.

For the January event, the maximum count-rate is recorded in the time interval 0000-0100 UT January 25, and the recorded increase amounts to 10.6%.

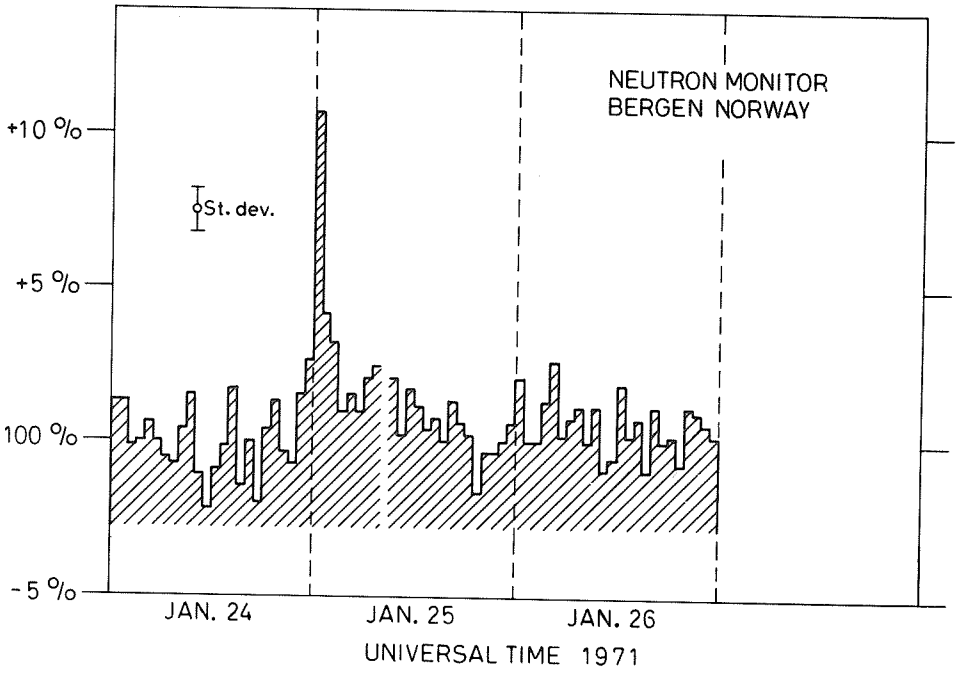

Fig. 1. Bergen neutron monitor data for the January 24, 1971 event.

Rocket Measurements of Energy Spectra of Protons and Alpha Particles during the January 24, 1971 Solar Event

by

H. Hempe and M. Witte
Institut für Reine und Angewandte Kernphysik
Universität Kiel, 23 Kiel, G.F.R.

During the ESRO-PCA campaign 1971 two Centaur rockets were launched from Kiruna 13.5 and 35.7 hours after the proton flare on January 24, 2308 UT. Preliminary energy spectra of protons between 22 and 133 Mev and alpha particles between 22 and 110 Mev/N are presented.

The experiment consisted of a dE/dx-E- scintillator telescope with an energy dependent geometry factor between 3.6 and 1.7 cm^2sr for 22 and 133 Mev protons, respectively. Coincident pulses in the dE/dx- and the E-scintillator were analysed by two 256-channel pulse height analysers. The channel numbers together with the response of the anticoincidence detector were transmitted in realtime as a 21-bit word through the IRIG 19 telemetry channel. To be able to correct for deadtime effects in this channel the counting rates of two- and threefold coincidences were transmitted through a separate telemetry channel.

For 280 seconds flight time above approximately 75 km two-dimensional pulse height distributions were constructed for unique identification of protons and alpha particles.

Figure 1 shows the energy spectra of protons and alpha particles during the first flight (F1) on January 25, 1238 UT and the second flight (F2) on January 26, 1050 UT.

The intensities have been corrected for deadtime effects of 95.5% during F1 and 46.5% during F2. The error bars include statistical and estimated systematical errors. Due to pile up and saturation effects caused by the high particle fluxes during the first flight, the uncertainties in the energy spectra of F1 might still be larger than indicated.

The data points at lower energies are obtained by the Utrecht Group [van Beek, 1972] in a rocket flight from Kiruna on January 26, 1322 UT, 2.5 hours after F2. During this period the proton flux, as measured by ATS-1, decreased by only 20%.

The energy spectra are gradually steepening as a function of energy. Conversion to a rigidity spectrum (Figure 2) shows that the alpha particles are well fitted by an exponential law

$$dN/dP = \text{const} \exp(-P/P_o) \text{ with } \begin{matrix} P_o = 80 \pm 20 \text{ MV for F1} \\ P_o = 86 \pm 18 \text{ MV for F2} \end{matrix}$$

The proton spectra are flattening towards lower energies and are bending over at approximately 200 MV which is probably due to geomagnetic screening. According to recent calculations of Smart et al. [1969] the daytime vertical cutoff of Kiruna is approximately 500 MV.

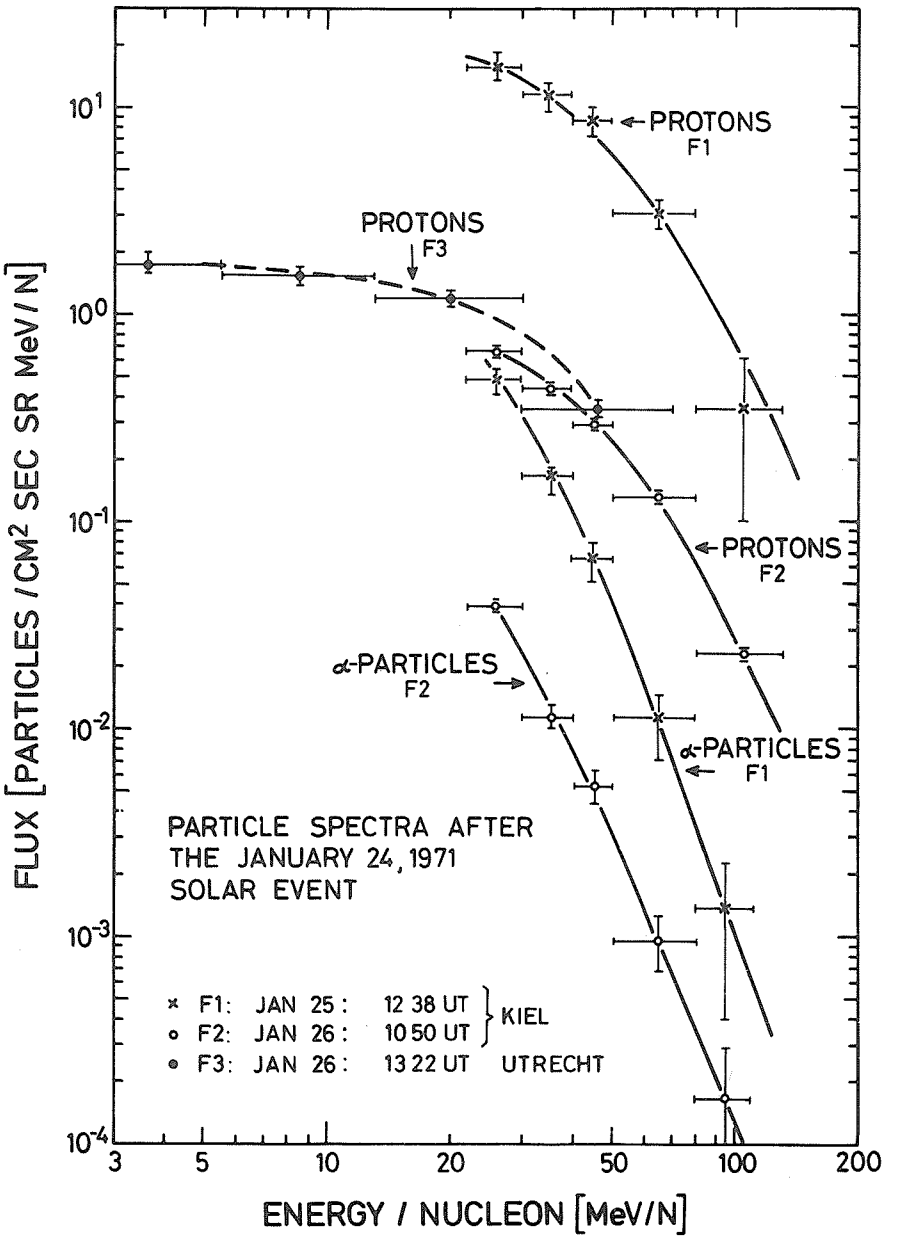

Fig. 1. Energy/nucleon spectra of protons and alpha particles obtained with an E-dE/dx telescope 13.5 and 35.7 hours after the January 24, 1971 solar event.

Intensity points at lower energies are measured by the Utrecht Group 2.5 hours after F2.

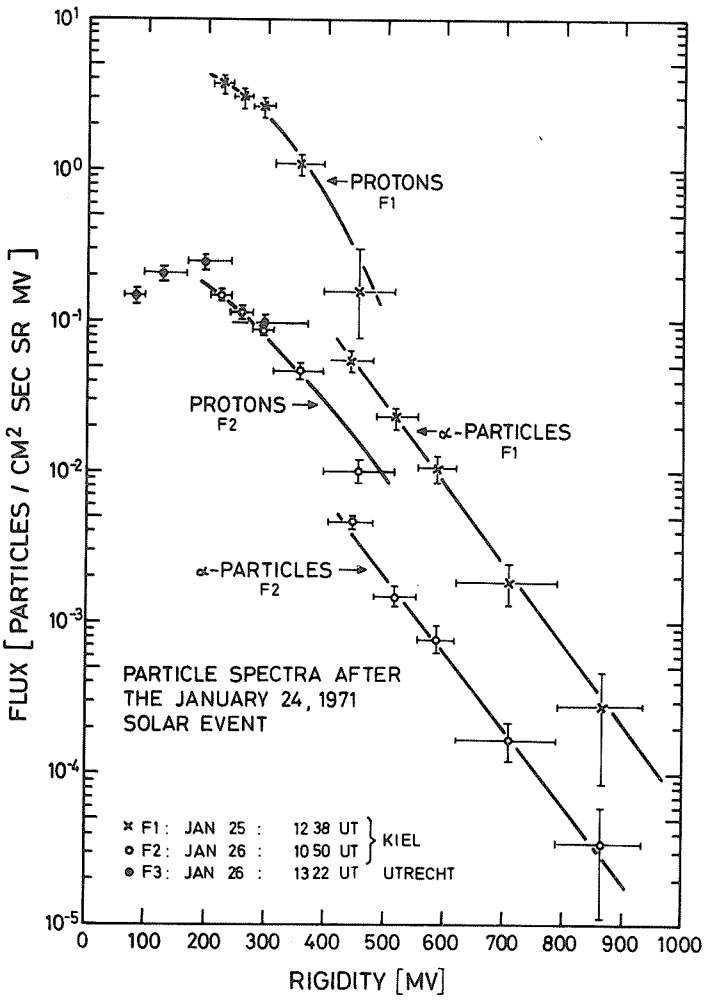

Fig. 2. Rigidity spectra of protons and alpha particles obtained with an E-dE/dx telescope 13.5 and 35.7 hours after the January 24, 1971 solar event.

Acknowledgement:

We wish to thank Dr. de Feiter and Dr. van Beek, Utrecht, for making their data available to us.

REFERENCES

VAN BEEK 1972 Annual ESRO-Report.

SMART, D. F., M. A. SHEA and R. GALL 1969 Iso-rigidity contours in the polar regions interpolated from trajectory-derived vertical cutoff rigidities, Proc. 11th Int. Conf. on Cosmic Rays, Budapest, 1969, Paper MO-136.

Cosmic Ray Solar Flare Event of January 24, 1971

by

M. Arens, H. F. Jongen, J. Skolnik
Natuurkundig Laboratorium, Universiteit van Amsterdam
Amsterdam

and

L. D. de Feiter
Laboratorium voor Ruimte-Onderzoek
Utrecht

ABSTRACT

On January 24, 1971 at 2335 UT an increase in counting rate was measured by high-latitude Neutron Monitors, probably caused by solar particles accelerated in the flare of importance 2B at N18 W44 at 2300 UT January 24, 1971. The differential rigidity spectrum was found to be a power law spectrum with exponent $\gamma = 5.5$.

The intensity-time profile is consistent with the ADB-model of Burlaga with an absorbing boundary at about 2 A. U.

Introduction

On January 24, 1971, at 2300 UT a solar flare of importance 2B was observed at N18 W44. Between 2335-2340 UT an increase in the counting rate of high-latitude Neutron Monitors was recorded, most probably caused by energetic particles of this flare. From the data of the Calgary and Sulphur Mountain Neutron Monitors the absorption length for the solar particles in the atmosphere is calculated. The fractional increase in intensity is then computed with the method of the 2-attenuation lengths [McCracken, 1962]. Using the model for the propagation of solar particles as proposed by Burlaga [1967] the time profile for the data of the Deep River Monitor is investigated.

Calculation of the Atmospheric Absorption Length for the Solar Particles

As is well known [e.g. McCracken, 1962], the absorption length, λ_f, of energetic solar particles is different from the absorption length λ_g, of galactic cosmic rays due to the relatively low energy of the flare particles. λ_f is calculated from the data of two neighboring Neutron Monitor stations at different atmospheric depths: Calgary and Sulphur Mountain [Wilson et al., 1967]. It is found that $\lambda_f = 102 \pm 3$ gr/cm^2, in agreement with values of λ_f given earlier [McCracken, 1962; Wilson et al., 1967].

Station	Altitude	R_c	$\lambda_{geomagn.}$	$\Phi_{geomagn.}$
Sulphur Mt.	2283 m	1.14 GV	58.16°	300.33°
Calgary	1128 m	1.09 GV	58.30°	302.13°

The fractional increases reduced to 1030 gr/cm^2 are calculated with the 2-attenuation lengths method for periods of 15 minutes. The results are summarized in Table 1.

Spectrum of the Solar Flare Particles

For the construction of the spectrum of the solar flare particles we used the galactic proton spectrum of May 1965 [Gloeckler and Jokipii, 1967] and the specific yield functions as given by Lockwood and Webber [1967]. From the Deep River data we deduced a 10% reduction, due to the 11-year modulation, at the moment of the flare as compared with May 1965. This modulation was taken into account for the calculation of the galactic component.

With the fractional increases in intensity for the stations with R_c between 1-5 GV and the specific yield functions the differential rigidity spectrum was found to be a power law spectrum with spectral index $\gamma = 5.5 \pm 0.5$. Because of the errors involved in this deduction it is difficult to get an impression of changes of the spectrum during the event.

Table 1

Percent increase in Neutron Monitor counting rate corrected with the 2 - attenuation length method

	R_c	UT 2330-2345	UT 2345-2400	UT 0000-0015	UT 0015-0030	UT 0030-0045
Dumont d'Urville	0.05	12.2	18.0	18.0	12.2	10.8
Ft. Churchill	0.21	4.0	--	11.9	10.2	7.3
Kiruna	0.54	3.5	14.8	14.1	10.4	8.5
Oulu	0.81	2.6	12.7	12.1	9.4	8.6
Deep River	1.02	4.0	10.8	11.3	9.2	8.3
Kerguelen Is.	1.19	3.8	7.7	8.7	8.1	6.8
Uppsala	1.43	5.4	7.6	9.8	7.0	7.8
Kiel	2.29	1.7	3.7	2.8	2.0	1.7
Utrecht	2.76	2.2	2.7	2.1	1.1	1.4

ADB Model

The model for the propagation of solar particles as proposed by Burlaga [1967] was applied to the Deep River data for this event. For the increasing phase the model predicts a dependence of the intensity as a function of time as:

$$F(t) = K_1 \exp(-S_r/t)\ t^{-5/2} \quad \text{with}$$

F intensity increase, K_1 a constant, S_r=2.5 t_m, t_m time of maximum intensity; t is counted from the injection time t_o. The best fit for a straight line through the data of the plot

$$\ln \{F(t)\ t^{5/2}\} \quad \text{versus} \quad t^{-1} \quad \text{with } t_o \text{ as parameter was obtained for}$$

t_o= 2320 UT (Fig. 1)

From the slope of this line S_r is found to be: S_r= 118 min. ± 17 min. so t_m = 47 min. The measured value of t_m with t_o = 2320 UT is: t_m = 40 - 45 min. The agreement between these values may be considered reasonable.

As has been shown by Snyder [Snyder et al., 1963] there exists a linear relationship between the solar wind velocity and ΣK_p:

$$v = (8.44 \pm 0.74)\ \Sigma K_p + (330 \pm 17) \quad \text{km/sec.}$$

The solar wind velocity is related to the angle Θ_1 between the earth-sun line and the interplanetary magnetic field line connecting with the earth as:

$$\Theta_1 = 32900/v \quad ^\circ\text{West [Burlaga, 1967].}$$

For January 24, 1971 ΣK_p = 17+; this yields v = 476 ± 30 km/sec. and Θ_1 = 69 ± 4 °West.

Following Burlaga [1967] and Lockwood [1968] t_m being a linear function of Θ_o^2, Θ_o being the angle between the flare position on the sun and the origin of the interplanetary magnetic field line connecting with the earth, Θ_o can be calculated from:

$$\Theta_o^2 = \frac{10(t_m - a)}{g} \quad \text{with constant a = 40 min. as derived}$$

from Burlaga's Figure 6. For g Burlaga gives the value: g = 6.5 ± 0.5 hours. Using this value and Θ_1 as derived earlier, the following estimate for the flare position is obtained: Θ_f = 45 ± 5 °W. The visual flare was observed at W44.

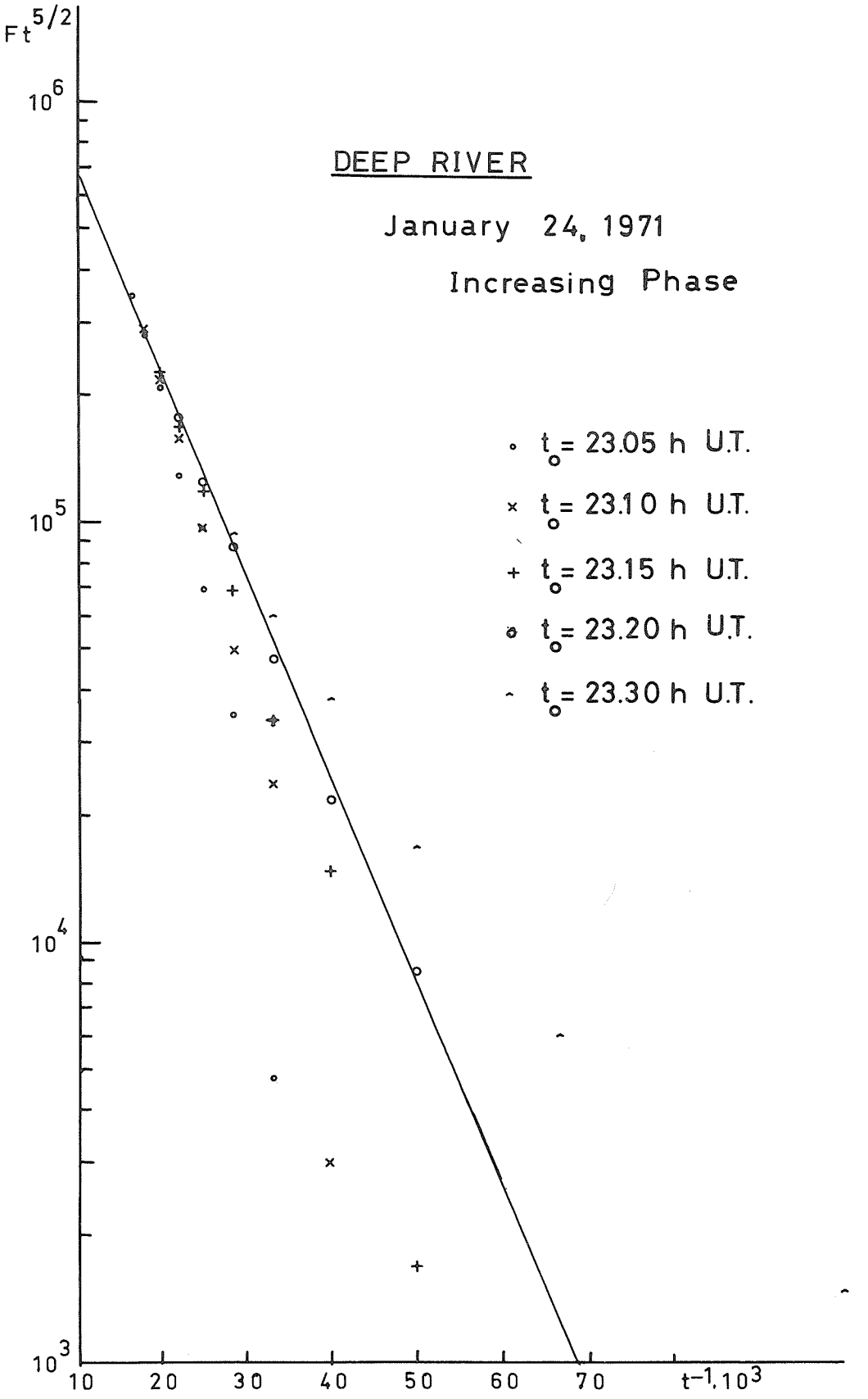
Ft^5/2
10^6
10^5
10^4
10^3
DEEP RIVER
January 24, 1971
Increasing Phase
t_o = 23.05 h U.T.
t_o = 23.10 h U.T.
t_o = 23.15 h U.T.
t_o = 23.20 h U.T.
t_o = 23.30 h U.T.
10
20
30
40
50
60
70
t^-1.10^3

Fig. 1.

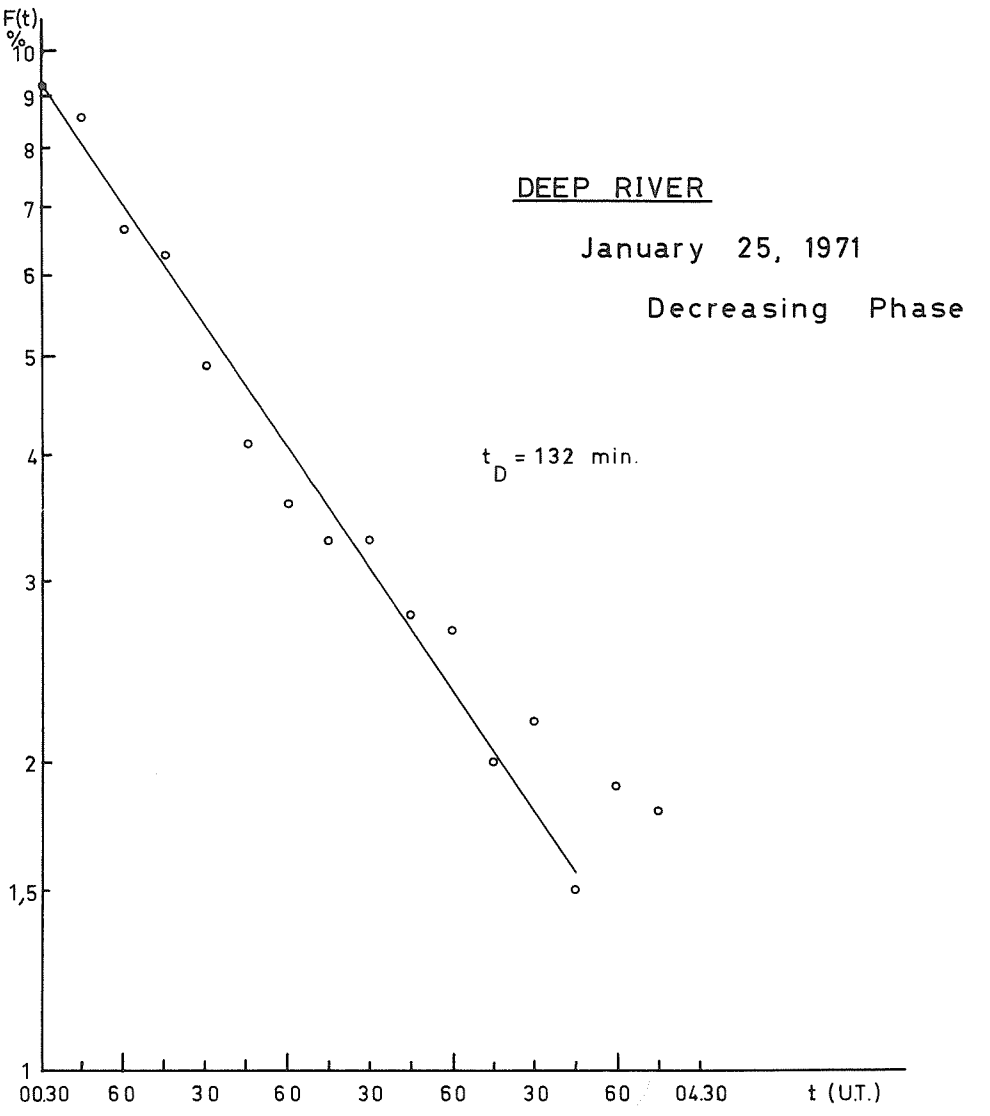

Fig. 2.

For the decreasing phase of the flare event the Burlaga model predicts an intensity versus time dependence as:

$$F(t) = K_2 \exp(-t/t_D) \quad \text{with}$$

F intensity decrease, K_2 a constant and t_D the decay time-constant. The slope of the line ln F(t) versus t for the early part of the decreasing phase, Figure 2, yields: t_D = 132 min. ± 16 min. With this value of t_D the position of the absorbing boundary:

$$\frac{r_1}{r} = \left\{ \frac{\pi^2 \; t_D}{10 \times t_m - g\Theta_o^2} \right\}^{1/2}$$ is found to be:

r_1 = 1.8 A. U.

Acknowledgments

We thank the following investigators for promptly sending their data: Professor A. Fréon (Dumont d'Urville, Kerguelen Is., Pic du Midi), Dr. R. Palmeira (Churchill, Dallas), Dr. H. Hauska (Kiruna, Uppsala), Professor P. J. Tanskanen (Oulu), Dr. J. F. Steljes (Deep River), Dr. T. Mathews (Calgary, Sulphur Mountain), Dr. O. Binder (Kiel), Professor H. Debrunner (Jungfraujoch). The Utrecht Cosmic Ray Monitor station is operated with financial support of the Netherlands Organization for Pure Scientific Research (Z.W.O.).

REFERENCES

BURLAGA, L. F. 1967 J. Geophys. Res., 72, 4449

GLOECKLER, G. and J. R. JOKIPII 1967 Ap. J., 148, L 41

LOCKWOOD, J. A. and W. R. WEBBER 1967 J. Geophys. Res., 72, 3395

LOCKWOOD, J. A. 1968 J. Geophys. Res., 73, 4247

McCRACKEN, K. G. 1962 J. Geophys. Res., 67, 423

SNYDER, C. W., M. NEUGEBAUER and U. R. RAO 1963 J. Geophys. Res., 68, 6361

WILSON, B. C., T. MATHEWS and R. H. JOHNSON 1967 Phys. Rev. L., 18, 675

Scintillation Monitor, Bologna, Italy. 15-Minute Observations

by

M. Galli, L. Fiandri
Istituto di Fisica "A. Righi"
Università degli Studi di Bologna

M.R. Attolini
Laboratori T.E.S.R.E.
Consiglio Nazionale delle Ricerche, Bologna

Figure 1 presents for January 21-27, 1971 the total ionization (T), the atmospheric pressure at ground level (P), and the hard components: 45° inclined towards West (W), 45° inclined towards East (E) and vertical cubical coincidences (V).

Table 1 presents the data from the scintillation monitor at Bologna. The tabulated data should be read with a decimal point after the second figure of each number. The numbers are deviations in % units from a fixed value of pressure corrected data at the end of each 15-minute interval.

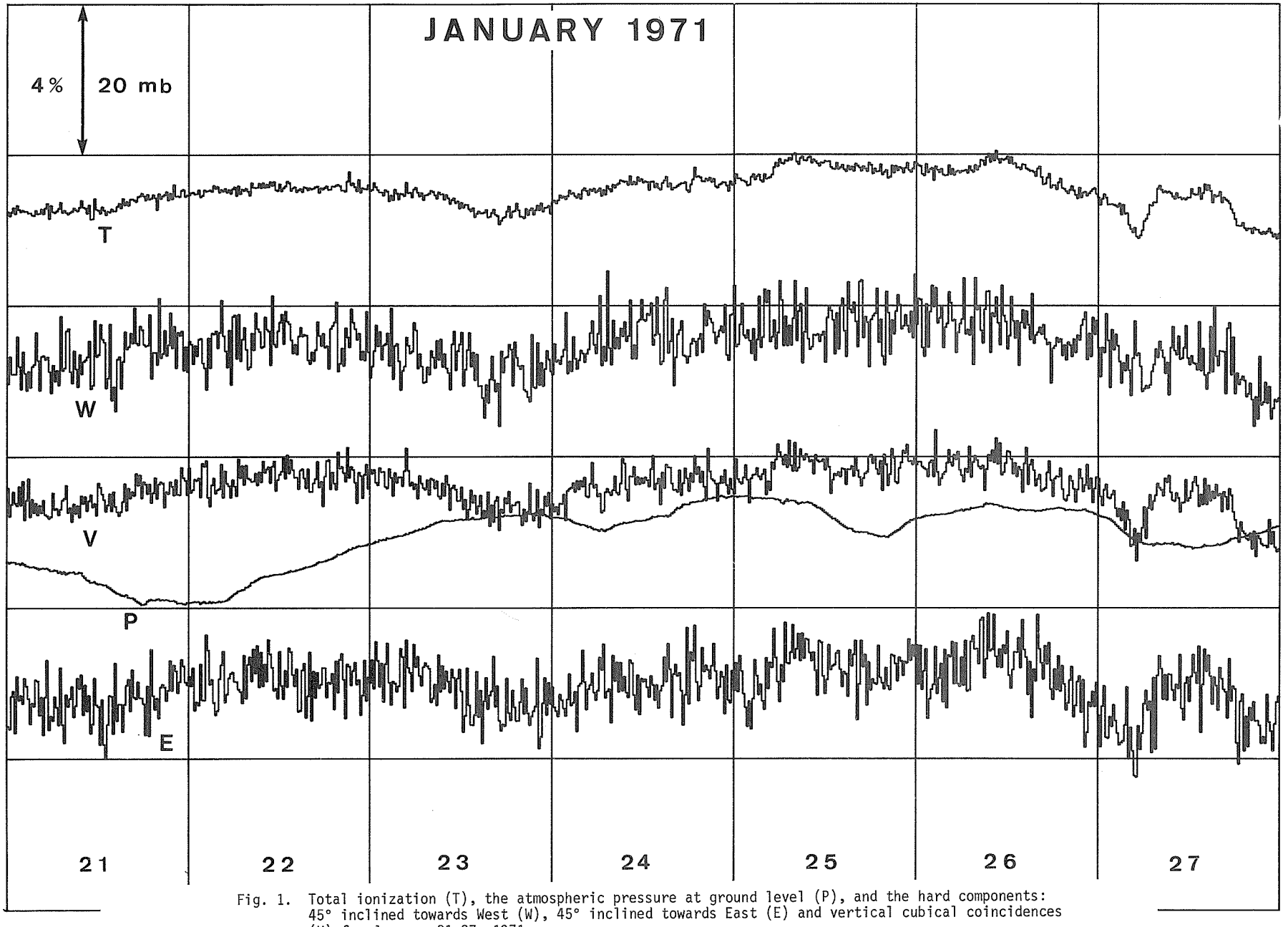

Fig. 1. Total ionization (T), the atmospheric pressure at ground level (P), and the hard components: 45° inclined towards West (W), 45° inclined towards East (E) and vertical cubical coincidences (V) for January 21-27, 1971.

Table I

15-MINUTE COSMIC RAY DATA AT BOLOGNA DURING JANUARY 24, 25 1971

Scintillation Monitor for Cosmic Rays
Location Bologna 44.5 N 11.35 E 50 m a.s.l.
Tabulated Deviations in percent units from a fixed value of pressure corrected totals, at the end of each interval

* Total Ionizing Component counts under 5 gr/sqcm * S.D. 0.084%
* Coincidence counts 45 degrees inclined towards West filtered by 10 cm of lead * S.D. 0.54%
* Vertical Cubical coincidence counts filtered by 10 cm of lead * S.D. 0.30%
* Coincidence counts 45 degrees inclined towards East filtered by 10 cm of lead * S.D. 0.54%

Bar. coeff. 0.20 percent/mb
January 24, 25 1971

	Minutes at End of Interval																			
U.T. hours	15	30	45	60	Mean	15	30	45	60	Mean	15	30	45	60	Mean	15	30	45	60	Mean
1200–1300	4.27	4.30	4.28	4.07	4.23	4.63	4.60	4.79	4.76	4.69	5.31	5.46	5.39	5.22	5.35	5.05	5.11	4.90	4.64	4.93
1300–1400	4.29	4.30	4.14	4.24	4.24	5.07	3.96	4.23	5.23	4.62	5.68	6.03	5.14	5.30	5.54	5.20	4.96	4.56	4.96	4.92
1400–1500	4.12	4.08	4.26	4.33	4.20	4.25	3.45	3.53	5.15	4.10	5.43	4.75	5.59	5.18	5.24	4.35	4.81	4.94	5.70	4.95
1500–1600	4.42	4.16	4.25	4.08	4.23	5.48	3.75	4.06	4.66	4.49	5.80	5.73	5.72	5.30	5.64	5.05	6.05	5.38	4.10	5.14
1600–1700	4.13	4.14	4.18	4.22	4.17	2.89	3.64	4.25	4.36	3.79	5.13	5.14	5.08	5.65	5.25	5.25	5.50	5.20	5.28	5.31
1700–1800	4.25	4.25	4.28	4.07	4.21	4.60	3.69	3.67	3.49	3.86	4.99	5.31	5.70	5.44	5.36	4.81	3.90	4.70	6.48	4.97
1800–1900	4.02	4.22	4.35	4.67	4.31	3.66	4.00	4.13	4.06	3.96	5.10	5.57	5.34	6.03	5.51	4.46	5.83	5.61	6.54	5.61
1900–2000	4.42	4.44	4.41	4.31	4.40	3.69	4.13	4.26	3.77	3.96	5.55	5.74	5.34	5.62	5.56	5.04	4.55	4.93	5.95	5.12
2000–2100	4.30	4.37	4.33	4.40	4.35	5.05	4.48	4.87	4.66	4.76	5.22	4.85	6.23	5.62	5.48	5.32	5.48	5.36	5.13	5.32
2100–2200	4.29	4.37	4.17	4.14	4.24	4.56	4.30	4.01	4.19	4.26	5.42	5.38	5.30	4.84	5.24	5.47	6.06	5.33	4.60	5.36
2200–2300	4.22	4.24	4.28	4.28	4.25	4.35	4.46	4.30	5.03	4.53	5.31	5.49	5.32	5.66	5.44	4.91	5.31	5.18	4.20	4.90
2300–2400	4.19	4.05	4.30	4.21	4.19	3.70	3.56	4.76	4.78	4.20	5.26	5.03	5.43	5.15	5.22	5.49	4.56	4.49	5.34	4.97
0000–0100	4.25	4.49	4.38	4.38	4.38	5.54	3.92	3.98	4.51	4.49	5.03	5.95	5.42	5.34	5.44	4.82	5.55	4.79	5.74	5.22
0100–0200	4.33	4.32	4.29	4.19	4.28	5.06	4.22	4.15	4.36	4.45	5.30	5.46	5.79	5.40	5.49	5.33	4.73	4.37	3.87	4.57
0200–0300	4.21	4.42	4.49	4.35	4.37	4.08	3.74	4.39	3.56	3.94	4.79	5.44	5.53	5.54	5.32	4.53	3.80	4.60	5.63	4.64
0300–0400	4.44	4.48	4.33	4.29	4.38	4.11	5.25	3.90	4.17	4.36	5.71	5.49	5.41	5.55	5.54	5.21	4.71	4.98	4.54	4.86
0400–0500	4.49	4.37	4.39	4.41	4.42	5.44	5.09	5.40	4.05	5.00	5.67	5.01	5.36	5.12	5.29	4.32	5.68	4.87	5.56	5.11
0500–0600	4.48	4.67	4.79	4.70	4.66	4.18	4.62	3.87	4.29	4.24	5.86	5.68	5.94	6.34	5.95	5.43	6.46	5.69	5.05	5.66
0600–0700	4.89	4.79	4.77	4.86	4.83	5.66	5.15	3.95	4.72	4.87	6.13	6.00	5.80	6.06	6.00	4.52	5.49	5.05	6.62	5.42
0700–0800	4.84	4.92	4.87	5.01	4.91	3.95	4.48	3.96	4.67	4.27	5.73	6.44	5.78	5.63	5.90	5.55	5.53	5.83	6.56	5.87
0800–0900	5.04	4.82	4.75	4.92	4.88	5.66	4.08	4.86	5.05	4.91	6.38	5.63	5.72	6.21	5.99	5.67	5.92	6.32	5.61	5.88
0900–1000	4.96	4.86	4.85	4.93	4.90	3.49	4.31	5.47	4.13	4.35	6.02	5.93	6.08	6.01	6.01	6.33	5.67	6.19	6.17	6.09
1000–1100	4.96	4.79	4.88	4.83	4.87	3.85	3.92	4.24	4.22	4.06	5.88	5.92	5.56	6.06	5.86	5.82	5.61	5.83	5.35	5.65
1100–1200	4.78	4.71	4.80	4.79	4.77	4.25	4.06	4.23	4.32	4.21	5.91	5.88	5.89	5.94	5.91	4.69	6.14	6.10	5.20	5.53

6. IONOSPHERE

HF Doppler Observation Associated with Cosmic Ray Increase of January 24, 1971

by

Minoru Tsutsui and Toru Ogawa
Ionosphere Research Laboratory
Kyoto University, Uji, Kyoto, Japan

From the time dependence of the ground-level cosmic ray and the lack of outstanding geomagnetic activity on January 24-25, 1971, this cosmic ray event is thought to be an F-type increase. An impulsive flare, therefore, is thought to precede the sudden increase of this type cosmic ray event. In general, the most remarkable characteristic of a flare which radiates solar cosmic rays is the fact that it is followed by the IVμ type solar radio burst. It is well known that the IVμ type solar radio burst has a good correlation with sudden ionospheric disturbances (SID's) according to results of various ionospheric observations. HF Doppler observations detect it as a sudden frequency deviation (SFD). So the time relation of these phenomena, i.e., solar flare, solar radio emission, cosmic rays and SFD, is expressed in Figure 1. In this figure, the time of start and maximum phase of the solar flare, the solar radio emission and the neutrons of cosmic rays are the results from the observations of Manila, Toyokawa and Deep River, respectively. The HF Doppler was observed at Uji (Kyoto).

The SFD recorder trace from the spectrogram is shown in Figure 2. This record consists of two frequency signals; one is JJY 5 MHz which is one of the standard radio frequencies in Japan and the other belongs to BPV 10 MHz whose station is at Shanghai. Distances from Uji to JJY and BPV are about 360 and 1400 km, respectively.

The frequency shifts Δf of the received signals are proportional to the time ratio of the increment of electron density ΔN, ($\Delta f \propto [dN/dt]$), to the change in a non-deviative layer. In the present case, there is a good correlation between Δf versus time for the 10 MHz signal which is reflected from the F layer and the time ratio of increasing flux of solar radio emission at 9000 MHz observed at Toyokawa. In the trace of the 5 MHz signal, a similar shape is seen. It is well known that Doppler frequency shifts Δf are inversely proportional to the frequency used f, $\Delta f \propto f^{-1}$, when the refractive index changes in a non-deviative region. Judging from this fact and these two traces, it seems that the present burst affects the region lower than the E layer, which is not the reflecting point but rather the non-deviative region for these two waves. The 5 MHz signal, however, vanished at 2318 UT because of the wave absorption accompanied with the increment of electron density in the D or lower E layer. This lasts until 0045 UT (0945 JST) on January 25. In the trace of 10 MHz signal, the effect of multipass propagation can be seen about 0000 UT (0900 JST) on January 25. It might be thought that this effect is due to the arrival of cosmic rays in the upper ionosphere, but this is unclear.

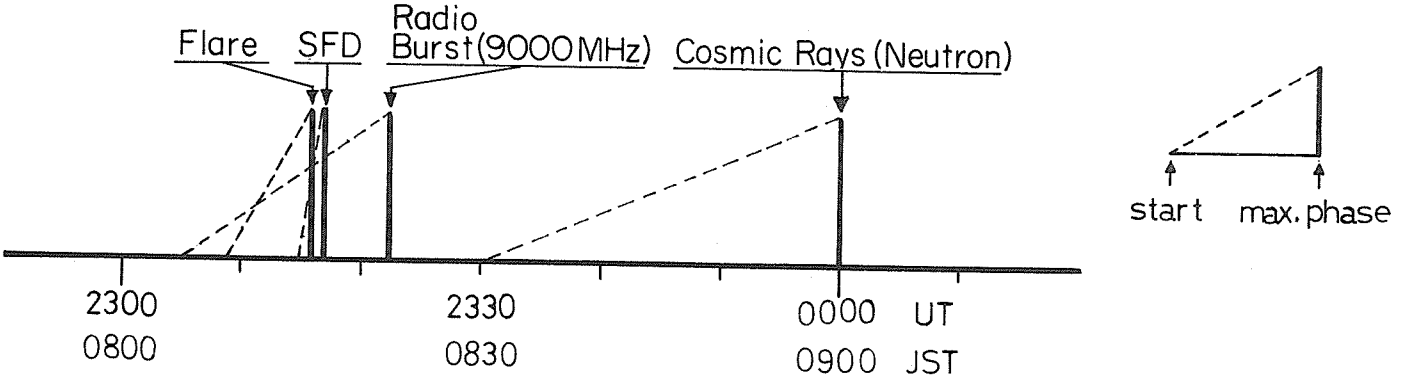

Fig. 1. The time relation of start and maximum phase of solar flare, SFD, solar radio emission and cosmic rays.

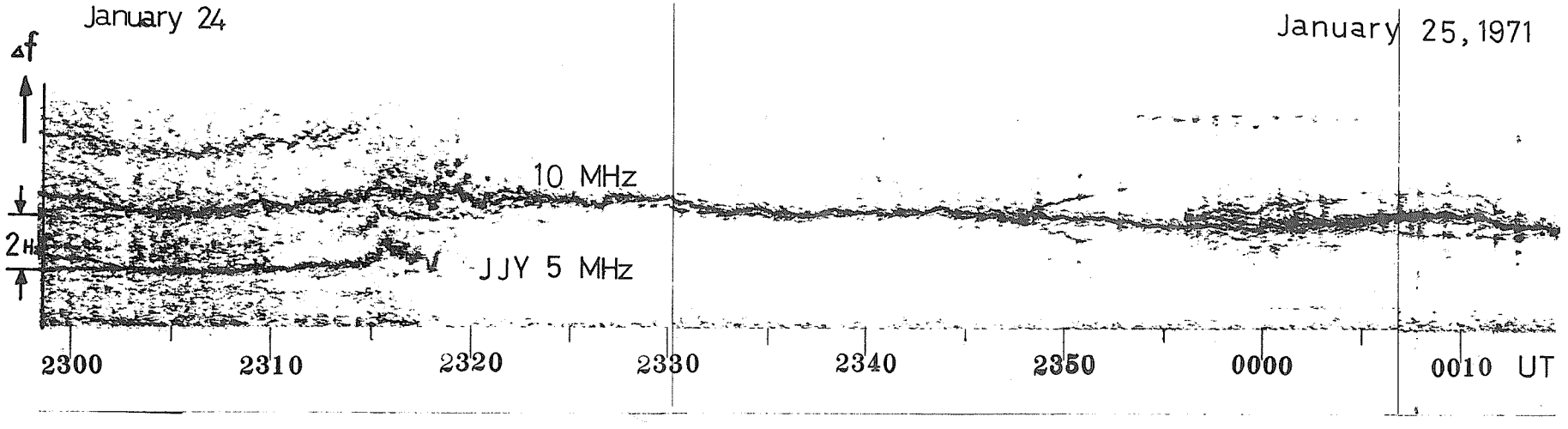

Fig. 2. HF Doppler record associated with cosmic ray increase of January 24-25, 1971.

EFFECTS OF THE JANUARY 1971 SOLAR PARTICLE EVENT ON POLAR VLF PROPAGATION

JOHN P. TURTLE
POLAR ATMOSPHERIC PROCESSES BRANCH
AERONOMY LABORATORY
AIR FORCE CAMBRIDGE RESEARCH LABORATORIES
BEDFORD, MASS. 01730

Measurements of VLF propagation in polar cap regions are made at the AFCRL Geopole Observatory at Thule AB in Greenland as a monitor of D-region particle precipitation disturbances. During the solar particle event on 24 January 1971 two VLF transmitters were being monitored; one was GBR (16.0 kHz) in England and the other was NPG (18.6 kHz) in Washington. These paths are shown in Figure 1.

The effects of the 24 January 1971 particle precipitation event on the amplitude of the signals from the two transmitters are shown in Figure 2. No phase data is presented as the crystal standard used at that time was not stable. No SPA effects were detected on either path as the sun was below the horizon over all of the GBR path and most of the NPG path. Particle precipitation effects first occurred at 2335 UT on 24 January. Amplitude attenuation on the NPG-Thule path reached a maximum of about 14 dB at 1300 UT on 25 January. The attenuation produced by the polar cap disturbance on the GBR-Thule path was much larger than on the NPG path due to the effect of the 900 km of the Greenland ice cap which the signal crosses. Because of the attenuation the GBR signal was lost until 29 January. The maximum attenuation on this path must have been more than 30 dB. The signals did not return to normal levels until 2 February 1971. The discontinuities in the data on 30 January and 5 February indicate that there were additional disturbances on these days.

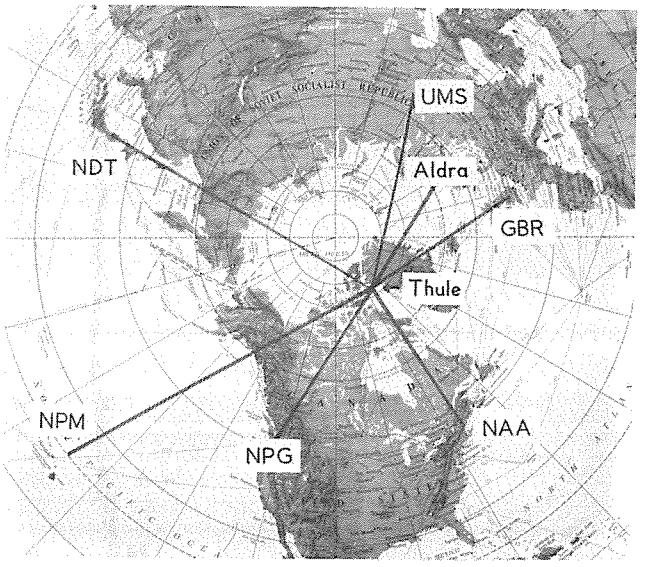

Fig. 1 Polar VLF Propagagation Paths to the Geopole Observatory

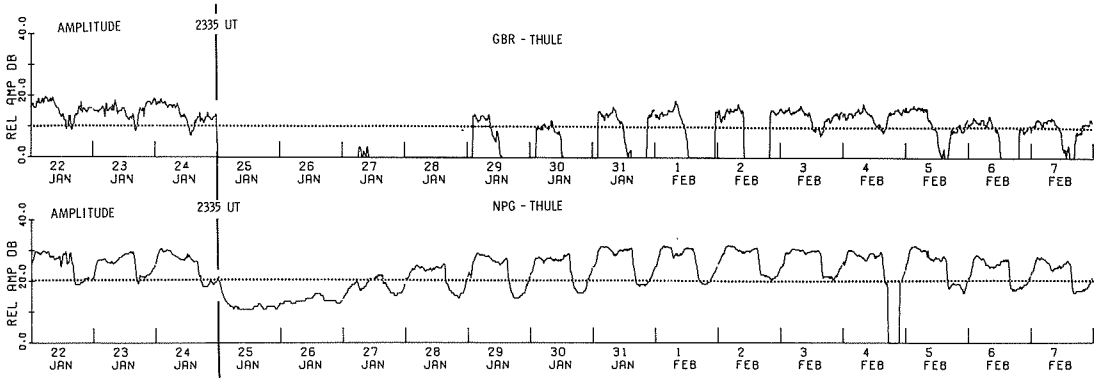

Fig. 2 VLF Amplitude Data for the January 1971 Solar Particle Event
(The dotted line is an arbitrary reference level)

30 MHZ RIOMETER DATA FOR JANUARY 1971 SOLAR PARTICLE EVENT

RAYMOND J. CORMIER
IONOSPHERIC RADIO PHYSICS BRANCH
IONOSPHERIC PHYSICS LABORATORY
AIR FORCE CAMBRDIGE RESEARCH LABORATORIES
BEDFORD, MASS. 01730

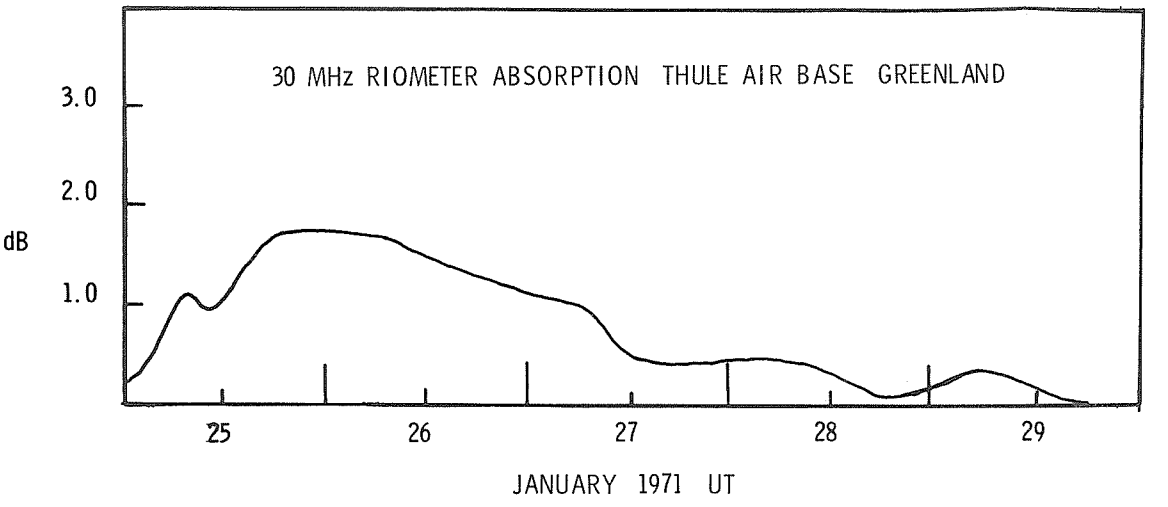

AFCRL Geopole Observatory 30 MHz Riometer Data
for January 1971 Solar Particle Event

Cormier, R. J. 1971 Geophysics & Space Data Bulletin
Vol. VIII; No. 1
AFCRL Bedford, Mass. 01730

The January 1971 Solar Cosmic Ray Event

by

A. J. Masley
Space Sciences Department
McDonnell Douglas Astronautics Company
Huntington Beach, California

Introduction

The McDonnell Douglas Polar Observatories are located at McMurdo Sound, Antarctica (77°51'S, 166°43'E) and at magnetically conjugate Shepherd Bay, N. W. T., Canada (68°49'N, 93°26'W). These stations, at a geomagnetic latitude of 80°, are located inside the polar cap regions, removed poleward from the auroral zones to minimize auroral interference.

Radio techniques are used which allow effects taking place at altitudes from 30 to 90 kilometers to be observed with ground-based equipment. Riometers are operated which measure the signal strength of galactic radio noise at 30 and 50 MHz. The ionization produced by the interaction of the charged particles with the atmosphere increases the electron density so that radio waves passing through the ionosphere are significantly absorbed. The absorption of the radio waves at a given frequency is proportional to the square root of the intensity of charged particles. This technique is sensitive to protons from about 5 to 100 Mev. Other equipment operating at the stations includes magnetometers and photometers at 3914 Å and 5577 Å.

January 24, 1971 Event

McMurdo 30 MHz riometer absorption began to increase at 2352 UT January 24 after about 30 minutes of radio noise at 30 and 50 MHz. The entire event was observed in continuous daylight at McMurdo (See Figure 1). The absorption increased to 8.5 dB at 0600 UT January 25. The absorption varied near this level for 24 hours reaching a maximum of 11.8 dB at 1800 UT January 25. The ionosphere at Shepherd Bay was illuminated down to 30 km for 8 hours each day. The maximum absorption observed during sunlight periods was 6 dB at 2000 UT January 25. The event gradually decreased to background on January 30.

Acknowledgement

This work was supported by the Polar Programs Office of the National Science Foundation under Contract NSF-C393 and the McDonnell Douglas Independent Research and Development Program.

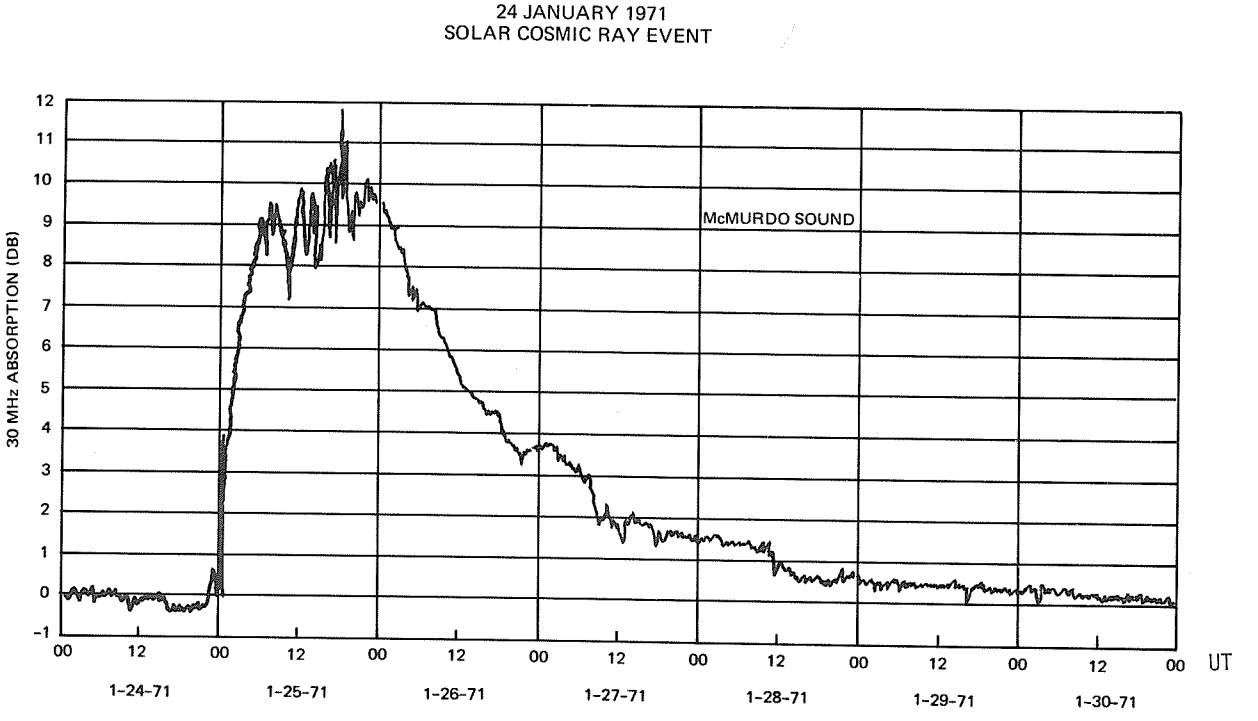

Fig. 1. 30 MHz riometer absorption data for McMurdo Sound, January 24-30, 1971.

Riometer Observation of the Solar Cosmic Ray Event of January 25, 1971

by

William M. Retallack, Warner L. Ecklund and Herbert H. Sauer
NOAA-Environmental Research Laboratories

This laboratory has for several years operated riometer observing sites on the Antarctic Continent with the support of the National Science Foundation. The data reported herein were obtained at frequencies of 29.85 MHz and 50.0 MHz, from sites at South Pole, Byrd Station, and Vostok. The data from Vostok is obtained through a cooperative program administered by the Arctic and Antarctic Institute, Leningrad. The geographic coordinates and approximate L-values of these observing sites are tabulated below.

TABLE I

Station Name	Geographic Coordinates		L
	Latitude	Longitude East	
Byrd	-80.02	240.47	7.23
South Pole	-90.00	-	14.02
Vostok	-78.27	-106.5	>45.

The riometer observations for this period are shown in Figure 1. During this period solar protons were observed by several satellites (as reported in "Solar-Geophysical Data") to arrive in the vicinity of the earth and were detected by several ground-based sensors. Details of these observations will undoubtedly be represented elsewhere in this publication.

As will be seen from the figures, the event as observed by riometer represents a fairly "classical" case of PCA, although the first day shows considerable structure. During this period, the observing sites were continuously illuminated and the profiles do not, therefore, exhibit the characteristic day-night effect of PCA.

The data from Vostok indicates that the first measurable PCA occurred late on 24 January consistent with the direct particle observation by ATS-1, although Byrd and South Pole did not respond until several hours later.

REFERENCES

Solar-Geophysical Data, Number 318, Part I, "Prompt Reports", February 1971, U. S. Department of Commerce, (Boulder, Colo., U.S.A. 80302)

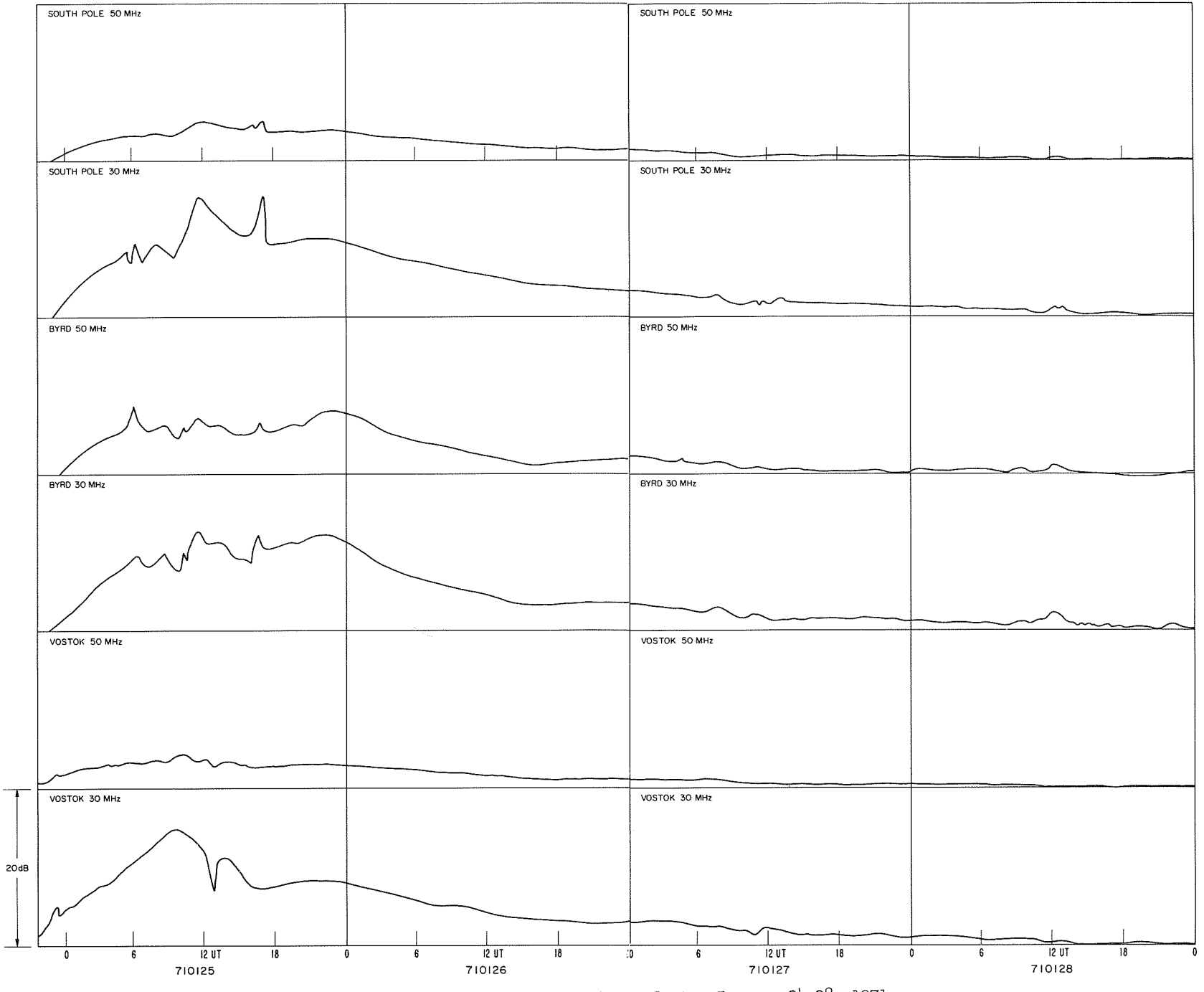

Fig. 1. Riometer observations during January 24-28, 1971.

Polar Cap Absorption of January 24, 1971 by Riometer Data in the Arctic and Antarctic

by

V. M. Driatsky and V. A. Ulyev
The Arctic and Antarctic Research Institute
Leningrad, USSR

The present study is concerned with one of two strongest Polar Cap Absorption events recorded in 1971. PCA data were obtained by riometers installed at the Soviet Arctic and Antarctic stations. Table 1 presents the station list, their geographical positions, invariant latitudes and the Sun's altitudes.

Table 1

STATION LIST

	Station name	Geographic positions		Φ'	Sun's altitude 26 January 1971		Notes
		latitude	longitude		noon	midnight	
1.	North Pole 19	80°38'N	143°22'E	73.4°N	- 9°26'	-28°10'	Positions for Jan. 26, 1971
2.	Heiss Island	80 37	58 03	73.8	- 9 25	-28 11	
3.	Cape Zhelaniya	76 57	68 35	70.3	- 5 47	-31 49	
4.	Dixon Island	73 30	80 14	67.2	- 2 18	-35 18	
5.	Amderma	69 46	61 41	63.9	+ 1 26	-39 02	
6.	Salekhard	66 32	66 32	61.0	+ 4 36	-42 12	
7.	Vostok Station	78°27'S	106 52	84.3°S	+30 20	+ 7 16	Data received by radio
8.	Mirny	66 33	92 01	76.8	+42 15	- 4 39	-"- -"-
9.	Molodezhnaya	67 10	45 51	67.6	+41 38	- 4 02	-"- -"-

NOTES: Riometer frequencies: Vostok St. - 30 and 50 MHz, Mirny - 31.8 and 40 MHz, other stations had riometers at 32 MHz.
Antennas at Vostok station are cophasal directed to zenith; at other stations antennas are of Yagi directed to North Pole.

Polar Cap Absorption, 24-29 January 1971

This event seems to be associated with a solar flare of importance 2B, recorded on 24 January at 2314-2332 UT on the western side of the solar disk (N19 W49) [Solar-Geophysical Data No. 318].

Explorer-41 observed the enhancement of a proton flux which started at 0000 UT, 24 January. The proton flux with energies Ep >10 Mev reached maximum F = 1171 $cm^{-2}sec^{-1}sterad^{-1}$ at 1300 UT, 25 January [Solar-Geophysical Data No. 328]. Figure 1 shows PCA intensity variations by the data of 9 riometers. All these data are divided into three groups.

The first group covers the data of North Pole-19 Station (NP-19) and Heiss Island Station. Both these stations are situated in the area of the polar night. The ionized region in the lower ionosphere responsible for the PCA was not lit by the solar rays at these stations. The absorption started to increase at about 0000 UT, 25 January, reaching its maximum value (approximately 2 dB) by the end of the day. On 29 January the absorption actually died out.

The second group covers a number of stations. They are Cape Zhelaniya, Dixon Island, Amderma, Mirny, Molodezhnaya. These stations experienced varying degrees of day and night. This is most pronounced at Mirny. At Cape Zhelaniya and Dixon Island where in January there is still a polar night and where for a half of the day the sun's altitudes are negative (approximately - 5° and -2°, respectively), the increase of the absorption was registered at local noon.

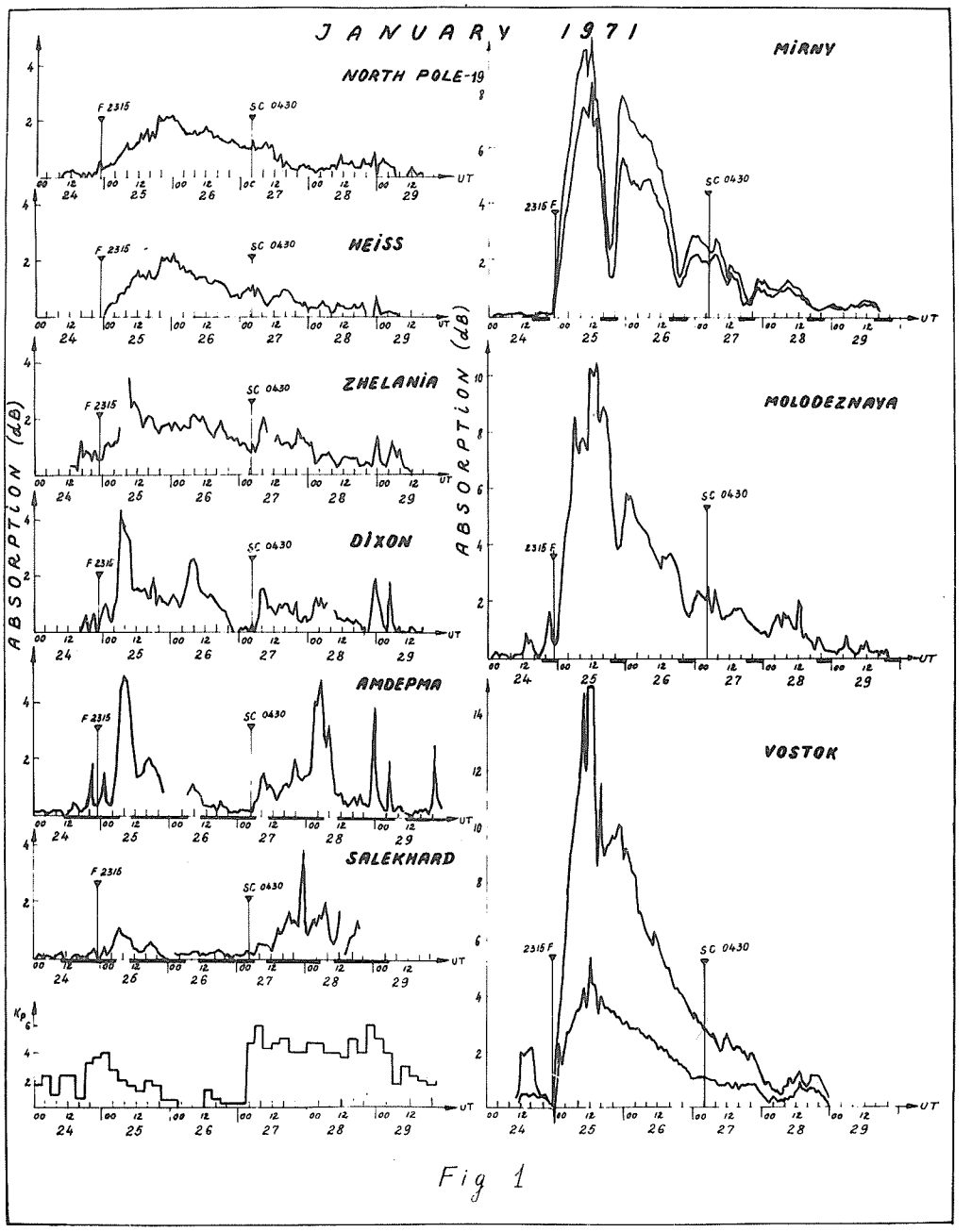

Fig 1

Fig. 1. Variations of PCA intensity and Kp geomagnetic index over the period 24-29 January, 1971.

The variations of Mirny and Molodezhnaya PCA intensity during daytime seem to be attributed to the midday recovery effect.

And finally the third group covers Vostok Station which is in the zone of polar day. The onset of the absorption was at 2322-2356 UT on January 24. It was difficult to establish more exact time of PCA onset owing to the Sun's strong radio emission, recorded by the station riometer at this time. The sun's altitude at midnight was + 7°16', that is conditions were approaching equilibrium [Leinbach et al., 1965]. That is why PCA intensity variations followed the variations of the proton flux density. No day-night effect was observed at this station. The absorption maximum falls on 1230 UT, therefore it coincides with the maximum of the proton flux.

Comparing the PCA data of the first and the third groups assuming the proton fluxes over the Northern Polar Cap and the Southern Polar Cap to be equal [Chivers and Hargreaves, 1965] we can see that the ratio of the daytime absorption to that of the nighttime ranges from 4 to 8.

The geomagnetic disturbance of the sc type was manifested as a short-time (15 minutes) absorption enhancement. The magnetic storm which follows the sc resulted in the decrease of the cutoff rigidity at the edge of the Northern Polar Cap, manifested by the PCA increase at Salekhard, Amderma and Dixon Island.

REFERENCES

CHIVERS, H. and I. K. HARGREAVES	1965	Planetary and Space Science, 13, 583.
LEINBACH, H., D. VENKATESAN and R. PARTHASARATHY	1965	Planetary and Space Science, 13 1075.
	1971	Solar-Geophysical Data, 318 Part I; 328 Part II, U.S. Department of Commerce, (Boulder, Colorado, U.S.A. 80302).

Ground Based Ionospheric Observations from the Danish Geophysical Observatories in Greenland during the January 24 Event 1971

by

J. Taagholt and V. Neble Jensen
Ionosphere Laboratory
Technical University of Denmark
DK-2800 Lyngby, Denmark

The ionosphere data published below are reduced data based on routine measurements made at the field sites:

Narssarssuaq	(geomagnetic coordinates:	Lat. N 71.4° Long. E 37.1°)
Godhavn	(geomagnetic coordinates:	Lat. N 80.0° Long. E 33.1°)
Thule	(geomagnetic coordinates:	Lat. N 89.1° Long. E 357.5°)

All three observatories, situated on the west coast of Greenland, are run by the Ionosphere Laboratory, a division of the Danish Meteorological Institute. The vertical sounder used at Narssarssuaq is a modified C-3/4, at Godhavn a J-5, and at Thule a C-4.

Additionally, Cosmic Noise Absorption (CNA) data obtained by means of IONLAB-Riometer at 30 MHz are shown from the same observatories as well as from Station Nord (geomagnetic coordinates: Lat. N80.7° Long. E134.5°), Sdr. Strømfjord (geomagnetic coordinates: Lat. N77.6° Long. E34.8°), and Godthaab (geomagnetic coordinates: Lat. N75.0° Long. E29.7°).

The three latter stations are operated for the Ionosphere Laboratory by the Greenland Technical Organization, Telesection.

Due to technical problems, the vertical soundings at Thule are missing for the January event.

The riometer recordings at Station Nord were established in May, 1971, and, therefore, no CNA data exist from Nord for the January event.

January 24 Event

The CNA data (see Figure 1) show a short absorption event starting about 1200 UT on January 24, more pronounced at Narssarssuaq and Godthaab with a maximum of about 2 dB and a duration of about 2-3 hours. At Sdr. Strømfjord and Godhavn the same event is seen, but with less than 1 dB absorption. At Thule no absorption at all is observed. The maximum absorption occurred at 1300 UT, corresponding to 1000 LMT on the f-plot (see Figure 2), where at Narssarssuaq, a pronounced increase in f-min is seen.

Beginning at 0000 UT on January 25 the absorption increased during the next 12 hours very smoothly at the trans-auroral station and very irregularly at Narssarssuaq, situated in the auroral zone. The maximum absorption arrives first at the southern station and about 6 hours later at Thule. The maximum absorption is most pronounced at the southern station, about 9 dB at Narssarssuaq, and about 5 dB at Godhavn, but only 2 dB at Thule. The day-time absorption shows the typical solar radiation effect, especially for January 25, where the absorption during sunlight periods is superimposed on absorption caused by the normal radiation corresponding to the solar angle. The uniformity, especially at the four southern stations, shows that the absorption event covers a great area, but with reference to the Thule data, does not seem to cover the total polar cap as the September event did (see p. 410 of this report).

On January 25 the f-plot shows a "black out" from 0400 UT, although the CNA data do not show higher absorption than during the 1300 UT event the day before. The same feature is seen on January 26, where hours without "black out" correspond to the hours with maximum absorption. This fact can perhaps be explained in that the short event during January 24 caused a very thin absorption layer which did not effect the 5-7 MHz signal from the vertical sounder but caused absorption at the 30 MHz riometer frequency.

January 26 data show again the common effect with stronger absorption during sun-light hours and lower during night hours, but not as pronounced as on January 25. During January 27 the general feature is that the absorption decreases, but auroral absorption seems to have large variations, most pronounced at Narssarssuaq, with the maximum between 0800 and 0900 UT corresponding to the "black out" observed at Narssarssuaq during the same hours (0500 and 0600 LMT).

As seen from the Narssarssuaq data, f-min is as high as 5 to 7 MHz between 1200 to 2100 UT on January 26, corresponding to 1.5 - 3 dB absorption on the 30 MHz riometer data.

On the f-plot January 26 from Narssarssuaq the solid curve represents the monthly median [Olesen and Taagholt, 1968] for foF2 from the same station's 1960 data. (This year is chosen because

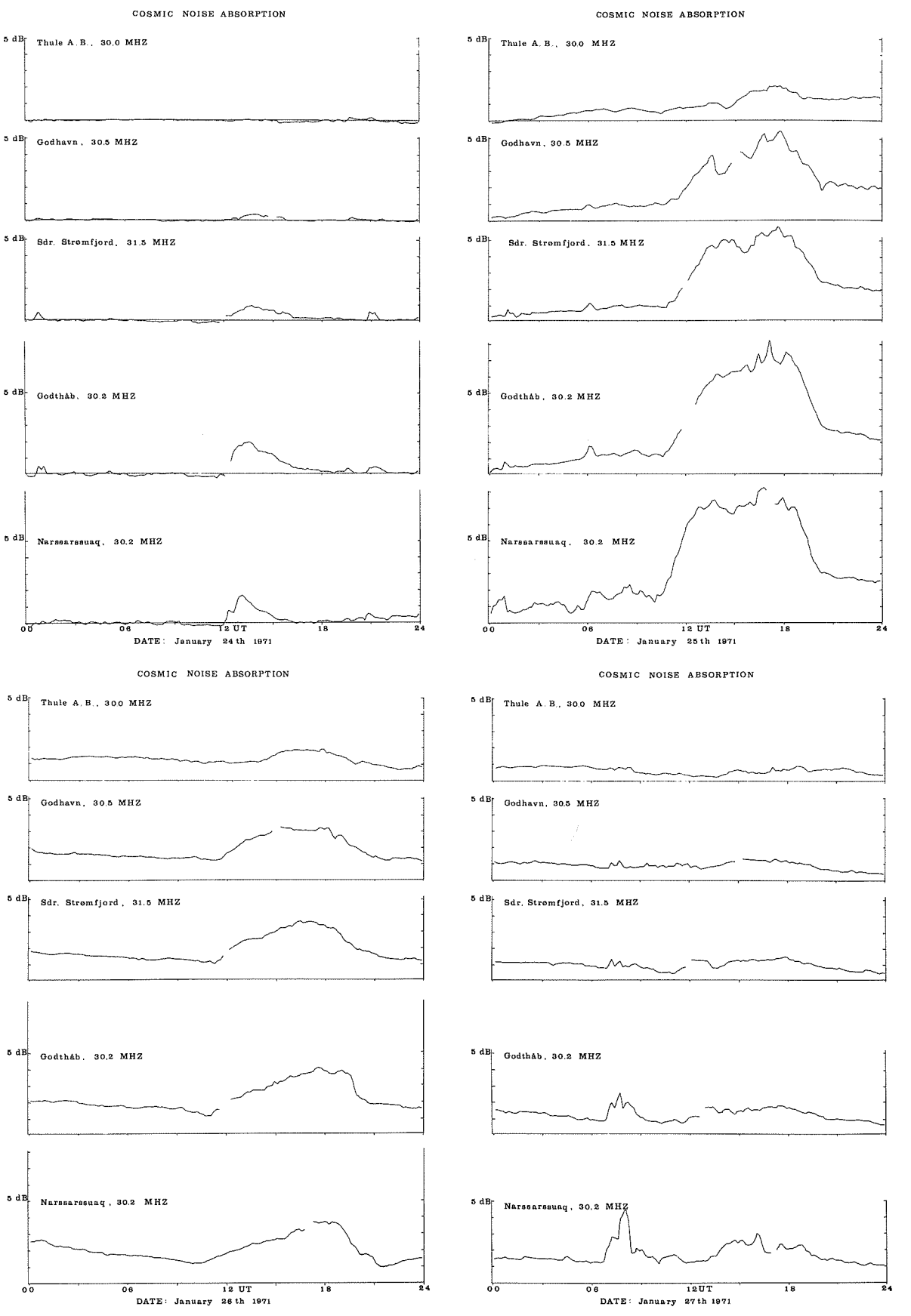

Fig. 1. 30 MHz Riometer data from January event.

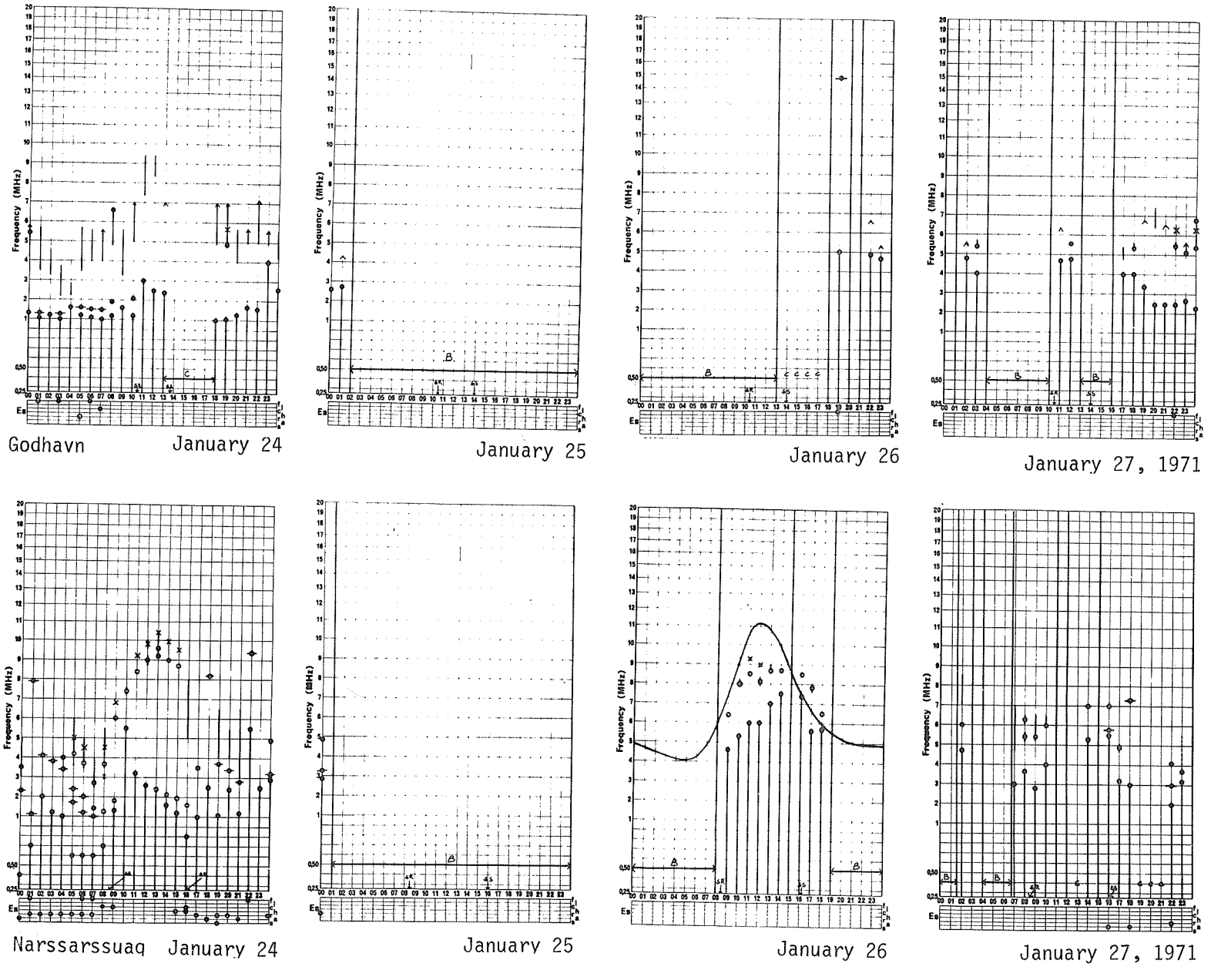

Fig. 2. f-plots from Godhavn and Narssarssuaq for January event. Smooth curve on f-plot January 26 from Narssarssuaq is monthly median foF2 from 1960 data.

it is three years after sunspot maximum, as is 1971).

The data indicate that although the absorption is higher during the day, the critical frequency is observed because the foF2 > fmin only during the day hours.

REFERENCES

OLESEN, J. K. and J. TAAGHOLT 1968 Ionosphere Data 1951-1966 Narssarssuaq and Godhavn, Greenland, IONLAB Report R14, 1-64.

Ionospheric Observations in Kiruna of the PCA Event of 24 January 1971

by

C. Jurén and J. Svennesson
Kiruna Geophysical Observatory
S-981 01 Kiruna 1, Sweden

Introduction

Ionospheric observations from Kiruna which may be related to the outstanding PCA event of January 24, 1971, and the associated geomagnetic event are collected and presented in synoptic Figures. Reproductions of magnetometer and riometer records are given in separate Figures. Ionosonde records from observing stations other than Kiruna have been included in the synoptic Figures to show the latitudinal variations.

The coordinates of the stations are given in the table below:

	Geographic		Corrected geomagnetic[+)]	
	Latitude	Longitude	Latitude	Longitude
Kiruna	67.8°N	20.4°E	64.8°N	104.2°E
Lycksele	64.6	18.7	61.7	100.6
Uppsala	59.8	17.6	56.9	97.1

The riometer records from Kiruna are replaced by records from Down Range Station, ESRANGE, when, for longer periods, the riometer records in Kiruna are highly affected by radio interference. These records are marked with the letters DRS.

The ionosonde data used are from the bulletins published by the Research Institute of National Defense, Stockholm, Sweden.

The geographic coordinates of the transmitters of the VLF signals shown in this data report are as follows: NAA (17.8 kHz) 44.6°N, 67.3°W; NLK (18.6 kHz) 48.2°N, 121.9°W; and HAIKU (13.6 kHz) 21.4°N, 157.8°W.

The PCA Event of 24 January 1971

The particle emitting flare was of importance 1B and occurred in the position N19 W50 with the onset time 2309 UT. The optical flare was associated with observations of an X-ray flare and type IV radio emission. A ground level increase of about 12% at Deep River started about half an hour later (≃ 2340 UT). (The above data are taken from "Solar-Geophysical Data").

The PCA onset was observed in Kiruna at 2347 UT on the VLF NAA (17.8 kHz) - Kiruna signal. The proton event had a maximum on 25 January and declined slowly until normal conditions were reached around 2-3 February 1971. The ionospheric effects observed both by VLF and radio wave absorption were of medium intensity.

A moderately severe magnetic storm started with a sudden commencement on 27 January, 0430 UT and lasted until 29 January. The ionosphere remained moderately disturbed through February 1, 1971.

A general view of the event as observed in Kiruna is shown in Figure 1.

VLF Propagation

The PCA event was observed as a phase advance and an amplitude decrease starting at 2347 UT on 24 January 1971 on the signal of frequency 18.6 kHz from NLK. The onset occurred during a geomagnetically moderately disturbed period when the phase was anomalously low.

A maximum phase advance of ≃ 35 μs and a maximum amplitude decrease of ≃ 15 dB compared to the normal levels were observed before noon on 25 January. No signal was received between 1400 UT and 1800 UT on 25, 26 and 29 January owing to transmitter maintenance. The VLF signal recovery started about 1800 UT on 25 January and the normal phase and amplitude levels were reached around 2 February.

No effect was observed on VLF of the magnetic storm on 27-28 January.

[+)] G. Gustafsson, Arkiv för geofysik, 5, 595, 1970.

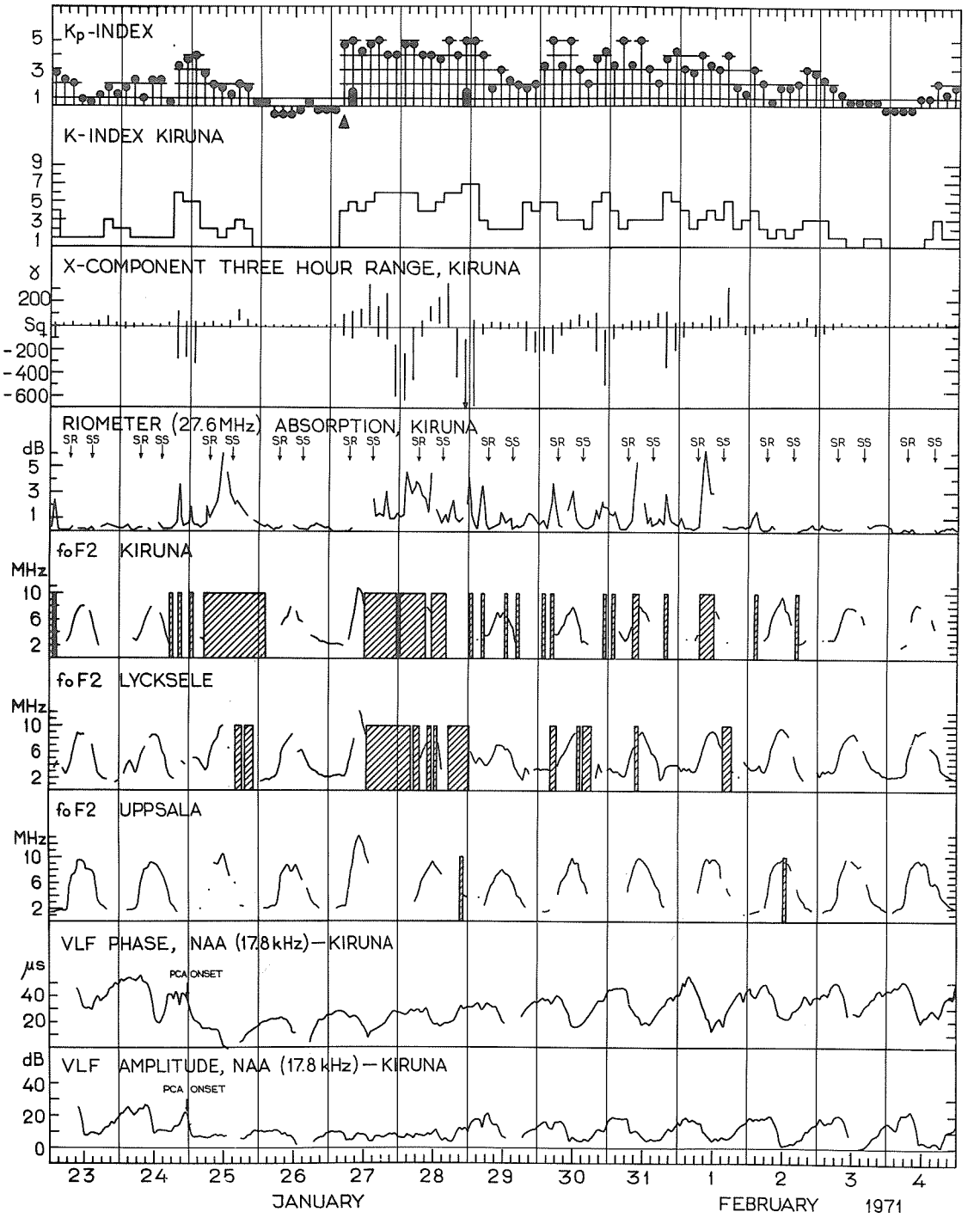

Fig. 1 Survey of ionospheric effects as recorded in Kiruna and nearby observatories. The foF2 plots are presented in the order of decreasing latitude.

The riometer absorption curve shows the maximum absorption during each hour. One-hour values of the critical frequency foF2 have been plotted. The hatched areas indicate periods when the critical frequency was not measured due to black-out, and empty areas correspond to periods when foF2 could not be measured for other reasons. The onset of the PCA is observed on the phase and amplitude records of the VLF signal.

Radio Wave Absorption

The records of cosmic radio noise at 27.6 MHz show some auroral type absorption around midnight on 24-25 January. The common effect of a PCA, i.e. strong absorption during day and weak absorption during night, started around 0600 UT on 25 January and showed a maximum value of absorption of ≃ 6 dB around 1130 UT. However, very little absorption was recorded on January 26.

High values of absorption with large variations (auroral type) were observed from 27 January to 1 February. A smaller superimposed effect of PCA absorption is also observed during the main phase of the geomagnetic storm on 27 and 28 January. A maximum value of ≃ 8 dB was recorded during the magnetic bay ≃ 2230 UT on 28 January. The original riometer records are reproduced in Figure 2.

The absorption is manifested in the plots of the critical frequency of the F2-layer as black-out. A period of continuous black-out was observed in Kiruna between 25 January 0600 UT and 26 January 0300 UT, while only short periods of black-out occurred in Lycksele. The particle precipitation evidently reached further to the south after the sudden commencement on 27 January, and black-out then occurred more frequently in Lycksele. Black-out was recorded also in Uppsala on 28 January 2200 UT during the peak of geomagnetic activity.

The absorption observations indicate that the PCA effects moved to the north of Kiruna on 26 January after the time of the PCA maximum. The cut-off latitude was lowered after the sc of the magnetic storm and PCA effects were again seen in Kiruna and Lycksele on 27 and 28 January.

Geomagnetic Activity

The PCA onset occurred during a moderately geomagnetically disturbed period around midnight on 24-25 January. After the geomagnetically extremely quiet day of January 26 (Kp sum 2+) a moderate geomagnetic storm started with sc on 27 January 0430 UT. The sudden commencement was followed by pulsations for several hours. A positive magnetic bay in the X-component started around 1230 UT and reached a maximum deflection of +340 γ from the Sq curve around 1345 UT. The positive bay changed into negative deflection around 1800 UT. At 2258 UT the X-component was deflected -600 γ and the Z-component +320 γ from the Sq curve. This indicates that the main activity occurred to the south of Kiruna.

The strongest geomagnetic disturbance was observed in Kiruna between 2200 and 2300 UT on 28 January. The magnetogram showed maximum deflections from the Sq curve of -830 γ for the X-component and +400 γ for the Z-component. The Y-component varied between large positive and negative deflections. It is concluded also in this case that the main activity occurred to the south of Kiruna which is also confirmed by ionosonde observations. During the following nights the magnetic activity in Kiruna was moderate (see Figure 1). Reproductions of the original Kiruna magnetograms are shown in Figure 3.

KIRUNA, VERTICAL RIOMETER 27.6 MHz
1970

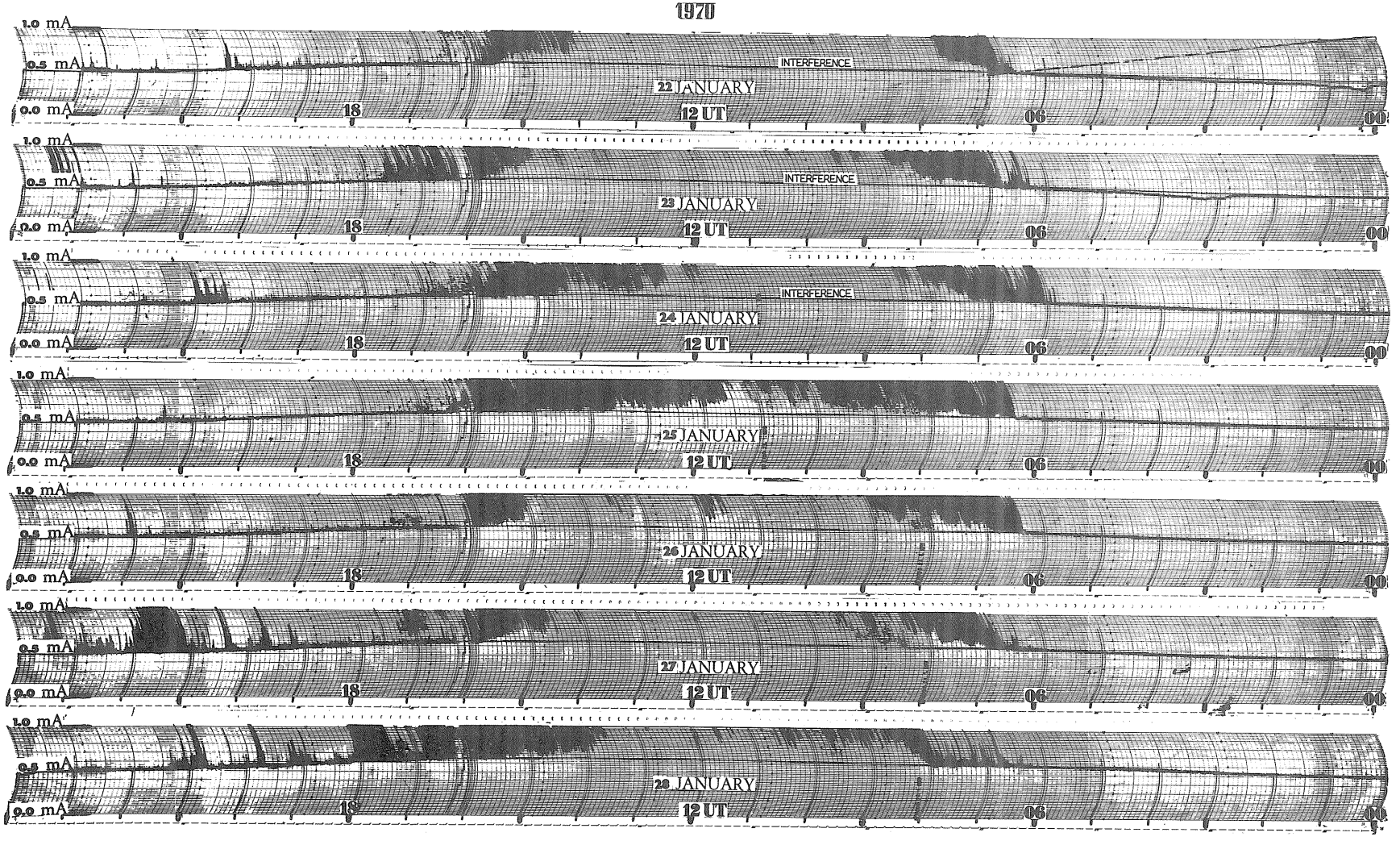

2a

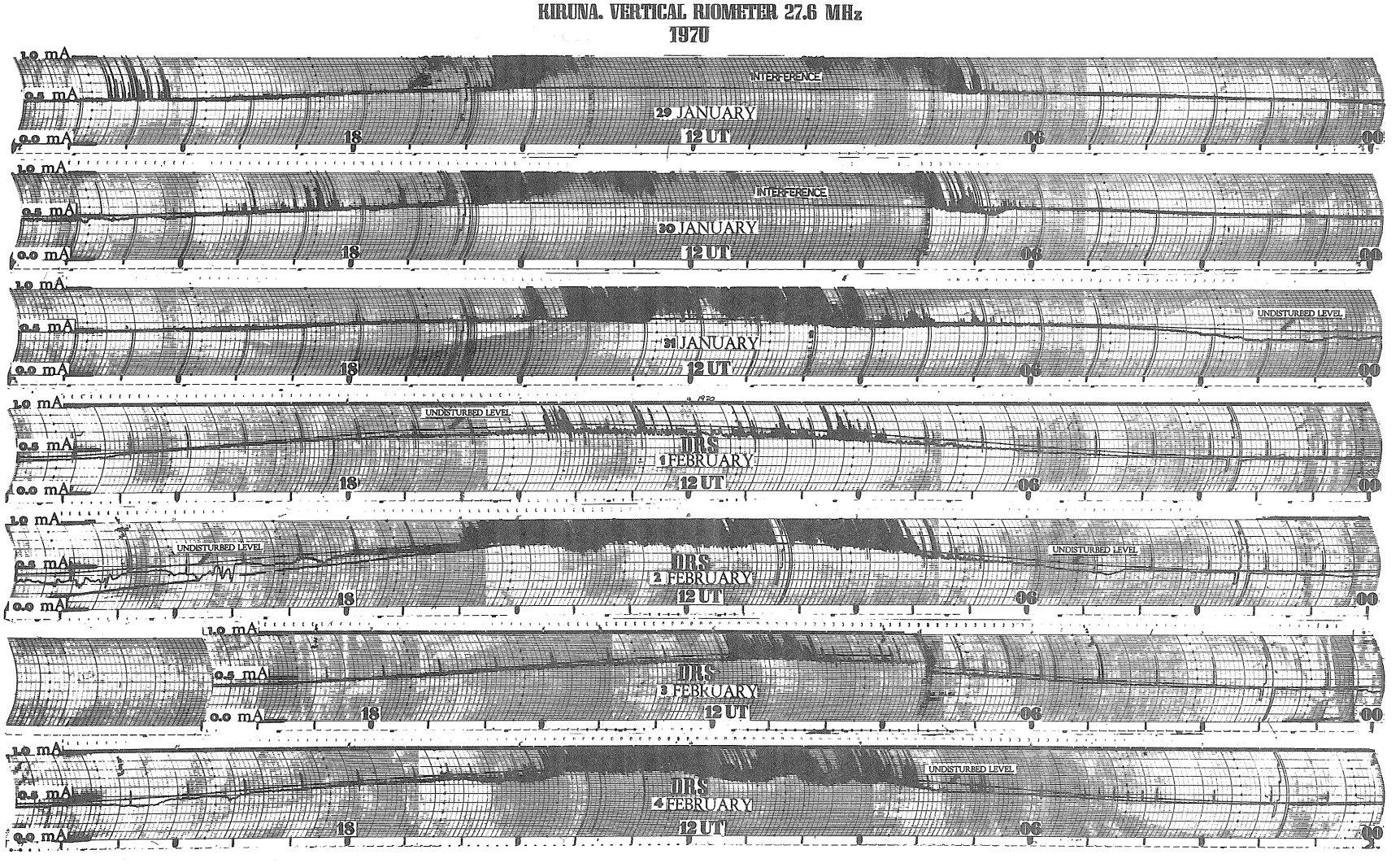

2b

Fig. 2 Riometer records from Kiruna 27.6 MHz receiver. In case of severe interference in Kiruna, the less disturbed records of the Down Range Station (DRS) at ESRANGE, (27.6 MHz), have replaced the Kiruna records. The reproductions are extracted from "Kiruna Geophysical Data".

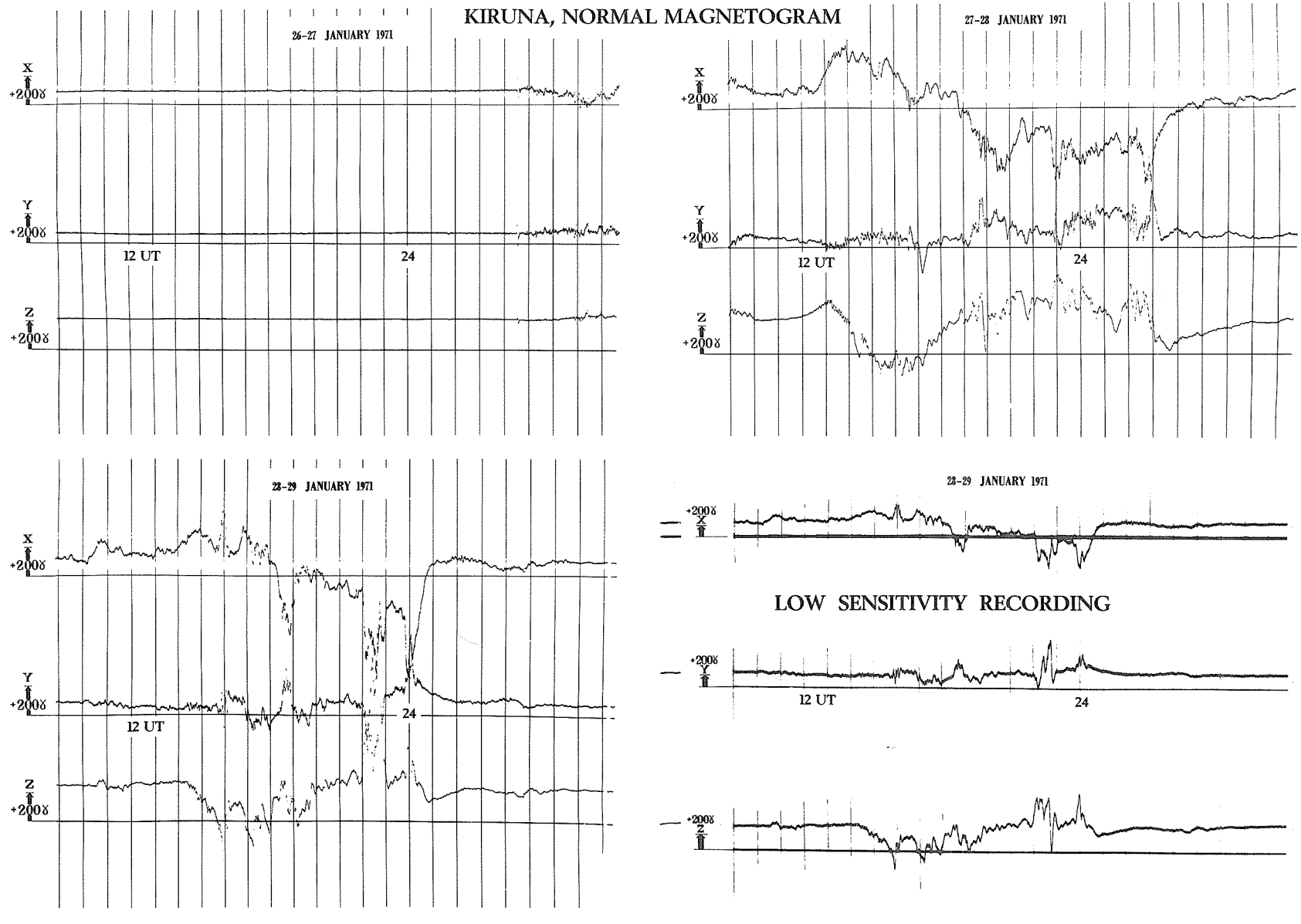
KIRUNA, NORMAL MAGNETOGRAM
26-27 JANUARY 1971
27-28 JANUARY 1971
28-29 JANUARY 1971
28-29 JANUARY 1971
X
Y
Z
+200γ
12 UT
24
LOW SENSITIVITY RECORDING

3a

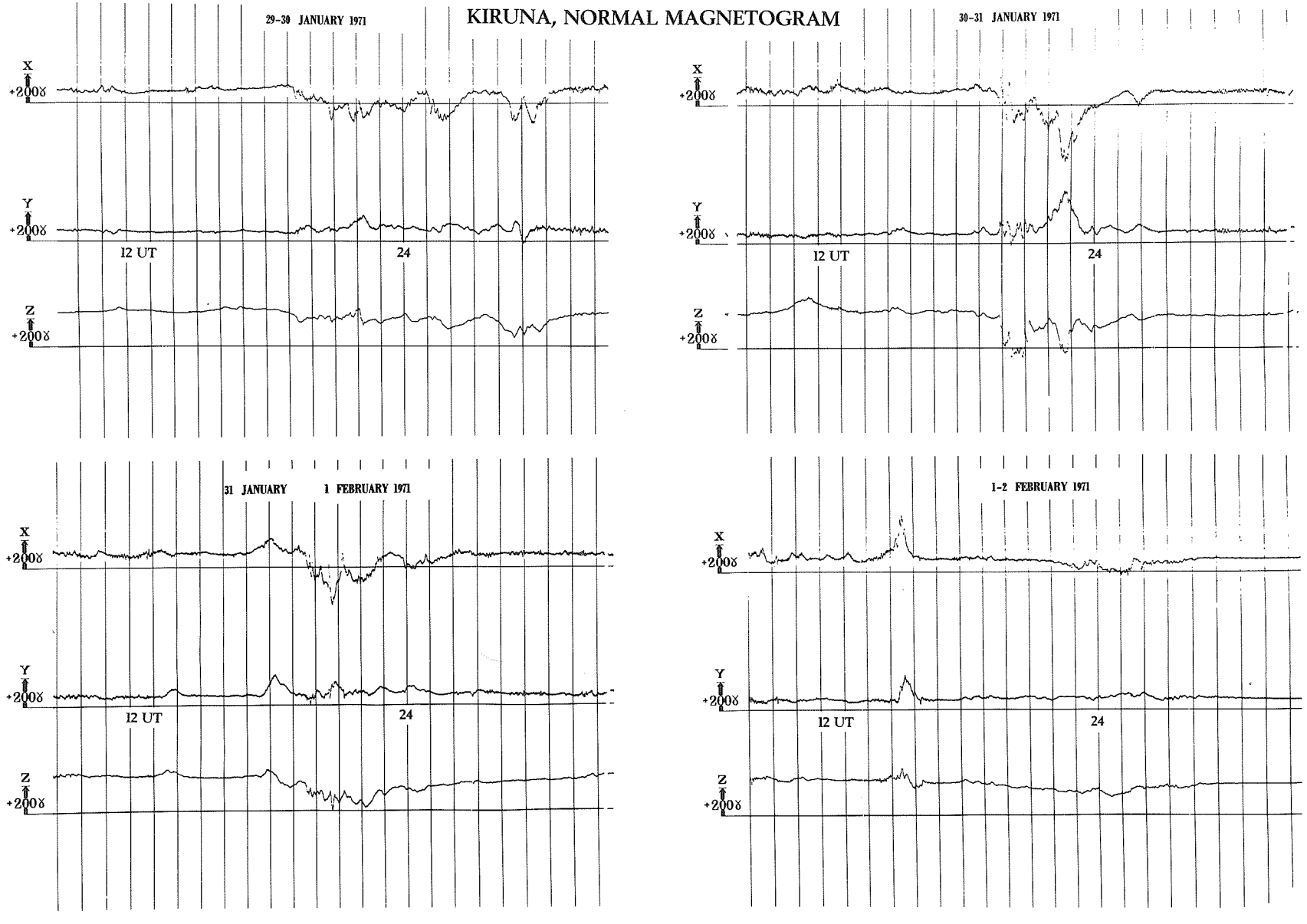

3b

Fig. 3 Kiruna normal magnetograms. For the most disturbed period, 28-29 January, the record of a low sensitive magnetometer is added to the normal magnetograms.

Report on Ionospheric and Whistler Activity at the Panská Ves and Průhonice Observatories on January 24, 1971

by

P. Triska, F. Jiricek and J. Lastovicka
Geophysical Institute
Czechoslovak Academy of Sciences
Prague, Czechoslovakia

The ionospheric measurements made at the Panská Ves (50°32'N, 14°34'E) and Průhonice (49°59'N, 14°33'E) Observatories during the proton flare event of January 24, 1971 were not very fruitful. The ionosonde at Průhonice was not functioning. The main part of this event accompanied by an X-ray burst occurred at night. In the morning on January 25 the SID-monitoring records no longer exhibited any flare influence nor any irregular or unusual phenomena. Usable and reliable data were obtained only from absorption (A3; LF and HF) and whistler measurements.

The HF-absorption measurements show that the day-time absorption on 25, 26 and 27 January was very close to the monthly median values of absorption, i.e., these days were free of the excessive winter absorption. In such a case the LF night-time absorption data can give us direct information about the proton flare influence on the lower ionosphere. The general night-time absorption characteristics for both measuring paths (272 kHz - reflection point 49°34'N, 16°03'E; 185 kHz - reflection point 51°09'N, 14°06'E) are given in the following Table:

Night	24/25	25/26	26/27	27/28
272 kHz	small rise after midnight	B_0 1825-2050 UT; normal	normal	normal
185 kHz	normal	normal	normal	increase

A small absorption rise at 272 kHz after midnight 24/25 January is not confirmed by absorption measurements at 185 kHz. The bay-like absorption disturbance (B_0) observed at 272 kHz on 25/26 seems unlikely to be connected with the proton flare event, because it is confirmed neither by our 185 kHz measurements nor by multi-frequency measurements made at Kuhlungsborn [HHI, 1971]. Both these effects are perhaps connected with the period of geomagnetic storminess (ssc - 1930 UT, 24 January according to NOAA [1971] or they are more or less of random origin. An enhancement of absorption on the night of 27/28 January and during the following nights is due to the magnetic storm which started at 0430 UT on January 27. Thus our LF-absorption data lead to the conclusion that the proton flare event of 24 January exhibited no detectable effect in the night-time lower ionosphere above Central Europe.

The VLF observations are made at the Panská Ves Observatory in the frequency range of 0.9 - 12 kHz between 50 - 52 minutes of each hour. According to these observations the VLF activity in the interval of 24 - 27 January was lower than the average activity. Thus it is not possible to follow the variation of the electron-whistlers dispersion during the three days following the proton flare event. The dispersion of about 60 $s^{\frac{1}{2}}$ as observed on January 25 in the afternoon can be considered to be normal according to the statistical results from long term observations at Panská Ves [Jiricek, 1970; Jiricek, 1971]. Only the VLF emission occurring on 25 January 0650 - 0652 UT could be considered as a manifestation of disturbed conditions. It was a relatively weak chorus in the frequency range of 1.5 - 3.5 kHz.

REFERENCES

HEINRICH-HERTZ INSTITUT 1971 HHI Geophys. Data, 22, January 1971, Berlin.

JIRICEK, F. 1970 On the Determination of Propagation Paths of Mid-Latitude Whistlers for Purposes of Estimating the Magnetospheric Electron Density, Studia geoph. geod., 14, 402 - 413.

JIRICEK, F. 1971 Whistler Activity in Central Europe during the Period of Increasing Solar Activity from 1964 to 1968, Trav. Inst. Geophys. Acad. Tchecosl. Sci. 1969, No. 313, 281-289, Academia, Praha.

NOAA 1971 Solar-Geophysical Data, 319 Part I, U.S. Department of Commerce, (Boulder, Colorado, U.S.A. 80302).

The Ionospheric Disturbances over Japan Associated with Solar Flare on January 24 and Geomagnetic Storm from January 27 to February 1, 1971

by

Yugoro Takenoshita
Akita Radio Wave Observatories, Radio Research Laboratories
Akita-Shi, Akita-Ken, Japan

This short note consists of two parts. The first part contains some development of HF wave absorption and of height variation of the D-region in the ionosphere associated with a solar flare on January 24, 1971, and the second part contains traveling ionospheric disturbances from January 27 to February 1, 1971 during geomagnetic disturbed interval.

Field intensities of JJY (2.5 MHz and 5 MHz) have been measured at Akita Radio Wave Observatories. The field intensities of JJY on both frequencies at Akita suddenly decreased lower than threshold at 0809 UT on January 25, 1971 (135° EMT) when a solar flare occurred. The most severe absorption might be more than 30 dB on both frequencies. They returned to measurable level after two hours on 5 MHz and after one and a half hours on 2.5 MHz, and recovered to normal level about seven hours after the event occurred.

TABLE 1

Particulars of the Transmitter and Receiver, JJY (5 MHz and 2.5 MHz)

Transmitters

Location	Koganei, Lat. 35°42'N, Long. 139°31'E
Power	2 kW
Antenna	Vertical, half-wave length
Distance	450 km

Receivers

Location	Akita, Lat. 39°44'N, Long. 140°08'E
Antenna	Vertical, a quarter of a wave length
Bandwidth	750 Hz at 2.5 MHz, 6 kHz at 5 MHz
Calibration	Once a week

Furthermore, the field intensity and phase of a low frequency wave at 40 kHz (JG2AS) transmitted at Kemigawa station were measured at Akita. The phase height of the D-region where an LF wave is reflected can be estimated from the measured phase and field intensity. When the solar flare occurred, the measured phase and field intensity at 40 kHz suddenly changed their values. It was estimated that the phase height of the D-region dropped down more than 20 kilometers. This phase height did not recover to normal height until the intensities of JJY returned to their normal level seven hours after the flare occurred. Figure 1 shows the progress of the JJY intensities and the phase height at 40 kHz.

TABLE 2

Particulars of the Transmitter and Receiver, JG2AS (40 kHz)

Transmitter

Location	Kemigawa, Lat. 35°38'N, Long. 140°04'E
Power	1 kW
Antenna	Vertical, head loading
Distance	450 km

Receiver

Location	Akita, Lat. 39°43'N, Long. 140°08'E
Antenna	Loop
Bandwidth	500 Hz
Calibration	Once a week
Phase Correspondence	4/1000 cycle

After about fifty-three hours from the event, a geomagnetic storm, accompanied with sudden commencement, began at 0430 UT on January 27. This storm did not develop as severely. Besides, the northern hemisphere was in winter at this period, and the ionospheric electron density did not

generally decrease very much. Short-term variations of the electron density in the F-region, however, were observed during this geomagnetic storm. The periods of electron density variation varied from two to four hours. The diurnal variation of foF2 on January 26 was very typical of the very quiet geomagnetic field. After January 26, however, short-term variations were frequently observed in the same manner at all four ionospheric observatories in Japan. If one compares the time of maximum foF2 among the different observatories, it was found that the ionospheric disturbance traveled over Japan. It was, however, sometimes difficult to find correspondence among each time of maximum foF2 at the different observatories, because it seemed that several disturbances were superposed one on the other. Some combinations of times of maximum foF2 at three selected observatories were used to estimate the traveling speed of the disturbances, when the ionospheric disturbances seemed to be isolated from one another. Each estimated speed is shown in Figure 2 at time (UT) corresponding to observation at Akita. Figure 2 shows also geomagnetic activity by means of Kp (geomagnetic planetary index). It is necessary to explain two points. The first point is that each observation was made every quarter of an hour. This sampling speed appears rather slow considering the observatory network. The second point is that the disturbances with speeds of about 350 meters sec^{-1} and 10 meters sec^{-1} are in the same category as T.I.D.s.

Nevertheless, Figure 2 indicates that speeds of T.I.D. followed geomagnetic activity, reaching high speeds when the geomagnetic activity was at a high level.

TABLE 3

Radio Wave Observatories of Ionospheric Observation in Japan

Observatories	Latitude	Longitude	Observatories	Latitude	Longitude
Wakkanai	45°23.6'N	141°41.1'E	Kokubunji	35°42.2'N	139°29.3'E
Akita	39°43.5'N	140°08.2'E	Yamagawa	31°12.1'N	130°37.1'E

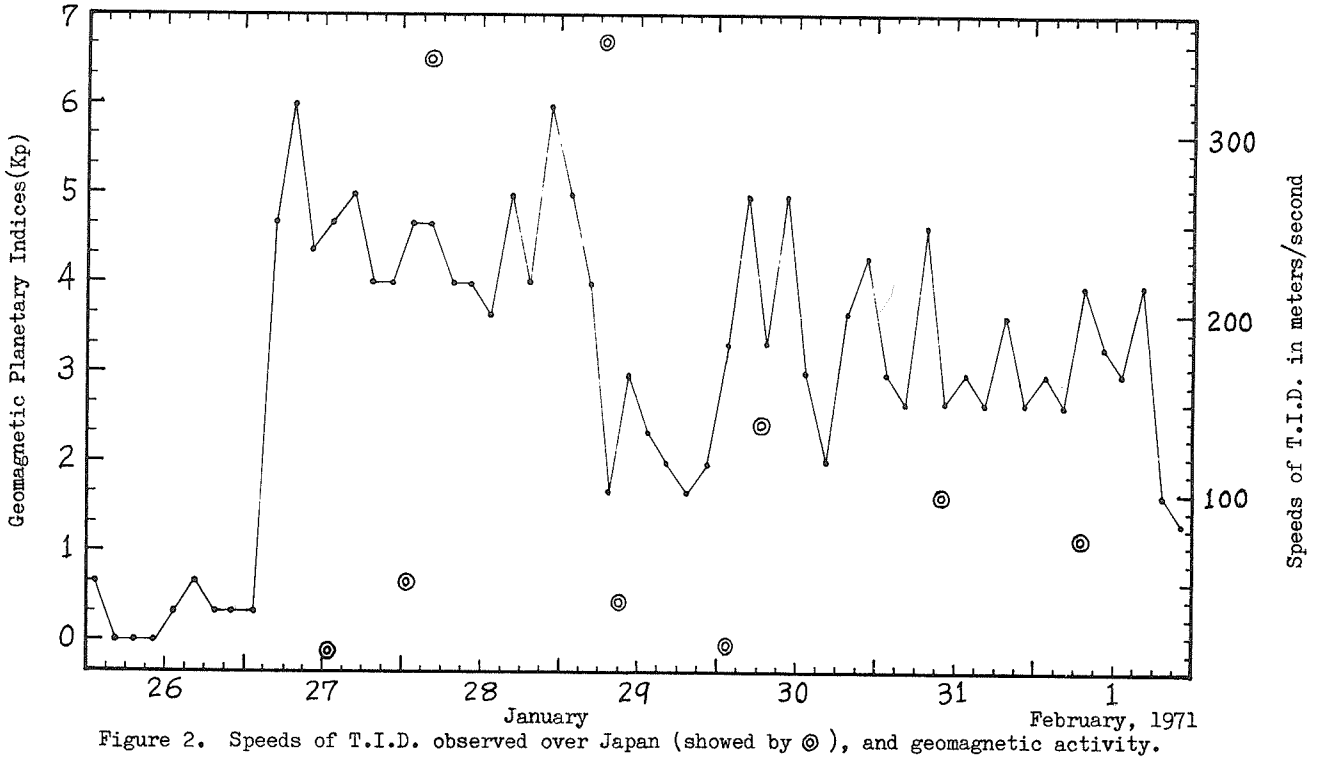

Figure 2. Speeds of T.I.D. observed over Japan (showed by ◎), and geomagnetic activity.

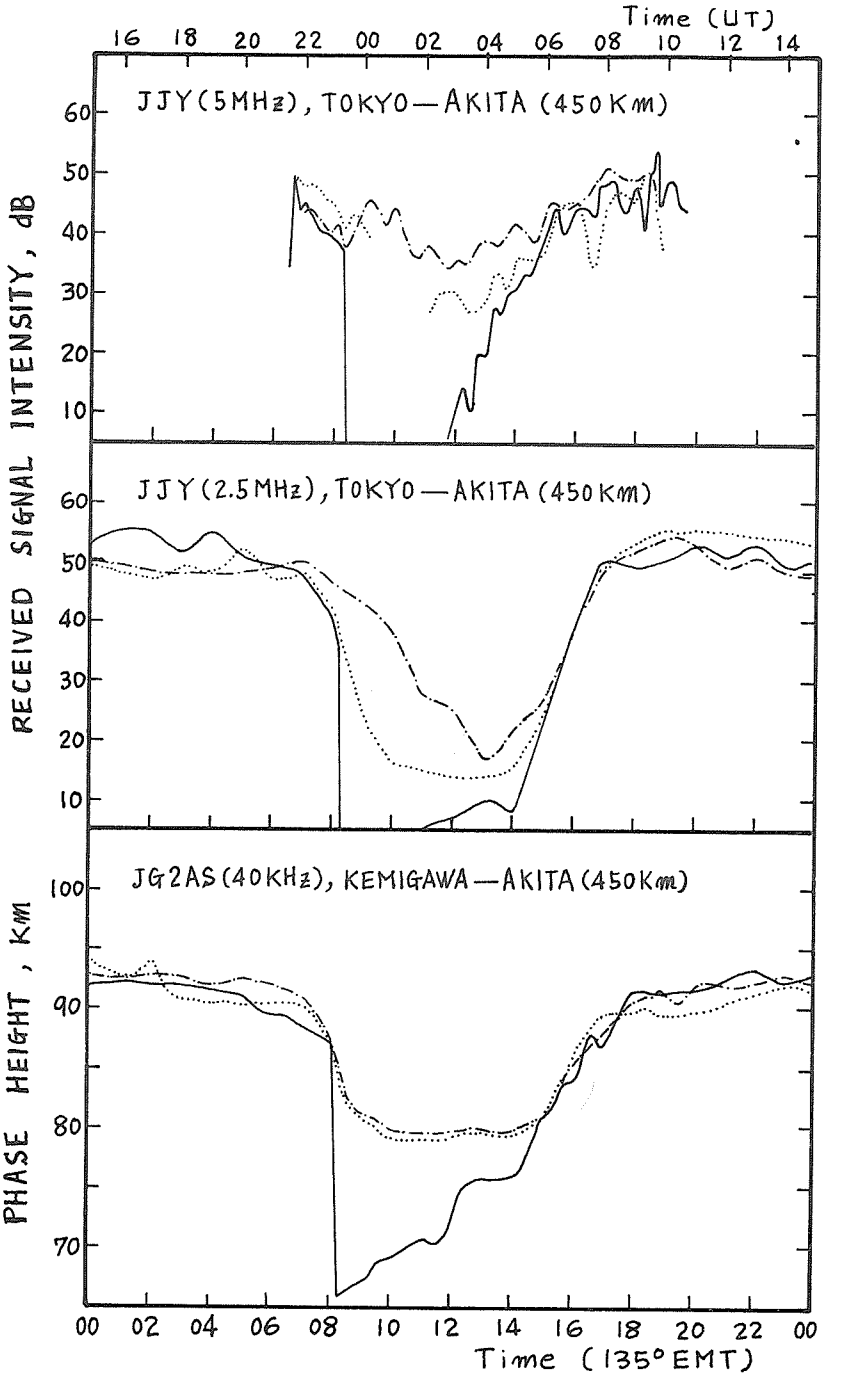

Figure 1. Some of the SIDs associated with a solar flare beginning at 0809 on January 25, 1971 in 135°EMT.
·····: 24, ——: 25, -·-·-: 26 in January, 1971

Lower Ionosphere Affected by Proton Event

by

K. Bibl
Lowell Technological Institute Research Foundation

At the Maynard, Massachusetts, ionospheric station of Air Force Cambridge Research Laboratories, a digital ionosonde has been measuring pulse amplitudes as function of frequency every quarter of an hour since 1 November 1970. Digitally integrated output data are, after recording on magnetic tape, compressed by computer processing and displayed with a special digital font printer as multidimensional patterns of which Figure 1 is an example. The upper boundary of the dark area is the top frequency (mostly fxF2) of the overhead F-region ionization while the lower boundary represents fbEs or fmin respectively.

The readable numbers represent the maximum amplitudes of the echo traces in the height range between 150 and 650 km. Between consecutive numbers lie 5 dB differential absorption on this representation. But on the tapes two additional less significant binary bits are available for inspection. Thus the amplitude resolution is one dB.

Although the absolute calibration of the frequency dependence of the amplitudes was not always maintained over the year, the method is excellent for day-to-day and short-term variation in absorption because it monitors continuously about 100 frequencies.

This outstanding frequency diversity gives the erratically varying amplitude measurements sufficient significance to discover even small changes in absorption. On 24 January 1971 a large increase in absorption due to increase in ionization of the lower ionosphere occurred during the ground proton event long after local sunset. The absorption reached a good fraction of the daytime value. In Figure 2 the difference between the amplitude value at 1815 75° WMT (2315 UT) and the average of the two adjacent quarter-hour measurements has been plotted for every second monitored frequency.

An increase of absorption for this quarter hour by about 12 dB at 2.0 MHz decreasing to 1 dB at 7 MHz is apparent, although the variation around a steadily decreasing frequency-dependent attenuation function is large. This large variation is a normal feature of absorption measurement due to interaction of several modes with almost equal amplitude and delay. In this common case the phase relation of the different modes determine the momentary total amplitude and lead to a high variance in the frequency dependence of the amplitudes.

The strong enhancement in absorption during a short time is certainly surprising. Synoptic studies must be undertaken to determine if protons not following the line of sight are responsible for the ionization of the lower ionosphere or if the atmosphere is penetrated twice in grazing incidence by the high-energetic protons.

In contrast to this relatively short event which made simple analysis possible the ground proton event of 1 September 1971 was by far more extended in time and did not show a clear time pattern of the absorption.

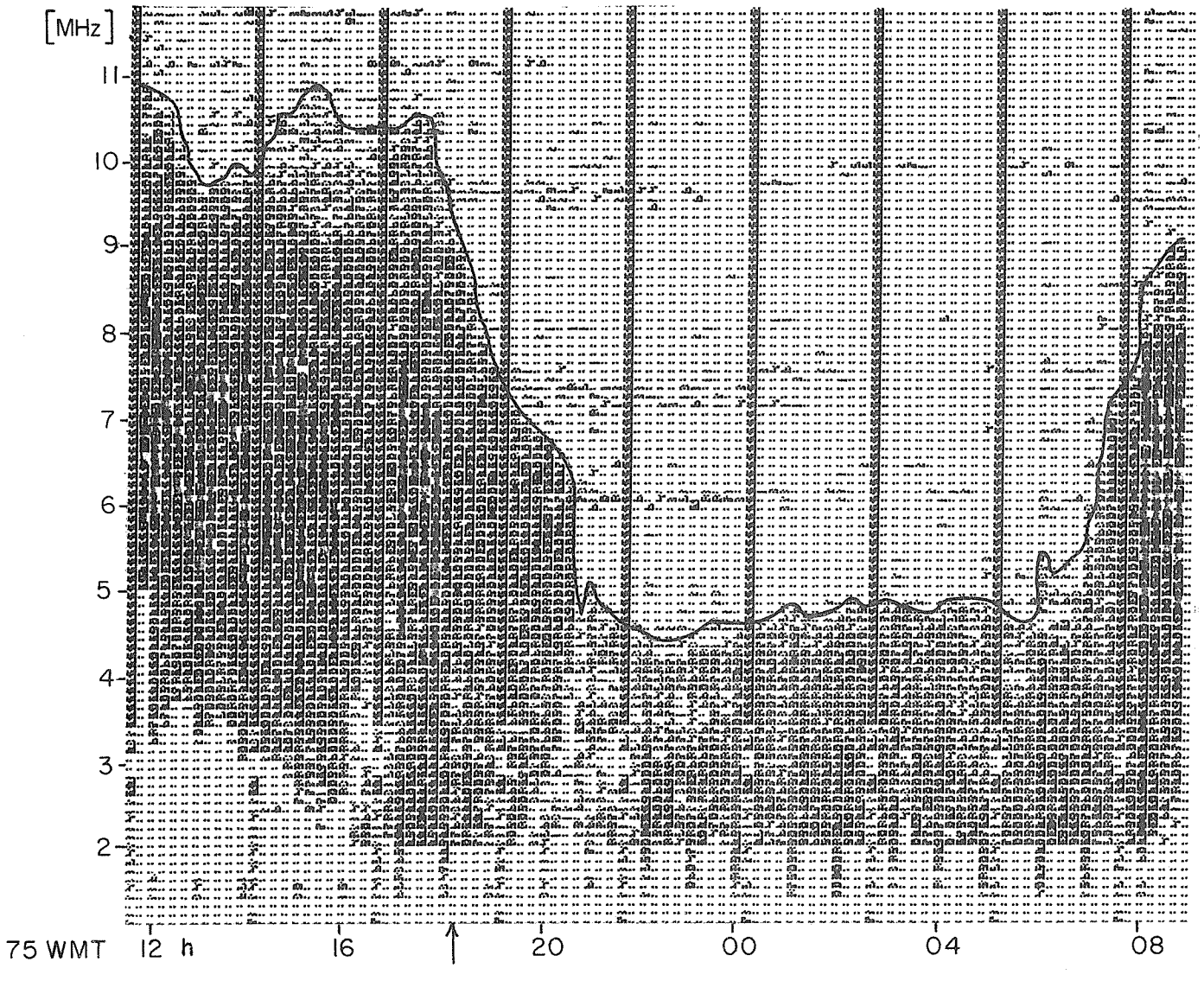

Fig. 1. GROUND PROTON EVENT AT 1809 75 WMT 24 JAN 1971
DIURNAL AMPLITUDES AND f_t(F(T)) AT MAYNARD, MASS.

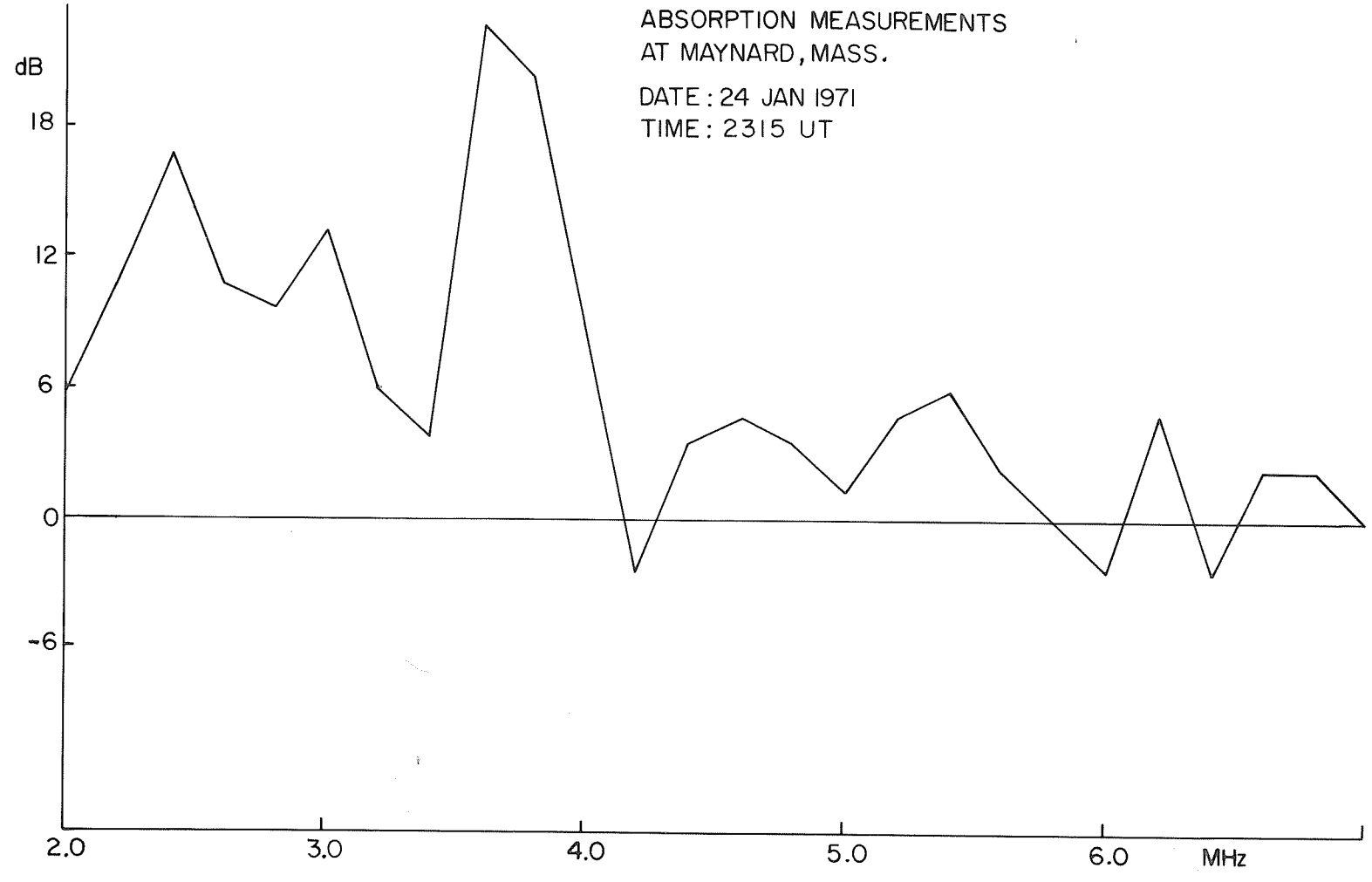

Fig. 2. Difference between the amplitude value at 2315 UT (1815 75°WMT) and the average of the two adjacent quarter-hour measurements for every second monitored frequency.

"Ionospheric Characteristics Associated with the Solar Activity of January 24, 1971 at Manila"

by

J. J. Hennessey, S. J. and Florencio Rafael, Jr.
Manila Observatory
Manila, Philippines

Despite the well known vagaries of the F-region of the ionosphere, ionospheric characteristics generally have a definite dependence on the elevation of the sun. These effects have a regularity in their diurnal pattern which can be disrupted to a greater or less degree by unusual solar activity. The extent of disruption by a solar flare should, in some way, be related to the local time of the event. The solar event of 2309 UT, 24 January 1971 (0709 LT, 25 January 1971 at Manila) occurred about an hour after sunrise. As this flare time corresponds to the start of the diurnal appearance of the regular E-layer and the period of continued increase of the F-layer from its pre-dawn dip, the flare-induced variations at Manila deserve consideration.

Since the F-region was not totally "blacked out" by the effects of the solar radiation on the lower ionospheric regions the ionograms successively provide a description by implication of the changes in the lower regions. Some notable features which appear and claim our attention in the F-region are: a) post-flare variations in foF2; b) recovery of the F-layer; c) restoration of multiple echoes; d) bifurcation; e) hpF2 values. The E-region recovery is also informative of the lower ionosphere regions.

a) Post-flare variations in foF2. Fortunately during a few hours after this event ionograms were taken at five-minute rather than the usual fifteen-minute intervals. For comparison of critical frequency F2 variations, the medians of the corresponding time values of three days before and three days after were taken (See Fig. 1). Just before the start of the flare at 2309 UT there is the expected agreement. The pre-dawn dips are quite comparable though the event day has a slightly lower value occurring fifteen minutes later than the control day values. During the first hour a slight increase in ionization density over that of the median becomes apparent. For example, at 2330 UT the flare day value of this density is greater than the control day median by approximately 26 percent. A rapid increase in the slope of the curve, of critical frequency versus time, is clearly noted. Just prior to the start of the flare, i. e. at 2300 UT, the flare day value is 17 percent greater. By 0000 UT the corresponding density values are close to one another.

Thereafter from 0000 to 0130 UT (25 January) the ionization densities show a definite increase much beyond the corresponding values of any of the control days. There is an evident concentration of additional electrons in the F2-layer. However the diurnal trend is maintained so that from 0130 UT the F2 critical frequencies decrease in value to a low of 9.2 MHz an hour after local noon. A rise in values follows in the next four hours to 12.5 MHz at 0900 UT.

In Summary then, the diurnal F2-layer trend is not greatly disrupted by this early daylight flare. But the ionization density following the start of the flare rises to greater than normal values. The time rate of drop, thereafter, is more rapid at its start from a higher value than those of the control days, and at its end is at a much lower value. (See Fig. 1).

b) Recovery of the F-layer. The most noticeable feature of the ionograms after the start of the flare is twofold: the absence of usual radio noise (this does not affect numerical characteristics) and the high f-min values. At 2332 UT the minimum frequency value for the F-trace was 5.4 MHz taken from the polaroid and at 2337 UT from the film ionogram. (See Fig. 2)

A careful reading of minimum frequency values for the F-region at 5-minute intervals manifests a general but not smooth decrease. At 2355 UT the f-min was 5.6 MHz, i. e. 0.6 MHz greater than the f-min on the previous record. By 25/0215 UT with the appearance of the definite E-layer the f-min, now being in the E-region, further decreases. By 0645 UT the f-min values have decreased to frequencies comparable with those of the control days.

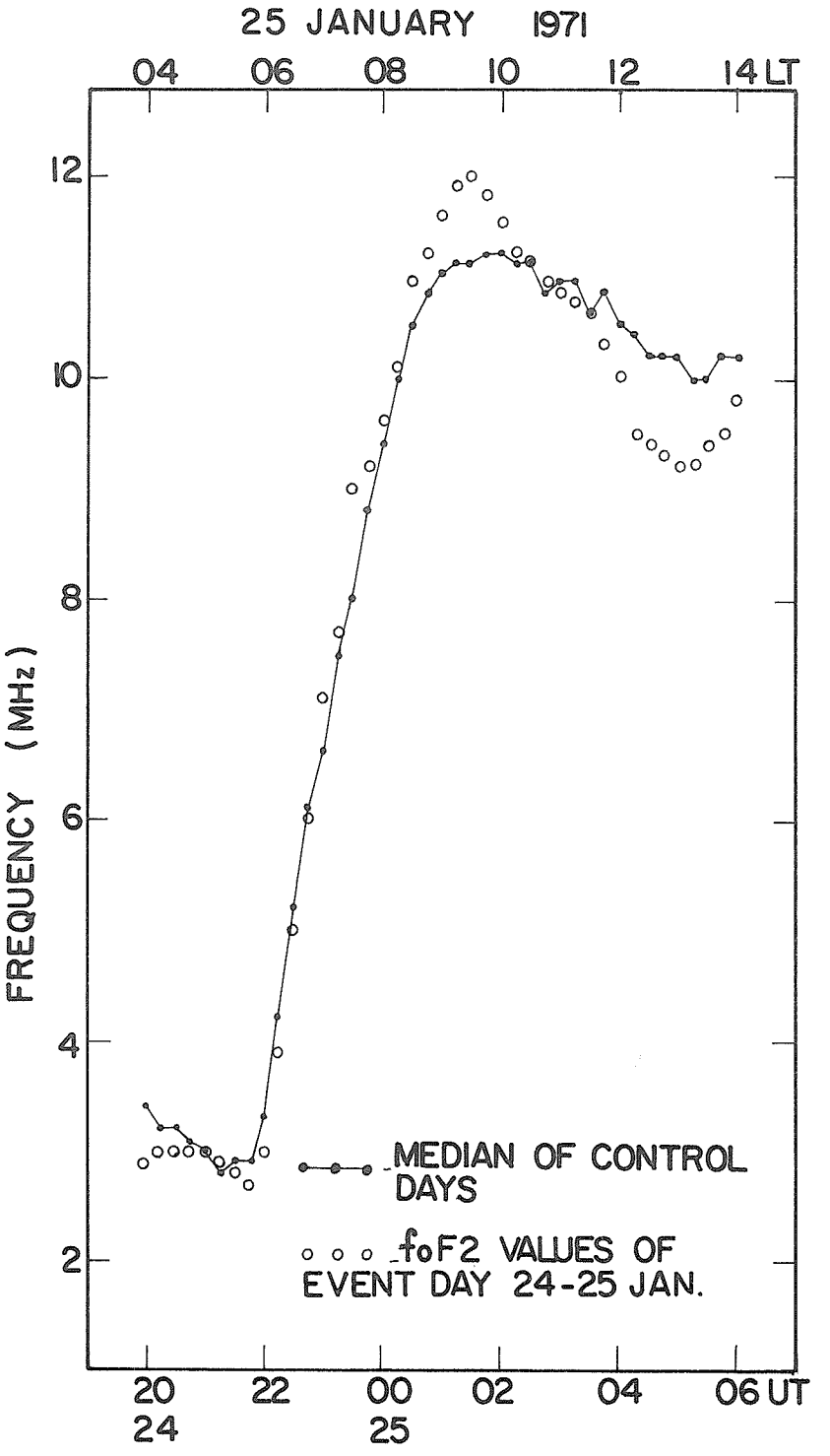

FIG. 1. foF2 vs median of control days.

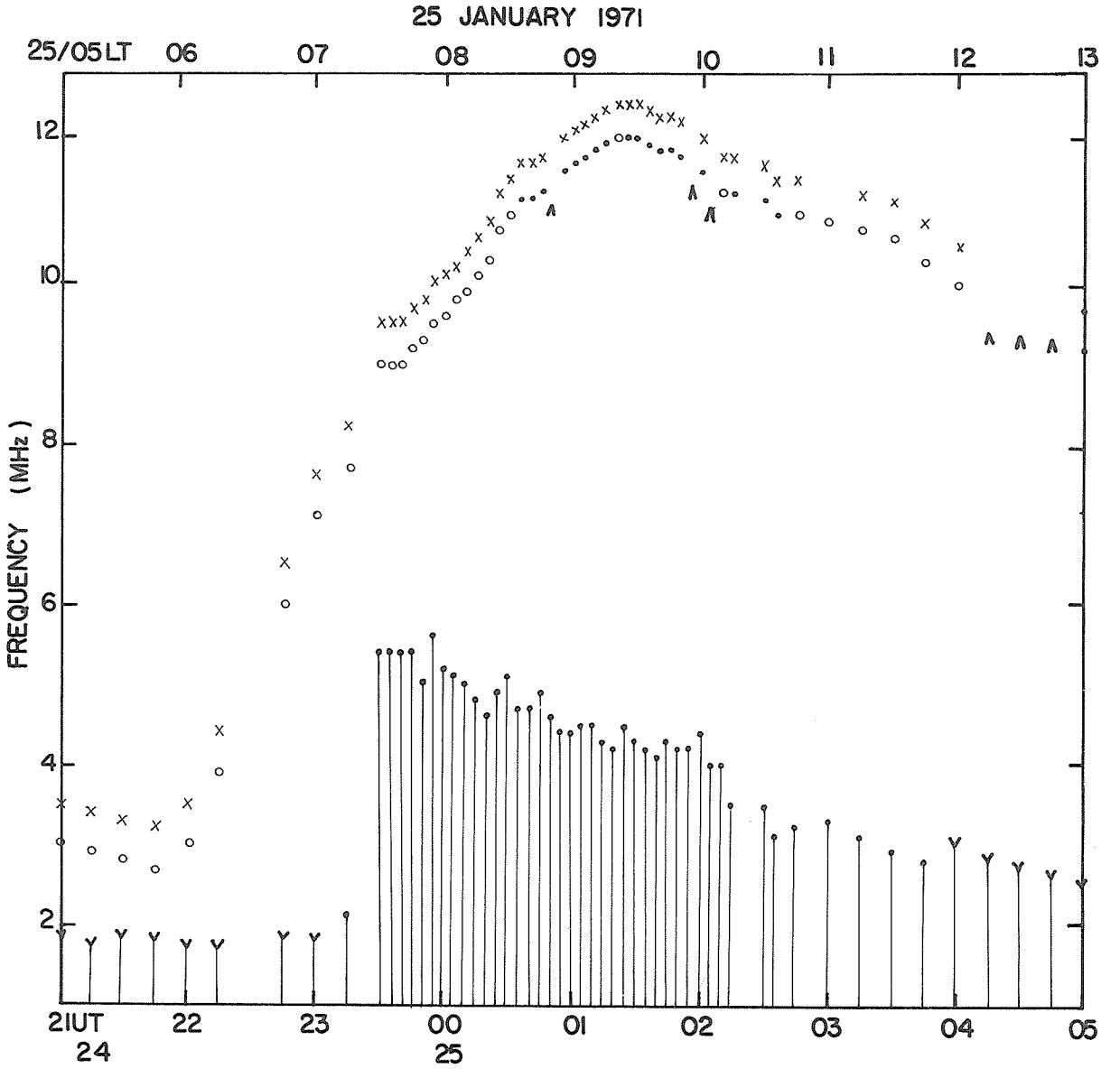

FIG. 2 f -PLOT FOR F2 AND f - MIN.

c) Restoration of Multiple Echoes in the F-region. The existence of multiple echoes of the F-trace is an indication that lower regions do not completely absorb or totally reflect the radiated energy. Hence this vertical incidence energy at high frequencies passes through the lower regions several times. Before the solar event, at 24/2301 UT at least three multiple echoes can be seen on the expanded scale record. Other records show multiple echoes, i. e. at 2300 UT on regular gain two additional echoes appear. Quite interestingly the 2315 UT ionogram still shows two multiple echoes indicating that the X-rays have not yet adequately ionized the D- and E-regions for absorption. The next ionogram at 2337 UT shows no multiple echo but high absorption. Only at 25/0120 UT does a weak multiple echo occur at twice the virtual height of the regular F-trace. A study of the next eight ionograms taken at five minute intervals shows variation: for example, the multiple echo at 0125 UT is weaker than the one at 0120 UT. (The diurnal gain setting of the ionosonde recorder remained the same during this period.) A weaker multiple trace has a shorter frequency range. The 0135 UT and 0140 UT records manifest multiples extending to higher frequencies but not as high as foF2. This restoration of multiple echoes for the F-region gives evidence that the lower ionosphere does not lose its ionization linearly with time during the recovery period.

d) Bifurcation of the F-layer. After the event starts in the ionosphere only the highest frequencies of the F-region appear on the ionograms. At 2337 UT frequencies from 5.4 MHz to 9.0 MHz can be seen. As early as 25/0040 UT the F1 layer shows indistinctly but is missing on subsequent ionograms for 25 minutes. At 25/0130 UT the F2 layer is fully formed and the F1 layer comes in but in an "L" condition preventing a definite foF1 value. So the F-region is stratified but not sharply so.

By 0159 UT the F1 trace is formed and at its low frequency end shows a descent in virtual height with increase in frequency. This is due to E-region retardation. The ionosonde is now able to expose the full F-trace.

e) hpF2 values. In the hour before the flare hpF2 was lower than the corresponding control day median but not lower than the values on particular days. About four hours after the flare the hpF2 values exceed those on any of the control days. Due to retardation this F2 layer seems to depart from a parabolic layer.

The E-region recovery. Six minutes (2315 UT) after the start of the flare the E-region (on an otherwise complete ionogram) appears to show a slightly higher f-min than that for corresponding control days. This may be transitional in the formation of the D-region. Immediately subsequent ionograms show values for f-min of 5.4 MHz (See Table I) with a gradual restoration of the E-layer over

Table I. Recovery Times

Appearance of	Time (UT)	Time After 2309	Appearance of	Time (UT)	Time After 2309	Time (UT)	f-min (MHz)
F1 layer	0040	1h 31m	E layer	0140	2h 31m	2300	1.8
F1 reappearance	0105	1h 56m	Es type h	0201	2h 52m	2315	2.1
						2337	5.4
F1 complete	0159	3h 50m	Es type l	0230	3h 20m	0215	3.5
F-1 1/2	0330	4h 21m	Es type c	0359	4h 52m	0645	2.1

a six hour period. The normal E-layer appears but very faintly at 0140 UT and disappears at 0155 UT. At 0215 UT it grows stronger and remains throughout the day. From 0201 the sporadic E appears and types h, l and c are manifest during the next two hours. These times and conditions indicate how the D-region has affected the higher E-region.

Mid-Latitude Total Electron Content during Cosmic Ray Event January 25-26, 1971

by

J. A. Klobuchar
Air Force Cambridge Research Laboratories
Bedford, Massachusetts

and

M. J. Mendillo
Astronomy Department, Boston University
Boston, Massachusetts

Continuous measurements of the ionospheric total electron content (TEC) using the Faraday rotation technique are routinely made from Sagamore Hill, Hamilton, Massachusetts, by monitoring the VHF signal from the geostationary satellite, ATS-3. The TEC of the mid-latitude ionosphere consists mainly of the integrated electron densities of the F-region; that is, the lower layers contribute a negligible amount to the total. The equivalent vertical TEC values for January 25-26, 1971 are shown in the Figure below. The dashed curves give the monthly median behavior for the month. The small vertical arrow indicates the approximate time of the commencement of ground level cosmic ray increase. The January period was magnetically quiet, as indicated by the Ap values in the Figure. Geomagnetic storms typically cause large scale changes in TEC which last several days while large solar flares produce effects of much smaller magnitude and shorter duration. For this period, however, no changes occurred in TEC which could be directly associated with the cosmic ray increase.

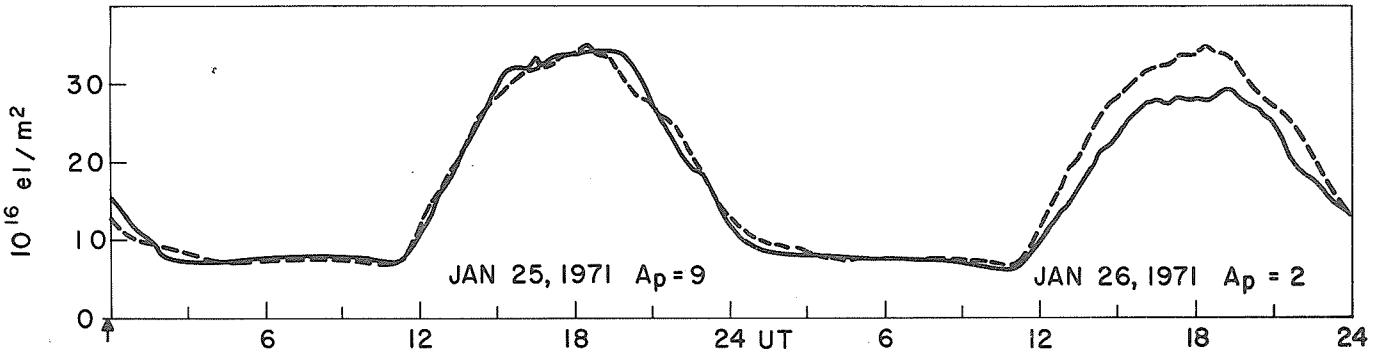

EQUIVALENT VERTICAL TOTAL ELECTRON CONTENT OBSERVED FROM SAGAMORE HILL, HAMILTON, MASS.

Polar Cap Disturbance of January 24, 1971, Observed on the Phase of VLF Waves

by

Y. Hakura
Radio Research Laboratories
Koganei, Tokyo, Japan

T. Ishii, T. Asakura, and Y. Terajima
Inubo Radio Wave Observatory
Radio Research Laboratories
Choshi, Chiba, Japan

Phase measurements with a cesium frequency standard of VLF waves propagating over great distances have been made at Inubo Radio Wave Observatory, Choshi, Chiba, Japan (35°42'N, 140°52'E). Among them, transpolar VLF waves provide a very sensitive method of detecting solar proton events at the middle latitude [Nakajima et al., 1970]. The transpolar signal paths for NAA-17.8 kHz, GBR-16.0 kHz, and WWVL-20.0 kHz are shown in Figure 1, in which the corrected geomagnetic latitudes of 60° and 70° are shown by two elliptical lines.

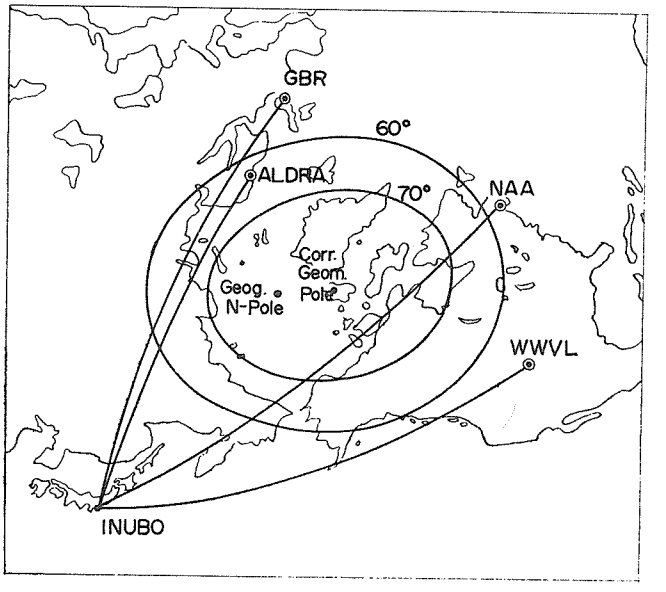

Fig. 1. Transpolar signal propagational paths.

Figure 2 shows solar proton flux with energy greater than 10 Mev [Solar-Geophysical Data, December, 1971], phase deviations in the NAA and GBR signals from their calm levels, and geomagnetic Kp indices on January 22 through February 4, 1971. A major polar cap disturbance started at about 2340 UT on January 24, in association with the solar proton event observed by the satellite Explorer 41. The Kp-associated phase deviations are also seen. Occurrence times of optical, radio, and x-ray flares, associated sudden phase anomalies SPAs, polar cap disturbances PCDs and proton event are shown in Table 1.

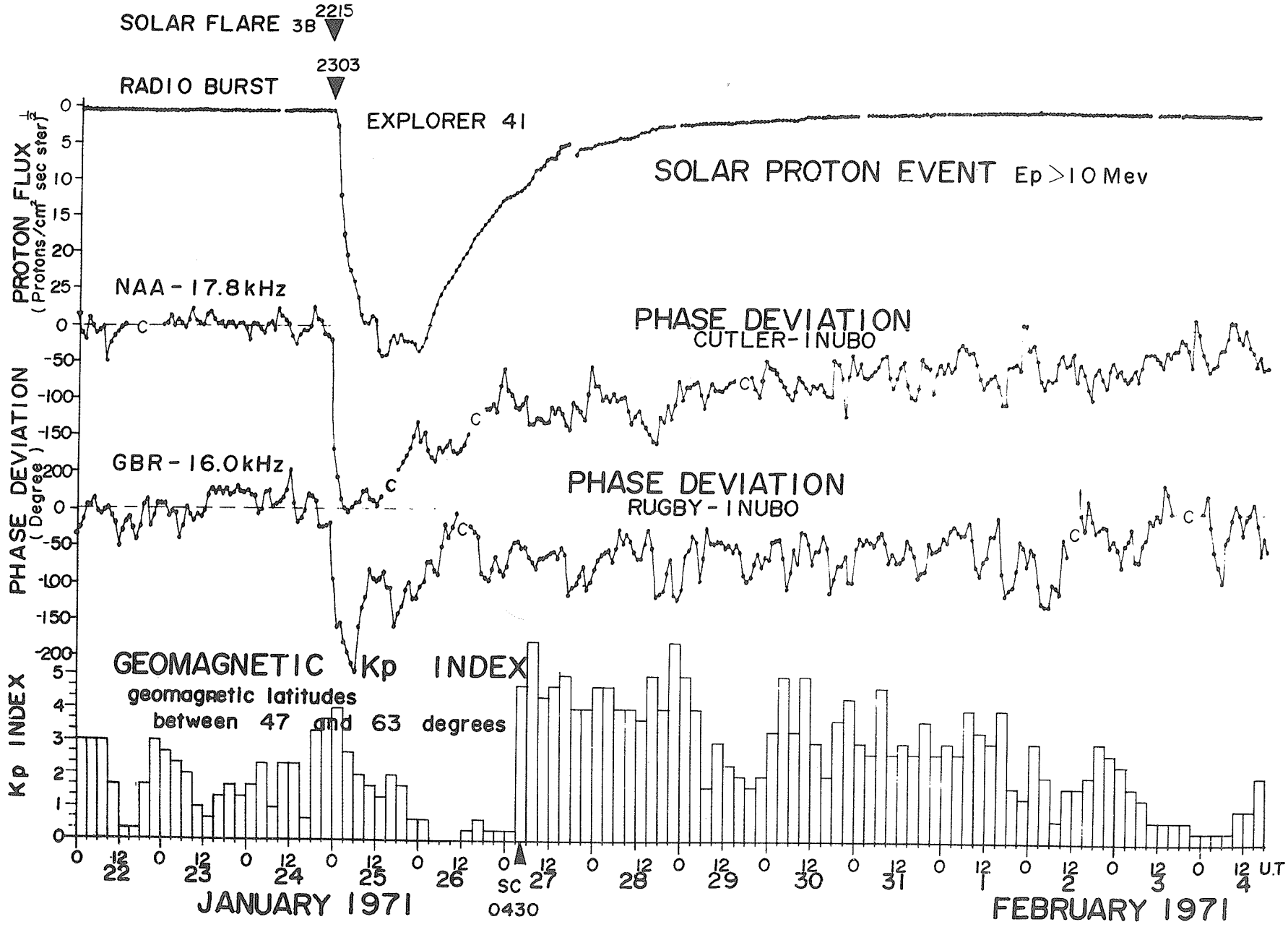

Fig.2 Polar Cap Disturbance of January 24, 1971

Table 1

SPA's and PCD's observed at Inubo and related solar-terrestrial events of January 24, 1971

Event		Start time	Max. time	End	Phase deviation, or Importance, or Flux
SPA	NAA-17.8 kHz	24/2308	2327	2336D	67°
	WWVL-20.0 kHz	2310	2341	0123	126°
Optical flare (N18, W49 in McMath plage region 11128)		2215	2331	0020	3B
Radio burst at 3750 MHz (Toyokawa)		2303	2324	2355	3.45×10^{-19} w $m^{-2} Hz^{-1}$
X-ray (1-8 Å) burst Explorer 37		2304E	2347	0953	0.49 erg $cm^{-2} sec^{-1}$
PCD	NAA-17.8 kHz	24/2338	25/0312	01/ 22	261°
	GBR-16.0 kHz	2341	0444	15	195°
Solar proton	Explorer 41 (E>30 Mev)	2400E	07	03	408 $cm^{-2} sec^{-1} ster^{-1}$
	(E>10 Mev)	2400E	14	17	1152
	ATS 1 (20 - 40 Mev)	2340			
	Neutron monitor (Deep River)	2340	0010		12 % above background

D = after
E = before

REFERENCES

NAKAJIMA, T., T. ISHII, K TSUCHIYA, A. SAKURAZAWA and Y. HAKURA 1970 Results of special observations for the Proton Flare Project 1969: Polar cap disturbance of June 7, 1969, observed on the phase of VLF waves, J. Radio Res. Labs., Japan, 17, 49-54.

1971 Solar-Geophysical Data, 328 Part II, December 1971, U.S. Department of Commerce, (Boulder, Colorado, U.S.A. 80302), 68-79.

The Effects of Solar Proton Event and Associated Geomagnetic Disturbance on the Phase of VLF Signals Received at Leicester, UK

by

J. W. Chapman and R. E. Evans
Department of Physics
Univeristy of Leicester
Leicester, U. K.

Introduction

This paper presents the effects of the period of enhanced solar proton flux and geomagnetic disturbance on the phase, recorded at Leicester, UK, of VLF radio signals propagated over medium and long distance paths. Details of the transmissions are given below.

Transmitter	Frequency (kHz)	Path Length (km)
NAA	17.8	4900
Trinidad	12.0	7200

The NAA-Leicester path lies between geomagnetic latitudes (Φ) of 55° to 60°, while (Φ) is less than 40° for about half the Trinidad-Leicester path and hence charged particle effects might be expected to have the least influence on the signals for this circuit.

The Disturbance of January-February 1971

Figure 1 shows the observed phase path variations for the period 24 January - 13 February 1971, together with other relevant data taken from the NOAA Bulletins of "Solar-Geophysical Data". A marked disturbance occurs on the NAA phase, the effect being larger at night than by day so that the amplitude of the diurnal phase variation is considerably reduced. The initial effect commences with the onset of enhanced proton flux, producing a phase advance of about 0.15 λ on the nights of 25-26 and 26-27 January. The transmitter was off from 1400 to 1800 UT on 25 and 26 January so that the effect on the daytime phase is uncertain, but appears to be very small. The major effect is associated with the occurrence of the magnetic storm having sudden commencement at 0430 UT on 27 January. The daytime phase is advanced by up to 0.2 λ on 27 January, while the night-time phase advance is almost 0.5 λ on the night of 27-28, when there are also marked phase fluctuations. The overall effect at night is substantially the same until 30-31 January, and then a slow recovery begins which is not complete until at least 9 February, long after the disappearance of the magnetic disturbance. The maximum daytime phase advance of about 0.25 λ does not occur until 30 January at the earliest (phase advance due to enhanced solar x-radiation makes the daytime effect uncertain), while recovery is complete by 8 February.

The effects on the Trinidad phase appear to be very similar to those for NAA, though as expected they are smaller. There is little or no change immediately following the increase in proton flux, but the sudden commencement is followed by an advance in both night-time and day-time phase. This effect is more marked at night (maximum 0.2 λ on 27-28 January) and again recovering more slowly than the disturbance in the magnetic field. Unfortunately there is a gap in the data between 3 and 8 February so that the recovery time is uncertain, but recovery is probably complete earlier than for NAA.

Discussion

The effects of the disturbance of January-February 1971 are very similar to those obtained for the same paths in March 1970 [Jones, 1971], although that event probably did not extend to such low latitudes since the perturbation of the Trinidad phase was smaller. There are separate effects due to the initial solar proton event and to the arrival of the lower energy plasma associated with the sudden commencement magnetic storm, and the well known "storm after-effect" is also present. Similar behavior is seen on other high and medium latitude long path records, e.g. (i) the October-November 1968 event on NSS-Leicester [Jones, 1970]; (ii) the same event for NPG (now NLK), Hawaii and Trinidad-Tromsö [Larsen, 1970]; (iii) the February 1965 event on NPG-Farnborough [Belrose, 1968].

The reason for the after-effect is not yet understood. The most obvious possibility is the continued precipitation of charged particles into the atmosphere. Lauter and Knuth [1967] have proposed steady leakage of high energy electrons from the outer radiation belt which has been over-filled by the solar plasma during the strong compression of the earth's field. Alternatively, a change in atmospheric structure has been suggested by Belrose [1964], the change in composition occurrring at auroral latitudes at the time of the storm and the delayed effect arising because of the time of travel to mid-latitudes. Yet another explanation of delayed effects has been proposed by Volland [1967] in terms of heat conduction waves originating in the magnetosphere.

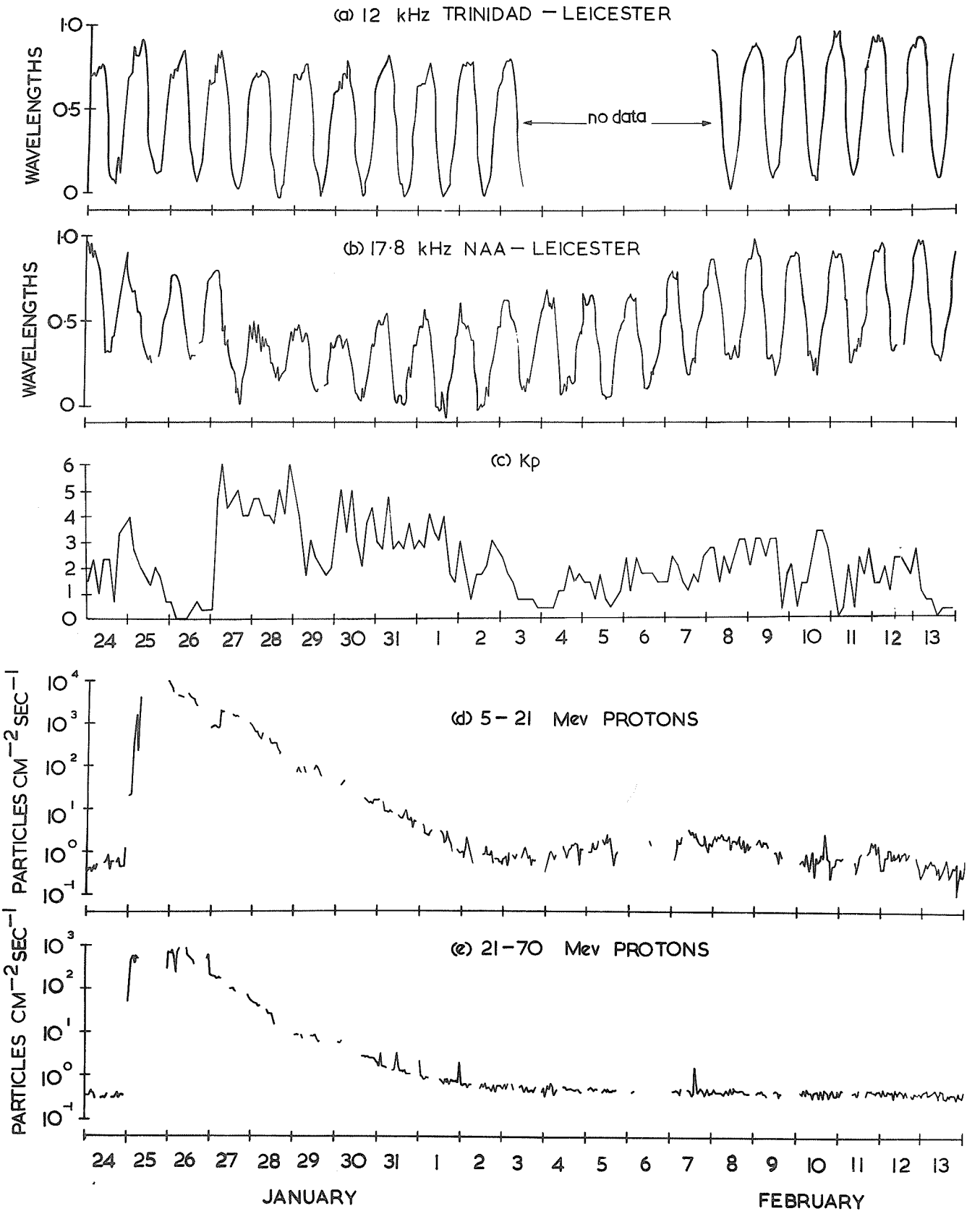

Fig.1. DATA FOR THE JANUARY—FEBRUARY 1971 EVENT. (a) and (b) VLF PHASE; (c) Kp; (d) and (e) ATS—I SOLAR PROTON FLUX.

REFERENCES

BELROSE, J. S. 1964 The Oblique Reflection of Low Frequency Radio Waves from the Ionosphere, AGARDograph 74: Propagation of Radio Waves at Frequencies below 300 kc/s, (Ed. W. T. BLACKBAND, Pergamon Press), 149.

BELROSE, J. S. 1968 Low and Very Low Frequency Radio Wave Propagation, AGARD Lecture Series 29, Radio Wave Propagation, IV-25.

JONES, T. B. 1970 Long Path VLF Observations of the Ionospheric Disturbances Resulting from the Solar Proton Event of October-November 1968, World Data Center A, Upper Atmosphere Geophysics, Report UAG-8, 282.

JONES, T. B. 1971 VLF Radiowave Observations of Ionospheric Disturbances during the Period 4-18th March, 1970, World Data Center A, Upper Atmosphere Geophysics, Report UAG-12, 247.

LARSEN, T. R. 1970 VLF Phase and Amplitude Measurement during the PCA Event October 31-November 6, 1968, World Data Center A, Upper Atmosphere Geophysics, Report UAG-8, 279.

LAUTER, E. A. and R. KNUTH 1967 Particle precipitation at medium latitudes after magnetic storms, J. Atmosph. Terr. Phys., 29, 411.

VOLLAND, H. 1967 Heat Conduction Waves in the Upper Atmosphere, J. Geophys. Res., 72, 2831.

1971 Solar-Geophysical Data, 318 Part I, February 1971; 319 Part I, March 1971; 320 Part I, April 1971, U.S. Department of Commerce, (Boulder, Colorado, U.S.A. 80302).

Ionospheric Effects from Solar Particles during January 24 - February 3, 1971

by

G. Nestorov and P. Velinov
Geophysical Institute
Bulgarian Academy of Sciences
Sofia, Bulgaria

Introduction

There exist two different types of influence of solar particles on the ionosphere during solar flare activity. The first type is determined by high energy particles of dozens of Mev energy or even more. In the case of more powerful flares even relativistic solar cosmic rays are generated with energy in the Bev range as is the case of January 24, 1971. This influence usually coincides with SID effects of solar electromagnetic radiation and involves the ionosphere at all latitudes. Shortly after these arrive, the main flux of Mev particles and the well-known PCA phenomena begin.

Usually about two days after that, further disturbances arise as a result of the soft particle emission during the flare. This second type of event is comparatively long-lived and often results in ionospheric and geomagnetic storm activity. Normally this second type effect is much more frequent - the soft energy particles result from almost every powerful flare. Only the important flares generate high energy particles; relativistic cosmic rays are generally rarely generated.

The ground-level cosmic ray increase on January 24, 1971 was caused by high energy solar particles and relativistic solar cosmic rays, while on January 27 a geomagnetic storm accompanied by particle precipitation occurred, i.e. during the studied period January 24 - February 3, 1971 are clearly demonstrated all types of influences of the solar particles on the ionosphere. Furthermore, the main effect takes place during the night of January 24 - 25 when the influence of the electromagnetic solar radiation is absent. It should be emphasized that the solar cosmic ray effect we investigated on May 4, 1960, which took place at local noontime, required the separation of SID contributions from the effect of the particles [Nestorov and Velinov, 1966]. That is why the investigation of the solar particle influence on January 24 under purely night conditions is especially of interest to us. For this purpose in this paper we shall present the radio wave observations about this effect and about the period after it, as well as certain qualitative and quantitative interpretations of the corresponding complex of phenomena.

Solar Cosmic Ray and High Energy Particle Effects on the Low Ionosphere

The sudden increase of the cosmic ray flux on January 24, 1971, 2330 UT observed by a number of stations [Solar-Geophysical Data] was attended by ionospheric anomalies in the middle geomagnetic latitudes. At the Ionospheric Observatory Sofia (42.6°N, 23.4°E) various effects in the range of long, medium and short radio waves were recorded.

In the night of January 24 - 25 was observed a great increase of the absorption of the frequency 164 kHz, path length 1720 km. The height of the signal reflection in the night is $h \leq 90$ km, while the equivalent frequency $f_i = f \cos i \simeq 25$ kHz (i.e. the path can be related to the conditions of propagation of VLF; "i" is the angle of incidence). As can be shown by the lower part of Figure 1 the excessive absorption ΔL starts somewhat before 2200 UT on January 24 while at the maximum cosmic ray flux (around 2400 UT) it reaches 15 dB. The time course of the absorption L_{164} is shown by a heavy line and dots while the signal fluctuations as the result of the polarizing and interferential fading are marked by vertical dotted lines. The course of the monthly median values L_{med} is shown by small circles and dashes. In the upper part of Figure 1 is shown the time course of the cosmic ray flux of the Deep River Neutron Monitor [Solar-Geophysical Data]. It can be seen that the absorption anomaly reaches its maximum about two hours after the cosmic ray flux. The anomaly ends shortly after 0400 UT.

The sudden and considerable increase of the absorption on 164 kHz on January 24 - 25, 1971, is due to the excessive nondeviating absorption in the cosmic ray layer as a result of the increase of the primary cosmic ray flux after 2330 UT on January 24. The additional absorption is a measure for the increase of the electron production rate in CR layer [Nestorov and Velinov, 1966]. Since the ionization can be obtained in an independent way by the increased cosmic radiation, a possibility opens up for a comparison of the calculated results by an ionospheric as well as by a direct method.

Under the influence of the relativistic solar cosmic rays arising as an additional ionizing source in the night CR layer, the electron production rate q will increase by δq. The relative variation $\delta q/q$ can be determined by the data of the variation of the nondeviating absorption of the radio waves $\delta L/L$ passing through the night CR layer and reflected by the higher situated E-layer [Velinov, 1968 and 1971]:

$$\frac{\delta q}{q} = \frac{\delta L}{L}\left(2 + \frac{\delta L}{L}\right) \qquad (1)$$

where L is the mean absorption in the quiet period (in our case we take the median values of L), δL is the change of the absorption from the level of the median values.

On the other hand $\delta q/q$ could be calculated according to the equation of the variation of the electron production rate of the height of h:

$$\frac{\delta q(h)}{q(h)} = \frac{\delta \rho(h)}{\rho(h)} - \delta R_c \, W_q(R) + \int_{R_c}^{\infty} W_q(R) \, \frac{\delta n(R)}{n(R)} \, dR \qquad (2)$$

where $\delta\rho/\rho$ and $\delta n/n$ are relative variations of the atmospheric density and differential spectrum of primary cosmic rays, respectively; δR_c is the change of geomagnetic cutoff rigidity; $W_q(R)$ is the coefficient relating the variation of $\delta q/q$ to δR_c, and to $\int(\delta n/n)dR$. If $\delta q/q$ is measured in percentage, and R_c in BV, then $W_q(R)$ is measure in % BV^{-1}. The analytical aspect of $W_q(R)$ is found by Velinov [1971]:

$$W_q(R) \simeq \frac{\gamma - 1}{R} \qquad (3)$$

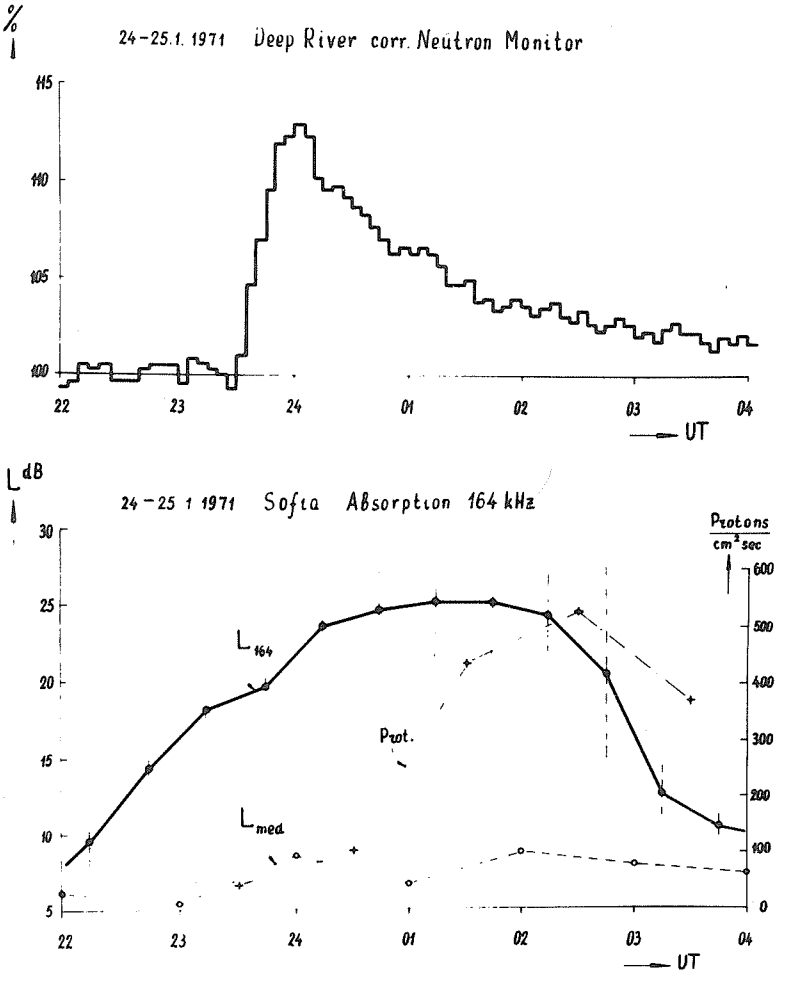

Fig. 1. The variations of the cosmic rays, high energy protons and absorption 164 kHz during the night of January 24 - 25, 1971.

where $\gamma \simeq 2.5$ is the power of the differential spectrum of cosmic rays $n(R) = KR^{-\gamma}$. Equation (2) is analogous to the equation for the CR intensity variation [Dorman, 1963]. In accordance with equation (2) the electron production rate variations may be divided into three classes corresponding to the three classes of CR variations: I Class - variations of the atmospheric density, II Class - geomagnetic variations and III Class - variations of the primary cosmic rays. The III Class is the biggest and most important and interesting class of variations which are of extraterrestrial origin. They are connected with the change of the energetic spectrum far from the Earth. In our case of January 24 - 25, the penetration of the relativistic solar cosmic rays has been attended by moderate geomagnetic disturbances as the 3-hour Kp index reaches the value 3 - 4. This shows that all the terms of the equation (2) must be taken into account.

First of all we shall determine the Class III variations, starting with the increase of cosmic ray intensity and apply the method of connecting coefficients [Dorman, 1963]. For this purpose we shall make use of the neutron component of the cosmic rays recorded at stations with geomagnetic cutoff rigidity R_c close to cutoff in the reflection point of the signal 164 kHz, where $R_c = 5$ BV:

Pic-du-Midi	$R_c = 5.6$ BV,	$\delta N_n/N_n \simeq 2\%$
Dallas	$R_c = 4.35$ BV,	$\delta N_n/N_n \simeq 1.3\%$

From these data by means of the equation:

$$\frac{\delta N_n}{N_n} = \int_{R_c}^{\infty} W_{CR}(R)\, \frac{\delta n(R)}{n(R)}\, dR \qquad (4)$$

(W_{CR} is the connecting coefficient between the primary and the secondary cosmic ray variations) may be determined the function $\delta n(R)/n(R)$ which substituted in equation (2) gives the Class III variations

$$(\delta q/q)_{III} \simeq 0.1$$

Taking into consideration the moderate geomagnetic disturbance in which the 3 hour Kp index reaches Kp $\simeq$ 3 - 4 (i.e. $\Delta H \simeq 50\ \gamma$) can be determined the Class II variation [Velinov, 1971]:

$$(\delta q/q)_{II} \simeq 0.04$$

For Class I variation we have no data but there are certain facts about the growing density of the atmosphere ρ so that we can obtain for the total variation

$$(\delta q/q)_{I} \leq 0.2$$

This value, however, gives an insufficient explanation of the ionospheric disturbances on January 24 - 25. Thus, for instance, on January 25, 0000 UT L = 9 dB, ΔL = 10 dB, whence according to (1)

$$\delta q/q = 3.4$$

and after 2 - 3 hours is reached the value of

$$\delta q/q \simeq 10,$$

i.e. the relativistic solar cosmic rays lack a flux of about 2 orders, in order to explain the observed ionospheric effect. That is why we should expect the existence of another more powerful source of ionization in the high atmosphere at a height below 90-100 km. As such, high energy solar particles of over 20 Mev can be attracted, which arrive a short time after the relativistic solar cosmic rays resulting in PCA phenomena. Actually in the interval 0000-0600 UT on January 25 from ATS-1 (1966-110 A) are observed hourly average fluxes of 10^2 - 5×10^2 protons $cm^{-2}sec^{-1}$ in the energy range 21 - 70 Mev, from Explorer 41 (1969-53 A) are observed 2.5×10^3 protons $cm^{-2}sec^{-1}$ with E>30 Mev and 5×10^2 protons $cm^{-2}sec^{-1}$ with E>60 Mev. Similar Vela proton counters showed 2640 particles cm^{-2} sec^{-1} with E>25 Mev [Solar-Geophysical Data]. The main problem is how a part of these particles has been able to penetrate as far as the middle latitude ionosphere where the geomagnetic threshold is large. The estimates of Velinov [1966, 1968 and 1970] show that for an explanation of the experimentally obtained $\delta q/q \simeq 10$ it is sufficient for 1 proton $cm^{-2}sec^{-1}$ with $E \geq 20$ Mev to penetrate to this region. Perhaps the geomagnetic disturbance Kp = 3 - 4, with the whole night of January 25 reaching ΣKp = 14, was a factor causing a very small part (0.03 - 0.3%) of the main solar particle flux to be precipitated at middle latitudes, thus causing the PCA event.

In confirmation of this the following facts are noted: a.) the comparison of the absorption course L_{164} (Figure 1) with that of the flux of protons 21 - 70 Mev, observed at ATS-1, shows a certain correspondence between the two courses; b.) the large fluctuations in the field strength are characteristic of the penetration of the high energy proton fluxes; c.) the absence of an ionospheric effect on January 25 - 26 while the powerful PCA event continued (ATS-1 recorded in 21 - 70 Mev range a maximum flux of 845 protons $cm^{-2}sec^{-1}$) but geomagnetic disturbance is absent - Kp = 0 - 1, and during the whole night $\Sigma Kp = 4$. Thus on January 25 - 26 there has been no precipitation of high energy particles. The effect under discussion expresses the PCA influence on the middle latitudes. Naturally the low and middle latitude PCA influence should be verified by some other special cases in the Sun-Earth space.

Effects in the Middle and Low Ionosphere during January 23 - February 3

The absorption time course of 155 kHz (path length 380 km), 164 kHz and 593 kHz (path length 140 km) during the period of January 23 - February 3, 1971 is shown in Figure 2. In the same Figure the course of the geomagnetic index Ap for the same period is indicated by small circles and dotted lines.

The observed ionospheric effect schematically expressed in Figures 1 and 2 compared with results of previous investigations gives ground for the following qualitative geophysical interpretations. The time variations of the absorption shown in Figure 2 for three frequencies reflect the ionization conditions of the region 80 to 120 km in the given period.

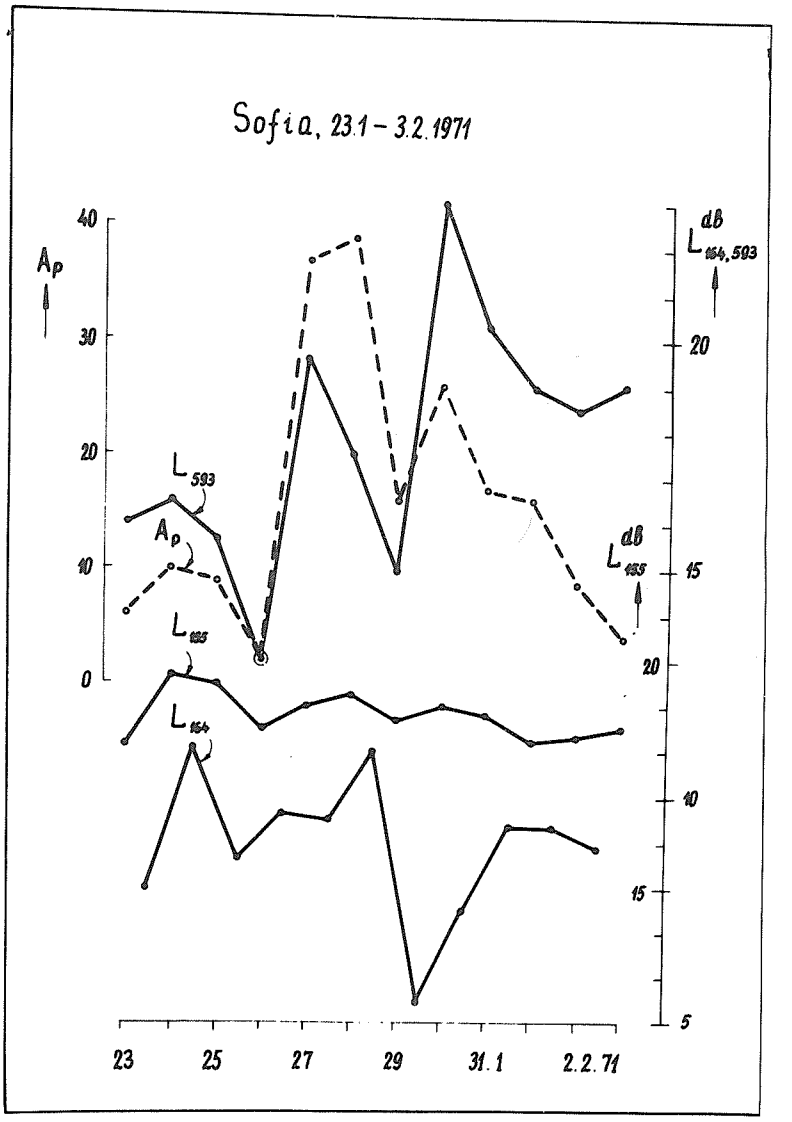

Fig. 2. The variation of the absorption of different frequencies during the period January 23 - February 3.

From previous investigation [Nestorov and Velinov, 1968; Nestorov, 1969] it is known that during the time of geomagnetic disturbances or storms (ssc) about two days after the disturbance maximum, the night absorption 593 kHz considerably increases. A smaller maximum of L is obtained in the ssc night. The case under consideration presents a similar picture. A normal maximum of L_{593} is obtained on January 27 while a secondary large increase of L_{593} is reached two days after the maximum of Ap, i.e. on January 30. The increase of ΔL over the monthly median is the measure of the increased electron production rate in the range 85 - 120 km and for the flux of soft particles also at these heights.

It is easily observable that the absorption course L_{164} after January 27 is opposite to L_{593}. This is in accord with the previous results about the behavior of the night absorption L_{164} after geomagnetic anomalies [Nestorov, 1972a, b]. The increase of L_{164} on January 24 - 25 as already explained is connected with the increased high energy particle flux during the same time.

On the contrary in the course of L_{155} no essential changes can be observed which corresponds to the normal behavior of the night absorption on this path for the period of 15 years [Nestorov, 1969 and 1970]. Only in exceptional cases after geomagnetic storms the absorption L_{155} partially decreases. The complex of the observations of the absorption of various equivalent frequencies (25.75 and 480 kHz) on the indicated paths outlines the following physical state of the mesosphere and low thermosphere in the given period.

The sudden increase of cosmic rays on January 24 - 25 is due to the powerful solar flare on January 24 starting at 2310 UT. This flare is connected with the generation of particles in all energy ranges including plasma, which is indicated by the geomagnetic storm on January 27 at 0430 UT. The influx of energy particles in the high atmosphere at the height of 80 - 120 km adds to the increase of the electronic concentration at this range of height and to the increase of the absorption of waves crossing the same region (L_{593} on January 30). The height of the signal reflection L_{593} during the night is about 120 km. The increased electronic concentration in the layer is followed by an increase of its gradient, which decreases the deviation and the total absorption of the signal 164 kHz (L_{164} on January 29 - 30). Between these two L curves out of phase there must exist a frequency under which the signal will neither increase nor decrease; actually a compensation effect of the frequency is observed ($f_i \simeq 75$ kHz, the signal 155 kHz in the night is reflected at the height of about 95 km).

Although at present there does not exist a generally accepted theory of the role of the fluxes of charged particles in the ionization of night E-layer, certain estimations of the effects in the studied period will be given on the basis of the method of Velinov [1969]. Suppose the particle flux I dissipates its energy between the heights h_1 and h_2 (in our case about 80 - 120 km). It would cause an additional electron production rate Δq connected with the corresponding additional absorption ΔL by means of equation (1) as

$$I = \frac{2Q(h_2-h_1)}{E_K} \Delta q \qquad (5)$$

$Q \simeq 30$ ev is the energy required for 1 electron ion pair; E_K is the energy of the particles (if they are of different energies, instead of E_K must be substituted $E_{K,eff}$ depending on the spectrum of the particles). The factor 2 takes into account that the particles equally dissipate their energy in the ionization and excitation of the atmospheric components.

From Figure 2 can be seen that

$$L_{27.1} \simeq 19.5 \text{ dB and } L_{30.1} \simeq 23 \text{ dB},$$

but since the median value for January is $L_{med} = 16$ dB

$$\Delta L_{27.1} \simeq 3.5 \text{ dB and } \Delta L_{30.1} \simeq 7 \text{ dB}$$

by means of equation (1) is obtained

$$(\Delta q/q)_{27.1} \simeq 0.5 \text{ and } (\Delta q/q)_{30.1} \simeq 1.1.$$

In the studied height interval in the night a medium electron concentration can be accepted under quiet conditions $N \simeq 10^3$ cm^{-3} and an effective recombination coefficient $\alpha_e \simeq 3\text{x}10^{-7}$ cm^{3}sec^{-1}, i.e. $q = 0.3$ cm^{-3}sec^{-1}. Therefore as additional electron production rate on January 27 and 30, we receive

$$\Delta q_{27.1} \simeq 0.15 \text{ cm}^{-3}\text{sec}^{-1} \text{ and } \Delta q_{30.1} \simeq 0.3 \text{ cm}^{-3}\text{sec}^{-1},$$

while for the necessary proton flux with $E_{K,eff} = 300$ kev

$$I = (1 - 2)\text{x}10^2 \text{ protons cm}^{-2}\text{sec}^{-1} \qquad (6a)$$

is obtained. In case electrons precipitate with $E_{K,eff} = 40$ kev, equation (5) gives

$$I = (0.75 - 1.5)\times10^{3} \text{ electrons cm}^{-2}\text{sec}^{-1}. \qquad (6b)$$

Factually the values (6) represent the number of particles with pitch angle in the cone of losses θ_1. The total number of particles can be determined when in the denominator of equation (5) is substituted also the function

$$k(\alpha) = \int_0^{\theta_1} \sin^{\alpha+1}\theta \, d\theta \Big/ \int_0^{\pi/2} \sin^{\alpha+1}\theta \, d\theta$$

as the parameter α determines the kind of the distribution of the particles. For latitudes $\lambda_m \simeq 41°$, Bulgaria, the parameter of McIlwain is 1.8, but in $\alpha = 0 - 2$ the function $k(\alpha) = 6\times10^{-2} - 5\times10^{-3}$.

Ionospheric Effect in the F2-Layer

In addition to the described physical condition of the night ionosphere it is suitable to show the behavior of the F2-layer observed at a fixed frequency f = 7.67 MHz during the same time period. The necessary time variation of Δt for the evolution of the F2-layer from sunrise to the level $N = 7\times10^{5}$ cm^3 required for the reflection of the signal, under a quasi-vertical incidence path length of 12 km, together with the variation of the Ap index and the velocity of the solar wind [Solar-Geophysical Data] are given in Figure 3. From Nestorov [1972c, d] it is known that during geomagnetic storms Δt considerably increases while in certain cases reflection is absent during the whole day which shows that foF2 < f. In the studied case the maximum Δt is later than the maximum of Ap and $\bar{V}$ by one day. This is the usual relaxation of Δt in the presence of an ssc. The good correlation of $\bar{V}$ with Δt is of interest which indicates the considerable influence of the solar wind on the anomalous state of the F2-layer.

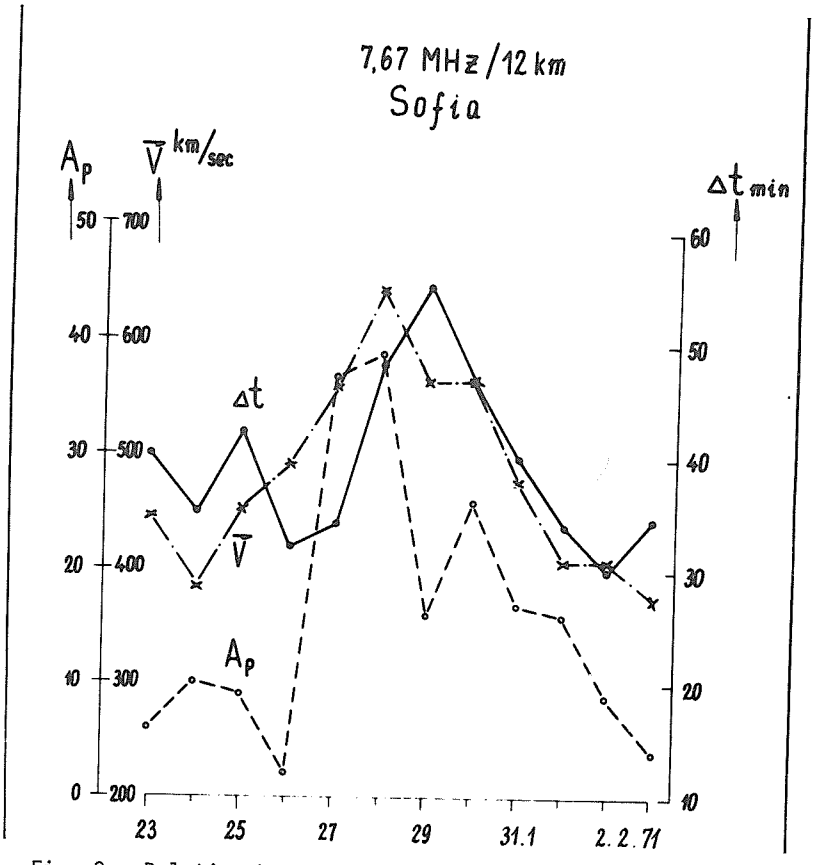

Fig. 3. Relation between solar wind velocity, the time of delay Δt of the F2-layer and geomagnetic index Ap.

REFERENCES

1971 Solar-Geophysical Data, 318 - 320 Part I, 1970-1971, U.S. Department of Commerce, (Boulder, Colorado, U.S.A. 80302).

DORMAN, L. I. 1963 Cosmic Ray Variations and Space Research, Publ. Hause Acad. Sci., U.S.S.R.

NESTOROV, G.	1969	Effect by Solar Corpuscular Fluxes on the Night Low Ionosphere in Middle Latitude, Proc. Geophys. Inst. Bulg., 14, 53.
NESTOROV, G.	1970	The Cosmic Ray Layer in the Low Ionosphere is a Reality, Compt. rend. Acad. bulg. Sci., 23, 57.
NESTOROV, G.	1972a	Positive Disturbances in the Night Ionosphere in the Mesopause Region during Geomagnetic Anomalies, Compt. rend. Acad. bulg. Sci., 25 (in press).
NESTOROV, G.	1972b	Lower Ionosphere at Medium Latitudes during Geomagnetic Disturbances, Proc. Geophys. Inst. Bulg., 18, 40.
NESTOROV, G.	1972c	Solar Control over the F2-Layer Evolution after Sunrise, Compt. rend. Acad. bulg. Sci., 25 (in press).
NESTOROV, G.	1972d	Geomagnetic Control over the F2-Layer Evolution after Sunrise, Compt. rend. Acad. bulg. Sci., 25 (in press).
NESTOROV, G. and P. VELINOV	1966	Effect of Solar Cosmic Rays on Low Ionosphere, Compt. rend. Acad. bulg. Sci., 19, 1011.
NESTOROV, G. and P. VELINOV	1969	Effects in the Night Lower Ionosphere as a Result of Particle Precipitation on Middle Latitudes, Solar Terrestrial Physics, Acad. Sci., U.S.S.R., 1, 181.
VELINOV, P.	1966	One Expression for the Ionization in Ionosphere from Cosmic Rays, Compt. rend. Acad. bulg. Sci., 19, 109.
VELINOV, P.	1968a	On Ionization in the Ionospheric D-Region by Galactic and Solar Cosmic Rays, J. Atmosph. Terr. Phys., 30, 1891.
VELINOV, P.	1968b	Relationships Between the Cosmic Ray Variations and the State of Low Ionosphere, Compt. rend. Acad. bulg. Sci., 21, 115.
VELINOV, P.	1969	On the Influence of Corpuscular Fluxes in the Magnetosphere on Night Ionosphere, Compt. rend. Acad. bulg. Sci., 22, 33.
VELINOV, P.	1970	Solar Cosmic Ray Ionization in the Low Ionosphere, J. Atmosph. Terr. Phys., 32, 139.
VELINOV, P.	1971	On Variations of the Cosmic Ray Layer in the Lower Ionosphere, J. Atmosph. Terr. Phys., 33, 429.

7. AURORA

The Auroral-Zone Effects of January 24 Event over Cola Peninsula

by

B. E. Brunelli, L. S. Evlashin, S. I. Isaev, L. L. Lazutin,
G. A. Loginov, G. A. Petrova, V. K. Roldugin, N. V. Shulgina,
G. V. Starkov, G. F. Totunova, and E. V. Vasheniuk
Polar Geophysical Institute, Academy of Sciences of USSR,
Apatity, Murmansk Region, USSR

Description of the 24-27 January event is given here using the same set of stations, observational technique and the manner of presentation as in our previous report [Brunelli et al., 1971]. The development of the January 24 proton event as seen from our data begins with the neutron monitor cosmic ray intensity increase, related to a 15-minute period, at 2330 UT. At 0600 UT January 25 the gradual increase of the riometer absorption began at Loparskaya, following the changing of the luminosity condition of the D-region of the ionosphere and revealing all other features typical for a PCA. This type of absorption was observed for two days with no appreciable geomagnetic effects. 53 hours after the beginning of the cosmic ray burst the magnetic storm began with the sudden commencement, accompanied by auroral absorption and intense aurora.

Figure 1 presents hourly values of the Apatity neutron monitor data. The solar cosmic ray burst has an amplitude of 15% and was preceded by a prolonged (∿5 days) but moderate (∿3%) decrease of intensity and followed by a rather large (∿7%) Forbush decrease simultaneous with the magnetic storm. From January 25 to 27 eight flights of radiosondes with single G-M counters as detectors were provided. During the ascent time of the flights the absorption spectra of the solar protons was measured and recalculated into energy spectra. Summary time of a measurement varied from 20 minutes to one hour. Temporal features of solar proton events are presented in Figure 2 where NM measurements during first few hours are combined with balloon measurements (>150 Mev level) provided later. The same spectra are shown in Figure 3. Figure 4-6 present the time history of the January event based on the data of ionosonde operations in Murmansk and also riometers with frequency 9 and 25 MHz, magnetometer, photometer and patrol spectrograph at Loparskaya.

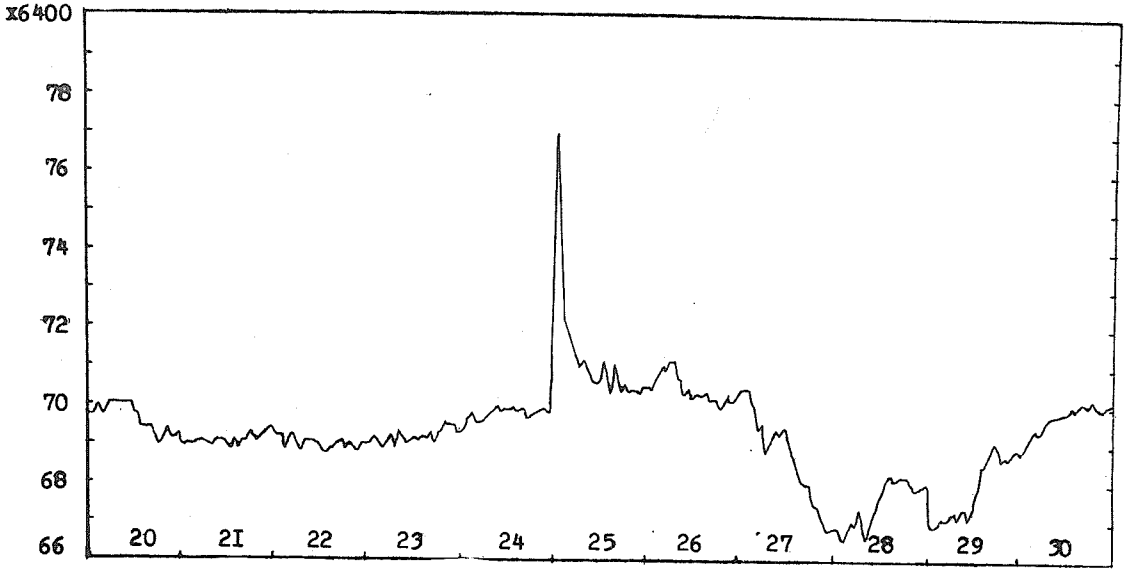

Fig. 1. Corrected hourly values of neutron monitor counting rate, Apatity, January 20-30.

Before the cosmic ray burst on January 24 moderate activity appeared at 1730 UT in the sporadic E-layer with fairly large blanketing frequencies and magnetic disturbance with sc at 1930 UT. The increase of luminosity and absorption began 5 minutes later and developed within an hour into a strong magnetic bay with aurora and rather large absorption. Immediately after the burst a new disturbance was registered by all the observational devices except the all-sky cameras which did not operate because of the bad weather. At 0445 and 0515 UT the ionosonde showed a black-out condition caused by the decreasing of foF2 falling below fairly high fmin.

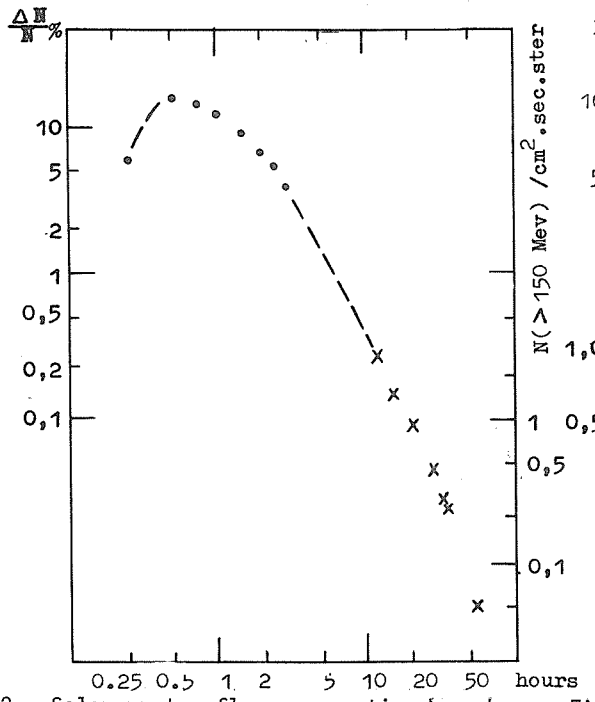

Fig. 2. Solar proton flux versus time based on neutron monitor data, dots, and balloon measurements, crosses. 2330 UT January 24 is assumed as a start.

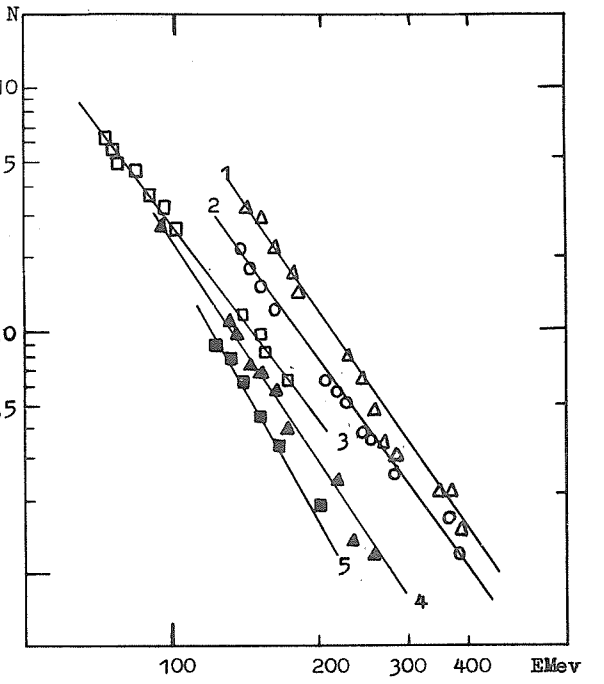

Fig. 3. Solar cosmic ray spectra from balloon measment data. Starting times: 1 - 1030 UT, 2 - 1420 UT, 3 - 2020 UT January 25, 4 - 0130 UT and 5 - 0450 UT January 26.

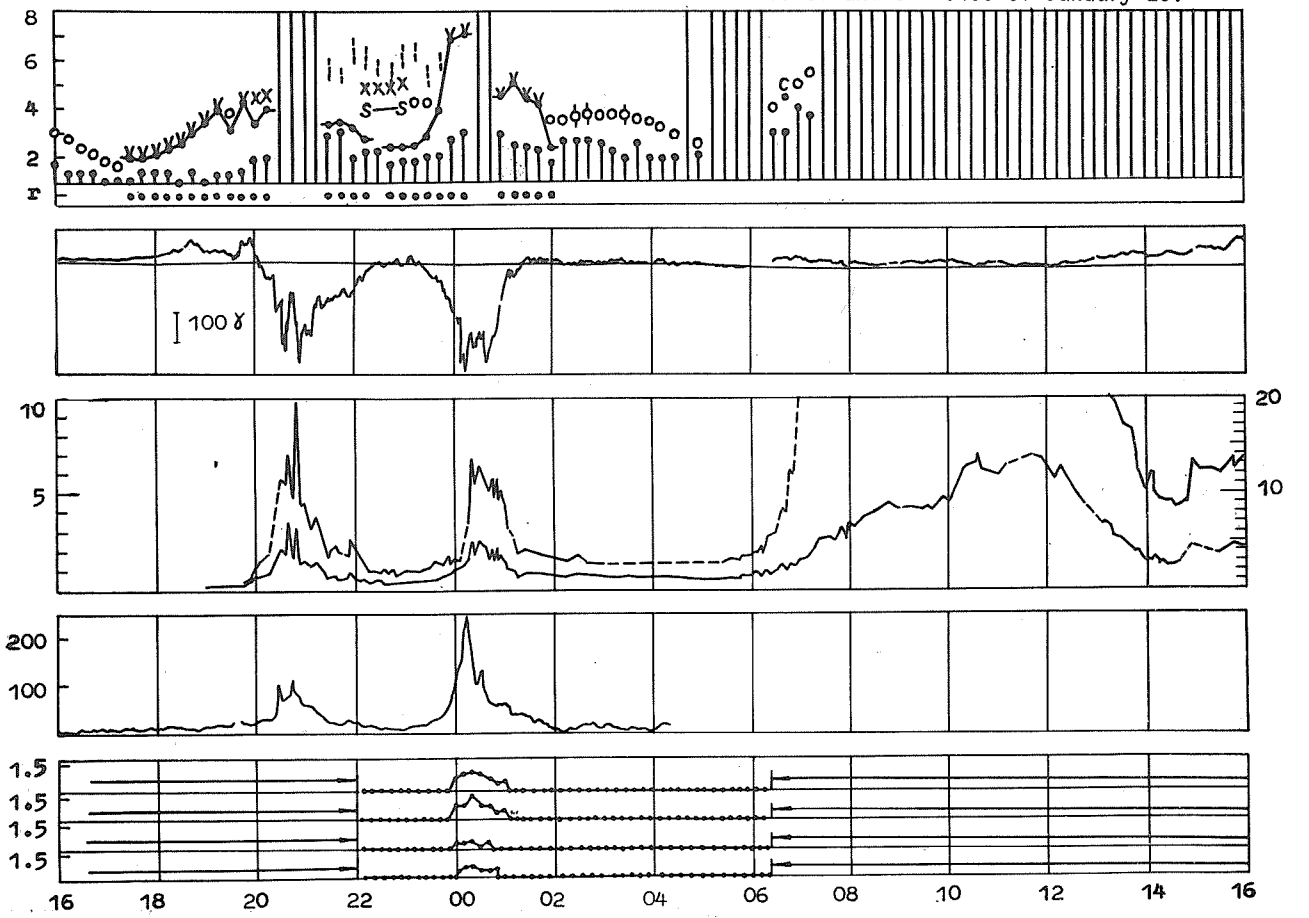

Fig. 4. Ground-based data January 24-25: f-plot, Murmansk ionosonde; geomagnetic H-component on this day and undisturbed level; riometers 25 and 9 MHz left and right scales, respectively; photometer (arbitrary units) and patrol spectrograph (scale in kR above the night sky level) (Loparskaya).

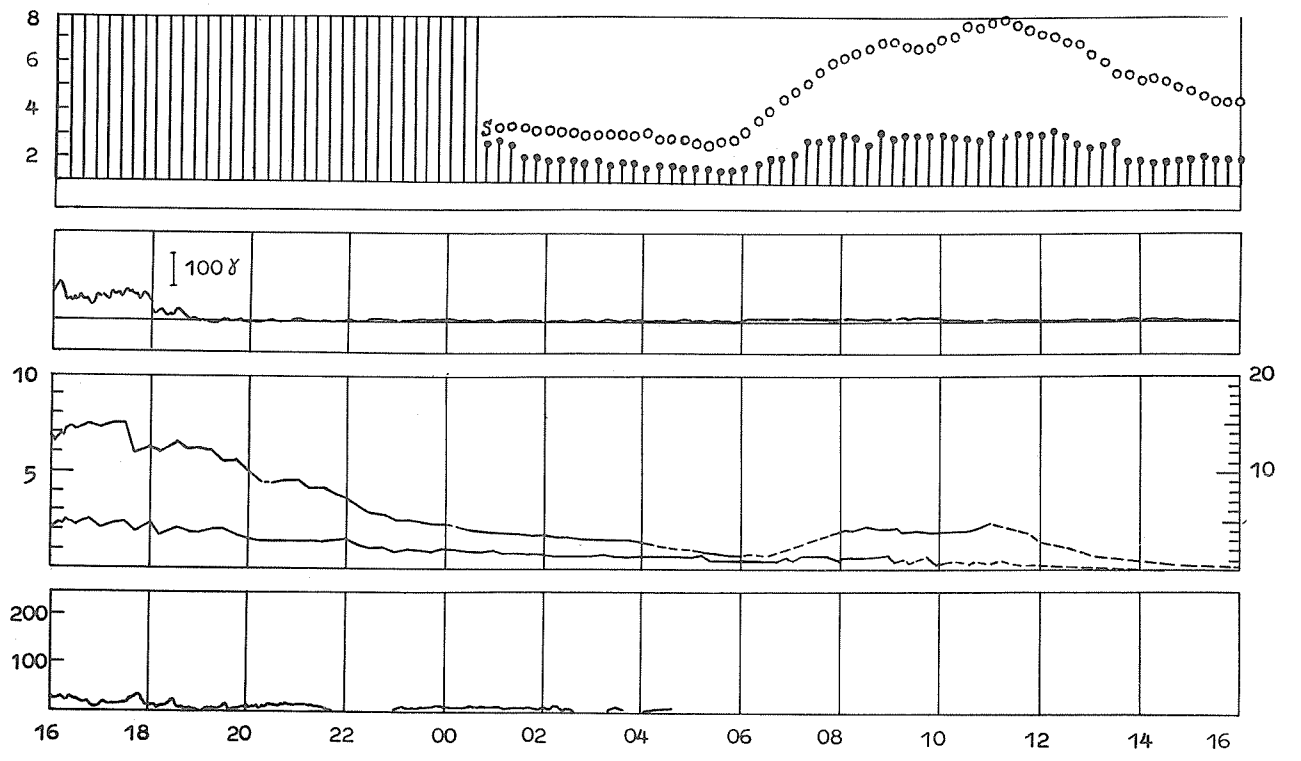

Fig. 5. The same as Fig. 4, January 25-26.

At 0640 UT the increase of the riometer absorption revealed all the features of a PCA: gradual change of absorption value, large day to night ratio (7 for the first day and 3.5 for the second one), day-time recovery well-defined on January 26, 1000 UT (Figure 5). Some unusual peculiarities are marked in the behavior of absorption in evening hours on January 26. The decrease connected with the transition to the night time conditions occurs rather fast. At 1400-1500 UT absorption passes through the minimum and then through a rather broad maximum. The time of minimum coincides with the positive magnetic disturbance. The deflection of absorption from the normal variation may be attributed to the change of cut-off rigidity or in other words the position of the boundary of the region of particle penetration into the polar cap. PCA values on January 26 were rather weak and decreased to zero near 1400 UT. The ionosonde on this day registered the signals from the F-layer despite the increased minimum frequencies. Behavior of the F-region did not differ significantly from usual.

Associated with the proton event a large magnetic storm took place on January 27 and 28 (Figure 6) with sudden commencement near 0430 UT January 27. First auroral disturbances began at 0700 UT as an absorption increase and positive magnetic bay. Second positive bay and associated black-out began at 1230 UT. During this bay in the twilight the all-sky camera shows aurora on the northern half of the sky. The following is the description of the development of geomagnetic activity and aurora during this night: Figures 7(1) - 7(12) present some key points. At 1515 UT there appeared a westward traveling (with velocity about 2.5 km/sec) loop opened to the east. Two successive locations of that are given in Figure 7(1). Between 1524-1527 UT a similar but less intense loop passed over Loparskaya (Figure 7(2)). This figure does not show other aurora located equatorward of the loop. Rather bright ray-structured arcs were also seen. Between 1541-1548 UT (Figure 7(3)) a new loop opened to the west appeared in the northern part of the sky. The positive magnetic disturbance, as was mentioned above, began near 1230 UT. The brightening of the aurora and the appearance of loops coincided with the negative magnetic bay superposed on the positive one. The behavior of aurora and geomagnetic field at this first phase of the storm (1515-1548 UT) is typical for the evening sector of an auroral oval: twice (Figures 7(1) and 7(2)) the northern part of the surge [Akasofu, 1968] passed over the Cola Peninsula moving slowly polewards, faster from the midnight sector of the auroral oval to the evening one. Figure 7(3) shows the southern part of the surge; the character of magnetic variation (negative bay over positive one) also corresponds to the passing surge [Akasofu, 1968].

At 1600 UT the luminosity of auroral forms decreased because of the shifting of aurora northward and southward from the zenith. The largest luminosity is observed near the southern horizon. At 1635 UT (Figure 6; 7(4)) the all-sky background luminosity suddenly increased. This increase is followed by the generation of a homogeneous arc drifting southward. At 1700-1850 UT (Figure 7(5)) the auroral form is seen mostly only near the south horizon.

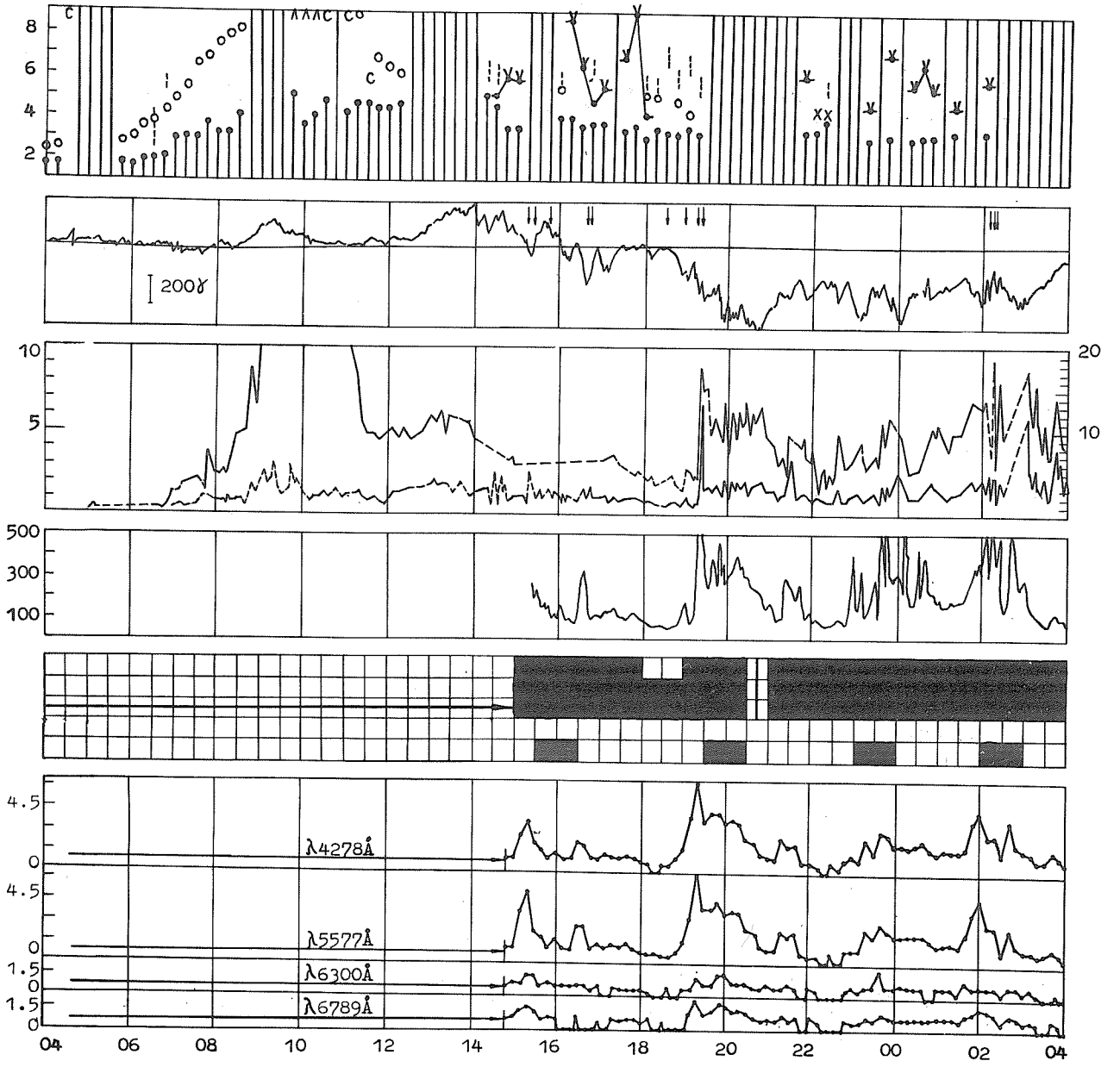

Fig. 6. The same as Fig. 4, but with changed scale values and additional ascaplot, January 27-28.

A southward location of the aurora indicates the development of a strong ring current. The magnetic field at this time is nearly normal. This does not exclude, however, the possibility that the decrease connected with the ring current is approximately equal to the increase of the field connected with the positive bay. The division of the zone into two separate ones near 1600 UT may be connected with an increase of the ring current. At 1845 UT the equatorial arc brightened. At 1851 UT (Figure 7(6)) began the poleward movement of the arc. There was a burst on the riometer and photometer and a decrease of H down to -230 γ. From this moment to the end of the storm the H value is always negative. At 1915 UT (Figure 7(7) - 7(9)) the strongest substorm began with an absorption value of 7 dB at 25 MHz with a sharp burst on the photometer, larger background and fast poleward movement of twisted rayed arcs. The poleward aurora boundary went out of sight. Between 2130-2250 UT aurora went to the southern part of the sky and the background disappeared.

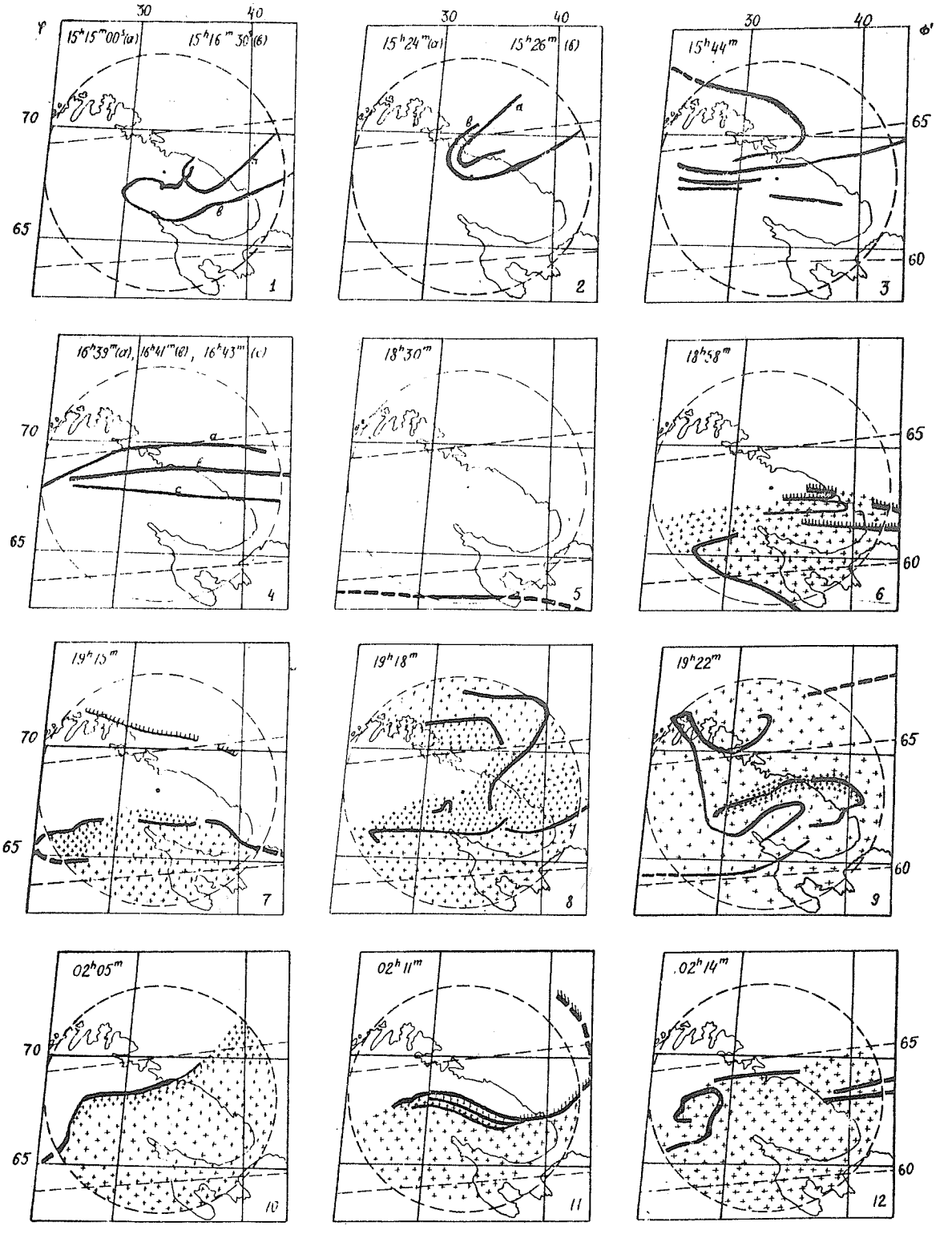

Fig. 7. Aurora maps for January 27-28. The position of homogeneous and rayed arcs is shown; the density of crosses shows the intensity of diffuse glow. The auroral height is assumed 100 km. Dashed circles define the basic field of sight of the all-sky camera. The peculiarities near border of frame are given by dashed lines.

The trigger disturbance appearing at 1851 UT before the main substorm seems interesting. In spite of a small amplitude this disturbance showed all the important features of a substorm. In the main disturbance it is unusual that the luminosity and absorption rates differ from the magnetic field one: a sharp increase of luminosity has no associated change in the magnetic field; the minimum of the magnetic field occurs at 2040 UT, i.e. delayed more than an hour as compared with the luminosity burst. At 2300-0200 UT January 28 occurs a number of bursts with poleward expansions and increases of the background. The burst with the clearest northern boundary formed by one arc or by the system of arcs is shown in Figures 7(10) - 7(12). Between 0300-0500 UT appeared auroral spots accompanied by irregular pulsations of brightness with a period near 10 seconds (Pi-1). These spots gradually shifted to the north horizon and their brightness decreased. Pi-2 pulsations also took place during this night, especially at 1948, 2254 and 0224 UT. The appearance of the spots and pulsations in the morning hours is typical for strong disturbances.

The above considered magnetic storm occurred after the solar proton burst, in spite of the existence of some individual peculiarities, it has all the characteristic features of a strong magnetic storm. The geophysical disturbances are observed at different longitudinal sectors of the oval thereby keeping the important features of an auroral substorm of corresponding oval sector.

REFERENCES

AKASOFU, S. -I. 1968 Polar and Magnetospheric Substorm, D. Reidel, Dordrecht, Holland.

BRUNELLI, B. E., L. S. EVLASHIN. S. I. ISAEV, L. L. LAZUTIN, G. A. LOGINOV, V. K. ROLDUGIN, G. V. STARKOV, N. S. SHULGINA, G. F. TOTUNOVA, and E. A. VASILKOVA 1971 Auroral-zone events of March 1970 on data of Cola Peninsula stations, World Data Center-A, Upper Atmosphere Geophysics Report UAG-12, 325-336.

Zenith Intensities of the OI 5577A and 6300A Radiation Inside The Polar Cap during the January 1971 Solar Particle Event

James G. Moore
Polar Atmospheric Processes Branch
Aeronomy Laboratory
Air Force Cambridge Research Laboratories
Bedford, Massachusetts 01730

The zenith intensities of the red and green lines of atomic oxygen at 6300A and 5577 A, respectively were measured during the nighttime hours of the period 24-28 Jan. 1971 with interference filter photometers. Calibration of the intensities was accomplished by a comparison with the absolute intensities measured by a calibrated spectrometer. The photometric data were scaled and absolute intensities of the emission lines and the ratio of 6300A/5577A radiation were determined and plotted by computer. The results are shown in Figures 1 and 2 for the entire observation period.

Examination of the figures shows the green line average intensity starting off at a value of approximately 300 Rayleighs on the night of the 24th and building to a value of 500 Rayleighs during the night of the 25th-26th Jan and then decreasing to a value of 250 Rayleighs on the 27th and 28th of January. This behavior is also reflected in the hourly averages of the high energy protons ($E_p > 60$ MEV) measured by Explorer 41 (See this issue) during this same interval as well as by riometer measurements at 30 MHz [Cormier, 1971]. This is typical of a polar glow aurora associated with a PCA [Sandford, 1963, 1967, 1969; Weill, 1962].

During certain times, the OI green line (5577A) shows rather sharp intensity increases. These are associated with discrete sun-aligned arcs as shown in a sample of frames from the all-sky camera film taken during this same interval, (Figure 3). The intense arc at 0445-0448 UT 27 Jan saturated the green line photometer, so the red-green ratios at this time are to be disregarded. A faint sun-aligned arc is seen on originals of the all-sky camera film at 0639-0643 UT and 0810-0814 UT 27 Jan 1971, although they are barely visible in the accompanying photographs. North is to the right and east is at the bottom in all photographs. The date and Universal Time are also shown. Some internal reflections of the orientation lights are also present.

The OI red line (6300A) shows enhancements throughout most of the night of 24-25 Jan which are not associated with corresponding enhancements of the OI green line (5577A). These are of the nature of undulations above an average intensity and are not associated with visual arc structures. The same situation obtains from 0830 UT-1240 UT 27 Jan and from 2100 UT 21 Jan to 1230 UT 28 Jan. Average intensities of the OI red line started out low and remained low until a slow increase around 0900 UT on 26 Jan. The red line was again high at 2100 UT on 26 Jan and

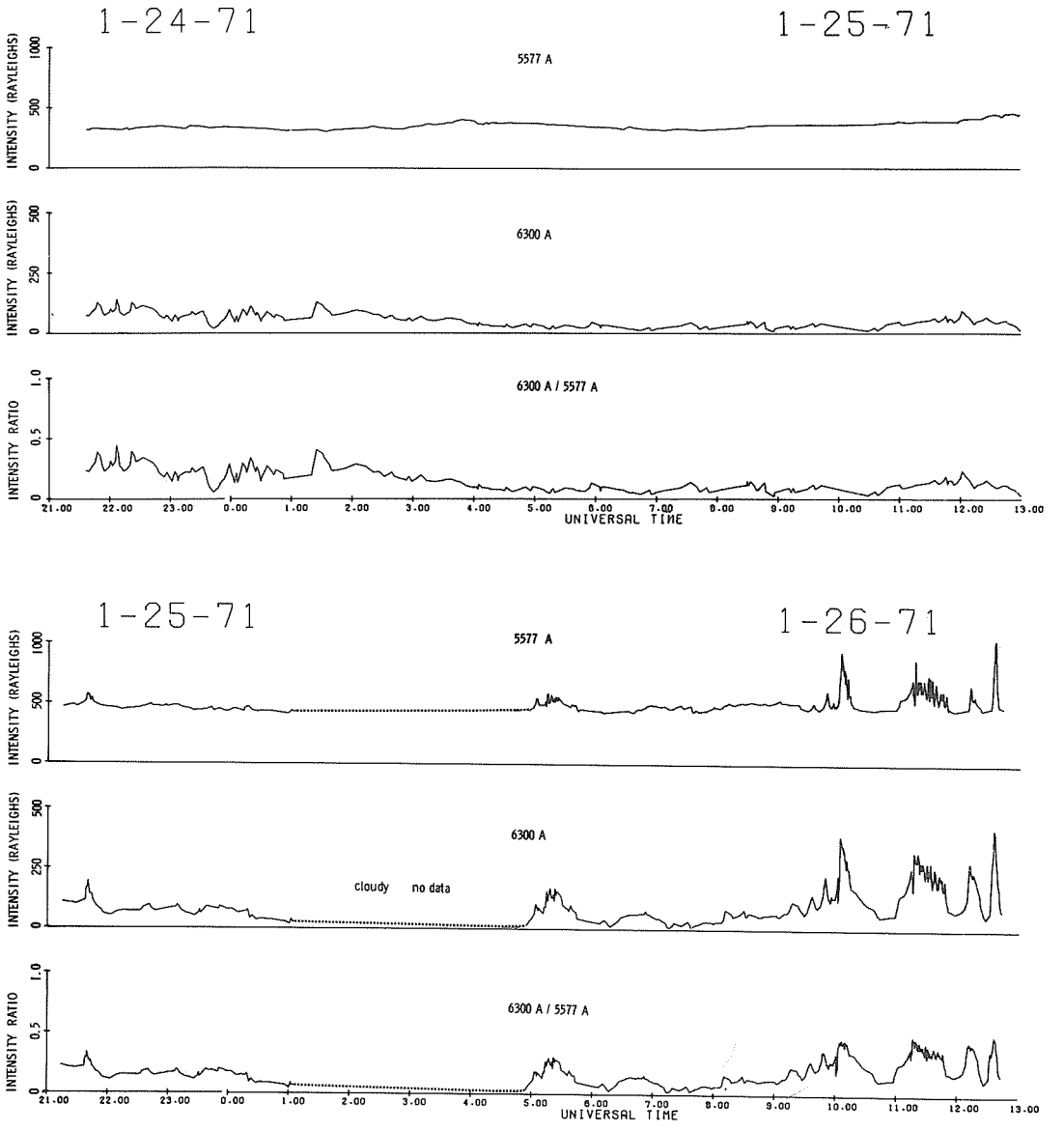

FIGURE 1 Zenith intensity versus Universal Time of the OI emission lines at 5577A and 6300A. The intensity ratio 6300A/5577A is also plotted. The dashed lines in the lower part of the figure represent a cloudy period when the data were not scaled. The period of sharp intensity increases in both the 5577A and 6300A curves are times when the presence of discrete sun-aligned arcs has been noted on the all-sky camera film.

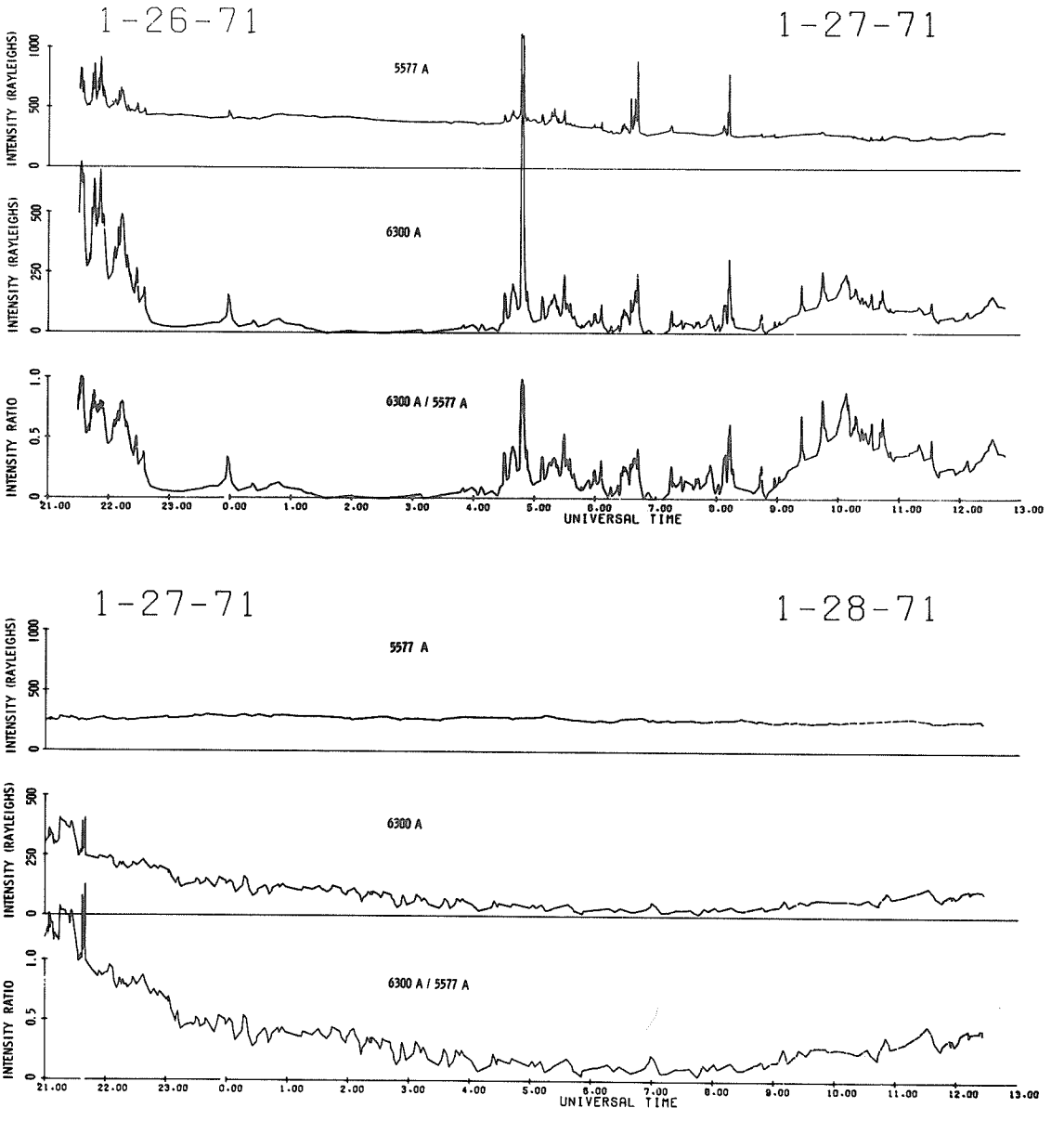

FIGURE 2 Zenith intensity versus Universal Time of the OI emission lines at 5577A and 6300A. The intensity ratio 6300A/5577A is also plotted. The period of sharp intensity increases in both the 5577A and 6300A curves are times when the presence of discrete sun-aligned arcs has been noted on the all-sky camera film.

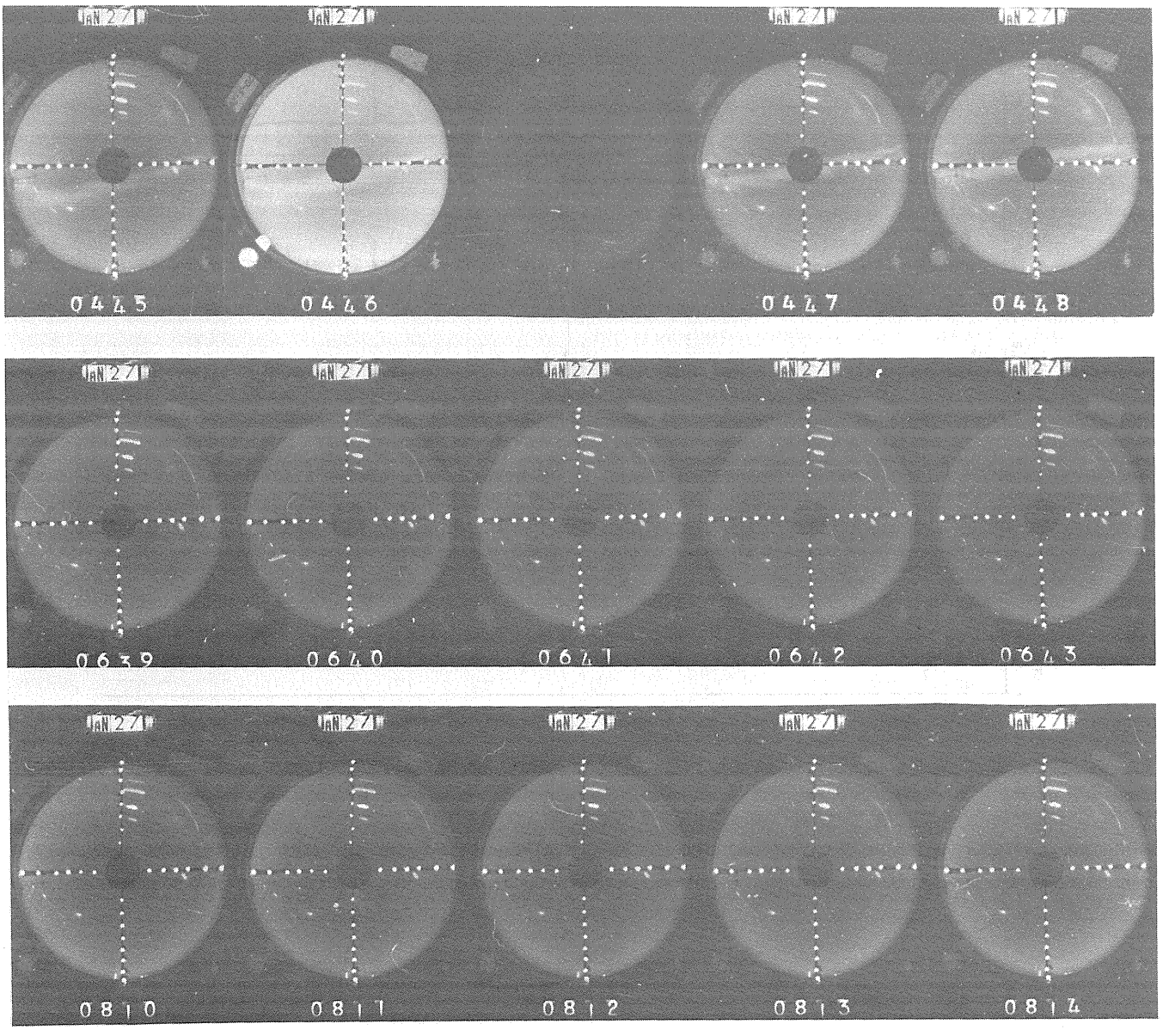

FIGURE 3 A reproduction of the all-sky camera film taken during January 27, 1971 at Geopole. Date and time in UT is indicated on each frame. North is at the right of each frame while East is at the bottom. Local midnight occurs at approximately 0422 UT. Discrete sun-aligned arcs are visible in the frames 0445-0448 UT and are barely visible in the frame at 0642 UT and in the frames 0811 to 0813 UT.

decreased rapidly to a low value at 2300 UT. It remained low until approximately 0900 UT on 27 Jan when an increase began. The red line remained high until a decrease began at 2100 UT on 27 Jan. There does not seem to be correlation (positive or negative) between Kp and 6300 in agreement with Sandford [1968, 1969] and Silverman et al. [1962]. Local magnetic K-indices, which have been found to be a much better parameter than Kp as an indicator of polar magnetic activity [Sharp et al., 1966; Feldstein and Starkov, 1967; and Sandford, 1968] were not available for correlation.

The red-to-green ratio (6300A/5577A) in the discrete sun-aligned arcs has been determined by integrating the intensities after the airglow levels have been subtracted. These ratios and the red-to-green ratios of the airglow as well as the ratio of the auroral to airglow ratios are listed in table 1 along with the Universal Time and the zenith height of unrefracted sunlight.

TABLE 1
Red-to-Green Ratios

Universal Time		Aurora	Airglow	Aurora/Airglow	Zenith height of Unrefracted Sunlight
2146	26 Jan	1.57	0.49	3.20	240 km
0645	27 Jan	0.62	0.11	5.40	900 km
0816	27 Jan	1.18	0.12	9.83	700 km

The height of lower bordersof weak-rayed arcs and bands in the polar cap has been determined to lie in the range of 145 to 180 km by triangulation from all-sky camera pictures [Starkov, 1968]. Examination of Table 1 shows that when the F region is illuminated 2146 UT 26 Jan, the red/green ratio for both the airglow and the aurora are enhanced over that obtained when the F region is not illuminated. The ratio of the red/green ratio in the aurora to that in the airglow makes this fact stand out more vividly. This indicates the vertical extent of the sun-aligned arc ranges from 145 km to F-region heights.

ACKNOWLEDGMENTS

I wish to thank personnel of the Polar Atmospheric Processes Branch, AFCRL, for operation of the optical equipment at Geopole and to personnel at Regis College for the data scaling. Mr. Gary Mullen of the Polar Atmospheric Processes Branch, AFCRL, has been especially helpful in computer processing of the data.

REFERENCES

CORMIER, R. J.	1971	Geophysics and Space Data Bulletin, Vol. VIII, No. 1, AFCRL, Bedford, Mass. 01730.
FELDSTEIN, Y. I. and G. V. STARKOV	1967	Dynamics of auroral belt and polar geomagnetic disturbances, Planetary Space Sci., 15, 209.
SANDFORD, B. P.	1963	Optical studies of particle bombardment in polar cap absorption events, Planetary Space Sci., 10, 195.
SANDFORD, B. P.	1967	Polar-glow aurora, Space Research, 7, 836.
SANDFORD, B. P.	1968	Variations of auroral emissions with time, magnetic activity and the solar cycle, J. Atmos. Terr. Phys., 30, 1921.
SANDFORD, B. P.	1970	Optical Emission over the Polar Cap, The Polar Ionosphere and Magnetospheric Processes, Edited by Skovli (Gordon and Breach, N.Y.).
SHARP, R. D., J. E. EVANS and R. G. JOHNSON	1966	Measurements of particle precipitation at the south pole, Planetary Space Sci., 14, 85.
SILVERMAN, S. M., F. WARD and R. SHAPIRO	1962	The correlation between the 5577A night airglow intensity and geomagnetic activity, J. Geophys. Res., 67, 2255.
STARKOV, G. V.	1968	Auroral heights in the polar cap, Geomag. Aeronomy, 8, 28 (English), 36 (Russian).
WEILL, G.	1962	Sur une aurore polaire d'un type nouveau, Compte Rendu Acad. Sci., Paris, 254, 3402.
WEILL, G.	1963	Une contraction de la zone aurorale antarctique observee au cours de la phase initiale des tempetes geomagnetiques, Compte Rendu Acad. Sci., Paris, 256, 985.

3914A, 5577A, and 6300A INTENSITY MEASUREMENTS AT THULE DURING JAN 24-29, 1971

WILLIAM N. HALL
POLAR ATMOSPHERIC PROCESSES BRANCH
AERONOMY LABORATORY
AIR FORCE CAMBRIDGE RESEARCH LABORATORIES
L. G. HANSCOM FIELD
BEDFORD, MASS. 01730

The figure shows the intensities of the 5577A and 6300A atomic oxygen and the 3914A band of N_2^+IN emissions recorded by the patrol spectrograph at the AFCRL Geopole Observatory, Thule AB, Greenland during JAN 24-29, 1971. The patrol spectrograph is a Perkin-Elmer model 173 developed for use during the IGY [Devlin et al. 1964] and the observing program used is essentially unchanged from the IGY and IQSY. The spectrograph integrates the optical emissions for the duration of the exposure and the intensity is reported as an average over the period of the exposure which may last up to 108 minutes every 2 hours. The first and last exposure of each night are less than 108 minutes and the exposure length is represented by the length along the time axis of the datum bar. Data for exposures of 11 minutes duration taken at solar depressions less than 12° during twilight are indicated by dots.

The triangles denoted SSC and SPE refer to Storm Sudden Commencements and to a Solar Proton Event [reported in Solar-Geophysical Data, numbers 318 and 324]. The time for the SPE refers to the time of enhancement of the 21-70 Mev channel on the ATS-1 satellite.

The 3914A emission increased rapidly after the onset of the SPE and decayed consistent with the behavior of Explorer 41 integral proton fluxes [Solar-Geophysical Data number 328]. Superimposed are twilight effects and enhancements associated with HIgh Latitude Discrete Auroras (HILDA's) following SSC's. The diagonal dashed lines at 0400-0600 UT on January 29 indicate the intensity was less than threshold of detection of the spectrograph and not a data gap.

The 5577A intensities were also enhanced during the SPE with further increases associated with HILDA's. These increases are in addition to a background level of 250-300 rayleighs before (not shown) and after the SPE. The behavior of both the 3914A and 5577A intensities was consistent with previous studies of the effects of SPE's [Sandford 1970].

The 6300A intensities showed typical diurnal variations [Stromman et al. 1971] with enhancements during HILDA's. The 6300A intensities did not show increases (and were not expected to) which could be associated with the SPE.

REFERENCES

Devlin, J. J., N. J. Oliver and A. Carrigan. 1964. Auroral Spectrograph Data; Vol. 25; Annals of the I.G.Y.; New York; Pergamon

Sandford, B. P. 1970. Optical Emission Over the Polar Cap; in The Polar Ionosphere and Magnetospheric Processes; 299-321; ed. by G. Skovli; New York; Gordon and Breach.

Stromman, J. R., B.N. Maehlum and J.K. Olesen. 1971. Storm Time Variations in the High Latitude Fluxes of Low Energy Electrons Inferred from OI (6300A) Observations; Planet. Space Sci.; 19; 540-543.

U.S. Dept. Of Commerce. 1971. Solar-Geophysical Data; No. 318, Part I, Feb. 1971; No. 324; Part II, Aug. 1971; No. 328, Part II, Dec. 1971, Boulder, Colorado

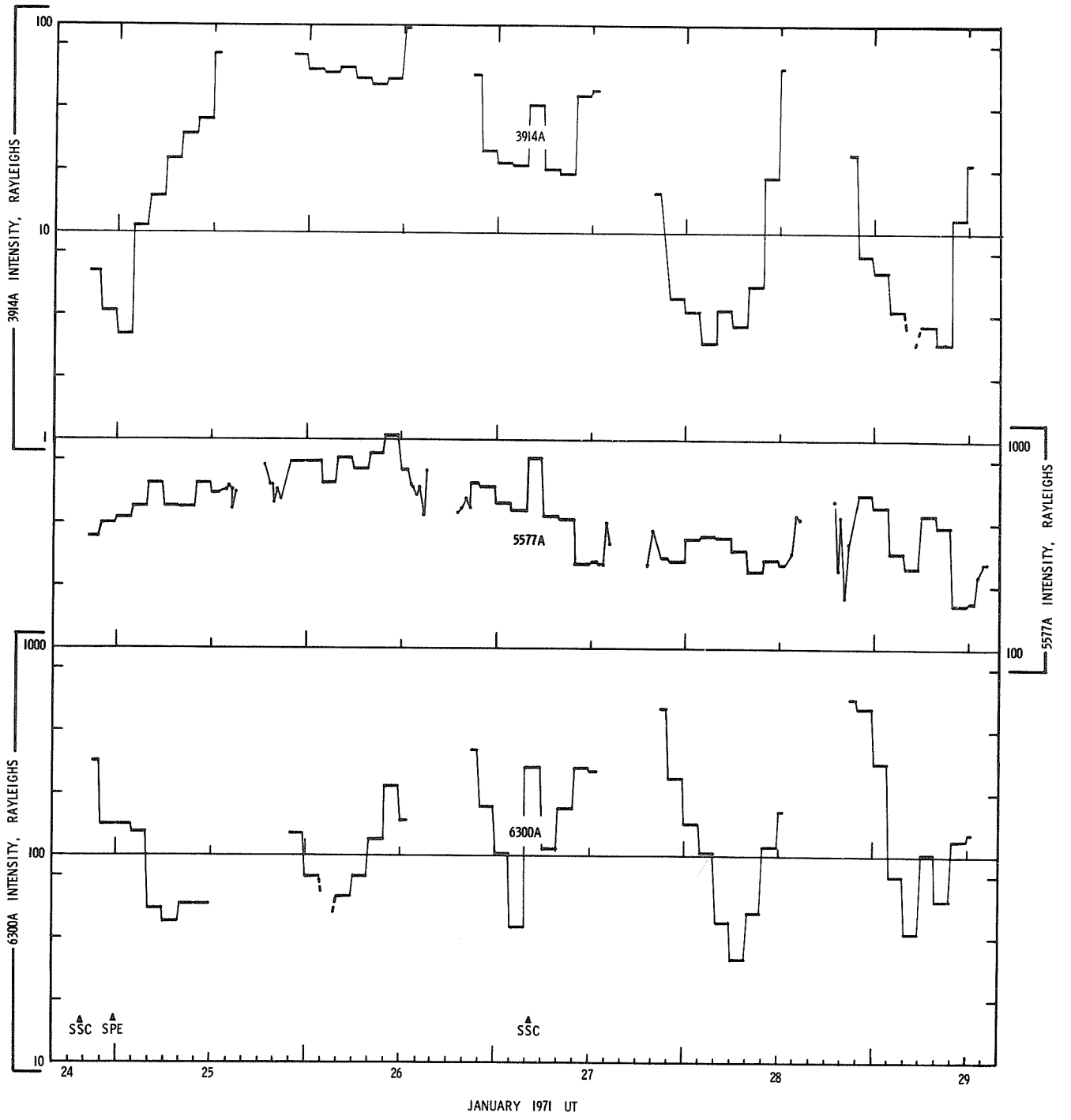

Optical Intensity Measurements at AFCRL Geopole Observatory, Thule AB, Greenland during January 1971

8. GEOMAGNETISM

Provisional Equatorial Dst

by

M. Sugiura
Laboratory for Space Physics
Goddard Space Flight Center, Greenbelt, Maryland 20771

Provisional equatorial Dst is plotted below for the period January 20-31, 1971. The Dst data presented here are provisional. The base line, which is based on extrapolations of the base lines for the four observatories, Kakioka, Hermanus, San Juan, and Honolulu, from the 1957-1970 series [Sugiura and Poros, 1971], will be redetermined later when the final Dst values are calculated.

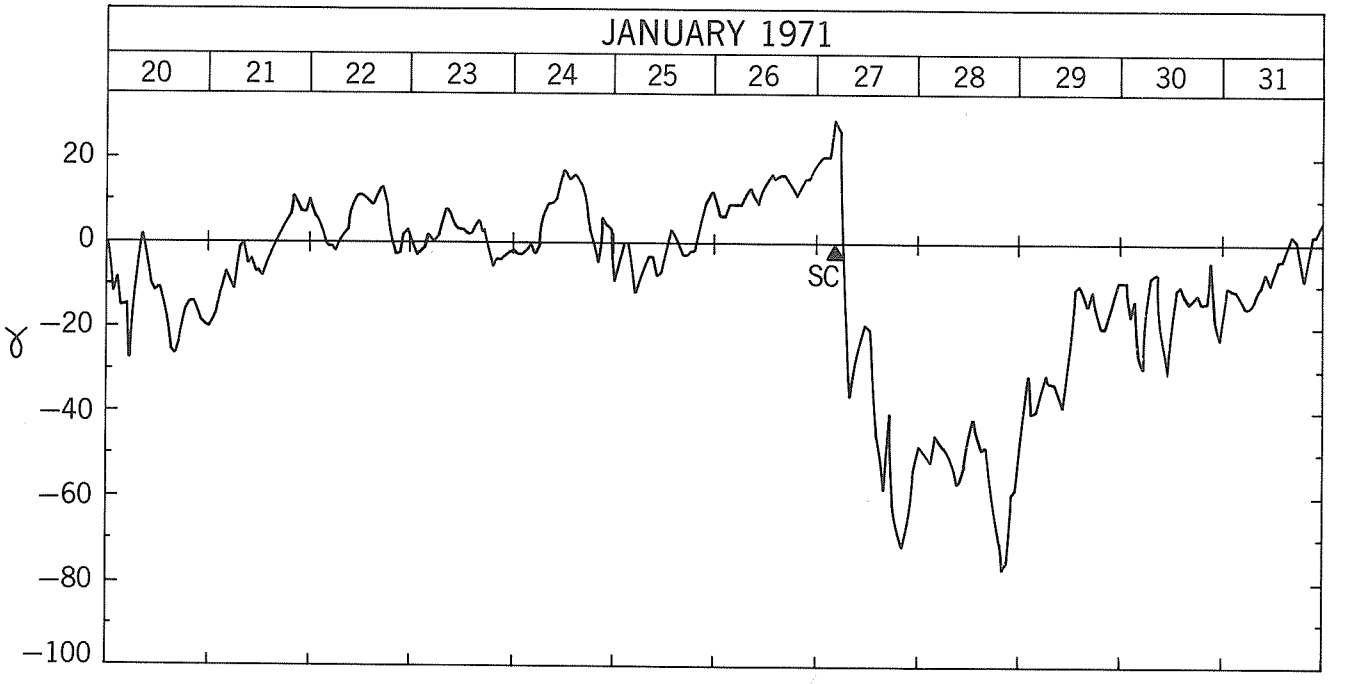

PROVISIONAL EQUATORIAL D_{ST}

REFERENCE

SUGIURA, M., and D. J. POROS — 1971 — Hourly values of equatorial Dst for the years 1957 to 1970, Goddard Space Flight Center, X-645-71-278.

K-Indices for January 23-31, 1971

by

D. van Sabben
International Service of Geomagnetic Indices
Royal Netherlands Meteorological Institute
DeBilt, Netherlands

The geomagnetic K-indices from the individual observatories for January 23-31, 1971 are given below. Please refer to IAGA-Bulletins 12, or IAGA-Bulletin 32 for definition of the symbols.

JAN

	23	24	25	26	27	28	29	30	31
BT	2333 2355	3334 4355	5444 4543	3313 2223	4665 5554	5534 4637	7544 4333	3444 3565	4444 6574
CC	3332 1543	3223 4544	5433 5542	2111 1212	2555 6665	4437 5766	6433 4543	5344 4656	3333 6564
DI	3332 1554	3323 4566	6443 4762	2211 1111	1466 7786	6646 6878	7334 4565	5545 5677	5444 5675
TI	3332 2653	2225 5455	4333 4652	2221 1211	2477 7988	4557 7989	6336 5665	4437 7667	4343 7785
PB	3232 3443	2316 5444	4436 4531	1111 1111	1564 6655	3457 5665	4426 4433	4326 4455	4475 5564
TR	4210 1223	4311 1266	5232 3430	0000 0101	1553 4465	5544 4556	6323 2244	5544 3266	4333 3365
GO	2323 2321	2223 3334	3444 4442	2222 1222	2454 5443	3444 4334	4323 3422	3524 4434	2234 5334
MM	3212 0132	2211 1166	5222 3330	1100 0000	0355 5675	6635 4677	7322 2254	4533 3366	4233 3365
KI	4111 1132	2111 1165	5221 2320	0000 0000	0454 5666	6644 5667	7322 2254	5533 3256	4233 3365
SO	3111 1232	2211 1154	5121 2330	0000 0000	0344 6676	6634 5667	7312 2243	4433 3255	3232 3354
WE	1110 0121	1114 4112	3223 3320	1000 0000	0376 8865	3457 7777	5326 3311	2225 6324	2163 5242
CO	1111 0221	1205 5122	3324 3420	0000 0000	0375 7645	3447 5656	4326 4311	3325 4433	2254 5333
RY	5432 2233	5422 2255	5553 3331	1111 1221	1574 6676	7655 5567	7533 2335	5634 4356	5354 3445
DO	3221 1222	1211 2143	3222 1320	0000 0000	0454 6665	5534 3767	6323 2223	3424 3254	2232 3243
YA	2321 1442	1325 5245	5333 3431	2110 0011	2556 5666	5537 5867	7336 3543	4425 6433	3353 6564
NU	3111 0122	1111 1133	3211 1220	0000 0000	0443 4554	4323 3656	5312 2233	3423 3344	2232 3443
LE	2111 0111	1201 1043	3110 1210	0000 0000	0343 4555	5533 3556	5311 1112	3433 2144	2132 2242
MG	2110 1322	1114 5134	4223 2321	0210 0000	1355 5643	4436 4765	6335 4432	3425 4345	3353 5443
LN	3222 2232	1222 2233	3222 2331	1101 1000	1444 4555	4333 3656	5323 2233	3434 3344	2233 4443
LO	3211 2221	1212 2143	3122 1320	0000 0000	0454 5554	4533 3567	5313 2223	3434 2354	2232 3343
SI	1120 0121	1114 3133	3323 2321	0000 0000	0375 7844	3447 5645	4325 4211	2325 4233	2263 3232
SV	2110 0232	0012 3244	3212 1330	0000 0000	0444 4444	4423 4666	4212 2332	3424 3354	3132 4342
RS	3221 1222	1222 2143	3222 1321	0000 1100	1444 4554	4332 3556	5312 2223	3434 2254	3232 3343
KN	3122 1333	1212 3244	3222 1331	1111 1010	1444 4455	4434 4656	5333 3333	3434 3354	3233 4453
MO	3121 2232	1212 2234	3222 1331	1111 1111	1444 4454	4333 3656	5323 2233	3434 3344	3232 4453
ES	3211 0221	1202 2044	3211 1210	0000 0000	0444 3444	4333 2446	4312 2222	3424 2244	3232 3343
ME	2121 0121	1113 3223	3223 2221	1110 1211	1497 6734	4556 5645	4325 3212	3436 4333	3274 3332
HL	3332 2333	2223 3355	4333 3332	2222 2222	2455 4444	4443 4445	3333 3333	4434 4454	3343 4344
MN	3211 1222	1212 2244	3112 1220	0000 0000	0344 4444	5333 3656	5312 2223	2425 2354	3132 3352
WN	3222 1132	2212 2144	4222 1321	1000 0100	1454 4555	5433 3656	5413 2233	3534 2254	3232 3443
WI	3221 1222	2212 2155	4221 1320	1000 1010	0454 4555	5533 3557	5423 2233	3535 3255	3243 3353
IR	2222 1332	1123 3234	3323 3331	1221 1111	2465 5555	4525 3656	5444 3433	2435 4455	3453 5443
SW	3222 2232	2222 3243	3222 2322	2222 2222	2444 4454	4333 3556	5422 2233	3434 3354	3232 3343
NI	3221 1232	2222 2144	3222 1320	1000 1000	1444 4454	4433 3556	5413 2233	3534 3354	2232 3343
VL	2211 2221	1212 2144	3122 1220	0010 1110	0344 4444	4432 2445	4422 2222	3434 2154	2132 3343
BE	3222 1232	1222 2244	3222 2321	1111 2111	1444 4444	4433 3656	5313 2233	3424 2354	2232 3343
HA	2221 1221	1211 2044	4211 1220	0000 0100	0443 3544	4432 2546	4422 3222	3434 2244	3232 3343
KV	3222 3332	1213 3244	4223 2331	1121 2110	1454 5454	5434 4656	5423 3333	3535 3355	3232 4453
MA	2222 1221	2113 1143	2221 2211	0000 0000	0343 3444	4332 2545	3322 2222	3434 3244	2222 3443
DB	3221 2221	1223 2144	3223 1221	1001 1010	1444 4444	4333 3546	4423 2223	3434 3254	3232 3343
PR	3221 1232	2212 2244	3222 1321	1011 1000	1444 4554	4433 3555	5413 2233	3434 3354	2232 3343
LV	2221 2223	2213 2333	2211 2321	1111 1121	2244 4434	4323 3445	3322 2223	3324 2254	3333 3342
KD	1121 0222	0032 3334	3222 1330	0020 0000	0455 5554	5314 6666	5323 3333	2425 4354	3132 4242
VI	1121 0121	1114 4122	3323 2220	0000 0000	0355 5543	4555 5443	5424 3221	3425 4324	2263 3332
NE	2121 0111	1103 3122	3323 1220	0000 0000	1365 5543	3545 3333	4313 3211	3424 3333	2253 2332
FU	2211 1121	1211 2143	3212 1211	1110 0100	1433 3444	4422 2545	4312 2222	3424 2244	2232 3232
CF	3212 1222	1201 2144	3221 1221	0000 0000	0444 4444	4333 3545	5422 3223	3424 3244	3233 3343
HB	3112 2222	2223 3244	4223 1321	1021 2000	1444 5454	5433 3656	5423 3233	3535 3354	3232 3453
UB	2222 1332	2123 4244	3232 3331	1321 0001	3465 6655	5535 4666	5444 4433	3436 5455	3453 5443
JO	2221 1111	1212 2133	3222 1210	0000 1100	0343 3334	3443 2337	4312 2211	2425 3234	2132 2222

SA	3121	1222	2323	3133	4322	3333	2310	1112	2465	5553	3455	4555	5334	4323	3435	4345	3342	4343
TY	3322	3222	2223	3344	3223	2322	1132	2111	1544	5454	5443	3556	5433	3233	3535	3354	3332	3353
OD	3222	1331	2213	2244	3223	2330	1111	1111	1454	5454	4423	4555	4323	2333	3435	3355	2243	4343
KK	2221	2222	----	----	-323	1332	3423	2122	3454	5444	4444	5655	3343	3332	3435	3544	4343	4342
OT	2210	1111	1122	2033	3222	2110	0000	0000	0453	4433	5454	4326	3312	3212	3425	3124	3253	3222
SU	2122	3322	1223	3344	3213	1321	1020	1111	0444	5335	4423	4555	3223	3322	3335	3255	3142	3242
GC	3121	0121	1212	2144	3221	1320	0000	0000	0444	5454	4433	4546	5423	2223	3435	3254	3243	3343
MT	2111	1220	1113	3133	3222	3220	1100	0000	1365	5543	3325	3545	5324	3322	3435	4244	2242	4332
VK	2422	1333	1333	4224	4432	3322	2222	2222	3565	5553	3435	4655	5443	3333	3426	4445	2243	4443
AT	3331	2332	1333	3244	4323	3431	1133	1111	2455	5555	4535	4656	5334	4323	3446	4355	4244	4442
LG	3210	0121	1102	2045	4211	1220	0000	0000	0443	4444	5532	2546	4422	1122	4523	2255	2242	3343
AQ	3111	0122	1111	1044	3221	1221	1000	0000	0343	5444	4322	4545	5312	2223	3424	1254	3132	3342
TF	2212	2231	2324	3244	3223	2431	2233	2111	2445	6544	4433	3655	5333	3323	3335	3255	3243	4342
TK	1001	0221	0101	2133	3222	2430	0000	0000	0565	6554	4324	4656	5314	4323	2435	4355	3243	4342
IK	3111	1121	1212	2144	3222	1321	1000	0000	0443	5444	5333	3555	4322	2232	3424	3354	2132	3342
CI	2211	1121	2212	2043	3233	1210	1000	0000	0444	5444	4432	3436	4423	2323	3424	3254	3232	3243
TL	2221	0211	1101	2143	3111	1210	0100	0100	1333	2324	4422	2435	3211	1212	3313	2154	1131	3143
FR	2211	1111	1222	2033	3322	2122	1000	0100	0443	4343	4443	3325	4322	2212	3425	3234	3152	3232
PE	3101	0111	1121	1033	3211	1220	0000	0100	1353	5344	4333	4546	5323	3223	2424	2254	2131	3342
AK	3332	1222	3212	1133	3322	2432	2222	1000	0444	5655	5445	5665	5544	3443	3324	4443	4433	3332
SM	2232	2222	2222	2244	3223	2321	2122	2221	2344	4334	3533	2335	4322	2322	3334	3254	2233	3333
AE	2223	2120	2213	3344	2123	2320	1112	3300	0443	5334	4333	5446	2323	3323	3414	3244	3032	3343
SF	3222	3232	2223	3444	3233	2331	1014	3321	1443	5445	5434	5547	3323	4---	----	----	----	----
KA	1111	1221	1113	3234	3222	3321	0100	0000	1464	4433	3334	3544	5223	3322	3425	3234	2132	4332
KS	3122	1221	1112	2144	4222	2432	2111	1111	1554	7535	5433	3556	5332	3312	4435	3355	3242	4343
AV	2212	1111	1211	1133	3122	2211	1111	1110	1444	3433	3333	4436	3323	2222	3423	3244	2132	3232
DS	2222	1212	1223	3143	4333	2221	1000	0111	1454	5454	4544	4434	6423	3312	4535	3235	3253	3333
TU	2221	0211	1213	3133	4232	1321	1000	0000	1454	5443	3444	3323	6423	3211	3515	3235	2242	2233
KY	1111	0221	1113	3134	3222	3320	0100	0000	0465	4433	3334	3534	5323	3322	3425	3234	2232	4332
QU																		
ML	2224	2333	2223	3344	4332	2322	1232	2112	2556	6434	5433	5556	4333	2223	3335	3354	3334	3343
SZ	2111	1121	1112	1332	2221	2111	1001	3111	1433	6434	4334	4436	3322	3322	3423	3344	3123	2343
LP	2211	1221	2322	3233	4432	3332	2111	1111	3475	5453	3344	3635	4343	4333	4446	5333	4343	4333
TA	2111	1122	1101	1043	31-1	1311	----	----	---3	5444	43--	3446	2312	2223	34-4	2144	---2	2343
HO	2120	0122	1213	2033	3212	2121	1000	0000	0463	4432	4334	2333	4323	1212	3423	3234	3242	2222
TE	1222	2132	1211	2143	4332	3323	2112	2243	2453	4452	2544	3455	5332	3222	3535	2---	----	-322
AL	2222	1232	1213	3233	3232	2431	1111	1111	0464	6444	3213	4546	4332	3323	3336	3354	2233	3342
SJ	0100	0100	1100	1133	3320	0010	0000	0000	0443	4453	2423	2434	5322	2212	3334	1235	3131	3221
MB	2111	1231	1111	2133	2212	1221	1001	1111	1443	5543	3224	5435	3412	2322	3422	3334	3122	3232
MU	3322	2222	2333	3233	4432	3333	3220	1011	4575	5454	2334	4634	4433	4333	5546	4333	4443	4333
GU	2222	1111	1223	3123	4222	2211	1101	0001	1464	4332	3214	2533	3323	3322	5425	4223	3232	3223
BA	2010	0122	1100	1043	2221	0321	1000	0000	0444	6324	4322	2446	2322	2223	3322	1244	3120	3342
MC	2021	2022	1103	2044	2221	2221	0000	0000	0444	6443	4422	2445	4212	2222	3423	2244	3234	3242
TG	4353	2222	3241	2132	5443	3431	3232	0011	5565	5453	2354	3625	4343	4333	5546	4343	5252	4333
LU	1010	0221	1112	2233	2221	2320	0001	3320	0433	5554	3211	3455	1211	2222	3334	2233	2122	3232
PM	2111	0121	1223	3124	3222	2221	2210	0011	1464	4443	3315	3533	2323	3321	4425	2234	2232	3232
HU	1111	2443	1222	3344	3222	2442	1001	2332	0443	4655	4433	4455	5323	4422	3433	4434	3223	4432
PP	1110	0011	0102	2032	2221	1011	0100	0001	1352	3422	3313	2323	4323	223-	3423	2133	2131	1122
TN	2223	2322	2133	2333	3333	3331	2132	2201	2344	6335	3323	3555	3233	3313	3335	3253	3333	3232
PI	1100	0211	1100	2---	----	-321	1000	0220	0454	4453	4433	3364	5422	3423	4434	3335	3333	3334
GN	2021	0321	1103	2234	4222	2340	1000	0001	2343	6544	3215	3654	5334	2322	4423	3243	2221	4223
HR	2122	1221	1203	2143	3222	3331	1001	0000	1345	5543	3323	4446	3224	3313	3434	4243	2133	4242
AC	----	----	----	----	----	----	----	1111	1553	5544	3322	3324	5322	34--	4322	2224	3222	3333
TO	3231	1221	2213	3234	-332	2220	-210	0001	1563	5533	3325	4544	4434	3321	3434	3234	2332	3233
AM	1221	0100	2303	3012	4332	0110	0000	0000	1563	4421	2334	4433	4423	1100	3534	3124	2342	2232
TW	1111	1322	1201	1133	3231	2331	1000	0120	1553	5443	3423	4344	5323	4433	4333	2334	3223	3342
MI	233-	0321	2325	5224	4443	3421	2111	0022	2585	7764	4447	6677	3426	3322	3525	5434	3353	6342
MY	4454	4333	3545	4245	5655	4432	2323	2223	3776	4344	5554	4635	5554	3423	4676	4365	4666	4344
MW	4543	2353	3543	4375	6552	4432	2211	1222	1584	4545	6564	5656	6433	3334	5645	3367	4553	4454
NL	3211	1221	3222	3244	4332	2231	0111	2212	1354	4456	6553	2577	5522	2323	3734	3246	3333	3333
SB	3332	3444	3423	3346	5443	3453	2211	2234	3454	4543	4434	3334	5333	4433	4435	4444	4342	4554
VO	3344	4332	3443	4334	5454	4432	2233	3222	2556	4442	4444	4334	5434	3312	4454	4344	3344	4333

Solar Wind Velocities and Geomagnetic Activity Associated with the Cosmic Ray Increases of January 24, 1971 and September 1, 1971

by

S. Krajcovic
Geophysical Institute
of
The Slovak Academy of Sciences
Bratislava, Czechoslovakia

Initially, we consider the geomagnetic activity from January 17, 1971 to January 31, 1971. The beginning of this critical period is characterized by one Q day (maximum Kp = 3-; minimum Kp = 0+; ΣKp = 13-). The five following days (Jan. 18-22) are characterized by disturbances with ΣKp values lying between 16o and 32-. January 23, 1971 is a Q day of the order of 13o for ΣKp. The two following days are comparable with respect to the geomagnetic activity with the days of the preceding subperiod (before Jan. 17) and are followed by one Q day with the minimum magnetic activity of the total critical period, i.e. ΣKp = 2+.

On the beginning of January 27, 1971 there appeared an ssc at 0024 UT of an important magnetic storm, the duration of which is about two days. The sum of planetary K-indices decreased on January 29, 1971 to the value of 22-, and then it was followed by one disturbed day (January 30, 1971) which has evidently no association with the cosmic ray increase on January 24, 1971. All of this is illustrated on the upper part of Figure 1.

The second critical period analysed in the present paper begins on August 25, 1971 and ends on September 8, 1971. This situation is shown in the lower part of Figure 1. At the beginning of this period two normal days are followed by two quiet days, August 27-28, 1971. Two more normal days follow these. The end of August 1971 is characterized by an important disturbed day (with respect to September 1, 1971) during which the maximum ΣKp reached the value of 33o.

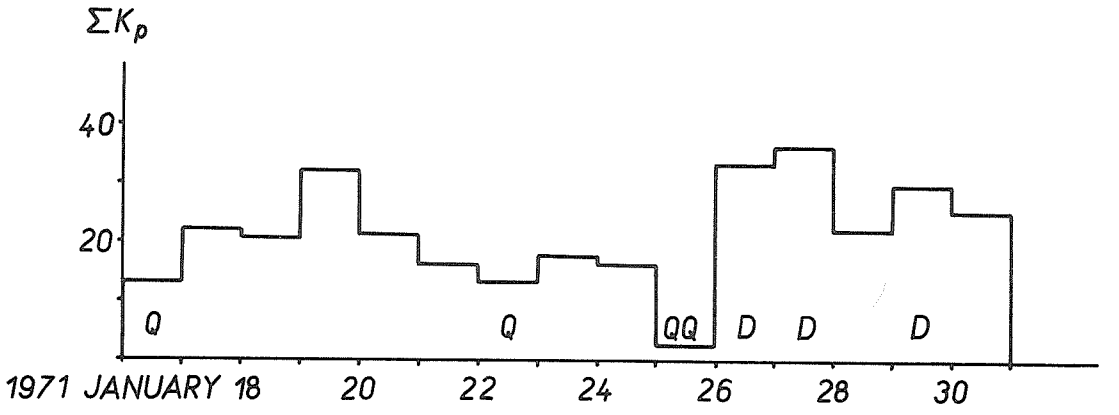

Fig. 1a. Geomagnetic activity of the period January 17-31, 1971 as characterized by ΣKp for each day. D, Q and QQ refer to disturbed, quiet and very quiet days, respectively.

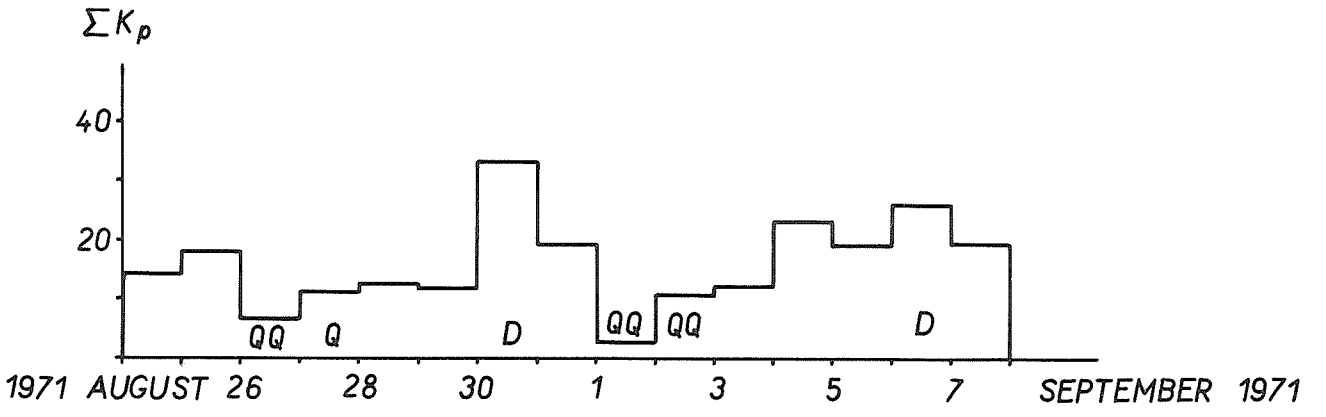

Fig. 1b. Same as Figure 1a for the period August 25-September 8, 1971.

Even if the day of September 1, 1971 is termed a normal one, it is very important to notice that the values of three-hour indices are of order of 2o, i.e. they are practically on the threshold of the disturbed subperiod.

The most important difference noted in comparing the geomagnetic activity of the critical days of the above mentioned periods (namely, January 24, 1971 and September 1, 1971) is the following:

a.) September 1, 1971 is preceded by one disturbed day and followed by two QQ days, then by one day that is rather quiet;

b.) January 24, 1971 is preceded by one quiet day and followed by one normal and one quiet day, this subperiod preceding an important geomagnetic storm (see Figure 1).

It is noted that the disturbed day on September 7, 1971 has evidently no association with the studied cosmic ray increase of September 1, 1971.

In Figure 2 we can see the time distribution of the solar wind velocities registered during both studied periods aboard Vela 3 and Vela 5 satellites (three hours or daily averages) and aboard Pioneer 6 and Pioneer 7 satellites (hourly averages during selected days).

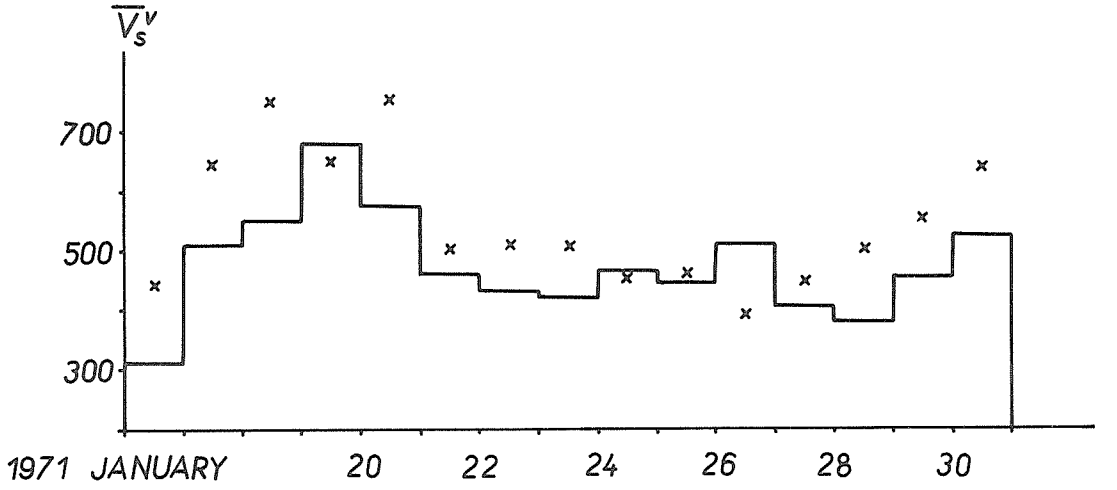

Fig. 2a. Time distribution of the solar wind velocities for the period January 17-31, 1971. Vela 3 and Vela 5 values (heavy line) are three hour or daily averages. Pioneer 6 and Pioneer 7 values (x's) are hourly averages during selected days.

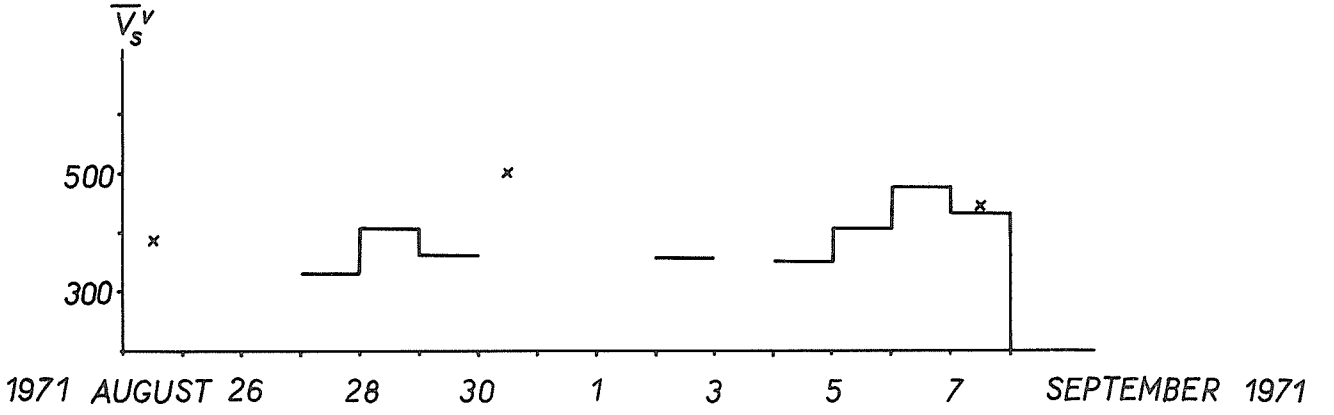

Fig. 2b. Same as Figure 2a for the period August 25-September 8, 1971.

By comparing Figures 1 and 2 we can state that the correlation among the solar wind velocities and Kp-indices is rather good. In addition we note that the solar wind velocities observed aboard Pioneer 6 and Pioneer 7 are, generally speaking, greater than those observed aboard Vela 3 and Vela 5 satellites. The reason for this is evidently the fact that the Pioneers' solar wind velocities are averaged over shorter time intervals (one hour) than those of the Velas' (three hours or one day).

The time distribution of cosmic ray increases for the above mentioned periods is plotted on Figures 3a and 3b, respectively. The curves represent only the smoothed values of cosmic ray indices (pressure corrected smoothed hourly totals) of Alert Neutron Monitor for selected periods which are published in "Solar-Geophysical Data".

At first glance it seems that both curves plotted on Figure 3a and 3b, respectively, are very similar, but in fact they vary greatly. The first curve (Figure 3a) is characterized at its beginning by the mean level of cosmic ray indices of the order of 104-106%. At the end of the "critical" day, we observe a sudden increase of cosmic ray indices to the level of 115%. After maximum, it decreases again in about 6 hours to 106%, remaining at this level for about two days. On the beginning of January 27 we observe a sudden decrease, the minimum of which is reached at noon of the following day. Recovery to the previous level begins on January 29, 1971 and is accomplished by noon of January 30, 1971.

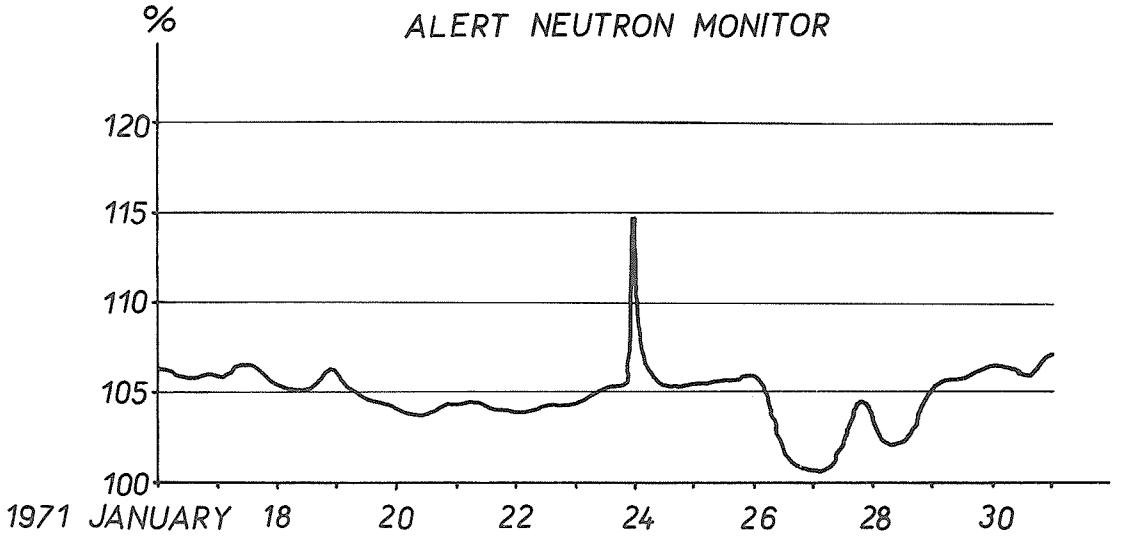

Fig. 3a. Time distribution of cosmic ray increases for January 17-31, 1971 from the Alert Neutron Monitor (pressure corrected smoothed hourly totals).

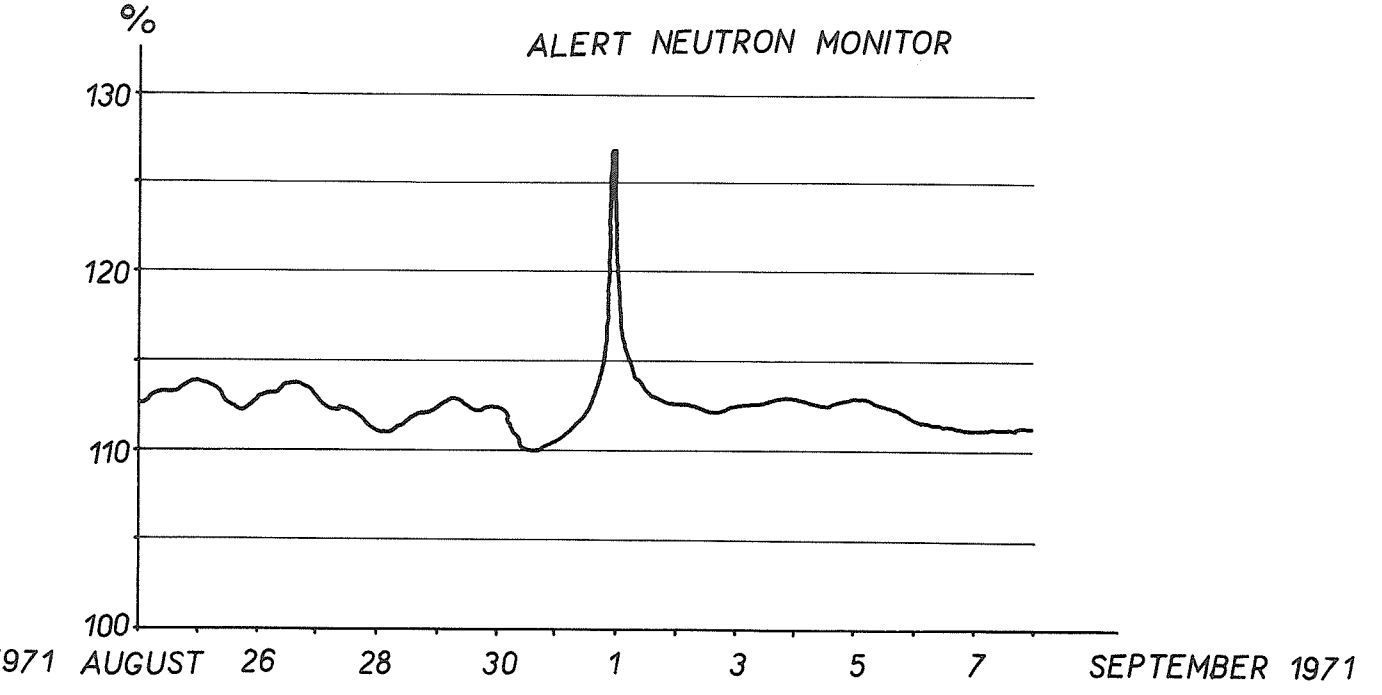

Fig. 3b. Same as Figure 3a for the period August 25-September 8, 1971.

Notice that the days of January 27-28, 1971 are the days when an important geomagnetic storm was registered on the Earth's surface. Thus we are correct in stating that the above mentioned depression of cosmic ray indices was caused by a stronger interplanetary magnetic field that had occurred during the period of geomagnetic storm. The above mentioned depression of cosmic ray indices was seen by other cosmic ray stations, e.g., Calgary, Deep River, Sulphur Mountain, etc.

The situation on the second "critical" day (September 1, 1971) is quite different. The first interval of this period is characterized by an oscillation of cosmic ray indices among the range of values 112 to 114% and then by marked increase to 127% on September 1, 1971. The value of the cosmic ray indices decreases during the next 12 hours to 112% and then oscillates among the values 112-113% until September 7, 1971, when the earlier level is again reached.

In this case the cosmic ray increase was not followed by a geomagnetic storm observable on the Earth's surface. The reason for this is found in the location of the eruption on the solar surface, about 39° behind the western edge of the solar disk, while in the January analyzed data the position of the eruption as a source of solar cosmic radiation is defined by the coordinates N19 W50.

The occurrence of a magnetic storm in the second case can be confirmed only on the basis of the measurements aboard Pioneers and Velas, respectively, of solar wind velocities and proton densities. These data were not available at time of preparation of this contribution.

In conclusion, it is evident that the experimental data obtained by other scientists in space experiments or in ground-level observations, when published, can contribute to a more complete analysis of the above mentioned events of cosmic ray increases and related phenomena.

Recurrent Tendencies in Geomagnetic Activity at the Time of Increased Cosmic Radiation at the Earth's Surface on 24 January 1971 and 1 September 1971

by

Jaroslav Halenka
Geophysical Institute
Czechoslovak Academy of Science
Prague, Czechoslovakia

The purpose of these comments is to show whether and in what way recurrent tendencies are reflected in geomagnetic activity in the neighborhood of the studied GLE's. These may contribute independent data on the nature of the interplanetary medium with a view to the propagation of solar energetic particles.

GLE 24 January 1971, Day 22 of Geomagnetic Rotation No. 1880

The effect occurred in a weakly disturbed interval with slight geomagnetic activity. On the 0 day (24 January 1971) ΣKp = 17+ (Ap = 10). Kp = 4o in the first three-hour interval of day +1 was also the highest value over the whole interval from day -3 to day +2. On day 22 of the previous (-1) rotation ΣKp = 24o with Kp max = 4+, thus showing weak geomagnetic activity. In rotation -2 around the 22nd day there was a marked minimum of geomagnetic activity (29 November - 2 December 1970, the first half of the day), which reflected the complete absence of an external perturbing factor. In the +1 rotation after the GLE there was weak stable geomagnetic activity, ΣKp = 16 and Kp max = 3o; the +2 rotation showed slightly increased geomagnetic activity with an ssc and Kp max = 5- on day 22; climax occurred in the +3 rotation with an ssc on day 21 and Kp max = 8- during the last interval of day 21 and subsequent Kp max = 7- during the first interval on day 22 with ΣKp = 33o (Ap = 36). The decrease of geomagnetic activity during the +4 rotation terminates the series of disturbances.

The investigated case occurred between two clearly recurrent increases of geomagnetic activity, also commencing with ssc on days 16 and 25, in which the activity of longer duration was on a moderately increased level. It is separated from them on both sides by well-defined decreases of geomagnetic activity on days 21 and 24, which can be observed during several rotations. The repetition of some of the details in the course of the geomagnetic activity, which might have a recurrent nature, for the immediate vicinity of the studied effect is shown in Figure 1. For the moderate smoothing of the random fluctuations of the Kp-index, running means over three consecutive three-hour intervals were applied. The long-term comparison of the daily sums of Kp on days -1, 0 and +1 during rotations Nos. 1873 to 1887, shown in Figure 3a, is remarkable and indicates that the agent causing the geomagnetic activity displayed systematically similar properties over a comparatively wide interval of 3 days during the individual rotations.

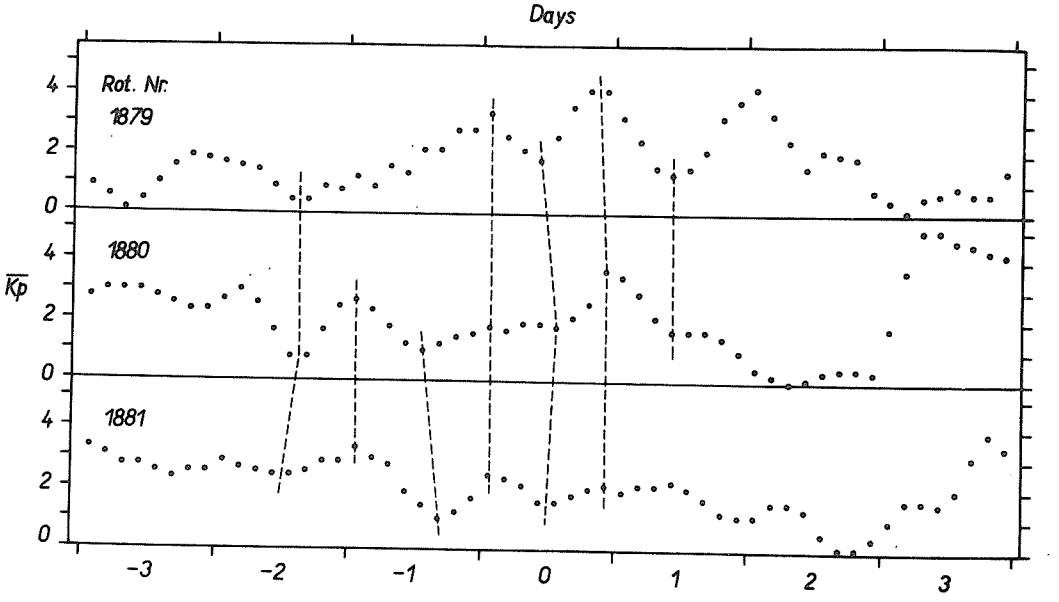

Fig. 1. Kp for rotations 1879-1881.

GLE 1 September 1971, Day 26 of Geomagnetic Rotation No. 1888

The effect occurred during a weakly disturbed period at the time of the decline of activity. On the day 0 (1 September) ΣKp = 19o (Ap = 10), the Kp max = 5o in the first and eighth three-hour intervals of the preceding day also represent the highest values within a wide interval around day 0. An ssc occurred in the eighth interval on day -2. In the previous (-1) rotation on the day 26 ΣKp = 18- with Kp max = 4+ and weak activity on the decline similar to rotation -2, in which the series of disturbances appeared at an even lower level of activity; however, an ssc was observed on day 25. The characteristic feature of the investigated case, the decreasing nature of the degree of disturbance in the course of day 26, was also preserved in the +1 rotation (ΣKp = 18o) and partly also in the +2 rotation, when the series of disturbances was terminated.

The investigated event was separated at both ends from the neighboring activity by marked, clearly recurrent decreases of geomagnetic activity on days 24 and 27, which can clearly be observed in many rotations. The repetition of several details in the close vicinity of the studied event, which might have a recurrent nature, is shown in Figure 2, again with the help of the curves of the Kp-index smoothed by running means over three three-hour intervals. The comparison of the daily Kp-index sums on days -1, 0 and +1 during rotations Nos. 1881 to 1894 is illustrated in Figure 3b, and in comparison with the GLE of 24 January 1971 is not as good, which shows that the agent causing the geomagnetic activity could have had different properties in the transverse direction in some of the rotations during the appropriate three-day interval.

On the whole it may be said that the recurrent tendencies in the fine time structure of geomagnetic activity in the closest neighborhood of the investigated events was not particularly marked. However, it was at least outlined. As regards the occurrence of increases and decreases of geomagnetic activity over the period of several days around both GLE's, the recurrent tendency is indisputable in general features. One may assume, therefore, that in the corresponding intervals the conditions for the propagation of energetic particles (particularly as regards the GLE of 24 January 1971) were comparatively stable over a long period, and that with a view to the geomagnetic activity in neither of the cases was there a question of forming a substantially new structure within the appropriate sectors of the interplanetary medium.

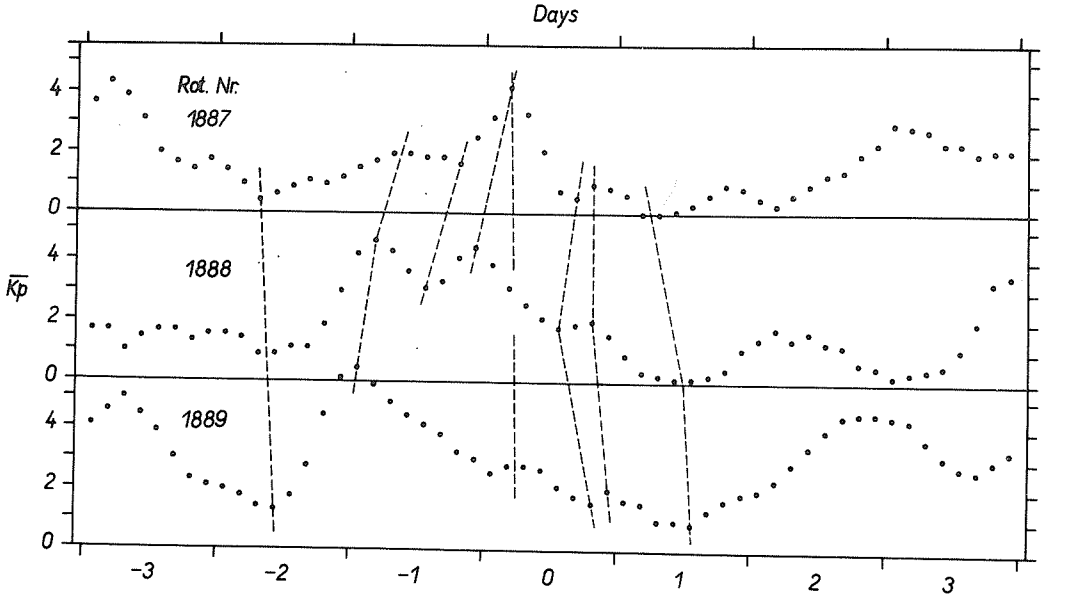

Fig. 2. Kp for rotations 1887-1889.

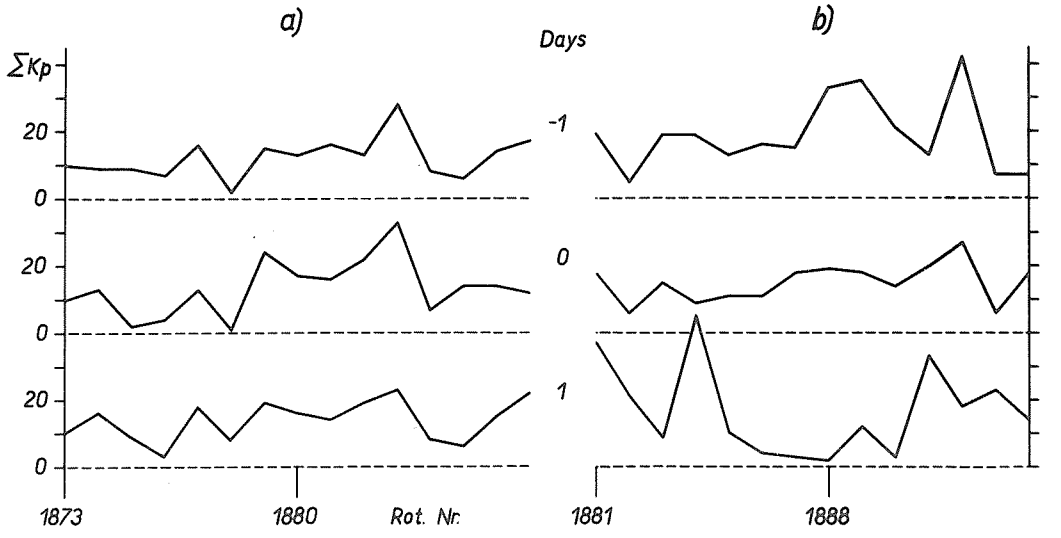

Fig. 3. Kp running means over three consecutive three-hour intervals.

Geomagnetically Active Plages and Flares Observed during the Interval Including January 24, 1971

by

M. C. Ballario
Osservatorio Astrofisico di Arcetri
Florence, Italy

Abstract

The moderate geomagnetic disturbance observed on January 24 (Kp max = 4) is related to an S proton flare recorded on January 22 (Time-lag of about 2 days).

On January 24 proton flares of importance 2, 1 and S are observed. They are related to the sc geomagnetic storm (Kp max = 6) of January 27 (Figure 1).

The other geomagnetic storms and disturbances observed during the intervals January 7 - February 13, including the selected days, are well correlated either with CMPs of positive plages or with occurrences of "specific flares", namely proton flares (Figure 1).

Introduction

Solar phenomena occurring during the interval January 7 - February 13, 1971, are examined.

In Figure 1 are marked:

A. The CMPs of all recurrent and non-recurrent plages as given in the McMath calcium plage list (Solar-Geophysical Data, Part I, Boulder, Colorado).

B. The CMPs of recurrent positive plages only.
The positive plages are never associated, before the meridian transit, with spot-groups type C or greater but, at the most, with spot-groups type A or B (spots without penumbra).

The CMPs of positive plages are generally associated with geomagnetic storms or disturbances; the correlation being about 78% [Ballario, 1970a].

On the contrary the negative plages are associated, before the meridian transit and at least for part of their life, with spot-groups type C or greater (spot with penumbra).

The CMPs of negative plages, as well as their CMPs in the subsequent rotations, are generally associated with quiet or slightly disturbed geomagnetic conditions [Ballario, 1970a], unless a resurgence takes place.

It is also seen that the CMPs of non-recurrent plages, whatever the associated spot-group type may be, are geomagnetically inactive.

The subdivision into negative and positive plages, depending on the associated spot-group type, is based on the Fraunhofer Institut Solar Maps.

The plage subdivision into recurrent and non-recurrent is given in the McMath calcium plage list. However, we have to note that, particularly when the active centers show only very small and negligible plages which appear and disappear during their life, some classified non-recurrent plages may be considered as recurrent ones. Thus, in this regard, some changes have been made.

C. The geomagnetic index Kp (Bartels).

D. The geomagnetically active flares.

We are not able, at present, to give the characteristics distinguishing the geomagnetically active flares from the inactive ones. Only "a posteriori" we may correlate geomagnetic storms and disturbances with flare occurrences.

In a previous paper [Ballario, 1970a] we have found that 48% of importance 2 and 3 flares, 53% of importance 1 proton flares and 21% of importance S proton flares were followed by geomagnetic storms or disturbances with Kp maximum value $\geq$ 4+ (time-lag of about 2 days), while the others were followed by quiet or slightly disturbed geomagnetic conditions. On the other hand it is well known that importance 1 and S flares are geomagnetically inactive.

In some cases the geomagnetic storms or disturbances are related both with CMPs of positive plages and with flare occurrences. Only when there are not CMPs of positive plages associated with the disturbance, can we consider the flare entirely responsible for the disturbance itself.

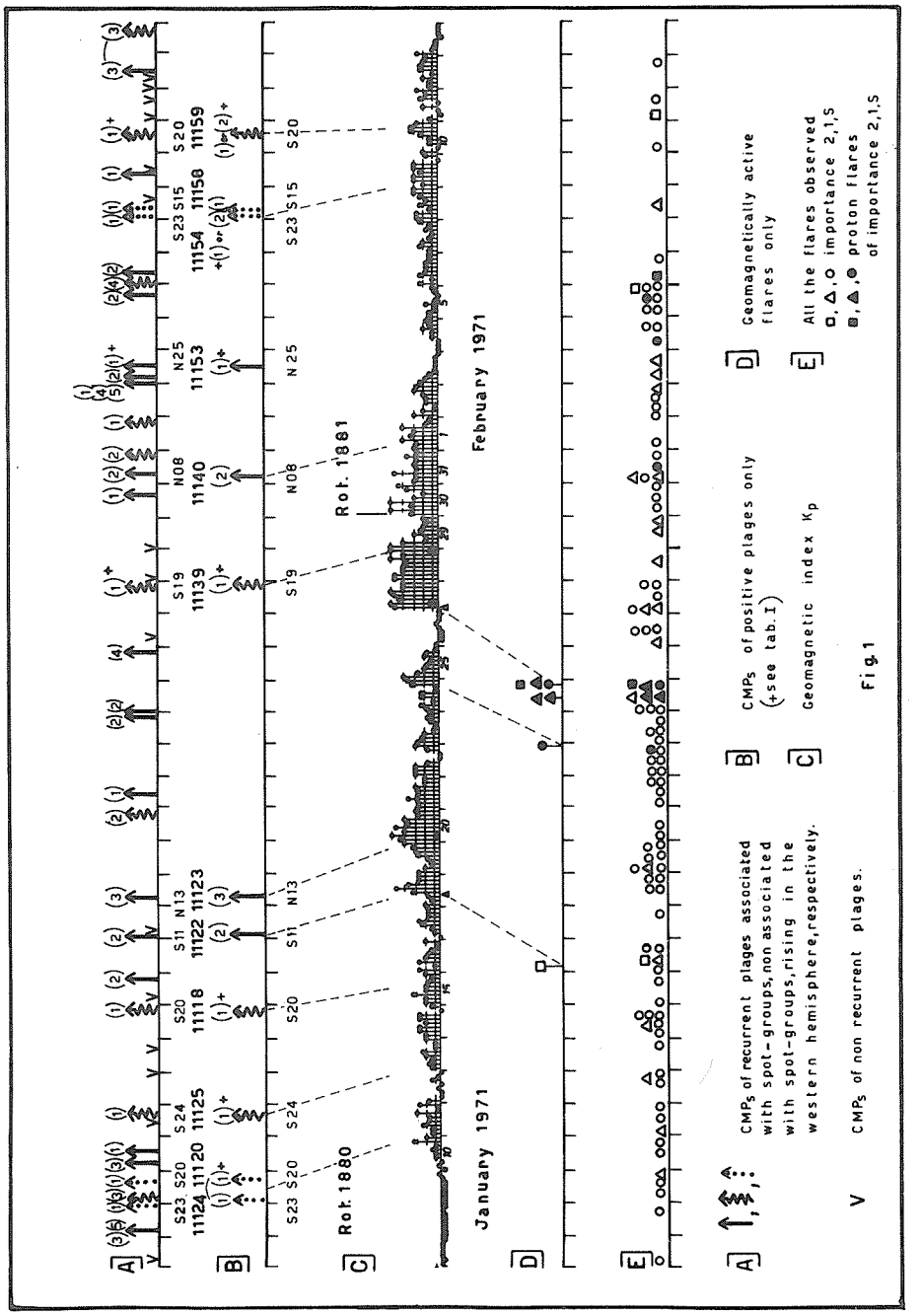
A
B
C
D
E
Rot. 1880
Rot. 1881
January 1971
February 1971
A CMPs of recurrent plages associated with spot-groups, non associated with spot-groups, rising in the western hemisphere, respectively.
V CMPs of non recurrent plages.
B CMPs of positive plages only (+see tab. I)
C Geomagnetic index Kp
D Geomagnetically active flares only
E All the flares observed
□, △, ○ importance 2,1,S
■, ▲, ● proton flares of importance 2,1,S

Fig. 1

Table 1

CMPs of plages recorded during the interval Jan. 7 - Feb. 13, 1971 and their subdivision into positive and negative plages.

Mc Math Data						Characteristics	Remarks (group type from Fraunhofer Institut solar maps)
CMP 1971	Lat.	Hel. long.	McMath plage number	Return of region	Age		
Jan.							
7.3	S30	47°	11107	New	1	non-rec. negative	- -
8.3	N18	33	11108	11073	3&5	recurrent "	E groups in the prec.rot.
9.0	S23	24	11124	New	1	rec. positive+(a)	Rising in the W hemisph.
9.1	S13	23	11110	11078	3	rec. negative	D groups in prec. rot.
9.6	S20	16	11120	New	1	rec. positive+(a)	Rising in the W hemisph.
10.2	N10	7	11112	11077	3	rec. negative	E groups in the prec. rot.
10.6	S04	3	11111	New	1	rec. "	Eastern E groups
11.5	S13	351	11114	New	1	non-rec. "	- -
11.6	S24	350	11125	New	1	rec. positive+(b)	Rising in the W hemisph.
13.0	S10	332	11116	New	1	non-rec. negative	- -
13.7	N11	322	11117	New	1	non-rec. " -	- -
14.9	S20	307	11118	New	1	rec. positive+(c)	No spots
15.2	S15	303	11121	New	1	rec. negative	Eastern C groups
15.8	N19	295	11119	11084	2	rec. "	G groups in the prec. rot.
17.1	S11	278	11122	11087	2	rec. positive	A,B. groups
17.2	N08	276	11131	New	1	non-rec. negative	- -
18.2	N13	263	11123	11088	3	rec. positive	Experiences a resurgence
20.8	S10	229	11127	11090	2	rec. negative	C groups in the prec. rot.
21.3	N20	222	11128	New	1	rec. "	Eastern E groups
23.8	N11	189	11129	11096	2	rec. "	Eastern D groups
24.0	S14	187	11130	11095	2	rec. "	Eastern J groups
25.8	N15	163	11133	11097	4	rec. "	Eastern J groups
26.3	S01	156	11138	New	1	non-rec. "	- -
27.7	S19	138	11139	New	1	rec. positive+(d)	No spots
28.0	N19	134	11135	New	1	non-rec. negative	- -
29.2	N04	118	11136	New	1	non-rec. "	- -
30.7	S12	98	11134	New	1	rec. "	Eastern D groups
31.3	N08	90	11140	11105	2	rec. positive	Experiences a resurgence
31.8	N25	84	11143	11102	2	rec. negative	J groups in the prec. rot.
Feb.							
1.9	S07	69°	11144	11106	4	rec. negative	D groups in prec. rot.
3.0	N13	55	11137	11108	1&4&5	rec. "	Eastern F groups
3.0	S14	55	11142	11124	2	rec. "	Eastern C groups
3.5	N25	48	11153	New	1	rec. uncertain+(e)	- -
5.7	S22	19	11142	11124	2	rec. negative	Eastern C groups
6.0	N21	15	11146	11108	4	rec. "	E,D groups in prec. rot.
6.3	S05	12	11145	11111	2	rec. "	Eastern H groups
8.0	S23	349	11154	New	1	rec. positive+(b)	Visible in the W hemisph.
8.0	S15	349	11158	New	1	rec. positive	Rising in the W hemisph.
8.3	N09	345	11148	New	1	non-rec. negative	- -
9.3	N15	332	11152	New	1	rec. "	Eastern C groups
9.4	S40	331	11147	New	1	non-rec. "	- -
10.6	S20	315	11159	New	1	rec. positive+(c)	Visible in the W hemisph.
11.0	N11	310	11150	New	1	non-rec. negative	- -
11.4	S10	304	11160	New	1	non-rec. "	- -
11.7	S10	300	11151	New	1	non-rec. "	- -
12.3	S06	293	11161	New	1	non-rec. "	- -
12.4	N20	291	11150	11119	3	rec. "	G,H groups in prec. rot.
13.9	N23	271	11155	11119	3	rec. "	" " " " "

Table 1 continued

+(a) Plages 11124 and 11120 at L = 24° and L = 16° are probably the same plage recurrent with the negative plage 11142 at L = 19° (CMP: 5.7 February).

+(b) Plage 11125 at L = 350° is probably recurrent with the positive plage 11154 at L = 349° (CMP: Feb. 8.0).

+(c) Plage 11118 at L = 307° is probably recurrent with the positive plage 11159 at L = 315° (CMP: Feb. 10.6).

+(d) Plage 11139 at L = 138° is probably recurrent with the negative plage 11165 at 16S and L = 140° (CMP: Feb. 23.8).

+(e) Plage 11153 develops in the following part of the negative plage 11137.

Table 2

Importance 2 flares and importance 2,1 S proton flares observed during the interval Jan. 7 - Feb. 13, 1971 (from Quarterly Bulletin on Solar Activity)

Date 1971	Time U.T.	Max U.T.	Position	Imp.	App. and corr. aerea	Charac.	McMath Region	Proposed correlation between Kp max. and flare max. (time-lag of about 2 days)
Jan.								
16	0804 1030	0830	18N-65E	2N	2.6 -	ELWZ	11128	Kp max = 5- on Jan. 18.6
22	2338 2435	2415	19N-23W	SB	1.0 1.2	U	11128	Kp max = 4 on Jan. 25.1
24	1436 1500	1445	21N-47W	1N	1.3 2.1	LU	11128	Kp max = 6 on Jan. 27.3
24	1706 1803	1723 1730	18N-45W	1N	1.6 -	FU	11128	
24	2035 2120	2039 2048	19N-50W	SN	1.0 -	EKU	11128	
24	2215 2231	2227	20N-48W	1N	1.9 -	FU	11128	
24	2308 2530	2315 2331	18N-49W	2B	4.1 -	KU	11128	
31	1114 1153	1116	12S-12W	SB	1.9 1.9	UZ	11134	Geomagnetically inactive
Feb.								
4	0827 0855	0834	04N-31W	SN	- 1.0	U	11137	" "
5	1546 1558	1546	08S-09E	SN	1.1 1.1	EUV	11145	" "
5	2221 2320	2225	09S-02E	2N	- -	SV	11145	" "
6	0438 0607	0507	17N-23W	2N	6.0 6.8	SU	11137	" "
11	0428 0608	0504	28N-60W	2F	2.2 -	FGHL	11146	" "

E. All the flares observed as given in the Quarterly Bulletin on Solar Activity.

The Events of January 7 - February 13

Plages

The CMPs of recurrent and non-recurrent plages observed during this interval and their subdivision into positive and negative plages are presented in Table 1 and marked in Figure 1A.

The positive plages are 11 in number and one is uncertain (McMath No. 11153). Their CMPs are marked in Figure 1B. Some of these positive plages, given as non-recurrent in the McMath calcium plage list, may be considered as recurrent ones (see footnotes of Table 1).

Broken lines relate the CMPs of positive plages with geomagnetic storms or disturbances (Figures 1B, 1C).

Flares

The data referring to importance 2 flares and importance 2, 1, S proton flares are presented in Table 2. They are 13 in number and only seven of them (five of which occurred in the same day) are followed by geomagnetic storms or disturbances.

These geomagnetically active flares are marked in Figure 1D.

Broken lines relate the maxima of the flares with the maxima of the storms or disturbances (Figures 1D, 1C).

Conclusion

The behavior of the geomagnetic index Kp during the interval under examination may be interpreted taking into consideration either the CMPs of recurrent positive plages and/or flare occurrences.

Particularly we note:

a.) The moderate geomagnetic disturbance of January 24 (Kp max = 4) is entirely due to the proton flare of importance S recorded on January 22 (time-lag of about 2 days), since no CMPs of recurrent positive plages are correlated with the disturbance itself.

b.) Also the sc geomagnetic storm of January 27 is entirely due to the five proton flares of importance 2, 1, S occurring on January 24.

c.) The sc geomagnetic disturbance of January 18 is related both with the CMPs of a recurrent positive plage (McMath No. 11122) and to an importance 2 flare occurring on January 16.

d.) The geomagnetic storms of January 20 and January 29 are related to CMPs of recurrent positive plages (McMath Nos. 11123 and 11139, respectively).

e.) The CMPs of recurrent negative plages and of non-recurrent plages are associated with quiet or slightly disturbed geomagnetic conditions (see the period February 2 - February 8; plage No. 11153 is probably a negative plage as stated in the footnotes of Table 1).

f.) Only for the geomagnetic disturbance of January 30 we are not able to give an interpretation since neither CMPs of recurrent positive plages nor flare occurrences are related with it.

The results here obtained are in good agreement with those found in examining the solar and geomagnetic phenomena recorded during the year 1968 [Ballario 1970a] and in other selected intervals [Ballario 1969a, 1969b, 1970b, 1971, 1972].

REFERENCES

BALLARIO, M. C. 1969a On the special events of March 1966, Ann. Geophys., 25, fasc. 1, 135-146.

BALLARIO, M. C. 1969b The EQSY 27-day recurrence sequence for 1964, Mem. SAIt., 40, fasc. 3, 271-294.

BALLARIO, M. C. 1970a Solar and geomagnetic events of the year 1968, Ann. Geophys., 26, 459-473.

BALLARIO, M. C. 1970b On the solar and geomagnetic events of Oct.-Nov., 1968, World Data Center A Upper Atmosphere Geophysics Report UAG-8, 231-238.

BALLARIO, M. C. 1971 March 1970: Solar and geomagnetic events, World Data Center A Upper Atmosphere Geophysics Report UAG-12, Part III, 349-358.

BALLARIO, M. C. 1972 On the geomagnetically active flares of September 1963, Mem. SAIt, in press.

Comments on the Special Intervals of January 24 and September 1, 1971

by

Bohumila Bednárová-Nováková
Geophysical Institute, Czechoslovak Academy of Sciences, Prague

An explanation of the geomagnetic activity in both special intervals and their immediate vicinity with a view to solar activity.

Special Interval, January 24, 1971

Two active centers with sunspots (Figure 1) passed through the Solar Central Meridian on January 23. One was in the north with spot type C16 January 23 (C14 January 24) and had filaments at the circumference of the field towards the equator and one directly on the equator; the other was in the south with spot type E27 January 23 (E30 January 24). Thus, we have two groups of sunspots on either side of the equator. This is a classical case of the Central Meridian Passage of two fields after which geomagnetic calm occurs [U. Becker, 1953; A. Stastná, 1964]. The reason for this is that the corona is split in the region between active centers as a result of two close, strong local magnetic fields, so that the space above the center of the visible solar disk is plasma-free. The bound filament with the northern region also indicates the separation of the fields. The geomagnetic disturbance only occurred after the Central Meridian Passage of the eastern limits of both active centers, where the connection between the northern and southern hemispheres was indicated by a small filament, located in a nearly meridional direction, which vanished between January 23 and 24. Conditions existed there for the generation of a narrower coronal stream which, after having reached the Earth's magnetosphere, caused an increase in geomagnetic activity [B. Bednárová-Nováková, 1961; B. Bednárová-Nováková and J. Halenka, 1969]. A disturbance with a short duration occurred at the end of January 24 (the last three-hour interval) and at the beginning of January 25 (the first three-hour interval). This was followed by complete geomagnetic calm. The storm with an sc began on January 27 after the Central Meridian passage of the circumferential unstable filament in the southern hemisphere, which belonged to region E27 on January 23. Part of this filament was located in a nearly meridional direction. The coronal formation has its largest dimension above this filament, corresponding to the length of the filament, similar, e.g., to the case of the 1968 corona in the NW, photographed during the total solar eclipse of September 22, 1968 [B. Bednárová-Nováková, in manuscript]. A stream of this type, if oriented radially above the center of the solar disk, is pointed directly at the Earth and the coronal plasma may affect the geomagnetic field.

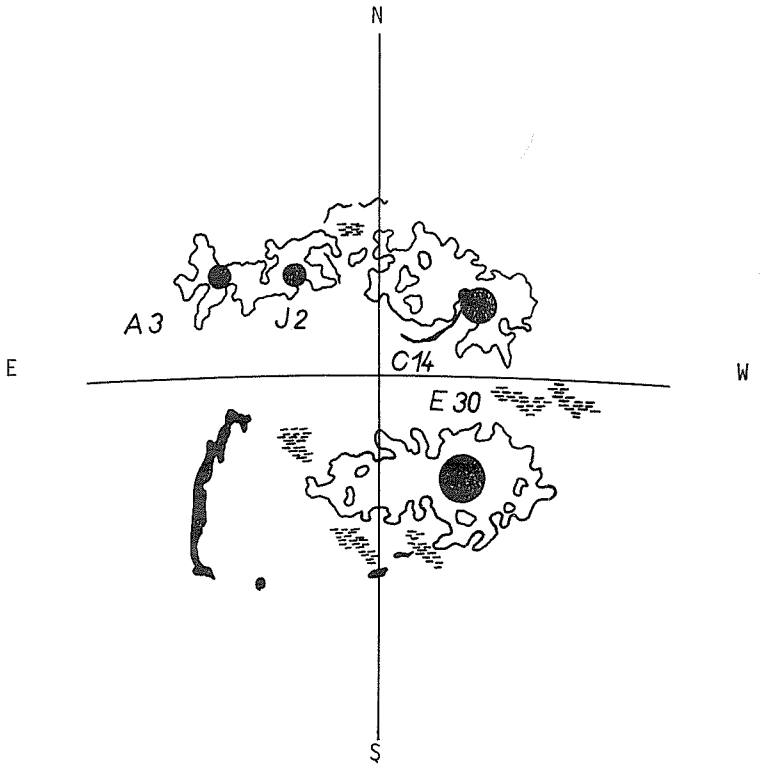

Fig. 1. Drawing based on Fraunhofer Institut's Map of the Sun from January 24, 1971.

Special Interval, September 1, 1971

A central floccular field with an unstable filament passed through the Central Meridian on August 29, 1971. A sudden commencement of a geomagnetic storm followed on August 30, which was the result of the formation of a coronal stream above the center of the visible solar disk. Another disturbance, subsequent to the storm and ending on September 1 (Figure 2), may be attributed to the equatorial wing of a minimum-shape corona forming after Central Meridian Passage of an unstable filament in the southern hemisphere and to several other filaments in the northern hemisphere on August 30. If suitably oriented, conditions are created for the coronal plasma to reach the Earth's magnetosphere. It can be said that the cosmic radiation propagating from the Sun on January 24 and September 1, 1971 had no connection with the geomagnetic activity following, as has already been pointed out in several other cases [J. Halenka, 1968; J. Halenka, 1971].

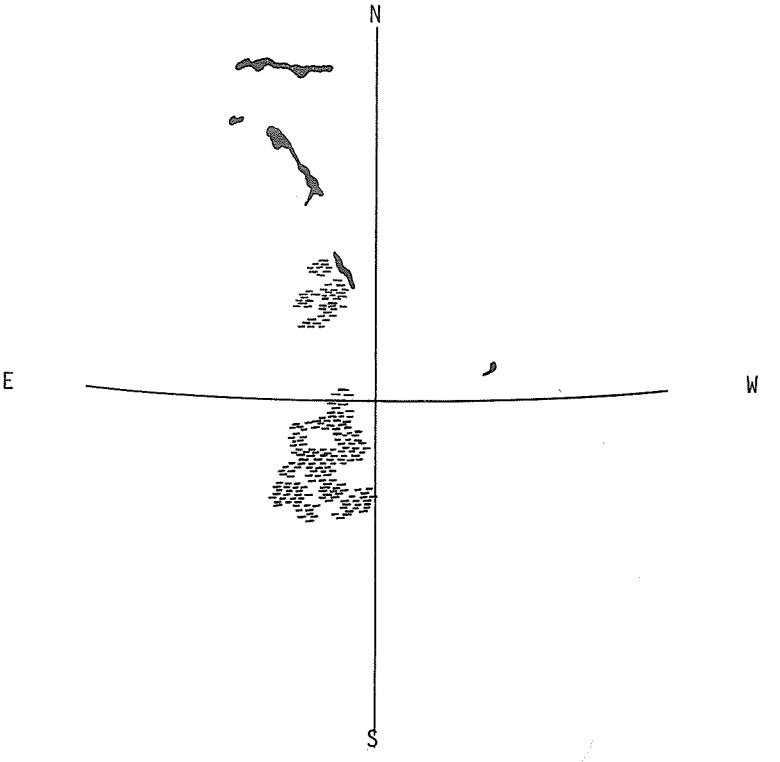

Fig. 2. Drawing based on Fraunhofer Institut's Map of the Sun from September 1, 1971.

REFERENCES

BECKER, U. 1953 Uber eine Beziehung zwischen erdmagnetischer Unruhe und der Anordnung der Sonnenflecken, Mitt. Fraunhofer Inst., Freiburg Br., II, 195.

BEDNÁROVÁ-NOVÁKOVÁ, B. 1961 Storms in IGY and IGC and Occurrence of Some Kinds of Filaments, Studia geoph. et geod., 5, 138-163.

BEDNÁROVÁ-NOVÁKOVÁ, B. and J. HALENKA 1969 A Universal Interpretation of the Generation of Geomagnetic Storms Using Features of the Solar Corona, Planet. Space Sci., 17, 1039-1044.

BEDNÁROVÁ-NOVÁKOVÁ, B. Solar Corona and Geomagnetic Activity (in manuscript)

HALENKA, J. 1968 On Correlating "Cosmic" Flares with Geomagnetic Storms, Geofysikální sborník 1967, No. 279, 367-386.

HALENKA, J. 1971 Geomagnetic Activity and the Solar Situation in the Neighborhood of Proton Effects, Geofysikální sborník 1969, No. 309.

STASTNÁ, A. 1964 Geomagnetic Activity after Passage of Two Different Configurations of Sunspot Groups through Central Meridian of Sun, Studia geoph. et geod., 8, 174-181.

Geomagnetic and SID Effects of the 24 January 1971 GLE

by

J. E. Salcedo
Manila Observatory
Manila, Philippines

On the occasion of the Ground Level Event (GLE) of 24 January 1971 many and various geophysical effects were recorded. A study of these effects will help to understand better conditions and mechanisms in the sun, in the earth's atmosphere and in planetary space and their interrelationships.

During the initial activities of McMath region 11128 before 2310 UT on the 24th, a geomagnetic substorm existed which could be the cause of subsequent enhancements of ionospheric conductivities. Figure 1 shows that typical solar wind velocities of about 400 km/sec prevailed until the first onset of 5-21 and 21-70 Mev protons. A 50 km/sec increase was measured by Vela spacecrafts. This increase in solar wind velocity was not significant enough to cause any disturbance in the geomagnetic field. The proton peak occurred some 10 hours, from ATS-1 data, after the H-alpha flare event, and still no impressive geomagnetic effect could be noticed except for the very mild storm in progress. During the steady decline of the protons on the 26th, the X-component of the geomagnetic field calmed down with a prevailing increase of about twenty gammas over the smooth S_Q. This calmness in the enhanced X-component of the geomagnetic field lasted until the ssc on the 27th. A phenomenon, such as this, can be attributed to the nearly constant heavy influx of charge (protons in general) into the earth's magnetic field buffering it from ordinary external disturbances.

Also from Figure 1 no other significant solar activity occurred during the period shown, between the great solar event and the geomagnetic ssc. Starting on the 27th at 0431 UT, the ssc was evidence of the arrival of the shock front [Tam and Yousefian, 1972] emanated from the flash phase of the solar flare explosion. This shock front comprised of solar gusts, arrived 53 hours and 08 minutes from the time of the peak centimeter burst, i.e., 2323 UT of the 24th. The solar shock can be described to consist of a classical front of waves with 3 peaks, each succeeding the other at a little over two minute intervals. The solar gust is calculated, from the transit time, to have an average velocity of 772 km/sec. Although this speed is not fast compared with 1100 km/sec velocity of previous big events, it induced a fast compression rate in the geomagnetic cavity. Then, this high compression rate can be attributed to a relatively dense composition of the solar wind which compressed the geomagnetic field X-component to 32 gammas in only a minute and a half at Manila.

The great solar event occurred at about 0700 of the 25th Manila local time. Short-wave transmissions via the F-region showed increased absorption of 7.0 dB on 9.6, 12 and 15 MHz and only 4.0 dB on 18 MHz. A total SWF did not occur because of nearness to sunrise. The shortwave stations monitored in Manila are northerly because of Manila's location at the west edge of the Pacific. Only Japanese and Chinese stations are conveniently receivable. Other factors present in longer distance transmissions make identification of SWF from eastern sources ambiguous.

Another impressive effect on the D-region was displayed on the SPA (Sudden Phase Anomaly) monitors. The NLK (Seattle-Manila 18.6 kHz) path showed a 246° phase advance. The GBR (Rugby-Manila 16.0 kHz) and NDT (Tokyo-Manila 17.4 kHz) paths had 35° and 33° phase advances, respectively. The major portion of the GBR path was still in darkness when the solar event took place. The NDT path, though one hour east of Manila, was not fully exposed due to the winter tilt. If these SPAs were to be normalized, i.e., maximum lit path [Wisdom, 1971] a 500-degree phase advance could be attained. Wisdom showed that normalized SPA exceeding 120° for NLK, 115° for GBR and 80° for NDT, fall into the category of a major SPA.

The main event of 2322 UT, the 2B flare, was preceded by at least four other significant events in McMath region 11128 within three hours. After the big event, all was quiet except some ten hours later, at a different region, McMath 11130, a sub-flare erupted. This makes the 2322 UT 2B flare a good specimen in the study of subsequent behavior of the geomagnetic field.

Figure 2 reveals certain characteristics of the plasma shock front, responsible for the ssc, nearly retained until its arrival on earth. The three outstanding initial peaks in the dekameter total power intensity were also manifested in the geomagnetic storm commencement, indicating a common causative agent: the plasma front. It is worthy of note that the peaks in the ssc are widely separated, 5.6 minutes against 2.6 minutes in the dekameter profile. Due to the 1.5×10^8 km course the solar wind shock front travelled, the earlier waves moved fast - thus more widely separated on arrival. The shock front while being propagated outward into the corona was excited into plasma oscillation (an accepted mechanism in the generation of Type IV dekametric events). The denser the plasma, the more intense the dekameter emission. These three peaks, therefore, suggest that the shock front is comprised of bunches of plasma waves. The same waves, on arrival at the earth compressed the geomagnetic cavity at three peak intervals. This cavity, having an extremely low resonance, could not respond to the detailed wave composition of the compressing plasma front. Thus only three smooth but distinct peaks were displayed in the analog recorder.

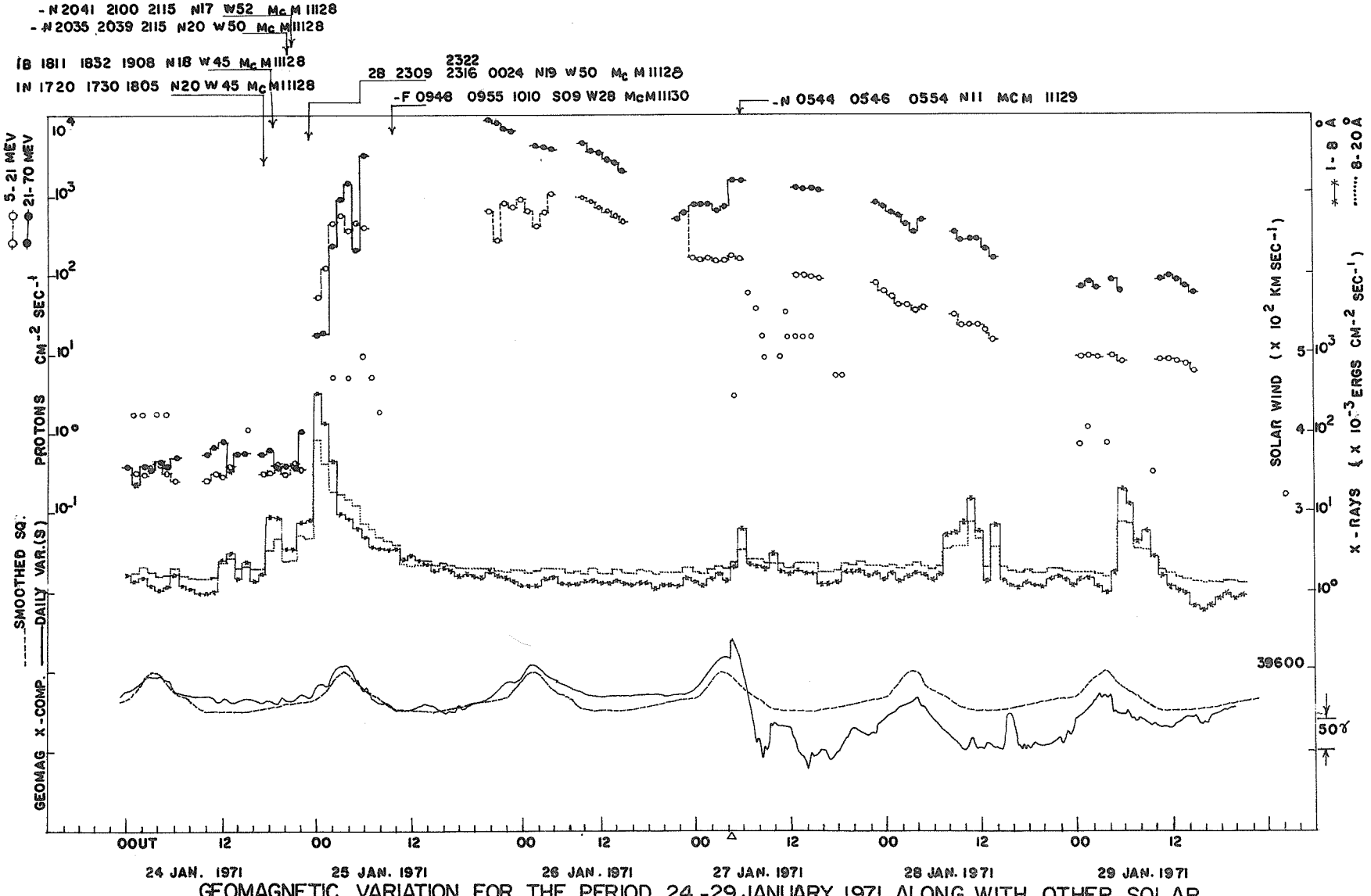

FIG. 1 GEOMAGNETIC VARIATION FOR THE PERIOD 24 -29 JANUARY 1971, ALONG WITH OTHER SOLAR EMISSIONS DURING THE GLE, AT MANILA.

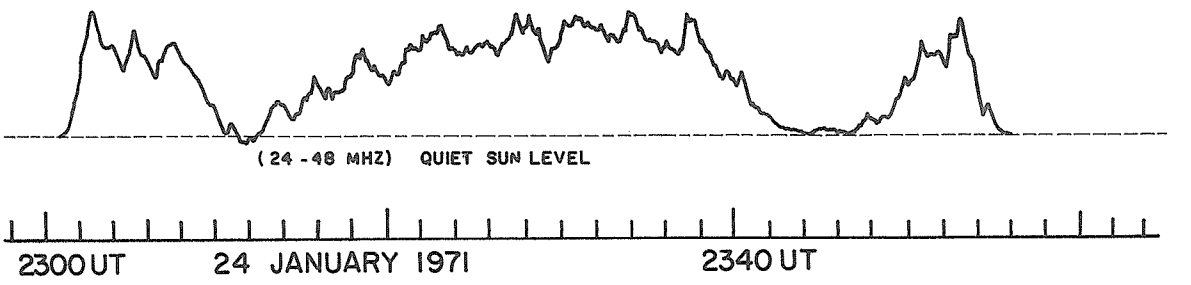

TOTAL POWER PROFILE OF THE DEKAMETRIC TYPE IV EMISSION

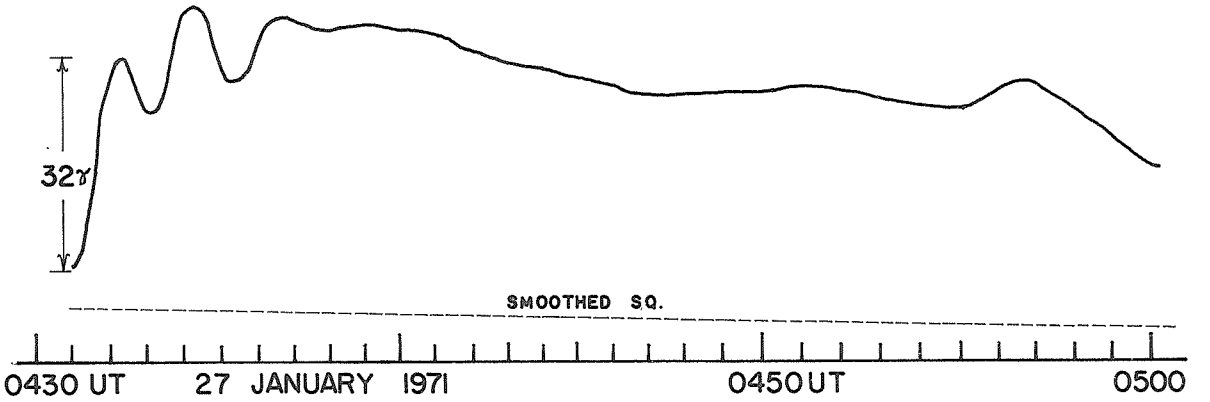

DETAIL OF THE GEOMAGNETIC SSC IN THE X - COMPONENT

FIGURE 2. RADIO AND GEOMAGNETIC EVENTS ASSOCIATED WITH THE 24 JAN. 1971 GLE OBSERVED AT MANILA.

The Tables below describe the behavior of the D-region during the solar event both as an absorbing and as a reflecting layer. The lower the frequency, the earlier the SWF reached maximum absorption. Recovery was in the reverse order; 18 MHz was first and 9.6 MHz last. The average max time for the SPAs was also about the same with the SWFs, at 2342 UT.

Table 1

SWF Events 24-25 Jan 1971

Freq (MHz)	Start	Max	End	Abs.(dB)
9.6	2308	2340	0315	7.0
12	2307	2341	0300	7.0
15	2309	2343	0256	7.0
18	2306	2344	0235	4.0

Table 2

SPA Events 24-25 Jan 1971

Sta.Freq(kHz)	Start	Max	End	Phase Advance (°)
NLK 18.6	2306	2340	0300	246
NDT 17.4	2308	2347	0200	33
GBR 16.0	2317	2328	0134	35

Radio and H-alpha peak times agree to within a minute, 2323 and 2322 UT, respectively. The X-ray max time, particularly the softer ones and the EUV which are responsible for ionizing the D-region, cannot be far behind, if not within, the radio and H-alpha max times. Castelli and Richards [1971] showed excellent agreement between EUV and centimeter radio start time and time of burst maximum. From Tables 1 and 2, an appreciable delay of twenty minutes exists, on the average, between H-alpha and radio times and maximum SID times.

Peak absorption and peak reflection of signals by the ionosphere imply maximum electron density has been attained. The data in the Tables showed continued ionization had prevailed for about twenty minutes after the centimeter radio max time. Secondary ionization: freed electrons have acquired exceedingly higher energies than usual, then reimparted to neighboring particles by collision, thus, prolonging the ionization process. More studies are being done to explain this time lag and to determine if it can be a useful indicator for extremely big events, such as, a GLE.

The author thanks AFCRL for supporting this work, and J. J. Hennessey and V. L. Badillo for their encouragement.

REFERENCES

CASTELLI, J. P. and D. W. RICHARDS 1971 Observations of Solar Bursts at Microwave and Extreme Ultraviolet Wavelengths, J. Geophys. Res., 76, 8409.

TAM, C. K. W. and V. YOUSEFIAN 1972 Effects of Interplanetary Magnetic Field on the Propagation of Flare-Generated Inter-Planetary Shock Waves, J. Geophys. Res., 77, 234.

WISDOM, W. A. 1971 Normalization Procedures for Sudden Phase Anomaly Events, (To be published).

On Geomagnetic Pulsations at the Time of Solar-Terrestrial Events of January 24, 1971 and September 1, 1971 at the Budkov Observatory

by

Karel Prikner
Geophysical Institute
Czechoslovak Academy of Sciences
Prague, Czechoslovakia

Introduction

The solar-terrestrial events of January 24 and September 1, 1971 belong to the category of phenomena which do not connect up directly with sudden marked disturbances of the geomagnetic field. However, they are usually related to the development of the conditions in the geomagnetic field in the course of the subsequent days or weeks. Therefore, it is necessary to investigate comprehensively their regularities from the point of view of forecasts of geomagnetic activity.

For purposes of investigating the behavior of the short-period variations of the geomagnetic field during both periods, the records of a normal magnetic apparatus of the Bobrov system (recording speed 20 mm/hr) and of a rapid-run induction variometer with a permalloy core (15 mm/min) of the IVJ-2 type, located at the Budkov Observatory (geomagnetic longitude and latitude Λ = 96° 02'E Φ = 49° 01'N) were used. The K-indices for the 3-hourly intervals were determined for the Průhonice Observatory (Λ = 97° 18'E Φ = 49° 54'N).

Significant Disturbances in the Geomagnetic Field

The degree of disturbance of the geomagnetic field during both intervals is characterized by the run of the K-indices, adopted from the Průhonice Observatory and shown in Figures 1 and 2. The interval between January 22 and 24 did not display any significant sudden disturbances. Not until 1930 UT on January 24 was an ssc observed (amplitude about 13γ), which was followed by a storm with a relatively short duration and recovery in the course of January 25. The whole of January 26 was very calm. At 0430 UT of January 27 a very sharp ssc was recorded (amplitude about 22γ) with a subsequent severe storm, the effects of which could be observed until the end of January.

Beginning August 31 a geomagnetic storm with a gradual commencement was in evidence, the effects of which could still be observed on the morning of September 1. On the same day, after 1900 UT, a bay disturbance developed in the H-component with an amplitude of about 26γ, lasting roughly 1.5 hours. The interval between September 2 and 4 is again relatively calm. A sharp ssc* with an amplitude of about 15γ was recorded at 1646 UT on September 4, which was followed by a geomagnetic storm.

Geomagnetic Pulsations

The most typical pulsation in the region of the Budkov Observatory is the day-time Pc3 pulsation. Owing to their most frequent occurrence during magnetically calm intervals, they were chosen as a means for studying the characteristics of the short-period variations in both intervals considered.

Several days on either side of January 24 and September 1, 1971 samples of the Pc3 pulsations were taken roughly in one-hourly intervals. Provided they were recorded, this applies to the whole period of their usual daily occurrence. In accordance with Hirasawa [1969] and Jacobs [1970] this period is roughly between 0300 and 1900 UT at the observatories mentioned above. The periods (T) and the double amplitudes (A), as the max. oscillation of the pulsation, in the X (NS) component of the records were measured in the samples. These data were not measured on August 31 because the field was too severely disturbed by a geomagnetic storm. For the same reason the measurements in both cases were terminated by the onsets of the geomagnetic storms of January 27 and September 4, 1971.

For each day, independently, the average daily value of both the quantities measured, $\overline{T}$(s) and $\overline{A}(\gamma)$, were also determined. The results for the interval around January 24 are in Figure 1 and the results for the interval around September 1 are in Figure 2. For purposes of comparing the degree of disturbance during both intervals with the variations of the pulsation characteristics, the run of the K-indices has been introduced into both the Figures. Apart from this the average daily values $\overline{T}$ and $\overline{A}$ are recorded for both intervals in Table 1.

The intervals were not evaluated for the evening and morning hours of January 22 and 23, and January 23 and 24, respectively. This was due to a failure of the recording instrument, which also occurred just prior to the interval investigated.

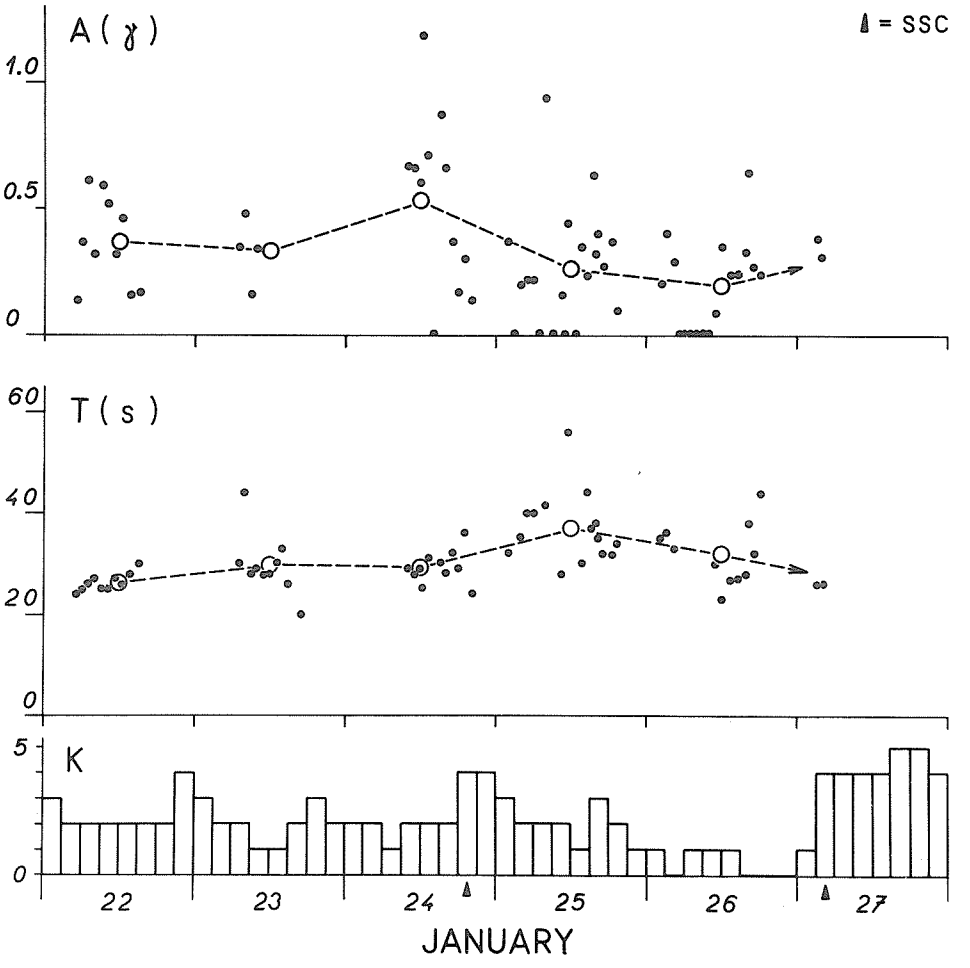

Fig. 1. Measured values of the amplitudes (A) and periods (T) of Pc3 pulsations (Budkov) for the studied interval in January 1971 (dots) and the run of their average daily values (circles). The run of the Průhonice K-indices has been included.

Discussion

In the course of both the evaluated intervals a smaller variation in the values of the average daily period $\overline{T}$ and a more marked variation in the average daily value of the amplitude $\overline{A}$ of the samples of recorded pulsations appeared. The value of $\overline{T}$ in both cases increased after the set date (in January roughly from about 29 seconds on January 24 to 37 seconds on January 25 and in September gradually and over a longer interval from 28 seconds on September 1 to 39 seconds on September 4).

The values of $\overline{A}$ on January 24 and September 1 were relatively high (Table 1). In both cases they decreased markedly during the subsequent days by more than 50% of their original value (from $\overline{A} \simeq 0.527\gamma$ on January 24 to $\overline{A} \simeq 0.194\gamma$ on January 26, and from $\overline{A} \simeq 0.770\gamma$ on September 1 to $\overline{A} \simeq 0.132\gamma$ on September 3, 1971). In some of the hourly intervals no pulsations could be observed on the records at all. In comparison with the run of the K-indices the subsequent period has the character of a rapid decrease in the overall level of disturbance of the magnetic field, simultaneous with decreasing activity in the range of short-period variations.

As already mentioned above, both the intervals with decreased levels of activity are followed by geomagnetic storms with sharp ssc's. This phenomenon can be observed frequently. One should point out that similar behavior was also observed in $\overline{T}$ and $\overline{A}$ during the interval immediately preceding the geomagnetic storm of March 8, 1970, which is discussed elsewhere [Prikner 1971].

In both the cases studied there is a clear time relation between the overall decrease of the level of disturbance in the geomagnetic field (K-indices) and the pulsation characteristics ($\overline{T}$, $\overline{A}$). These features in the behavior of the pulsations are in agreement with the results of Jacobs [1970], etc. According to the conclusions of Troitskaya et al. [1967], the velocity of the solar wind in

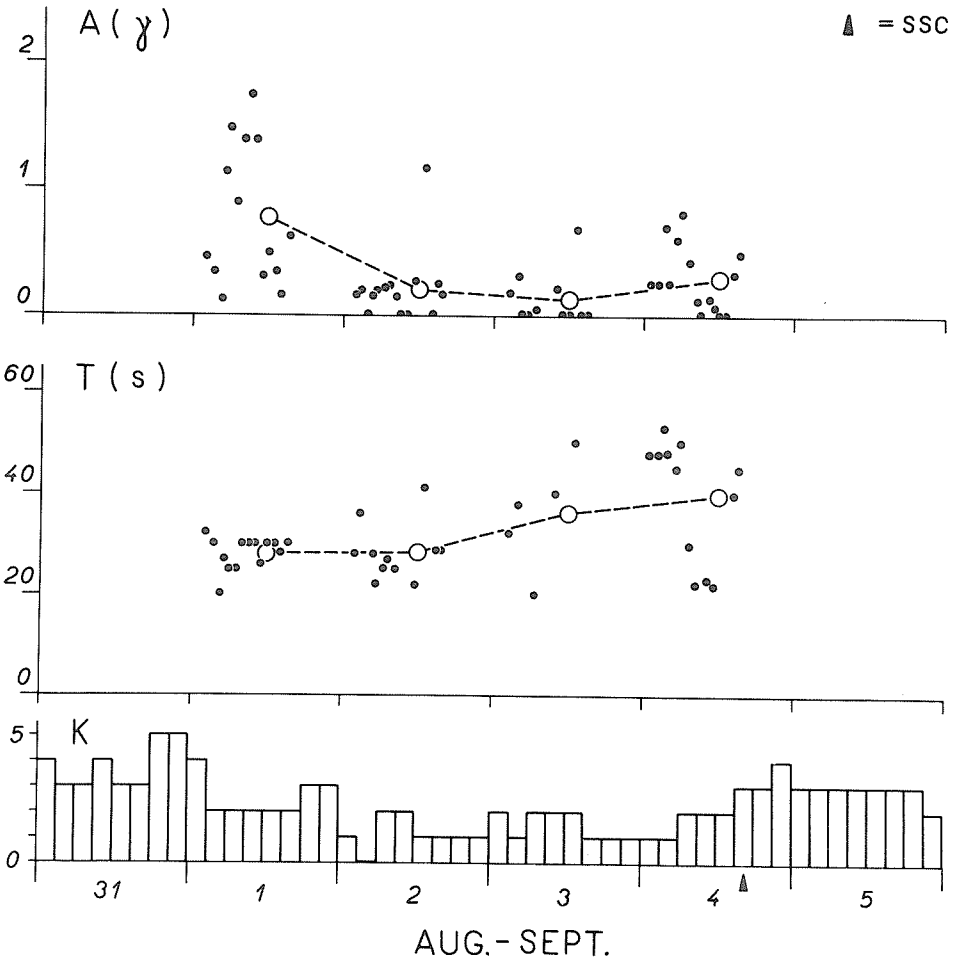

Fig. 2. The same as in Fig. 1 but for the interval in September 1971.

the vicinity of the Earth should have decreased slightly during the intervals investigated. Now, consider the interpretation of the changes in the pulsation characteristics as in Prikner [1968]. In this interval of a relatively low level of activity of the geomagnetic field, one may expect an increase in the size of the resonator in which the pulsations are generated or a certain decrease in the average velocity of the HM-waves in the Earth's magnetosphere. This may be connected with the expansion of the lower layers of the magnetosphere (plasmasphere) as a result of heating or of the expansion of the resonator - magnetosphere when the plasma pressure of the solar wind decreases at the boundary of the magnetosphere. The said processes result in a gradual increase of the period of the recorded pulsations, in a decrease of their amplitudes, and possibly even in their vanishing from the record. This could be actually observed in the observatory data used.

With a view to forecasting geomagnetic activity, the comprehensive study of these intervals is interesting. The study is important principally because of their connection with the geomagnetic storms which follow them.

Table 1

Date (1971)		$\overline{T}$ (s)	$\overline{A}$ (γ)
January	22	26.3	0.366
	23	29.6	0.332 ?
	24	29.2	0.527
	25	37.0	0.261
	26	32.0	0.194
August	31	storm	storm
September	1	28.0	0.770
	2	28.3	0.212
	3	36.0	0.132
	4	39.5	0.299

REFERENCES

HIRASAWA, T. 1969 Worldwide Characteristics of Geomagnetic pc-Pulsations with the Period From 10 to 150 Seconds During Active-sun Years. Rep. Ionos. Space Res. Japan, 23, 281-293.

JACOBS, J. A. 1970 Geomagnetic Micropulsations. Physics and Chemistry in Space 1, Spring.-Verl., Berlin, Heidelberg, New York.

PRIKNER, K 1968 Resonance of a Plane HM-wave in the Lower Magnetosphere and pc Pulsations with Periods of 5 to 40 Seconds Occurring During Geomagnetic Storms. Studia Geoph. et Geod., 12, 224-230.

PRIKNER K. and J. STRESTIK 1971 The Properties of Geomagnetic Pulsations at the Time of the Magnetic Storm of March 8th, 1970. World Data Center A, Upper Atmosphere Geophysics Report UAG-12, Part III, 401-404.

TROITSKAYA, V. A., O. V. BOLSHAKOVA and R. V. SHCHEPETNOV 1967 On the Possibility of Introduction of the Solar Wind Index W_{SW} With Applications of Properties of Micropulsations of the Electromagnetic Field of the Earth. IUGG Assembly, Zürich.

The Cosmic Ray Event of January 24, 1971, and the Micropulsation Activity

by

Jagdish Chandra Gupta
Earth Physics Branch
Energy, Mines and Resources, Ottawa, Canada

On January 24, 1971, at about 2335 UT the counting rate of cosmic rays increased suddenly by about 12% above the background level. A few minutes earlier a flare of importance 3B was reported to have erupted in the McMath plage region 11128. And, about 52 hours later a world-wide moderate intensity ssc geomagnetic storm was recorded by the magnetometers. It is most probable that whereas the high energy particles ejected from the sun due to the flare were responsible for the observed cosmic ray increases the bulk of the low energy particles which arrived several hours later caused the storm.

In order to study the micropulsation activity following this cosmic ray event the normal run magnetograms showing Pc5 activity and the rapid run magnetograms showing the pulsational activity in the Pc3, 4 period range were examined from several observatories described in Table 1.

Table 1

Stn. No.	Station	Geographic		Geomagnetic	
		Latitude	Longitude	Latitude (N)	Longitude (E)
1.	Alert	82.5°N	62.3°W	85.7°	168.7°
2.	Resolute Bay	74.7°N	94.8°W	83.1°	287.7°
3	Mould Bay	76.2°N	119.4°W	79.1°	255.4°
4.	Baker Lake	64.3°N	96.0°W	73.9°	314.8°
5.	Leirvogur	64.2°N	21.6°W	70.3°	71.6°
6.	Fort Churchill	58.7°N	94.3°W	68.8°	322.5°
7.	Great Whale River	55.3°N	77.8°W	66.8°	347.2°
8.	Abisco	68.3°N	18.8°E	65.9°	115.3°
9.	Kiruna	67.8°N	20.4°E	65.3°	115.7°
10.	College	64.9°N	147.9°W	64.6°	256.1°
11.	Dõmbas	62.1°N	9.1°E	62.3°	100.1°
12.	Meanook	54.6°N	113.3°W	61.9°	300.7°
13.	Sitka	57.1°N	135.3°W	60.0°	275.0°
14.	St. John's	47.6°N	52.7°W	58.7°	21.4°
15.	Ottawa	45.4°N	75.6°W	57.0°	351.5°
16.	Victoria	48.5°N	123.4°W	54.3°	292.7°
17.	Tucson	32.2°N	110.8°W	40.4°	312.2°
18.	San Juan	18.4°N	66.1°W	29.9°	3.2°
19.	Honolulu	21.3°N	158.1°W	21.1°	266.5°

The chart records examined do not give any indication of special pulsational activity starting simultaneously with the cosmic ray event. And, one could say with confidence that any regular or irregular pulsational activity seen on the records would have been present whether or not the cosmic ray event occurred. In other words the entry of the very high energy particles into the magnetosphere did not trigger any conditions which might lead to micropulsation activity.

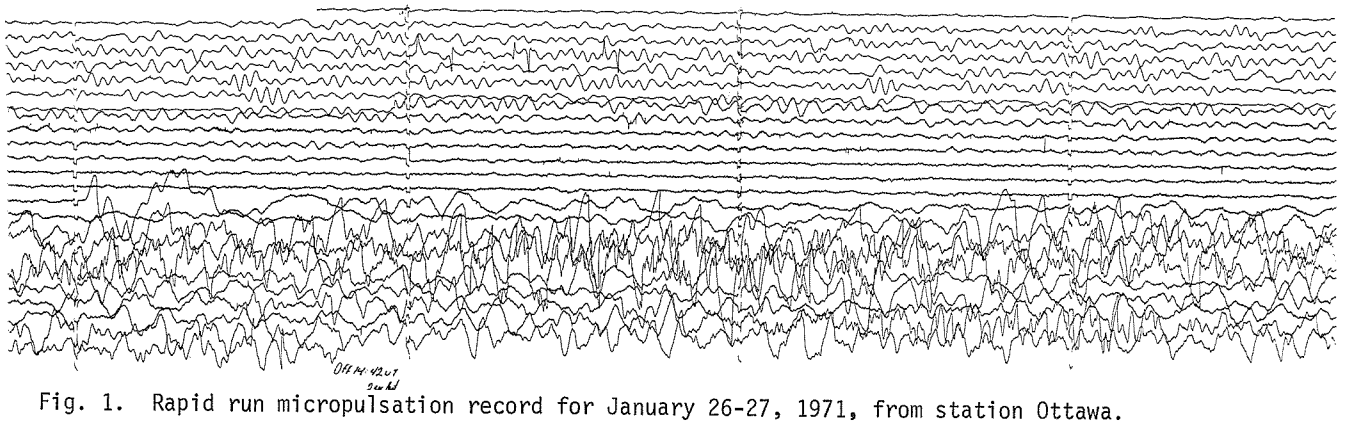

Fig. 1. Rapid run micropulsation record for January 26-27, 1971, from station Ottawa.

The rapid run Ottawa magnetogram for January 26-27 is shown in Figure 1. Simultaneously with the ssc a Pi2 developed and was seen on Ottawa, Meanook, Baker Lake and Resolute Bay records; because of instrumental problems the Meanook rapid-run records are not analysed further. The pulsational

activity was in the Pc3, 4 period range and rather sinusoidal in nature a few hours prior to the Pi2 appearance on the records. Following the Pi2 irregular pulsational activity dominated the charts and often rendered them unusable, especially at Ottawa. For stations Resolute Bay, Baker Lake and Ottawa in Table 2 are shown:

(1) the average amplitude of the largest Pc3, 4 pulsation whenever present in all the 15 minute intervals lying between 1630 UT on January 26 to 0430 UT on January 27 (column 3 and 4);

(2) the amplitude of the dominant cycle of the Pi2 which developed at 0430 UT on January 27 (column 5);

(3) the average amplitude of the largest Pi pulsations in each of the 15 minute intervals during 0430 to 0630 UT on January 27 (column 6).

Table 2

Station	Component	Amplitude (nT)			
		Pc3	Pc4	Pi2 at ssc	Pi's after ssc
Resolute Bay	Y	-	0.8	9.2	1.9
Baker Lake	X	2.0	1.9	14.0	13.9
Ottawa	H	1.3	1.1	3.5	2.9

Clearly the amplitudes of pulsations, Pc's or Pi's are largest in the auroral zone (Baker Lake in general is on the northern border of the auroral zone). The Pi amplitudes seem to fall much more rapidly than those of Pc's on either side of the auroral zone.

Some high latitude normal run magnetograms showed Pc5 activity more distinctly than others during the intervals preceding the ssc and after the peak of the substorm (seen at high latitudes) which followed ssc. Most striking example is that of Great Whale River where Pc5 activity predominates in all three components (Figure 2). There is a recognizable difference between the pulsational activity before and after the substorm; the former is more sinusoidal and of small amplitude and the latter is irregular and of large amplitude. The amplitude and the period of the largest pulsation in the Pc5 period range, in each hour, are measured from the normal magnetograms for the intervals 0000-0400 UT and 1000-1400 UT on January 27; the later interval begins closer to the end of the substorm. The computed average values are given in Table 3 for several stations, a majority of which lie at high latitudes. It is seen clearly from the Table that whereas the amplitudes increased, the periods of the Pc5 pulsations decreased after the substorm activity. The amplitude of the pulsations was largest at Churchill prior to the substorm and at Great Whale River after the substorm. This indicates an inward movement of the surface at which HM waves responsible for Pc5 oscillations are generated. After the substorm the amplitudes are found to be large at Great Whale River and 70° to the West at College. However the amplitudes are found to be smaller at Churchill and Meanook. In the latitudinal extent the amplitudes in general are found to decrease rather rapidly but Kiruna and Abisco which lie between the latitudes of Great Whale River and College show much smaller amplitudes. This tends to indicate a sectorial effect to be prevailing. Therefore these observations support the idea of Obertz and Raspopov [1968] according to which the region of excitation of Pc5 is localized in space. Even with the small amount of data used here the effect of increasing magnetic activity on the amplitudes and on the periods of Pc5's is clearly demonstrated.

Acknowledgements

I wish to express sincere thanks to Messrs. G. Jansen van Beek and E. I. Loomer, and to Drs. E. R. Niblett and P. H. Serson for help and comments. Also thanks are due to Mr. William Paulishak of the World Data Center A for Solar-Terrestrial Physics for supplying the desired normal magnetograms from several observatories.

REFERENCES

OBERTZ, P., and O. M. RESPOPOV 1968 Study of the Spatial Characteristics of Type Pc5 Geomagnetic Micropulsations, Geomag. Aeron. VIII, 424-427.

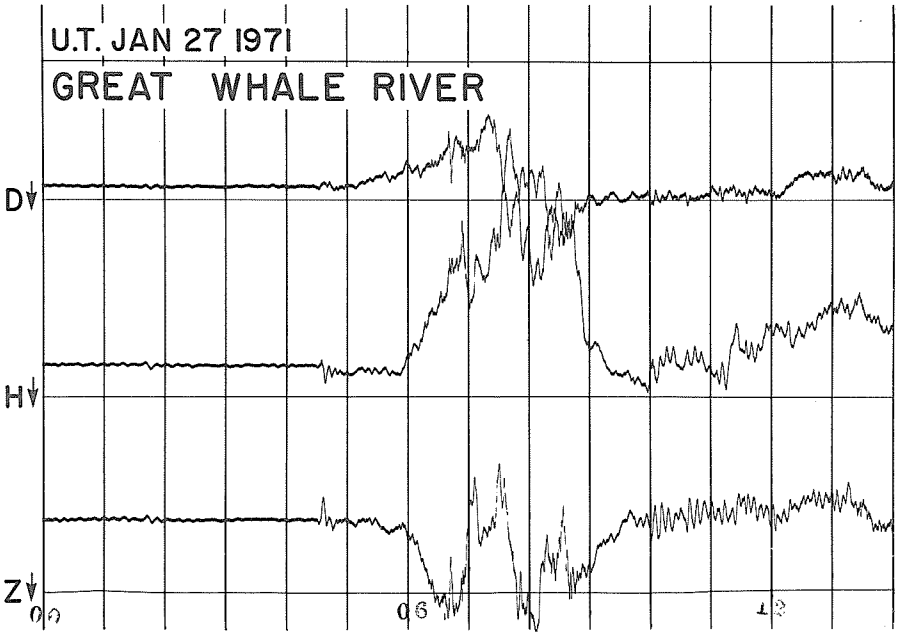

Fig. 2. Portion of standard photographic magnetogram for Great Whale River, January 27, 1971.

Table 3

Average amplitude and the average period of the largest cycle of the Pc5 micropulsations on January 27, 1971, in the H(or X) components.

Station	Before the Substorm 0000-0400 UT (Kp=0_+) Amplitude (nT)	Period (sec.)	After the Substorm 1000-1400 UT (Kp=6_0) Amplitude (nT)	Period (sec.)
Alert	7	297	46	288
Resolute Bay	13	459	24	252
Mould Bay	13	320	28	198
Baker Lake	12	374	33	310
Leirvogur	4	540	27	420
Fort Churchill	22	549	51	400
Great Whale River	13	580	80	405
Abisco	7	450	40	396
Kiruna	4	450	30	392
College	8	528	70	342
Dombas	3	489	9	330
Meanook	4	477	49	342
Sitka	2	348	7	328
St. John's	-	-	6	310
Ottawa	-	-	12	275
Victoria	1	369	3	387
Tucson	2	520	6	340
San Juan	-	400	2	380
Honolulu	2	500	6	300

Cosmic Ray Event of January 24, 1971 and the Geomagnetic Variations

by

J. C. Gupta and E. I. Loomer
Division of Geomagnetism
Earth Physics Branch
Department Energy, Mines and Resources
Ottawa, Canada

ABSTRACT

In the McMath plage region 11128 several flares of relatively low importance occurred on January 24, 1971. The largest flare, Group 36350 [Solar-Geophysical Data], began at 2215 UT with maxima at 2316 and 2335 UT, and importances of 1B and 3B, respectively. Most probably the large cosmic ray increases recorded by the neutron monitors near 2330 UT were associated with the very high energy protons ejected from this flare. A moderate intensity ssc geomagnetic storm occurred about 52 hours after the eruption of these flares. It was apparently caused by the impact on the magnetosphere of the solar wind modulated by the relatively low energy plasma ejected from the solar flares of that day. An analysis is included for the complex polar substorm which followed the ssc.

The movement of the auroral electrojet in the oval to the west and north and the rotation of the oval to the west were inferred from the magnetic effects.

Data were insufficient to distinguish between the Akasofu and Feldstein equivalent current models, and to determine the mechanism of the intensification of activity at the northern edge of the oval. The anomalous nature of the current vectors at Godhavn and College remains to be explained.

It is the purpose of this report to examine the geomagnetic activity following a large and sudden cosmic ray increase, which started about 2335 UT on January 24, 1971. The magnetic activity for a few days (January 24-27) before and after the occurrence of this event is shown by the three hourly Kp indices in Table 1. Clearly January 24-25 showed about average activity, January 26 was a very quiet day and the disturbance started early on January 27.

Even though several tens of flares erupted during January 22-24 in the McMath Plage Region 11128, only some of the important ones are noted in Table 2 [see Solar-Geophysical Data, 1971]. Amongst these flares was Number 6 which was of importance 3B and most likely produced particles in a wide energy spectrum. However, the possibility that flare Number 7 is a strong source of particles with different energies may not be discounted.

Table 1

Kp JANUARY 1971

Date	Three-Hour Universal Time Intervals								
	1	2	3	4	5	6	7	8	ΣKp
24	2-	2+	1o	2+	2+	1-	3+	4-	17+
25	4o	3-	2o	2-	1+	2o	2-	1-	16o
26	1-	0o	0o	0o	0+	1-	0+	0+	2+
27	0+	5-	6o	4+	5-	5o	4o	4o	33o

Whereas the relativistic particles emitted during a flare arrive at the earth's orbit in a matter of a few minutes, the bulk of the flare particles takes about 20-72 hours and produces si's or ssc's on magnetic records. In the case under study the cosmic ray increase of January 24 occurred about 20 minutes after the first maxima of Group 36350 [SGD, No. 323, 1971] (see Table 2). Based on this transit time it is most probable that the relativistic protons with energies in the neighborhood of 1 Bev [Pinter, 1970] from this flare were responsible for the observed intense increase in cosmic rays at high latitudes. About 52 hours later on January 27 at 0430 UT a moderate intensity ssc geomagnetic storm was recorded by various observatories. Simultaneously a Forbush decrease was recorded by the neutron monitors.

Table 2

Grouped Reports ≥ 1 JANUARY 1971

Flare No.	Date	Max	Approximate Location	Plage No. McMath	Importance
1	23	0414	N19 W21	11128	1B
2	24	1814	N17 W46	11128	*1B
3		1830	N16 W45	11128	1N
4		2045	N19 W50	11128	1N
5		2316	N19 W50	11128	*1B
6		2331	N18 W49	11128	3B
7	25	0250	N19 W51	11128	*3F

*second brightening.

To explain these observations it is suggested that the moderate/low energy plasma ejected from various flares of McMath plage region 11128 on January 24 modulated the background solar wind, the impact of which on the magnetospheric boundary was mainly responsible for the observed storm. Moreover, the compressed geomagnetic cavity under the influence of this solar wind seems to have prevented the background galactic cosmic rays from entering into the magnetosphere and thus giving rise to the observed Forbush decrease. It is interesting to note that a similar ssc storm and a Forbush decrease were recorded about 48 hours after the cosmic ray event of November 18, 1968 [Kawasaki and Akasofu, 1970].

For a few observatories (see Table 3) H-component variations on January 27, digitized from normal magnetograms at 1 min-interval, are shown in Figure 1. The well-defined ssc occurred at 0430 UT on January 27. This ssc was followed by a world-wide storm. The bulk of the particles from the flares of January 24 had reasonable transit time to cause the observed ssc and the main phase decrease of the storm.

Polar substorm 0600-1000 UT

The ssc of 0430 UT was followed by a complex polar substorm beginning about 0600 UT and lasting for approximately 4 hours. The pronounced structuring of the traces at a number of stations, (see for example GWR (H), Fig. 1), strongly suggests that 3 separate substorms occurred in this interval. In this analysis 3 substorms have been identified which agree approximately in times of occurrence with the main H- and Z-bays on the Leirvogur and Dixon Island traces.

Analysis of Magnetic Data

The stations used in the analysis are shown in Figure 2. H(X), D(Y) and Z perturbations were measured from the quiet level (Kp=0) preceding the ssc, and expressed in the geomagnetic coordinate system X^1, Y^1, Z. It is probable that the currents which give rise to polar magnetic substorms are three dimensional and flow along field lines as well as in the ionosphere. However, to describe the development of the substorm, equivalent ionospheric line current vectors have been calculated, using both the horizontal and vertical components of the perturbation vector, following the procedure outlined previously by Loomer and Jansen van Beek [1971]. Plots of current vectors for a number of instants during the storm are given in Figure 3.

Sequence of Magnetic Events

The growth of the auroral electrojet is evident in the midnight sector at 0555 UT when gradual positive Z and negative H bays begin at Great Whale River (Fig. 4). At 0615 UT an impulsive event was observed at Leirvogur in the early morning sector, and at Meanook, Victoria and College in the evening sector. No unusual features were observed at Great Whale River at this time.

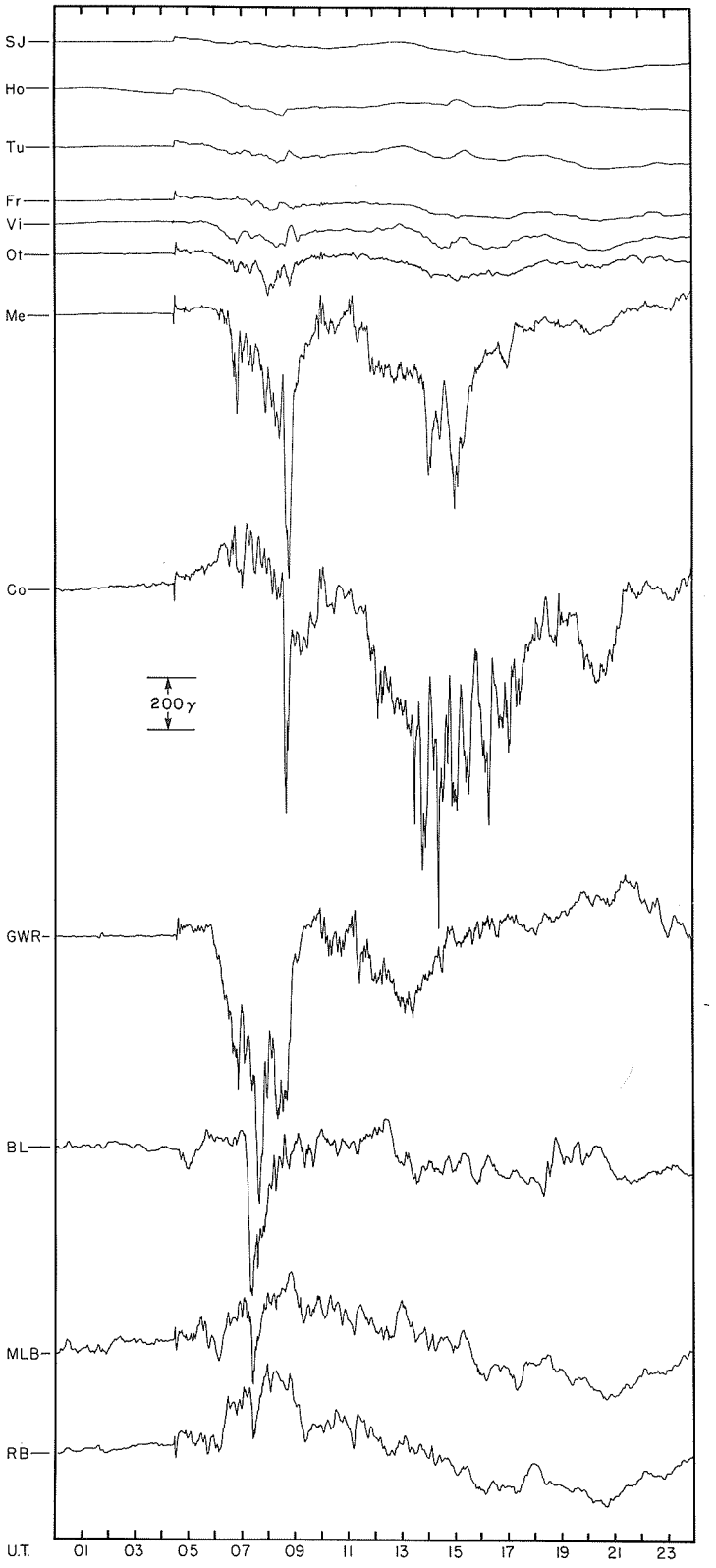

Fig. 1. H(X) magnetogram traces drawn from 1 minute digitized data. X-traces are shown for Baker Lake, Mould Bay and Resolute Bay for January 27, 1971.

Table 3

	Station	Geomag. Co-ords. Lat.N	Long.E		Station	Geomag. Co-ords. Lat.N	Long.E
* Al	Alert	85.7	168.7	Co	College	64.6	256.1
RB	Resolute Bay	83.1	287.7	DI	Dixon Is.	62.8	161.7
Go	Godhavn	80.0	33.1	Me	Meanook	61.9	300.7
MLB	Mould Bay	79.1	255.4	Si	Sitka	60.0	275.0
BL	Baker Lake	73.9	314.8	Ot	Ottawa	57.0	351.5
Na	Narssarssuaq	71.4	37.3	Vi	Victoria	54.3	292.7
Leir	Leirvogur	70.3	71.6	Fr	Fredericksburg	49.6	349.8
Ch	Fort Churchill	68.8	322.5	Tu	Tucson	40.4	312.2
PB	Point Barrow	68.4	240.7	SJ	San Juan	29.9	3.2
GWR	Great Whale River	66.8	347.2	Ho	Honolulu	21.1	266.5
Ab	Abisko	65.9	115.3				

* see note following REFERENCES

The expansive phase of the first substorm to be clearly identified is believed to begin with the sharp negative Z-bay at 0640 UT (Figure 4) which was superimposed on the positive Z-bay at Great Whale River and Churchill. The bay lasted for 5 minutes and suggests an abrupt northward surge at this time in the midnight sector. The intensity of the storm at 0640 UT is maximum near Great Whale River when ΔH was about 420 γ, and Churchill, with the electrojet flowing to the south of these stations (Figure 3). Current intensity at Great Whale River was 3.7×10^5 amps.

The next outstanding magnetic effect is the sudden commencement of the principal negative X-bay at Baker Lake at 0652 UT. This may be interpreted as the effect of a westward surge which originated at 0640 UT between Great Whale River and Churchill, and travelled along the 70° geomagnetic parallel with a speed of approximately 1 km/sec [Akasofu, 1968; Loomer and Jansen van Beek, 1972].

The movement of the electrojet to the north of Great Whale River is seen on the magnetogram (Figure 4) as a positive indentation of the negative H-bay from 0650 to 0710 UT with maximum at 0700 UT, together with the change in sign of the Z-perturbation, which becomes negative about 0700 UT. Very similar effects are observed in the X- and Z-components at Churchill, and the majority of stations in and near the oval register an impulsive change in field around this time. The intensification of the electrojet and its movement to the west and north are clearly shown on the current vector plots for 0654 and 0700 UT. At 0710 UT, when X reaches its greatest negative value at Baker Lake, the electrojet is already decreasing in intensity there. The largest current values for these times are recorded at Baker Lake (5.2×10^5 amps at 0700 UT), and Godhavn. ΔH was maximum at Great Whale River (650 γ at 0654 UT) and Narssarssuaq (800 γ at 0700 UT).

The continued movement of the electrojet to the north and west is evident in the negative X- and Y-bays beginning about 0710 UT at Resolute Bay and Mould Bay. A westward-travelling surge seen at Baker Lake at 0652 UT and travelling at 1 km/sec could be expected to reach the Resolute Bay, Mould Bay area near 0710 UT, and the effects observed at this time at Resolute Bay and Mould Bay may result directly from the expansion of the storm which developed in the midnight sector at 0640 UT. However, independent substorm activity at the northern edge of the oval [Akasofu, 1970; Rostoker, 1971; Loomer and Jansen van Beek, 1971] is also a possible explanation. Latitude profiles in ΔX^1 would appear to support this interpretation, but owing to the limited number and unequal distribution of observatories available for this analysis, it is not certain how reliable such profiles are. Current vectors at 0728 and 0742 UT are maximum at Resolute Bay and Godhavn (4.6×10^5 amps at 0742 UT). ΔH remains maximum at Narssarssuaq and Great Whale River (1050 γ at 0742 UT). It is apparent from Figure 3 that the electrojet is flowing westward around the oval at all longitudes at 0742 UT.

At 0806 UT the current is again maximum at Great Whale River (5×10^5 amps) and the electrojet is appreciably south of the station. A new substorm apparently begins around this time. No outstanding effects of this storm are evident in the oval, owing perhaps to the lack of auroral zone observatories

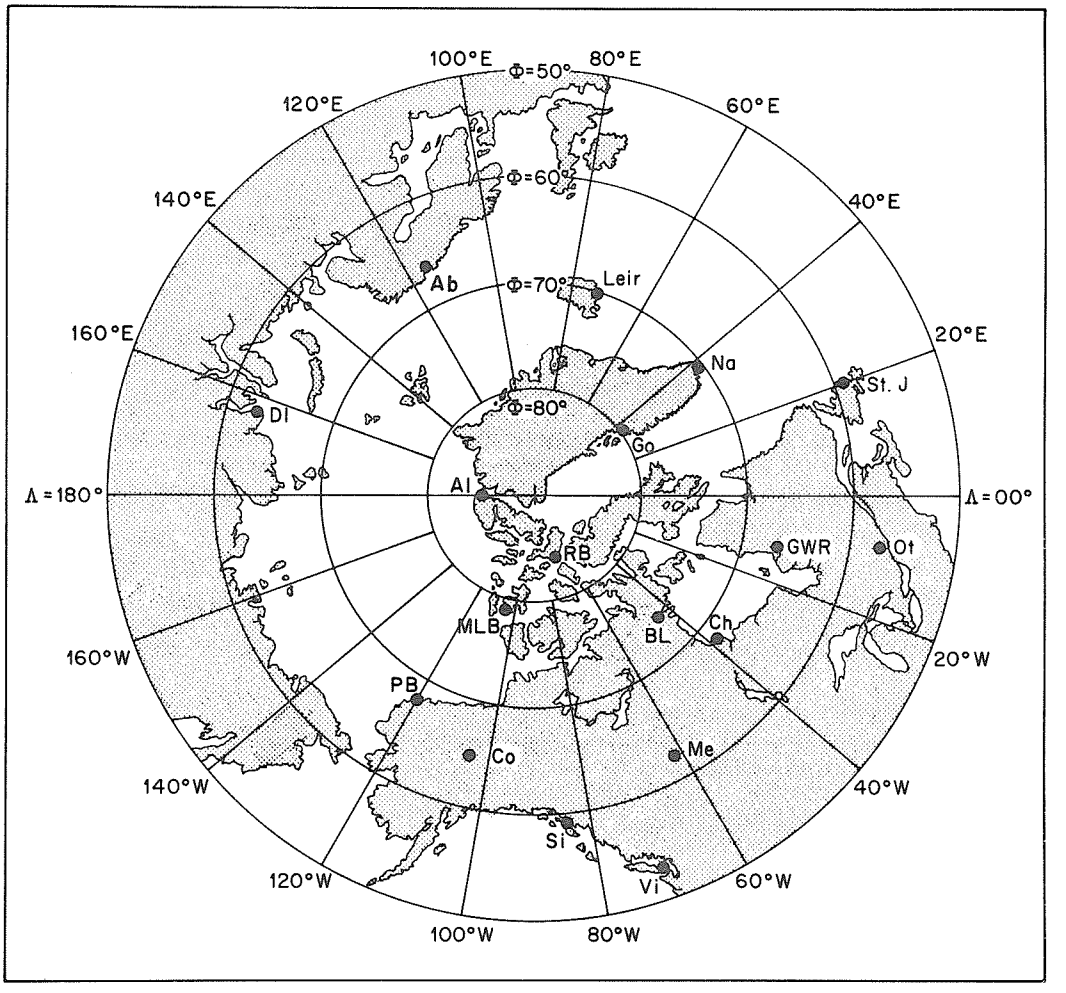

Fig. 2. Map in geomagnetic coordinates showing the stations used for this analysis.

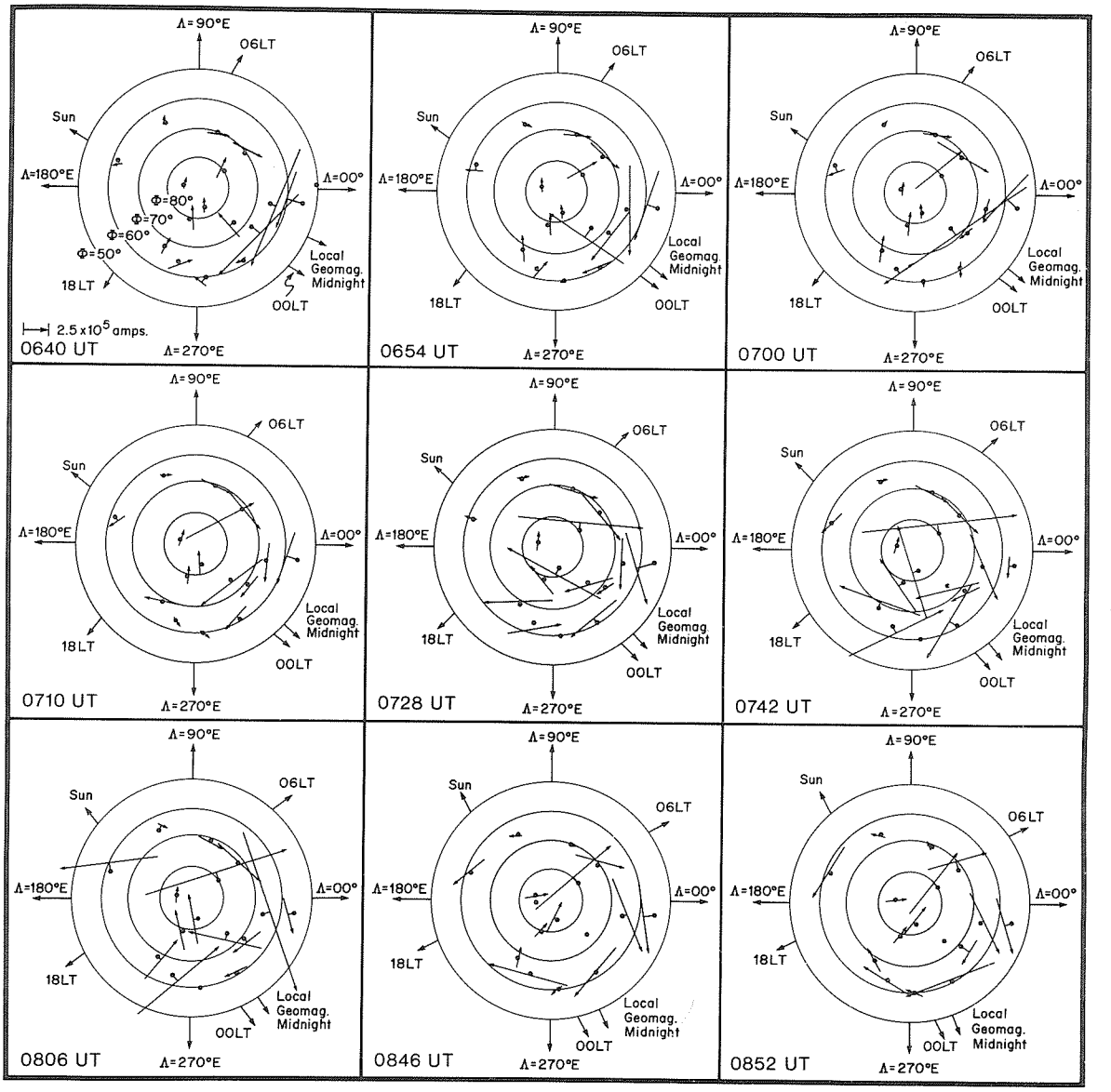

Fig. 3. Current vector plots for selected times. Key to location of stations is given by Figure 2.

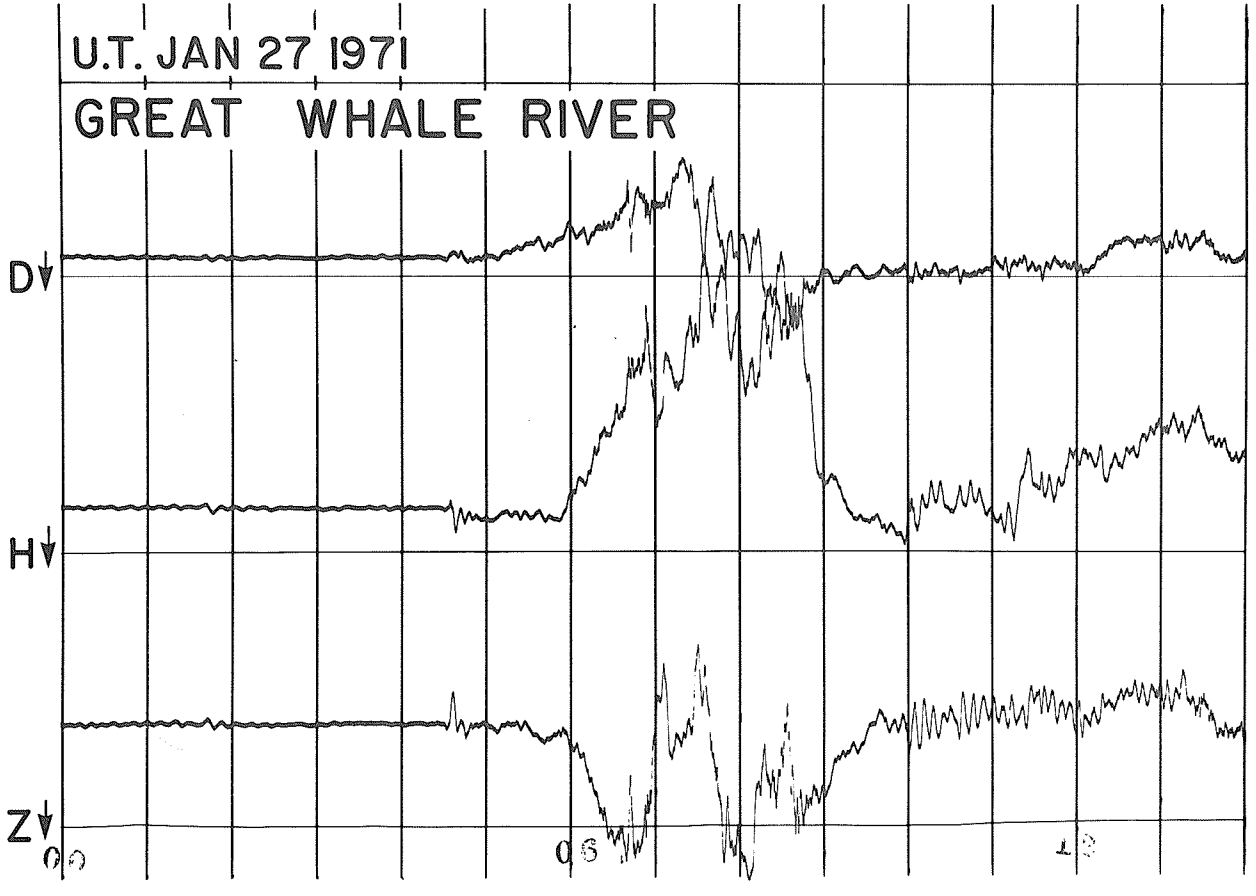

Fig. 4. Portion of standard photographic magnetogram for Great Whale River, January 27, 1971.

between Churchill and Point Barrow. However, a very clear D transitional bay occurred at 0829 UT at Tucson, situated in longitude between Great Whale River and Meanook, suggesting that the center line of the substorm, or demarcation line, passed over Tucson from east to west at this time.

The third substorm was first seen at Meanook at 0835 UT with the sudden commencement of the main negative H-bay. By 0840 UT College is also under the influence of the primary electrojet. Prior to this College was south of the oval and in a predominantly eastward current flow. The movement of the area of maximum intensity of the electrojet westward form Great Whale River to Meanook and College is evident in the current vector plots for 0846 and 0852 UT. At 0852 UT ΔH was greatest at Meanook when it exceeded 1000 gammas. Current intensity was 2.8×10^5 amps. Very clear examples of D transition bays are seen at Meanook where D changes from east to west at 0852 UT and at Victoria where the changeover is at 0859 UT. Following Rostoker's model [1966] and using the method given by Loomer and Jansen van Beek [1972], the velocity of the demarcation line relative to the sun-earth line was 0.9 km/sec at the latitude of the Meanook and College current vectors at 0852 UT. This is in good agreement with the results of Rostoker et al. [1970].

Discussion and Summary

Substorm activity ended rather abruptly around 1000 UT. A strong southeasterly current flow was recorded at Dixon Island on the current vector plots drawn for the 3 substorms. There were insufficient data in the day sector to distinguish between the Akasofu and Feldstein models [Akasofu, 1968] of equivalent current flow. On some of the plots the orientation of the current vectors at Alert, Abisko, Dixon Island, College and Point Barrow strongly suggests a two-celled current system. However, it is difficult to explain the strong persistent northeastward current flow at College prior to 0840 UT.

The early growth of the electrojet at Leirvogur and Great Whale River may be an illustration of the initial phase of the substorm identified by Loomer and Jansen van Beek [1971], and probably identical with the growth phase believed by Rostoker [1972] to precede the explosive (or expansive) phase of the substorm.

The intensification of the storm and the movement to the west and north of the storm center was most clearly seen in the magnetic effects associated with the first substorm. The magnetic events which followed the impulsive bay at 0640 UT at Great Whale River and Churchill suggested that a westward surge travelling at 1 km/sec preceded the extension of the electrojet into the evening sector, approaching Baker Lake at 0652 UT and flowing within 2-2½° of Resolute Bay at 0728 and 0742 UT. Alternatively, the intensification of activity at Resolute Bay and Mould Bay may have been the result of a separate substorm occurring at the northern edge of the auroral oval. The large current vector at Godhavn was unexpected, and is perhaps best explained by the northward expansion of the electrojet in the midnight sector.

The very large current vector at Great Whale River at 0806 UT, around the time assumed for commencement of the second substorm, is an example of the return of the center of the storm in the recovery phase to an area near the pre-expansion position, considerably east of the local midnight meridian, noted by Loomer and Jansen van Beek [1971].

Although much information concerning the development of substorms may be inferred from magnetic data alone, a more complete analysis of this substorm will be published elsewhere.

Acknowledgement

We would like to extend sincere thanks to Mr. William Paulishak of the World Data Center A for supplying us with the magnetograms and to Mr. G. Jansen van Beek for very helpful discussions and assistance in computations.

REFERENCES

AKASOFU, S. -I. 1968 Polar and Magnetospheric Substorms, Astrophysics and Space Science Library, 2, D. Reidel Publishing Co., Dordrecht, Holland.

AKASOFU, S. -I., et al. 1970 Results from a Meridian Chain of Observatories in the Alaskan Sector (I), Preprint of Report of Geophysical Institute, Univ. of Alaska.

KAWASAKI, K., and S. -I. AKASOFU 1970 Geomagnetic Disturbances during the Period November 16 - 21, 1968 Associated with the McMath Plage Regions 9760 and 9780, World Data Center A, Upper Atmosphere Geophysics Report UAG-9, 92-102.

KISABETH, J. L. and G. ROSTOKER	1971	Development of the Polar Electrojet during Polar Magnetic Substorms, J. Geophys. Res., 76, 6815.
LOOMER, E. I. and G. JANSEN VAN BEEK	1971	Magnetic Substorms, December 5, 1968, Pub. Earth Phys. Br., Vol. 41, No. 10.
LOOMER, E. I. and G. JANSEN VAN BEEK	1972	Polar Magnetic Substorms 0300-0600 UT, December 5, 1968, Pub. Earth Phys. Br., Vol. 42, No. 4.
PINTER, S.	1970	Solar Cosmic Ray Event on 18 November 1968, World Data Center A, Upper Atmosphere Geophysics Report UAG-9, 26-29.
ROSTOKER, G.	1966	Midlatitude Transition Bays and Their Relation to the Spatial Movement of Overhead Current Systems, J. Geophys. Res., 71, 79-95.
ROSTOKER, G., et al.	1970	Development of a Polar Magnetic Substorm Current System, Report of Univ. of Alberta, Killam Earth Sciences, May 8.
ROSTOKER, G.	1972	Polar Magnetic Substorms, Rev. Geophysics and Space Physics, 10, 157-211.
	1971	Solar-Geophysical Data, 323 Part II, U.S. Department of Commerce, (Boulder, Colorado, U.S.A. 80302).

Note

Owing to a large induction anomaly, care must be exercised in using Alert magnetic data. In their paper "The Extension of the Alert Geomagnetic Anomaly through Northern Ellesmere Island, Canada" (Canadian Journal of Earth Sciences, Vol. 8, No. 1, 1971), O. Praus et al. show that Alert magnetic perturbations are not seriously affected by the anomaly unless the magnetic component transverse to the strike of the anomaly is appreciably larger than that along the anomaly. The strike of the anomaly is approximately N.E. to S.W. For Alert perturbations used in this analysis the components along and transverse to the anomaly are similar in magnitude, and the equivalent line current vectors calculated from the Alert data should not be seriously distorted by the anomaly.

USCOMM-NOAA-ASHEVILLE,NC-1-73-1325